(NASA-CR-162828) SLICING OF SILICON INTO SHEET MATERIAL. SILICON SHEET GROWTH DEVELOPMENT FOR THE LARGE AREA SILICON SHEET TASK OF THE LOW COST SOLAR ARRAY PROJECT Final Report, (Varian Associates, Lexington, G3/44

N80-19623

Unclas
47485

JET PROPULSION LABORATORY
CALIFORNIA INSTITUTE OF TECHNOLOGY
PASADENA, CALIFORNIA

DOE/JPL 954374-10

SLICING OF SILICON INTO SHEET MATERIAL

FINAL REPORT

September 21, 1979

Varian Associates
Lexington, Massachusetts

S-100-F
DOE/JPL 954374-10

SLICING OF SILICON INTO SHEET MATERIAL

Silicon Sheet Growth Development for the Large Area Silicon Sheet Task of the Low Cost Solar Array Project

FINAL REPORT

By

J. R. FLEMING
S. C. HOLDEN
R. G. WOLFSON

September 21, 1979

Reporting Period January 9, 1976 to September 30, 1979

JPL Contract No. 954374

Varian Associates
Lexington Vacuum Division
121 Hartwell Avenue
Lexington, Massachusetts 02173

This work was performed for the Jet Propulsion Laboratory, California Institute of Technology, under NASA Contract NAS7-100 for the U. S. Department of Energy (DOE).

The JPL Low-Cost Solar Array Project is funded by DOE and forms part of the DOE Photovoltaic Conversion Program to initiate a major effort toward the development of low-cost solar arrays.

This report contains information prepared by the Lexington Vacuum Division of Varian Associates under JPL subcontract. Its content is not necessarily endorsed by the Jet Propulsion Laboratory, California Institute of Technology, National Aeronautics and Space Administration or the U. S. Energy Research and Development Administration, Division of Solar Energy.

TABLE OF CONTENTS

APPENDICES

LIST OF FIGURES

LIST OF TABLES

SUMMARY

Complete results, from raw data to interpretation to recommendations, of a program to investigate the use of multiblade slurry sawing to produce silicon wafers from ingots are presented in this report.

During the course of this program, the commercially available "state of the art" process was improved by 20% in terms of area of silicon wafers produced from an ingot. The process was improved 34% on an experimental basis. Production of 20 wafers per centimeter length of 100 mm diameter ingot is now possible on a production basis.

Economic analyses presented show that further improvements are necessary to approach the desired wafer costs, mostly reduction in expendable materials costs. Tests which indicate that such reduction is possible are included, although demonstration of such reduction was not completed.

A new, large capacity saw was designed and tested. Performance comparable with current equipment (in terms of number of wafers/cm) was demonstrated. Improved performance was partially demonstrated, but problems (both mechanical and of unknown origin) precluded full demonstration of improved performance.

1.0 INTRODUCTION

The process of slurry sawing is an ancient one: its origins are prehistoric. The basic elements are relative motion between a workpiece and a blade or blades, generally toothless, and the introduction of an abrasive, carried in a liquid, which performs the actual cutting. The process was probably originally developed because the blade can be much softer than the workpiece.

Varian Associates (and our predecessor, National Research Corporation) have been manufacturing slurry saws for almost two decades. Over 800 of the model 686 (recently replaced by the similar model 7176) are being used in various industries slicing materials ranging in hardness from hard steels to almost fully dense alumina. Our experience with these varied materials has allowed us to select materials and operating conditions that are workable for almost any desired and possible result. Optimizing the process for a given material and desired result still requires experimentation.

Some features of the process as used in Varian equipment are as follows. Precision rolled AISI 1095 steel blades, fully hardened, are assembled into a blade package by alternating blades with precision rolled, fully hardened AISI 1095 steel spacers at each end of the blade as shown in Figure 1. (Multiple blades must be used because the relatively slow material removal rate must be offset by cutting multiple wafers simultaneously.) Blades range in thickness from 150 μm (.006 in.) to 250 μm (.010 in.), and spacer

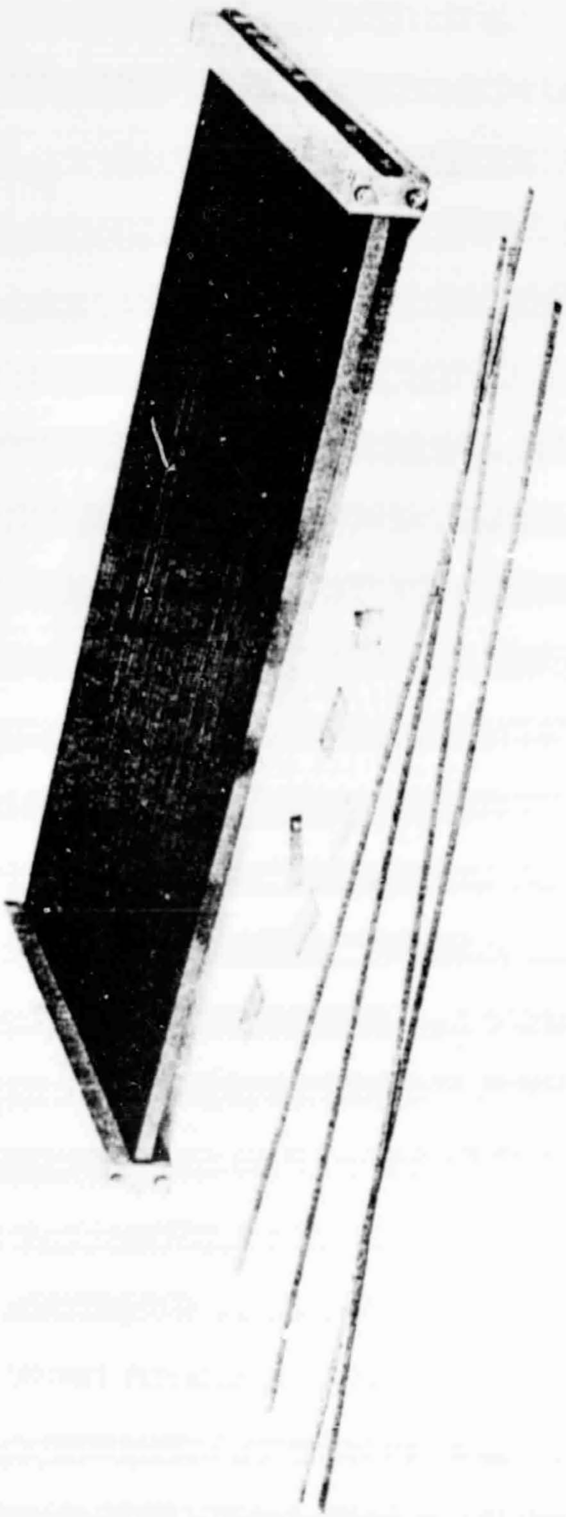

Figure 1. Multiblade Pin Package and Components

thicknesses range from 300 μm (.012 in.) up. The blade package is held together temporarily by either glue or pins passing through the spacers and clamping the assembly.

The blade package is inserted into a bladehead, the spacer stacks are compressed to provide frictional blade clamping (patented) and the blades are stretched to 1.33×10^3 N/mm^2 (1.93×10^5 psi). This elongation is necessary to add to the stability of the blades and prevent "wandering" as the cut progresses. Since the bladehead reciprocates on hand-scraped ways to provide the relative blade-workpiece motion, the next step is to align the blades precisely relative to the stroke direction.

With the blades installed, the workpiece is glued to a glass or ceramic submount which is glued to a workholder. The workholder is then clamped to a vertical feed mounted below the bladehead. The feed is raised pneumatically until the workpiece contacts the blades.

A slurry is now poured over the assembly. This slurry consists of an oil-based vehicle (usually PC oil, manufactured by Process Research Corporation) mixed with silicon carbide abrasive (boron carbide is sometimes used with harder workpieces). Useful abrasive sizes range from #320 to #1000.

With the bladehead reciprocating, the pneumatic feed providing a constant cutting force, and the slurry providing cutting action, the workpiece is abraded away. The blades usually wear much more slowly that the workpiece, but have a finite lifetime. The slurry also has a finite lifetime because of debris accumulation, and no

commercial application has yet found it profitable to separate and reuse the oil and abrasive. Thus, oil, abrasive, and blades are "expendables" and their lifetime can affect the economics of optimization significantly.

The slurry sawing process has several characteristics which make it a promising method for production of silicon wafers (from ingots) for solar cells. The machinery is simple and relatively low cost. It requires little skill to operate (although skill is required in setting up the machine). Once running, it requires little operator attention. In many cases, the "kerf loss" or amount of waste material is significantly lower than with other methods, which is a very important factor in the manufacture of solar cells where the wafer cost is a large portion of the final device cost.

With these facts in mind, a study was undertaken under the auspices of the LSA project, administered by the Jet Propulsion Laboratory. This study included several phases, which were: 1. a parameter and potential study, in which we investigated the effect of various parameters and assessed the state of the art and potential of slurry sawing as applied to slicing 100 mm (4 in. nominal) diameter silicon ingots; 2. an equipment design and process modification phase, in which we designed, fabricated, and tested new equipment (specifically a large capacity saw) and tested process modifications which showed potential to reduce the cost of wafers. Concurrently with these studies, economic analyses were performed to assess the results and guide further work.

This report is the final report under the current contract. In the interest of maintaining a logical progression, the first section covers Phase I, the second section discusses the economic analysis and its implications, and the third section covers the actions taken in Phase II as a result of the economic analysis.

2.0 PHASE I: ANALYSIS

2.1 Efficiency of the Cutting Process

It is desirable to obtain a measure of how well the microscopic cutting process works. This is difficult to do directly, because the cutting interface cannot be observed directly. An indirect measure, which we call "efficiency", has been developed and proved useful.

The development of the efficiency parameter begins with the theory of abrasive wear [1]. An abrasive particle is modeled by a conical indenter described by an angle Θ as shown in Figure 2. Under a small load ΔL, the indenter generates a contact area related to the load and work material hardness, H,

$$\pi r^2 = \Delta L/H \qquad (1)$$

The projected area of the indenter below the work material surface, in a plane perpendicular to that surface, is

$$A_p = r\,x = r^2 \tan\Theta \qquad (2)$$

---

[1] Ernest Rabinowicz, Friction and Wear of Materials, John Wiley & Sons, New York (1965).

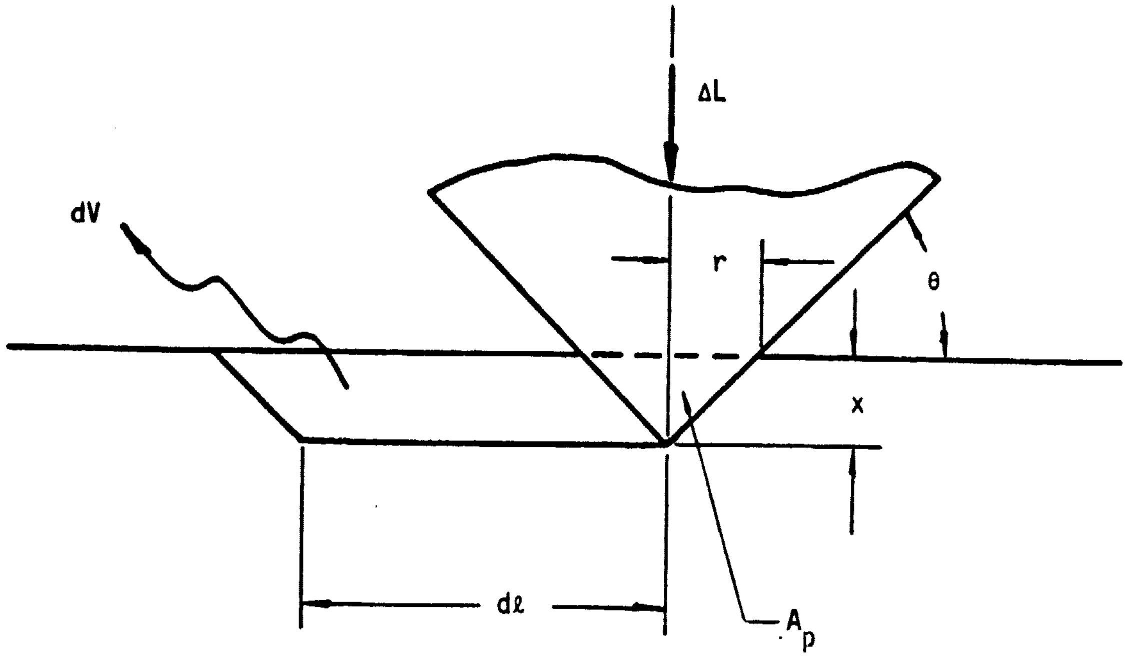

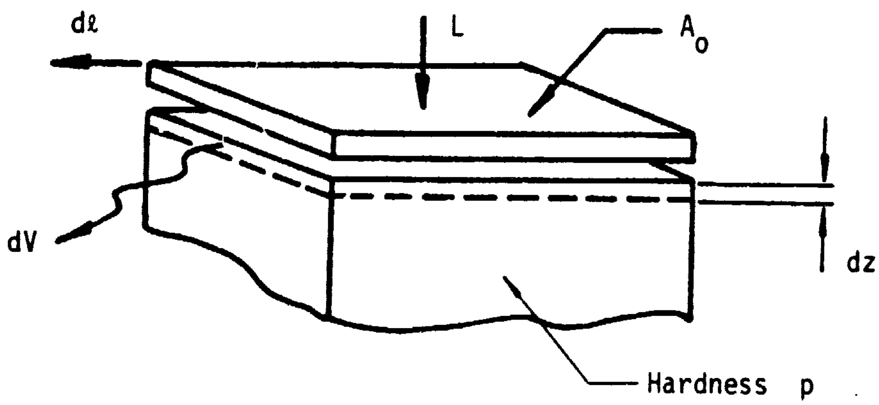

Figure 2. Models of Planar Abrasive Wear

If the indenter is moved laterally by an amount $d\ell$, the volume of work material swept out by the indenter will be

$$dV = A_p d\ell \tag{3}$$

Substituting for A_p from (2) and r^2 from (1),

$$dV/d\ell = \Delta L \tan\Theta/(\pi H) \tag{4}$$

Equation 4 is an idealized removal rate for a single grain. If there are multiple cutting grains under a total load L with some average indenter geometry $\overline{\tan\Theta}$,

$$dV/d\ell = L\overline{\tan\Theta}/(\pi H) \tag{5}$$

Note that if $\overline{\tan\Theta}$ is calculated from Equation 5 using experimentally measured values, then $\overline{\tan\Theta}$ is a measure of how well the cutting process is working at a given load, material hardness, and sliding distance. This is because $\overline{\tan\Theta}$ is affected not only by abrasive geometry, but also by all factors other than load, hardness, and sliding distance which affect the cutting process.

However, Equation 5 is not directly suitable for measuring the efficiency of slurry sawing since, as discussed below, the cutting is non-planar and forces which do no work affect the cutting significantly.

In order to develop an efficiency parameter for slurry sawing, it is first necessary to develop an expression for the cutting rate in planar abrasive wear. In terms of the rate of relative motion $d\ell/dt$ and the total nominal area of contact A_0 as shown in the lower half of Figure 2, the cutting rate dz/dt is

$$dz/dt = (dV/d\ell)(d\ell/dt)(1/A_0) \qquad (6)$$

Substituting for $dV/d\ell$ from (5),

$$dz/dt = (d\ell/dt)(1/A_0)L\overline{\tan\Theta}/(\pi H) \qquad (7)$$

In slurry sawing, the shape of the wear trough is similar to that shown in Figure 3. Since the applied load L is not normal to the cutting surface, the previous equations are not directly applicable. Physically, "wedging" of particles contributes to material removal, so the above equations generally underestimate the cutting rate.

If we consider a small area of the trough, and let the local normal force divided by the area be denoted by normal pressure p_n, Equation 7 becomes

$$dz_n/dt = (d\ell/dt)p_n\overline{\tan\Theta}/(\pi H) \qquad (8)$$

where dz_n/dt is the cutting rate normal to the surface.

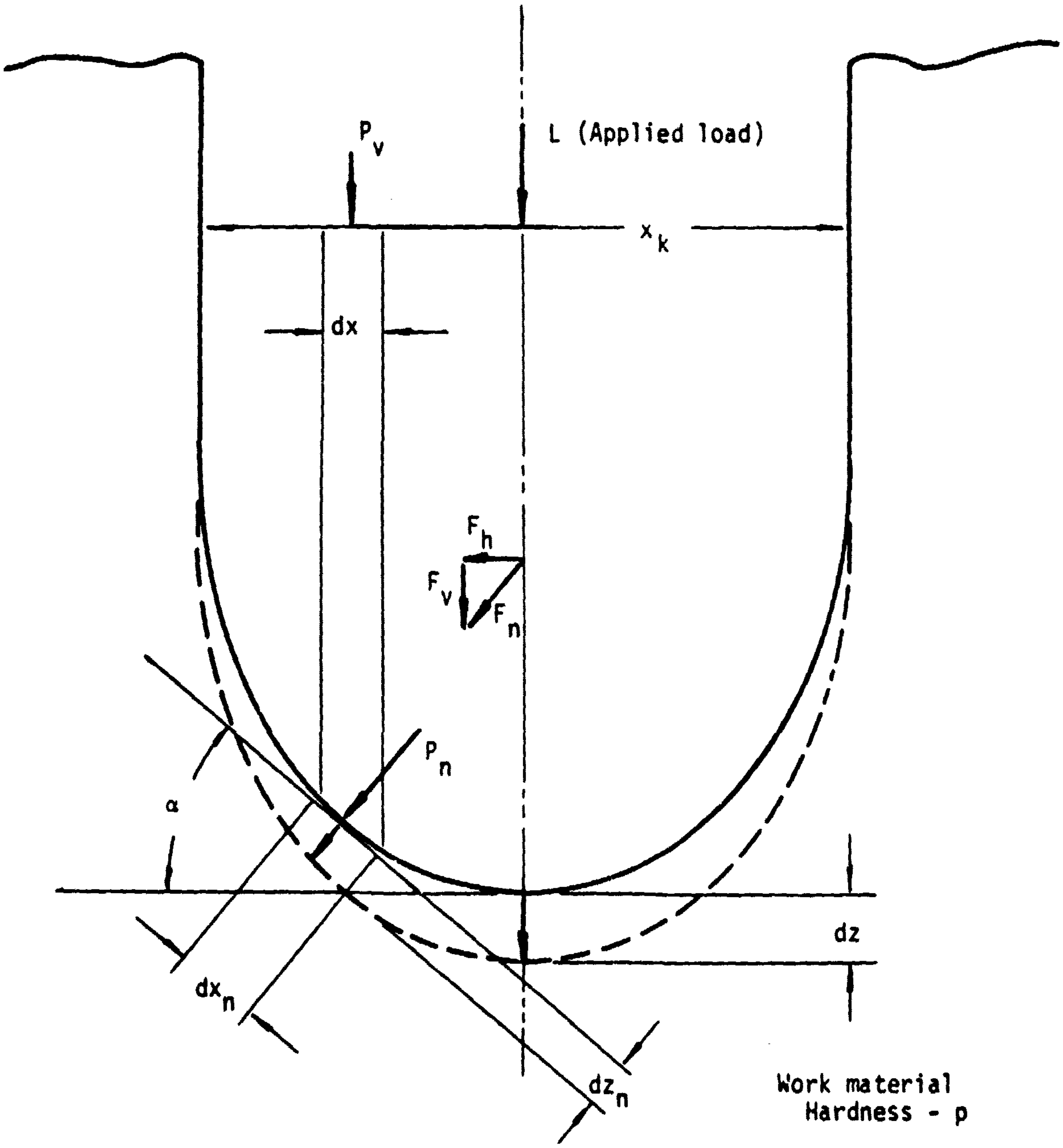

Figure 3. Model of Non-Planar Abrasive Wear

It is necessary that all portions of the blade progress at the same vertical rate, so

$$dz_n/dt = \cos\alpha \, dz/dt \qquad (9)$$

Also, the vertical component of the indentation pressure must be supplied by the vertical applied pressure, or

$$P_v dx = p_n dx_n \cos\alpha \qquad (10)$$

Or, since from elementary trigonometry $\cos\alpha = dx/dx_n$,

$$P_v = p_n \qquad (11)$$

Solving Equation 8 for p_n , substituting for dz_n/dt from (9) and for p_n from (11) yields

$$P_v = (dt/d\ell)(dz/dt)\pi H\cos\alpha/\overline{\tan\Theta} \qquad (12)$$

Multiplying P_v by dx and by y_k , the "kerf length" or length of blade engaged with the work (into the paper in Figure 3), gives the portion of the total applied load L due to the contact over the width dx . Integrating over the kerf width yields the total applied load L . Noting that only α is a function of x in (12), the result is

$$L = (dt/d\ell)(dz/dt)\, 2\int_0^{x_k/2} \cos\alpha dx \; \pi H y_k/\overline{\tan\Theta} \qquad (13)$$

Defining $\bar{\varepsilon} = \overline{\tan\Theta}\, x_k/(2\int_0^{x_k/2} \cos\alpha dx)$ and $A_o = x_k y_k$ and rearranging Equation 12, we obtain

$$dz/dt = (d\ell/dt)(1/A_o)L\bar{\varepsilon}/(\pi H) \qquad (14)$$

This is the equation for cut rate in slurry sawing. It is exactly the same as Equation 7 except $\bar{\varepsilon}$ replaces $\overline{\tan\Theta}$. Therefore, since $\overline{\tan\Theta}$ is a measure of the efficiency of a planar abrasive wear process, $\bar{\varepsilon}$ is a measure of the efficiency of slurry sawing.

It is useful to approximate the increase in efficiency of slurry sawing over planar abrasive wear. If the trough in Figure 3 were flat-bottomed, the wear process is planar $(\alpha(x) = 0)$, and $\bar{\varepsilon} = \overline{\tan\Theta}$ as expected. If the trough is a half circle $(\alpha(x) = \sin^{-1}2x/x_k)$, integrating the definition of $\bar{\varepsilon}$ yields $\bar{\varepsilon} = 1.27\,\overline{\tan\Theta}$. Thus, the wedging action in slurry sawing increases the cutting rate about 27% over planar abrasion.

Recapitulating, Equation 14 may be solved for $\bar{\varepsilon}$ in terms of variables that are easily measured experimentally:

$$\bar{\varepsilon} = (dz/dt)x_k y_k \pi H/(L\ d\ell/dt) \qquad (15)$$

where dz/dt is the cut rate, x_k is the width of the slot worn by the blade, y_k is the length of the slot, H is the work material hardness, L is the vertical load per blade, and

$d\ell/dt$ is the rate at which the blade slides over the work. A later discussion, under Phase II, will show that the actual contact length is much less than y_k , but this does not affect the validity of $\bar{\varepsilon}$ as an efficiency measure: it does make it impossible to predict a cut rate from first principles using Equation 14.

2.2 Blade Stability and Deflections

One parameter of great interest is the cutting load per blade. Higher cutting loads increase cutting rate, while lower loads decrease wafer dimensional variation. Experimental work performed by Varian, both under this contract and otherwise, shows that the maximum load per blade for most purposes (trade-off between cut rate and wafer accuracy) is approximately 558 grams/blade/mm of blade thickness (500 oz./blade/inch of blade thickness). Some analyses have been performed to try to place this empirical result on a sound analytical footing.

The analysis presented in this section has been partially supplemented by a more exact analysis performed under Phase II, but is included here for completeness.

Figure 4 illustrates a steel blade of length ℓ_B , thickness t_B , and height h_B . The blade is tensioned to a uniform stress σ_0 and the endpoints are fixed. There are two phenomena which affect the stiffness of such a blade; the "intrinsic stiffness" due to the fact that the blade is made of steel, and

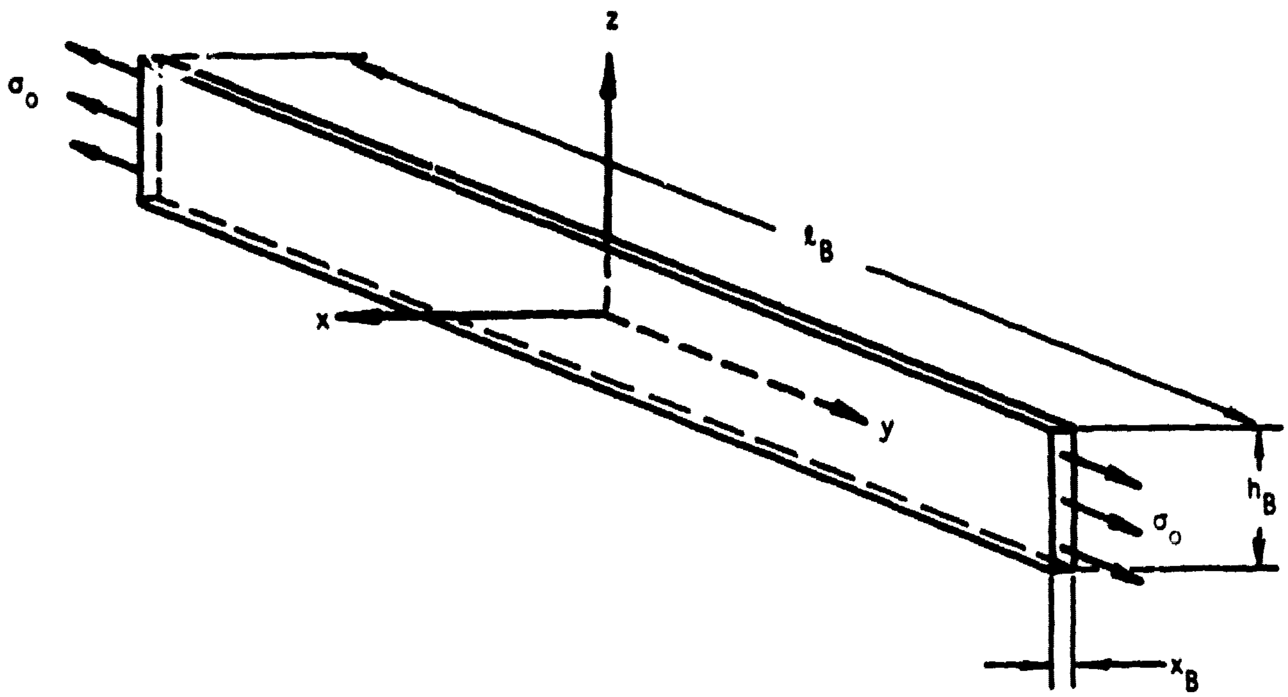

Figure 4. Geometry of a Tensioned Blade

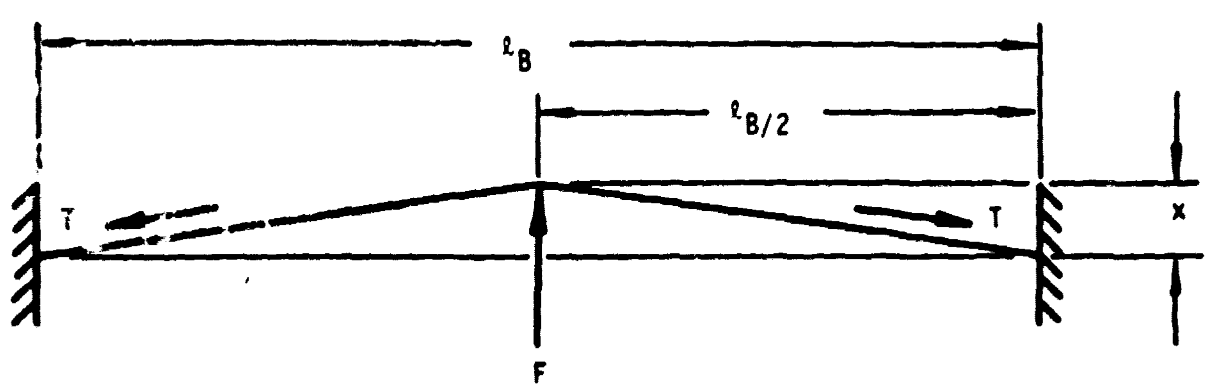

Figure 5. Central Deflection of a Tensioned String

the "induced stiffness" or "taut string effect" due to the fact that any deflection of the blade causes the tension to increase. In Varian slurry saw blades, the taut string effect dominates (this will be shown more formally in the Phase II analysis, where it will be shown that the intrinsic stiffness is about 10% of the induced stiffness). The following analysis includes only the induced stiffness, and thus calculated displacements are larger than the real ones (upper bounds) and forces that cause a given displacement are lower bounds.

If a taut string is deflected by a central force as shown in Figure 5, the relationship between force F and displacement x is (in terms of tensioning force T)

$$F = 2T \sin(\tan^{-1}(2x/\ell_B)) \qquad (16)$$

since the applied force F must balance the component of the tension force T in the direction of F . For small angular deflections, Equation 15 is closely approximated by

$$F = 4Tx/\ell_B \qquad (17)$$

Since $T = \sigma_o h_B t_B$,

$$F = (4\sigma_o h_B t_B/\ell_B)x \qquad (18)$$

Equation 18 applies equally to horizontal or vertical deflections since the intrinsic stiffness is not included.

The response of the blade to a twisting moment M may be calculated by considering the blade to be made up of many strings of infinitesimal height dh_B, assuming that the blade rotates around its centerline, and summing the contributions of each string. Since this analysis will be repeated with more detail and accuracy under Phase II, details of the derivation will not be presented. The relationship between moment M, twist angle Θ, and maximum deflection x_m is, from this analysis (see Figure 6)

$$M = (\sigma_0 t_B h_B^3 / 3\ell_B)\,\Theta$$

or $$M = (2\sigma_0 t_B h_B^2 / 3\ell_B)\,x_m \qquad (19)$$

Considering the effect of cutting load, the most obvious problem is that of torsional buckling under excessive load. Buckling will occur when a small rotational perturbation Θ as shown in Figure 7 causes an upsetting moment due to the cutting force to exceed the restoring moment given in Equation 19. Since the upsetting moment is Fx_m, the simplest critical buckling load F_c^0 is given by

$$F_c^0 = 2\sigma_0 t_B h_B^2 / 3\ell_B \qquad (20)$$

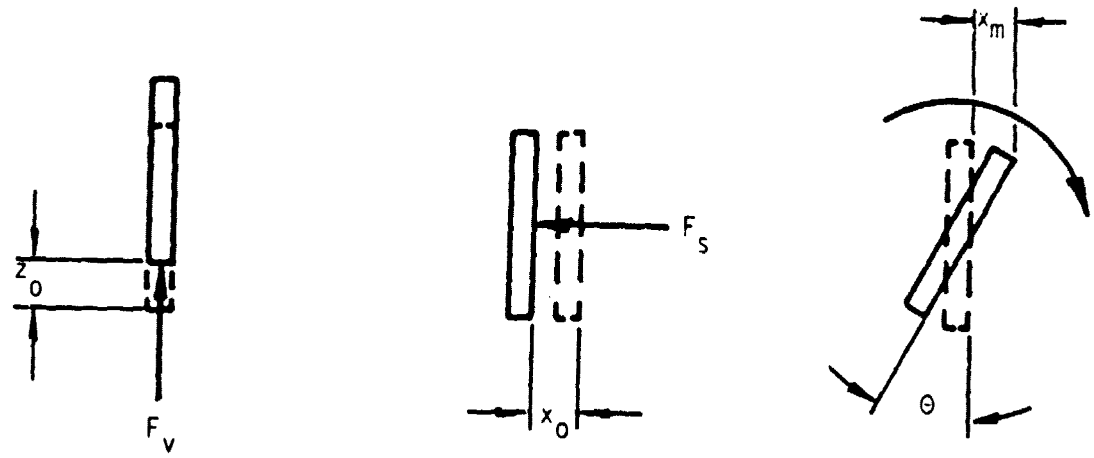

Figure 6. Modes of Blade Deflection

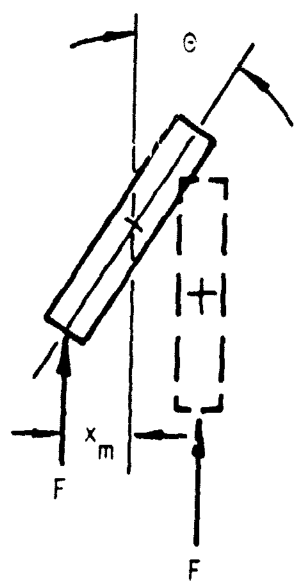

Figure 7. Geometry of Torsional Buckling

A typical blade may be described by ℓ_B = 381 mm (15 in.), h_B = 6.35 mm (.25 in.), t_B = .15 mm (.006 in.), and $\sigma_0 = 1.406 \times 10^5$ g/mm^2 (2×10^5 psi). The buckling load F_c^0 is then 1490 grams or 10^4 grams/blade/mm of blade thickness. This analysis is obviously unable to explain the blade wander observed when blades are loaded more than 5.58×10^2 grams/blade/mm of blade thickness.

If the unloaded blade is tipped as shown in Figure 8, the initial angle Θ_0 will reduce the buckling load. Considering this configuration in the same manner as above, the new buckling load F_c is related to F_c^0 by

$$F_c\ (1 + \Theta_0/\Theta) = F_c^0 \qquad (21)$$

Since Θ_0 will be significantly less than 1 radian and Θ will be of the same order of magnitude, assuming an initial tilt is insufficient to decrease the buckling load to the same order as the empirical maximum load.

This analysis is, therefore, of little use in predicting the onset of blade wander. It cannot be taken as a proof that blades do not buckle torsionally: the failure of the analysis may be due to oversimplification of the problem.

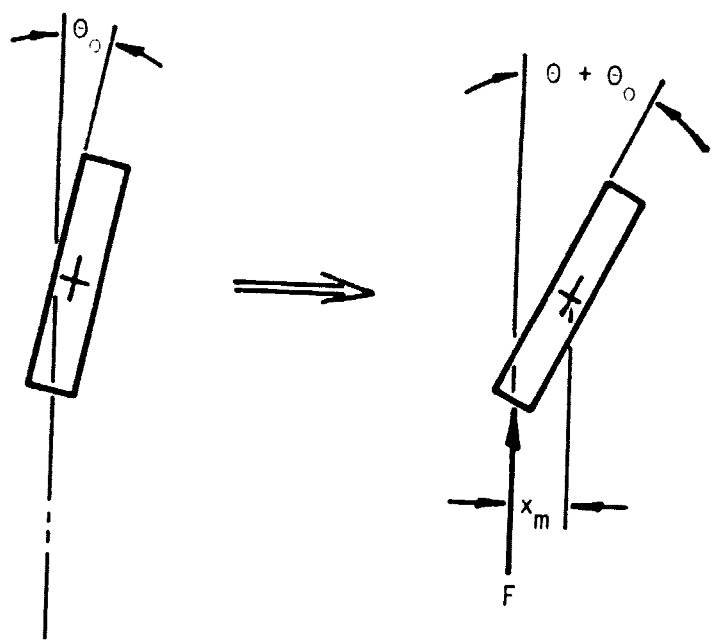

Figure 8. Geometry of a Pre-Tipped Blade

2.3 Statistics of a Blade Package

As stated earlier and shown in Figure 1, a blade package for a Varian multiblade slurry saw consists of blades separated from each other by spacers at each end of the blades. Both blades and spacers are precision rolled to very close thickness tolerances to obtain good blade alignment. Varian saws are designed so that the end blades of a package may be aligned with the stroke, generally within a runout of 3.2×10^{4} mm/mm (1.3×10^{-5} in./in.). Even though the blade pack components are extremely precise, the large number of components may lead to the well known "stacking tolerance" problem: since the position of the end of a blade within the pack is determined by the stacking of many parts, and the error in position is determined by adding many errors (some in one direction and some in another), a significant position difference between the ends of the blade may result. This misalignment of the blade relative to the stroke results in kerf losses larger than expected, and thinner (more fragile) wafers. It is, therefore, of interest to consider the statistical question of expected misalignment.

Statistically, there is an expected value of blade thickness $E(t_B)$ and an expected value of spacer thickness $E(t_s)$. There are also expected values for the errors e in these quantities, $E(e_B)$ and $E(e_s)$. These expected errors are zero if the sign of the error is considered. If the absolute value of the error is considered, the expected values are non-zero. Considering

absolute values of errors, the expected value of any component thickness can be given in terms of the nominal thickness t and the errors as

$$E(t) = t \pm E(e) \qquad (22)$$

If N such components are stacked, the expected thickness of the stack is $NE(t)$, but if we, again, consider the absolute value of the expected error, the expected error in stack thickness $E(e_N)$ is given from elementary statistics as a sum involving binomial coefficients $\begin{bmatrix} n \\ m \end{bmatrix} = n!/((n-m)!\,m!)$

$$E(e_N) = (E(e)/2^N) \sum_{m=o}^{N} \begin{bmatrix} N \\ m \end{bmatrix} \left| N-2m \right| \qquad (23)$$

Luckily, in slurry sawing the blade packages of interest contain over 100 elements, and for N greater than 100, Equation 23 can be well approximated by

$$E(e_N) = 0.798\, E(e)\, N^{1/2} \qquad (24)$$

Returning to blade packs, the runout Δ of a blade relative to a neighboring blade is given by the difference in expected errors between the two ends 1 and 2 of the blade

$$\Delta = \left| \pm E(e_{b1}) \pm E(e_{s1}) - (\pm E(e_{b2}) \pm E(e_{s2})) \right| \qquad (25)$$

Equation 25 is the difference between two similar stacking errors and is, therefore, equal to the stacking error of twice as many components. Therefore, combining Equations 25 and 24, the expected runout of the N^{th} blade relative to the first is

$$\Delta_N = 0.798\ (2N)^{\frac{1}{2}}\ [E(e_s) + E(e_b)] \tag{26}$$

Since both end blades are aligned in Varian saws, Equation 26 does not directly apply to the absolute alignment of a blade. Considering the effect of aligning both ends, the runout of blade number N in a package containing N_B blades is

$$\begin{aligned}\Delta_N &= 1.129\ [E(e_s) + E(e_b)]\ N^{\frac{1}{2}}\ (0 < N \leq N_B/2)\\ &= 1.129\ [E(e_s) + E(e_b)]\ (N_B - N)^{\frac{1}{2}}\ (N_B/2 \leq N \leq B_B)\end{aligned} \tag{27}$$

The maximum expected runout occurs at the center of the pack $(N = N_B/2)$ and is

$$\Delta_{max} = 0.798\ [E(e_s) + E(e_b)]\ N_B^{\frac{1}{2}} \tag{28}$$

and the average runout is easily calculated to be

$$\Delta_{ave} = 0.532\ [E(e_s) + E(e_b)]\ N_B^{\frac{1}{2}} \tag{29}$$

Two important caveats must be noted. First, any factor (such as dirt or bent components) which interferes with perfect stacking will increase misalignment. Second, the expected errors are much smaller than the tolerances of the components since tolerances are maximum value, and since if all similar components are taken from the same lot of steel (as has been Varian's practice) both the tolerances and expected error values will be lower than if multiple lots were used.

Some rough measurements were made in order to gain an understanding of the order of magnitude of the terms appearing in Equations 28 and 29.

First, a random sampling of spacers from one lot of steel were measured by two techniques (high precision mechanical micrometer and ADE 6033T non-contact thickness gauge). The results are shown in Figures 9 and 10. Neither measurement method is sufficiently precise to instill any confidence in the results, but the expected value of spacer thickness error may be approximated as

$$E(e_s) = .001 \text{ to } .0024 \text{ mm} \quad (.000039 \text{ to } .000096 \text{ in.}) \tag{30}$$

The difference in blade errors $E(e_b)$ is not the blade-to-blade error, but is related to the expected change in thickness from one end to the other. The ADE 6033T was used for this

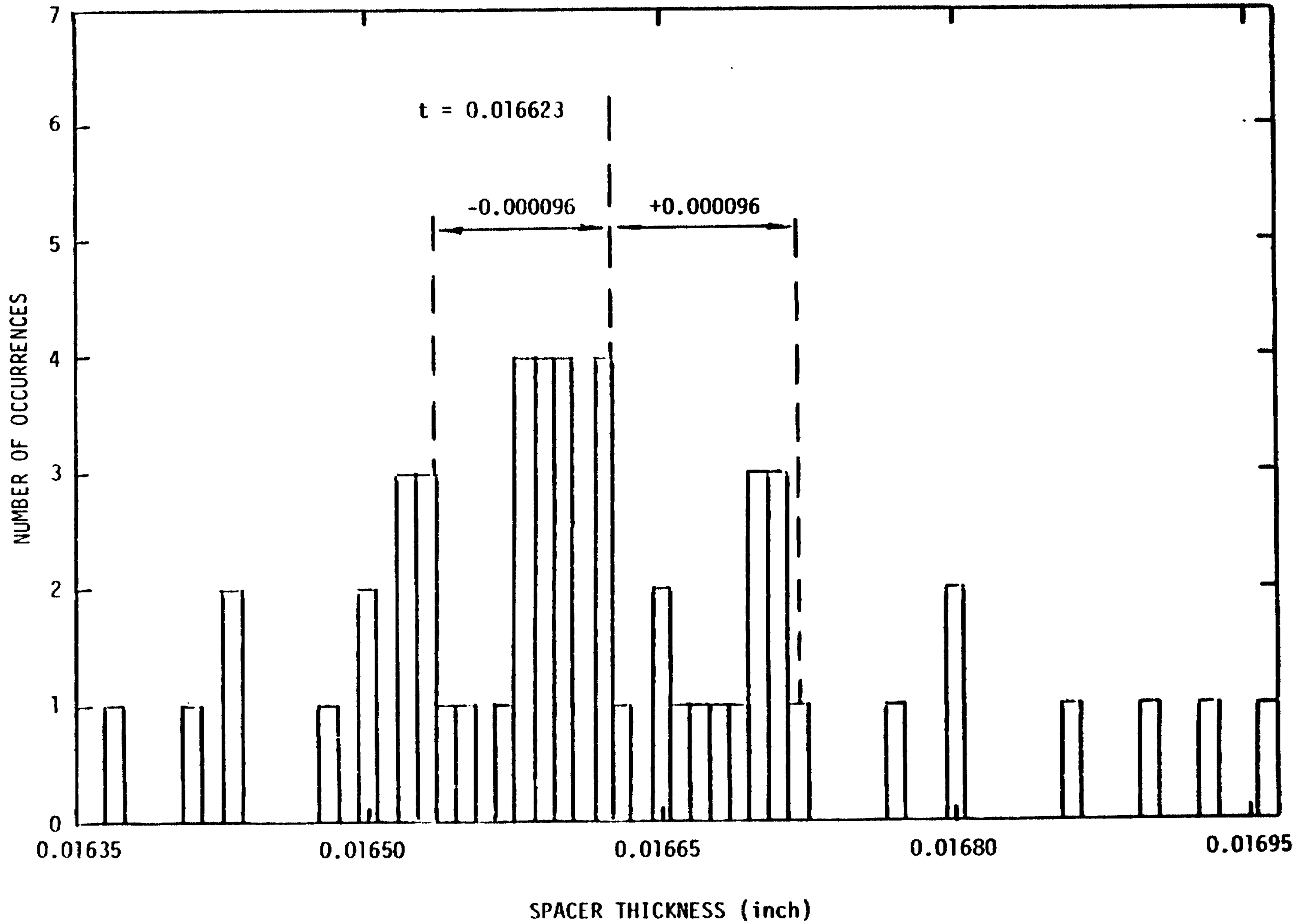

Figure 9. Distribution of Spacer Thicknesses (Mechanical Measurement)

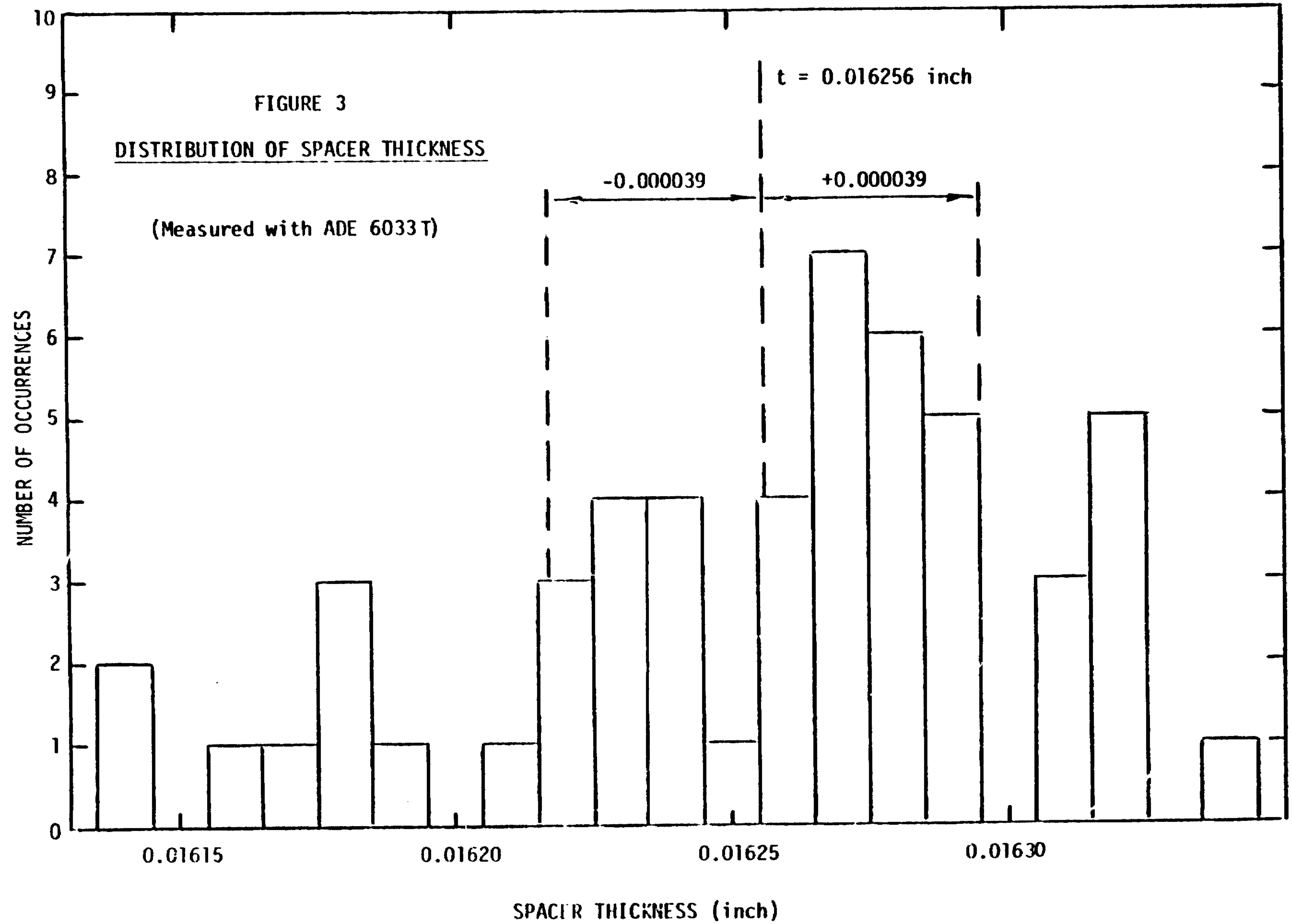

Figure 10. Distribution of Spacer Thicknesses (Non-Contact Measurement)

measurement, and the results are shown in Figure 11. Assuming that the mechanical system, if it could be used, would yield about three times the error measured in the ADE system (as was found in the spacer measurements) and noting that the runout error measured here equals $2^{\frac{1}{2}} E(e_b)$,

$$E(e_b) = .001 \text{ to } .003 \text{ mm} \quad (.000036 \text{ to } .000108 \text{ in.}) \tag{31}$$

From Equations 28 and 29, for a 225 blade package,

$$\Delta_{max} = .023 \text{ to } .061 \text{ mm} \quad (.00090 \text{ to } .0024 \text{ in.}) \tag{32}$$

$$\Delta_{ave} = .015 \text{ to } .041 \text{ mm} \quad (.00060 \text{ to } .0016 \text{ in.})$$

A blade package (225 blades) was tensioned and aligned in a standard bladehead. (This work was actually performed under Phase II but is reported here for continuity.) A precision inspection bench was used to measure the exact position of each blade. Figure 12 shows the resultant information reduced to average runout over a 305 mm (12 in.) length. The average runout is .041 mm (.0016 in.) . This converts to .050 mm (.0020 in.) average runout over the full 381 mm (15 in.) length, very close to that predicted in Equation 32.

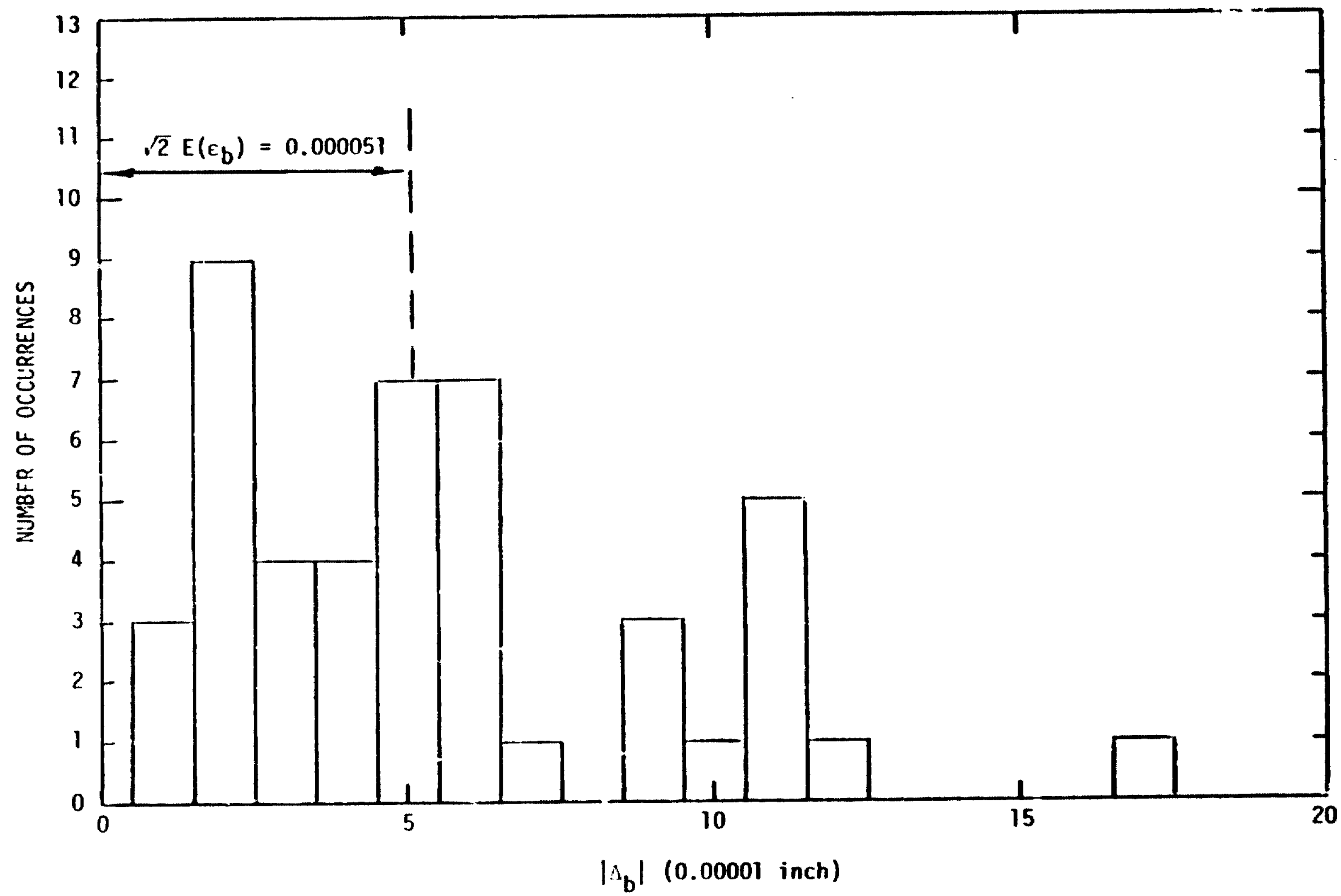

Figure 11. End-to-End Change in Blade Thickness (Non-Contact Measurement)

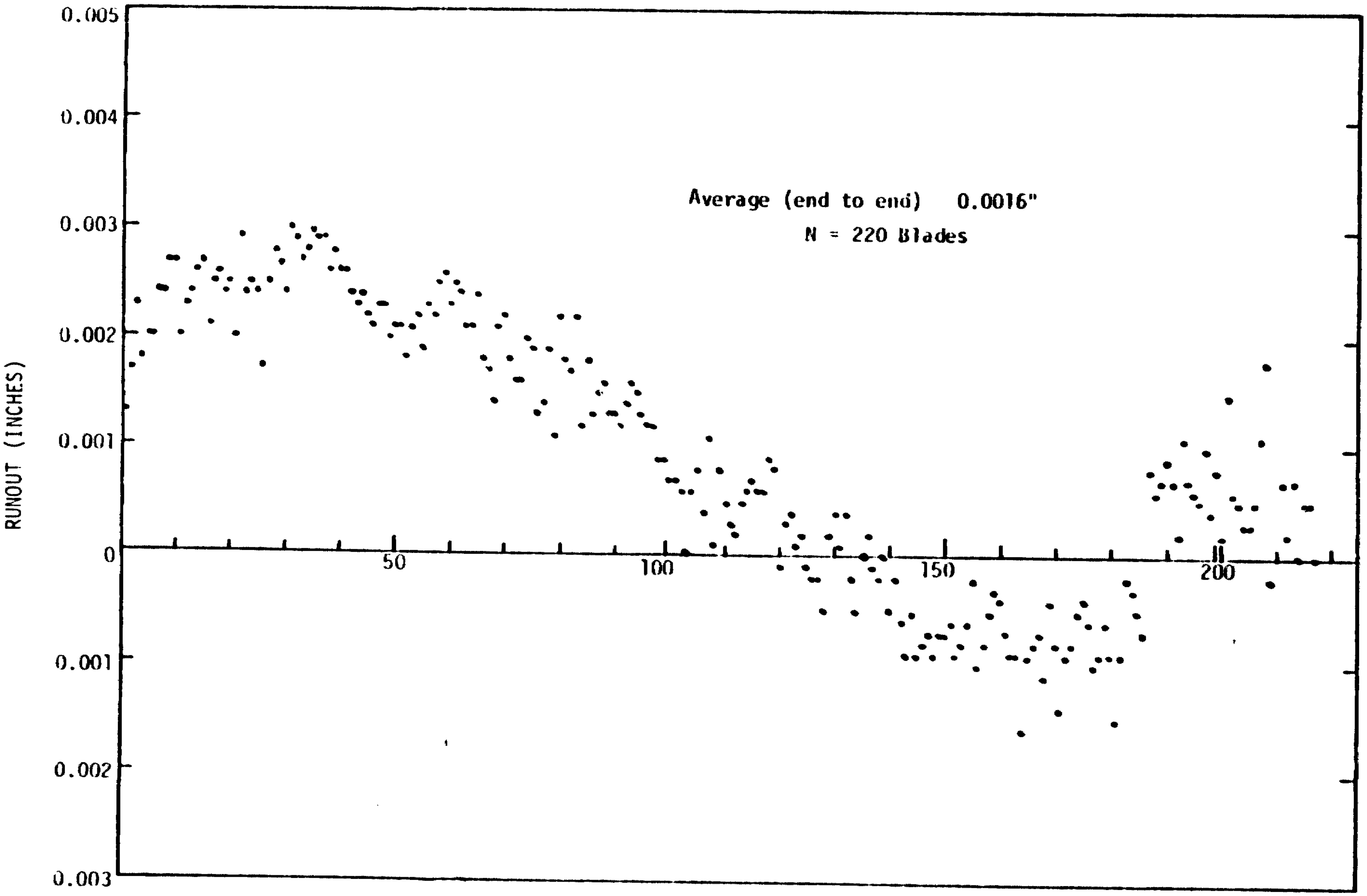

Figure 12. Blade Misalignment Within a Package (Over a 12 Inch Length)

The conclusions that may be drawn from the above are first that Equations 28-31 form a good basis for predicting runout, and second that the runout in the 200-300 blade range used in production saws is probably not quite large enough to significantly affect the process. Even though expected runout grows as the square root of the number of blades, very large saws with many blades may exhibit problems due to runout.

It is also worth noting that runout can cause wafer breakage. From Equation 18, the stiffness of a tensioned blade at the center is about 2×10^3 g/mm. At the end of the stroke, this stiffness could be as high as 5×10^3 g/mm. If the blade runs out, half the runout displacement applies a force to the wafer. For runouts on the order of .05 mm, the force applied is of the order of 125 grams. It is easy to believe that this force can break wafers in the .25 - .3 mm thickness range.

2.4 Reduction of Blade Cost by Looser Tolerances

Much of the cost of the blade material is due to the very accurate dimensional and material specifications. It may be possible to reduce the cost of blades by specifying less accurate material.

One of the specifications is the "straightness". Nominally, the edges of the blade stock are straight when viewed perpendicular to the wide dimensions of the stock. Processing variations,

however, result in these edges being curved. The amount of curve is the straightness. The standard groups of straightness are normal, accurate, and extra accurate (these groups are quantized below). Currently, blade stock is bought as extra accurate, costing 10-15% more than otherwise identical normal straightness stock. An analysis has been carried out on the effect of straightness with a view to saving the expense of extra accurate stock. The analysis concerns the deviation of a blade from the nominal cutting plane (defined by the lower corners of the end blades in a tensioned pack).

Consider a blade with dimensions shown in Figure 13. Defining ρ as the radius of curvature at any point (initially ρ_0), and y_c as the y coordinate of the blade centerline taken through the point, geometrical considerations lead to a formula for the strain due to bending:

$$\epsilon^b_{xx} = \frac{y-y_c}{\rho} - \frac{y-y_c}{\rho_0} \text{ , all others zero} \tag{33}$$

Since the stress is uniaxial, the only strains due to tension are:

$$\epsilon^t_{xx} = \Delta L/L$$

$$\epsilon^t_{yy} = \epsilon^t_{zz} = \nu\Delta L/L \tag{34}$$

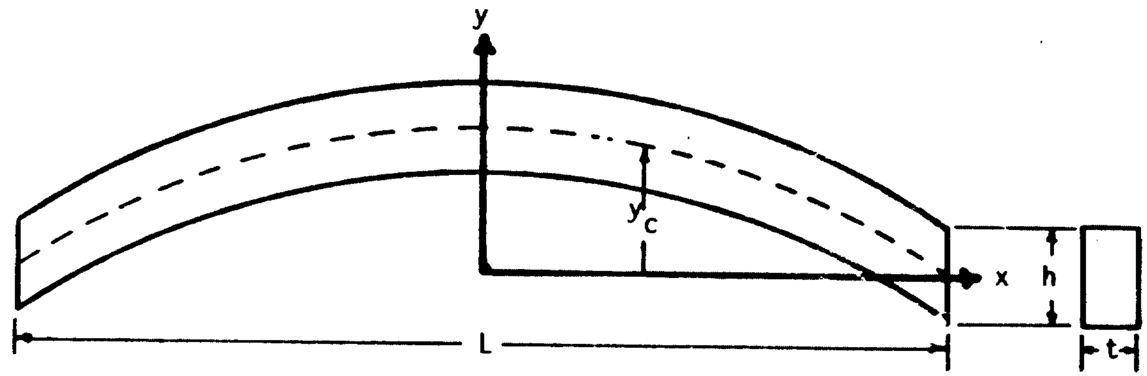

Figure 13. Geometry of a Curved Blade

And, assuming elasticity,

$$\sigma_{xx} = E\left(\varepsilon^{b}_{xx} + \varepsilon^{t}_{xx}\right) = E\left(\frac{y-y_c}{\rho} - \frac{y-y_c}{\rho_o} + \frac{\Delta L}{L}\right) \qquad (35)$$

Considering a free body, moment equilibrium and simple beam theory and superposition lead to

$$\sigma_{xx} = (1-12(y-y_c)/h^2)E\Delta L/L \qquad (36)$$

Equating Equations 35 and 36 and solving for $\frac{1}{\rho}$,

$$\frac{1}{\rho} = \frac{1}{\rho_o} - \frac{12\, y_c \Delta L}{h^2 L} \qquad (37)$$

It is possible to express ρ in terms of the first two derivatives of y with respect to x, y' and y''. Defining the curvature in Figure 13 as positive,

$$1/\rho = -y'' / (1 + (y')^2)^{3/2} \qquad (38)$$

If y' is very small, the relationship is simpler; $(1/\rho = -y'')$. However, since the final equation will be solved numberically, there is no need to drop the nonlinear term. Substituting Equation 38 in Equation 37 and solving for y'' ,

$$y'' = \left(\frac{12\, y_c\, \Delta L}{h^2 L} - \frac{1}{\rho_0} \right) (1 + (y')^2)^{3/2} \qquad (39)$$

With boundary conditions

$$y = y_0 \text{ @ } x = \pm L/2 \qquad (40)$$

Equations 39 and 40 comprise an ordinary boundary value problem. If the nonlinear term is dropped, an analytical solution does exist in the form of an infinite series. It is more convenient to solve the problem numerically for the few cases of interest, especially since the blade thickness does not appear.

The solution is more convenient if Equations 39 and 40 are restated. First, since y is not initially known (because of Poisson contraction, $y_c \neq y$ + constant), identify $y = y_c$ to solve for the centerline position. Second, shorten the interval by using symmetry to define the boundary condition $y' = 0$ @ $x = 0$. Third, nondimensionalize by defining new variables.

$$x^* = x/L \quad y^* = y/L \quad \rho_0^* = \rho_0/L \quad \beta = 12L\Delta L/h^2 \qquad (41)$$

The restated problem is

$$y_c^{*''} = (\beta\, y_c^* - 1/\rho_o^*)\,(1 + (y_c^{*'})^2)^{3/2} \tag{42}$$

$$y_c^* = 0 \text{ @ } x^* = -0.5$$

$$y_c^{*'} = 0 \text{ @ } x^* = 0$$

The only remaining task in the formulation is to define ρ_o. The straightness tolerance is stated in terms of the maximum deviation B from a chord of length A (usually 2.44 m or 8 ft.). Assuming the curve to be an arc of a circle,

$$\rho_o = (A^2 + 4B^2)/8B \tag{43}$$

Values of A, B and ρ_o for various tolerance grades are shown in Table 1. Values of $1/\rho_o^*$ and β are shown in Table 2. The values are all based on a length L = 381 mm (15 in.) and extension ΔL = 2.54 mm (0.1 in.).

The problem was solved on an HP-97 calculator. The boundary value problem was converted to an initial value problem by a "shooting method" combined with a fourth order Runge-Kutta integration scheme. Resulting values of $y_c^{*'}$ @ $x^* = -0.5$ are shown in Table 3. A fourth order Runge-Kutta scheme was then used

TABL:: 1

BLADE CURVATURE PARAMETERS FOR VARIOUS STRAIGHTNESS GRADES

	A m (in)	B m (in)	ρ_o m (in)
Normal	2.4384 (96)	11.906 (15/32)	62.429 (2457.8)
Accurate	2.4384 (96)	5.9531 (15/64)	124.85 (4915.3)
Extra Accurate	2.4384 (96)	2.7781 (7/64)	267.53 (10533)

TABLE 2

NONDIMENSIONAL PARAMETERS FOR VARIOUS STRAIGHTNESS GRADES AND BLADE HEIGHTS

Blade Height h mm (in)		Straightness Grade Normal	Accurate	Extra Accurate
12.700	β =	72	72	72
(1/2)	$1/\rho_o^*$ =	6.1029×10^{-3}	3.0517×10^{-3}	1.4241×10^{-3}
6.3500	β =	280	280	280
(1/4)	$1/\rho_o^*$ =	6.1029×10^{-3}	3.0517×10^{-3}	1.4241×10^{-3}
4.7625	β =	512	512	512
(3/16)	$1/\rho_o^*$	6.1029×10^{-3}	3.0517×10^{-3}	1.4241×10^{-3}

TABLE 3

NONDIMENSIONAL SLOPE, $y_c^{*'}$, AT END OF BLADE

Blade Height h mm (in)	Straightness Grade Normal	Accurate	Extra Accurate
12.700 (1/2)		3.5950×10^{-4}	1.6777×10^{-4}
6.3500 (1/4)	3.6472×10^{-4}	1.8237×10^{-4}	8.5109×10^{-5}
4.7625 (3/16)	2.6971×10^{-4}	1.3487×10^{-4}	6.2939×10^{-5}

to calculate y^* between $x^* = -0.5$ and $x^* = 0.5$. A step-size Δx^* , of 0.02 was used for all the integrations. Analysis of the problem with different stepsizes indicates that the results are at worst good to 3-4 significant figures. (Ten decimal digit arithmetic was used for all calculations, with the results rounded after the calculations.)

Figures 14 - 16 show the position of the blade centerline, relative to a chord, after tensioning. It is interesting that tensioning does not significantly reduce the difference between the straightness grades even though a larger moment is developed in the less straight blades. This cannot be due to the relative magnitudes of extension stress and bending stress, since no extension stress terms appear in Equation 42.

The figures also show that the maximum deviation of a normal straightness tensioned blade from a chord is in the range 2.5 μm (10^{-4} in.) to 25 μm (10^{-3} in.). Currently, no attempt is made to align the blade ends on the cutting plane; the error due to normal straightness blades is likely to be smaller than the error due to misalignment. Therefore, we conclude that normal straightness blade stock can be used without any degradation in the cutting process, saving about 10-15% in the cost of blades.

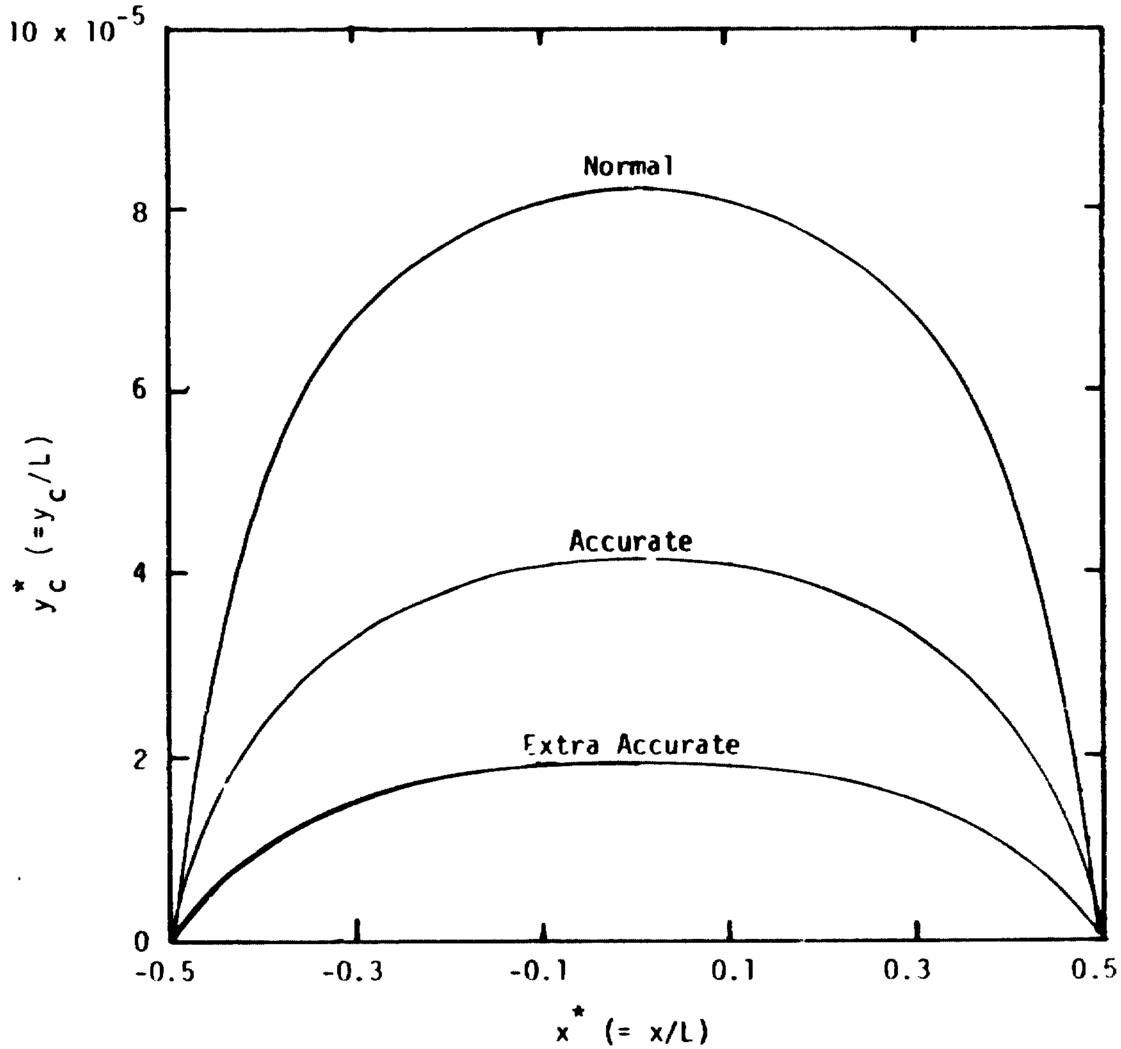

Figure 14. Centerline Shapes of 12.5 mm (1/2 in.) High Blades Under Tension

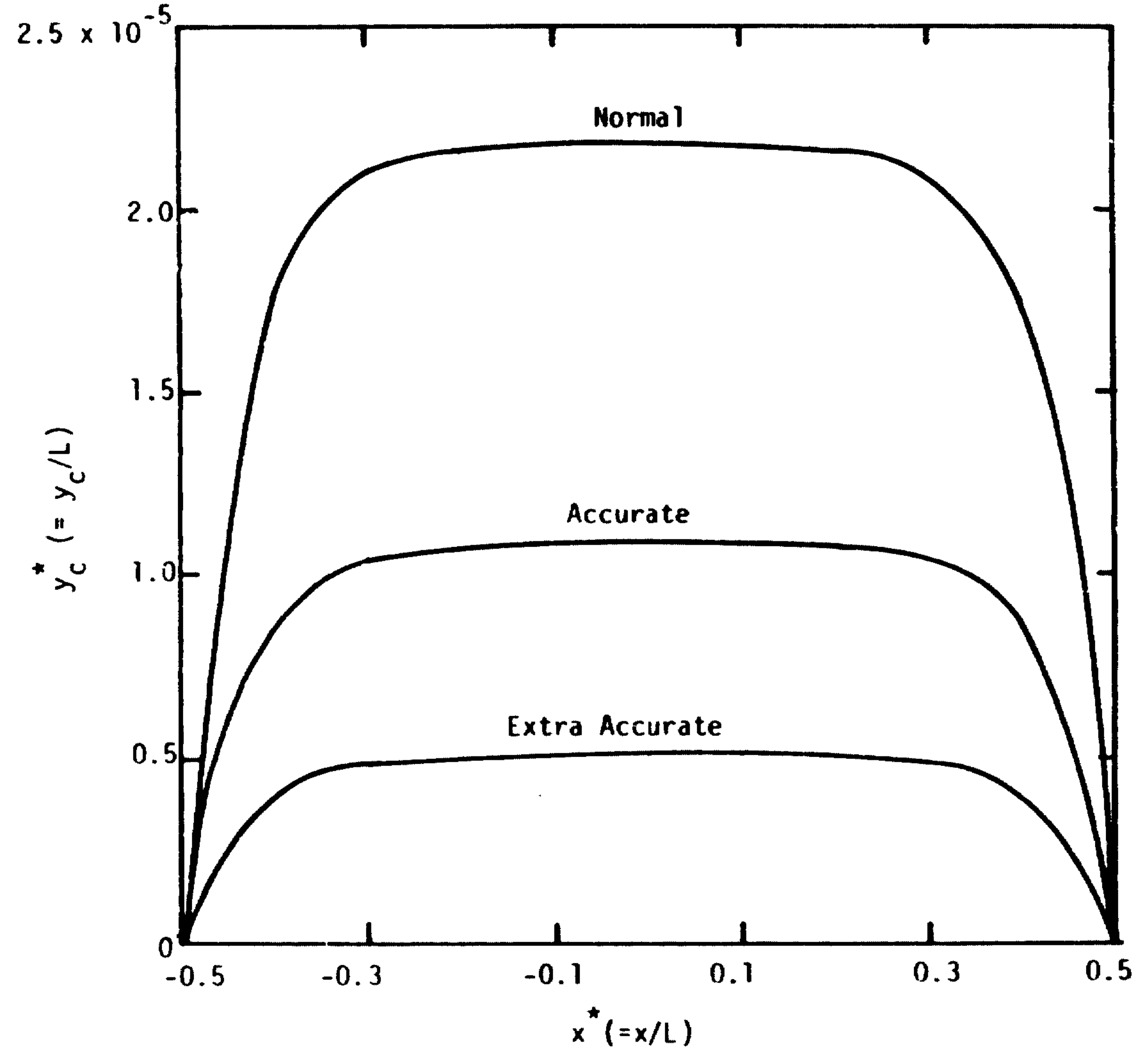

Figure 15. Centerline Shapes of 6.4 mm (1/4 in.) High Blades Under Tension

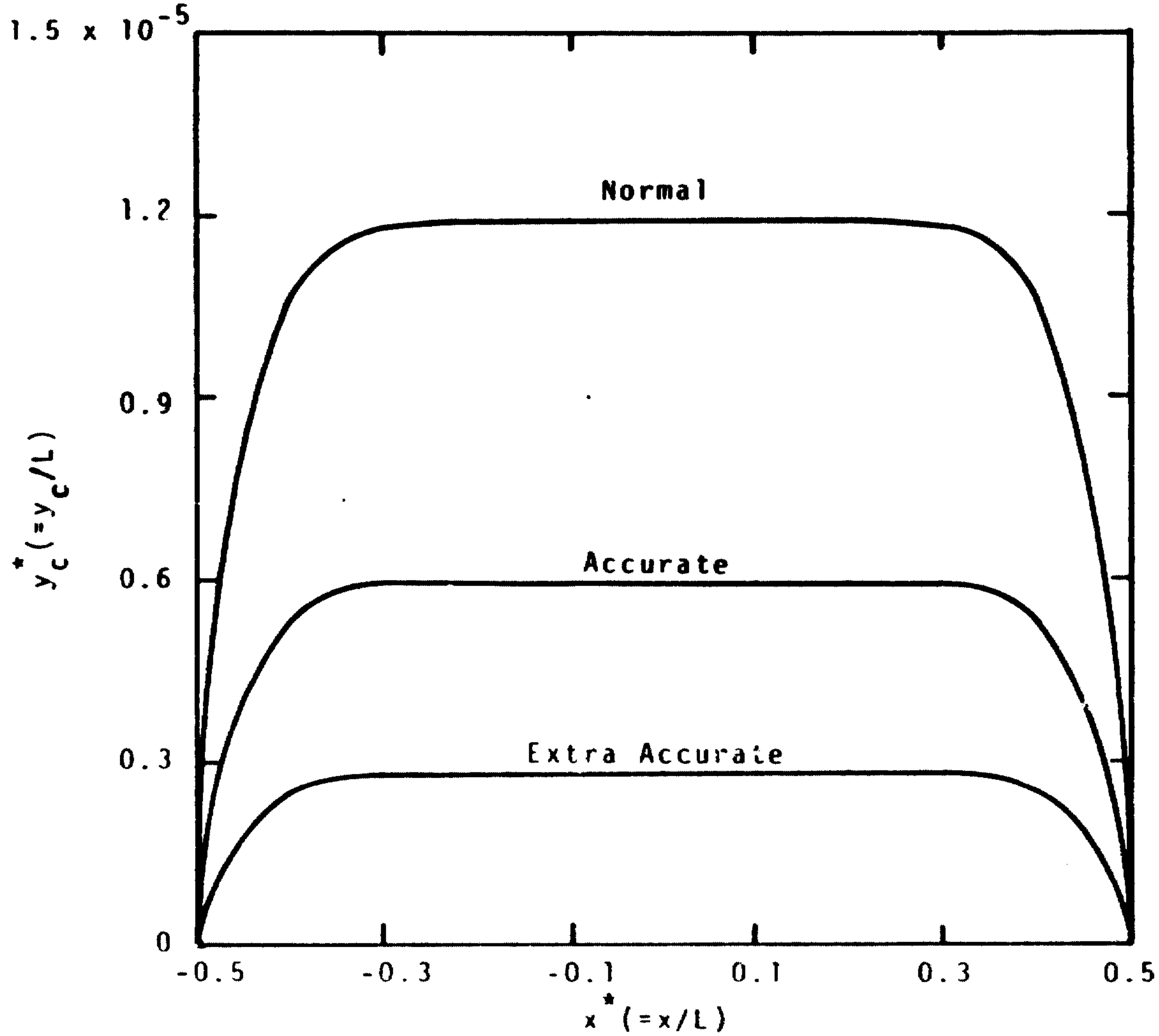

Figure 16. Centerline Shapes of 4.8 mm (3/16 in.) High Blades Under Tension

3.0 PHASE I: EXPERIMENTAL PROGRAM

3.1 Equipment

A modified Varian 686 slurry saw was used for the slicing tests. The saw is shown in Figure 17 and a closeup of the bladehead, containing a blade pack and ingot, is shown in Figure 18. The modifications installed consisted of an improved drive bearing system, RPM indicator for accurate reciprocation rate measurement, immersion lubrication for the vertical feed, fully enclosed slurry return system, pulsed static slurry application system, and facilities for mounting a dynamometer to the vertical feed platen (for measuring cutting and drag forces).

There are several performance limitations in this saw which are important when considering economics. The mass of the bladehead limits the reciprocation speed to 120 strokes/min. The bladehead can only accept a package 185 mm (7.5 in.) wide, and can apply a maximum of 4×10^5 N (90,000 lb.) tensioning force: one or the other of these maxima determines the largest package of a given blade and spacer size that can be used. Since the feed is pneumatic, air cylinder friction makes operation difficult with low (20 or less) numbers of blades or low total cutting forces.

3.2 General Experimental Program

The testing program began with a series of tests to characterize the response of the system to relatively large

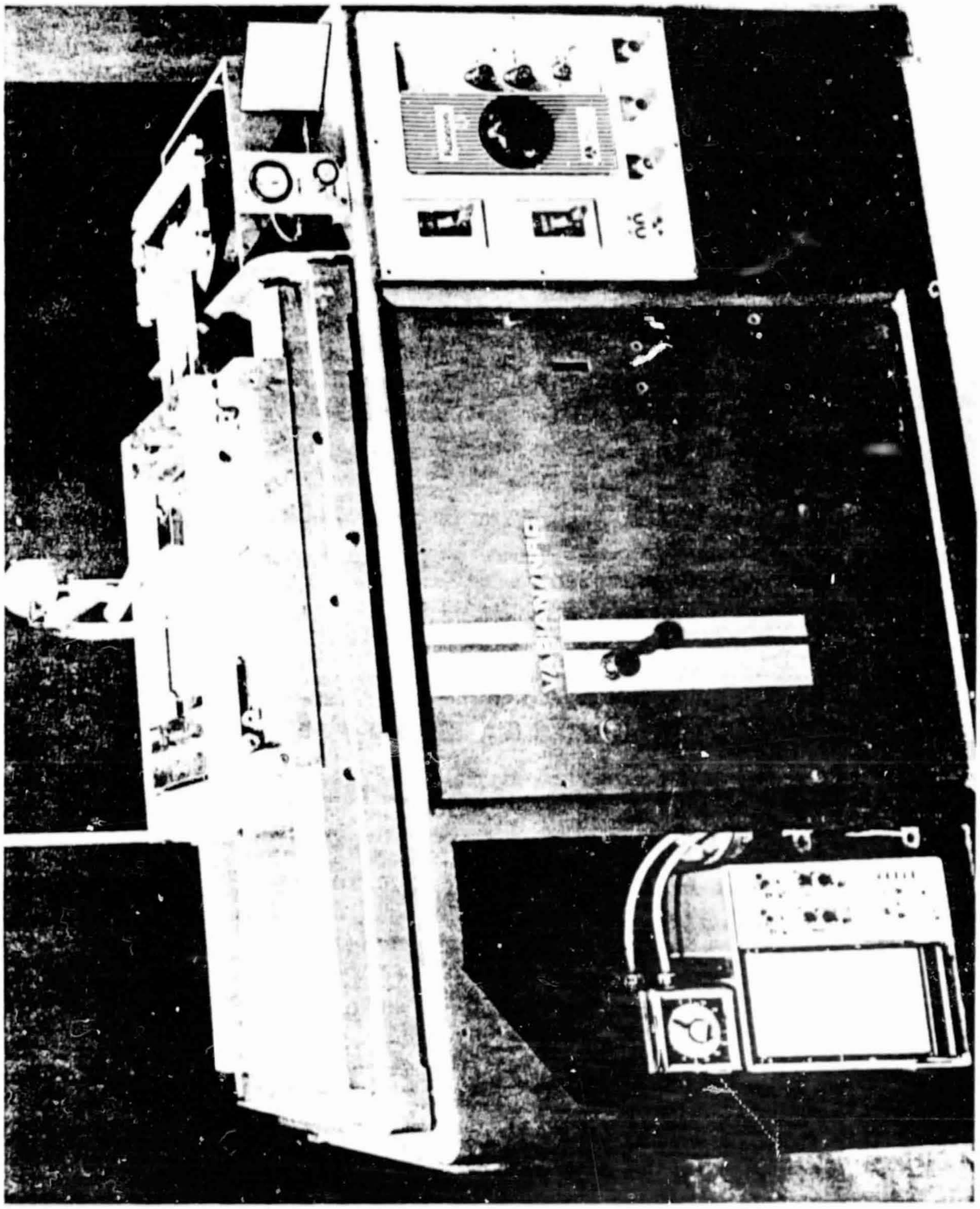

Figure 17. Modified Varian 686 Wafering Saw

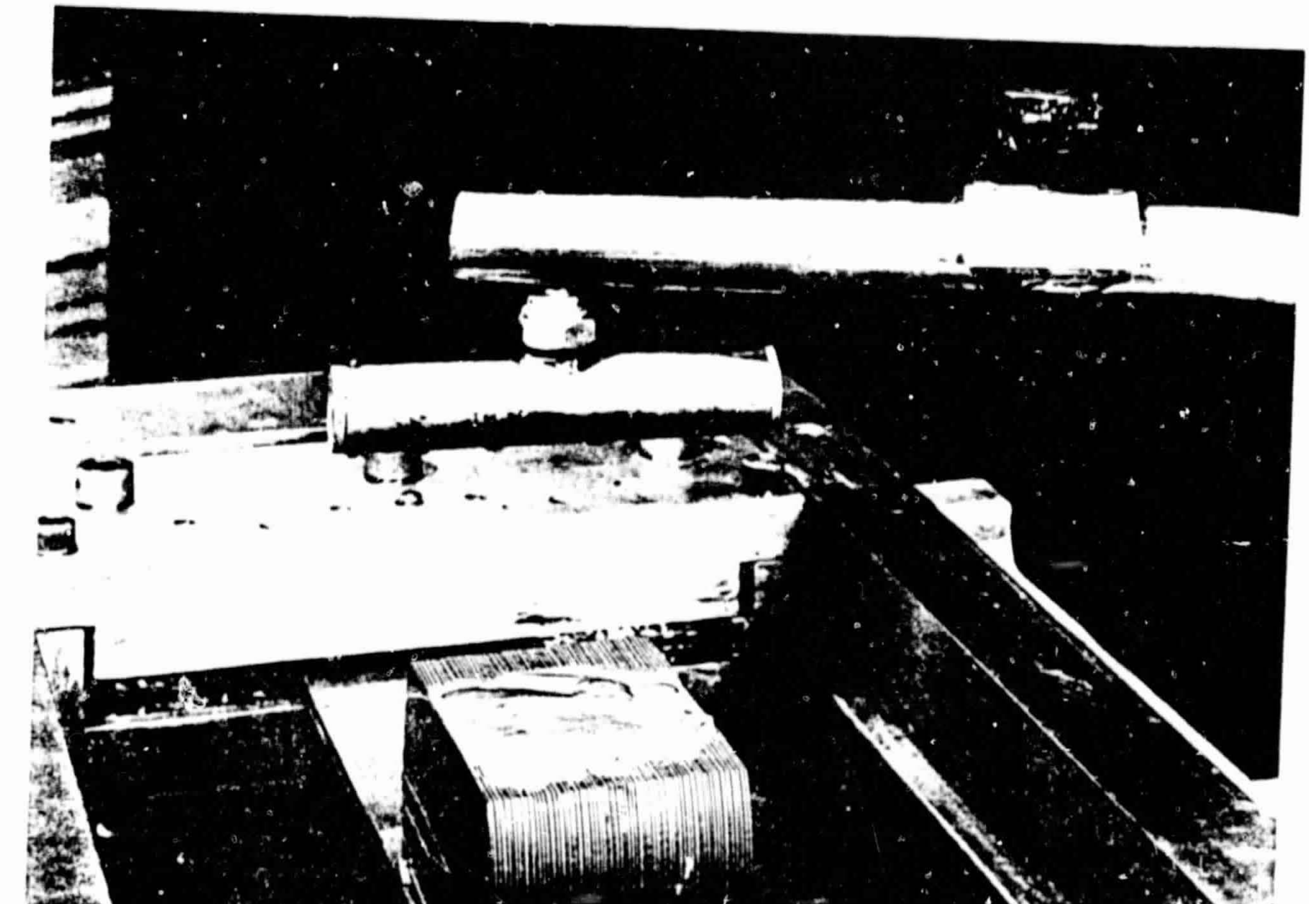

Figure 18. Slicing a 10 cm Silicon Ingot with a Multiblade Slurry Saw

variations in parameters, and to establish a baseline from which to proceed. Tests in this series were numbered 1-XXX where XXX is the test number.

After obtaining preliminary results, a testing program to improve the system by changing abrasive and blades was carried out. Abrasive tests were numbered 2-XXX and blade tests were numbered 3-XXX as above.

Concurrently with the abrasive and blade program, "production" runs were carried out. These runs generally used the full saw capacity and were designed to assess the state of our knowledge or provide wafers to solar cell manufacturers. These runs were numbered P-XXX.

Tests are discussed in general below. Tables of all the relevant information for each test will be found in the Appendices.

3.3 Parameter Study

Preliminary Slicing - 10 cm ingot: #1-001

A 10 cm ingot of silicon was sliced with 0.020 cm thick blades, 0.024 cm thick spacers, a cutting load of 113 grams per blade, average blade speed of 68 cm/sec, with a slurry of PC oil (Process Research) and #600 SiC abrasive (Micro Abrasives) mixed with 0.24 kg abrasive per liter of oil. Total cutting time was 30.6 hours, and the ingot cross-section was 82.6 cm^2. This test used the best slicing technique known by Varian for silicon. It provided the starting reference for large ingot slicing. Wafers averaged 0.055 cm thick.

Variations in Blade Load: #1-011 to #1-015

A standard rectangular block of silicon with a 2.5 cm kerf length and 5.0 cm height was cut with the same conditions as in #1-001, except that the blade load for each test was varied from 57g, 113g, 270g to 283g per blade. At 283g (#1-015), the blades wandered severely, causing broken wafers, eventually breaking the workpiece from the submount. In the other tests, cutting rate increased and wafer accuracy decreased with increasing cutting force.

Variations in Kerf Length: #1-021 to #1-024

Again, the "Standard" cutting conditions of #1-001 were used, but the size of the ingot was varied. At 113g of blade load, 1.25 cm by 2.50 cm high, 5.00 cm by 2.50 cm high, 6.88 cm square and at 10.6 cm diameter silicon workpieces were sliced. Cutting rates and kerf loss decreased and wafer accuracy generally improved as the kerf length increased.

Variation in Blade Size: #1-031 to #1-034

A standard silicon block, 2.5 cm kerf length by 5.0 cm high, was cut with blades 0.020 thick by 1.27 cm high, 0.015 cm by 0.63 cm, 0.015 cm by 1.27 cm and 0.010 cm by 0.48 cm. A cutting force of 113 g was used for all but the 0.010 cm thick blades (57 g was used). Test #1-012 was the basic reference and standard for this series. The cutting rate with 0.015 cm blades was slightly better (10%) than with 0.02 cm blades. Despite the 50% reduction of cutting force, 0.010 cm thick blades cut at a rate 70% of that of 0.020 cm

blades. Wafer accuracy was degraded as the blade thickness decreased. No general trend as to the effect of blade height could be characterized.

Blade Speed, Abrasive Mix: #1-041 to #1-043

In Test #1-041, a 2.50 cm block was sliced at a 113 g blade load. The blade speed was varied from 20 to 81 cm/sec. The cutting rate increased in proportion to bladehead speed. The high shock load developed at 120 RPM caused the block to break away from the submount, destroying the wafers.

For the early tests, slurry was made of 0.24 kg of #600 SiC abrasive per liter of PC oil. Two tests were made with 0.12 and 0.48 kg/l, using 2.50 cm kerf length and 113 g of blade loading. Cutting rate increased by 25% as the abrasive mix increased fourfold.

<100> vs. <111> Silicon: #1-051 to #1-054

A series of early tests (all using <111> silicon) were duplicated with <100> silicon. It had been anticipated that the non-isotropic hardness and fracture behavior of silicon might lead to a difference in cutting rate. However, these tests indicated that there is no difference in slicing of the two orientations, and more recent tests where the two orientations are used interchangeably support this result even further. In Tests #1-053 and #1-054, 0.041 cm spacers were used, resulting in wafers 0.033 cm thick.

Abrasive Size: #1-061 to #1-063

Blocks of silicon 2.5 cm by 5.0 cm high were sliced with 0.020 cm blades at 85 grams of blade load, using #1200, #1000 and #800 SiC abrasive. The mixture of abrasive to oil was reduced initially to maintain a consistent number of abrasive points per unit area of slurry film. During the tests more abrasive was added and the slurry was thinned with 30 SUS mineral oil in order to maximize the cutting rate. The optimum cutting rate and kerf loss each decreased as the abrasive particle size decreased. Wafer thickness was more consistent, but slice taper degraded as the finer abrasives were used.

3.4 Slurry Composition and Application

The preliminary testing had shown that #600 SiC abrasive gave the highest slicing productivity, and that larger ingots provided improved wafer accuracy with slightly better slice productivity. A slight effect of increased abrasive density resulting in higher cutting rates had also been noted. #800 SiC abrasive had shown lower kerf loss and adequate cutting rate (70% that of #600 SiC). A series of tests were designed to explore the cutting efficiency of #600 abrasive, the reduction of kerf width from #800 abrasive, and a possible improvement in slurry applications technique.

10 cm Ingot, #600 SiC: #2-001

A 10 cm ingot of silicon was sliced with 0.020 cm blades and 0.030 cm spacers, using 113g per blade, as before, but with an abrasive mix of 0.48 kg/l of oil (as in #1-043). The total cutting time was 19.17 hours, an increase of more than 40% in the cutting productivity over previous tests. Also, the resulting wafers were 0.024 cm thick, and none had broken during cutting. Many wafers (~30%) of the 143 produced were broken during subsequent handling and cleaning.

Increased Abrasive Mix, Increased Cutting Load: #2-002

A 7.62 cm square block of silicon was sliced with 0.020 cm blades and 0.041 cm spacers, using the pulse slurry applicator and an abrasive mix of 0.96 kg/l of #600 SiC. At a cutting force of 113 g, the cutting rate was lower by 30 to 40% compared with those expected from #2-001. The blade load was increased to 170 and then 227 g with proportional increases in rate, and without an apparent degradation of wafer accuracy.

New Application Technique: #2-003

The pulse slurry system was, again, used, but to repeat Test #2-001. With 0.041 cm spacers, the wafer thickness was 0.0318 cm. Total cutting time was 18.25 hours, only 5% faster than #2-001. The pulse slurry system was shown to be effective in generating high cutting rates and good wafer accuracy.

#800 SiC, 10 cm Ingot: #2-011

A 10 cm ingot was sliced at 113 g using 0.020 cm blades and 0.041 cm spacers. The cutting rate with #800 SiC (0.48 kg/l) was slightly better than early tests with #600 (#1-001, #1-024), and improved over the rates experienced earlier with #800 SiC (#1-063). Wafers were 0.0362 cm thick. The load was raised to 170 g and to 227 g during the test and the cutting rate increased proportionally.

#800 SiC, 7.62 cm Square Ingot: #2-012

A 7.62 cm square ingot was sliced under conditions similar to #2-011. Wafer production rate was only 57% that of #2-011, indicating, as in #2-002, that a square workpiece cannot be sliced as fast as a round one. Under 170 g of blade load, the cutting rate increased proportional to load. Wafer thickness was 0.0355 cm.

#600 SiC, Thin Oil: #2-031

Again, a 10 cm diameter ingot was sliced, as in #2-003, with #600 abrasive mixed 0.48 kg/l. The PC oil was diluted with 30 SUS mineral oil in a ratio of 3:1. The less viscous slurry did not change the cutting time (19.9 hours), but did produce wafers less accurate than in #2-001 and #2-003.

Large Slurry Volume: #2-004 and #2-005

A 38 liter volume of slurry was used in two simultaneous tests. The slurry was mixed with the standard 0.48 kg/liter of #600 SiC abrasive. The same blade package was used to cut through two 10 cm ingots. The large volume of slurry was meant to reduce

the effects of viscosity increase of the standard 7.6 liter slurry volume as the silicon debris is accumulated.

Cutting time for the first ingot was 21.5 hours with otherwise standard conditions of cutting. The kerf loss with 0.020 cm blades was 0.0255 cm, similar to other tests. There was a reduction of average slice taper to 0.007 cm, but this is the same as the first "improved" 10 cm ingot slicing test, #2-001.

The second ingot took 26.5 hours to slice, due to the necessary reduction of bladehead stroke to compensate for the worn blades. The blades began to break after 60% of the ingot was sliced. The height of the worn blades was about 0.254 cm (60% worn) at this point. More than 80% of the blades survived to the end of the cut where the height of the worn blades was 0.150 cm. Slice taper in this ingot was 0.0015 cm, typical for the worst cases of 10 cm wafering.

No improvement in slice taper resulted from the large slurry volume, and it was found that 60% height loss may be a practical limit to blade wear. In both tests, slice thickness was 0.025 cm.

Slurry Lifetime: #2-006A, #2-006B, and #2-006C

A 7.6 liter batch of slurry (0.48 kg/liter of #600 SiC) was being used to slice a series of 10 cm silicon ingots. For each ingot, a new blade package was installed. At various points, samples of the slurry were collected and analyzed as discussed later to indicate the mechanism of slurry failure.

In #2-006A, kerf loss was 0.0255 cm and slicing time was 27 hours. The reduction of cutting rate is not explained, since the conditions were identical to #2-003 (18.2 hours). Wafer accuracy was normal and slice taper was 0.0016 cm, similar to previous tests. The cutting time for #2-006B was 26.25 hours and taper was identical to #2-006A. In this case, kerf loss was only 0.0238 cm, less than in #2-006A.

In both cases, wafers were 0.025 cm thick, and 125 slices were produced in each. The cutting did not seem to degrade during these two runs.

A third 10 cm ingot (125 slices per ingot) was sliced with the same 7.6 liter volume of slurry. Approximately half way through the third ingot, severe slice breakage occurred and the test was aborted.

In each test of the 2-006 series, a fresh blade package was used. The blades were 0.20 mm thick by 6.35 mm high, with 0.30 mm spacers. Wafers were 0.25 mm thick. 113 grams of blade load was used in each case with a sliding speed of approximately 58 cm/sec.

The first two tests (2-006A & B) were nearly identical in cutting rate, and slice accuracy. However, breakage of the slices began to occur near the end of the second run. Breakage was even more severe in the final run (2-006C), but the cutting rate was reduced by nearly 50%. It appears that the useful lifetime of slurry is approximately full saw capacity (225 wafers)

of 10 cm silicon ingot for a 7.6 liter volume of slurry. However, a more severe limitation appears to be the breakage of thin wafers that occurs before cutting speed is diminished.

The build-up of debris in the slurry oil causes an increase in the viscosity of the slurry. This viscosity increase will cause higher drag loads on thin wafers and may limit the access of slurry to the blades. Samples of slurry oil were taken at various stages of the 2-006 tests to evaluate the condition of the silicon carbide abrasive as the slurry performance deteriorated.

Slow Speed: #2-021

A 10 cm ingot was sliced with a bladehead speed of 35.5 cm/sec, half of that normally used. Total cutting time was 54.5 hours. Even though the cutting time was long, the efficiency (0.96) was similar to the efficiency of early cuts and of tests with square workpieces. As speculated in previous reports, the shape of the workpiece promotes bounce of the vertical feed. This motion may increase flow of abrasive into the cutting region under the blades. With square workpieces, this bounce is limited. The slow machine speed also limited the vertical feed bounce even with the round workpiece, resulting in the lower cutting efficiency. The cutting time was expected to be at least 40 hours due to the slow bladehead speed, and using the high cutting efficiency of round workpieces with improved slurry mixture.

The wafers produced at this slow speed were the most accurate to date. The kerf loss was higher than normally seen in 10 cm diameter ingots, but this may be due to the longer time available for material removal beside the blades under the reduced cutting efficiency.

Boron Carbide Abrasive: #2-041

A standard 10 cm ingot was sliced with a 7.6 liter volume of slurry made with an 0.48 kg/liter mix of #600 B_4C abrasive. This abrasive is harder than SiC and is expected to give a longer lifetime to the abrasive grains. Total cutting time was 14.8 hours, a reduction of 25% compared with SiC. However, the abrasive keff loss was 0.0084 cm, an increase of 70% over the typical abrasive kerf loss with #600 SiC abrasive. This is an increase of 14% in total kerf loss using the 0.020 cm thick blades.

Wafer accuracy in general was degraded compared to #600 SiC abrasive slicing. However, slice taper was improved compared with typical 10 cm slices, except for the lower taper seen in Test #2-004 (38 liter slurry volume).

Thinned Slurry Oil - #2-025

To test the premise that oil viscosity controls slice taper and the apparent "life" of slurry, a mix of 0.36 kg of #600 SiC per liter of PC oil was used at the start of a 10 cm silicon ingot slicing test. At 50% and 75% through the ingot, 30 SUS mineral oil was added to lighten the slurry. Total mix of the light oil was 20% at the end of the test.

Total cutting time was 27 hours and the thinning did not impact any factor of wafer accuracy and, in fact, reduced the cutting efficiency normally experienced with similar slurry conditions.

Thin Spacers (0.20 mm) - #2-022

A pinned blade package with 0.20 mm thick blades and 0.20 mm thick spacers was used to explore the thinnest slicing possible with silicon ingots. Upon tensioning to 50% of full blade tension, (90 kg per blade), the spacers collapsed by buckling under the compression applied by the front lips of the bladehead.

A second package of an epoxy bonded type and the same blade and spacer size was then tensioned. The epoxy between the spacers suppressed the buckling mode until 70 to 80% (135 kg per blade) of full tension was reached.

With the present blade package geometry 0.25 to 0.30 mm spacers will be the practical limit. This allows 0.20 to 0.25 mm thick slices to be produced. Thin blades will reduce the allowable spacer size by as much as 15%.

Slurry Mix (0.24 kg/l) - #2-023

An 0.24 kg/liter mix of #600 SiC slurry was used to slice a 10 cm ingot with 113 grams of blade load. Total cutting time was 27.5 hours and it is apparent that cutting efficiency is reduced from that experienced with 0.48 kg/liter mixes (1.19 vs. 1.60). There was no improvement in wafer accuracy, blade wear or kerf loss with the light slurry mix.

High Cutting Force (225 g/blade) - #2-024

A 20 cm ingot was sliced with 0.20 mm thick blades, 0.41 mm spacers and 225 grams per blade of cutting force. A standard

0.48 kg/liter slurry mix with #600 SiC abrasive was used. Cutting time was 17.2 hours.

Even though the cutting rate was higher than normal, cutting efficiency was low (1.00). It appears that the abrasive density is saturated for cutting ability at the higher cutting force. A heavier slurry mix may reduce cutting time at high loads even further.

High Slurry Mix, High Load - Test #2-026

A standard 10 cm silicon ingot was cut using a 0.96 kg/liter mix of #600 SiC abrasive and a cutting force of 225 grams per blade (each twice normal). Total cutting time was 13.5 hours and cutting efficiency was high, peaking at 1.69. The test was intended to test the match of cutting load and abrasive concentration in MS slicing. Previous tests where load was increased without a change in abrasive mix, a reduction of cutting efficiency was noted. In this case, cutting efficiency compared favorable with standard conditions (0.48 kg/liter and 113 grams per blade). The result was a reduction of cutting time which nearly scaled with the increase in load (two times). However, even though a relatively thick spacer (0.40 mm) and standard (0.20 mm) blades were used, and slice thickness was nearly 0.36 mm, only 26% of the wafers survived the cutting operation. Blade wear was comparable to standard cutting (wear ratio of 0.045).

3.5 Zirconia-Alumina Abrasive - Test #2-042

Zr_2O_2 - Al_2O_3 abrasive was obtained to substitute for the standard #600 SiC. The abrasive appeared rather rounded and almost porous under SEM examination. The particle size was comparable to the silicon carbide, and a cutting test was run. A 10 cm silicon ingot was cut with 0.20 mm blades and 0.30 mm spacers. The abrasive mix was increased to 0.60 kg/liter to adjust for the 25% higher density of the zirconia-alumina and provide for an abrasive particle packing similar to that used with standard silicon carbide cutting. At 113 grams per blade (standard for 0.20 mm blades), the cutting efficiency was only 20% that seen with SiC abrasive. Severe breakage occurred with the thin slices, and the cut was aborted after completing 1.5 cm of depth into the 10 cm ingot in 12 hours.

The zirconia-alumina had been tried because in standard abrasive applications (grinding belts, etc.), it has shown greatly improved lifetime over silicon carbide and other abrasives. However, for MS slicing, the small scale shape of the particles seems to be a more significant criterion. The cleaved silicon carbide particles effectively concentrate cutting stresses to provide fracture of the silicon, and thus facilitate cutting. The zirconia-alumina was more rounded, with no sharp edges. The cutting forces are more distributed in contact with the silicon, and silicon fracture was significantly supressed. Perhaps only in the case of MS slicing, particle shape is most critical, and

other abrasive material characteristics are likely not important.

The rounding of fresh zirconia-alumina was far more apparent than silicon carbide particles used to their "full" lifetime.

3.6 Blade Materials

Thin Blades: Tests #3-001 and #3-002

The first priority in testing possible changes in blade materials was to attempt cutting of large silicon ingots with 0.010 cm thick blades. Two separate efforts were made with 0.010cm thick, 0.63 cm high blades with 0.041 cm thick spacers. In both Test #3-001 (10 cm diameter ingot) and #3-002 (7.62 cm square) severe blade wandering resulted and the partly sawn wafers broke off. Both tests provided blade loads of 28 to 85 g per blade. In Test #3-002, a few blades broke during the cut. Cutting rates, considering the loads used, approached very impressive rates, comparable to the rates in #2-001.

0.010 cm Thick Blades: #3-021

A package of 0.010 cm thick blades was used to cut a rectangular block of silicon with 7.62 cm kerf length. Blades were 0.476 cm high, as opposed to the 0.635 cm high blades used in previous cutting tests with thin (0.010 cm) blades. A cutting force of 57 grams per blade was used, and cutting efficiency of approximately 1.0 resulted, indicating a proper cutting mechanism. The slurry consisted of 7.6 liters of PC oil with 0.48 kg/kiter of #600 SiC abrasive.

The blade breakage that had plagued the earlier tests in the thin blade series did not occur until nearly the end of the cut. The blades had been elongated to 0.254 cm, the elongation used successfully with thicker (0.02 cm) blades, and corresponding to 80% of the yield strength of the blade steel.

However, severe blade wandering occurred from the beginning of the cut. Throughout the test, blades would distort so severely that wafers regularly broke out of the workpiece. The blades all assumed a "tipped" or buckled cutting configuration, and the direction of overturning could be determined by the work appearance of the blades. The blades are made of a blued steel, and under the action of the abrasive, the bluing is worn away.

Typically, a blade wears only near its lower edge. The tipped blades showed a lack of bluing on the "downward" side of the blade. Associated with that wearing was a loss of blade thickness to 0.0075 cm. In a normal cut, thickness loss is negligible and blades wear away only on the bottom edge.

In a given area of the blade package, blades overturned in the same direction. Across the package, the overturning direction would gradually change from one side to the other. The lack of random overturning indicates that the buckling of blades is governed by improper vertical blade alignment determined by the blade package assembly or tensioning impact on the overall blade alignment.

The steel used in this cut was of a different tensile strength than previous thin blade cuts (205 kg/mm^2 compared to 215 kg/mm^2), but was identical to the steel used in 0.020 cm thick blades. The harder material of the previous thin blade cuts might have contributed to the higher breakage, but the mechanism is not obvious.

The only wafers remaining from the cut were ones that were excessively thick, due to divergent blade wandering, and thus strong enough to survive the cut.

<u>0.015 cm Thick Blades: #3-031</u>

A cut using 0.015 cm thick blades, 0.635 cm high, was made in another rectangular workpiece with a kerf length of 7.62 cm. The standard slurry volume (7.6 liters) and mix (0.48 kg/liter of #600 SiC) were used with 85 grams of cutting force per blade.

The cut was surprisingly successful, with the wafer accuracy among the best recorded in this program. The cutting efficiency was very impressive, especially considering the lower efficiency normally experienced with rectangular workpieces.

The blade wear was even more impressive, with a resulting wear ratio of 0.027, 68% of the previous lowest wear ratio with 0.020 cm thick blades.

The wafers had a noticeable difference in shape compared to other cuts. The normal wafer surfaces are slightly convex, with the appearance of reduced kerf loss as the slurry path from the ingot exterior is increased. However, in Test #3-031 the wafers are slightly concave.

Thin (0.15 mm) Blades - #3-032

0.15 mm by 6.35 mm blades and 0.40 mm spacers were used to slice a 10 cm silicon ingot into 100 wafers. 85 grams of load and 0.48 kg/liter mix of #600 SiC abrasive was used. Total cutting time was 26 hours. Cutting efficiency was typically 1.45 with a maximum of 2.43. Wafer accuracy was comparable to 0.20 mm blades. Wafer thickness was 0.343 mm with 0.216 mm kerf loss, a savings of 35 microns of kerf loss. Blade wear ratio and height loss were also comparable to 0.20 mm blades.

Cutting results were not similar to those of #3-031 (0.15 mm blades) where high slice accuracy, low blade wear and slightly concave wafer surfaces resulted. The anomaly of Test #3-031 has not been explained.

Thin Blades - #3-033

A package of 0.15 mm thick blades with 0.30 mm spacers was used to slice a 10 cm silicon ingot. Slurry mix was 0.24 kg of #600 SiC per liter of PC oil. With 85 grams of blade load, slicing time was nearly 29 hours.

The light slurry mix was used to control the cutting of thin wafers with 0.15 mm blades. The cutting time was longer than in Test #3-032 (0.48 kg/l). Typical cutting efficiency was 20% less with the lighter mix and maximum cutting efficiency was 30% lower.

Wafers were 0.255 mm thick, however, the yield was less than 70%. Slice taper was 20 microns.

Thin Blades (0.10 mm) - #3-041

A package of 0.10 mm thick by 6.35 mm high blades and 0.30 mm spacers was made using a controlled assembly procedure in order to avoid package assembly related blade misalignment. As in previous efforts, blade breakage began to occur within 15 minutes of the start of cutting. The failure seems to be a fatigue problem as approximately 3,000 cycles of bladehead motion (15 minutes) is required to cause failure. A slight blade misalignment will cause a cutting path for a blade that causes it to be distorted on each stroke. This periodic deflection may induce stresses sufficient for fatigue failure of the blades.

Thin Blades, High Cutting Force - Test #3-034

0.15 mm thick blades were used again in slicing a 10 cm ingot, with 0.40 mm spacers, a slurry mix of 0.36 kg/loter and a cutting force of 140 grams per blade (85 used previously). Cutting time was 19.8 hours, slice thickness was 0.33 mm and yield was 100%. Wafer accuracy was good, but kerf loss savings from 0.20 mm blades was only about 0.03 mm, indicating a slightly excessive loss of silicon (0.02 mm). This test did indicate the possibility of stable cutting with 0.15 mm blades.

A heating mounting block was used in #3-035, allowing immediate demounting of wafers after cutting is completed. Normally, after slicing, blades must be withdrawn through the sliced ingot in order to facilitate demounting. It was felt that this would cause breakage of thin slices, consequently the new technique was devised. It appears that the technique is successful in avoiding unnecessary breakage of thin slices (approx. 0.25 mm thick).

Thin Blades, Thin Wafers - Test #3-035

0.15 mm blades were used with 0.30 mm spacers to slice a 10 cm silicon ingot. Blade force of 85 grams and slurry mix of 0.36 kg/liter was used with #600 SiC. Cutting time was 29.5 hours with a peak efficiency of 2.10, higher than similar cutting with a lower slurry mix. Wafer yield was over 98% with 118 blades cutting. Slice thickness was 0.24 mm, and kerf loss was only 0.21 mm. The total silicon used per slice was 0.45 mm, the lowest to date. This corresponds to a conversion of 10 cm silicon ingot to sheet of 22.2 slices per cm of ingot, or 0.95 m^2/kg of starting silicon ingot.

Thin Blades, Abrasive Concentration - Test #3-036

A partial 10 cm silicon ingot (25% of top cropped from another cutting test) was cut with 0.15 mm blades and 0.30 mm spacers. A higher cutting force (113 grams) and abrasive mix (0.48 kg/liter) was used to duplicate Test #3-035. Total cutting time for the smaller ingot was 26.2 hours, indicating that cutting rate was much less than with #3-035. The only suspect was a minor variation in the abrasive particle size, as similar results were observed with the same batch of #600 SiC abrasive in other cutting underway at the same time in the Varian slicing laboratory. The effect of a small reduction in abrasive particle size on cutting rate was seen in early cutting tests. Since, the process seems to be sensitive to particle size, variations in cutting rate must be expected due to minor changes in abrasive grading.

As in previous efforts, blade breakage began to occur within 15 minutes of the start of cutting. The failure seems to be a fatique problem as approximately 3,000 cycles of bladehead motion (15 minutes) is required to cause failure. A slight blade misalignment will cause a cutting parth for a blade that causes it to be distorted cn each stroke. This periodic deflection may induce stresses sufficient for fatigue failure of the blades.

3.7 Production Tests

Full Production Demonstration - Test #P-001

A 10 cm silicon ingot was sliced as a full production demonstration for Solar Power Corp. to produce silicon wafers of the same thickness as they use today. The results were analyzed as part of this effort. The wafers from Test P-001 were 0.48 mm thick, and kerf loss was 0.26 mm. Total cutting time was 19 hours and the maximum saw capacity of 225 wafers was sliced.

The blade load was 170 grams since the thick slices were produced. Cutting rate seemed to "saturate", with the higher load not resulting in a scaled increase in cutting rate. However, the slice accuracy and surface profile were of high quality, indicating that the cutting process was controlled.

This result leads to a general observation about the interaction of slurry mixture (in this case 0.48 kg of #600 SiC per

liter of PC oil) and cutting force. At a given cutting force, an increased density of abrasive in the oil causes increased cutting rate with a reduction of wafer accuracy attributed to loss of cutting "control". However, Test P-001 indicates that the suitable mix of slurry may increase as blade load is increased. The abrasive mix establishes the number of particles involved in cutting on each blade. Higher particle densities may improve average cutting rate, but a degree of rolling may result, causing wandering and reduced wafer accuracy. For higher blade loads, the optimum cutting condition may be met when each abrasive particle carries a certain load. A higher particle density on the blades may be required for the proper balance of cutting rate and "control" of blades.

Full Production Demonstration - #P-002

A second slicing demonstration for Solar Power Corporation was evaluated as part of this contract work. Again, the full machine capacity of 225 blades was used to slice a 10 cm diameter silicon ingot. 0.20 mm blades and 0.36 mm spacers were used in the blade package. #600 SiC mixed at 0.36 kg/liter of slurry oil were used with the standard 7.6 liter slurry volume. 113 grams of blade load and a 65 cm/sec sliding speed resulted in a cutting time of 23½ hours.

Wafers were 0.303 mm thick and total kerf loss was 0.257 mm. Yield was better than 94%.

Full Production Demonstration - Test #P-003

0.20 mm blades and 0.30 mm spacers were used to slice a 10 cm silicon ingot, using the full saw capacity of 225 blades (0.20 mm thick and 6.35 mm high). 113 grams of blade load and 0.48 kg/liter of #600 SiC abrasive resulted in a cutting time of 25.33 hours. Slice yield was only 76%, resulting from a collapse of the spacers within the blade package upon tensioning. At 80% full tension, the sound of collapsing spacers was heard, but the test was continued. The collapse was not disastrous to the cutting process, but did seem to cause the reduction of slice yield and poor slice accuracy. The average wafer thickness was 0.246 mm compared to earlier results with thicknesses of 0.251 mm. The difference appears to be related to the larger package size, and a correspondingly higher average blade misalignment.

Full Production Demonstration, Thin Blades - Test #P-004

A full bladehead capacity of 300 0.15 x 6.35 mm blades with 0.30 mm spacers was used to cut a 10 cm diameter silicon ingot. The available ingot length was 12.4 cm, allowing 271 wafers to be cut simultaneously. Cutting time was 35 hours, and wafer thickness was 0.25 mm, with a kerf loss of 0.20 mm. However, the wafer yield after cleaning was only 33%. With only 115 blades cutting, the same conditions had resulted in nearly 100% yield. This supports an earlier conclusion that blade alignment is the limiting factor in MS slicing with the present machine configuration.

In all cases of successful thin wafer slicing, a change to larger numbers of blades results in an increase in slice breakage, a reduction of slice accuracy, and a slight increase in kerf loss. The effect is more severe when thin (less stable) blades are used. In the Fourth Quarterly Report, it was shown that the cumulative packing tolerance of blades and spacers was expected to result in longitudinal blade misalignment from 200 to 500 microns. A vertical misalignment is expected as well. This misalignment will reduce the load carrying capacity of the blade, perhaps to a point where blade overturning will occur readily and cutting action cannot be sustained. It was shown earlier that the theoretical buckling load of a perfectly aligned blade is 10 times the loading actually experienced in MS slicing. Longitudinal misalignment (runout) can set up lateral loads on wafers during a cutting operation, and with thin slices (0.25 mm thick) fracture can easily occur.

An increase in number of blades, a reduction of blade thickness or tension or length (lower blade stability) can all limit the thickness to which slices can be cut. The fundamental problem source is the stacking of blade thickness variations, and the cure will be addressed in the extension (Phase II) of this contract,

Full Production Demonstration, Thin Blades - Test #P-005

P-004 was duplicated, except that a thicker (0.35 mm) spacer was used with the 300 0.15 mm blades. Ingot length allowed 234 wafers to be cut simultaneously. Cutting time was 32 hours and 83% of the wafers survived the cutting/cleaning process. This

improvement was due to the 0.05 mm thicker wafers (0.30 mm) and their higher strength, but it still shows the tradeoff presently required for large numbers of blades simultaneously. This run completed the cutting tests for the initial contract (Phase I).

3.8 Other Experiments

Cutting Force History - Dynamometer Results

A Dynamometer was used to record the vertical and horizontal components of force occurring during slicing experiments. The instrument was fabricated to give a full scale sensitivity of as low as 8.9 N (2 lbf) vertical and 4.4 N (1 lbf) horizontal when used with a Hewlett Packard Model 7402A Oscillographic Recorder with 17403A AC carrier preamplifiers. It utilizes a full-wave bridge of semiconductor strain gauges. The results showed that the performance of the vertical feed system is predictable and may cause problems with thin wafers.

The vertical feed has a set of four preloaded ball bushings which guide four posts from an upper platen. There is a preload friction which must be overcome in order to move the platen upward or downward. Assuming this to be a constant F_f, and the feed system to have an effective weight W, the pressure, p, applied to the cylinder area A_p results in a cutting force F_c which depends on the direction of motion, x, of the fixed platen (positive upward).

$$F_c = p\,A_p - W - F_f \frac{\dot{x}}{|\dot{x}|}$$

When no load is applied in cutting, the feed will rise on an applied air pressure of 0.25 N/mm^2 (37 psi) and will fall when the pressure is lowered to 0.15 N/mm^2 (22 psi). With the air cylinder having 1.5×10^3 mm^2 (2.36 in^2) of area, the effective weight of the system is 311 N (70 lbf) and the feed friction is 80 N (18 lbf) in either direction.

This means that, when the cutting force is applied in the normal fashion a load increment of 160 N(36 lbf)will result if the feed must move downward during the stroke of the bladehead. This occurs at the beginning of cutting since the bottom of blades do not lie parallel to the stroke plane of the bladehead, and the feed is forced downward at one end of each stroke. (See Figure 19 (a)). As the blades wear, each end is radiused and the feed must respond downward at each end of the stroke to compensate. Figure 19 (b) and (c) shows the accumulation of this condition during slicing Test #1-063. Figure 20 shows that the peak forces at the end of the stroke are about 160 N (36 lbf) above the average applied cutting force. As the stroke rate is increased to 1.7 sec^{-1}, the force increases by 31 N (7 lbf) and the peak forces become more severe. This is due to inertia of the feed imposed by the abrupt end configuration of the worn blades (high local acceleration). This peak load is applied to the work at the end of each stroke, and corresponds to an increment of 58 grams per blade when 140 blades are used.

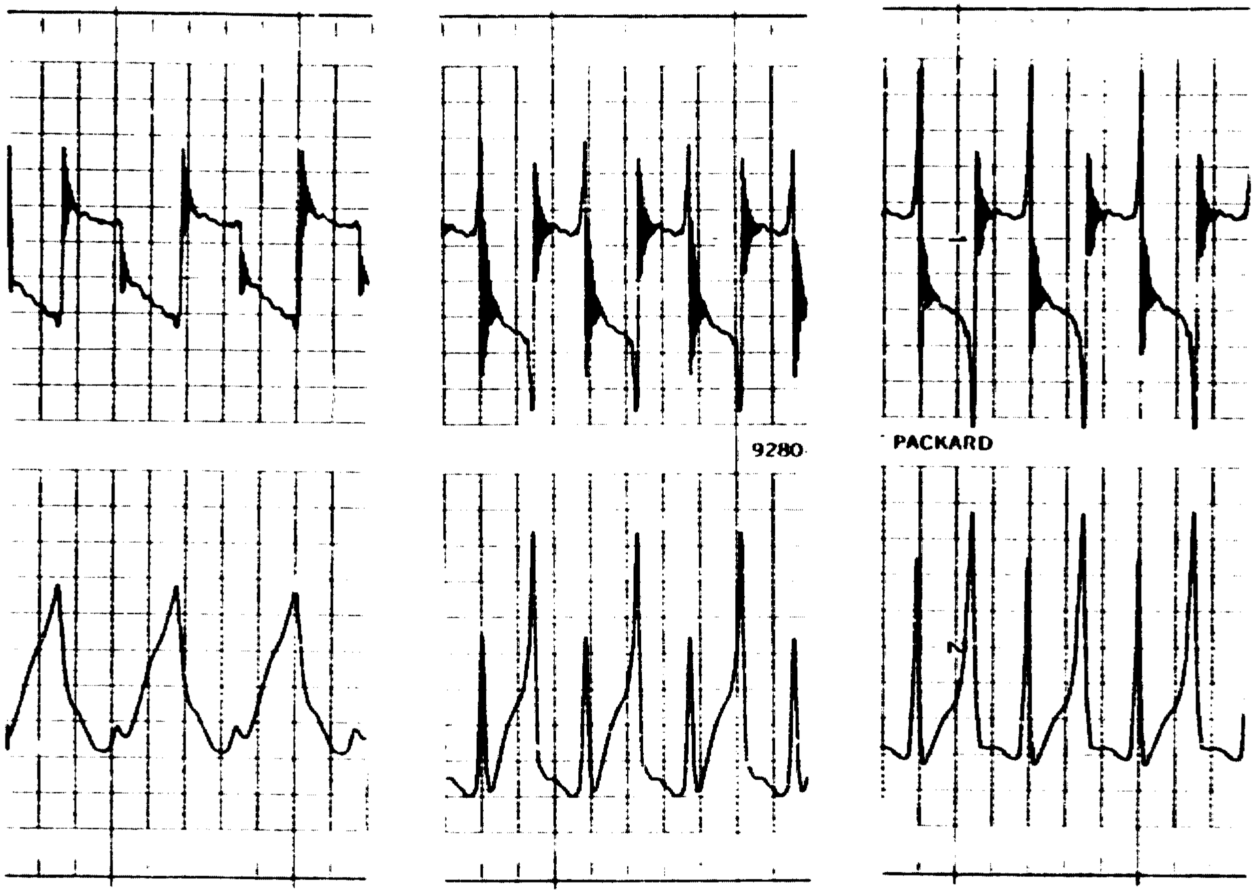

(a) (b) (c)

Horizontal Cutting Force

50 lbf full scale
0.1 sec/mm

Vertical Cutting Force

100 lbf full scale
0.1 sec/mm

CUTTING TEST #1-063

Figure 19. Development of Cutting Force During Slicing

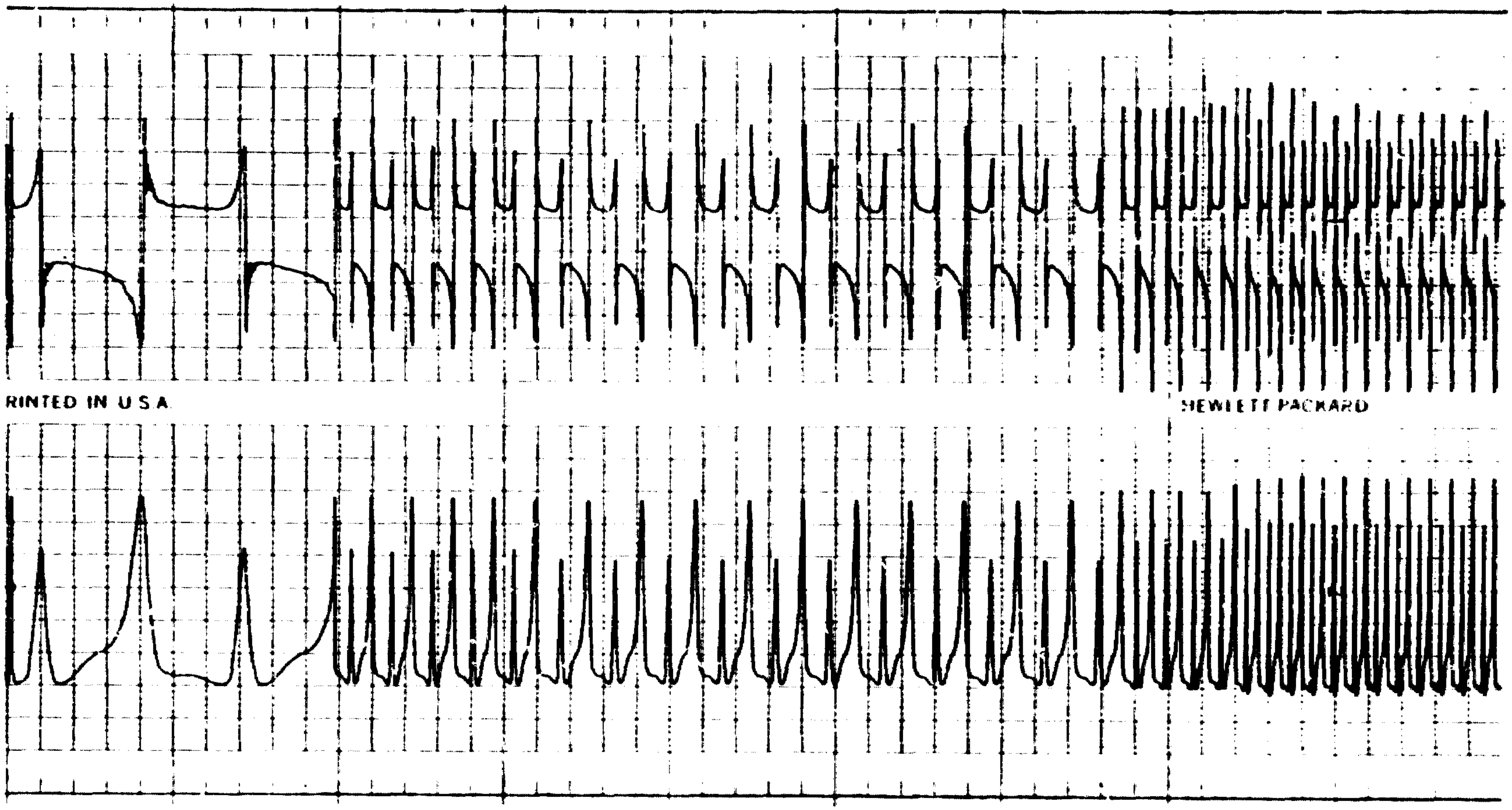

Top: Horizontal Cutting Force (50 lbf FS)
Bottom: Vertical Cutting Force (100 lbf FS)

0.1 sec/mm Horizontal Scale
Cutting Test #1-063

Figure 20. Variation of Cutting Force with Increasing Reciprocation Rate

SEM Study of Abrasives

Samples of unused #600 silicon carbide abrasive and slurry samples from various stages of the slurry lifetime test series 2-006 were photographed using a scanning electron microscope. Also viewed were fresh samples of #600 Boron Carbide and a blade edge used in a slicing test. These micrographs are shown in Figures 21 through 25.

Used abrasive was separated from the slurry oil by sequentially diluting with chlorethane, allowing particles to settle and pouring off the diluted oil.

The particle size for all #600 abrasive was 10 microns on the average. The size of particles did not appear to decrease from fresh to fully used slurry. However, the used abrasive was decorated with particles of silicon 0.4 to 1 micron in diameter.

There was no large scale change in the appearance of the silicon carbide through the cutting history of the slurry. However, there was occassionally a build-up of silicon or steel along the sharp edges of the silicon carbide. This condition appears similar to the built-up edge (BUE) on the wear land of machine cutting tools (Figure 24). The accumulation of particles adhering to the cutting edges of silicon carbide may effectively blunt the edges and reduce the tendency to cut the silicon workpiece.

The appearance of the silicon carbide was such that the possibility of abrasive breakdown or blunting causing a limit to slurry life was not apparent. Instead it appears that silicon debris (perhaps causing viscosity increase) may be the limit to the lifetime of cutting ability of slurry.

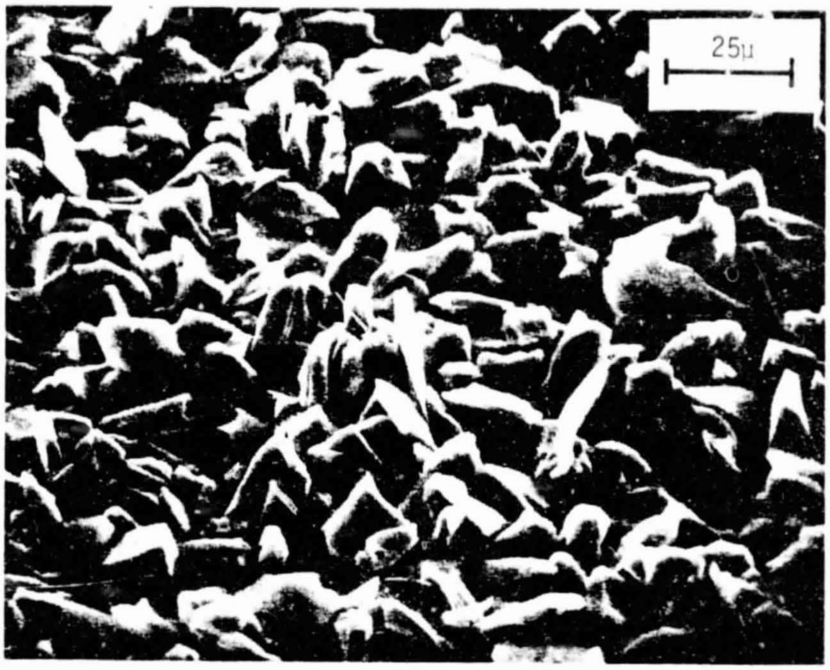

a) 700X

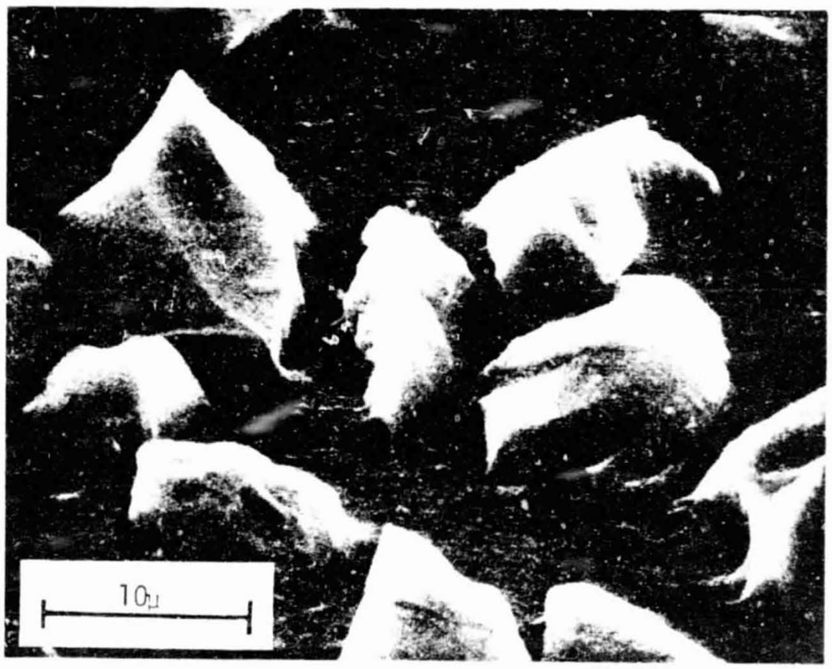

b) 3,000X

Figure 21. Urused #600 SiC Abrasive

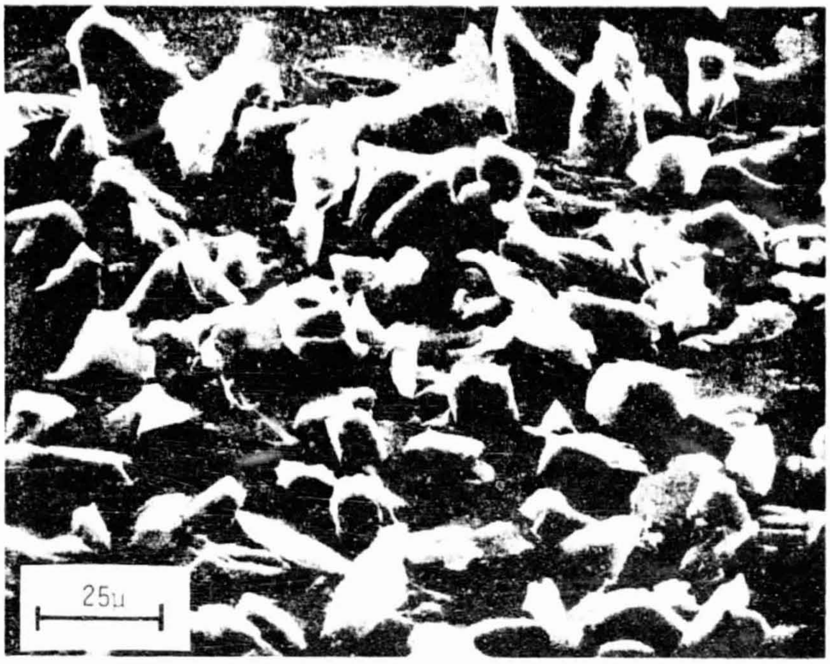

a) 700X

b) 3,000X

Figure 22. Unused #600 B_4C Abrasive

a) 700X

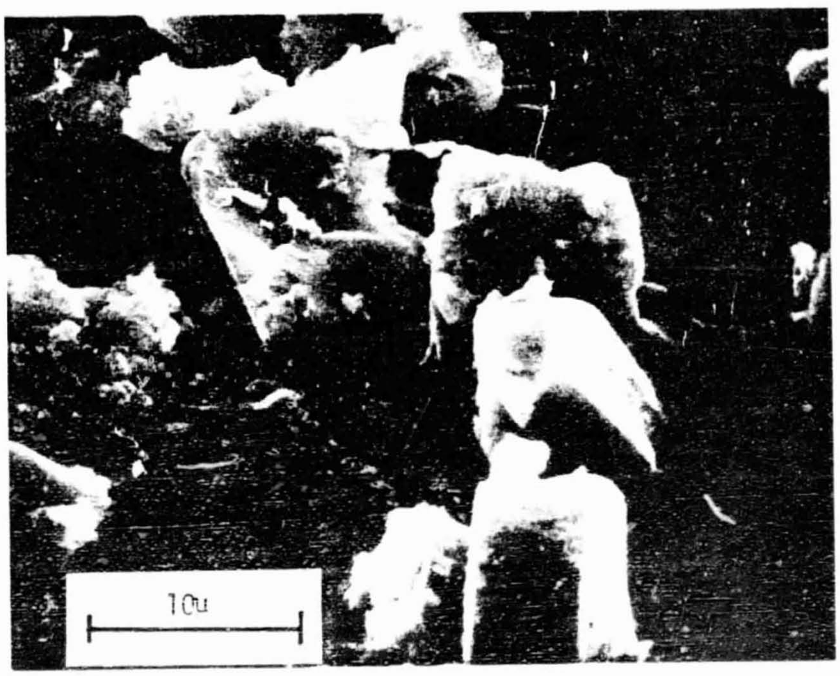

b) 3,000X

Figure 23. Used #600 SiC Abrasive

(Separated from slurry used in Test 2-006A through 2006C. Silicon abrasion to 78.0 cm^3/liter of oil and 163 cm^3/kg of abrasive)

a) 20,000X
RETENTION
OF
SHARP
EDGES

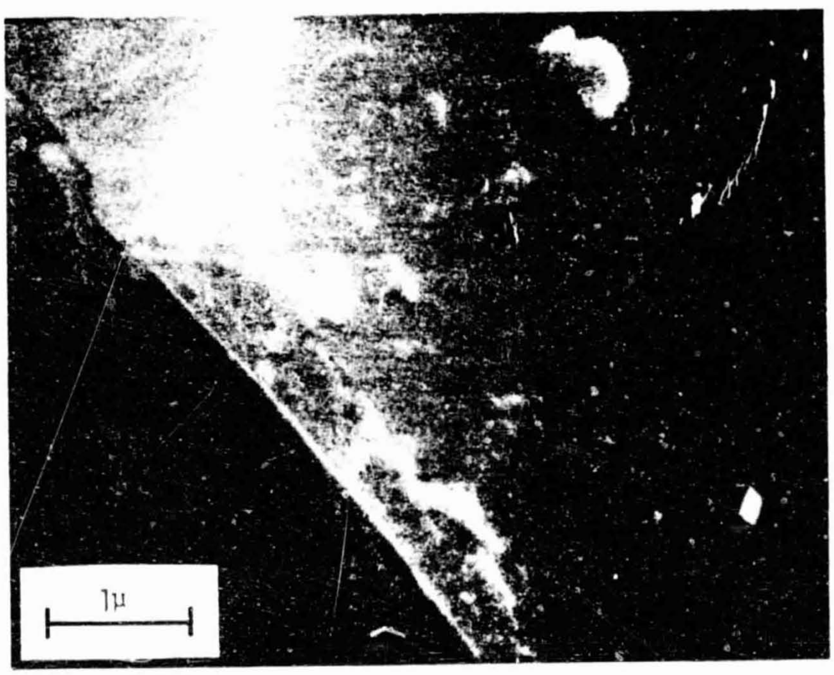

b) 20,000X
BUILDUP
OF
DEBRIS

Figure 24. Detail of Used #600 SiC Abrasive

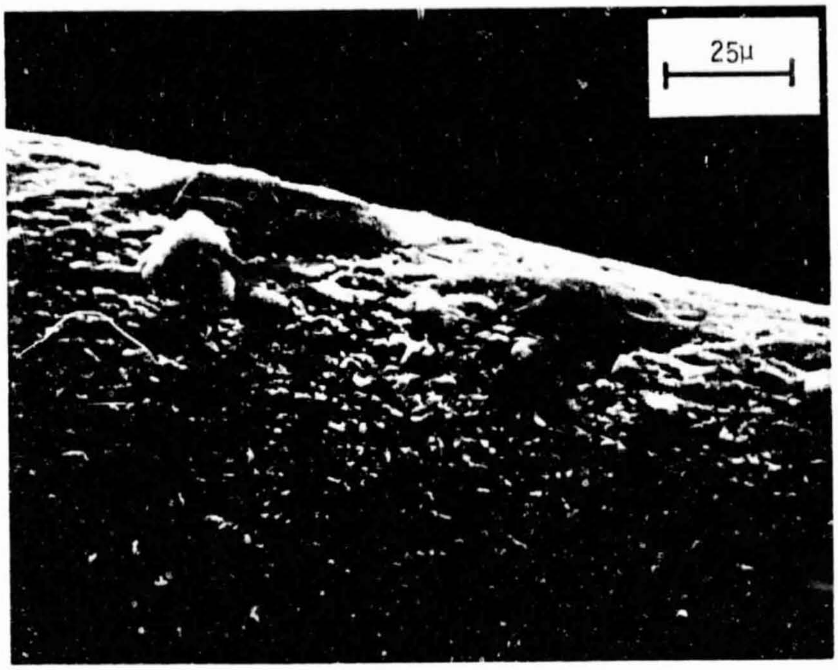

a) 700X

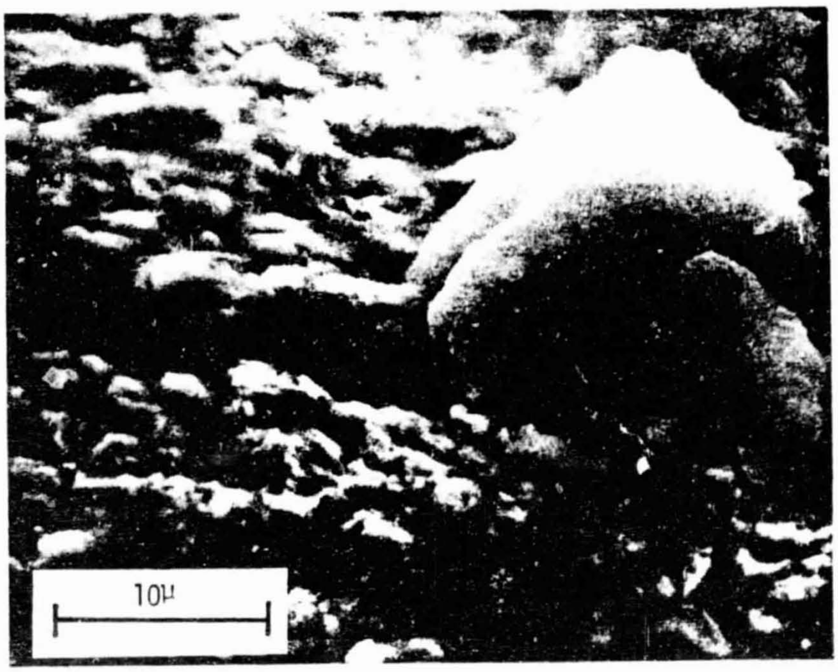

b) 3,000X
IMBEDDED
ABRASIVE
ARTICLE

Figure 25. Cutting Edge of a Used Blade (From Test #3-031)

Also, it is apparent that the major difference between silicon carbide and boron carbide abrasive is a slightly larger particle size for boron carbide. The cleaved, sharp particles are both of similar shapes.

Figure 25 shows an abrasive particle which has remained imbeded in a blade. This is not a common occurrence, but the imbedding of abrasive particles was never assumed to be permanent. Instead, a quasi-static imbedding is most likely.

Etching Study of Surface Damage

A procedure for the step-etching of as-sawed silicon wafers was devised. Saw-induced damage is revealed by dislocation etch pits and varies appreciably with sawing conditions, and the damage has been found to extend inward more than a few microns. As shown by Figure 26 for a wafer from cutting Test #1-011, the dislocation density remains above 10^4 per cm^2 until a depth of 18.8 μ (0.74 mil) is reached, and its value is 640 per cm^2 at 27.8 μ (1.11 mil). In slicing Test #1-014, where blade loading was 4 times higher, the damage density at the surface is lower than in #1-011, but the slope of the damage vs. depth curve is lower.

The step-etching procedure is conventional. A satisfactorily nonselective and conveniently slow etchant was developed from the commonly used 3 HNO_3 (conc.) : 1 (HF (conc.) : 1 CH_3COOH (glacial) chemical polishing reagent by increasing the proportion of nitric acid to 30:1:1. This composition gives sufficient oxidizing power to maintain planarity, while the greatly reduced rate of oxide

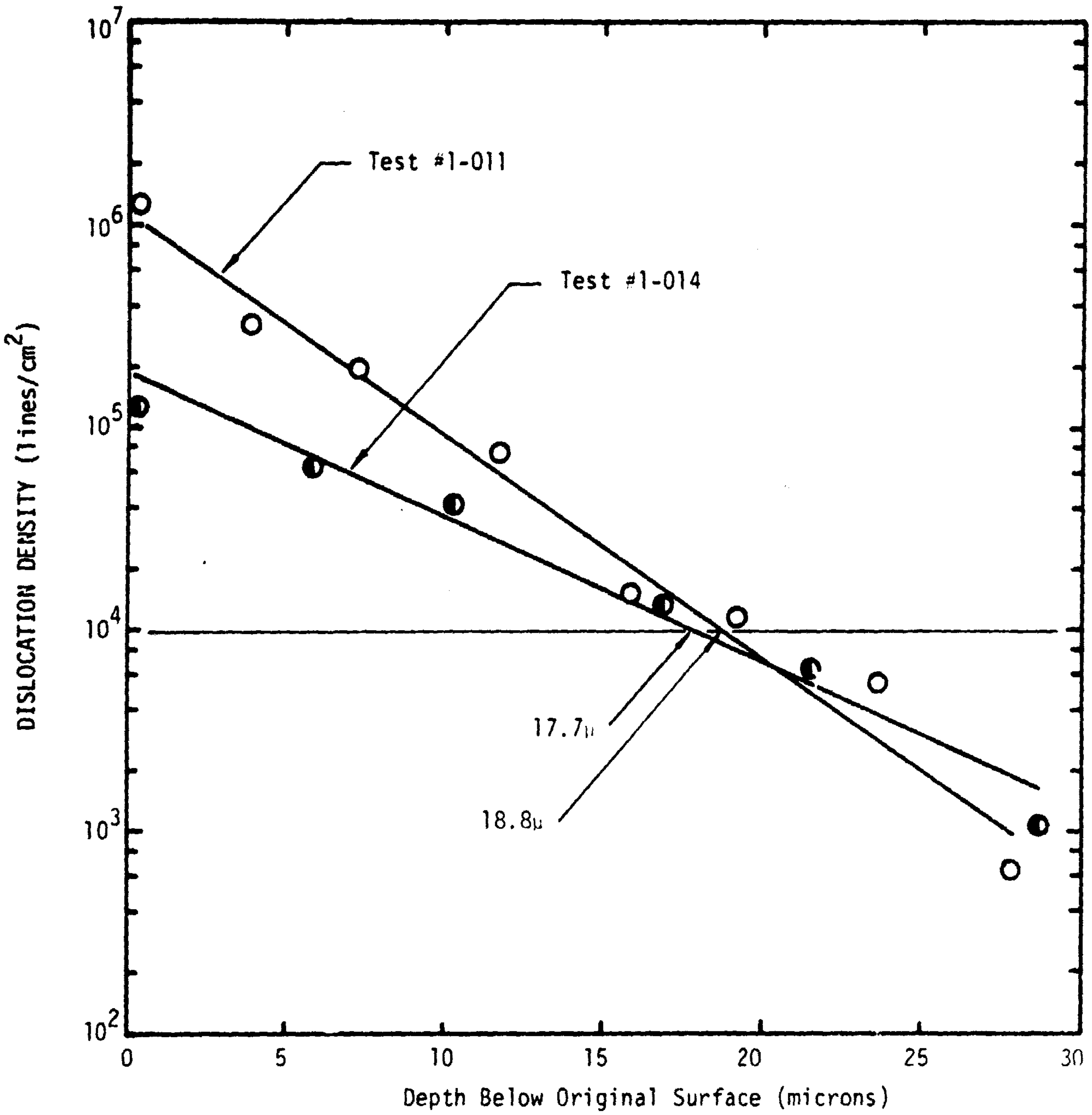

Figure 26. Dislocation Density as a Function of Depth

removal yields an effective etch rate of approximately 2μ per minute. The Wright etchant is used to reveal defects, and ceresine (microcrystalline) wax is used to mask against etching; the wax is readily removed by chloroethylene with ultrasonic agitation. Step heights are measured with a Sloan Dek Tak surface profilometer.

SEM Study of Wafer Surface Damage

Figures 27 - 32 show SEM micrographs of etched and unetched surfaces of wafers sliced with three different abrasives. The etched surfaces were prepared using a 5 minute Wright etch. Measurements indicated that 4 microns of surface was removed. (We have been told that the unetched surfaces resemble lightly etched surfaces. This is probably because the wafers were washed in Alconox, an alkaline detergent which produces some etching action.)

All surfaces indicate a fine (1 to 10 micron) interspacing of cracks. These are likely Hertzian fractures produced as abrasive particles passed over the surface. The network appears to result in material removal by intersection of cracks producing free silicon particles. Figure 27b shows a void from which a particle was formed.

The etched <100> surfaces show the remnants of major cracks oriented 90° apart. Presumably these are cracks which were oriented along <111> planes and propagated deeper than the rest. The cracks appear to be no deeper than 5 to 10 microns. The Wright etch has caused the cracks to widen into a coarse topography after minimal material removal.

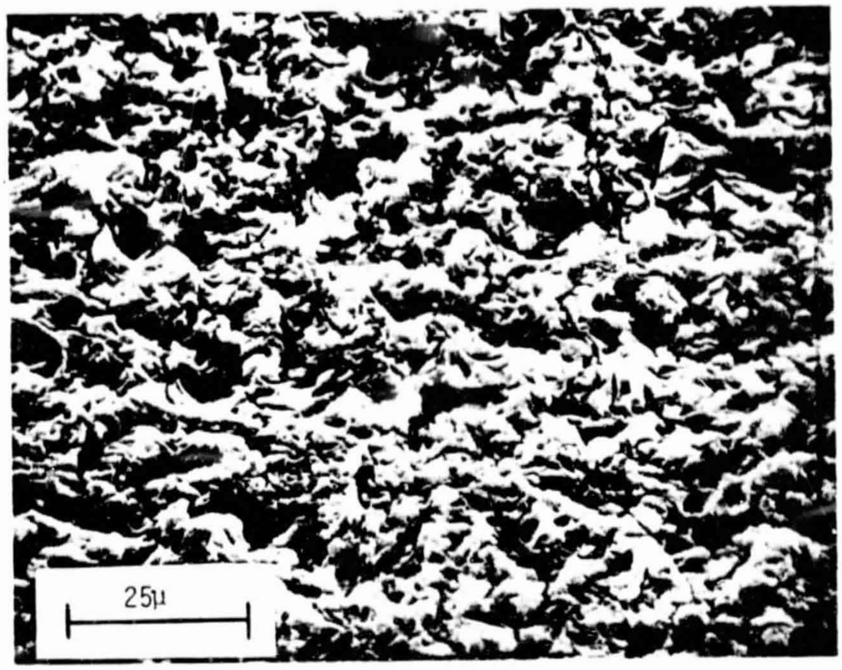

a) 1,000X

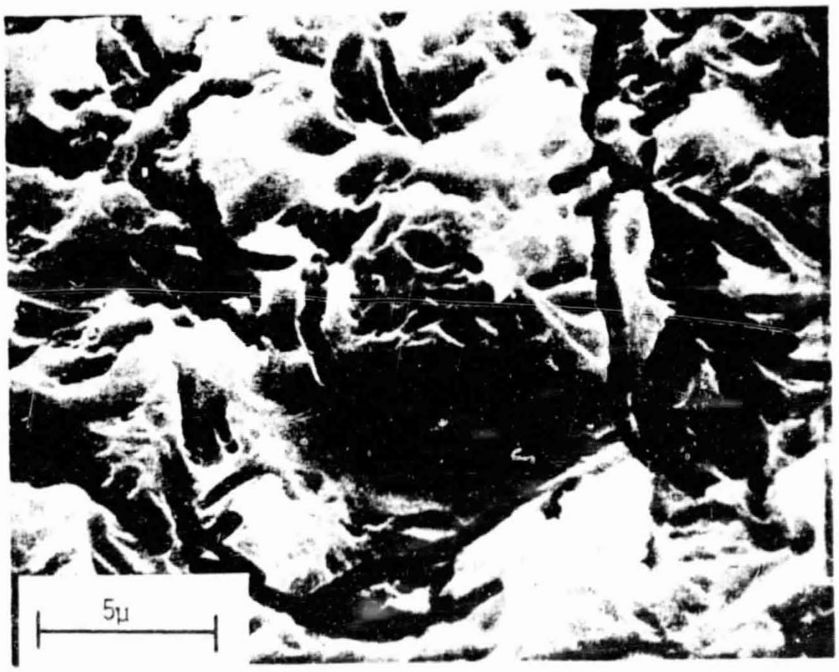

b) 5,000X

Figure 27. "Unetched" Surface of an MS Sawn Wafer

({100} Surface viewed at 45° from normal. #600 SiC abrasive used -- Test #2-001)

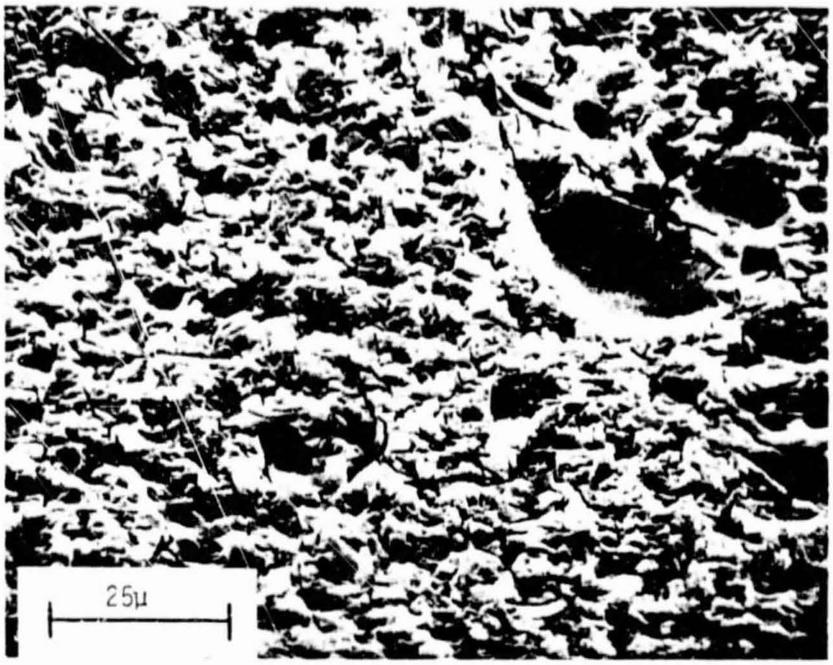

a) 1,000X

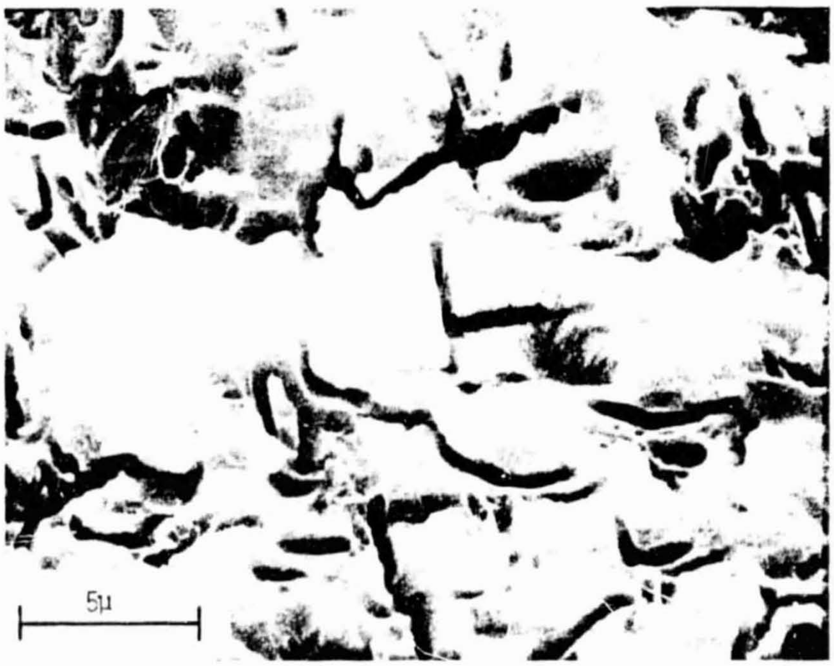

b) 5,000X

Figure 29. "Unetched" Surface of an MS Sawn Wafer

({100} Surface viewed at 45°. #800 SiC abrasive - Text #2-011)

PRECEDING PAGE BLANK NOT FILMED

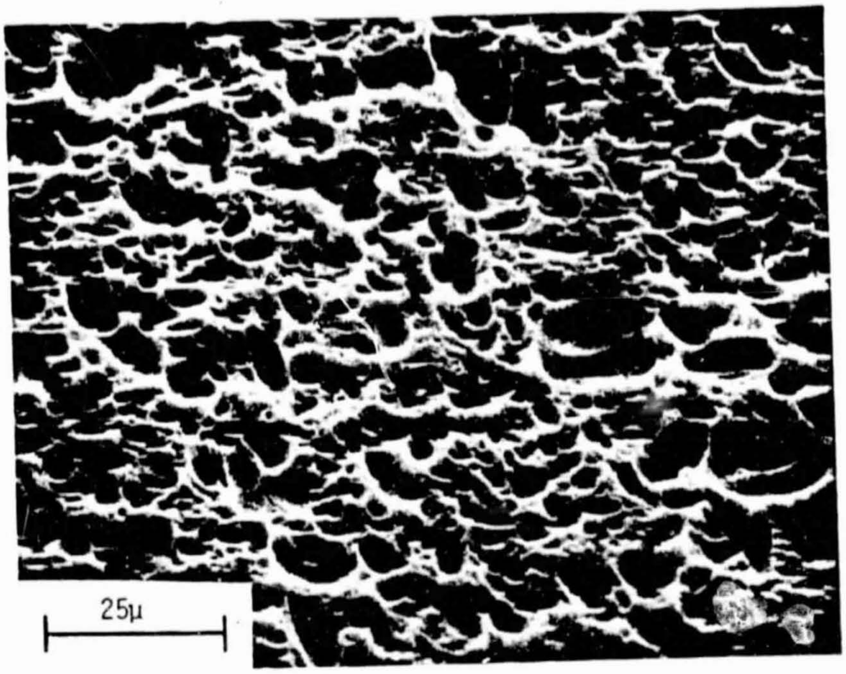

a) 1,000X

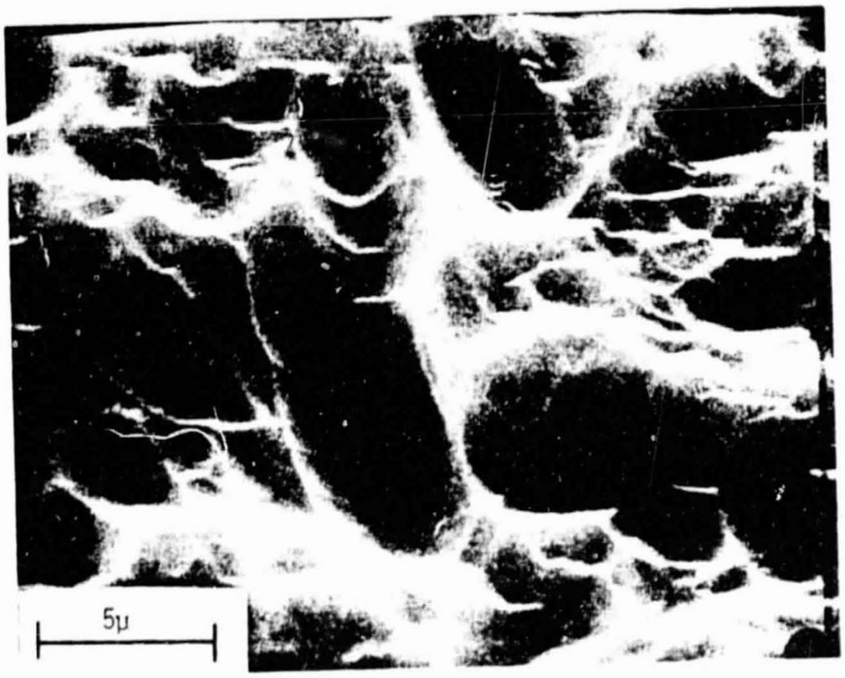

b) 5,000X

Figure 30. Etched Surface of an MS Sawn Wafer

({100} Surface viewed at 45°. #800 SiC abrasive - Test #2-011.
4μm removed with 5 minute Wright etch)

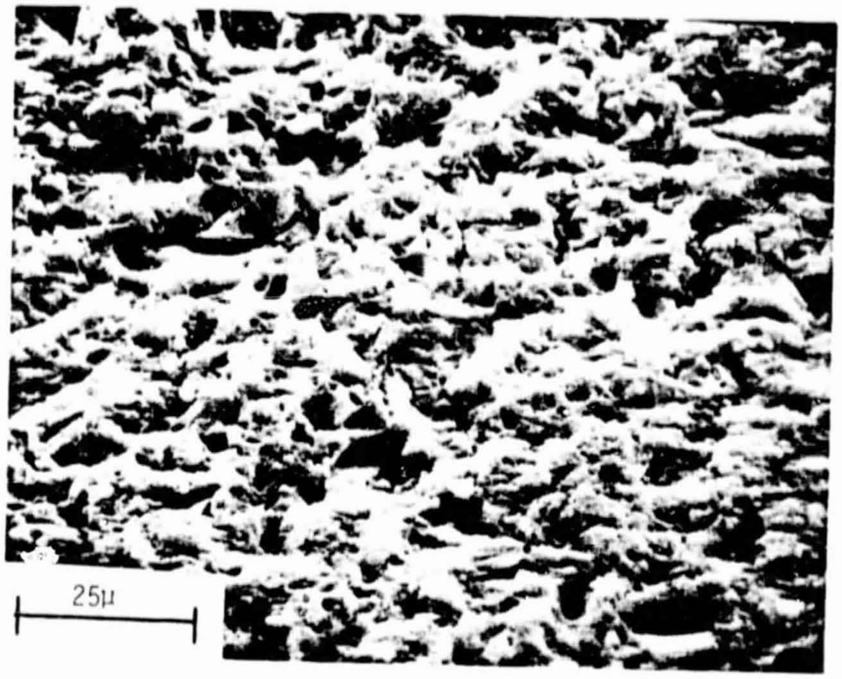

a) 1,000X

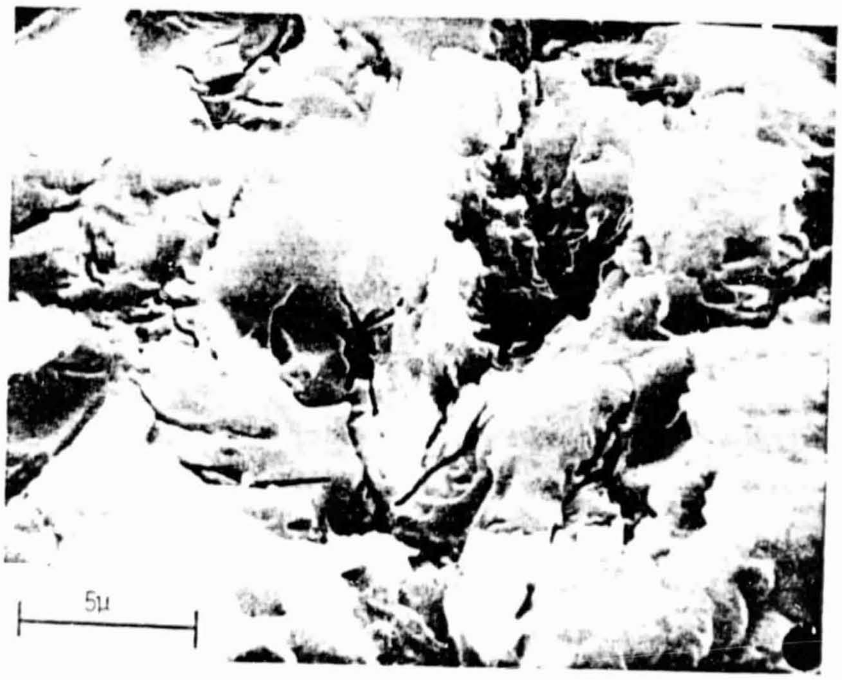

b) 5,000X

Figure 31. "Unetched" Surface of an MS Sawn Wafer

({100} Surface viewed at 45°. #600 B_4C abrasive - Test #2-041)

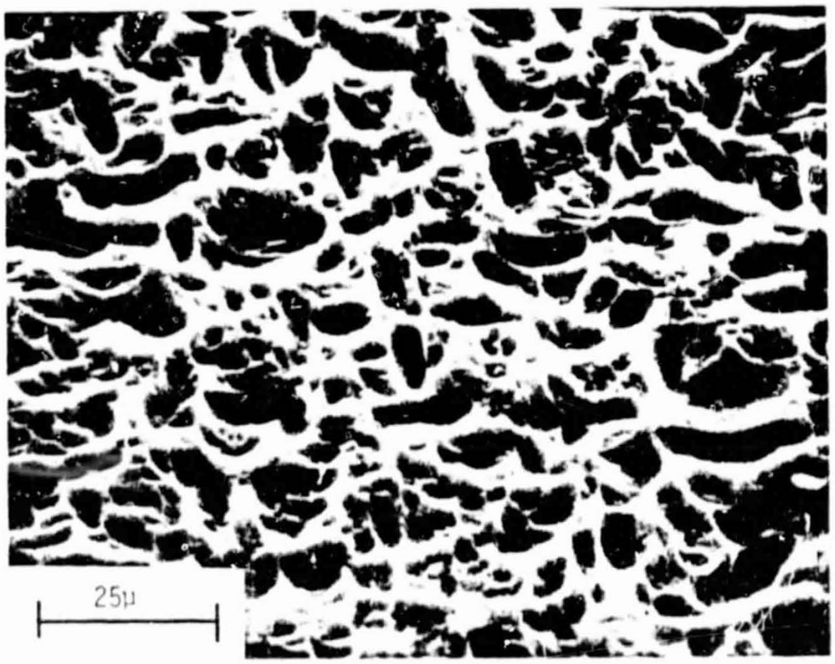

1,000X

Figure 32. Etched Surface of an MS Sawn Wafer

({100} Surface viewed at 45°. #600 B_4C abrasive - Test #2-041. 4µm removed with 5 minute Wright etch)

The surface sliced with finer (#800) silicon carbide abrasive has a finer crack network. The particle voids (Figure 12a) are much larger (30 microns than with #600 SiC. This result is even obvious under a low power optical microscope. The #600 Boron Carbide resulted in a crack network of a different appearance. The spacing is comparable to #600 SiC, but the cracks are much finer. They did not seem to open as much as those produced with #600 SiC. The etched wafer appears the same, however.

3.9 Wafer Characterization

Although it is generally agreed that solar cell wafers need not meet the specifications for dimensional variation used in the semiconductor industry, there must be some standards. Wafer-to-wafer thickness variation, taper, bow, and thickness all affect the choice of handling methods and process steps. Characterization of wafers is also important in guiding the experimental program.

Under Phase I, two types of measurements were used to characterize wafers. 20 wafers per run were measured in a Bausch & Lomb bench micrometer (accurate to .0001 in.). Thickness of each wafer was measured at 9 points, 8 around the edge and one at the center. From these measurements standard formulae were used to calculate average wafer thickness, standard deviation of average thickness, average thickness variation within a wafer and its standard deviation, the average of standard deviations of thickness variations within a wafer and its standard deviation, and average

taper. Also, one or two wafers from each run were traced on both sides using a Sloan Dek-Tak surface profilometer. Traces were run in both the with-stroke and cutting directions. These traces were used to measure bow (here defined as the difference between average thickness from above and maximum thickness between two planes tangent to two points on each side of the wafer), taper, and surface roughness.

The results for each test are presented in the appendices and discussed below.

C-2

4.0 PHASE I: DISCUSSION AND CONCLUSIONS

4.1 Parameter Study

Effects of Load, Ingot, Size, Sliding Speed

Figure 33 shows abrasion rate as a function of feed load for Tests #1-011 through #1-015 (the curve marked "typical" does not include the initial portion of the test when the system "settles down" or the final portion when the blades slow as they are allowed to cut into the submount to avoid excessive taper at the end of the cut). It can be seen that load and abrasion rate are almost linearly related. At 283 g/blade, the workpiece broke up due to severe blade wander. Both bow and taper increased with increased load.

Later tests (#2-024, #P-001, #2-026) showed that this linear relation does not always hold: efficiency is reduced at high loads, indicating the process is not working as well as possible, and this is confirmed by the fact that the abrasion rate did not increase to the level predicted by Figure 33. Increasing the proportion of abrasive in the slurry raised the cutting efficiency to normal levels and caused the abrasion rate to scale with the load: a new problem was manifested in the fact that the yield was low with very thick wafers. Since thin wafers are quite important for economic reasons, we feel that our "standard" loads of 558 g/blade/mm of blade thickness are the best choice.

Results of various tests showed that the abrasion rate is independent of kerf length (i.e., work dimension in the stroke

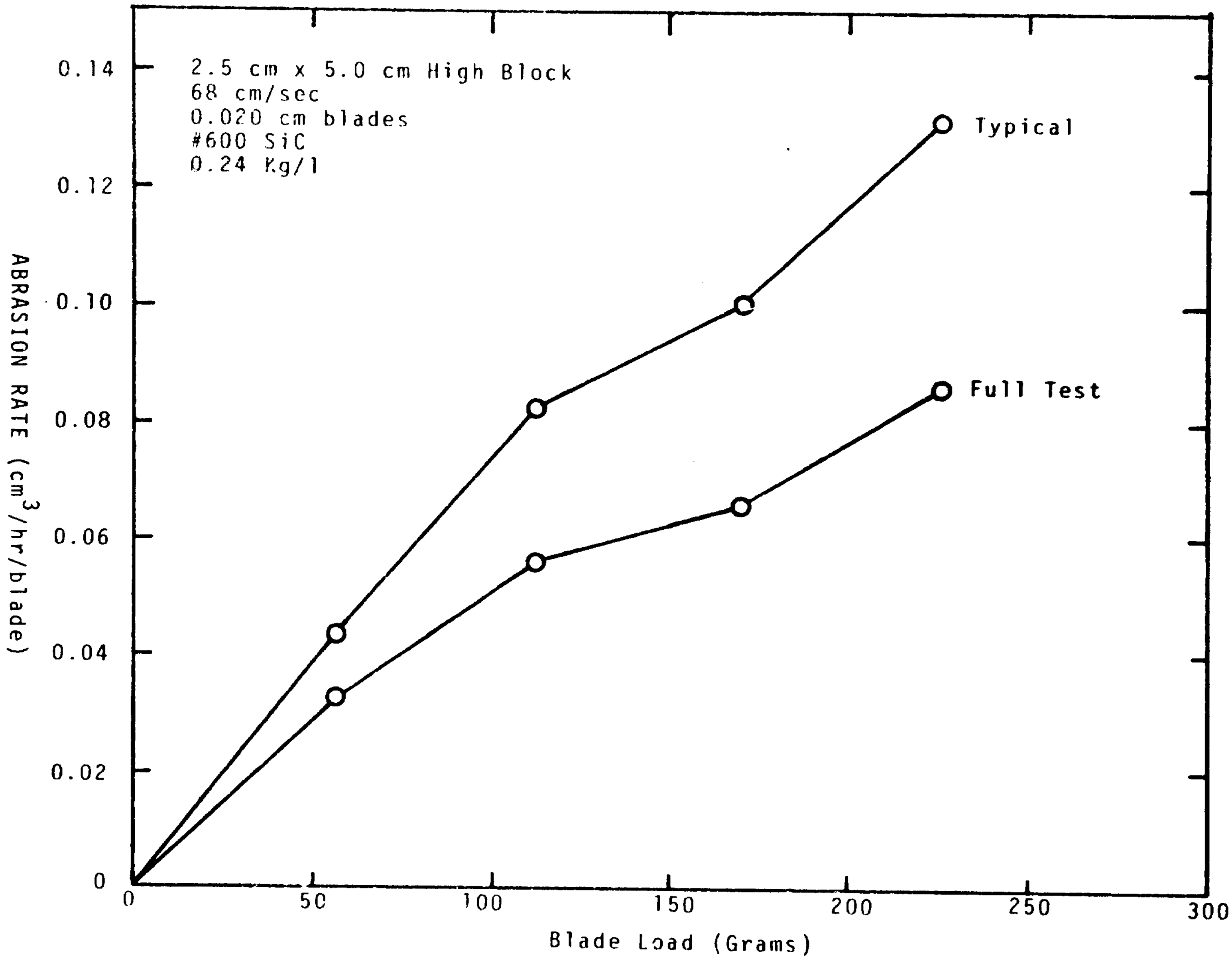

Figure 33. Abrasion Rate as a Function of Blade Load

direction) for lengths between 20 and 110 mm. Kerf length is, therefore, not a significant variable.

Figure 34 shows the abrasion rate as a function of maximum sliding speed during a stroke. The arrows indicate that the abrasion rate following a change in speed was low, and increased as the saw "settled in". At 81 cm/sec, the workpiece broke up. It seems that higher reciprocation rates are a valid method of increasing productivity without increasing expendables: however, the current saw is incapable of making a significant improvement because of the limitation on reciprocation rate imposed by bladehead mass, and the lack of facilities for absorbing the higher shock loads generated at higher reciprocation rates.

Kerf Width and Abrasive Size

Results of several tests indicate that abrasion rate is constant as the kerf width changes from .2 to .35 mm. Thus, kerf width is not an important variable in calculating cut rate.

Figure 35 shows both abrasion rate and "productivity" for various abrasive sizes (all from Micro Abrasives Corporation). The large reduction in rate as the particles get smaller is insufficient to offset the reduction in kerf loss. In addition, the smaller abrasives (higher numbers) resulted in significant increases in dimensional variation. #600 seems the best choice of abrasive size.

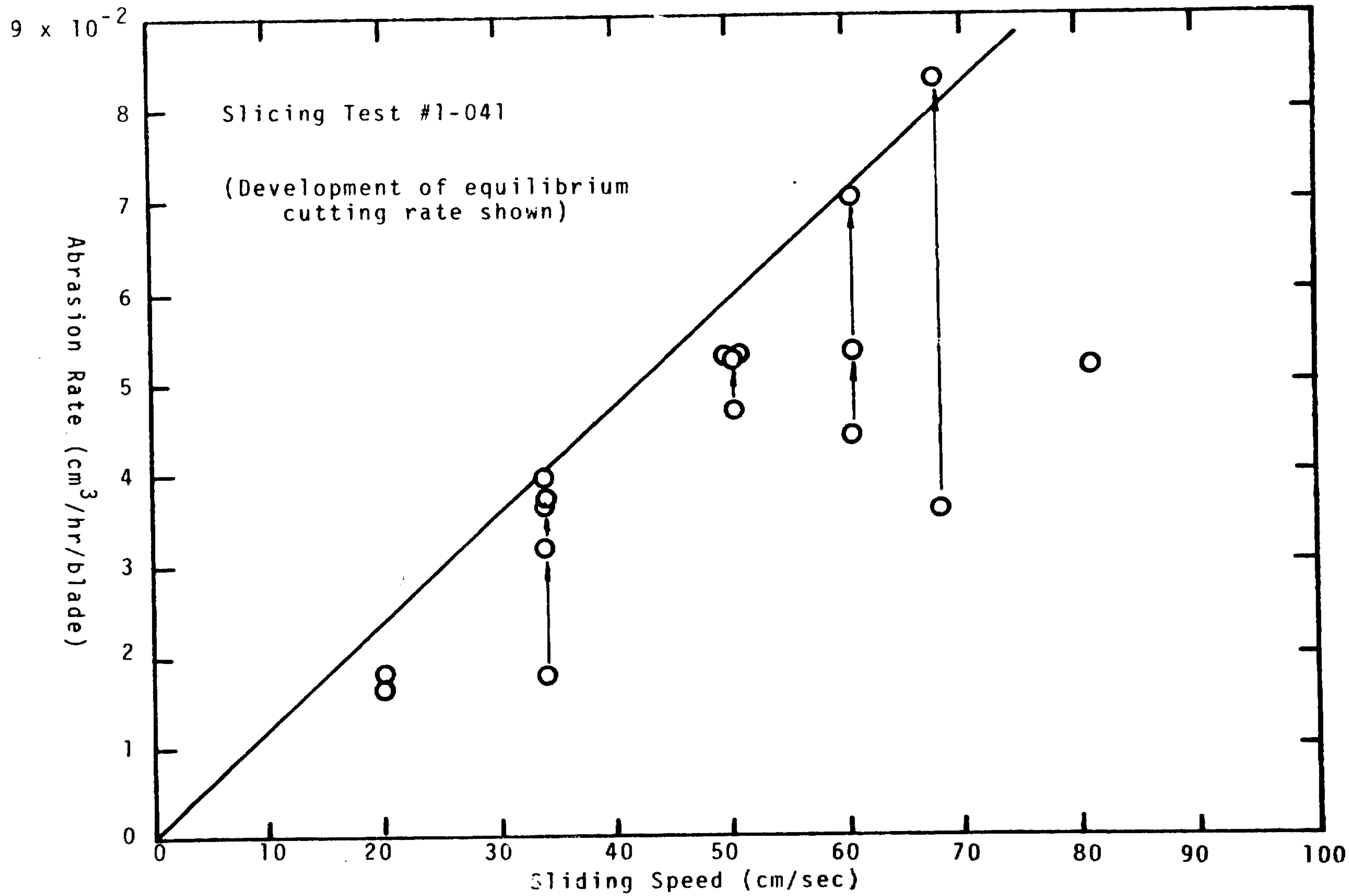

Figure 34. Abrasion Rate as a Function of Sliding Speed

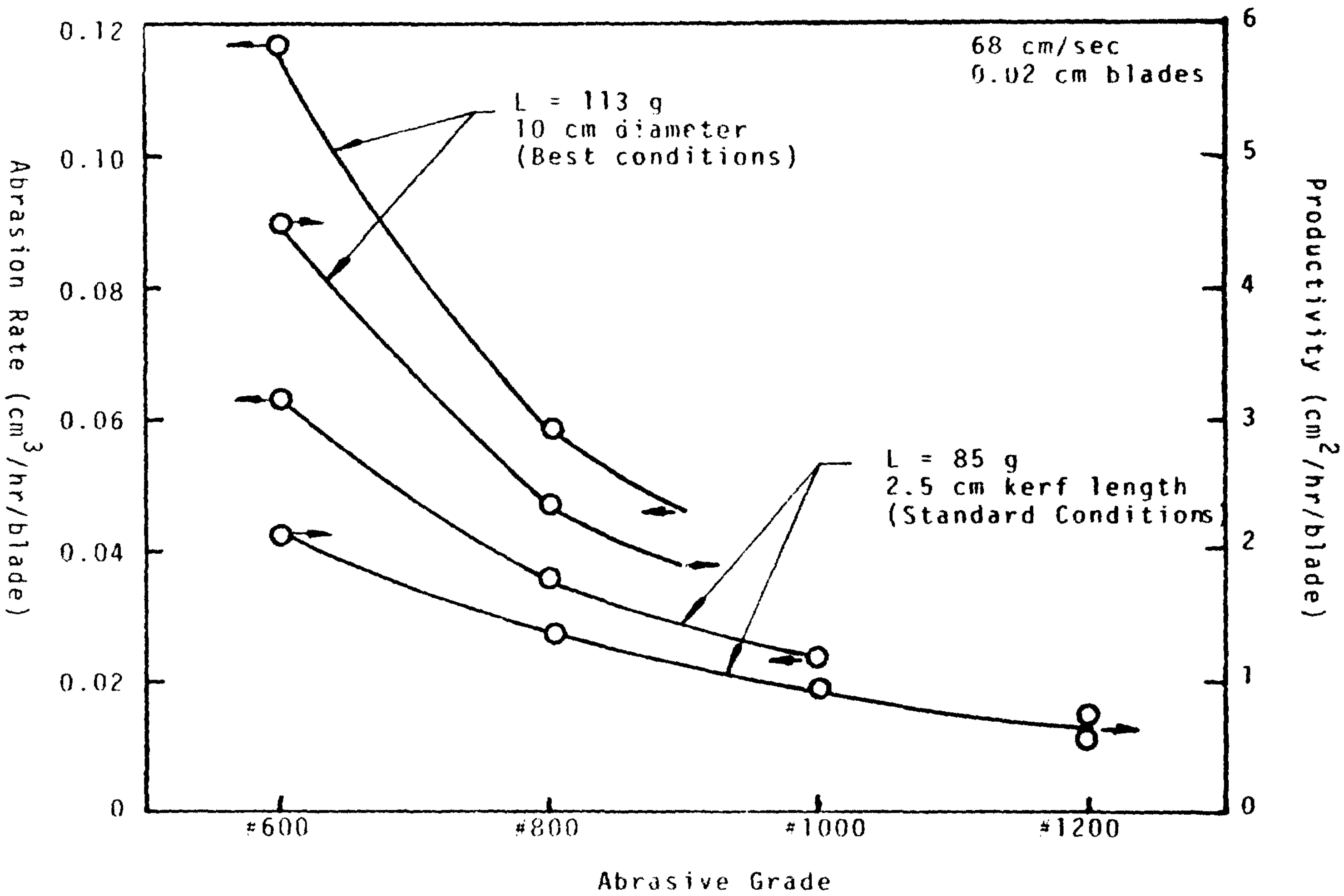

Figure 35. Abrasion Rate and Productivity for Various Grit Sizes

Blade Wear

Blade wear for a full cut through a 100 mm diameter ingot is typically 2.5-3mm. Therefore, a 6.35 mm (.25 in.) high blade is useful for one such cut. A 12.7 mm high blade should be useful for 2 and perhaps 3 such cuts. (Note that shorter strokes must be used for successive cuts because of wear, so the height loss in each succeeding cut is greater than the preceding cut.) 12.7 mm high blades will probably be necessary for 125 mm diameter ingot, and will definitely be necessary for 150 mm diameter ingots, since blade wear is proportional to wafer area.

4.2 Abrasive and Slurry

Slurry and Abrasive Lifetime

Tests using the same slurry (#2-006 A, B, C) showed that the slurry is definitely "worn out" after slicing two 100 mm ingots, and somewhat worn out after one ingot. SEM studies of the abrasive show that the abrasive is not significantly degraded. We hypothesize that the "wearing out" mechanism is debris accumulation, and abrasive is recyclable.

Thinning the slurry, to attempt to reduce viscosity increase, had no effect other than a reduction of efficiency.

Abrasive Concentration

Experimental results indicate that there is an optimum abrasive concentration, and that it is a function of blade thickness. 0.48 kg/l (4 lb/gal) is preferable for .2 mm (.008 in.) blades, while 0.36 kg/l (3 lb/gal) is optimum for .15 mm (.006 in.) blades.

It seems likely that this relationship will also hold for .1 mm (.004 in.) blades. As noted above, abrasive concentration should also be increased as cutting loads increase to maintain efficiency.

Boron Carbide and Zirconia-Alumina Abrasives

Higher cutting rates were obtained using boron carbide abrasive. However, kerf loss also increased. It is likely that there is a sizing incompatibility between #600 silicon carbide and #600 boron carbide: these small sizes are separated in settling tanks, so density differences make it impossible to obtain uniform sizing between different abrasive types.

Boron carbide is approximately 10 times more expensive than silicon carbide. In view of the SEM studies of used silicon carbide which found no significant degradation, and, therefore, the likelihood of being able to recycle silicon carbide, the added expense of boron carbide is not justified.

Zirconia-alumina abrasive, which is much more "rounded off" than silicon carbide, yielded very inefficient cutting. This abrasive is not suitable for slurry sawing.

4.3 Blades

In any slicing technique, the loss of material during the slicing process is important. We, therefore, concentrated on reducing the blade thickness in order to reduce the kerf loss and understand the problems associated with thinner blades.

Initial "best effort" blades were .2 mm (.008 in.) thick (#1-001 and others). Significant problems were initially encountered with attempts to use .15 mm (.006 in.) blades, but eventually we were successful. (#P-005, #3-035, #3-036 and others.) Success was obtained by scaling both the abrasive concentration and cutting load by blade size.

No successful cuts were obtained with .1 mm (.004 in.) blades. Blade breakage and wander were severe. In order to use these blades, we feel that alignment of the blades should be improved and a shock absorbing system to reduce shock loads will be necessary. We do not now feel that blades thinner than .1 mm will be useful in the near future.

4.4 Miscellaneous

Spacer Thickness

It was found that spacers thinner than .3 mm (.012 in.) are not useable because of spacer buckling. 0.3 mm spacers require the additional support provided by the epoxy blade package to prevent buckling. Since .3 mm spacers used with #600 SiC yield a .225-.250 mm (.009 - .010 in.) thick wafer, and thinner wafers are so fragile that they probably could not survive the cut without extensive shock absorbing and support, .3 mm spacers seem to be a reasonable goal. .35 mm (.014 in.) spacers were used successfully in several runs.

Wafer Demounting

Initially, wafers were demounted by dropping the feed (pulling the wafers down through the blades), which caused significant wafer breakage. We tried a crude heated workmount plate, which melted the Dekhotinsky cement used to secure the ingot, with success. We have found that groups of 10-20 wafers can be "wiggled off" without significant breakage, without using the heated mount. A heated mount might be more convenient in a production environment.

Blade Stability

The analysis of blade buckling presented earlier showed that buckling loads are an order of magnitude higher than nominal applied loads. However, dynamometer results also showed high shock loads due to blade wear at the stroke ends. The displacement forced by blade wear is probably beneficial in that it pumps the slurry around, flushing debris and introducing fresh abrasive; but the associated loads should be reduced by reducing feed mass and spring constant in order to increase blade stability (and life of .1 mm blades).

Blade Alignment

The statistical analysis of blade alignment showed that noticeable misalignment is expected in the best aligned package possible. In the currently produced saw, such misalignment is probably small enough so as not to affect the process significantly: however, in a larger saw, a redesigned package or external alignment device or both may be needed.

Surface Damage

Etching studies have shown that the extent of saw-induced damage is very small, on the order of 10-15 μm deep. Damage should not be a problem in solar cell fabrication.

Blade Tolerances

An analysis of the shape of a tensioned blade showed that the differences between "normal straightness" blade stock and the currently used "extra accurate straightness" stock are insignificant. The difference in cost between the two materials is 10-15%.

5.0 ECONOMIC ANALYSIS

Although the economic analysis of multiblade slurry sawing was carried out throughout the course of the contract, this is a convenient point to present the complete analysis as it stands at the end of the contract. This discussion of economics provides a convenient summary of the results of Phase I, and an introduction to and rationale for the investigation of Phase II.

All the analysis presented here is in the format of the IPEG (Interim Price Estimation Guidelines) of SAMICS (Solar Array Manufacturing Industry Costing Standards) as developed at JPL. All dollar values are 1980 dollars unless otherwise noted.

5.1 State-of-the-Art Economics

The first step in the analysis is to assess the economics of the best currently available process. In this state of the art assessment, we have decided to be conservative in the process specifications since the economics are so favorable to slurry sawing. The main impact of this decision is in the choice of blade thickness and spacer size. The state of the art factory is chosen to produce 5.2×10^4 m^2 of sheet per year.

General Parameters

Although we were successful in using 0.15 mm (.006 in.) blades to cut 0.3 mm (.012 in.) wafers during Phase I, for this

state of the art assessment, we chose to assume 0.2 mm (.008 in.) blades and 0.35 mm (.014 in.) wafers. A convenient conversion factor is the number of square meters of sheet produced for each kilogram of ingot used. Assuming a 100 mm diameter ingot (4 in. nominal) and a slicing yield of 95% gives a conversion factor for this process of 0.67 m^2/kg.

The cycle time, including one hour for teardown and setup (an experienced operator can easily better this) is taken to be 30 hours.

Equipment and Floor Space

The basic equipment must be chosen as the model 7176 wafering saw currently available from Varian. The current (August, 1979) market price for this saw is $24,500. The price in 1980 dollars will be taken as $25,000. It is reasonable (in light of known production practices) to assume that 95% utilization can be maintained, so 88 saws (83 active at any time) suffice to produce at the desired level. Our experience suggests that $140,000 in miscellaneous equipment is required.

The floor space required is approximately 5.6 m^2 (60 ft^2) per saw.

Labor

It is not unreasonable to assume 22 saws per operator. Experienced operators can easily maintain this level, spending 1/2 to 2/3 of their time actually setting up the saws, and the

remainder cleaning the saws and performing miscellaneous tasks. We know of one company that runs with 33 saws per operator.

We, therefore, take labor to be 4 operators and one foreman per shift. In accordance with JPL guidelines, we assume 4.7 shifts per day in order to operate 365 days per year.

Materials and Energy

For each run, one purchased blade pack will be required. 7.6 liters (2 gal.) of PC oil will be used for the vehicle, and 13.2 kg (6 lb.) of silicon carbide abrasive. Miscellaneous supplies (ingot submount, Dekhotinsky cement, etc.) total \$5.18 per run. 31.7 kw-h of electricity is required per run.

Results

Table 4 is a layout of the IPEG calculations for the state of the art system. The interim price goal for 1980 sheet generation is \$343/m^2 value added. Although this quantity must be allocated to ingot growth and wafering, the add-on cost from Table 4 of \$128/m^2 is only 37% of the allocation: the remaining 63% (\$215 m^2) should easily be sufficient for ingot growth. The conclusion is that a conservative assessment of the state of the art in slurry sawing shows that this process can easily meet the interim 1980 goals.

TABLE 4

STATE OF THE ART COST SUMMARY (1979)

		AMOUNT	UNIT COST	DIRECT COST	FULL ANNUAL COST
EQPT	saw	88	25,000	2,200,000	1,080,000
	miscellaneous	--	--	140,000	69,000
SQFT	floor space	5,370 ft^2	--	--	975,000
DLAB	operator	23	16,170	372,000	783,000
MATS	blade pack	23,135	96.50	2,233,000	2,903,000
	vehicle	46,270 gal.	3.80	175,800	228,500
	abrasive	138,800 lb.	2.50	347,000	451,000
	miscellaneous		--	120,000	156,000
UTIL	electricity	733 Mw-h	50	36,600	47,500
					6,643,000

QUAN = 51,500 m^2

VALUE ADDED = 128 $\$/m^2$

5.2 Onward to 1986

Through a long and continuous process of considering technical feasibility and effects of changes, we have constructed a scenario for development of the multiblade slurry sawing process. This scenario outlines the technical progress necessary to reach or approach the 1986 goals. Table 5 presents the highlights of the cumulative changes in this scenario (note that the years given are years in which these changes can be used in production: obviously, the equipment must be available several years earlier and process knowledge should be available on the order of a year earlier). Tables 6-8 contain the IPEG calculations for the scenario, and the individual changes are discussed below.

General Parameters

The conversion factor m^2/kg discussed above is extremely important to the add on cost. We feel that properly designed shock absorbing equipment will make it possible to cut 0.25 mm (.010 in.) thick wafers using 0.1 mm (0.004 in.) thick blades. Assuming a 95% wafer yield, the conversion factor is then the easily remembered 1.0 m^2/kg. We do not now see any way to increase this factor.

The ingot diameter is assumed to increase to 150 mm (6 in.) diameter. This has essentially no effect on the economics of the sawing process, but is used because analyses of Czochralski ingot growth indicate that this increase is necessary to make the growth process economical.

The cycle time must be maintained essentially constant at 32.6 hours. This means that for a 150 mm ingot the cutting rate must be increased by a factor of 1.3 to 4.6 mm per hour (note that this corresponds to approximately doubling the area production rate by which many factors scale). To achieve this, the reciprocation rate must be doubled: (work under Phase I showed that area production rate (equivalent to cut rate at constant ingot size) is proportional to reciprocation rate), again requiring equipment redesign.

Equipment and Floor Space

Since the equipment must be redesigned to achieve the above changes, we decided to use this fact to postulate a saw of larger capacity than currently available in order to affect three more areas. A saw which cuts more wafers per run with the same labor input will reduce the labor cost per wafer. It is reasonable that a single large capacity saw, cutting about three times more wafers than current equipment, will require less floor space than three conventional saws. Finally, it is also reasonable to assume that such a large saw could be sold for less than three conventional saws, reducing the capital investment per wafer. Our best (but not necessarily firm) estimate of the market price of such a saw is $77,000.

After studying the floor space required and building a prototype saw, we decided that the floor space required is 5.1 m^2(60 ft^2) per saw as before.

Labor

The large capacity saw is intended to require the same set-up time and attention as current equipment. Partly to introduce a small safety factor and partly to make the numbers easier, we assumed 20 saws per operator. As discussed below, significant savings can be affected by in-house blade pack fabrication: based on Varian's experience three assemblers per shift will be sufficient to supply our hypothetical 1986 factory.

Again, one foreman per shift and 4.7 shifts per day are required.

Material and Utilities

Expendable materials are a very important factor. Several significant reductions are possible in this area.

Blade packages are a very high cost item. Most large users of slurry saws assemble their own packages to lower this cost. It is easy to assume that this practice would be followed in a large wafer factory.

The cost of blade pack materials must also be reduced. During Phase I we showed that an immediate 10-15% reduction was possible by reducing straightness tolerances. Considering (by consulting with our supplier) the reductions possible by looser thickness tolerances (shown to be possible during Phase II), bright instead of blued stock, 12.5 mm (.5 in.) high rather than 6.25 mm (.25 in.) blades (necessary for 150 mm ingot and cheaper per pound), and high quantity pricing, we feel that the cost of blade and spacer steel can be reduced by 60%.

The cost of vehicle is also significant. Experimental work under Phase II showed that all the characteristics of PC oil are not necessary. We feel that a cheap vehicle, either mineral oil based (moderate cost, definitely recyclable) or water based (low cost, possibly recyclable) can be made which will cost 85% less per run than PC oil (including recycling in the case of mineral oil based vehicle).

Abrasive cost is extremely significant. Indeed, projected abrasive usage is a significant (about 1-5%) portion of current world production. In view of the lack of abrasive breakdown showed by the SEM studies under Phase I and the successful use of recycled abrasive under Phase II, we feel that 66% of the abrasive can be recycled after each run.

Electricity cost is somewhat significant, but we feel that the large saw will use essentially the same amount of electricity per wafer as current equipment (i.e., about 3 times as much per run).

5.3 Results and Discussion

The scenario analyzed by SAMICS results in wafering add-on costs in 1982, 1984, and 1986 of 82.8, 40.7, and 19.2 $\$/m^2$ respectively (1980 dollars). The goals for these same years for sheet generation add-on are 179.2, 53.2, and 25.5 $\$/m^2$. The amount left over for ingot growth is shown in Table 9. From analyses of ingot growth by Czochralski and HEM methods, there

TABLE 5

SCENARIO FOR SLURRY SAWING COST REDUCTION

(Cumulative Changes: Years are Those in Which Equipment is Installed in a factory)

1982 - current equipment
- 300 slices/run
- in-plant blade package fabrication
- 100 mm diameter ingot
- 3.5 mm/hr. cut rate
- 0.80 m^2/kg (including 95% slicing yield)
- low-cost slurry vehicle (40% of PC oil cost)

1984 - large capacity saw
- 900 slices/run
- 125 mm diameter ingot
- 0.89 m^2/kg (including 95% slicing yield)
- 33% abrasive reclamation

1986 - 1000 slices/run
- low-cost blade stock
- 150 mm diameter ingot
- 4.6 mm/hr. cut rate
- 1.0 m^2/kg (including 95% slicing yield)
- very low cost vehicle (15% of PC oil cost)
- 66% abrasive reclamation

TABLE 6

COST REDUCTION SCENARIO (1982)

		AMOUNT	UNIT COST	DIRECT COST	FULL ANNUAL COST
EQPT	saw	203	25,000	5,075,000	2,487,000
	miscellaneous	--	--	1,077,000	528,000
SQFT	floor space	12,390 ft^2	--	--	2,134,000
DLAB	operator	50	16,100	805,000	1,690,500
	assembler	14	14,300	200,200	420,500
MATS	steel	163,700 lb.	7.56	1,237,600	1,609,000
	vehicle	112,500 gal.	1.50	168,750	219,500
	abrasive	337,500 lb.	2.50	843,750	1,097,000
	miscellaneous	--	--	126,500	164,500
UTIL	electricity	1,260 Mw-h	50	63,000	82,000
					10,432,000

QUAN = 126,000 m^2

VALUE ADDED = 82.8 $\$/m^2$

TABLE 7

COST REDUCTION SCENARIO (1984)

		AMOUNT	UNIT COST	DIRECT COST	FULL ANNUAL COST
EQPT	saw	98	77,000	7,546,000	3,697,500
	miscellaneous	--	--	775,500	380,000
SQFT	floor space	6,000 ft^2	--	--	1,033,000
DLAB	operator	25	16,100	402,500	845,000
	assembler	10	14,300	143,000	300,000
MATS	steel	189,000 lb.	7.56	1,429,000	1,857,500
	vehicle	137,000 gal.	1.50	205,500	267,000
	abrasive	273,000 lb.	2.50	682,500	887,250
	miscellaneous	--	--	220,000	285,500
UTIL	electricity	1,872 Mw-hr	50	93,600	121,500
					9,674,250

QUAN = 238,000 m^2

VALUE ADDED = 40.7 $\$/m^2$

TABLE 8

COST REDUCTION SCENARIO (1986)

		AMOUNT	UNIT COST	DIRECT COST	FULL ANNUAL COST
EQPT	saw	122	77,000	9,394,000	4,603,000
	miscellaneous	--	--	560,000	274,500
SQFT	floor space	7,300 ft^2	--	--	1,257,000
DLAB	operator	30	16,100	483,000	1,014,500
	assembler	14	14,300	200,200	420,500
MATS	steel	266,000 lb.	3.08	814,500	1,065,000
	vehicle	186,000 gal.	0.56	104,000	135,500
	abrasive	186,000 lb.	2.50	465,000	604,500
	miscellaneous	--	--	298,200	387,500
UTIL	electricity	2,620 Mw-h	50	131,000	170,500
					9,932,500

QUAN = 517,820 m^2

VALUE ADDED = 19.2 $\$/m^2$

should be no problem in 1982, a possible problem in 1984, and probably a problem in 1986 of achieving the costs in Table 8 for ingot growth. We realize that, in this analysis, wafering consumes the majority of the allotted add-on cost, but we cannot honestly project greater cost reductions in the allowed time period.

During Phase II of the contract, we started the process of developing the technical improvements necessary to realize the process proposed above. The goals for Phase II were based on an earlier (but not significantly different) analysis than the one presented here. The remainder of this report deals with our thinking, methods, and results in this effort.

TABLE 9

LEFTOVERS FOR INGOT GROWTH ($\$/m^2$)

YEAR	WAFERING ADD-ON ($\$/m^2$)	SHEET GENERATION ADD-ON GOAL ($\$/m^2$)	CONSEQUENT INGOT GROWTH ADD-ON ($/kg)
1982	82.8	179.2	120.5 (@ .80 m^2/kg)
1984	40.7	53.2	14 (@ .89 m^2/kg)
1986	19.2	25.5	6.3 (@ 1.0 m^2/kg)

6.0 PHASE II: INTRODUCTION AND DISCUSSION OF GOALS

As a result of analyses essentially similar to that presented in Section 5, a Phase II program was started to further investigate and optimize multiblade slurry saws. Two standard Varian 686 saws, unmodified except for installation of a static, pulsed slurry application system, were purchased for use in cutting tests. A prototype of the large scale saw postulated for introduction in 1982 was designed, fabricated and tested. A small scale "lab saw" was also designed and fabricated in order to test the process under wider variation of parameters than is possible in a standard saw, and to use in investigation of the basic processes of slurry sawing. An ADE Microsense 6034 non-contact wafer measuring station was also purchased, so as to allow bow and taper measurements that correlate better with those made in industry.

The first major goal was identification and testing of a low-cost slurry. This included both cheaper vehicle and abrasive. The planned tasks were to analyze and test suspension oils, fabricate or purchase promising oils, enhance lifetime of slurry if possible, test mixtures of abrasive sizes (since abrasive is cheaper if the size range is wider), reclaim and test oil and/or abrasive , and finally identify and test a low cost system. The idea of testing water-based vehicle came later, and was included in the testing program.

In the area of blades, time was a severe limitation. Because blade stock is a long lead time item (8-12 months) and difficult to procure in quantities less than a few thousand pounds, it proved impossible to obtain all the variations we desired. We were able to test the effect of thickness tolerance and hardness variation. Major goals included further analysis of tolerance requirements, testing of the effect of lower cost blades, and specification of blade tolerances and hardness. The laboratory saw, a saw designed to use 1-10 blades between 254 and 750 mm (10 to 25 in.) long, run at high speeds, and provide precise cutting force control, was also a part of this task since we anticipated its initial use to be for blade tests.

In view of the statistically expected runout of a blade package (developed under Phase I), and in view of the increase in runout expected from using looser tolerance blade stock, we decided to try to improve the alignment of a blade package. Perhaps the most appealing method to do this is by complete blade package redesign: however, neither time nor resources were available to do this. Therefore, we included in the blade task a program to develop and test a saw-mounted "alingment device" to supersede the runouts imposed on a blade pack by the statistical nature of the blade-spacer stacking method of assembly.

In designing the large saw, much of the basic machine layout was forced by the specifications. The major impact of the specifications was that, in order to hold just over three times

as many blades, the bladehead mass must be on the order of ten times the current bladehead mass (since stiffness scales as the square of linear dimensions). When we considered that the reciprocation speed must be doubled, we decided not to try to move a mass on the order of one ton over distances on the order of eight inches at rates on the order of 200 strokes/min. This meant that the moving component functions had to be interchanged: the work must be reciprocated and the bladehead moved so that the blades feed into the work. Worries about sudden reversals of direction "throwing" wafers near the end of the cut led us to decide to include a control (flywheel) which "softened" the stroke reversals. Air cylinder feed is obviously unsuitable for moving the bladehead, so a motor and electronic feedback control were included. Also, since the system of blade tensioning used in the 686 (four bolts directly pulling on the clamp which holds one end of the blade pack) would be too complex (mostly in remembering the order of bolt tightening) and time consuming if applied to the large saw, we decided to include a new tensioning system. These requirements, plus miscellaneous designs such as slurry feed, lubrication, work mounting and addition of an alignment device developed under the blade task, defined the goals of the large saw design, fabrication, and testing task.

Several miscellaneous tasks were included, which were continued economic analysis, cell fabrication, evaluation of surface damage including optimized damage removal, and design,

fabrication, and use of a mechanical wafer strength tester to specify handling and cutting limitations of wafers.

In addition to the above formally stated goals, we made every attempt to demonstrate conversion factors (m^2/kg) as high as possible up to and including 1.0 m^2/kg (which corresponds to producing 25 wafers from each centimeter length of 100 mm diameter ingot). Also, during the course of Phase II, it seemed advantageous to install an end-of-stroke shock absorber or "bounce fixture" in one of the 686 saws in order to test our assumptions about decreased wafer breakage and increased life of 0.1 mm (.004 in.) thick blades in an otherwise known system.

The following sections will discuss in detail how we went about meeting these goals and the results of our efforts.

7.0 PHASE II: ANALYSIS

7.1 Geometric and Kinematic Fundamentals of Slurry Sawing

We hired a consultant, Prof. Guenter Werner of the M.I.T. Department of Mechanical Engineering, to investigate the theory of slurry sawing. Professor Werner is a specialist in the fields of grinding and lapping, and is one of the proponents of the theory that abrasive grains in lapping roll rather than cut like a lathe tool. The results of his analyses are presented below.

Rough Calculations Based on the Rolling Abrasive Model

Assuming the abrasive rolls rather than becoming entrapped in the blade and cutting (as seems likely, in lapping), several features of the slurry sawing process can be explained. First, earlier work showed that rounded abrasive (zirconia-alumina) cut poorly in spite of high hardness. If the abrasive rolls, the material removal mechanism must be one of impact (Hertzian) fracture, and rounded abrasive would be expected to cut poorly because of its tendency to roll smoothly and not provide the impact associated with the jerky rolling of more angular grains. Second, the low wear rate of the blades compared to the workpiece makes sense in light of the fact that the steel blades are much less sensitive to impact fracture than the very brittle workpiece.

It is interesting to approximate the number of impacts. Given a relative blade-workpiece motion $d\ell/dt$ and a grain diameter d_g, and assuming the grain contacts both the workpiece and blade and rolls without slip, the grain must rotate at a rate

$$R = (d\ell/dt)/\pi\ d_g \qquad (44)$$

In slurry sawing, $d\ell/dt$ is on the order of 600 mm/sec, and d_g is on the order of .03 mm. This leads to a revolution rate of 6×10^3 per second!

If we assume that the distance between the blade and workpiece is one grain diameter, and that the density of abrasive grains in that space is the same as in the overall slurry, then in terms of the "mix" $M(g/mm^3)$ and abrasive density $\rho(g/mm^3)$, the number of grains touching an area $A(mm^2)$ of the workpiece is

$$N_p = 6\ AM / (\pi\rho d_g^2(M/\rho + 1)) \qquad (45)$$

(Note that M is here taken to be the number of grams of abrasive added to $1\ mm^3$ of vehicle: the significant volume change leads to the correction term $M/(M/\rho+1)$ which is the actual density of particles in g/mm^3). For typical slurry sawing parameters $M = 3.6 \times 10^{-4}\ g/mm^3$ (.36 kg/l, 3 lb/gal), $\rho = 2.33 \times 10^{-3}\ g/mm^3$ (silicon carbide) and $d_g = .03$ mm, then

$$N_p/A = 300\ \text{particles}/mm^2 \qquad (46)$$

Although this number is somewhat large, the particles are not crowded: a simple calculation shows that average interparticle distances are 1 to 1.5 times the particle diameter.

Although the above numbers are interesting, the truly astonishing number arises when the number of impacts is considered. With all the above assumptions, the number N of particles passing through a unit width in unit time is

$$N = N_p(d\ell/dt)/2A \quad mm^{-1}sec^{-1} \tag{47}$$

And if a grain makes I impacts per revolution, the number of impacts I* on a unit area per unit time is

$$I^* = IN_p(d\ell/dt)/2\pi d_g A \tag{48}$$

Assuming I is 3 (somewhat conservative) and using the numbers above yields $I^* = 5 \times 10^6$ impacts per square millimeter per second!

The above analysis is admittedly crude and neglects such factors as slippage, non-ideal packing, fluid effects, etc. Even if the numbers are off by several orders of magnitude, it is believable that an extremely large number of impacts can occur, and the material removal can be explained by impact-induced microfracture.

Consideration of Cut Rate

In analyzing the cut rate from first principles, the actual blade-work contact area is extremely important. Thus, a consideration of the "fit" between blade and workpiece is essential.

a)

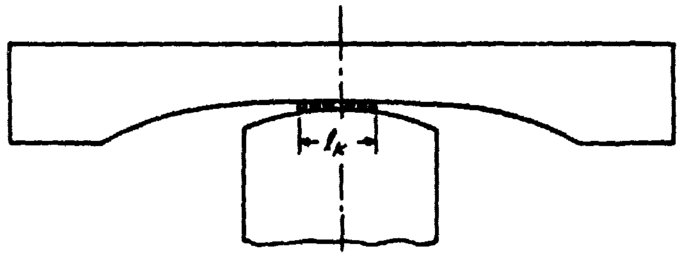

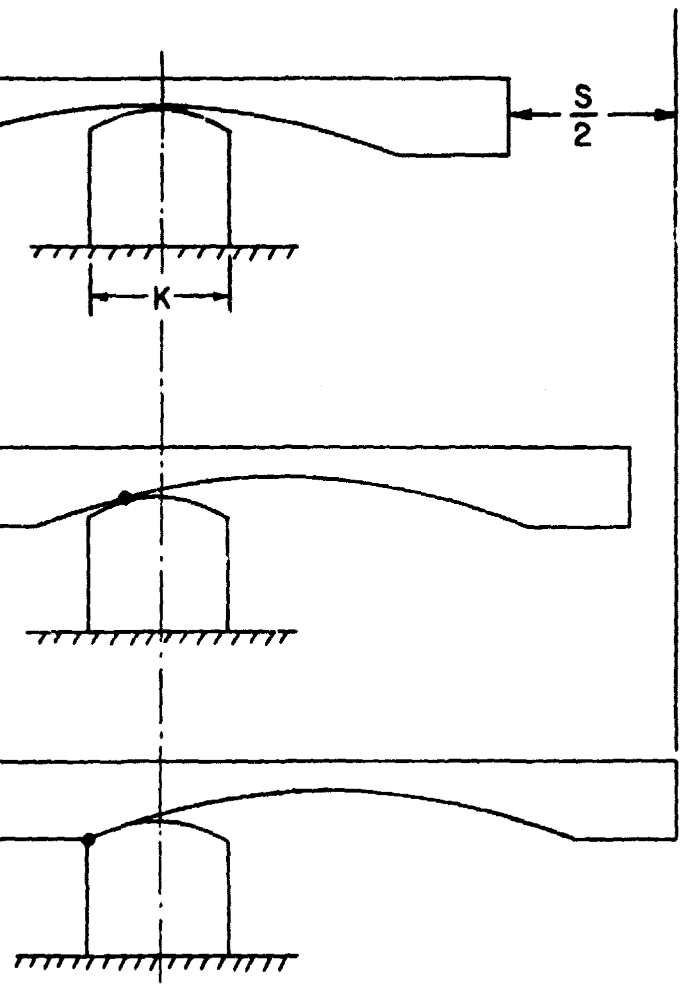

b)

Figure 36. Geometry of Worn Blade-Ingot Interactions

As the blade reciprocates, the ends of the blade are in nominal contact with the workpiece only at the ends of the stroke. Also, the sliding speed is maximum at the center of the stroke and zero at the ends. Under these conditions, the blade must wear more at the center than the ends. The shape of the worn portion of the blade must be a curve, of unknown shape but probably close to elliptical as shown in Figure 36(a).

The actual contact area will depend on both the blade and workpiece wear curves. Assuming that the blade and workpiece maintain contact (perhaps untrue at the very end of the stroke) and that the curve shapes are pseudo-static, the workpiece curve must be geometrically similar to and smaller than the blade curve.

Two such curves can only touch at a point. Because of non-idealities and the presence of grit the contact area will be small but finite, of length ℓ_k as shown in Figure 36(a). The size of ℓ_k is discussed below: since it will drop out of the analysis of cut rate, the discussion of ℓ_k is postponed.

Since, as the blade reciprocates, the contact point moves in a direction opposite to the blade motion as illustrated in Figure 36(b) the contact time t_c between the blade and a point on the workpiece is a function of actual contact length ℓ_k , sliding velocity $d\ell/dt$, nominal contact length K and stroke length S :

$$t_c = \ell_k S/((d\ell/dt)(S + K)) \qquad (49)$$

Combining Equations 49 and 48, the number of impacts per unit area of work surface in one stroke, N_i , is

$$N_i = I^*t_c \tag{50}$$

Each impact can be assumed to remove a volume which is proportional to the average load per grain L_g which in turn is proportional to feed force per blade F , kerf width w_k , contact length ℓ_k , and abrasive density N_p/A :

$$V_w = k_vL_g = k_vAF/N_p\ell_kw_k \tag{51}$$

where k_v is an unknown constant (?) with dimensions volume/force.

The cutting rate per stroke dz^*/dt is then the volume removed per impact from (51) times the number of impacts per second per unit area from (50):

$$\begin{aligned} dz^*/dt &= V_wN_i \\ &= k_vAFI^*t_c/N_p\ell_kw_k \\ dz^*/dt &= k_vFIS/2\pi d_g(S + K)w_k \end{aligned} \tag{52}$$

Finally, multiplying dz^*/dt by the number of strokes per minute R gives

$$dz/dt = k_vFISR/2\pi d_g(S + K)\, w_k \tag{53}$$

Equation 53 is the equation for cut rate as derived from a simplified rolling abrasive model. It agrees well with experiments in several ways: the predicted linear increase in cut rate with stroke rate, feed force per blade per unit blade width, and inverse of particle diameter are followed quite closely by the experiments under Phase I. The predicted less than direct increase of cut rate with stroke length is also true, although the magnitude has not been checked. It is reasonable to assume that the linear increase in cut rate with number of impacts per particle revolution is true, although we have no means of checking this. We conclude that the rolling abrasive model is the only one which has yet allowed the derivation of cut rate as a function of system parameters from first principles, and the resulting equation is reasonable, useful, but not yet proved to be true.

"Bounce"

One feature of the slurry sawing process is "bounce", a vertical motion of the ingot relative to the blade near the ends of the stroke. Bounce increases as blade wear increases. It is generally felt that the motion is beneficial since it creates a pumping action which flushes used slurry and introduces fresh slurry. However, the forces associated with this motion can break wafers and blades, so bounce must be controlled. Standard practice is to shorten the stroke when the bounce becomes excessive so as to remove the effect of the ends of the worn portion of blade.

Kinematic considerations of the rolling abrasive model led Professor Werner to an interesting analysis of bounce. Figure 37 shows a blade and workpiece in contact with geometrically similar but different size profiles as discussed above. It is apparent that when the blade moves, the ingot must move downwards with respect to the blade by a distance $B = c - d$.

Geometrically, the condition of similarity of the two profiles leads to

$$d = cK/(S + K) \tag{54}$$

Combining (54) with the relationship $B = c - d$,

$$B = c(1 - K/(S + K)) = cS/(S + K) \tag{55}$$

To make Equation 55 useful, we must consider the relationship between blade wear c and stroke length and kerf length.

Taking the cut rate of Equation 53, multiplying by K, and modifying the $S/(S + K)$ portion by raising to a power α $(o<\alpha<1)$ at Professor Werner's suggestion, we obtain the rate of cross section work removal in a plane parallel to the stroke:

$$dA_{cs}/dt = (k_V K FIR/2\pi d_g w_k)S^\alpha/(S + K)^\alpha \tag{56}$$

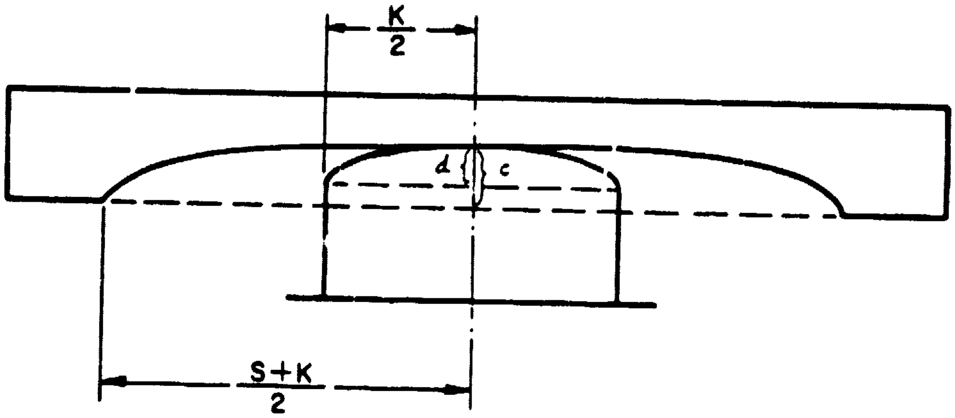

Figure 37. Model for Kinematic Analysis of Bounce

Multiplying by time, setting the total number of strokes $n = tR$, yields

$$A_{cs} = (k_v KFIn/2\pi d_g w_k)S^{\alpha}/(S + K)^{\alpha} \tag{57}$$

Now, from Figure 37, the blade wear can be approximated by

$$A_B = K_b\, c\, (S + K) \tag{58}$$

The ratio of blade to work wear has been found to be roughly constant; call this K_r. Taking the ratios of Equations 57 and 58 and setting $\gamma = Fk_v\, I/2\pi K_b K_r d_g w_k$

$$c = \gamma\, n\, S^{\alpha} K / (S + K)^{1+\alpha} \tag{59}$$

Substituting (59) into (55) gives the bounce in terms of stroke, nominal kerf length and number of strokes:

$$B = \gamma\, n\, S^{1+\alpha} K / (S + K)^{2+\alpha} \tag{60}$$

It is instructive to rewrite Equation 60 in terms of the ratio of stroke length to nominal kerf length $R_{sk} = S/K$:

$$B = \gamma\, n\, R_{sk}^{1+\alpha} / (R_{sk}+1)^{2+\alpha} \tag{61}$$

Equation 61 implies that the bounce (and blade wear!) as a function of R_{sk} has a maximum, easily calculated to be at $R_{sk} = 1 + \alpha$. Figure 38 shows the bounce as a function of R_{sk} for various values of α: the implication is that blade wear can be reduced by picking $R_{sk} < 0.5$. Of course, the non-constant nominal kerf length encountered in slicing round ingots would complicate and change the analysis. We have not yet had time to check this analysis experimentally.

Consideration of Actual Contact Length

It is possible to derive an expression for the actual contact length between the blade and workpiece. Assume that the gap g between the blade and work profiles at the end of the actual contact area is some fraction of the grain diameter

$$g = c_{\ell} d_g \qquad 0.5 < c_{\ell} < 1 \tag{62}$$

In the vicinity of the theoretical contact point, the profiles can be described by a blade profile radius r_b and a work profile radius r_w. As long as the angle between the two curves is small, geometrical considerations lead to

$$\ell_k = (2\, c_{\ell}\, d_g\, r_b r_w / (r_b - r_w))^{1/2} \tag{63}$$

The radii in (63) change with time and with position in the stroke. Since the actual curve shapes are not known, assume that

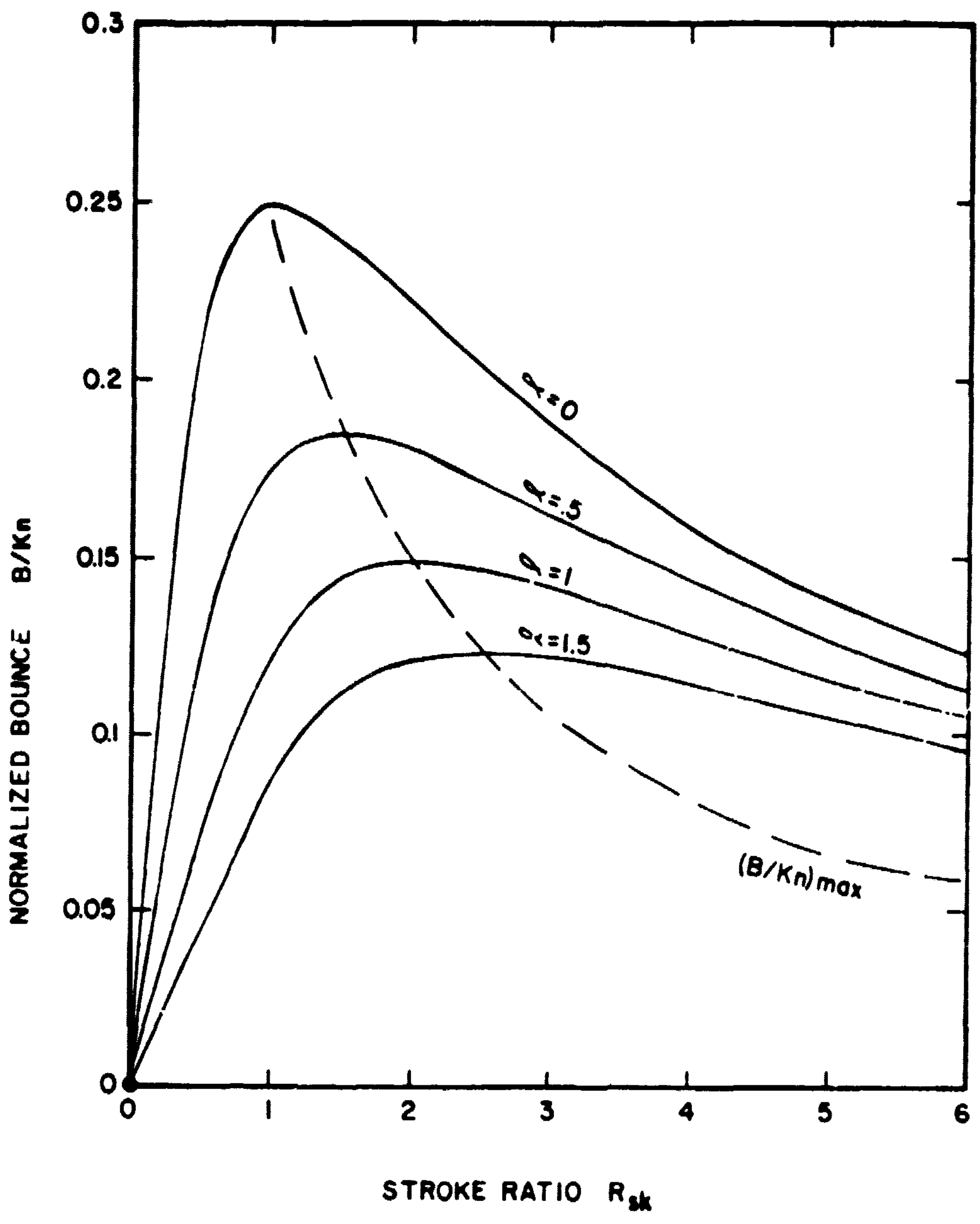

Figure 38. Normalized Bounce as a Function of Stroke Divided by Kerf Length

(Dotted line shows position of maxima.)

the curves are arcs of circles (i.e., ignore the dependence of radii on position). Then for small values of c and d (see Figure 37),

$$r_b = (S + K)^2 8c$$

$$r_w = K^2/8d \qquad (64)$$

Combining Equations 54 and 59 with Equation 64 leads to:

$$r_b = (S + K)^{3+\alpha}/(8\gamma n S^{\alpha} K)$$

$$r_w = (S + K)^{2+\alpha}/(8\gamma n S^{\alpha}) \qquad (65)$$

And combining Equations 64 and and 65 and setting
$\delta = d_g w_k \delta/F = K_v I/2\pi K_b K_r$ yields

$$\ell = d_g/2(c_\ell w_k/F\gamma n)^{1/2}(S + K)^{(3+\alpha)/2} S^{-(1+\alpha)/2} \qquad (66)$$

Thus, the contact length is directly proportional to grain size and depends in a more complex fashion on stroke and nominal kerf length. The dependence on square root of kerf width and inverse square root of cutting force is surprising in view of the physical model chosen, but may be true. We have as yet been unable to check this equation experimentally.

7.2 Further Analysis of Blade Buckling

We were puzzled by the fact that, although the analysis of blade buckling presented earlier predicted no torsional buckling under normal conditions, blades do deflect in a manner which strongly suggests torsional buckling. The following analysis was carried out in an attempt to resolve this question, and includes effects such as blade wear and kerf length.

Several assumptions were made to make the analysis feasible. First, the worn blade profile is assumed to be a straight line. Second, since the ingot will provide some support to the portion of the blade buried in the ingot, the portion of blade in the ingot is assumed to tip as a rigid body around the local centerline. Third, stress concentrations and redistribution of stresses at changes in cross section and changes of centerline position are ignored.

Restoring Torque and Stiffness

If the portion of a blade in the work is tipped by a small angle Θ, the restoring torque T_R may be written in the form

$$T_R = C\Theta \qquad (67)$$

where C is a constant function of blade properties, dimensions, and tension.

Considering the blade shown in Figure 39, the stiffnesses of each worn and unworn section of the blade must be considered.

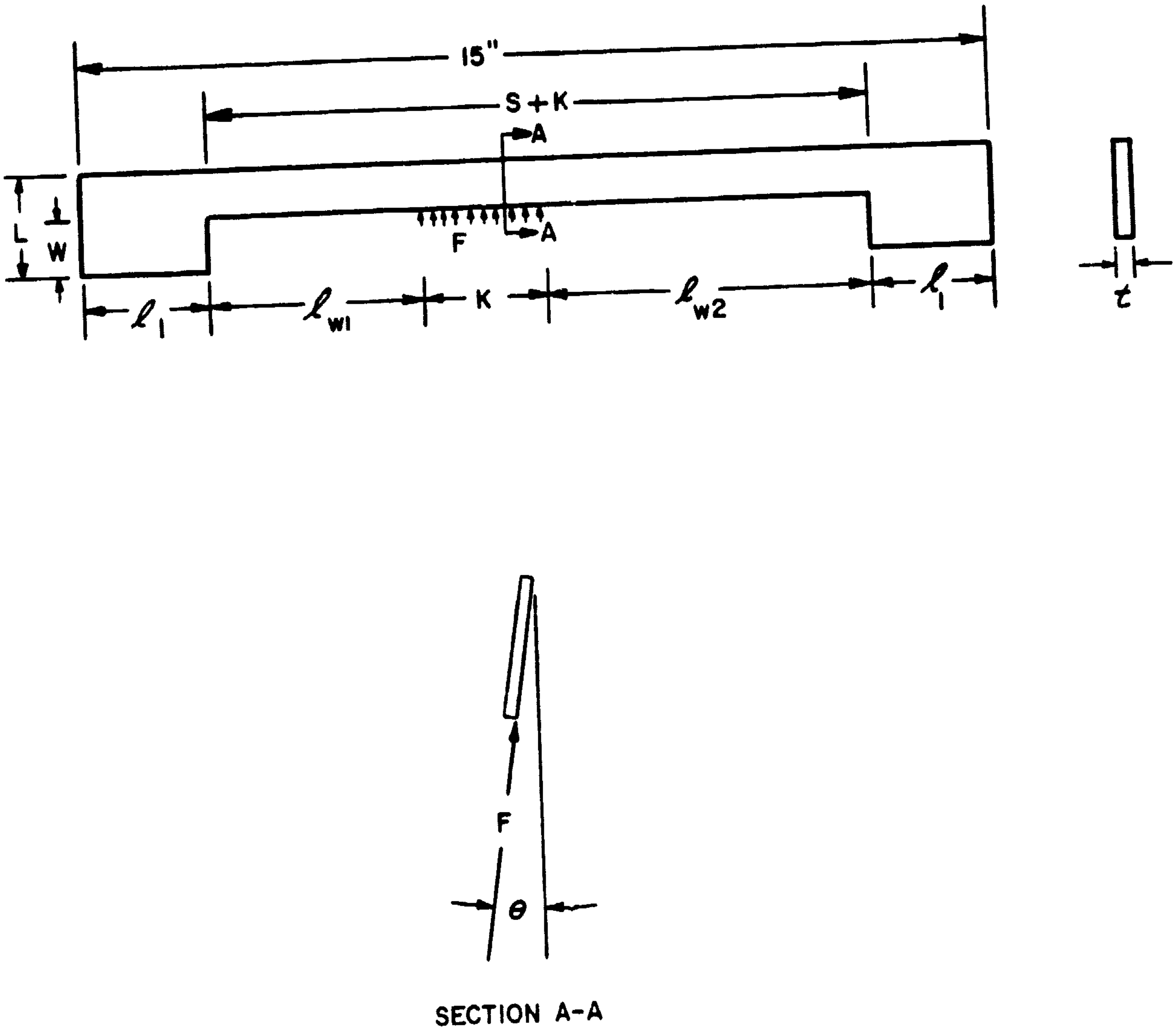

Figure 39. Blade Model for a More Complex Buckling Analysis

For any section i, the stiffness is of the form[2]

$$C_i = (\xi_i + \eta_i) / \ell_i \tag{68}$$

where ξ is a function mostly of blade material properties ("intrinsic" stiffness) and partly of pretension, and η is a function only of pretension.

Considering the combination of worn and unworn portions, the worn and unworn portions on one side of the work are in parallel, and the sections on each side are in series, so the overall stiffness is (noting that ξ and η do not depend on length, so ξ_1 and η_1 apply to both unworn portions and ξ_2 and η_2 apply to both worn portions)

$$\begin{aligned} C = {} & (\ell / (\xi_1 + \eta_1) + \ell_{w1} / (\xi_2 + \eta_2))^{-1} \\ & + (\ell / (\xi_1 + \eta_1) + \ell_{w2} / (\xi_2 + \eta_2))^{-1} \end{aligned} \tag{69}$$

Of course, we are interested mostly in the minimum stiffness during a stroke. Noting that $\ell_{w1} + \ell_{w2}$ = constant = L, using this relationship to eliminate ℓ_{w2} from (69), and setting $dC/d\ell_{w1} = 0$ gives

$$\ell_{w1} = \ell_{w2} = L/2 = \ell_w \tag{70}$$

---

(2) Biot, M.A., "Mechanics of Incremental Deformation", John Wiley and Sons, New York, N.Y. (1965).

Evaluation of Parameters

From Reference 2, ξ is the same as the stiffness of an untensioned member calculated using a modified shear modulus

$$G' = G - \sigma_T / 2 \qquad (71)$$

where σ_T is the tension.

For a rectangular cross-section of width t and height h[3]

$$\xi = J'G'$$

$$J' = ht^3 \, (1/3 + 0.21t\,((t^4/12h^4) - 1) / h) \pm 4\% \qquad (72)$$

(The expression for J' is an approximation to an infinite series of hyperbolic tengents; therefore h and t cannot be interchanged in Equation 72.)

With ξ defined by Equations 71 and 72, η may be calculated. From Reference 2,

$$\eta = J\sigma_T \qquad (73)$$

---

(3) Roark, R.J. and Young, W.C., "Formulas for Stress and Strain", 5th ed., McGraw-Hill (1975).

where J is the polar moment of inertia. From Reference 3,

$$J = th\,(t^2 + h^2)\,/\,12 \qquad (74)$$

Now the only unknown in the above equations is σ_T. One might expect σ_T to be a function of blade wear, but to a very close approximation this is not so due to the method of tensioning. Blade tension is specified in terms of elongation, usually 2.54 mm (0.1 in.) over the blade length of 381 mm (15 in.) This causes a strain $\varepsilon = 6.67 \times 10^{-3}$ and the stress may be calculated from strain times Young's modulus E.

In the calculation of stress, blade cross-section does not enter so the blade wear does not affect the pre-tension. This is actually slightly erroneous, since the jaws holding the blades deflect slightly (about 0.5 mm, .002 in.) during the tensioning. As the blades wear, their stiffness decreases and this allows the clamps to relax, slightly extending the blades and increasing the tension by about 1%. This change can certainly be ignored. Therefore,

$$\sigma_T = 6.67 \times 10^{-3}\,E \qquad (75)$$

Finally, Equations 68, 70, and 71 - 74 may be combined to define two stiffness parameters (note w is the amount worn)

$$s_1 = \ell^{-1}((G - \sigma_T / 2)(ht^3(1/3 + 0.21t((t^4/12h^4)-1)/h))$$

$$+ \sigma_T ht(h^2 + t^2)/12)$$

$$s_2 = \ell_w^{-1}((G - \sigma_T/2)(h-w)\, t^3\, (1/3 + 0.21t\, (t^4/12(h-w)^4$$

$$-1)\, /\, (h-w))) + \sigma_T(h-w)t((h-w)^2+t^2)/12)$$

And from Equations 69 and 67, the restoring torque T_R for an angular deflection Θ of the center section is

$$T_R = 2s_1s_2\Theta/(s_1 + s_2) \qquad (77)$$

Buckling

When the torque due to offset of the cutting force from the blade centerline is greater than the restoring torque, the blade will buckle torsionally. From Figure 38, the upsetting torque T_u is

$$T_u = F(h-w)\sin\Theta/2 \approx F(h-w)\,\Theta/2 \qquad (78)$$

Setting the torques from Equations 78 and 77 equal to find the point of buckling, the buckling feed force F_b is

$$F_b = 4\, s_1s_2 / ((h-w)(s_1 + s_2)) \qquad (79)$$

Calculation of Buckling Loads

The actual calculation of loads is more complex than before because of the increased complexity of the model. Also, some further manipulation is necessary since the blade wear w is not a constant.

An average blade wears on the order of 3.2 mm (.125 in.) during a cut on a 100 mm ingot. Assuming the wear rate to be constant, the wear can be written in terms of the cut depth d

$$w = 3.2\ d \times 10^{-2}\ \text{mm} \tag{80}$$

The kerf length K is, in terms of d and ingot diameter D

$$K = 2\ (d(D-d))^{1/2} \tag{81}$$

The unworn blade length is

$$\ell = (381 - S - D)/2\ \text{mm} \tag{82}$$

and the worn, unsupported length is

$$\ell_w = 191 - \ell - K/2\ \text{mm} \tag{83}$$

Typical cross-sections are

$$\begin{aligned} h &= 6.35\ \text{mm}\ (.25\ \text{in.}) \\ t &= .15\ \text{mm}\ (.006\ \text{in.}) \end{aligned} \tag{84}$$

For steel,

$$G = 7.9 \times 10^4 \text{ N/mm}^2 \ (11.5 \times 10^6 \text{ psi})$$

$$E = 2 \times 10^5 \text{ N/mm}^2 \ (29 \times 10^6 \text{ psi}) \qquad (85)$$

It is of interest to compute the amount of stiffness due to preload. Under no pretension, the stiffness per unit length is J'G' (see Equations 68, 71, 72, and 73 with $\sigma_T = 0$). For a pretension of 0 , the stiffness per unit length J'G' of a section of height 6.35 mm and thickness 0.15 mm is 556 Newton millimeters per radian per millimeter. From the same equations, the stiffness per unit length of the same section stretched to $\sigma_T = 1330$ N/mm² is 4.81×10^3 Newton millimeters per radian per millimeter. The "intrinsic" stiffness of an untensioned blade is therefore about 12% of the total stiffness of a tensioned blade, so the intrinsic stiffness is small compared to the "induced" stiffness but probably should not be ignored.

Results of Computations

The above equations were evaluated for the parameters given above for various values of cut depth d and for an ingot diameter D = 100 mm , and a stroke S = 203 mm (8 in.). Buckling loads were evaluated on an HP-97 programmable calculator for cut depths of 0 to 100 mm in steps of 1 mm.

The initial buckling load was found to be 15.5 N. This load increased to a maximum of 17.8 N at d = 15 to 17 mm . The buckling load then decreased to 6.3 N at the 100 mm depth.

This analysis agrees quite well with the independent analysis reported under Phase I in which the buckling load of a similar unworn blade (disregarding intrinsic stiffness) was found to be 14 N (viz. 15.5 N calculated from this analysis). Since typical loads for such blades are 0.82 N , and blade wander occurs almost from the beginning of the cut, the above analysis reiterates the conclusion that a torsional buckling analysis cannot explain the observed blade wander.

8.0 LARGE SAW DESIGN

8.1 General Considerations

As discussed earlier, many aspects of the large saw design were forced by the necessity to increase bladehead mass by a factor of about 10. This meant that the saw had to be a work-moving saw with the workpiece reciprocating and the bladehead fed into the work by an electric motor drive, controlled by a closed-loop force controller. In addition, an improved blade tensioning system was required.

The only major question remaining in the rough design was the layout of the ingot moving system, specifically how to arrange the components for maximum protection from slurry. Several concepts were considered (sketches will be found in the appendix), including an "upside down" arrangement in which the workpiece was suspended over the blades and the blades were fed upward. We finally decided to build a carriage consisting of a space frame, supporting the ingot, hanging from linear ball bushings. The frame was designed so that splash shields could be installed between the main part of the carriage and the bushings.

The major detailed design tasks were then design of the carriage drive system (including provisions for stroke adjustment), design of the bladehead and tensioning mechanism, and design of the cutting force controller. These tasks are discussed in detail below.

8.2 Cutting Force Controller Design

We decided to measure the cutting force by supporting the ingot on a spring-supported plate guided by precision ball bushings. This plate formed the top portion of the carriage. The distance between the plate and carriage could then be measured, and the known spring constant used to convert to force. This system had the additional advantage of allowing the ingot support to have low mass and low spring constant, reducing the shock force on the ingot associated with end-of-stroke bounce.

Model of Cutting Design

In order to design a closed loop control system, it is necessary first to derive a mathematical model of the dynamics of the cutting process.

The system defined above is illustrated schematically in Figure 40. A precision variable speed DC motor-generator is controlled by an input DC voltage E_i. The motor rotation is reduced through a gear system, and drives a lead screw which drives the bladehead and blades down into the ingot. A displacement transducer (LVDT, or linear variable differential transformer, used because the low spring constant desired required large deflections) measures the ingot displacement, and the LVDT conditioning module generates a DC output voltage proportional to ingot position.

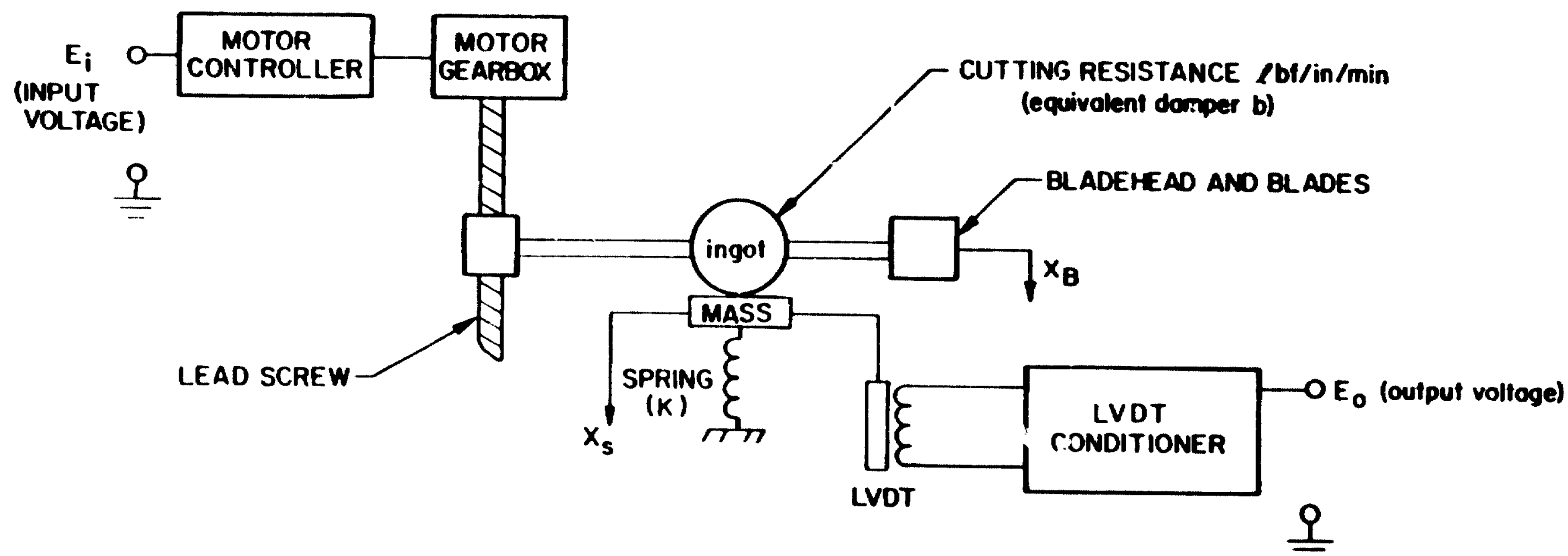

Figure 40. Model of Drive, Sawing, and Sensing Processes

This system is rather easily analyzed if the dynamic characteristics of the motor controller and LVDT conditioner are ignored. It turns out that the time constants in these two components are about 10-100 times less than those in the other components, so these dynamic characteristics can be ignored.

Assume, therefore, that the bladehead velocity is related to E_1 by a proportionality constant A, or

$$dx_B / dt = A E_1 \qquad (86)$$

In the cutting of the ingot, the cut rate will be a function of the force applied to the ingot. Assuming this function to be linear, the cutting interface is equivalent to a damper. The velocity difference across the damper is equal to the difference between blade and spring velocities, so the force on the damper is

$$F = b\,(dx_B / dt - dx_s / dt) \qquad (87)$$

The force on the damper is also equal to the spring force plus the inertial force due to the velocity of the mass, or

$$F = Md^2 x_s / dt + Kx_s \qquad (88)$$

Equating Equations 87 and 88, and using (86) to eliminate dx_B / dt

$$Md^2x_s / dt + bdx_s / dt + Kx_s = A\,b\,E_i \qquad (89)$$

The LVDT conditioner output is related to x_s by a proportionality, $E_0 = Bx_s$. Using this relation to eliminate x_s from Equation 87 and dividing through by M ,

$$d^2E_0 / dt + (b/M)dE_0 / dt + (K/M)E_0 = (A\,B\,b/M)\,E_i \qquad (90)$$

For the controller analysis, the Laplace transform of Equation 90 is desired. This is easily done. For notational convenience, define

$$A^* = ABb/M$$
$$b^* = b/M$$
$$K^* = K/M \qquad (91)$$

and the Laplace transform of (90) is

$$E_0 / E_i = A^* / (s^2 + b^*s + k^*) \qquad (92)$$

Controller Layout and Analysis

The controller block diagram, including the Laplace transform (transfer function) for each component, is shown in Figure 44. A reference voltage E_r (proportional to desired cutting load) is subtracted from the LVDT output to obtain an error signal E_e. Since we felt that relatively high frequency load variations (such as those induced by bounce at about 1-10 Hz) should not affect the cutting force control, the error signal passes through a low-pass filter. The filter output is then integrated, so small errors can lead to large speed changes in time, and fed back to the controller. (Note that the integrator in Figure 41 is not ideal; an ideal integrator has infinite DC gain $(A_i = 0)$. Since we were afraid that the gains involved might be large enough to approach the gain limit of an op amp, we decided to explicitly include the finite gain.)

The filtered error signal is also amplified and displayed on a null meter. This allows both monitoring of performance and nulling out the deadweight of the system before the run.

The system in Figure 41 is perhaps most easily analyzed by starting from an arbitrary point and multiplying transfer functions around the loop. Starting at the LVDT output E_o, E_e is given by

$$E_e = E_o - E_r \tag{93}$$

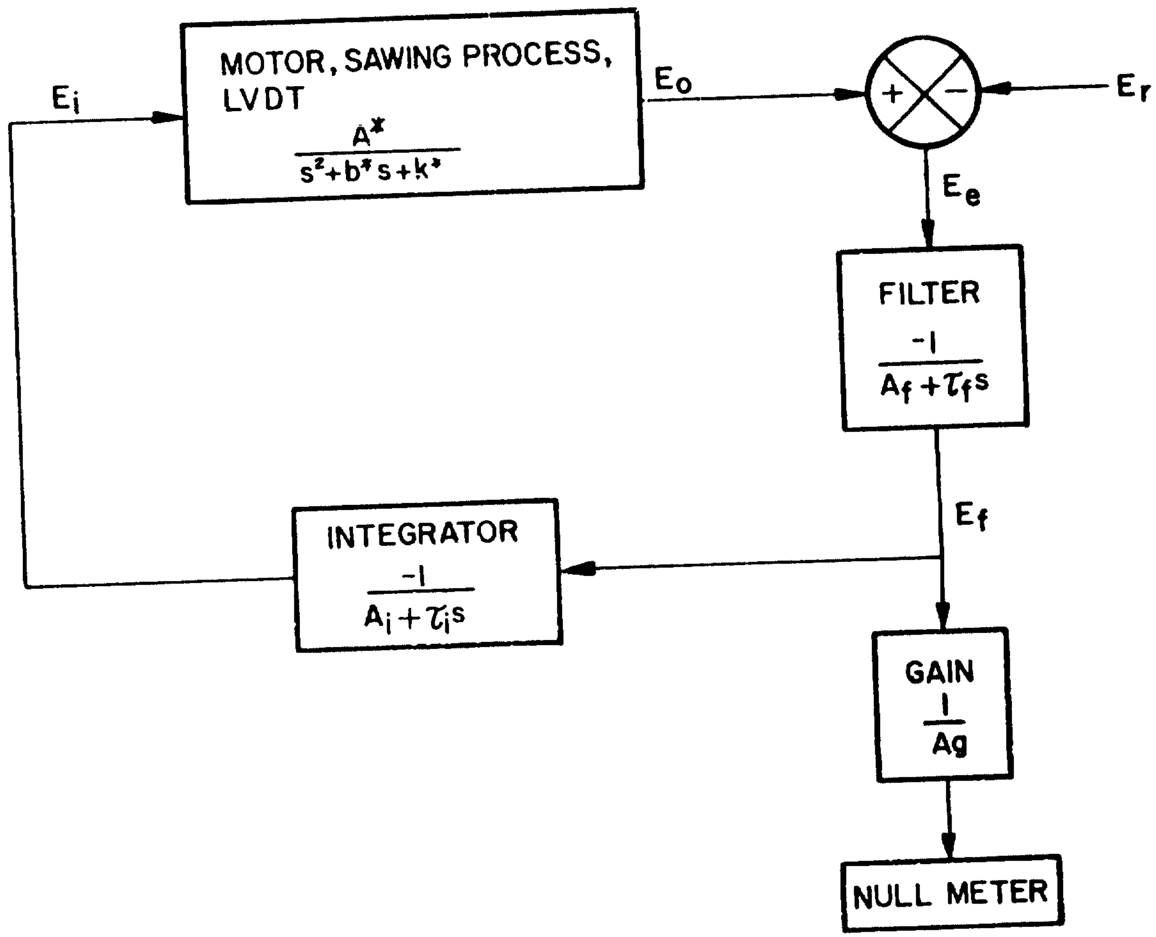

Figure 41. Cutting Force Controller Block Diagram

Multiplying E_e by the filter transfer function gives E_f

$$E_f = -E_e\,(A_f + \tau_f S)^{-1}$$

$$= (E_r - E_o)(A_f + \tau_f S)^{-1} \tag{94}$$

Proceeding in this fashion through the integration and sawing processes, we again obtain E_o :

$$E_i = (E_o - E_r)(A_f + \tau_f S)^{-1}(A_f + \tau_i S)^{-1}$$

$$E_o = (E_o - E_r)(A_f + \tau_f S)^{-1}(A_i + \tau_i S)^{-1}A^*(s^2 + b^* s + k^*)^{-1} \tag{95}$$

Defining some coefficients

$$a_1 = b^* + A_f/\tau_f + A_i/\tau_i \tag{96}$$

$$a_2 = A_f A_i/\tau_f\tau_i + k^* + A_f b^*/\tau_f + A_i b^*/\tau_i$$

$$a_3 = A_f A_i b^*/\tau_f\tau_i + A_i k^*/\tau_i + A_f k^*/\tau_f$$

$$a_4 = A_f A_i k^*/\tau_i\tau_f - A^*/\tau_i\tau_f$$

$$a_5 = -A^*/\tau_i\tau_f$$

and manipulating Equation 95 into the form E_o/E_r = some mess, by pure chance the mess becomes

$$E_o/E_r = a_5/(s^4 + a_1 s^3 + a_2 s^2 + a_3 s + a_4) \tag{97}$$

For perfect cut force control, E_o/E_r should be 1 . If the integrator were perfect, this would be true (after times long enough to let the system settle); but since the integrator is not ideal, the ratio E_o/E_r in steady state (s = 0) is

$$E_o/E_r = -A^*/(A_f A_i k^* - A^*) \tag{98}$$

and the parameters A_f and A_i must be chosen to make this ratio sufficiently close to 1 (Note, $A^* < 0$).

Also, for stability, all the roots of the denominator of Equation 97 must lie in the left half-plane (i.e., have negative real parts). The choice of parameters to meet these goals is discussed below.

<u>Choice of Controller Parameters</u>

The choice of controller parameters is made difficult by the fact that several of the sawing process parameters cannot be known exactly: only ranges can be given.

The motor controller is such that a -15 volt signal causes the motor to run at 5000 RPM. This is reduced through a 5000:1 gearhead, a 2:1 transmission, and another 5:1 gearbox. This gearbox turns a lead screw with a lead of 5.08 mm/rev (.2 in./rev). Thus, the proportionality constant between controller input voltage and bladehead velocity is

$$A = (5000\ \text{rev}/-15\ \text{V min})(1/5000)(1/2)(1/5)(5.08\ \text{mm/rev}) \quad (99)$$
$$A = -3.39 \times 10^{-2}\ \text{mm/min V} = -5.64 \times 10^{-4}\ \text{mm/sec V}$$

Several other parameters were picked arbitrarily. The LVDT sensitivity B and the table spring constant K were picked as

$$B = .394\ \text{V/mm}\ (10\ \text{V/in.})$$
$$K = 128\ \text{Newton/mm}\ (731\ \text{lbf/in.}) \quad (100)$$

The combined table and ingot mass is very close to 18.1 kg (40 lbm), so

$$M = (18.1\ \text{kg})(10^{-3}\ \text{sec}^2\ \text{N/kg mm})$$
$$M = 1.81 \times 10^{-2}\ \text{N sec}^2/\text{mm} \quad (101)$$

The cutting resistance b is more difficult to assess. However, in the range expected a cutting force of .83 N/blade (3 ozf/blade) results in a cut rate of about .05 mm/min (.002 in/min). Thus, b is approximately (for 1000 blades),

$$b = (1000 \text{ blades})(.83 \text{ N/blade})(1/.05 \text{ min/mm})(60 \text{ sec/min})$$
$$= 10^6 \text{ N sec/mm} \qquad (102)$$

For safety, we considered

$$5 \times 10^5 < b < 5 \times 10^6 \text{ N sec/mm} \qquad (103)$$

From these equations, a range of parameters in Equation (92) can be calculated using Equation 91:

$$-6.14 \times 10^3 > A^* > -6.14 \times 10^4 \ (\text{sec}^{-2}) \qquad (104)$$

$$2.76 \times 10^7 < b^* < 2.76 \times 10^8 \ (\text{sec}^{-1})$$

$$K^* = 7.07 \times 10^3 \ (\text{sec}^{-2})$$

The problem is then to choose A_f, τ_f, A_i, τ_i so as to make the roots of the denominator of (97) all have negative real parts, and minimize the difference of Equation 98 from 1.

The equation for which we need the roots:

$$s(s(s(s + a_1)+a_2)+a_3)+a_4 \tag{105}$$

With a_1-a_4 given by (96), is somewhat intractable: both the coefficients and roots vary greatly in magnitude, and slopes are steep in the vicinity of the roots.

We also did not have access to much computing power: an HP-97 programmable calculator was our computer. Extremely powerful algorithms can be implemented on this machine, but it is difficult to automatically include difficult cases such as the problem posed here.

We, therefore, arbitrarily restricted our search for parameters. The inverse of filter gain, A_f, was chosen to be 1. Since we could not optimize the controller response (e.g. by root locus methods) and it is more difficult to find accurate complex roots than real ones, we decided to choose parameters so as to make all roots negative real. Roots were first approximated with an "analytical" solution and refined by binary search.

With these restrictions, the following parameters proved suitable:

$$A_f = 1 \quad \tau_f = 0.1 \text{ sec} \tag{106}$$

$$A_i = 0.01 \quad \tau_i = 0.05 \text{ sec}$$

For the lower limit on b , the coefficients and roots of (105) are:

$$a_1 = 2.7600 \times 10^7 \qquad R_1 = -2.587 \times 10^{-2} \tag{107}$$

$$a_2 = 2.8153 \times 10^8 \qquad R_2 = -1.739 \times 10^{-1}$$

$$a_3 = 5.5272 \times 10^7 \qquad R_3 = -10.00$$

$$a_4 = 1.2421 \times 10^6 \qquad R_4 = -2.760 \times 10^7$$

and for the upper limit on b , the coefficients and roots are:

$$a_1 = 2.7600 \times 10^8 \qquad R_1 = -2.560 \times 10^{-2} \tag{108}$$

$$a_2 = 2.8152 \times 10^9 \qquad R_2 = -1.740 \times 10^{-1}$$

$$a_3 = 5.5207 \times 10^8 \qquad R_3 = -10.00$$

$$a_4 = 1.2294 \times 10^7 \qquad R_4 = -2.760 \times 10^8$$

(We do not mean to suggest that even most of the figures in Equations 107 and 108 are significant.)

The maximum controller error in percent is easily calculated from Equation 98 as

$$\text{percent error} = 100\ (1 - A^*/(A_f A_i K^* - A^*)) \tag{109}$$

and the maximum occurs with the minimum b and is 1.1 percent. This completes the controller design except for one small addition: a system to disable the loop and control E_i (motor speed) directly from the front panel was installed. This is a "cut rate control" system and was used in case of force controller failure. A schematic of the actual circuit will be found in the Appendix.

8.3 Carriage Drive

In order to minimize power requirements and smooth out the acceleration of the ingot, we decided to drive the carriage by a flywheel-connecting rod system. It was necessary to analyze the system to determine reasonable flywheel mass and connecting rod length.

Figure 42 shows a schematic representation of the system. In terms of the notation defined in Figure 42, it is most convenient to change notation slightly by defining

$$I^* = I/Mr^2 \tag{110}$$

$$L^* = L/r$$

$$c = \cos\Theta$$

$$s = \sin\Theta$$

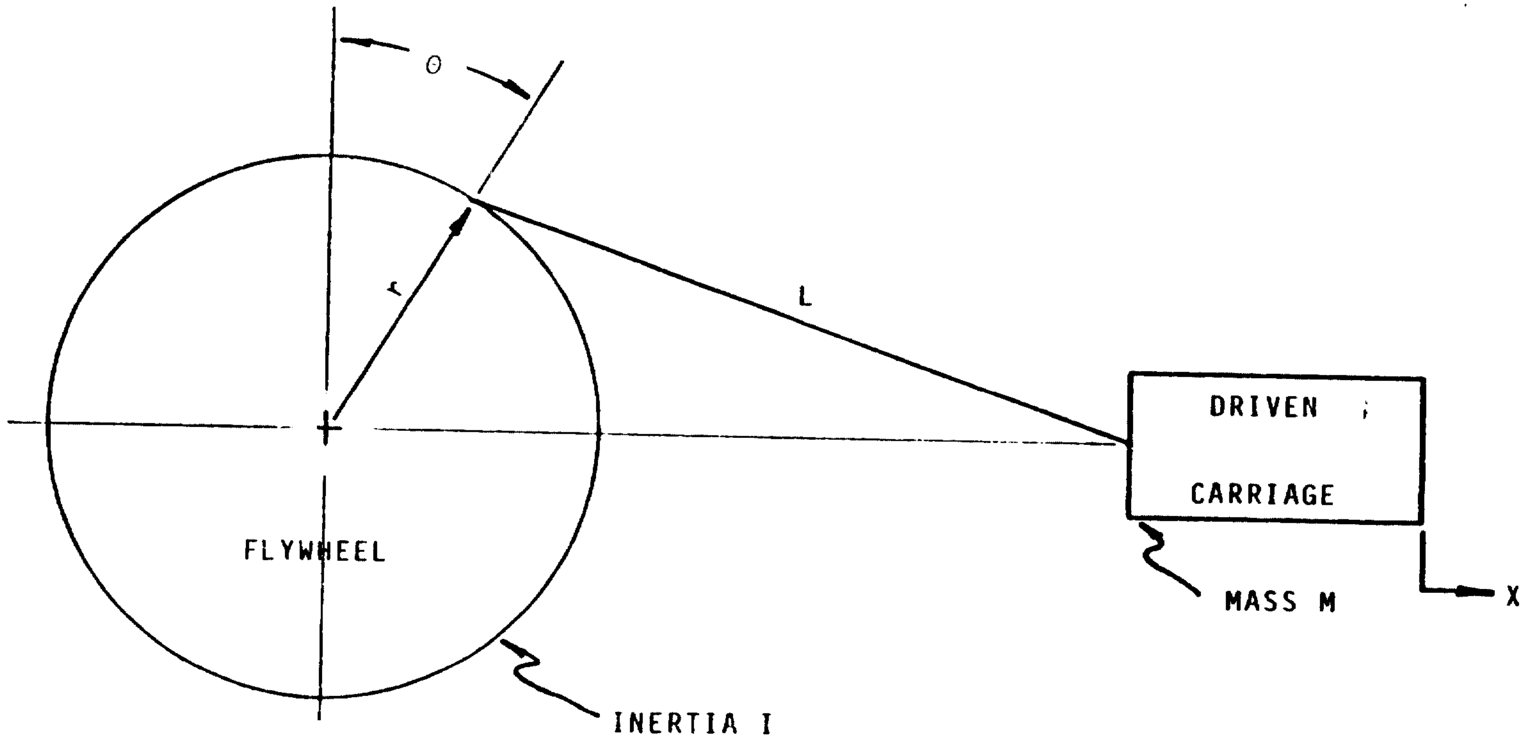

Figure 42. Schematic of Reciprocating Drive

Then, the equations of motion for this system are

$$d^2\Theta/dt^2 = (d\Theta/dt)^2(cs + c(3s^2-1)/L^* + sc(2s^2-1)/L^{*2} + c^3s^2/L^{*3} + c^3s^3/L^{*4})(I^* + c^2 + 2c^2s/L^* + c^2s^2/L^{*2})^{-1} \tag{111}$$

$$d^2x/dt^2 = rd^2\Theta/dt^2(c + sc/L^*) + r(d\Theta/dt)^2((1-2s^2)/L^* - s - c^2s^2/L^{*3})$$

The equations of motion were integrated numerically for natural motion using fourth order Runge-Kutta integration on an HP-97 calculator. The stroke length (2r) was chosen to be 254 mm (10 in.).

For the flywheel selection, the connecting rod was chosen to be infinitely long. For this condition, (111) reduces to

$$d^2\Theta/dt^2 = (d\Theta/dt)^2 cs/I^* \tag{112}$$

$$d^2x/dt^2 = -cd^2\Theta/dt^2 - sr(d\Theta/dt)^2$$

Figure 43 shows the simulation of one cycle of motion for various values of I^*. A value of $I^* = 3$ was chosen since the peak acceleration for this case is only 12% more than the sinusoidal ($I^* = \infty$) case.

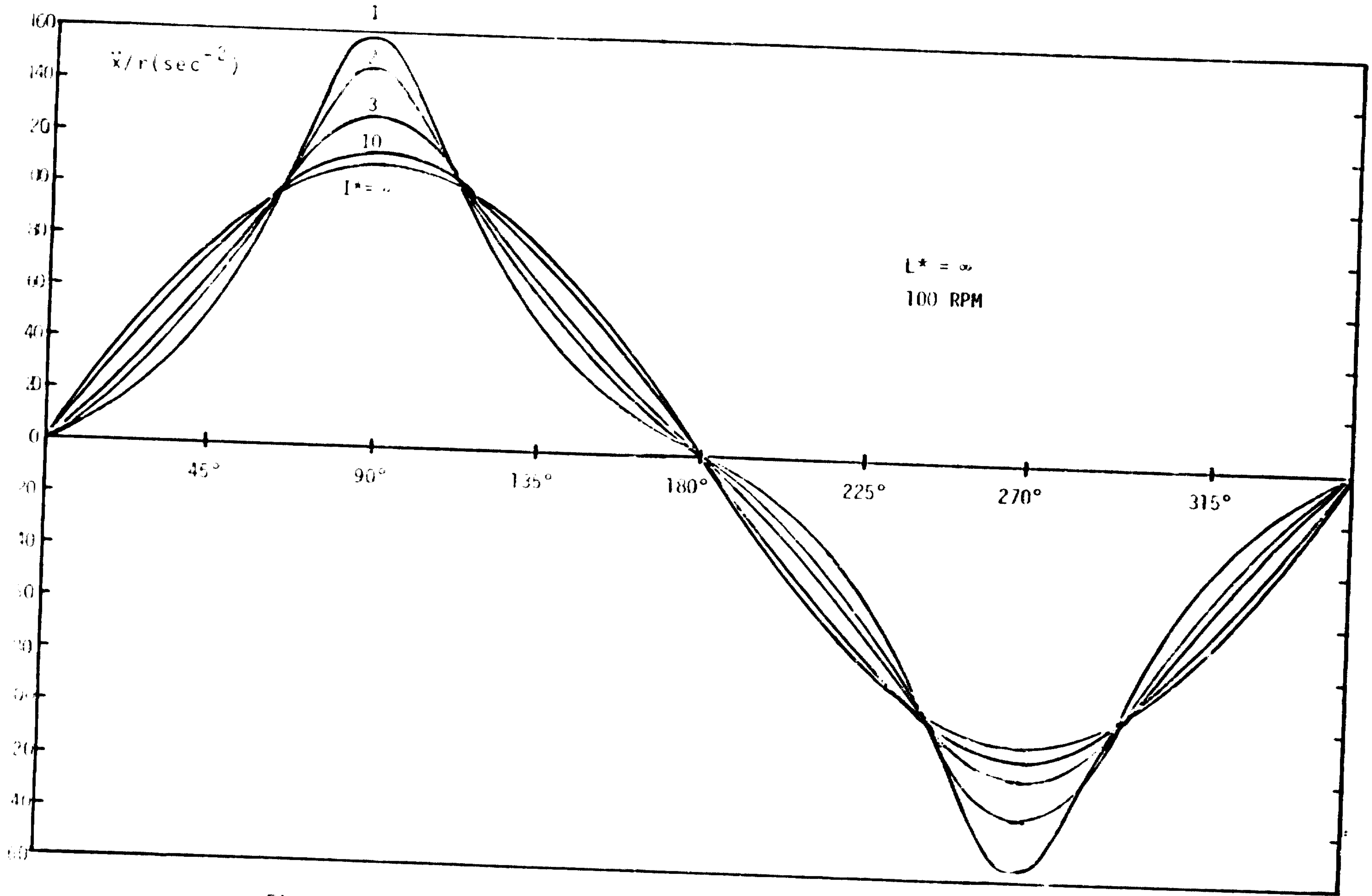

Figure 43. Natural Acceleration of a Flywheel Drive for Various Moments of Inertia

With $I^* = 3$, Equations 111 were then simulated for various values of L^*. The results are shown in Figure 44. Since a 13% increase in peak acceleration occurs for $L^* = 8$, a value of L^* greater than 8 was specified.

Figure 45 shows the system motion for $I^* = 3$ and various values of L^*.

Since the carriage mass is about 440 kg (200 lbm), the flywheel moment of inertia and connecting rod length can be calculated from (110).

The system requires some method of stroke adjustment. The system chosen is illustrated schematically in Figure 46. A disc, to which is mounted the connecting rod, is mounted off-center on the flywheel. The disc can be rotated around its own centerline, and the distance between centerlines and disc size are chosen so that the distance between the flywheel centerline and connecting rod end can be varied from 0 to 64 mm (0 to 2.5 in). A walking beam amplifies the resulting 128 mm (5 in.) maximum stroke by a factor of two, to allow continuous adjustment of carriage stroke between 0 and 254 mm.

Figure 47 is an isometric drawing of the system. A rod extends through the flywheel axle, and a pinion on the rod turns the disc through a ring gear. Another rod, surrounding the first rod, can be screwed in to clamp the disc between a plate and ring to lock the stroke by friction.

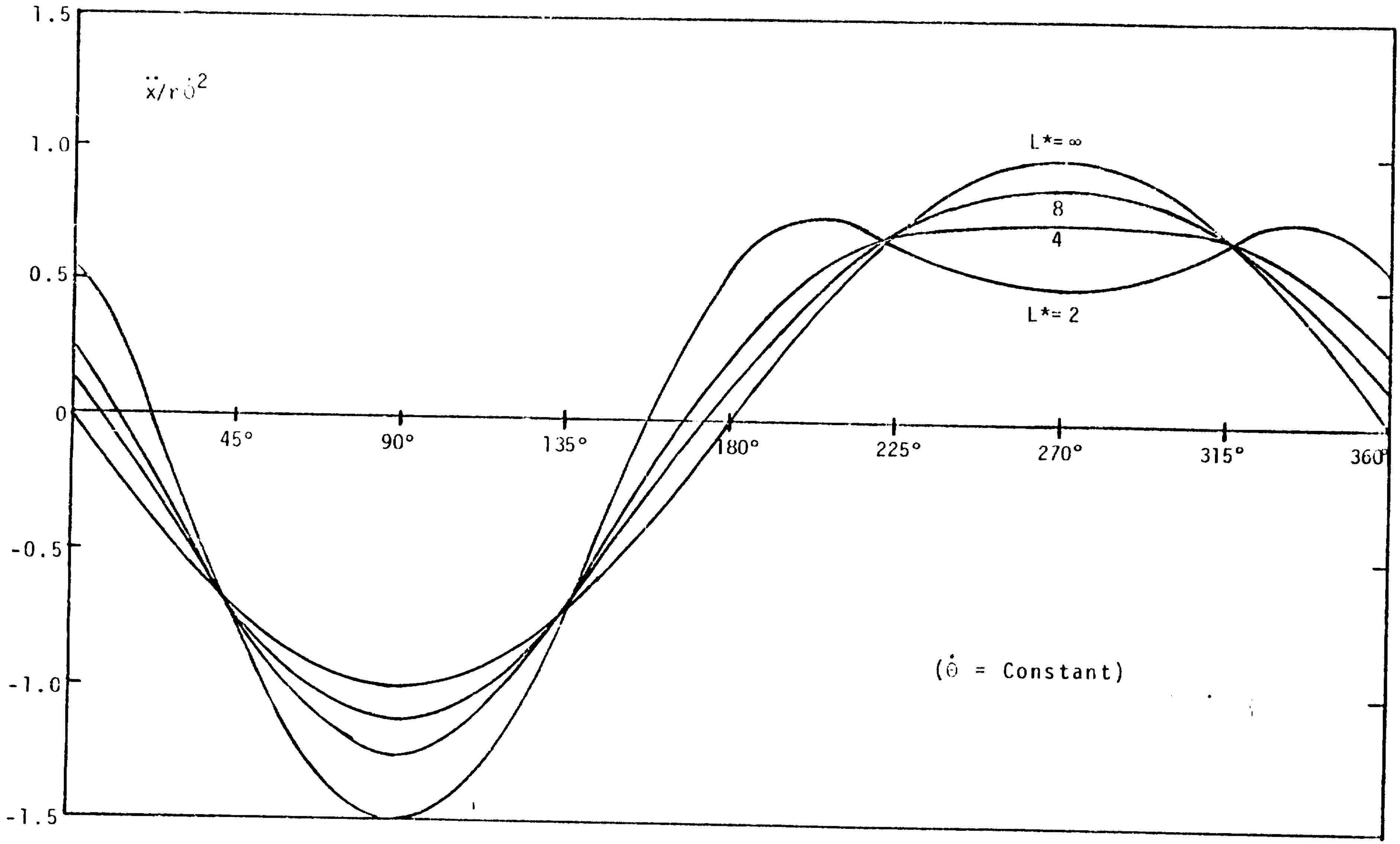

Figure 44. Acceleration of a Crank Drive for Various Crank Lengths

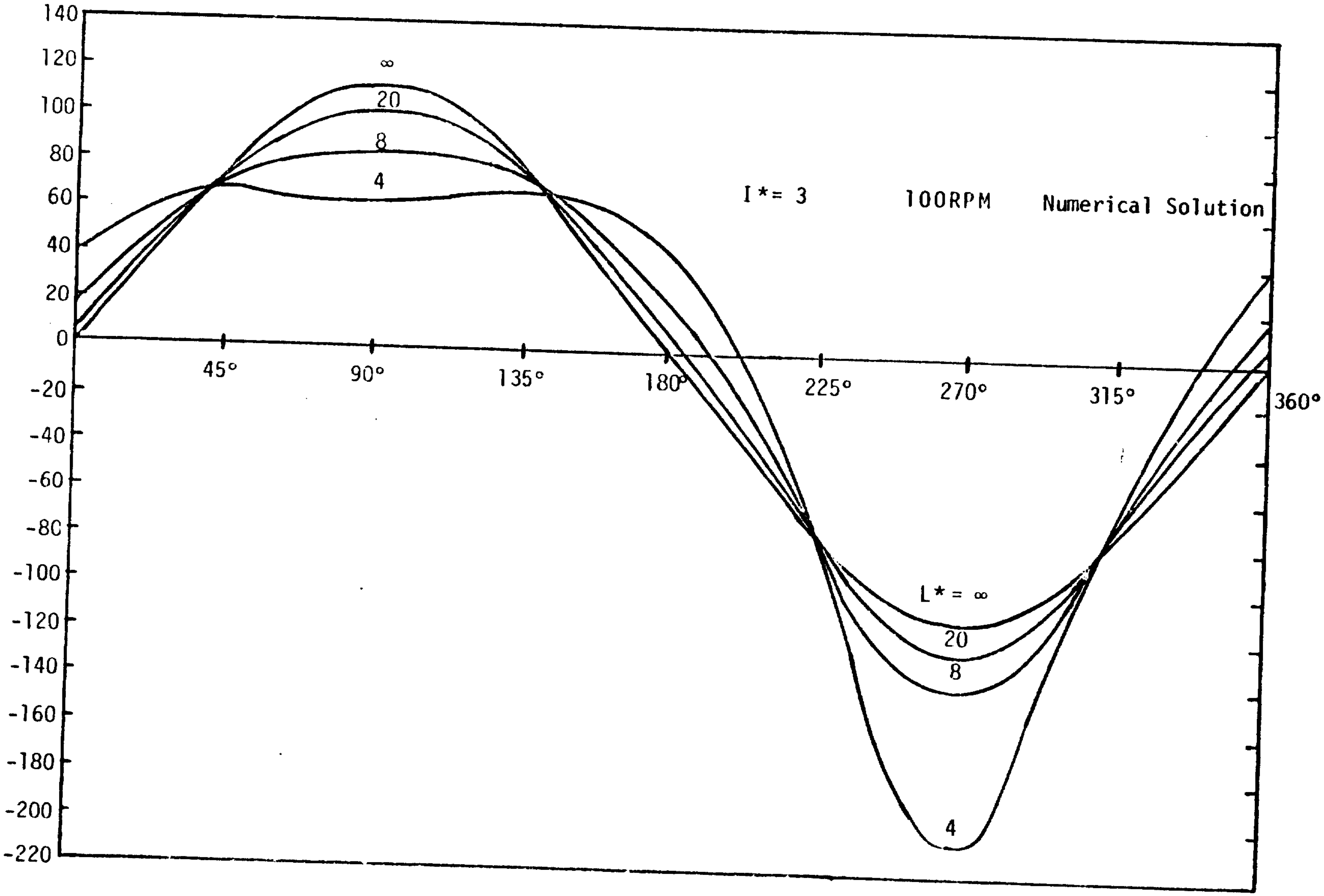

Figure 45. Natural Motion of a Flywheel Drive for Various Crank Lengths

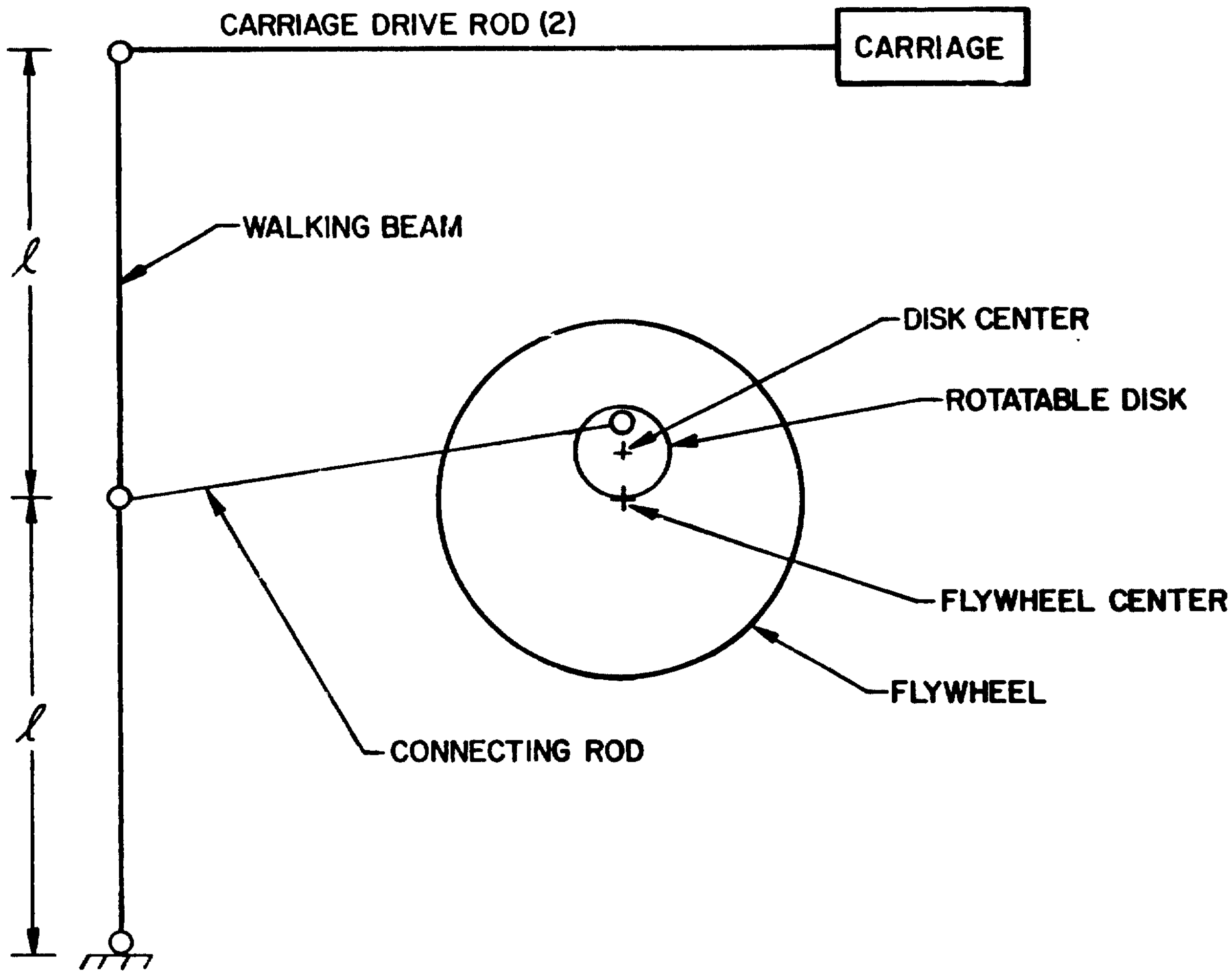

Figure 46. Schematic of Drive and Stroke Adjustment System

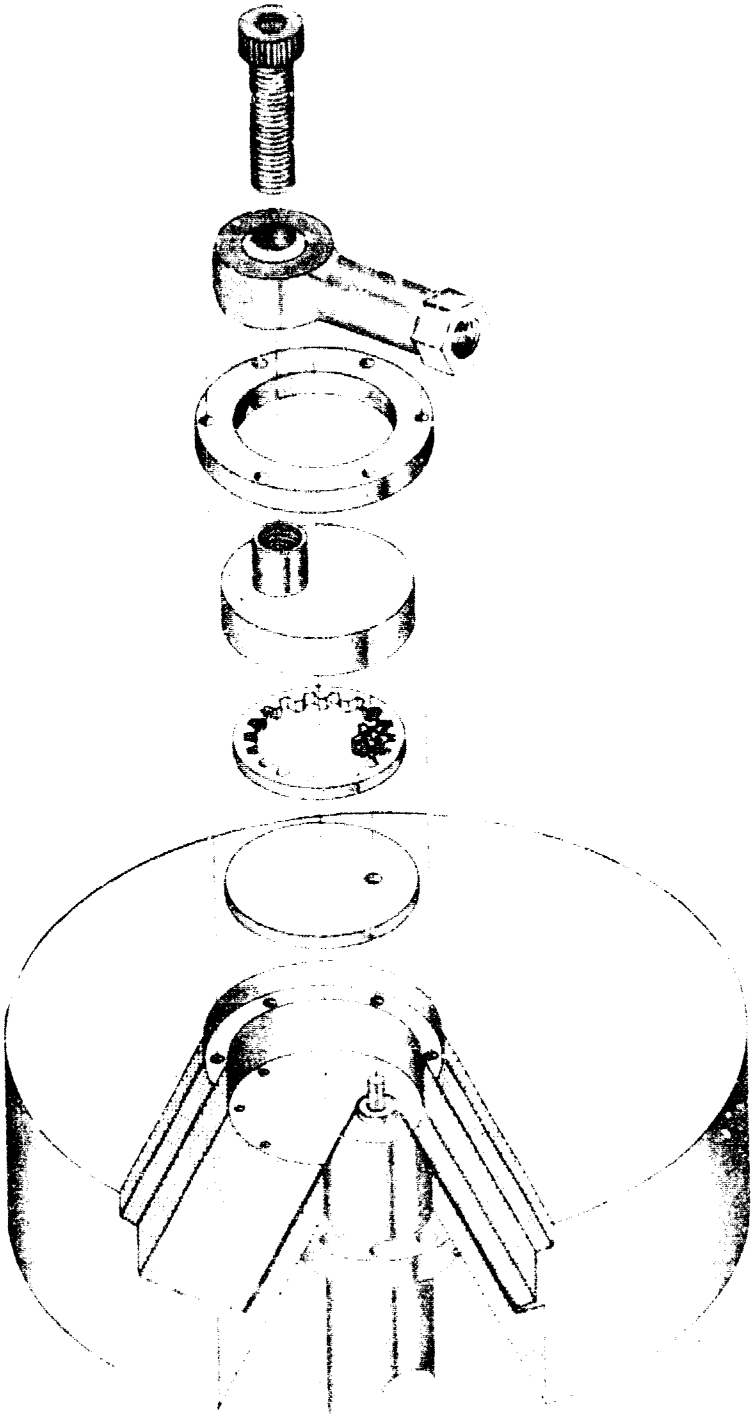

Figure 47. Flywheel and Stroke Adjustment System

This system was used in the large saw, and several disadvantages were noted. The relationship between stroke and adjustment rod rotation is sinusoidal rather than linear, making setting of a desired stroke difficult. The frictional locking mechanism failed several times, allowing the stroke to slip. Finally, the carriage drive rods must move up and down slightly as the walking beam sweeps through a stroke: this makes it difficult to seal these rods where they pass through the wall of the slurry containment area.

8.4 Bladehead and Tensioning System

The bladehead was designed as simply as possible, and the major components are shown in Figure 48.

At each end of the blade pack, a top jaw lifts off to expose a groove into which the spacers fit. The top jaw is then bolted to the lower jaw. Alignment between the jaws is maintained by a key.

One half of the tensioning mechanism is shown at the lower center of Figure 48. Four bars are assembled into a diamond shape (viewed from the top). The leftmost (partially shown) pack-holding jaw is fixed. As a bolt is tightened, two opposing corners of the diamond are drawn together, forcing the other two corners apart. This moves the moveable (rightmost) jaw away from the fixed jaw, extending the blade pack. An identical system on the other side of the blade pack insures even extension. Two

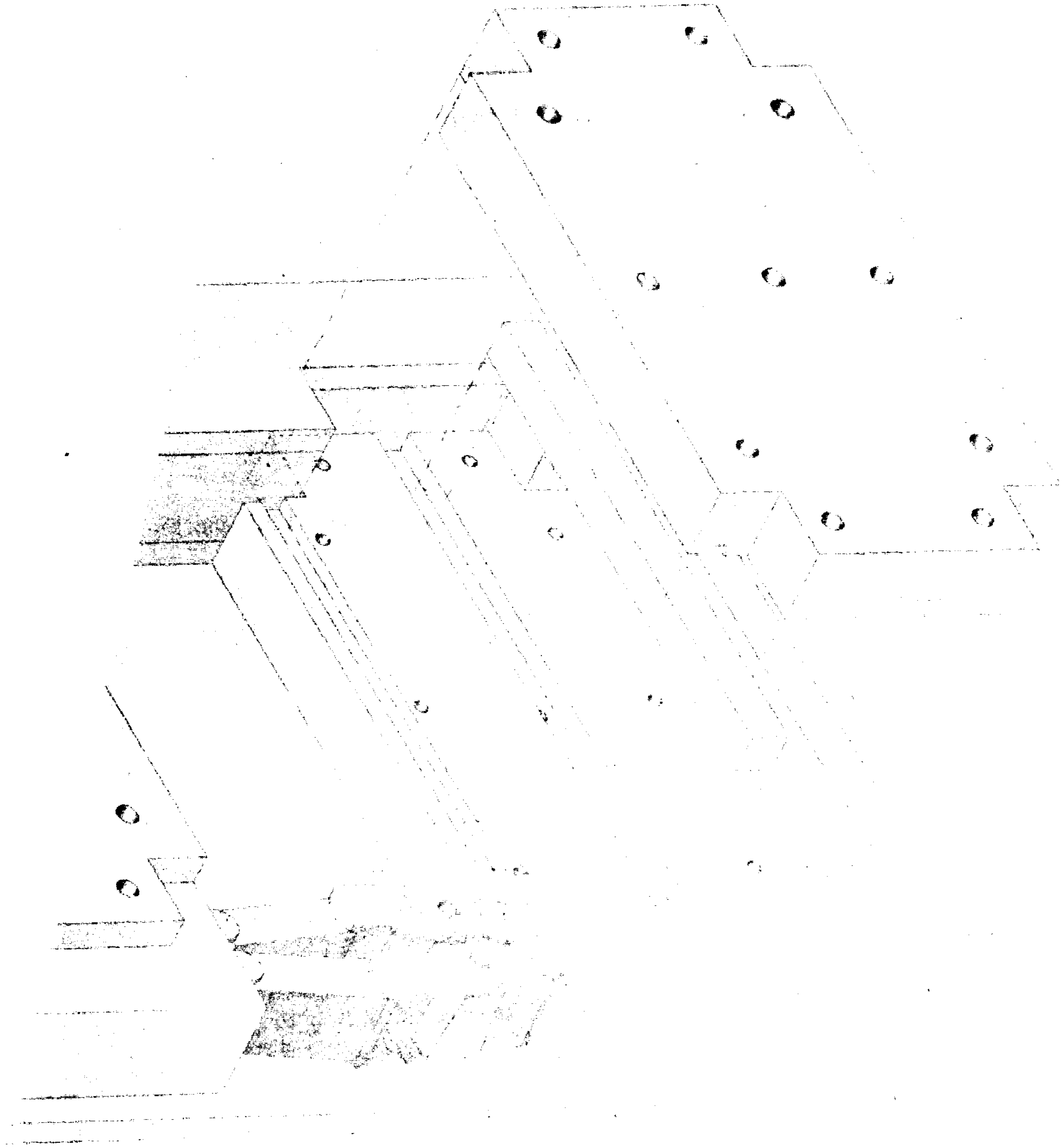

Figure 48. Bladehead and Tensioning Mechanism

of the four arms in each linkage are fitted with wedge blocks to allow adjustment of the system.

This system has the significant advantages of only two bolts, high mechanical advantage which increases during the tensioning process, and simple operation. Several serious disadvantages were noted after using the system: there is significant danger of locking the system by tightening the bolt too much (over-straightening the diamond shape), no bolts are available easily which last more than about 4 tensionings (hydraulic or pneumatic tensioning would be preferable, with bolts for holding), and the system is essentially unusable with pin-construction blade packs (in which the blades must be slipped to insure equal lengths) because it is difficult to set the wedge blocks so as to simultaneously allow sufficient mechanical advantage and prevent locking the system.

8.5 Miscellaneous Design

Figures 49-54 show the progressive assembly of the major saw systems. In Figure 49 the drive motor and chain to drive the flywheel are shown inside the tube-and-plate frame. Figure 50 shows the addition of the flywheel and stroke adjustment system. Figures 51-54 show sequentially the addition of the walking beam and carriage drive rods, carriage and carriage support system (splash guards not shown), bladehead with lead screws and guide

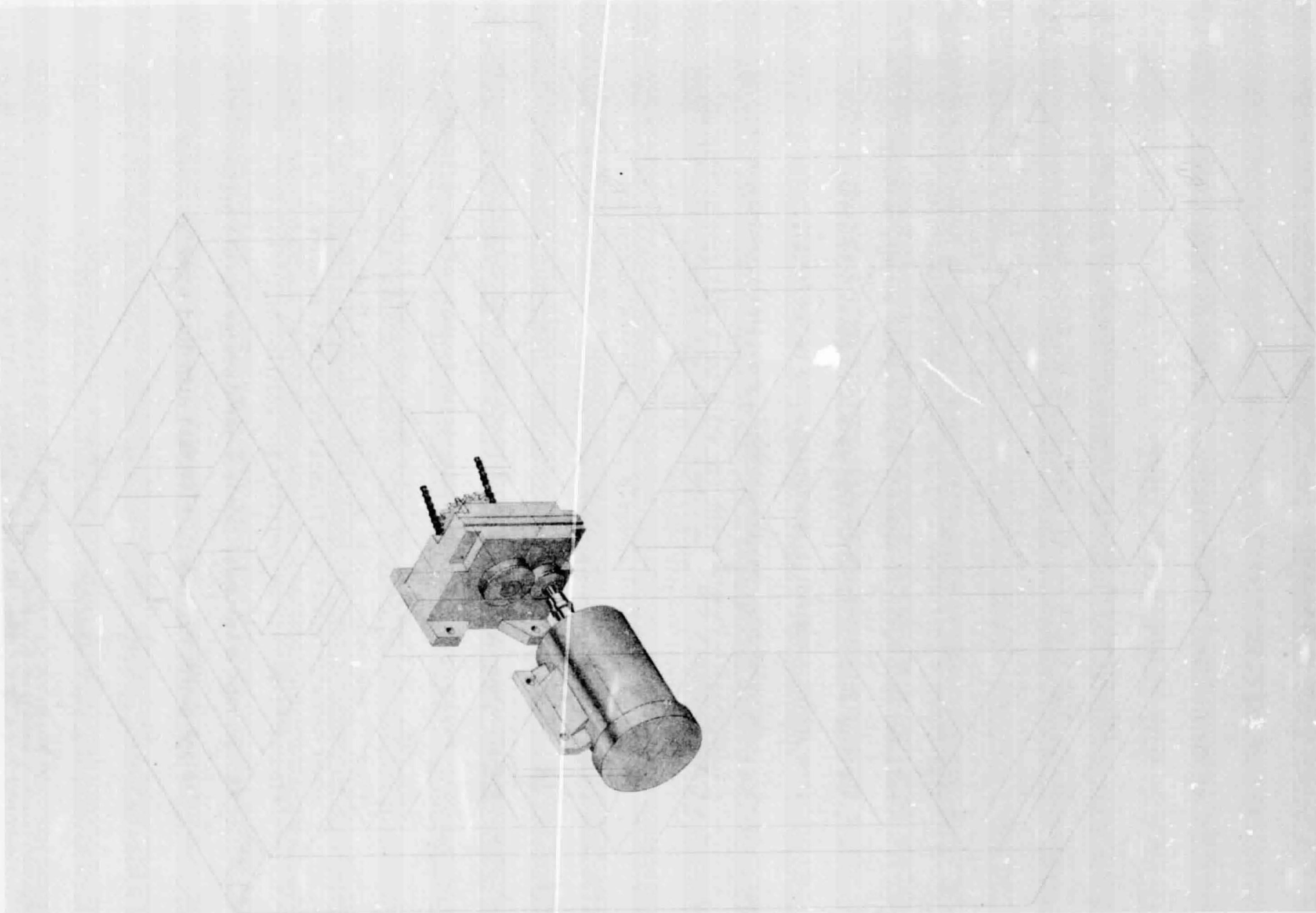

Figure 49. Large Saw Assembly: Frame, Carriage Drive, Motor and Gearbox

REPRODUCIBILITY OF THE ORIGINAL PAGE IS POOR

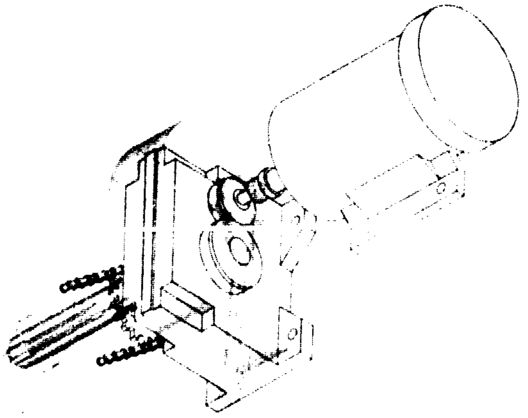

Figure 50. Large Saw Assembly: Addition of Flywheel and Stroke Adjustment

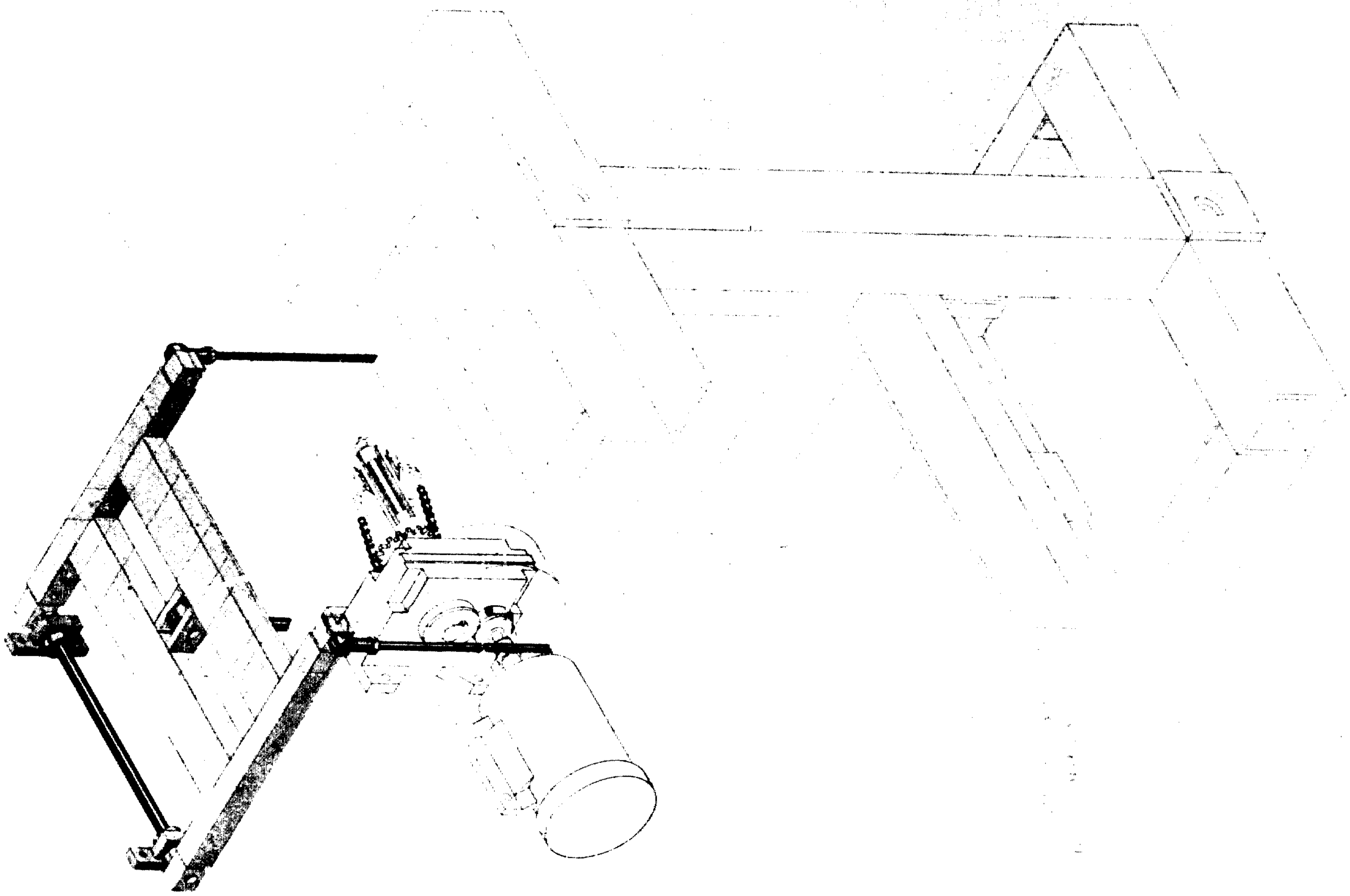

Figure 51. Large Saw Assembly: Addition of Walking Beam and Carriage Drive Rods

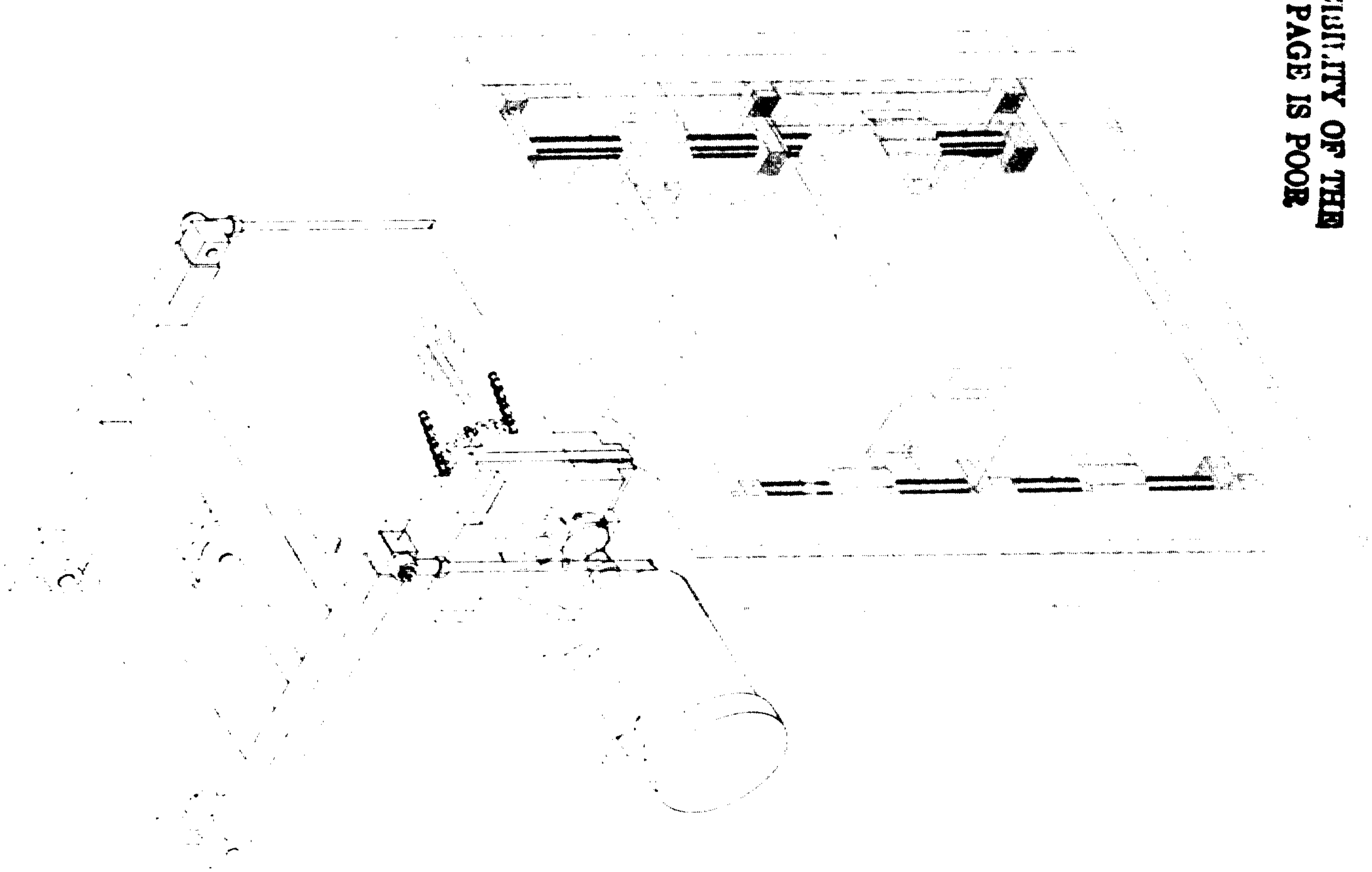

Figure 52. Large Saw Assembly: Addition of Carriage and Bushings

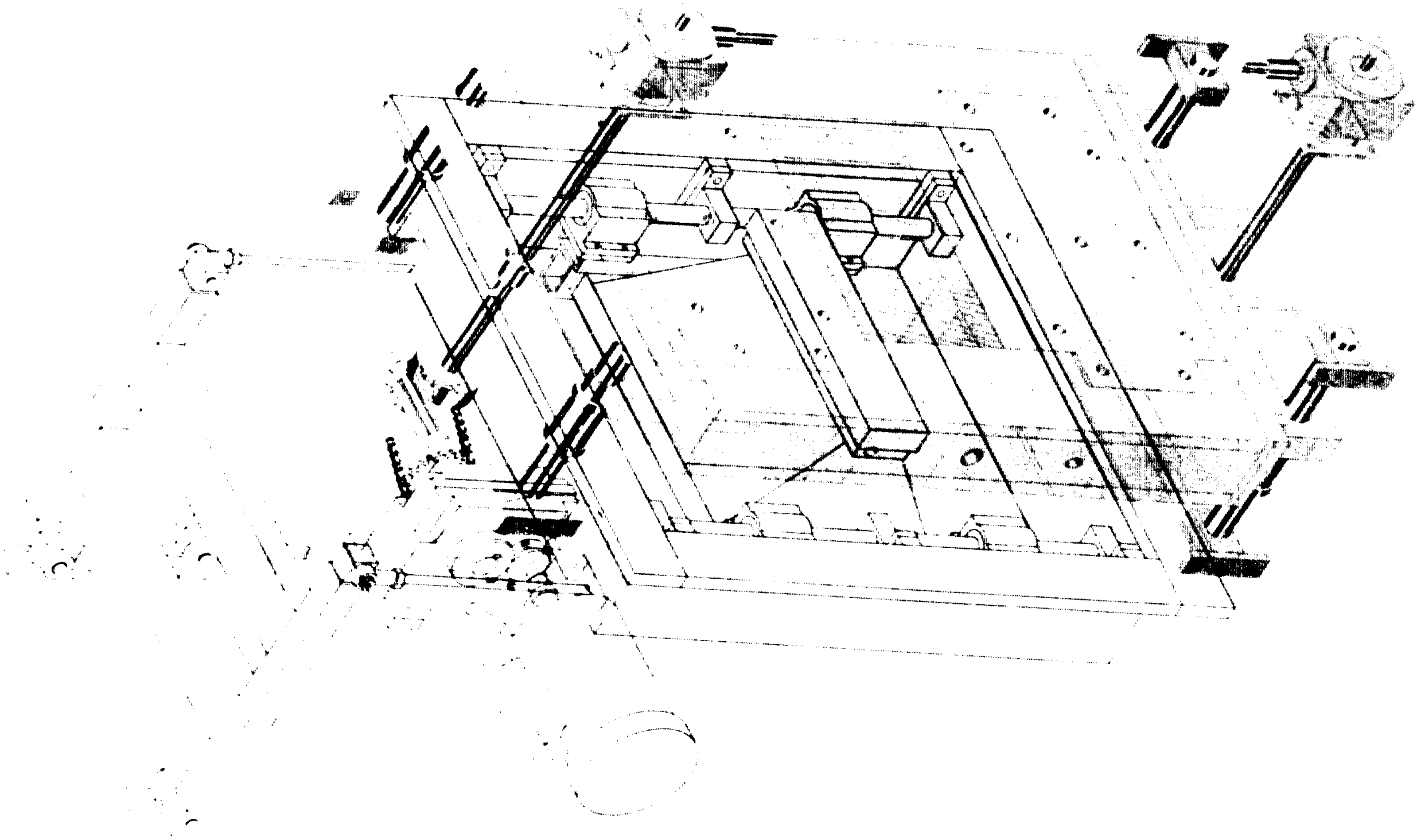

Figure 53. Large Saw Assembly: Addition of Bladehead, Bushings, and Lead Screws

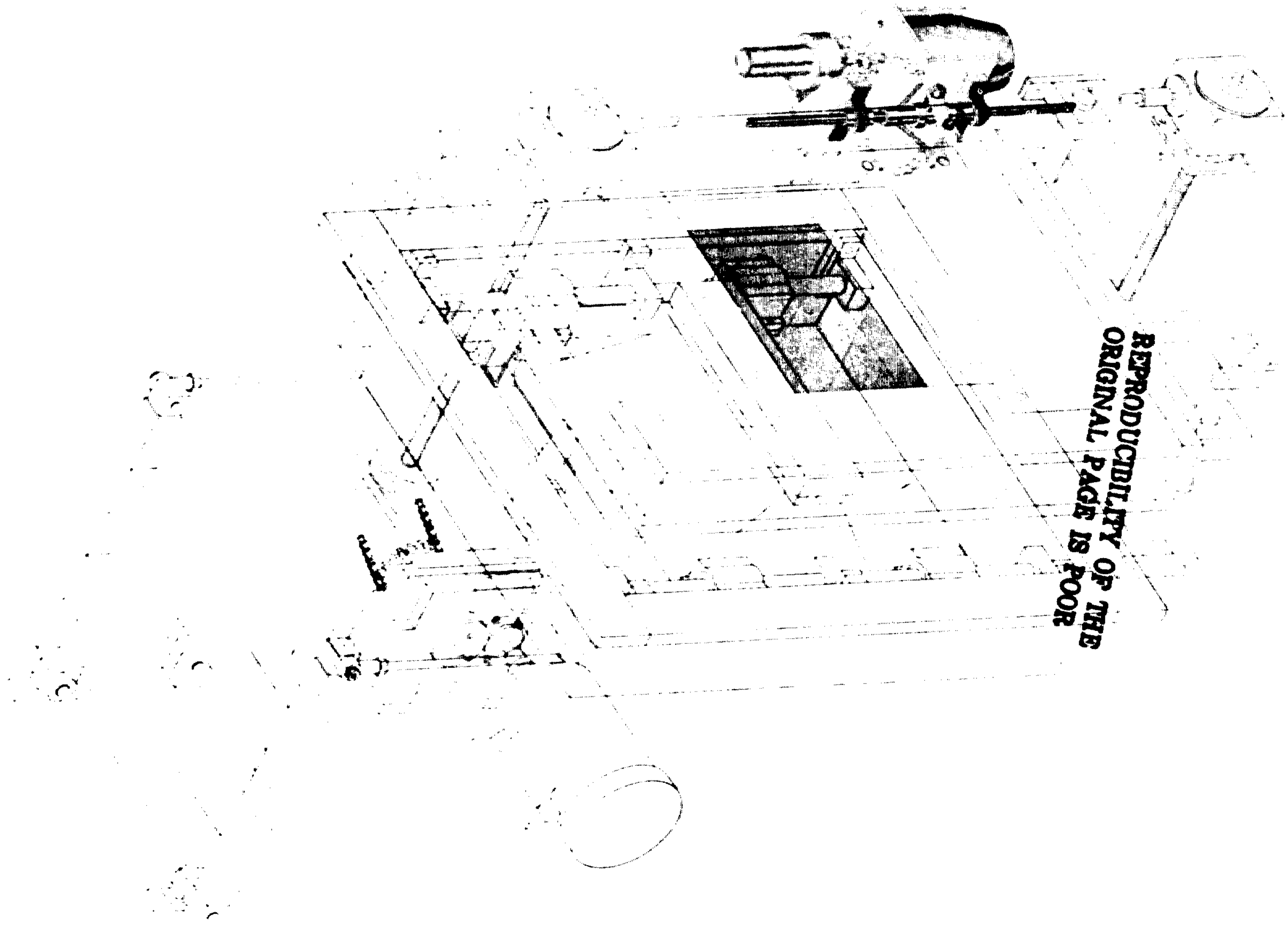

Figure 54. Large Saw Assembly: Addition of Bladehead Drive Motors and Shifter

bushings, and bladehead drive motors (small for cutting, large for bladehead positioning). Figure 55 is a photograph of the completed saw.

During the period of saw testing, we found that the LPM-205 module (Schaevitz Engineering) which was used to drive the Schaevitz MHR-500 LVDT was prone to breakdowns and had insufficient zeroing range. We replaced this module with a system of our own design. This consisted of a Burr-Brown 4423 oscillator generating a 10 kHz sine wave, feeding the LVDT through two complementary current-boosting transistors. The signal from the LVDT is in the form of two sine wave outputs at the drive frequency; the difference between these outputs is linearly proportional to core position. Our module passed each signal through a precision full wave rectifier, subtracted the result in a difference amplifier, shifted the level in another amplifier (providing zeroing over the full linear range), adjusted the level in a gain amplifier, and stripped off the 20 kHz (not 10 kHz, because of the full wave rectification) carrier in a four pole low-pass active filter (adjusted so response at 500 Hz was 97% of the DC response). This system worked very well; a schematic will be found in the Appendix.

As hinted earlier, we had serious problems with bearing lifetime due to slurry splashing. The carriage bearings had to be protected by bellows in addition to the splash shields. The rod-end bearings in the drive system and flywheel bearings were quickly

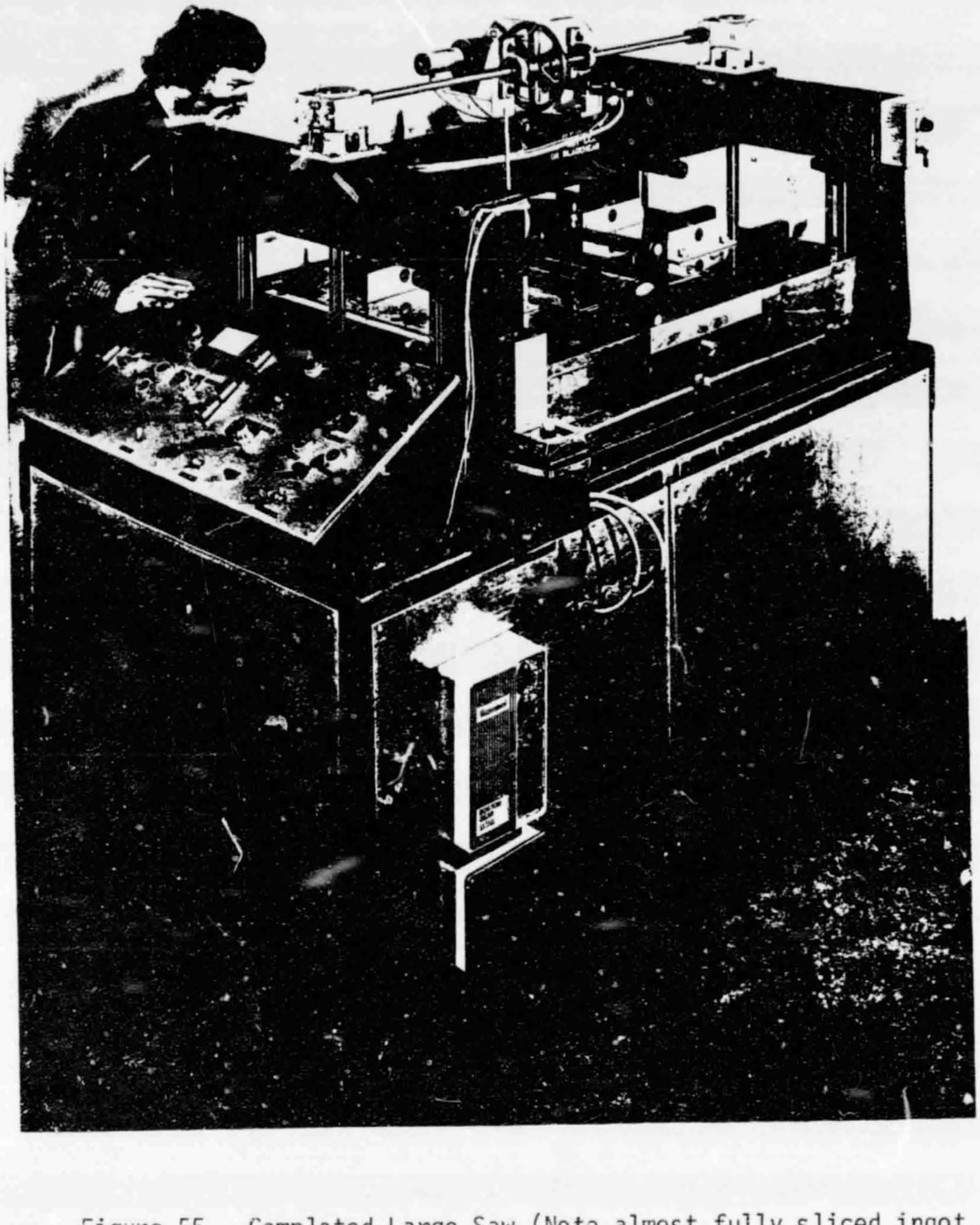

Figure 55. Completed Large Saw (Note almost fully sliced ingot.)

destroyed by slurry coming out on the carriage drive arms. The rod end bearings connecting the carriage drive arms to the carriage had very short lifetimes. These problems, all associated with the carriage drive arms, can only be solved by complete drive system redesign so the carriage drive arms can be sealed where they pass into the slurry area (or eliminated). As noted above, the stroke adjustment system could be significantly improved at the same time.

Slurry distribution was also a problem. Our standard static system, in which a sheet of slurry is provided by a slotted tube, proved insufficient to evenly distribute slurry across the blade pack. Most runs were made with a perforated tube dropping closely spaced streams, but this system clogged repeatedly. A spray system using tungsten carbide spray heads was designed and ordered, but at the time of writing (September, 1979) not all components had been received.

Measurement and display of bounce also proved difficult. A circuit was designed and installed which amplified the LVDT signal in a high pass filter, leaving only the AC component (peak-to-peak voltage proportional to bounce). Positive and negative peak-detect-and-hold circuits followed by a differential amplifier then sensed bounce. In spite of careful shielding and isolation, the long time constants (30 sec) required made this system useless because of noise sensitivity. In later runs we displayed the LVDT signal on an oscilloscope as an indication of bounce.

9.0 LAB SAW DESIGN

The lab saw was originally conceived as a small scale 686 saw. When we began to design the lab saw, it became evident that extensive redesign was necessary. In order to provide accurate cutting force with very small numbers (1-10) of blades, an electronic closed-loop control system was needed to replace the air cylinder feed. Because of the greatly variable blade length, a new waybed and slurry splash pan were needed. The bladehead drive system had to be moveable in order to allow the blade center to be placed at the stroke center and ingot center. Again because of greatly variable blade length, the bladehead and spacer clamping system had to be redesigned.

The cutting force controller was chosen to be the same as the large saw controller: design details are presented in an earlier section. For the lab saw, the parameters that are different from the large saw are:

$$M = 1.36 \times 10^{-2} \text{ N sec}^2/\text{mm (30 lbm)} \tag{113}$$

$$K = 16.3 \text{ N/mm (93 lbf/in.)}$$

With these parameter changes, Equations 99-109 yield choices of suitable gains and time constants:

$$A_f = 1 \qquad \tau_f = 1 \text{ sec} \tag{114}$$

$$A_i = 2 \times 10^{-4} \qquad \tau_i = 5 \text{ sec}$$

The lab saw was designed and fabricated with a controller as defined above. The extensive redesign necessary, coupled with extremely late delivery on several subcontracted items (such as the waybed) made the completion of the lab saw several months later than expected.

Two problems appeared when we used the lab saw. First, the spacer clamping mechanism was somewhat tricky and required great care to use properly. Second (and more important), since the force sensor for the cut force was mounted on the upward feeding mechanism (guided by a linear ball bushing), we had to install a bellows going from the feed top plate to the slurry pan to protect the mechanism from slurry. The nonlinear (due to fold separation) spring constant of the bellows turned out to be several times larger than typical feed forces, and was sensed by the sensor. Thus, the vertical feed traveled to a point where the bellows force equalled the feed force and stopped. Bellows with sufficiently low spring constants were not available, and preventing the force sensor from sensing bellows force would have required extensive redesign.

Since the lab saw had been completed too late to use in the blade tests with the blade materials we were able to obtain, and it required significantly more work to become generally useful, we decided to suspend lab saw work because of limited time and personnel.

10.0 EXPERIMENTS: PHASE II

10.1 General Remarks on Cutting Tests

As a result of the successes obtained under Phase I, we redefined our "baseline" or standard silicon cutting technique. This standard technique may be defined as follows. Blade pack parameters: .15 mm (.006 in.) thick by 6.35 (.25 in.) high blades, 381 mm (15 in.) clamped length, extended 2.54 mm (.1 in.), separated by .35 mm (.014 in.) thick spacers; this configuration cuts 20 wafers/cm of ingot. Slurry parameters: 7.56 ℓ (2 gal.) PC oil (37 ℓ or 10 gal. for the large saw) mixed with Micro Abrasives #600 SiC with .36 kg added to each liter of oil (3 lb. added per gallon of oil), applied by a static tube pulsing for 5 sec out of each 30 sec. Feed force: 0.83 N (3 ozf) feed force per blade. General: 100 strokes/min reciprocation rate, 203 mm (8 in.) initial stroke reduced by 6.35 mm (.25 in.) whenever bounce exceeded .64 mm (.025 in.), ingot diameter 100 mm. Unless otherwise noted, these conditions were used for all tests.

Each test was given a number of the form 2-XX-YY. 2 stands for Phase II. XX stands for the test series name: 01 for blade tests, 02 for lab saw tests, 03 for slurry (vehicle and abrasive) tests, 04 for solar cell demonstration and fabrication, 05 for miscellaneous techniques, 06 for tests of an alignment device to improve blade alignment, and 07 for large saw tests. YY then stands for the test number within that series.

10.2 Low Cost Blade Tests

Slightly Soft Blades: Tests #2-1-01, -02, -03, -04

We attempted to improve the cutting action of the overall system by using softer (by about 10%) blades. These blades cut faster in some other systems (for example, quartz), and we hoped the same might be true in cutting of silicon. The cost of softer blades is the same as for standard blades.

Tests #2-1-01, #2-1-02, and #2-1-03 were run using the softer blades, 1x, 1.6x, and 0.5x the standard abrasive concentration, and otherwise standard conditions. Serrations had been observed in the upper bladehead clamp jaws, caused by indentation by the relatively thin spacers we use. We have no evidence, but these serrations might cause spacers to "hand up" and prevent proper blade positioning. Therefore, we replaced the jaws.

Yields were 92% (#2-1-01), 100% (#2-1-02) and 7% (#2-1-03). The low yield of #2-1-03 was caused by blade breakage, but the reason for blade breakage is unknown. Dimensional parameters (bow, taper, thickness) of the wafers were normal or slightly worse than normal. Cutting times were very long: 38.5 hrs. (#2-1-01), 74.3 hrs (#2-1-02), and 43.75 hrs (#2-1-03). Blade wear in all cases was slightly greater than normal.

Since soft blades cut so slowly, we tried one more run, #2-1-04, using soft blades, a standard slurry mix, and 50% higher feed load. After the three previous runs, the bladehead jaws had

again become serrated: the faces were smoothed and a strip of blade stock was inserted between the spacers and jaws to prevent further serration. Again, we cannot trace any problems directly to these serrations, but the blade stock does provide a simple cure.

Cutting time was reasonable, 29.5 hours. Yield was less than 20%, for unknown reasons. Meaningful dimensional parameters could not be obtained since the over-range indicator on the ADE gauge was activated for about 80% if the wafers: this is an indication of poor wafers. We, therefore, conclude that softer blades offer no advantage in silicon wafering: harder blades might be useful to the cutting process, but are apparently not available except at higher cost.

Lower Accuracy Stock: Tests #2-1-05, -08, -09, -07

Test #2-1-05 was run using lower accuracy (T-1 instead of T-2 thickness tolerance), cheaper blade stock. While conditioning the blades by cutting a glass block, several blades broke. No obvious reasons for the breakage were apparent. We ran Test #2-1-07 to dunlicate #2-1-05. Because of availability, the saw equipped with the "bounce fixture" (discussed below) was used.

Cutting time was 48 hours, due to feed sticking caused by the bounce fixture. Yield was 79%. Wafer dimensional parameters were not significantly worse than average. This blade stock seems useable, although stacking tolerance associated blade misalignment may be a problem in large packs.

Continuing our investigation of cheaper blades, we ran Test #2-1-08 using a blade pack made from T-0 thickness tolerance blades. The thickness tolerances on these blades are 60% greater than the tolerances on our standard T-2 tolerance blades.

Blade thickness, spacer thickness, and all other conditions were standard. Severe wafer breakage occurred throughout the run, and no wafers survived. Cutting time was 40.5 hours due to feed sticking (the test was run on the bounce fixture machine because of availability). Blade wear was low (25% less than usual) but blade side wear was high (1/3 the blade thickness).

We repeated the test in Test #2-1-09, except we removed the bounce fixture. The results of the two tests were identical. We concluded that T-0 tolerance blades cannot be used to wafer 100 mm diameter silicon.

Increased Tension: Tests #2-1-06, -10

We ran Test #2-1-06 to gain preliminary understanding of the effect of blade tensioning on cutting and wafer quality. Tension in the blades was increased by 20% (3.05 mm (.12 in.) elongation, rather than 2.54 mm (.10 in.)). All other conditions were standard.

Cutting time was 35.5 hours. Yield was 95% after the cut; wafer breakage during cleaning reduced this to 64%.

Blade wear was slightly high, 3.12 mm (.123 in.), but not high enough to be worrisome. Surprisingly, wafer taper and bow were slightly high. Kerf loss was also slightly higher than normal.

It seems likely that higher tension should result in better wafers and, perhaps, shorter blade lifetime. The results of Test #2-1-06 seemed so contraintuitive that we repeated the test in Test #2-1-10. Blade elongation was increased 20% (to 3.05 mm, 0.120 in.). All other conditions were standard.

Cutting time was somewhat long, 41 hours. Yield was 90%. Worst mean values of wafer dimensional parameters were as follows: nonlinear thickness variation 52 μm (0.002 in.), centerline bow 92 μm (0.0036 in.). Comparable results from other runs using standard elongations were 65 μm (0.0026 in.) NTV and 133 μm (0.0052 in.) bow. Other parameters such as thickness standard deviation and non-worst case NTV and bow were also improved. (Due to the nature of the sawing process, wafer dimensional parameters differ between the withstroke and perpendicular-to-stroke directions.)

In two runs with the increased elongation, we have now obtained one average run and one better than average run. More testing is necessary to define the average result with the greater elongation. The increased elongation is very attractive because it improves one attribute of the process (wafer dimensional parameters) without degrading any other attributes (setup time, cost, etc.).

10.3 Lab Saw Tests

Qualification Tests: #2-2-01, -02

Test #2-2-01 was the qualification test for the lab saw. Ten standard length .15 mm by 6.35 mm (.006 by .25 in.) blades and .36 mm (.014 in.) spacers were used. 7.57 ℓ (2 gal.) of PC oil were mixed with 2.7 kg (6 lb.) of #600 SiC abrasive. In other words, the blade pack and slurry used were our standard "baseline" types.

Because of the bellows problem discussed earlier, the constant cutting force system could not be used. The constant cut rate option was used, cutting at a safe .85 μm/sec (.002 in/min).

The run went very well. Two wafers broke during a night shutdown: fingerprints were found in the residual oil on the ingot, and we assume someone on the second shift touched the wafers and discovered how fragile they can be. The wafers showed some ridges which we attribute to variations in spring constant as the bellows convolutions separated. The saw performed excellently both mechanically and electrically.

Test #2-2-02 was a duplicate of #2-2-01, intended to gain experience with the saw. Only three wafers resulted because of misalignment of the ingot with the stroke direction. However, the saw performed very well mechanically.

Blade Elongation in the Lab Saw: Tests #2-2-03, -04, -05

Since tests of increased blade elongation had given mixed results (see #2-1-06, -10) we decided to try to measure the effect of blade elongation variations in the lab saw. During this series,

we obtained several complete runs; however, it was discovered that the spacer clamping mechanism tended to allow blade slippage during tensioning, and thus the results were meaningless.

Because of the problems encountered with the lab saw and the high priority of other tasks, we discontinued work on the lab saw.

10.4 Slurry Tests

#500 SiC Abrasive: Test #2-3-01

A package of 150 0.15 mm thick blades and 0.41 mm spacers was used to cut a 10 cm silicon ingot. A change from #600 SiC abrasive (standard) to #500 SiC resulted in a cutting time of 24.5 hours, but an increase in kerf loss for 0.20 mm (with #600) to 0.24 mm. Yield was 67%, and slice bow and taper average 35 μ, which indicates a good controlled cutting action. However, the shift to the heavier abrasive gave an increase in kerf loss comparable to that saved by reducing blade thickness from 0.20 mm to 0.15 mm.

Lubrizol Suspension Oil: Tests #2-3-02, -03

Several tests were run using Lubrizol 5985, a suspension oil supplied by Lubrizol Corporation as a replacement for the standard PC oil. This oil exhibits high suspension power using a dissolved polymer suspension agent, and lower viscosity than PC oil. Test #2-3-02 was run using 0.15 mm blades and 0.30 mm spacers. All

conditions (tensioning, abrasive mix, abrasive, feed weight, etc.) were "standard", i.e. set at the values found to be best for PC oil.

Severe wafer breakage occurred during cutting. The yield was about 3%. The machine was checked for alignment, and it was found that the end of the bladehead well (against which the end of the blade pack is compressed) was significantly out of perpendicular relative to the feed (50 to 80 microns in 12 mm). The end blocks were shimmed to make them perpendicular to within 2.5 μm (.0001").

Test #2-3-02 was repeated, except the spacers were increased to .356 mm (.014") in order to increase wafer strength. The operator had difficulty aligning the blade pack, but was able to obtain alignment within tolerances (having the blade pack parallel to the stroke within 5 μm (.0002")).

Again, severe wafer breakage occurred during cutting. The yield was about 25%. The wafer surfaces were quite wavy, and some broken wafers were measured to be .102 mm (.004") thick. These results indicated that controlled cutting had not been achieved.

The question is "can controlled cutting be achieved with Lubrizol 5985"? The major differences between 5985 and PC (standard) are viscosity and suspension power. It is difficult to believe that the much higher suspension power of 5985 is detrimental; thus, the lower viscosity of 5985 is probably the major difference.

Viscosity affects mostly the drag forces and the abrasive transport quality during cutting. Lower viscosity should decrease drag forces; again, this should not be detrimental.

Therefore, the poor performance of 5985 is likely to be due to a change in the transport and distribution of abrasive.

Light Mix Lubrizol: Test #2-3-06, -09, -10

Since Lubrizol 5985 oil had not performed well under the same conditions as the standard slurry oil, we decided to vary the abrasive mix. Feeling that Lubrizol may provide a higher effective mix at the cutting interface due to the higher suspension power and lower viscosity, we decided to reduce the amount of abrasive.

For this test, the mix was 0.24 kg/l (2 lb/gal) and all other conditions were standard. Efficiency, abrasion rate, and productivity were slightly low. Cutting time was longer than usual, and kerf loss was high. Yield was only 19%. Slice taper and bow were slightly high.

We felt that since a slight improvement over previous tests was noted in the early stages of this test, we were going in the right direction.

Continunig the trend of Test #2-3-06, Test #2-3-09 was made at a mix of 0.12 kg/l (1 lb/gal). All other conditions were standard.

Kerf loss was reduced. Slice taper was increased slightly and slice bow increased significantly. All other measurements were comparable to Test #2-3-06. Yield was only 12%.

The low yield and high taper and bow were partly a result of blade breakage and wear. The blades were worn on the side by approximately 1/3 the thickness. The ratio of the number of blades worn on one side to the number worn on the other side was 10:1, indicated some asymmetry in the cutting process. This amount of wear is unprecedented in cutting any material in any condition. We cannot yet give a good reason for this wear. However, the early stages of cutting appeared quite good. It is possible that the abrasive was limiting the slurry life at the end of the cut. It appears that light mix is the correct approach for standard Lubrizol.

In order to find the point at which a Lubrizol slurry has too little abrasive, and to investigate the side wear problem, Test #2-3-10 was run with a 0.06 kg/l (½ lb/gal) mx. Yield was so low (4%) that only cutting time could be measured. The cutting time increased significantly. This has always been a good indication that the total amount of abrasive was too little; thus, it seems that a heavier mix is necessary with Lubrizol.

The high side wear occurred again. Measurements were made during the cut with the following results. At ¼ of the cut depth, side wear could not be measured; at ½ the cut depth, side wear was 0.05 times the blade thickness; at the end of the cut the side wear was 1/3 of the blade thickness.

These results indicate that the side wear is due to some effect which changes during a cut, perhaps the geometric changes

due to the round cross-section of the ingot or abrasive breakdown due to the small amount of abrasive used. Although Lubrizol with a light mix is economically attractive, we cannot use it until we resolve the side wear question. It still remained that the early cutting was better controlled and breakage occurred after 1/3 of the ingot has been cut.

Lubrizol Retest: Test #2-3-11

After discovering serrations on the bladehead clamp jaws, we retested Lubrizol 5985 suspension oil in Test #2-3-11 (between tests #2-1-03 and #2-1-04). Conditions used were those found earlier to be best, i.e. standard except for 1/3 standard abrasive concentration (0.12 kg/l or 1 lb/gal).

Cutting time was 32.7 hours. No wafers survived the run. After the test, the clamp jaws were found to be serrated again. We have no evidence that jaw serration even contributed to the breakage. Since the only major advantage of 5985 is easier recycling, and since we have been so far unsuccessful with 5985, we decided to concentrate on lower cost slurry fluids.

Lubrizol Additive (Imitation PC): Test #2-3-12

After much testing of viscosity and suspension power, we obtained a mixture of the polymer suspension additive used in Lubrizol 5985 with mineral oil which we felt was the best match possible with PC oil. The cost was not known, but since the

C-3

suspension power was less than LZ 5985, we felt it should be lower. The suspension and viscosity tests are discussed later.

In Test #2-3-12, a film appeared to form on the blades. Wafers broke very early in the run, the bladehead drive motor overheated, and motor fuses blew. This indicated very high drag forces, and we decided that LZ 5985 additive is not a promising additive.

Water Based Slurries: Tests #2-3-13, -14, -15, -18, -19, -22, -35, -37

After Lubrizol 5985 showed such disappointing results, we began to feel that vehicle suspension power may not be expecially important to the cutting process. In addition to the fact that LZ 5985 (with very high suspension power) worked poorly, we reasoned that once abrasive is transported to the cutting area, we could see no way in which suspension power could affect the cutting process itself. Based on this reasoning, water based slurry vehicle with its extremely low cost potential seemed interesting.

The viscosity of the fluid is probably important. Although we do not know the optimum viscosity for a slurry vehicle, it is unlikely that water (250 times less viscous than PC oil) is optimum: the water must be thickened. Acting on a suggestion from Dr. Leipold of JPL, we obtained a cellulose based water soluble polymer which can be used at low concentrations to increase

the viscosity of water up to 30,000 times. This was used to increase the viscosity of tap water to be within 5% of that of PC.

Since the blades are steel, corrosion is a strong possibility. A commercial corrosion inhibitor was used, at the minimum dilution recommended by the manufacturer, to prevent corrosion. A bactericide was also added. The thickener also produced a quite alkaline solution, pH 9-10.

Test #2-3-13 was run with this formulation. Initial cutting rates were quite high, approximately 50% faster than normal. After a night shutdown, we noted that slurry tended to dry and cake between the blades during shutdown, with consequent wafer breakage. This could be avoided by washing the blades on shutdown, or by running continuously.

At 12.5 mm (0.5 in.) cut depth, blades began to break. By 18 mm cut depth, about half the blades had broken and the test was aborted. Inspection of the blades showed that they had all cracked at the junction between the worn and unworn portions, at the end of the stroke. The fracture initiated at the cutting side (bottom) of the blade, and the initiation area showed the large-scale faceted appearance typical of intergranular cracking. After about 0.32 mm (0.013 in.) of crack length, the fracture surface character changed to the gray dimpled appearance of ductile fracture. No fatigue striations were discernable at 90X magnification.

We concluded that the fracture initiated by stress corrosion cracking with possible fatigue growth before the final ductile failure. The first possible cure considered was reducing blade tension. Assuming that the overall reaction is dominated by the initial reaction, $Fe \rightarrow Fe^{++} + 2e^-$, a quick calculation (assuming an exponential dependence of reaction rate on stress) showed that the blade stress had to be reduced over 200 times to allow a blade to make it through a 100 mm diameter ingot. Previous experience has shown that it is impractical to reduce the blade tension by more than a factor of about 1.3, because blades under lower tension wander more readily. Even if the calculated necessary reduction in blade tension is two orders of magnitude too high, suppressing stress corrosion by reducing blade tension is impractical.

The next step was to try a different corrosion inhibitor. Inspection of old lab notebooks showed that similar stress corrosion problems had occurred when using water to cool and flush debris away from diamond impregnated blades. Samples of the corrosion inhibitor which solved the problem were obtained, and a new batch of water-based vehicle (WBV) was prepared. A blade pack was tensioned, and WBV was pumped over it in a pulsed cycle as it would be while cutting. To encourage corrosion the top and bottom of the blade pack was abraded (with 320 grit sandpaper) five times during the test. After 100 hours of exposure to WBV without any breakage, we terminated the test and tried cutting silicon again.

Test #2-3-14 was run with the new formulation (WBV II). Cutting rates were comparable to standard rates. When shutting down, the blades were washed with water containing corrosion inhibitor, and the bladehead was reciprocated a few times to clean out the kerf slots. No problems were encountered when starting up after the night shutdown. Unfortunately, blade breakage occurred after the same number of cycles and in the same fashion as in the previous test.

It seemed that the major problem with WBV is stress corrosion. The first two tests used nitrite-based chemical inhibitors. Test #2-3-15 was run using WBV III, using a nitrite-free chemical inhibitor.

Results were quite similar to previous tests. Initial cutting rate was quite good. When the machine was shut down for the night, the blades were washed with water and corrosion inhibitor, and no problems were experienced with morning start up.

Unfortunately, severe blade breakage occurred at approximately the same point as in previous tests (1/8 to 1/4 the way through). We concluded that standard chemical corrosion inhibitors are not sufficient for this purpose.

Test #2-3-22 was run using a slurry of distilled water and abrasive, with no other additives. Other conditions were standard. This test was intended to provide a baseline by which to measure the performance of the various corrosion inhibitors we have tried or will try.

Cutting rate was reasonable, about .053 mm/min (.0021 in/min). At 23 mm (.91 in.) cut depth, blade breakage was so severe that we stopped the test. The blades were visibly rusted immediately after the test, even on the portions that were continously abraded.

It is tempting to conclude that the corrosion inhibitors we have used had either a detrimental or no effect. However, even though the blade steel was nominally identical to that used previously, some microstructural differences may be present. We feel that the visible rust, which we had not seen before, is an indication that corrosion was increased in the absence of inhibitors. Our conclusions were that corrosion inhibitor does indeed reduce corrosion; the inhibitors tested so far do not sufficiently reduce corrosion; and the difference in lots of steel is sufficient that blade lifetime in Test #2-3-32 cannot be directly compared with blade lifetime in previous water based slurry tests.

In Tests #2-3-15, -18, and -19 we tested soluble oil corrosion inhibitors. Two different oils were used: dilution was the manufacturers recommended maximum. Test #2-3-19 used the same formulation as Test #2-3-18, except the polymer thickener was not added. In all three tests, severe blade breakage occurred after 1-5 hours of cutting.

We hired a consultant, Prof. R. M. Latanision of M.I.T. (Director of the Corrosion Laboratory) to investigate the blade failures. Based on observation of the process and broken blades, he concluded that the fractures were caused by hydrogen embrittlement, the hydrogen resulting from corrosion. (He felt that the fracture surfaces are such excellent examples of hydrogen embrittlement fracture that he requested samples to use in class.) His opinion was that no corrosion inhibitor is available which would solve the problem: the solution would be to reduce blade hardness and/or change blade material. None of these alternatives is acceptable.

Dr. Paul Tung of JPL modified his fatigue test machine so as to allow testing of blades in aqueous environments.

A sample of Cortec VCI-309 anodic-cathodic-vapor phase corrosion inhibitor was delivered to Dr. Tung, along with blade samples, for fatigue testing. Dr. Tung reported that blades tested in distilled water broke "very quickly" but the spread was large; blades tested in 5 wt.% VCI-309 lasted more than 10^6 cycles (3 tests); and the one blade tested in 1 wt.% VCI-309 lasted more than 10^6 cycles.

If cycles in Dr. Tung's tests correspond to load cycles in the saw, these lifetimes correspond to 84 hours of cutting, which is much more than required for even two cuts through a 100 mm diameter ingot.

In light of these promising results, we ran Test #2-3-25 using a distilled water slurry vehicle containing 5% (by weight) of Cortec VCI-309. (5% is the maximum recommended concentration.) The results of the tests were promising, but not as good as hoped. The total running time was 21 hours, including three night shutdowns. One blade broke at 5 hours, 40 minutes; one blade broke at 9 hours, 5 minutes; and several blades broke between 13 hours and 21 hours. The vehicle tended to form a stable foam, which caked on the saw. After 21 hours, the cut had only progressed 25 mm (1 inch) into the work, and all the abrasive was trapped in dried foam. In view of the clogging of the machine, we shut down the run.

The fact that all but a few blades lasted at least 21 hours is heartening. Still, an acceptable water based vehicle must allow minimum blade lifetimes longer than this. One problem in testing is that the statistics are extreme rather than mean value statistics (i.e., we are interested in the lower tail of the blade lifetime distribution rather than the average). This makes it difficult to predict saw performance on the basis of relatively few laboratory tests.

We ran Test #2-3-37 using the same slurry as #2-3-35 with the addition of a Foam-a-cide 500, a commercial defoaming agent from the Angler Chemical Company of Plainville, MA. All other conditions were standard.

The defoaming agent did its job. The initial cut rate, however, was extremely slow (about 1/4 of usual). After 6.25 hours of cutting, at about 1/16 of the full depth of the cut, the workpiece broke loose and shattered against the bladehead. We decided this run was not promising and terminated it.

Although water-based slurry vehicle seems somewhat promising at this time, apparently much development work remains.

Abrasive Sizing Tests: Tests #2-3-01, -04, -05, -07, -08, -21, -30

In Test #2-3-01, a package of 150 0.15 mm thick blades and 0.41 mm spacers was used to cut a 10 cm silicon ingot. A change from #600 SiC abrasive (standard) to #500 SiC resulted in a cutting time of 24.5 hours, but an increase in kerf loss for 0.20 mm (with #600) to 0.24 mm. Yield was 67%, and slice bow and taper averaged 35 μ , which indicates a good controlled cutting action. However, the shift to the heavier abrasive gave an increase in kerf loss comparable to that saved by reducing blade thickness from 0.20 mm to 0.15 mm.

In Test #2-3-04, a mix of three abrasive sizes was used, with 1/3 of the standard mix (0.36 kg/liter) made up of each of #500, #600 and #800 SiC. Total cutting time was only 22.1 hours, less than with only #500 SiC. However, bow and taper were not as low as in #2-3-01 and kerf loss was nearly identical (0.246 mm). Yield was 83%, indicating a reasonably controlled cutting action.

The results indicate two aspects of MS slicing. Firstly, it appears that the largest particles in an abrasive mix control the cutting action and kerf loss. Secondly, the abrasive mix involving a broader range of particle size seems to maintain good cutting action. It is possible that the smaller particles help support the larger particles and allow them to perform their optimum cutting action.

For Test #2-3-05, the abrasive consisted of equal parts of #600 and #800 SiC. Other conditions were standard. This test was to investigate both reduction of kerf with mixed abrasive and the effect of the amount of spread in particle sizes.

Efficiency, abrasion rate, productivity and kerf loss were normal. The yield was very low, only 29%. Slice taper and bow could not be measured since the wafers activated the out-of-range warning on the measuring device.

The results of this test were encouraging in terms of using potentially cheaper abrasive, but controlled cutting conditions were not achieved. Cause of the low yield must be established.

Continuing the effort to lower the price of abrasive by using a broader spectrum of particle sizes, Test #2-3-07 was run using equal parts of #600, #800 and #1000 grits. Cutting force, cutting speed, ingot size, and suspension oil were standard. 0.15 mm x 6.35 mm blades with 0.40 mm spacers were used. An error was made in slurry mixing: only half the desired amount of abrasive was mixed, so the overall abrasive mix was 0.18 kg/l.

Cutting time was good, 23.2 hours. However, severe slice breakage occurred and the yield was only 3%. The blades, again, showed anomalous side wear, up to 1/3 the total thickness. The appearance of side wear may indicate that a wafer breakage is caused by a machine problem, although no measurements have supported this.

Test #2-3-08 was an attempt to reduce kerf loss and abrasive cost; a standard condition run was made using equal parts of #800, #1000 and #1200 grit abrasive.

Again, yield was very low (11%). Cutting time was long (about 44 hours) as before with #800 grit slurry. Kerf loss was slightly reduced: bow and taper were somewhat large. The mixture of #800 and smaller abrasives does not seem to offer any improvement over #800 alone.

The Norton Company supplied us with a sample of silicon carbide abrasive produced by a cheaper process. Although labelled as #500, the company claimed that it was equivalent to the #600 we currently use.

We tested this abrasive in Test #2-3-21. All conditions were standard. Cutting time was 25.5 hours; yield was 75%; kerf loss was high, .265 mm (.105 in.). Wafer dimensional parameters were average.

We concluded that the abrasive was workable, but was more similar to our standard #500 than #600.

At our request, Norton produced a new sample with smaller particle size. This sample, designated MCA 1632 by Norton, was tested in run #2-3-30. All conditions except the identity of the abrasive were standard.

The results were essentially the same as in Test #2-3-21. Cutting time was 30 hours, yield was 99%, taper was 51 μm (.002 in.), and bow was 44 μm (.0015 in.). All these results are quite good. Unfortunately, the abrasive kerf loss was 98 μm (0.004 in.) rather than the 60 μm (0.0024 in.) expected with #600 abrasive.

The results of these tests indicate that direct abrasive cost reduction is not promising: the major cost reduction is expected to come from recycling.

Mineral Oil Vehicles: Tests #2-3-16, -17, -20, -23, -25, -26, -27, -28, -32, -34, -36

Since such good initial cutting rates were found using water based slurry, we hypothesized that suspension power does not significantly affect cutting performance. We, therefore, ran Test #2-3-16 using 400 SUS mineral oil as the slurry vehicle. Viscosity (with abrasive) matched that of PC oil. All other conditions were standard.

Cutting rate was approximately normal but varied somewhat more than usual. During the run the ingot was significantly warmer than normal (110°F at one point vs. 90°F maximum measured on other runs). However, current draw was normal. Presumably the higher temperature was not due to increased heat generation but was due to decreased heat removal. This is surprising since mineral oil should have higher specific heat than and approximately the same thermal conductivity as PC oil.

Approximately halfway through the cut, the workpiece broke loose from the submount. The reason is not known: the temperature was too low to significantly soften the adhesive.

Measurements on the half-wafers indicated that they were not significantly worse than normal. The question of heat transfer and generation in mineral oil slurry was not explained.

We continued our investigation of slurry fluids in Test #2-3-17 by trying a high viscosity mineral oil. 600 SUS oil was used: all other conditions were standard. Slurry viscosity was approximately twice that of a standard PC oil slurry.

As the blades became buried, the drag forces increased greatly. The ingot heated to 43°C (27-30°C is normal) and the motor was drawing 10 A vs. 6-7 A normal draw. This caused several fuses to blow, and the run was stopped after 5.1 hours at a cut depth of 10 mm (.30 in.). No blades were broken, indicating that drag force is not a cause of blade breakage: the ingot was "the hottest ingot" the operator had ever seen.

Since the ingot and blade pack were still good, we replaced the slurry with a mixture of abrasive and 200 SUS mineral oil (about 2/3 the viscosity of a standard PC mixture). Current draw was slightly high (8.5 A) and two fuses blew before the end of the run, but the run was completed in 40.25 hours. Yield was 21%: wafers may have been broken or weakened by high drag forces. Wafer dimensional parameters were poor.

We concluded that mineral oil slurries may be workable, but will probably require a lubricity additive. (Lubricity is a poorly understood fluid property which is more important than viscosity when considering lubrication when clearances are very small.)

Test #2-3-20 used a mineral oil slurry mixed 10:1 by volume with lard oil, a standard lubricity additive. All other conditions were standard.

Drag forces were reduced, as shown by the reduced current draw in the motor. However, drag forces were still higher than with PC oil slurries. Several fuses blew during the run, and all wafers had broken by the time the cut was half finished, and the run was halted after 18.5 hours.

The lubricity approach seemed promising, and since good cutting was obtained in Test #2-3-19 (unthickened water), we decided to try thinner mineral oils with lard oil additive.

Test #2-3-23 was run using thin (100 SUS) mineral oil with lard oil added. Cutting time was reasonable, 36.75 hours. Yield was very low, 12%. Wafer dimensional parameters were poor, but not terrible; NTV was 120 μm (.0047 in.) and bow was 235 μm (.0093 in.). The cause of the low yield and high bow are unknown, but both problems probably stemmed from the same source. The drag force and fuse blowing problem was completely eliminated.

As a baseline comparison, we ran Test #2-3-26 which was a duplicate of #2-3-23 except that no lard oil was added. Cutting time was long, 61 hours. Yield was 73%. NTV was 100 μm (.004 in.) and bow was 256 μm (.012 in.). No fuses blew, but the ingot was noticeably warmer than usual during the cut.

Two more tests were run to test the effect of parameter variation on thin mineral oil-lard oil slurry. Test #2-3-25 was run under the same conditions as #2-3-23 except that we changed our machine setup procedure slightly. The standard method is to tension the blade pack and then align the blades with the stroke. We reversed this order: the procedure was much more difficult and time consuming, but probably resulted in better alignment of the central blades.

Cutting time was again long, 61 hours. Yield was 49%. Slice taper and bow were 92 μm and 128 μm respectively, an improvement over Test #2-3-23. However, the bow and taper were still somewhat high, and we feel that the difficulty of the different setup procedure is so high that the improvement achieved is not worth the extra work.

Since cutting time with mineral oil-lard oil slurries had been so long, we tried to speed up the cut in Test #2-3-27 by increasing the abrasive/vehicle mix to 0.48 kg/l (4 lb/gal). The reason for this change was our suspicion that the tortuous path followed by the slurry in returning from the ingot to the bucket allows buildup of settled sludge (when a non-suspension vehicle is used). Thus, the abrasive/vehicle ratio is constantly decreasing. Every 8 hours, we had been scraping up the sludge and remixing, but the ratio still varied during each 8 hour period. The increased amount of abrasive in Test #2-3-27 was intended to compensate for this settling.

As we hoped, cutting time was much improved, 26.5 hours. Unfortunately, yield was very low (5% or 7 wafers). The surviving wafers were excellent, with very low bow and taper. Although the wafers were too few to form a statistically significant sample, their high quality indicates that the cause of the low yield was not severe blade wander.

Previous tests with a slurry fluid of low viscosity (100 SUS) mineral oil with lard oil lubricity additive mixed 5:1 by volume have showed mixed results. The drag force problem can be eliminated. Cutting times have been made reasonable by increasing the amount of abrasive, which should not be necessary in newer saws due to decreased abrasive "laydown" in the return path to the slurry bucket. Yield has been poor, and wafer quality has ranged from poor to excellent.

In Test #2-3-28, we reduced the proportion of lard oil to 40:1, which is recommended for many applications. If the large amount of lard oil was causing the problem, this reduction should allow the yield to be raised. All conditions were standard except the abrasive mix, which was increased to 0.48 kg/l (4 lg/gal) as in Test #2-3-27.

Unfortunately, there was too little lard oil to prevent the drag force problem, and several fuses blew. At 41 mm (1.6 in.) cut depth the mineral oil/lard oil ratio was decreased to 20:1 by adding lard oil. No more fuses blew, but wafer breakage started almost immediately.

Final yield was 66%. Cutting time was 38.3 hours, bow was 198 μm (.008 in.) and taper was 87 μm (.0035 in.).

We conclude that mineral oil slurries with lubricity additives seem workable, but lard oil may not be the right additive.

Test #2-3-36 was run using an unusual abrasive. The Mosher Company, a local manufacturer and distributor of lapping equipment and supplied, provided a sample of Micro Abrasives #600 silicon carbide (our standard abrasive) which they had treated using a proprietary process to provide lubricity when suspended in oil. They claimed we could use this abrasive with straight mineral oil (100 SUS).

Unfortunately, this did not work. Even at 80% of standard reciprocation speed, fuses blew regularly from the beginning. We terminated the run after 1/16 of the cut, and concluded that the treated abrasive offered no improvement over the untreated abrasive in straight mineral oil.

In Test #2-3-34 we tried 100 SUS mineral oil mixed with cetyl alcohol lubricity additive and a surfactant to prevent abrasive clumping. The cetyl alcohol could not dissolve in the oil, so no cutting was attempted.

We feel that 100 SUS mineral oil with lard oil additive is a promising low cost slurry vehicle. Cost is about $1.20/gal in bulk. Due to the lack of suspension power, a few days settling allows one to easily draw off about 80% of the vehicle for reuse, reducing the cost of vehicle to about $.25/gal/run. Another advantage of this system is that the sludge can be resuspended in a less viscous medium such as water, making abrasive reclamation more convenient.

We feel that the problems encountered can be solved in time. It should be noted that the 7176 saw (which is the replacement for the 686) and the prototype both have much simpler slurry return paths, so sludge build-up should not be a problem.

Test #2-3-32 was run using a vehicle made up of 85% by volume 100 SUS mineral oil and 15% by volume White & Bagley #2213, a general purpose lubricity additive for metal cutting and grinding.

The initial cutting rate was low, about 70% of the usual rate with PC oil slurry. One fuse blew during the first day of running, and speed was decreased to 80 RPM. On the second day of cutting, about 1/8 of the way through the ingot, it proved impossible to run the saw over 30 RPM without blowing fuses and the run was stopped. Again, since insufficient lubricity was obtained at the highest recommended concentration, and also since it seemed that some component had evaporated or settled out causing higher drag than with 100 SUS mineral oil along, we did not investigate this system further.

<u>Cutting Oils: Tests #2-3-29, -31</u>

Previous testing of mineral oil slurry vehicle showed that drag forces are a major problem, cutting times may be made reasonable by proper choice of conditions, excellent wafers can be produced, and if drag forces are sufficiently reduced by

addition of sufficient lard oil, then the only problem left is low yield due to wafer breakage near the end of the run for unknown reasons.

It seems reasonable that some characteristic of the lard oil may be responsible for the wafer breakage. Thus, we decided to try additives different from lard oil, namely commercial cutting oils. The price was not a consideration in this series, since we have found that oils with little suspension power are easily recycled by one to two days settling, and if a workable oil proved too expensive, we would at least have a good starting point from which to develop low-cost low-suspension power slurry vehicles.

We consulted the White & Bagley Company of Worcester, MA and picked three test vehicles. W & B cutting oil #1 is a low priced, general purpose cutting oil. W & B cutting oil #2698 is a medium cost, very high sulfur-chlorine-fat content oil for hard to machine materials. Both oils are thin, on the order of 100-200 SUS. W & B HD soluble oil 2213 is an all-purpose extreme pressure additive for oil or water, containing no sulfur or fat but with a high chlorine content (covered in Test #2-3-32 above).

Test #2-3-29 was run using a vehicle of W & B cutting oil #1. All other conditions were standard. During the first quarter of the cut, fuses blew regularly and the saw could not be run over 60 RPM (60% of standard speed). We terminated the test and will not use W & B cutting oil #1 again as there seems to be no promise of making it work.

Test #2-3-32 was run, again using standard conditions, but using W & B cutting oil #2698. Results were identical to results of Test #2-3-29: blown fuses and inability to run the machine at full speed.

Our conclusions are that we have not yet found the proper mineral oil system, but such a system is workable. Further research is necessary, combining careful consideration of the necessary properties with judicious selection of additives for experimentation. It is unlikely that commercial cutting oils will prove suitable, in view of the results of Tests #2-3-29 and #2-3-31. The workable system will consist of mineral oil and a carefully selected one or two additive package.

Recycled Abrasive: Tests #2-3-33, -38

Much effort was spent before we succeeded in separating abrasive from PC oil. Filtration and cyclonic methods did not work. Since the order of magnitude difference in particle size and the difference in density between SiC and Si both tend to separate the two types of particles, we felt it was only a matter of time before we succeeded.

We finally did succeed in separating used abrasive from PC oil slurry. The apparatus was a Centrifugal Clarifuge manufactured by the Barrett Company, which cost $4,000 today complete (including recirculating pump and extra bowl). It consists of a spinning bowl having edges turned in at the top encased in a fiberglass housing. Liquid is poured or pumped into the center of the bowl,

and sludge is forced into the outside of the bowl while excess liquid flows over the edges of the bowl. The sample was 19 ℓ (5 gal) of used slurry containing approximately 33 kg (15 lb) of abrasive. The sample was poured through Barrett's demonstration unit five times at a flow rate of approximately 0.32 ℓ/sec (5 gal/min).

The cake formed on the inside of the bowl was obviously mostly silicon carbide with a skin of silicon (SiC is gray while the Si dust is brown). The cake was then washed in chlorothane twice to facilitate magnetic removal of steel dust from the blades and remove residual oil to make accurate weighing possible. A small amount of silicon dust was removed by this washing. Final recovery was 9.9 kg (4.5 lb) of abrasive, or 30%. This could be easily increased since much abrasive was lost by sticking to the bag in which it was transferred from Barrett to Varian, inefficient washing, sticking in the centrifugal bowl (from which the cake was scraped rather than washed), and the fact that the bowl had more capacity than was used by the small sample.

4.4 kg (2 lb) of recycled abrasive was mixed with 8.8 kg (4 lb) of new abrasive (33% recycled) and the mixture was tested in run #2-3-33. All other conditions were standard.

The results were an unqualified success. Cutting time was 28 hours. Yield was 100% on the saw: five wafers were broken during cleaning by an inexperienced klutz (also known as the author of this report). Wafer thickness was 276 μm (0.011 in). Taper

was 63 μm (.0025 in) and bow was 91 μm (.0036 in). These results are all either average or better than average. This test shows conclusively that use of 33% one-time recycled abrasive does not degrade performance in any way. Since further recycling would result in a very small percentage of abrasive recycled more than once, we feel confident that multiple recycling of abrasive at the 33% level will have no effect other than reduced cost.

As a check, we repeated Test #2-3-33 in Test #2-3-38. Cutting time was long (42 hours): yield was 98% (one blade broke). Because of time limitations we were unable to measure the wafers.

We conclude that 33% recycled abrasive is an excellent method of cost reduction.

10.5 Demonstration and Fabrication

Cell Fabrication, 10 cm Diameter: Test #2-4-01

0.15 mm blades and 0.36 mm spacers were used to cut a 100 mm silicon ingot with a standard 0.36 kg/liter mix of #600 SiC with PC oil and 85 grams of cutting force per blade. Cutting time was 22.4 hours and yield of the 0.314 mm slices was only 59%. Taper and bow were 70 μ. It was felt that the alignment of the blade stop in the bladehead (which is the vertical reference for blade alignment) may have impacted yield in this test. Alignment was carried out to try to correct this condition.

Machine Proof Test: Test #2-4-02

After end stop correction, the above test (#2-4-01) was repeated. 0.41 mm spacers were used resulting in 0.36 mm slices. Cutting time was again 22.4 hours with 50% yield. Bow and taper were 50-70 μ. The indication was that proper alignment existed, but that uncontrolled cutting leading to low yield had occurred.

The best explanation for poor cutting lies in the different slurry application technique used with the new test saws. A reciprocating slurry application, as opposed to pulse-type distribution, seems to increase the effective slurry mix. Higher mix generally has given reduced cutting time and wafer yield and accuracy. The preceding tests show these conditions. We, therefore, shifted to a pulse-type slurry applicator.

Wafer Dicing, Cell Fabrication: Test #2-4-03

MS slices, 0.35 mm thick were diced into 2 cm squares to be used for surface preparation and cell fabrication studies of MS slicing.

Cell Fabrication: Test #2-4-04

Three hundred 0.15 x 6.4 mm blades with .41 mm spacers were used to cut a 100 mm silicon ingot for surface preparation and cell fabrication studies. Cutting time was 28 hours, but yield was only 29%. Slice thickness was .322 mm and kerf loss was 0.237 mm. Slice breakage during the cutting process and poor yield with thin slices continued to plague this phase of the program.

N-type for Cell Fabrication: Tests #2-4-05, -06

In order to have N-type 100 mm diameter wafers available for cell fabrication, etching studies, etc. we ran tests #2-4-05 and -06.

Test #2-4-05 used a heavy slurry mix (0.48 kg/ℓ) in order to try to resolve the yield problems found above. 0.20 mm thick blades and 0.41 mm thick spacers were used. Cutting time was 36.5 hours, and yield was only 55%. Slice taper was 64 μm and bow was 113 μm.

Test #2-4-06 used standard conditions except a 204 blade epoxy type pack rather than the standard pin pack was used. 0.41 mm spacers were used. Cutting time was 40 hours, and yield was 64%. Slice taper and bow were 117 μm and 225 μm respectively.

Investigation of PC Oil Problems

Since mid-December 1977, we had been using PC oil from a 55 gallon drum, lot 67-k-26-2. When this drum was received, we noticed that the color was different from previous lots. Process Research confirmed that they had changed the base oil.

We checked a sample for viscosity and static suspension characteristics. The sample was insignificantly different from previous samples, so we used it as before.

In March 1978, we discovered that the oil from the bottom 1/4 of the barrel was significantly lower in viscosity than previously. The viscosity was only 15% of the standard value. Since we tap the oil from the bottom of the barrel, it seemed likely that the

clay platelets which thicken the oil and give it good suspension characteristics had settled and been drawn off earlier. Agitating the barrel increased the viscosity to 30% of the standard value.

We have no direct evidence that any cutting tests during the period December 1977-March 1978 were adversely influenced by loss of oil viscosity. However, the change in oil viscosity is an extra, unaccounted variable during a period of poor cutting results. Process Research agreed to replace the barrel, and we decided to keep the oil stirred to prevent viscosity and suspension power variations.

10.6 Miscellaneous Techniques

Cutting Enhancement: Test #2-5-01

Glass walls were mounted on either side of a 10 cm silicon ingot with standard conditions of MS slicing. This technique has been used very successfully with gallium arsenide and other materials. The cutting action seemed to proceed well, but the glass and ingot eventually broke loose. The result was complete fracture of the work, even though cutting time and blade wear appeared to be comparable to good cutting.

Machine Proof Test: Test #2-5-02

The second JPL saw was corrected for bladehead end stop vertical alignment (which aligns the blades vertically) and was used to cut a silicon ingot with 0.15 mm blades and 0.41 mm spacers. Cutting time was 23 hours, but yield was only 42%. The indication is that slurry mix and application technique were not suitably matched to allow good cutting.

Upside Down Cutting: Tests #2-5-03, -06, -07, -15

To determine the characteristics of slurry ingress to the blades during MS slicing, a special work holding fixture was installed on a standard Varian 686 MS saw to allow "upside-down" cutting of a 100 mm silicon ingot. 150 0.20 x 6.4 mm blades and 0.41 mm spacers were used with 113 grams of blade load. 0.48 kg/liter of #600 SiC was used as a slurry with "pulse-type" application to either side of the ingot.

Cutting time was 26.1 hours, yield was 100% and the bow and taper of the 10 cm slices was 36 and 44 microns respectively. Indeed the cutting process proceeded well in this mode and the slice accuracy was the best seen to date.

The work-holder tended to loosen and rock slightly at the end of each bladehead stroke due to the direction of loading in this cutting mode. For this reason a new test was scheduled to eliminate the rocking motion which may have cushioned the cutting shock to wafers and been responsible for the improvements noted.

A second upside down cut, #2-5-06, was run to isolate the effect of the upside down mode from that of the rocking work-holder experienced in Test #2-5-03. A rigid workpiece mount was used and cutting went very well until halfway through the ingot when the workpiece broke loose from the submount. This experience was sufficient to show that the reversal of gravity on the action of slurry was the useful improvement with this technique.

"Upside down" cutting (feeding the ingot downward) provided the best results (in terms of thickness variation, bow, and taper) obtained so far. Both previous upside down cuts used 0.2 mm (.008 in.) thick blades, so we decided to try, Test #2-5-07, upside down cutting with 0.15 mm (.006 in.) blades. All conditions, except for the direction of cut, were standard.

Cutting time was normal, 32.25 hours. Yield was 23%. Slice taper and bow were about normal, and kerf loss was slightly high. The reason for the poor performance compared to the first upside down cut is not known; it may possibly be because of the thinner blades.

Since the first test of upside down cutting yielded the best wafers obtained so far, and since subsequent tests all had problems not directly associated with the cutting process (e.g., ingot-submount separation), we ran Test #2-5-15 using a baseline blade pack (thinner blades than in the first run).

During the run, the ingot broke away from the submount once and the submount broke away from the mounting plate once. Both times the operator happened to be standing by the machine and was able to shut down immediately. Only five wafers were lost due to breaking loose.

Cutting time was slightly long, 35 hours. Yield was 92%. Wafer dimensional parameters were poor, because of steps caused by imperfect alignment on remounting. The high yield in spite of the problems is very encouraging. We were unable to pursue this technique because of time limitations.

Load Variations During Cutting: Tests #2-5-04, -05

Test #2-5-04 was run before Professor Werner's analysis (presented above). It was assumed that the cutting pressure at the blade/silicon interface was important to controlled abrasion and that variations in pressure due to ingot cross-section (at constant load) might cause some of the bow/taper variations seen in MS slices. Cutting force was varied to maintain constant pressute (based on nominal kerf length) with the maximum load being 113 grams per blade. 136 0.15 mm blades and 0.41 mm spacers were used. In order to suppress wafer fracture, a thin coating of epoxy was used on the perimeter of the ingot. The epoxy slowed the cut so severely during the early and late portion of the test that the overall slicing time was 63 hours. Yield was 71%, and the edge chipping seen in the past did not occur. The coating disturbs the cutting process so severely, however, that an alternate will be sought. Wafer accuracy in the vertical direction was degraded, but in the horizontal direction, it was greatly improved.

All analyses have indicated the blades should be stable (not subject to torsional buckling) at the feed loads used, by about an order of magnitude. However, blade wander does occur. We attempted to investigate whether torsional stability affects blade wander by altering the feed weight during Test #2-5-05 in order to keep the feed weight at a constant percentage of buckling load as calculated previously (second analysis). The maximum feed weight was the standard 85 g/blade (3 oz/blade). All other conditions were standard.

Since the feed force was low for most of the run, cutting time was long (78 hours). Yield was 67%. Wafers were poor. We concluded that "constant stability" actually degrades the cutting process.

Large Ingots: Tests #2-5-08, -09, -12

In Test #2-5-08, an attempt was made to slice a 150 mm (6 in.) diameter ingot. All conditions were standard, except for the blade pack. 0.2 mm (0.008 in.) thick blades were used for extra stability. 0.51 mm (0.02 in.) spacers were used for increased wafer strength. The blades were 12.7 mm (0.5 in.) high, twice the standard height. This change was made since blade wear correlated with total distance traveled in the cut, which for a constant cutting rate is proportional to wafer area. Since the 150 mm ingot yields wafers with 2.25 times the area of 100 mm wafers, we expected about 6.35 mm of blade wear: obviously 6.35 mm high blades could not be used.

Cutting speed was average. Severe wafer breakage occurred, with about 1/3 of the wafers broken at a 50 mm (2 in.) cut depth. At this point, the ingot broke loose from the submount, and the test was aborted. Blade wear was 1.25 mm (0.049 in.), as expected for that depth.

The wafer breakage was probably a result of poor initial cutting alignment, since the ingot was not ground to a cylinder (a flat was ground for mounting). The reason for breaking loose from the submount is not known.

In Test #2-5-09, we cut a 120 mm (5 in.) diameter ingot. The ingot was ground to a cylinder. All conditions were standard, except .41 mm (.016 in.) spacers were used for increased wafer strength.

Cutting time was slightly longer than expected, 53 hours (we expected about 48 hours from area considerations). Cutting speed near the end was slow, probably because the slurry was nearing the end of its effective lifetime. In addition, a regulator failure in the feed air system caused no cutting force for about 1/2 hour. Yield was quite good for a first try, 53%.

The wafer dimensional parameters have not yet been measured because the wafers are too large for our instruments. However, we now know that 120 mm diameter ingots can be cut my multiblade slurry saws with only 200-250 microns of kerf loss (150 micron thick blades and 12 micron abrasive).

Since we were successful cutting a 125 mm (5 in.) ingot, but the slurry lifetime seemed to be reached before the end of the cut, we decided to run Test #2-5-15 cutting a 125 mm ingot and add abrasive during the second half of the cut. All conditions were standard, except the spacers were .41 mm (.016 in.) for wafer strength.

Unfortunately, we were unable to test the abrasive addition concept because the wafers broke up approximately half way through the cut. The reason is not known: ingot residual stress or lack of a bounce fixture are possibilities.

Baseline Check: Tests #2-5-14, -16, -17, -18, -19

Tests run in the early portion of Phase II showed consistently low yields and problems. We decided to check our "baseline" conditions as defined in Section 10.1 to see if the problems were

caused by a bad baseline or if they arose from difficulties encountered in "pushing the limits" of slurry sawing.

Tests #2-5-16, #2-5-17, and #2-5-19 were run using 0.15 mm (.006 in.) blades and 0.36 mm (.014 in.) spacers. The first two tests were half capacity, while the third was full saw capacity. All conditions were standard.

Yields were 72%, 85% and 80% respectively. All other parameters (cutting time, wafer dimensional parameters) were normal.

Two tests were run to see if minor baseline modifications could produce significant improvements. Test #2-5-14 used 0.2 mm (.008 in.) blades and 0.3 mm (.012 in.) spacers. This yielded thinner wafers, but the same m^2/kg conversion factor. Test #2-5-18 used 0.15 mm blades and 0.36 mm spacers, but was run on a saw not previously used in this program.

Yields were 90% and 75% respectively. Again, all other parameters were normal.

In view of these results, we concluded that our baseline conditions are indeed good. Yields must be improved, but the best way to do this is to continue pushing the process to its limits and thereby learn more about the mechanisms responsible for low yield.

End-of-Stroke Shock Load Reduction: Tests #2-5-10, -11, -13, -20, -21, -22

As discussed above, both in the analysis and Phase I experimental section, unavoidable blade wear gives rise to "bounce", a vertical motion of the ingot. The motion and associated pumping action are felt to be beneficial, but the associated forces are detrimental, contributing to blade and wafer breakage and blade wander.

In order to reduce the shock load, we constructed a low-mass bounce fixture consisting of two parallel plates separated by springs and constrained to move only towards or away from each other by a miniature four post die set. This fixture was inserted between the workpiece and the feed system.

This was tested using standard conditions in Test #2-5-10, except the spacers were .4 mm (.015 in.). The fixture was so effective in isolating the shock from the feed system that the feed tended to stick. This was resolved by periodically stopping the machine and dropping the feed about 10 mm.

Cutting time was slightly long, 36 hours (probably because of feed sticking). Yield was 100% and it was noted that only one wafer had a noticeable edge chip. Wafer dimensional parameters were average, again probably because the feed dropping interrupted the process.

We decided to try to define the limits of blade and spacer thickness possible with the bounce fixture.

Test #2-5-11 was run using standard conditions except the spacers were 300 μm (.012 in.) thick. This spacing should yield 250 μm (.010 in.) thick wafers.

To prevent the feed sticking, the operator periodically stopped the machine, dropped the feed a short distance, and restarted. This caused some wafer breakage, and was discontinued about 2/3 of the way through the cut. Thereafter, the cutting rate was quite slow due to feed sticking.

Overall cutting time was 35.2 hours and yield was 77%, mostly due to the breakage discussed above. Average wafer thickness was 235 μm (.0093 in.). Taper and bow were 65 μm (.0026 in.) and 150 μm (.006 in.) respectively. The high bow can be attributed to the interruptions caused by the feed dropping.

We also tried Test #2-5-13 using .10 mm (.004 in.) blades and .41 mm (.016 in.) spacers, since we hoped that the reduced shock loads would extend the life of the thin blades. The large spacer was chosen because the blade packs were on hand, having been ordered for possible use with the alignment device. The blades were 4.8 mm (3/16 in.) high, rather than the standard 6.35 mm (1/4 in.) high, since that is the size Varian stocks in the thin blades.

Sincw we were testing blade lifetime rather than wafer quality, we cut a partially used half ingot.

Because of feed sticking, compounded by the low feed force necessary with the thin blades, it took 21.75 hours to cut the half-ingot. However, no blades broke. This is a very significant improvement over the typical .25 hour blade lifetime observed earlier, and indicates that the bounce fixture makes it possible to cut with the thinner blades.

We then ran another test (#2-5-20) of the thin .1 mm (.004 in.) thick blades: the conditions were identical to Test #2-5-13 except we cut a full ingot.

Cutting time was 75 hours. The blades were worn to about 0.5 mm (0.02 in.) height. The cut was not completed: the blades were within 12.5 mm (0.5 in.) of the bottom of the ingot when they began to break due to the long cutting time and consequent blade wear.

The failure to finish the cut can be attributed to feed sticking. This can be corrected by installing a redesigned feed. We were very encouraged by the long lifetime of thin blades possible with the bounce fixture.

The original bounce fixture exhibited feed sticking problems and was an add-on (which stuck up into the ingot mounting area and halved the machine capacity). The original fixture was also inadequately shielded against slurry and wore out quickly. To continue the investigation, we fabricated a built-in bounce fixture and electric motor feed with closed loop force control. Initial

tests had to be conducted using constant cutting rate, since the cabinets for the electronics (on order for six months) did not arrive until the end of the contract.

Test #2-5-21 was run to test the new bounce fixture. At the request of JPL, we used a 100 μm (0.004 in.) thick blade and 300 μm (0.012 in.) thick spacer to cut 25 wafers/cm. The cut rate chosen was 0.64 μm/sec (0.0015 in/min). All other conditions were standard.

From the beginning, the fixture rocked excessively with the stroke. Adjusting the cut rate (and, therefore, spring compression) made no difference. After 32 hours of cutting, most of the blades broke. They were worn to 38% of their original height. The blade wear was much more than expected. The cut depth was 57 mm, 57% of the full cut.

The fixture was a success in that the blade lifetime was significantly extended over that obtained without the fixture (.25 hour typical). It was not certain whether the bounce fixture pin-bushing fit was too loose or whether the pins and bushings were too small, causing the excessive rocking.

We obtained hardened, oversize dowel pins and hand-fit them to the bushings. We then ran Test #2-5-22, a duplicate of #2-5-21 (all conditions were standard except the blades were 100 μm (0.004 in.) thick and the spacers were 300 μm (0.012 in.) thick, cutting 25 wafers/cm, and the cut rate was set at 0.64 μm/min (.0015 in/min) because the constant force system was not installed).

Initially, little rocking was noticed. As the kerf length (and, therefore, drag force) increased, the rocking returned. After 34.5 hours, at 60% of full cut depth, severe blade breakage occurred, and we terminated the run.

Two runs of the new 686 bounce fixture have now yielded the same results, but significantly shorter blade lifetimes than obtained with the first crude model. The with-stroke rocking is probably the cause. Test #2-5-22 showed that the cure is to increase the pin and bushing diameters. However, time constraints again prevented us from testing this.

10.7 Blade Alignment Improvements

Technique of Blade Alignment

It was previously described that very small (approximately .1 micron) variations in blade and spacer thickness could result in rather significant (10 to 50 micron) vertical and horizontal mis-alignments of blades when accumulated over hundreds of components as in a typical multiple blade package. The blade used to cut very thin slices with a minimum of kerf loss must be capable of very accurate passage through the ingot without exerting loads on the very delicate slices. The blade is also constrained to be relatively unstable due to its narrow width, and is susceptible to load induced distortion. With even a small degree of blade misalignment, these conditions are worsened. It is the misalignment of blades that limits the MS process, and thinner blades of larger

numbers of components will increase the tendency of blades to wander. As noted before, blade pack redesign is probably the best solution, but we were unable to attempt this.

Figure 56 shows a schematic of a misaligned blade and a corrective procedure devised to minimize blade misalignment even with large numbers of blades. The blade package is relied upon to roughly space and tension the blades. A set of four positioning combs (rack gears) determines the final location of a blade. The repositioning of a blade is small, thus, loads are minor, but the four distances must be identical within a very small amount. By machining all four combs simultaneously, the variation between spacings is nearly zero and only depends on the run-out of the particular machining operation. In this way, improved alignment which does not depend on the package size is conceivable.

The effect may be to allow higher yield, thinner blades, higher cutting force, improved accuracy, thinner slicing by the MS technique.

Alignment Device: Tests #2-6-01, -02, -03, -04, -05

The alignment device was installed onto a package with 150 0.15 mm blades and 0.35 mm spacers. The installation was facilitated by positioning the rack gears into engagement with the blades prior to tensioning. Both end blades were parallel

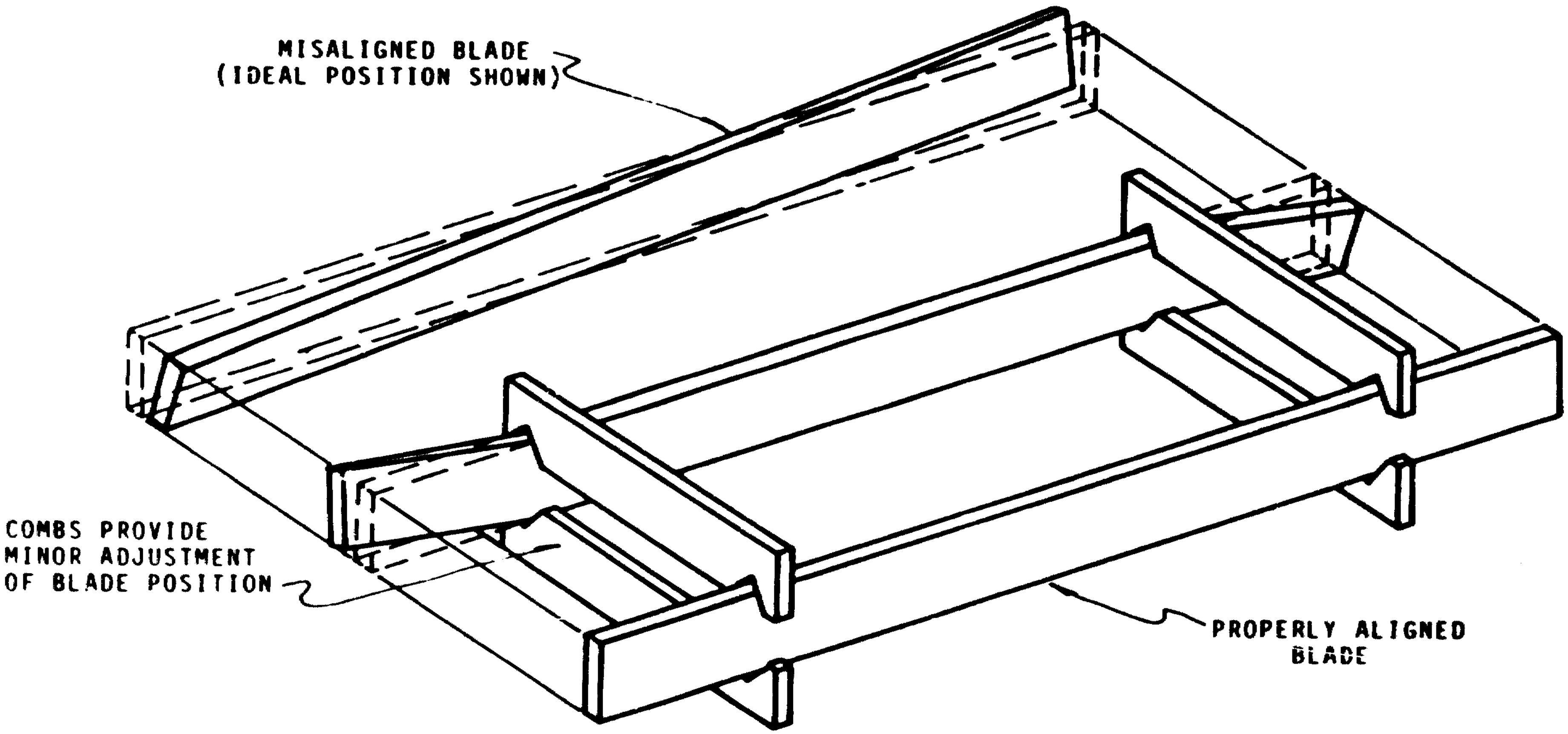

Figure 56. Schematic of Blade Alignment Device

within 2-3 μ, a distinct improvement over normal blade packages. By adjusting rack gear positions, a vertical runout of ± 3 microns was obtained in the four measurable points at the corners of the blade package. Slurry was a standard mix of 0.36 kg/liter. Total cutting time was 23 hours (faster than normal), however, the first half of the ingot was cut with a blade force of 127 grams, rather than 85 grams, by mistake. Total wafer yield was 81% (120 of 149). Slice thickness averages 287 microns with a kerf loss of 221 microns. Wafer accuracy was improved over the best cutting accuracy obtained with 0.15 mm blades. However, the difference was not significant enough to herald success of the alignment device at this point.

A second test of the alignment device was performed using a different installation technique. The blade package was first measured to assure that its width, after compression, could match the exact spacing of the rack gears. Opposing pairs of spacers were replaced with oversized spacers to achieve this condition. The package was fully tensioned, and then the width was adjusted by modulating the side compression. The rack gears were easily engaged at this point. All preliminary alignment went as before except that vertical alignment of one side of the package was off vertical by 75-125 microns. This was averaged over that end of the package, but the variation was not correctable since one gear seemed to be longer than the other. The rest was run with 150 0.15 mm blades, 0.35 mm spacers and 85 grams of blade load with a slurry mix of 0.24 kg/liter.

Cutting appeared to go well, but the ingot broke loose from the submount after half of the ingot had been cut. Measurements of the broken wafer pieces indicated 200 microns of kerf loss and 300 micron thick slices. Bow and taper measurements were not meaningful, but the surface profiles were very impressive. Four new sets of gears were purchased for further testing.

Two further cutting tests were performed using the multiple blade alignment device with identical conditions (0.15 x 6.4 mm blades, 0.36 mm spacers, 85 grams/blade loading, 0.36 kg/liter mix of #600 SiC abrasive).

In the first, #2-6-03, a set of gears used many times was installed. Blade parallelism was within 3 microns, but vertical alignment was, as in Test #2-6-02, out by 60 microns at one end of the pack. Cutting time was 28.3 hours and yield was 53% (10 cm slices). Taper and bow were 50-60 microns average in the vertical direction. Slice thickness was .273 mm with .235 mm kerf loss.

A new set of rack gears was installed for Test #2-6-04. Vertical alignment was only within 20-30 microns, but improved over previous tests. Cutting time was 32.3 hours and 66% yield resulted with 10 cm slices. Slice thickness was .267 mm and kerf loss was .241 mm. Bow and taper were not improved (80 microns average).

Since only minor improvements in slice accuracy resulted from tests with the alignment device, the next step in its test process was to test it using 300 blades (150 have been used previously).

In Test #2-6-05, the device was more difficult to install on the wider pack, but was installed without major problems. Cutting time was quite good, 23 hours. Blade side wear was slightly high (0.05 mm or 0.02 in. or 1/3 the original thickness), and yield was very low (no complete wafers). It seems that the alignment device offered little or no overall improvement even with a full pack. We now feel that the present configuration of the alignment device does not improve the cutting process significantly.

During the test, we monitored slurry temperature and viscosity. Viscosity varied from an initial 164 cps to a high of 330 cps and a low of 123 cps. Temperature varied from 24°C to 34°C. Temperature was, as expected, a function of how long the saw had been running. Surprisingly, viscosity correlated only with temperature. The lowest viscosity was measured at the end of the run. Since previous results indicate that slurry failure is a result of debris accumulation, this means that the debris does not increase viscosity, but may interfere physically with the slurry action.

10.8 Large Saw Tests

Initial Tests: Tests #2-7-01, -02

The first test of the saw was Test #2-7-01. Very conservative conditions were chosen. The blades were .2 mm (.008 in.) thick and the spacers were .41 mm (.016 in.) thick. 131 blades were cutting.

Tensioning and slurry were standard. The ingot reciprocated at 100 RPM.

Due to a failure in the LVDT excitation module, the constant feed force system could not be used: the constant cut rate system was used, cutting at a safe .85 μm/sec (.002 in/min).

No problems were encountered in setting up the saw. Cutting time was 29.7 hours. Yield was 98% at the end of the cut: cleaning breakage reduced this to 88%.

Continuing our initial testing of the large capacity prototype, we ran Test #2-7-02. Again, safe conditions were chosen: 125 blades, 0.2 mm (0.008 inch) thick, spaced 0.41 mm (0.016 inch) apart were used. The force control system was still inoperative, so a safe cut rate of 0.85 μm/sec (0.002 in/min) was selected. This test was intended to check some minor adjustments in the drive system and bladehead support.

After consulting with JPL, we decided to terminate the run 1/4 of the way through the cut and replace it with a full capacity test, #2-7-03.

Full Capacity Tests: Tests #2-7-03, -04, -05, -06, -07, -08, -09, -10, -11

For Test #2-7-03, we used our standard blade pack, 0.15 mm (.006 inch) thick blades spaced 0.36 mm (0.14 inch) apart. 975 blades were used, cutting an ingot 495 mm (19.5 inch) long.

A major problem occurred in the setup. The tensioning mechanism, as discussed earlier, is a toggle clamp type (two opposing corners of a diamond-shaped linkage are drawn together by a bolt, forcing the other two corners apart). The lengths of two adjacent arms are adjustable by wedge blocks. The wedge blocks as received were slightly too large, but were used in the first two runs since the higher mechanical advantage obtained when the corners come close together was not necessary to tension the small packs we were using.

For the full capacity run, we needed the maximum mechanical advantage, so we ground the wedge blocks. We assembled the tensioning mechanism and set the arm length to give an extension of 3.05 mm (0.120 inch) with no blades in the head (there are springs built in to give some resistance to extension). The 20% extra extension was to allow for better pivot seating with the extra force required for a full pack.

Unfortunately, the amount of pivot seating was grossly underestimated; in addition, the arms on one side were slightly unequal in length. Although we monitored the clamp positions during tensioning to avoid locking the toggle linkages by making them too straight, one side straightened completely at 70% of desired elongation, and resisted all our efforts to unlock it.

The only way to unlock the clamp was to cut all the blades to remove the locking force. Here again events conspired against us: a recent, unexpected blade pack order had depleted our supply of the 0.15 mm (0.06 inch) thick blade stock. The pack in the machine had been assembled by tearing down inventoried packs. A new stock of steel had entered customs, and was not expected in the plant for 5 days, by which time the yearly 2 week plant refurbishment shutdown would have started, and pack assembly area would not be working. Since we could not obtain more blade packs for about 3 weeks, we decided to run with the low blade tension we had obtained.

The run was started and we found that our normal sheet-type slotted slurry distribution pipe could not reach the edges of the pack. Wafer breakage started at the ends, and by the time the run was through all wafers were broken. However, we feel that the tensioning and slurry distribution problems were sufficient alone to account for the breakage. The fact that breakage did not start in the center, where the worst-aligned blade is expected, indicated that blade alignment may not be the limiting factor in use of the large prototype.

Test #2-7-04 was run using the same parameters as #2-7-03, and was also a full capacity test. The tensioning mechanism was properly adjusted, and full tension was achieved easily. A slurry dispenser tube with many small holes instead of a slot was used. This dispenser was acceptable but tended to clog, so a better solution for slurry dispensing must be found.

The run was extremely successful almost all the way through. Yield was 99%+ up to the last 10 minutes of the cut, at which point many wafers broke loose from the submount. Final yield was 36%. Cutting time was 36.7 hours. The wafers were quite good; bow was 66 μm (.0026 in.) and taper was 82 μm (.0032 in.).

When we inspected the submount where the wafers had broken away, the submount proved to clean of adhesive. Either insufficient adhesive was applied or the adhesive weakened from being held at working temperature too long. In either case, the run would have been extremely successful but for our error in bonding the work to the submount. As it was, the run was moderately successful.

In Test #2-7-05, we first tested the feed force controller. This controller uses the fact that the ingot is mounted on a spring loaded table, much like the bounce fixture. The deflection of this table is sensed by an LVDT, and the resulting signal is compared to a reference signal which is proportional to the desired total load. Depending on the results of the comparison, the motor driving the bladehead into the work is sped up, slowed down, or kept at constant speed. To avoid instability, the signal to the motor is the integral of the "error" or difference between the LVDT and reference signals.

The run started very well. Cutting rate was high, so we increased the load to full load very slowly.

About 1/3 of the way through the run, a banging noise was noticed. Hindsight shows that this was due to a worn bearing. The bearing had accumulated slurry due to insufficient slurry bucket sealing.

At the time of the run, we could not tear down the machine sufficiently to discover the worn bearing without terminating the run. It seemed (wrongly) that the noise was something banging against the inside of the slurry bucket, and that shortening the stroke reduced the noise for a while.

The operator continually shortened the stroke until the final stroke was about 50 mm (2 in.). Since the volume of blades worn away is roughly constant, this short stroke caused excessive blade height wear. With about 2.5 mm (.1 in.) of ingot left to be cut, blades started breaking. By the time the blades were sufficiently into the submount to remove the wafers, enough blades had broken to make the final yield 31%.

Cutting time was long, 41.6 hours, again because of the short stroke. NTV was 105 µm (.004 in.) and bow was 324 µm (.013 in.). These were also probably a result of excessive blade wear.

In spite of the problems, the feed force controller worked very well, and we still felt that our problems were associated with learning how to use the prototype.

The major problems we had noted at this point were: 1. short bearing lifetime due to insufficient slurry shielding, 2. electronics

failures due to the breadboard nature of construction, and 3. lack of an indication of end of stroke "bounce" so the operator had difficulty deciding when to shorten the stroke.

The bearing lifetime problem has not yet been solved. We also started design and construction of a more reliable, better built electronic system. A bounce readout was fabricated and installed, and the noise sensitivity was decreased by careful grounding and shielding.

Test #2-7-06 was run as a test of the bounce readout device. The blade pack was our "baseline" 150 μm (.006 in.) blade and 350 μm (.014 in.) spacer, yielding 20 wafers/cm. 940 blades were easily extended to full elongation. All other conditions were standard.

Some minor mechanical and electrical problems were encountered during the run (e.g., slurry drain blockage), but none were serious enough to cause termination of the run. Cutting time was 39 hours, although this number is somewhat suspect because of the large number of starts and stops to fix minor problems. Very near the end of the run, two groups of wafers broke off near one end of the ingot, totaling 90 broken wafers. Thus, cutting yield was 90%. Solely since we are not experienced with such large numbers of wafers and do not have enough casettes to hold them all, cleaning breakage reduced the yield to a still respectable 74%. Average wafer thickness was 267 μm (.0105 in.), taper was 124 μm (0.005 in.) and bow was 155 μm (0.006 in.).

Although the wafer thickness was somewhat low, the taper was somewhat high, and the bow was very high, we feel this run was very successful. The thickness, bow, and taper we attribute to the starting and stopping to fix minor problems. This run proved that the large saw is capable of producing high yield runs of 100 mm diameter silicon wafers, using baseline conditions, producing 20 wafers/cm.

Test #2-7-07 used .1 mm blades and .35 mm spacers to cut over 1000 wafers at 22 wafers/cm. The test was stopped due to excessive vibration and banging. We determined that slurry had entered the ball bushings which support the workpiece carriage, and the shaft on which the bushings ride was worn. We accomplished the difficult job of rotating these shafts, to bring fresh surface into contact with the bushings, without removing the ingot or blades.

When the run was restarted, some improvement in noise and vibration was noted but something else was obviously wrong. Investigation showed that the frictional stroke adjustment lock had slipped, the stroke had lengthened, and the ingot was banging against the bladehead. Since the ingot was severely chipped and the severe banging had fatiqued the LVDT connections (incapacitating the force controller), we terminated the run.

At this point we paused to rebuild the large saw as much as possible without making major design changes. The bladehead was removed, disassembled, cleaned, and reinstalled. The tensioning

bolts were replaced. All bearings were replaced. Bellows were added on the carriage support rods to protect them from slurry. Rubber curtains were added to the slurry pan for increased splash protection. A carriage drive rod sealing system was fabricated and installed: this system allowed the top of the walking beam to move vertically on ball splines, and the carriage drive rods passed through seals and ball bushings in the slurry pan wall. The drive rods proved too small to lift the top of the walking beam: they bent instead, so the system was removed for fear of fatigue problems. Splash guards were installed over bearings outside the slurry pan to protect them from slurry brought out on the carriage drive rods. A better-built force controller was installed. The bounce indicator circuit had proved unusable, so we used an oscilloscope to display the LVDT signal and read off bounce. The stroke adjustment system was cleaned of accumulated lubricant (which seemed to cause the slippage problem), the gears were replaced, and more screws were added between the friction ring and flywheel since failure of these screws under the frictional clamping force had been noticed. The slurry pan drain was enlarged to prevent clogging. Since slurry pump "starvation" had been noticed when slight drain clogging lowered the slurry level, we reworked the slurry bucket to allow the pump to sit lower in the slurry.

Test #2-7-08 was run using standard conditions. 975 blades were cutting. Initial cutting rates were quite high, so we increased the feed force to its full value quite slowly. No mechanical problems were noted. Almost halfway through the ingot, the wire connecting the carriage (going to the LVDT) to the slurry pan wall shorted from abrasion. The wire was spliced and lasted through the rest of the run. Problems were encountered when the perforated slurry dispenser tube kept clogging.

Wafer breakage started about the halfway point, and continued till the end. Most breakage occurred in the middle. Final was about 40-50%, and cut time was 28 hours. Wafers were not counted or measured.

Investigation revealed two problems. The operator noted that bounce could not be reduced for long by stroke shortening: the adjustment system may have been slipping. More obviously (after the run) and seriously, an IC failed in the LVDT module, causing feed forces to be about 2.5 times those set on the front panel.

We replaced and tested the IC, cleaned the stroke adjustment mechanism, and replaced the static dispenser system with a reciprocating electric pulsed dispenser similar to the standard 686 dispenser.

Test #2-7-09 was a duplicate of #2-7-08. The reciprocating slurry dispenser failed at almost halfway through the cut and was replaced with the perforated static tube. Some blades broke near the end. Within 5mm of the end of the cut a large section of wafers broke out, and yield was a low 20-30%. Cutting time was 30.5 hours. Wafers were not counted or measured.

We replaced the slurry dispenser again with a pneumatic reciprocating dispenser as used on the 686, except that the slurry was pulsed. Test #2-7-10 was run at the request of JPL to cut 25 wafers/cm using .10 mm blades and .3 mm spacers. A bumping sound was noticed during the run which seemed as if a carriage support bearing was worn. The machine was partly disassembled, and the bearings and rods seemed fine. A blade broke after 13 hours of cutting. At 17 hours, severe blade breakage started and at 20 hours the cut rate slowed, and the majority of blades and all wafers broke. Investigation showed that the stroke adjustment mechanism had once more slipped, allowing the ingot to bang against the bladehead. The high shock forces probably caused the blade breakage. The stroke adjustment system was reworked to include O-rings for increased friction.

In Test #2-7-11, we retreated from 25 to 22 wafers/cm, using .15 mm blades and .3 mm spacers. This run went very well until the very end. The only early problem was that the screws clamping the ingot to the carriage loosened at 43 mm cut depth, and the resultant rocking broke 10-15% of the wafers. Little breakage was noted until 91 mm depth (about 1 mm before entering the glass ingot submount) when all wafers broke. The wafers were extremely hot, almost too hot to touch, which is extremely unusual.

The reason for this problem is not definitely known. Some rocking of the spring-supported carriage top plate was noticed: the bushings may be slightly worn. When the slurry was mixed,

it seemed thick, but seemed normal during the run. After the run it seemed thick again. Several normal runs, both for JPL and others, were made using the same lot of oil and abrasive both before and after this run: an error may have been made in mixing the slurry.

10.9 Other Experimentation

Bladehead Accelerations

We have been considering the possibility that yield or accuracy could be improved by changing the nature of some machine functions rather than manipulating the basic abrasion system. Specifically, one possibility is that the "bounce" at the end of the stroke due to worn blades, while helping slurry transfer by creating a pumping action, may break wafers or cause blades to wander due to high shock loads. Tests concerning this are discussed below.

The other possibility we have considered is bladehead lifting with consequent cocking of the bladehead on the ways. This seems impossible at first glance, since the bladehead weighs 114 kg (250 lbs.) and the maximum feed force (with a full blade pack) is only 25.5 kg (56 lbs.). However, excellent results were obtained cutting upside down (pushing the ingot down onto the blades). The two differences in upside down cutting are the direction of gravity and the direction of the feed force. Since the bladehead is being pushed down onto the ways in upside down cutting, we felt it to be worthwhile to investigate the bladehead motions.

A quartz piezoelectric accelerometer with less than 0.9% cross-axis sensitivity was mounted on one corner of the bladehead for a standard run and an "upside down" run. Acceleration measurements were taken before, at the beginning, and during the run. The upside down run was made on the machine with the shock absorbing drive arm.

The significant results are shown in Figures 57, 58 and 59. Each figure includes one complete bladehead reciprocation, with the end-of-stroke points marked by the pulses they cause. The end of stroke points do not occur at the same point in each figure because the oscilloscope trigger and single sweep were not working properly together, so the sweeps were hand-triggered. We do not have the facilities to calibrate the accelerometer, so the vertical scales are not calibrated in acceleration. The vertical scale in each figure is 50 mV/major division. All measurements shown were taken at approximately 38 mm (1.5 in.) cut depth and an end-of-stroke bounce of 0.38 mm (0.015 in.) which is 1/2 the maximum we ever allow before shortening the stroke.

The vertical acceleration, Figure 57, is decreased greatly in the upside down mode. The lateral (horizontal and perpendicular to the stroke) acceleration is only slightly reduced; this means that cocking of the bladehead on the ways is unlikely. The acceleration in the stroke direction is also reduced in the upside down cut; this is probably due to the cushioned drive arm. The measured vertical acceleration in the standard configuration

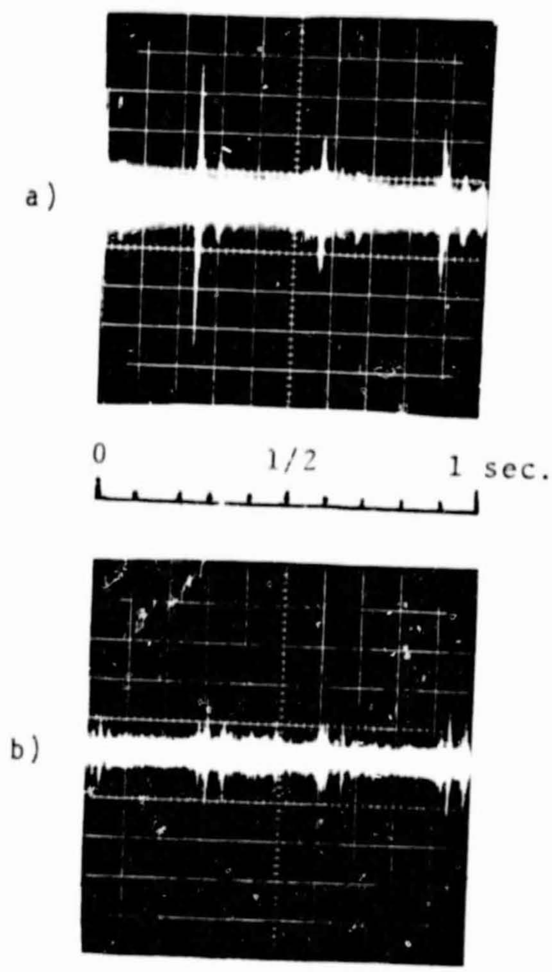

Figure 57. Vertical Bladehead Acceleration

a) Standard Cut

b) Upside Down Cut

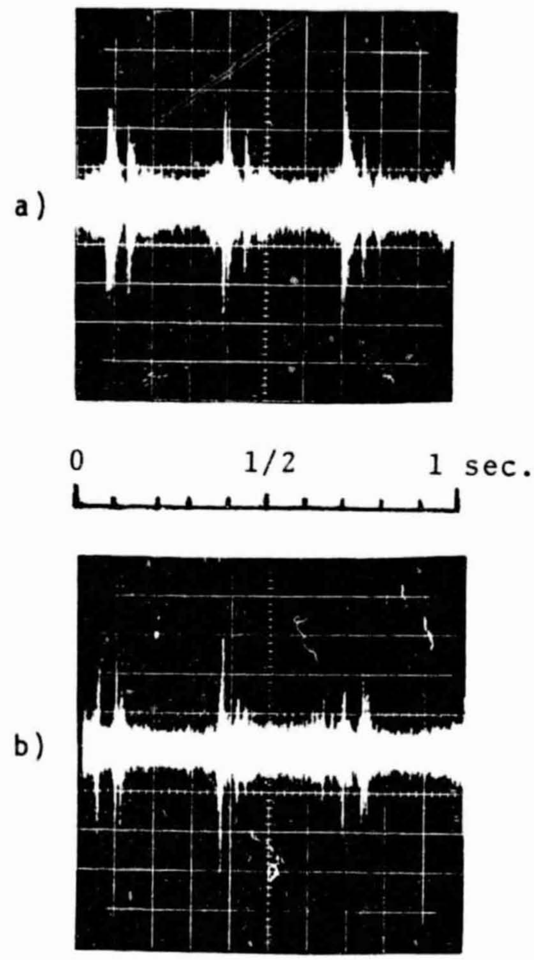

Figure 58. Lateral Bladehead Acceleration:
a) Standard Cut
b) Upside Down Cut

a)

b)

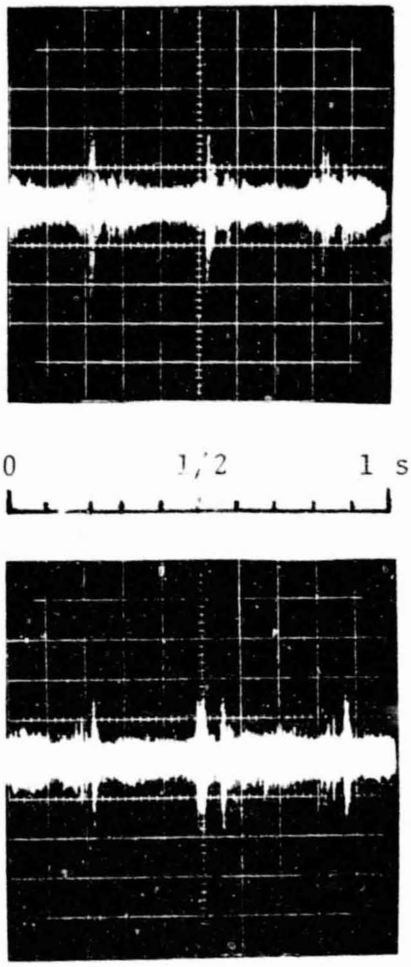

Figure 59. "With Stroke" Bladehead Acceleration:
a) Standard Cut
b) Upside Down Cut

indicates the magnitude of shock load resulting from the imposition of ingot "bouncing". This may be the current limit of thin silicon wafer slicing, and the source of cracked wafers.

Investigation of Suspension Media

We investigated the possibilities of using various oil or water based suspension media for slurry sawing. In the suspension tests, we worked with our standard suspension oil (PC oil) and a new oil manufactured by the Lubrizol Corporation (Lubrizol 5985).

Attempts to use straight 5985 were disappointing. The best results were obtained using 1/3 the amount of abrasive normally used in PC oil (0.36 kg/l). A portion of the wafer breakage problems may be traced to machine problems (poor yield in standard cutting tests). It is possible that some wafer breakage was due to abrasive failure, abrasive settling, or some other mode of failure, all due to the small amount of abrasive in the system.

In the meantime, we carried out a more structured investigation of the two suspension oils. The first steps were consideration of important differences and characterization of the two oils.

Comparison of 5985 and PC

The major differences between 5985 and PC are:

1. Different suspension power (5985 holds abrasive in suspension longer).
2. Viscosity (5985 is less viscous).
3. Suspension method (5985 uses a dissolved polymer, PC uses colloidal clay platelets).

We feel that the suspension method does not affect the cutting process significantly (although it may affect reclamation).

It seems likely that the suspension power and/or viscosity affect the cutting process through abrasive transport. The cutting process is controlled not by the actual abrasive mix but rather by the "effective mix" (i.e., a measure of the number of active particles at the cutting interface). Greater suspension power and/or lower viscosity might well increase the effective mix by transporting particles to the cutting interface more efficiently.

The first step in our systematic investigation must be to identify the important variables.

Characterization of Oils

The viscosities of both oils were measured using a Brookfield LVF viscometer with the #2 cylindrical spindle. The samples were 550 ml of the test fluid in a 600 ml Griffin low form beaker (KIMAX #14000). The spindle-beaker combination were calibrated with silicone oil viscosity standards (92 cps $\pm 1\%$ and 505 cps $\pm 1\%$). The temperature was $25° \pm 1°C$ in in all tests. The results are presented in Figure 60 and discussed below.

Suspension power was measured by static settling tests. 50 g of PC, 5985, or 5985 cut with 130 cps mineral oil were mixed with 20.85 g of #600 SiC (corresponding to a standard PC mix: note that the specific gravity of all the oils ranges from 0.89 to 0.91). These mixtures were shaken and allowed to stand until significant settling took place.

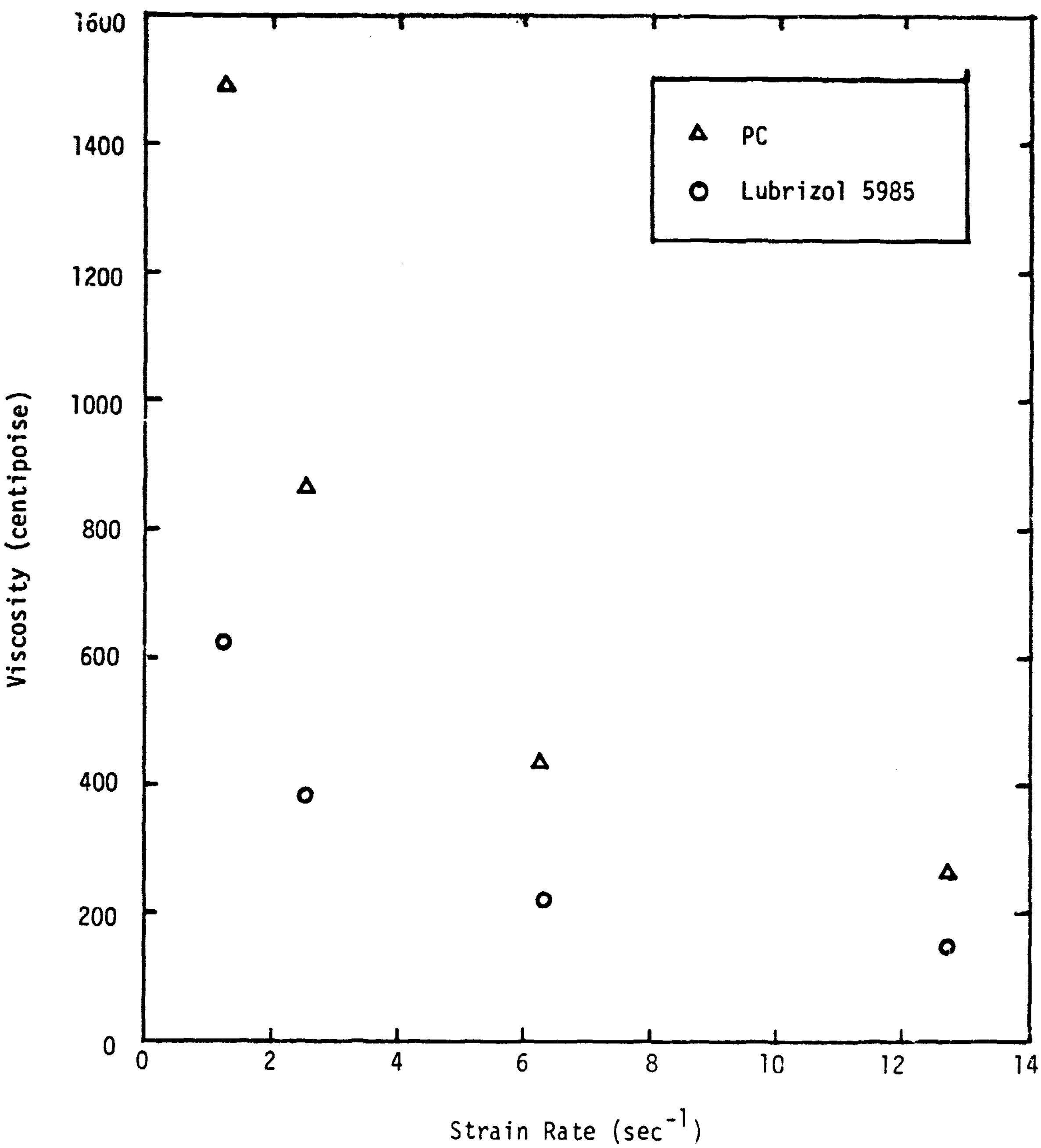

Figure 60. Viscosity of Suspension Oils

PC oil is a thixotropic fluid: the viscosity depends on both strain rate and history. The viscosity decreases asymptotically with time at a given strain rate. This is not surprising, since the clay platelets probably line up as shearing proceeds. The viscosities in Figure 60 are asymptotic viscosities.

PC settles by loss of suspension power. Both the platelets and abrasive settle, so that a clear oil area forms at the top, with a homogeneous mixture of abrasive and platelets below.

Lubrizol 5985 is a pseudo-plastic fluid (on the time scale investigated): the viscosity depends only on strain rate. Only the abrasive settles out: larger abrasive particles settle faster, so a three-layer structure forms: a thin layer of oil and suspension agent above a region of oil, suspension agent, and fine abrasive particles above a cake of fully settled particles.

It is essentially impossible to match 5985 and PC by diluting 5985. Consideration of Figure 60 shows that the viscosities can be matched at all strain rates by diluting 5985 with carefully tailored pseudo-plastic fluid (a difficult job !).* We do not know if the thixotropic nature of PC is important. However, it seems that a reasonable viscosity match may be obtained by mixing

---

* The strain rate in MS slicing varies during each stroke from 0 to approximately 10^5 sec^{-1} , with an average value of 5×10^4 sec^{-1}.

5985 with a mineral oil chosen to give a viscosity of around 250 cps at 12.5 sec^{-1}.

Matching suspension power is also difficult because 5985 forms a cake at the bottom and PC does not. On the basis of clear top area, it appears that a mixture of 40-45% 5985 matches PC best.

Blending

The blending tests concentrated on the viscosity and suspension power of the fluid. As discussed above, we considered viscosity and/or suspension power to be the important variables in a suspension fluid. If the viscosity and suspension power of PC could be matched, and this blend performed like PC in cutting, then we would have an easily variable suspension fluid with which to explore the effects of viscosity and suspension power.

In the blending tests, 53 different oil-additive blends were tested. LZ 5985 additive concentrations were varied from 0 to 30% by weight, and base oil viscosities were varied from 80 cps to 300 cps (at 25°C). Samples were prepared by successive dilution from the sample in each series with the highest additive percentage. Viscosities were measured at four strain rates using the Brookflied LVF viscometer with cylindrical spindles. 50 ml of each sample were then mixed with 18 g of #600 silicon carbide abrasive (corresponding to the standard 0.36 kg/l mix) and the mixture was allowed to settle in a sealed vial.

The results of the viscosity tests are too numerous (and not important enough) to present completely here. The large number of tests was necessary because of extremely nonlinear behaviour as a function of additive concentration. Sample results, for the blend finally chosen to match PC, are shown in Figure 61.

From Figure 61, it would appear that "imitation PC" is a poor match for PC in viscosity; however, these viscosities were measured without abrasive. For final matching, viscosities were measured in the settling vials (with abrasive) at 60 RPM using the #2 disk spindle (to avoid abrasive damage to the cylindrical spindle). Because of the small sample size and the disk spindle, strain rate could not be calculated: the strain rate was higher than any shown in Figure 61 and closer to that encountered in slurry sawing (10^4 sec^{-1} average). Therefore, this test was used as the final viscosity match. Surprisingly, adding abrasive to PC lowered the viscosity to 247 cps. Adding abrasive to imitation PC increased the viscosity to 247 cps. The reason for the unusual behaviour of PC when abrasive is added is not known.

As in the viscosity tests, the settling test results are too extensive to present fully. Typical results are shown in Figure 62. Since the slurry is stirred by the pump, we decided that the match should be on the basis of the shortest measurable settling time.

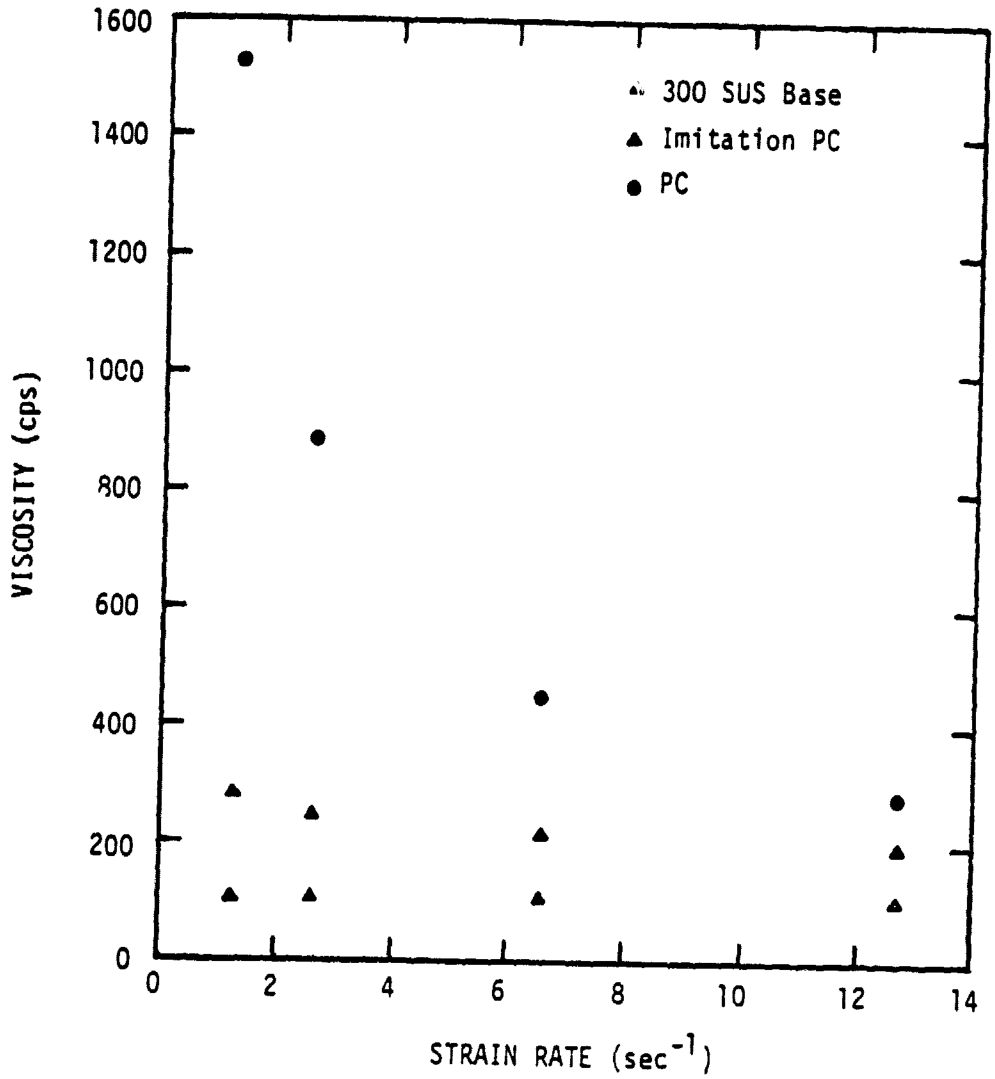

Figure 61. Viscosities of Various Blends

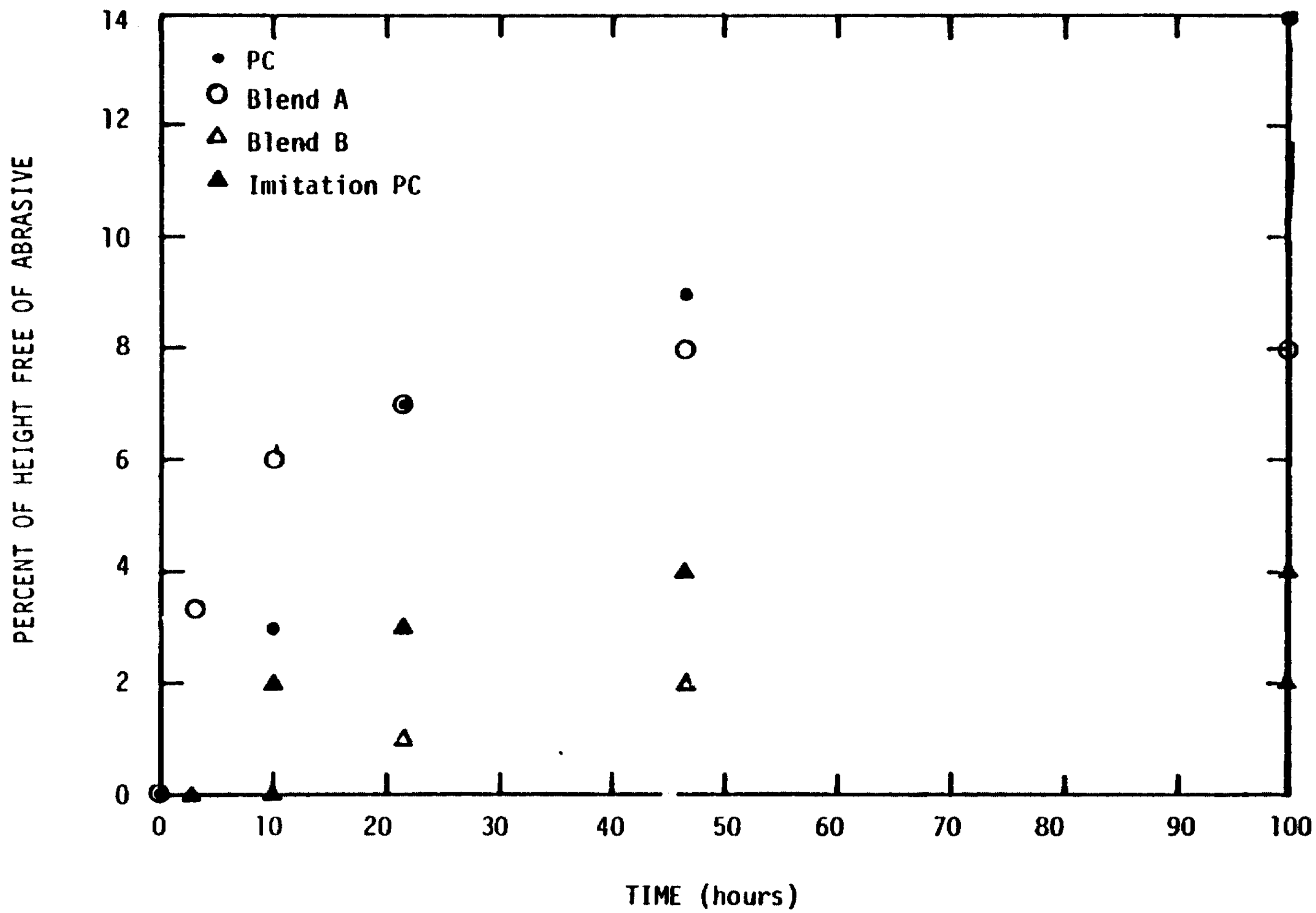

Fiqure 62. Sample Settling Test Results (Blend A is imitation PC base plus 17.5 wt.% additive; blend B is imitation PC base plus 22.5 wt.% additive).

Once we had defined imitation PC (80% by weight 300 SUS mineral oil (113 cps @25°C), 20% by weight LZ 5985 additive), we ran a cutting test to establish the similarity to PC. As reported earlier, a film formed on the blades. This caused high drag loads, leading to wafer breakage and motor overheating.

The reason why imitation PC behaved so differently from both PC and Lubrizol 5985 is not known. One possible explanation arises from an observed difference in settling between imitation PC and 5985. In imitation PC, the abrasive settles relatively fast and the additive remains in solution (as shown by the cloudiness of the cleared area). In 5985, the abrasive settles much slower and takes the additive with it. Although the concentration of additive in 5985 is unknown, it is certainly higher than 20%. It is possible that in 5985, the major effects on an additive molecule are due to neighbor additive molecules, while in imitation PC, the major effects are due to neighbor oil molecules. This difference could lead to deposition of additive on the blades, forming the above mentioned film. Also, "lubricity" (which is important to drag when clearances are small) was not considered here.

Cell Fabrication

A set of 20 silicon wafers cut on the MS saw was sent to Solar Power Corp. for fabrication into solar cells in their standard commercial processing line. The slices were 10 cm diameter with a nominal thickness of 300 μ. Of the twenty wafers,

only 1 survived the complete processing sequence. One was broken in shipment, 7 broke during the boron diffusion step and 11 others broke during other process steps. The remaining cell produced V_{oc} of o.55V, I_{sc} of 1.68A, maximum power (P max) of 0.67W and a fill factor of 0.725 at 100 mw/cm^2 illumination and 28°C. This represents an efficiency based on full wafer area of 8.53%, (8.97% based on 9.75 cm diameter applied cell area). Since the potting compound acts as part of the AR coating system for Solar Power's cells, the performance cited above is expected to improve by 10% in a completed panel. Therefore, the efficiency of this cell may be characterized as 9.4% based on the 10 cm wafer of 9.9% based on the size of the active cell applied.

Surface Damage Removal by Etching

Samples of standard MS sawn wafers were cut into 2 x 2 cm pieces and etched with either Nitric-HF (planar) or Transene Solar Cell Etchant 100 (texture) to remove variable amounts of surface material. Tables 10 and 11 show a summary of the average material removal from the groups of wafers. Figures 63 and 64 show the etch rate. The results indicate a wide range of consistent damage removal.

The wafers were fabricated into solar cells by an outside vendor. Cells were manufactured with AR coating. The cells were tested under AMO conditions with illumination of 135.3 mW/cm^2 at

TABLE 10

RESULTS OF MS SILICON WAFER ETCHING WITH NITRIC-HF ETCHANT *

DESIGNATION	NO. PCS.	ETCH TIME (min)	REMOVAL MICRONS/SIDE	STD. DEV.
01	24	0:00	- -	- -
02	24	0:20	2.60	0.05
03	24	0:40	4.64	0.09
04	24	1:10	6.95	0.22
05	24	1:40	8.13	0.16
06	24	2:20	12.04	0.31
07	24	3:20	15.06	0.28
08	24	4:15	19.13	0.41
09	24	6:30	31.95	0.51
10	24	8:30	44.44	1.28
11	24	11:00	52.61	0.95
12	24	15:00	61.38	0.81

* Wafer size 2 x 2 cm, Etch temperature 25°C

TABLE 11

RESULTS OF MS SILICON WAFER ETCHING WITH ANTIREFLECTIVE ETCHANT *

DESIGNATION	NO. PCS.	ETCH TIME (min)	REMOVAL MICRONS/SIDE	STD. DEV.
01	24	0:00	0	- -
02	24	1:00	1.51	0.16
03	24	2:00	2.93	0.39
04	24	3:00	6.31	0.51
05	24	4:00	7.64	0.45
06	24	5:20	9.96	0.69
07	24	8:00	15.79	1.16
08	24	10:00	15.91	1.34
09	24	15:00	24.55	1.34
10	24	20:00	29.86	0.95
11	24	25:00	40.05	1.97
12	24	35:00	52.32	2.47

* Solar Cell Etch - Type 100, Transene Co., Etch Temperature 101-103°C

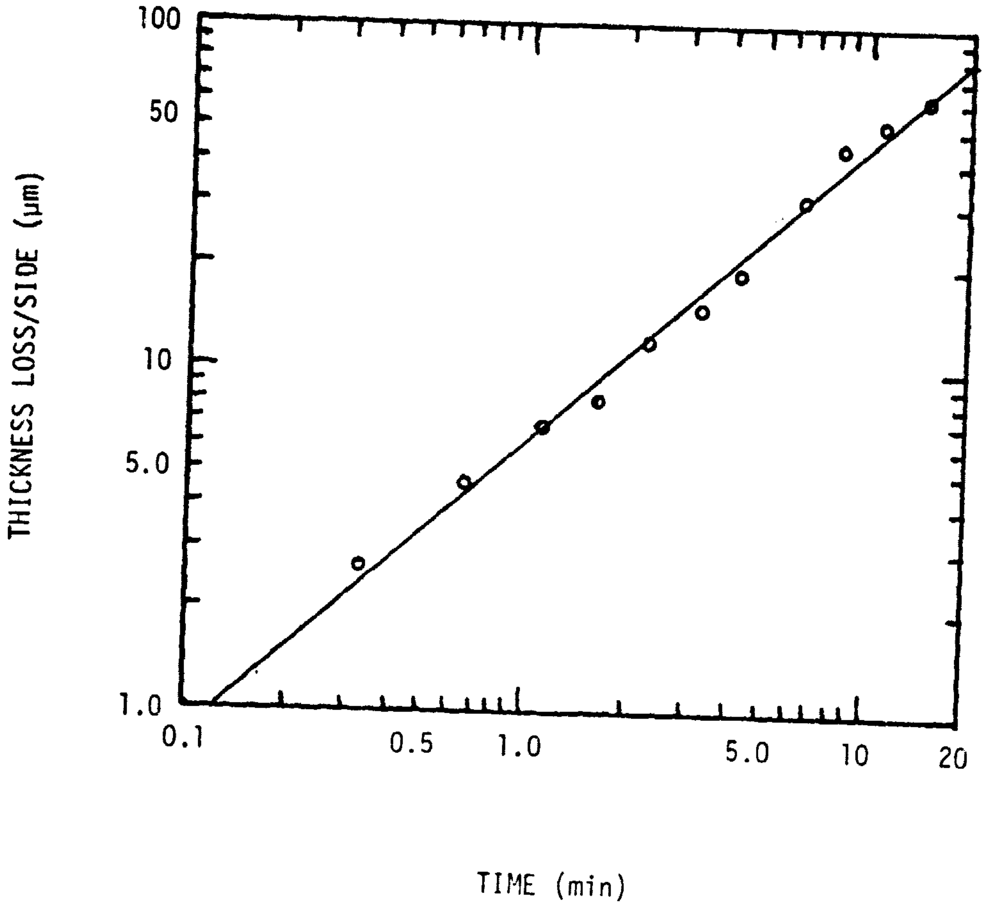

Figure 63. Thickness Loss (Based on Weight loss) from 20 x 20 mm Slices in Planar Etch. (T = 24°C. Line shown is least squares fit:

$\mu = \left\{6.09^{+0.92}_{-0.80}\right\} t^{(0.85 \pm 0.09)}$, 99% confidence level)

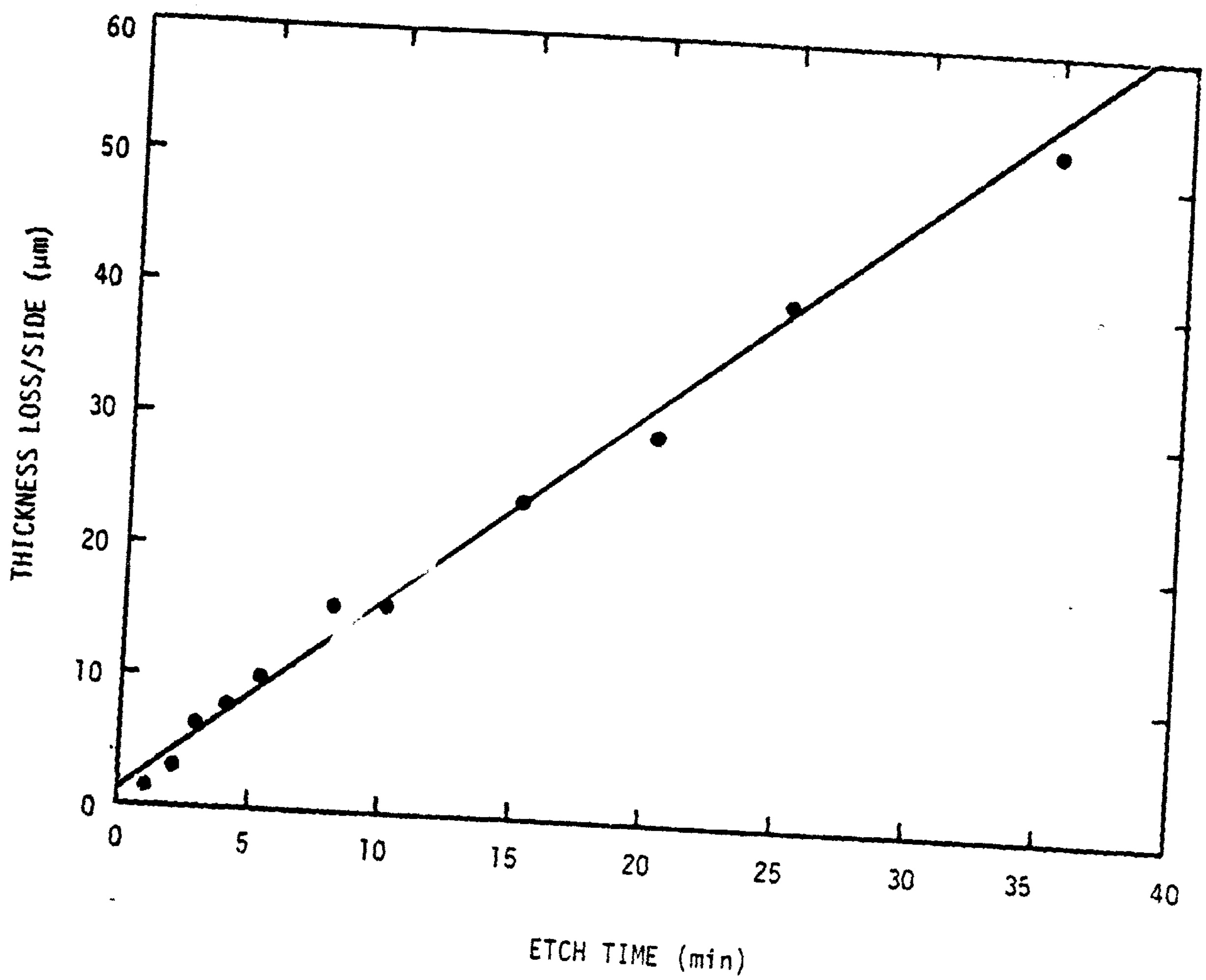

Figure 64. Thickness Loss (Based on Weight Loss) from 20 x 20 mm Slices in Antireflective Etch. (T = 102°C. Line Shown is least squares fit: $\mu = (1.17 \pm 1.49) + (1.53 \pm 0.12)t$, 95% confidence level)

28°C. The results are presented in Figures 65 and 66 and the raw data is contained in an appendix. (Some of the data was discarded in preparing Figures 65 and 66. "Outliers", the extreme values, were checked by computing the ratio of the standard deviations with and without each outlier. This statistic is tabulated. Outliers with less than 5% significance were rejected and the process repeated until no further outliers could be rejected.)

The efficiencies obtained are somewhat low and their range is somewhat high. However, the control (ID sawn) wafers for each group obtained average efficiencies of only 11.5% (4 wafers). It is likely that process optimization would allow fabrication of slurry sawn wafers as good as the ID sawn wafers.

The most significant result shown in both Figures 65 and 66 is that the optimum removal amount is in the range 5-15 μm per side. This agrees with previous work done at JPL and is extremely significant to the economics of the slurry sawing process.

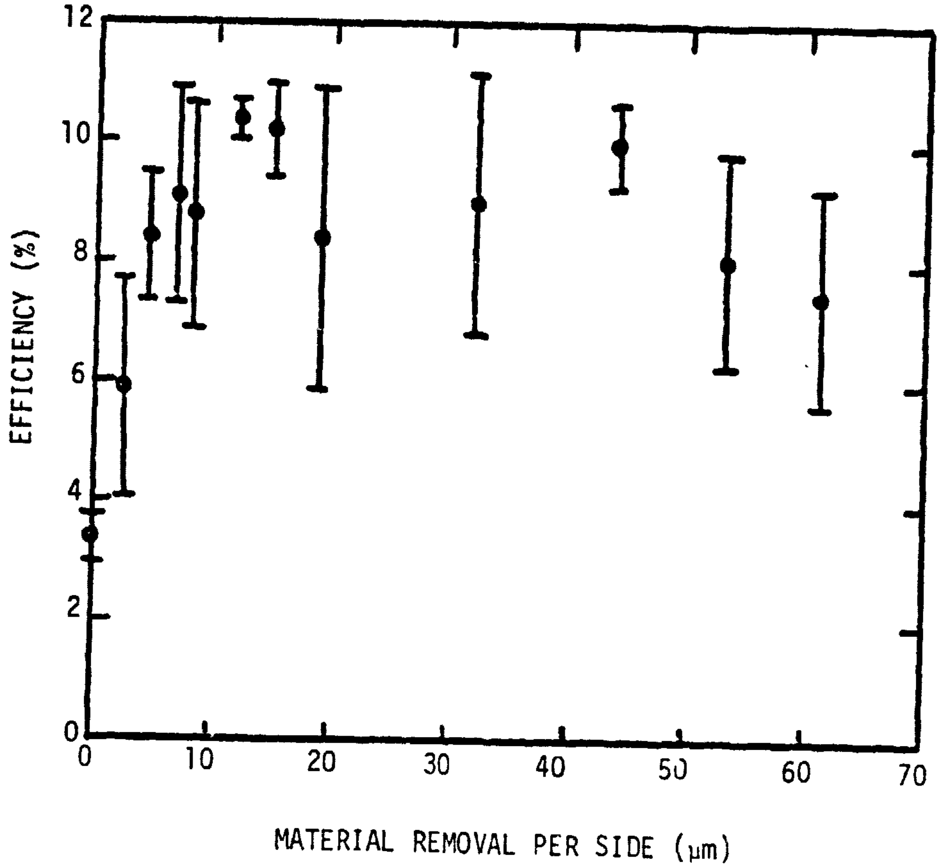

Figure 65. Efficiency vs. Material Removed in Planar Etch. (Bars indicate standard deviation.)

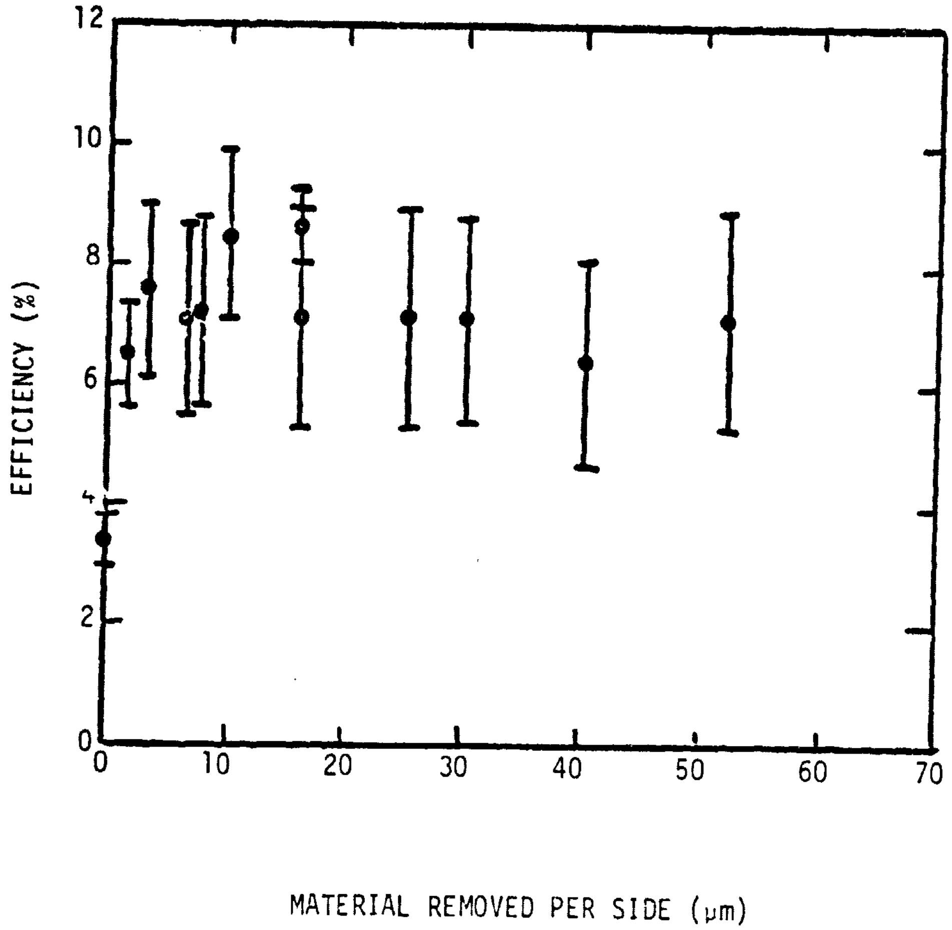

Figure 66. Efficiency vs. Material Removed in Antireflective Etch. (Bars indicate standard deviation.)

11.0 CONCLUSIONS

11.1 General

1. Multiblade slurry sawing may easily be used to produce 16.4 wafers/cm of 100 mm diameter ingot (0.2 mm blades and 0.4 mm spacers) or 17.9 wafers/cm of 100 mm ingot (reducing blade thickness by 0.05 mm) at commercially acceptable yields using commercial technology.
2. Careful use of commercial technology allows cutting of 19.7 wafers/cm of 100 mm ingot (0.15 mm thick blades and 0.35 mm spacers) at or near commercially acceptable yields.
3. Crystal orientation and polycrystallinity have no effect on the slurry sawing process.
4. Ingot residual stress can cause difficulties in the slurry sawing process.
5. 0.14 mm thick wafers can be cut from 125 mm diameter ingot using multiblade slurry sawing.
6. 21.9 wafers/cm of 100 mm ingot have been successfully cut on an experimental basis.
7. The rolling abrasive model of slurry sawing can be used to predict cut rates and other variables from first principles. This model requires further development and experimental verification before it can be used to improve performance.
8. The rolling abrasive model predicts low "bounce" as long as the stroke length to kerf length ratio is small.

11.2 Economics

1. 1980 and 1982 interim sheet generation goals are easily met using commercially available technology.
2. The 1984 interim sheet generation goals may be met by technically feasible extensions of current technology.
3. The 1986 sheet generation goals can be approached, but possibly not met, using feasible, but difficult, extensions of current technology.
4. Required extensions to current technology in order to approach the 1986 sheet generation goals are reduction of expendable materials cost (steel and pack assembly, slurry vehicle, and abrasive costs); reduction of wafer thickness (to 0.25 from 0.3 mm); reduction of blade thickness (from 0.15 to 0.1 mm); and reduction of capital equipment cost (by use of a new, possibly large capacity, saw).
5. The reduction of blade and wafer thickness mentioned above leads to the requirement of 25 wafers/cm or a conversion factor of 1.0 m^2/kg input (including a 95% yield).

11.3 Blades and Blade Packages

1. Blade packs of more than 200-300 blades may present difficulties in maintaining blade alignment.
2. "Add-on" systems to improve blade alignment were not successful.
3. Thin (0.1 mm) blades are susceptible to shock induced fatigue, and cannot be used in unmodified commercial equipment.

4. The lifetime of thin (0.1 mm) blades is extended by a factor of 100-250 by reducing end-of-stroke shock loads.
5. Required steel cost reductions are possible by relaxing straightness and thickness tolerances, doubling blade height, volume buying, and elimination of bluing. Relaxation of thickness tolerances will exacerbate the problem of alignment.
6. Blade wander cannot be explained by a simple or even somewhat complex torsional buckling model.

11.4 Slurry Vehicle

1. Commercial metal cutting oils and Lubrizol 5985 are unsuitable slurry vehicles.
2. The most important factor in oil-based slurry vehicle selection is "lubricity", a parameter which characterizes the drag force encountered with small clearances.
3. Suspension power is not important as long as mechanical stirring allows delivering abrasive to the cutting interface.
4. Mineral oils with sufficient lard oil added to provide lubricity yield good cutting but wafer breakage for unknown reasons.
5. Water-based vehicles exhibit severe blade stress corrosion problems.

6. "Soluble" oils and standard chemical cutting fluid corrosion inhibitors do not solve the stress-corrosion problem of water based vehicle.
7. Cortec VCI-309 is a good candidate for reduction of stress corrosion.
8. If the stress corrosion problem associated with water-based vehicles is solved, foaming and evaporation may be important problems.
9. Large scale (>80%) recycling of non-suspension vehicles is easy and practical.

11.5 Abrasive

1. Boron carbide and zirconia-aluminum oxide abrasive are not suitable for economic and technical reasons respectively.
2. #600 silicon carbide (as sized by Micro Abrasives Corporation: 10-30 μm diameter, 18 μm average) is the best cost-efficiency tradeoff.
3. Reduction of abrasive cost through manufacturing cost reduction or broader sizing is unlikely.
4. #600 SiC abrasive consisting of 66% new and 33% one time recycled is indistinguishable from new.
5. SEM studies of used SiC indicate no degradation.
6. Abrasive is most easily recycled using a centrifuge and perhaps washing.

11.6 Large Saw

1. The large saw is capable of producing high yield cutting 20 wafers/cm of 100 mm ingot.
2. It is uncertain whether the performance mentioned above is attainable consistently.
3. Significant mechanical problems have plagued large saw testing, especially problems arising from inadequate slurry shielding.
4. One test on the large saw came close to high yield production at 22 wafers/cm; breakage occurred with 90% of the cut completed, and the reasons for breakage are unknown.
5. Rebuilding of the large saw, including redesign of the carriage drive and stroke adjustment mechanisms, is necessary if further testing is to be carried out.

11.7 Wafers

1. 10-15 μm/side removed from a wafer by etching is sufficient to remove saw-induced damage.
2. Wafer breakage in downstream processing has been noted in systems not designed especially to handle slurry-sawn wafers.

12.0 RECOMMENDATIONS

Multiblade slurry sawing is a promising method for production of silicon ingots for solar cells. Further investigations should include:

1. Further analysis of the mechanisms of slurry sawing, including abrasive action and reasons for blade wander and breakage.
2. Consideration of optimum methods of shock load reduction.
3. Investigation of additives for mineral oil to provide a cheap, easily recyclable slurry vehicle.
4. Optimization of abrasive recycling techniques.
5. Reduction of capital equipment cost.
6. Redesign of either current equipment or the large saw to allow consistent high-yield operation with thin blades and spacers.
7. Blade package redesign to avoid misalignment caused by stacking errors.

We feel that the investigation of slurry sawing should be continued, and the recommendations above are the skeleton of a useful and practical program for such investigation.

APPENDIX I

PHASE I SLICING TEST SUMMARY

SLICING TEST SUMMARY

PARAMETER \ TEST		1-001	1-011	1-012	1-013
MATERIAL		(111)	(111)	(111)	(111)
LOAD (gram/blade)		113	57	113	170
SLIDING SPEED (cm/sec)		68	68	68	68
NUMBER OF BLADES CUTTING		128	119	119	119
ABRASIVE (grit size)		#600 SiC	#600 SiC	#600 SiC	#600 SiC
OIL VOLUME (liters)		7.6	7.6	7.6	7.6
MIX (kg/liter)		0.24	0.24	0.24	0.24
KERF LENGTH (cm)		10.8 max	2.50	2.50	2.50
INGOT HEIGHT (cm)		8.74	5.00	5.00	5.00
BLADE THICKNESS (cm)		.020	.020	.020	.020
KERF WIDTH (cm)		0.027	0.029	0.030	0.030
ABRASIVE KERF LOSS (cm)		0.007	0.009	0.010	0.010
AREA/SLICE (cm^2)		82.6	12.5	12.5	12.5
CUTTING TIME (total hours)		30:35	11:05	6:45	5:40
EFFICIENCY	(full test)	0.95	0.85	0.73	0.57
	(typical)	1.09	1.13	1.08	0.87
	(maximum)	1.20	1.29	1.10	0.90
ABRASION RATE	(full test)	0.073	0.033	0.056	0.066
(cm^3/hr/blade)	(typical)	0.084	0.044	0.083	0.1002
	(maximum)	0.092	0.050	0.084	0.104
PRODUCTIVITY	(full test)	2.70	1.13	1.85	2.20
(cm^2/hr/blade)	(typical)	3.09	1.50	2.76	[illegible]
	(maximum)	3.40	1.72	2.81	3.46
SLICE TAPER (cm)		+.0021	-.0011	-.0030	-.0018
ABRASIVE UTILIZATION (cm^3/kg)		138.2	23.6	24.5	24.5
OIL UTILIZATION (cm^3/liter)		33.2	5.7	5.9	5.9

SLICING TEST SUMMARY

PARAMETER \ TEST	1-014	1-015	1-021	1-022
MATERIAL	{111}	{111}	{111}	{111}
LOAD (gram/blade)	227	283	113	113
SLIDING SPEED (cm/sec)	68	68	68	68
NUMBER OF BLADES CUTTING	119	119	119	119
ABRASIVE (grit size)	#600 SiC	#600 SiC	#600 SiC	#600 SiC
OIL VOLUME (liters)	7.6	7.6	7.6	7.6
MIX (kg/liter)	0.24	0.24	0.24	0.24
KERF LENGTH (cm)	2.50	2.50	1.25	5.00
INGOT HEIGHT (cm)	5.00	5.00	2.50	2.50
BLADE THICKNESS (cm)	.020	.020	0.020	0.020
KERF WIDTH (cm)	0.034	- -	0.030	0.028
ABRASIVE KERF LOSS (cm)	0.014	- -	0.010	0.008
AREA/SLICE (cm^2)	12.5	12.5	3.12	12.5
CUTTING TIME (total hours)	4:55	- -	4:00	5:35
EFFICIENCY (full test)	0.56	- -	0.31	0.82
(typical)	0.86	- -	0.54	0.99
(maximum)	0.91	- -	0.55	1.12
ABRASION RATE (cm^3/hr/blade) (full test)	0.086	- -	0.023	0.063
(typical)	0.132	- -	0.041	0.076
(maximum)	0.140	- -	0.042	0.086
PRODUCTIVITY (cm^2/hr/blade) (full test)	2.54	- -	0.78	2.24
(typical)	3.89	- -	1.38	2.71
(maximum)	4.12	- -	1.40	3.06
SLICE TAPER (cm)	-.0039	- -	+.0007	-.0003
ABRASIVE UTILIZATION (cm^3/kg)	27.7	- -	6.1	22.8
OIL UTILIZATION (cm^3/liter)	6.7	- -	1.5	5.5

SLICING TEST SUMMARY

PARAMETER \ TEST		1-023	1-024	1-031	1-032
MATERIAL		{111}	{111}	{111}	{111}
LOAD (gram/blade)		113	113	113	57
SLIDING SPEED (cm/sec)		68	68	68	68
NUMBER OF BLADES CUTTING		119	119	119	135
ABRASIVE (grit size)		#600 SiC	#600 SiC	#600 SiC	#600 SiC
OIL VOLUME (liters)		7.6	7.6	7.6	7.6
MIX (kg/liter)		0.24	0.24	0.24	0.24
KERF LENGTH (cm)		6.88	10.64 max	2.50	2.50
INGOT HEIGHT (cm)		6.88	- -	5.00	5.00
BLADE THICKNESS (cm)		0.020	0.020	0.020	0.010
KERF WIDTH (cm)		0.030	0.027	0.031	0.022
ABRASIVE KERF LOSS (cm)		0.010	0.007	0.011	0.012
AREA/SLICE (cm^2)		47.3	91.7	12.50	12.50
CUTTING TIME (total hours)		21:35	39:40	8:00	8:00
EFFICIENCY	(full test)	0.86	0.82	0.63	0.89
	(typical)	0.99	0.95	0.97	1.04
	(maximum)	1.16	1.01	1.10	1.28
ABRASION RATE	(full test)	0.066	0.062	0.048	0.034
(cm^3/hr/blade)	(typical)	0.076	0.073	0.074	0.0402
	(maximum)	0.089	0.077	0.084	0.049
PRODUCTIVITY	(full test)	2.19	2.31	1.56	1.56
(cm^2/hr/blade)	(typical)	2.53	2.69	2.40	1.83
	(maximum)	2.96	2.86	2.72	2.25
SLICE TAPER (cm)		+.00122	+.0011	-.0022	-.0036
ABRASIVE UTILIZATION (cm^3/kg)		92.6	161.5	25.3	20.4
OIL UTILIZATION (cm^3/liter)		22.2	33.8	6.1	4.9

SLICING TEST SUMMARY

PARAMETER \ TEST		1-033	1-034	1-041	1-042
MATERIAL		{111}	{111}	{111}	{111}
LOAD (gram/blade)		113	113	113	113
SLIDING SPEED (cm/sec)		68	68	20-81	68
NUMBER OF BLADES CUTTING		127	127	119	119
ABRASIVE (grit size)		#600 SiC	#600 SiC	#600 SiC	#600 SiC
OIL VOLUME (liters)		7.6	7.6	7.6	7.6
MIX (kg/liter)		0.24	0.24	0.24	0.12
KERF LENGTH (cm)		2.50	2.50	2.50	2.50
INGOT HEIGHT (cm)		5.00	5.00	5.00	5.00
BLADE THICKNESS (cm)		0.015	0.015	0.020	0.020
KERF WIDTH (cm)		0.027	0.025	- -	0.030
ABRASIVE KERF LOSS (cm)		0.012	0.010	(.030 est)	0.010
AREA/SLICE (cm^2)		12.50	12.50	12.50	12.50
CUTTING TIME (total hours)		6:10	6:00	- -	8:50
EFFICIENCY	(full test)	0.72	0.68	- -	0.55
	(typical)	0.95	0.91	0.90	0.82
	(maximum)	1.16	1.01	1.03	0.94
ABRASION RATE (cm^3/hr/blade)	(full test)	0.055	0.052	- -	0.043
	(typical)	0.073	0.070	0.020 to 0.082	0.063
	(maximum)	0.089	0.077	0.023 to 0.094	0.072
PRODUCTIVITY (cm^2/hr/blade)	(full test)	2.03	2.08	- -	1.42
	(typical)	2.69	2.79	0.68 to 2.74	2.09
	(maximum)	3.29	3.09	0.77 to 3.13	2.40
SLICE TAPER (cm)		-.0002	+.0006	- -	-.0028
ABRASIVE UTILIZATION (cm^3/kg)		23.5	21.8	24.5	48.9
OIL UTILIZATION (cm^3/liter)		5.6	5.2	5.9	5.0

SLICING TEST SUMMARY

PARAMETER \ TEST		1-043	1-051	1-052	1-053
MATERIAL		{111}	{100}	{100}	{100}
LOAD (gram/blade)		113	113	113	170
SLIDING SPEED (cm/sec)		68	68	68	68
NUMBER OF BLADES CUTTING		119	119	119	127
ABRASIVE (grit size)		#600 SiC	#600 SiC	#600 SiC	#600 SiC
OIL VOLUME (liters)		7.6	7.6	7.6	7.6
MIX (kg/liter)		0.48	0.24	0.24	0.24
KERF LENGTH (cm)		2.50	2.50	5.00	6.98
INGOT HEIGHT (cm)		1.25	5.00	2.50	6.98
BLADE THICKNESS (cm)		0.020	0.020	0.020	0.020
KERF WIDTH (cm)		0.029	0.031	0.027	0.028
ABRASIVE KERF LOSS (cm)		0.009	0.011	0.007	0.008
AREA/SLICE (cm^2)		3.12	12.50	12.50	48.8
CUTTING TIME (total hours)		3:25	8:40	8:20	21:15
EFFICIENCY	(full test)	0.35	0.58	0.53	0.56
	(typical)	- -	0.95	0.84	0.82
	(maximum)	1.14	1.09	0.91	0.97
ABRASION RATE (cm^3/hr/blade)	(full test)	0.026	0.045	0.041	0.064
	(typical)	- -	0.073	0.064	0.095
	(maximum)	0.087	0.084	0.070	0.112
PRODUCTIVITY (cm^2/hr/blade)	(full test)	0.91	1.44	1.50	2.30
	(typical)	- -	2.35	2.38	3.37
	(maximum)	3.01	2.69	2.58	3.99
SLICE TAPER (cm)		+.0014	-.0034	-.0007	+.0015
ABRASIVE UTILIZATION (cm^3/kg)		3.0	24.0	22.0	95.1
OIL UTILIZATION (cm^3/liter)		1.4	5.8	5.3	22.8

SLICING TEST SUMMARY

PARAMETER \ TEST	1-054	1-061	1-062	1-063
MATERIAL	{100}	{111}	{111}	{111}
LOAD (gram/blade)	113	85	85	85
SLIDING SPEED (cm/sec)	55	53	55	55
NUMBER OF BLADES CUTTING	164	119	119	119
ABRASIVE (grit size)	#600 SiC	#1200 SiC	#1000 SiC	#800 SiC
OIL VOLUME (liters)	7.6	7.6	7.6	7.6
MIX (kg/liter)	0.24	.015-.12	0.24-0.36	0.12-0.24
KERF LENGTH (cm)	5.00	2.50	2.50	2.50
INGOT HEIGHT (cm)	2.50	5.00	5.00	5.00
BLADE THICKNESS (cm)	0.020	0.020	0.020	0.020
KERF WIDTH (cm)	0.028	0.025	0.025	0.027
ABRASIVE KERF LOSS (cm)	0.008	0.005	0.005	0.007
AREA/SLICE (cm^2)	12.50	12.50	12.50	12.50
CUTTING TIME (total hours)	10:40	21:10	17:30	14:05
EFFICIENCY (full test)	0.53	0.32	0.38	0.51
(typical)	0.91	0.33	0.51	0.78
(maximum)	1.13	0.39	0.62	0.90
ABRASION RATE (cm^3/hr/blade) (full test)	0.033	0.015	0.018	0.024
(typical)	0.056	0.015	0.024	0.036
(maximum)	0.070	0.017	0.029	0.042
PRODUCTIVITY (cm^2/hr/blade) (full test)	1.17	0.59	0.71	0.89
(typical)	2.01	0.59	0.95	1.35
(maximum)	2.50	0.70	1.16	1.55
SLICE TAPER (cm)	-.0008	+.0020	+.0007	+.0001
ABRASIVE UTILIZATION (cm^3/kg)	21.7	40.8	13.6	22.0
OIL UTILIZATION (cm^3/liter)	5.2	4.9	4.9	5.3

SLICING TEST SUMMARY

PARAMETER \ TEST	2-001	2-002	2-003	2-004
MATERIAL	{100}	{100}	{100}	Si {111}
LOAD (gram/blade)	113	113-170-227	113	113.4
SLIDING SPEED (cm/sec)	63	68	68	62.4
NUMBER OF BLADES CUTTING	143	115	142	142
ABRASIVE (grit size)	#600 SiC	#600 SiC	#600 SiC	#600 SiC
OIL VOLUME (liters)	7.6	7.6	7.6	37.9
MIX (kg/liter)	0.48	0.96	0.48-0.72	0.48
KERF LENGTH (cm)	10.0 max	7.62	10.0 max	10.0 max
INGOT HEIGHT (cm)	8.62	7.62	8.62	8.62
BLADE THICKNESS (cm)	0.020	0.020	0.020	0.02
KERF WIDTH (cm)	0.026	0.028	0.029	0.0255
ABRASIVE KERF LOSS (cm)	0.006	0.008	0.009	0.0055
AREA/SLICE (cm^2)	73.8	58.1	73.8	73.8
CUTTING TIME (total hours)	19:10	15:55	18:15	21:35
EFFICIENCY (full test)	1.41	- -	1.53	1.24
(typical)	1.65	1.09	1.70	1.74
(maximum)	2.20	1.30	2.53	2.11
ABRASION RATE (cm^3/hr/blade) (full test)	0.1001	0.102	0.117	0.0872
(typical)	0.117	- -	0.130	0.1223
(maximum)	0.156	- -	0.194	0.148
PRODUCTIVITY (cm^2/hr/blade) (full test)	3.85	3.65	4.04	3.42
(typical)	4.50	- -	4.49	4.79
(maximum)	6.00	- -	6.68	5.81
SLICE TAPER (cm)	+.0006	+.0011	+.0027	+.0007
ABRASIVE UTILIZATION (cm^3/kg)	75.2	25.6	55.5	14.7
OIL UTILIZATION (cm^3/liter)	36.1	24.5	40.0	7.05

SLICING TEST SUMMARY

PARAMETER \ TEST	2-005	2-006A	2-006B	2-006C
MATERIAL	Si {111}	Si {100}	Si {100}	Si {100}
LOAD (gram/blade)	113.4	113.4	113.4	113.4
SLIDING SPEED (cm/sec)	56.7	57.8	57.8	60.4
NUMBER OF BLADES CUTTING	144	125	125	125
ABRASIVE (grit size)	#600 SiC	#600 SiC	(#600 SiC)	(#600 SiC)
OIL VOLUME (liters)	(37.9)	7.6	(7.6)	(7.6)
MIX (kg/liter)	0.48	0.48	(0.48)	(0.48)
KERF LENGTH (cm)	10.0 max	10.0 max	10.0 max	10.0 max
INGOT HEIGHT (cm)	8.62	8.62	8.62	4.75
BLADE THICKNESS (cm)	0.02	0.02	0.02	0.02
KERF WIDTH (cm)	0.0247	.0255	.0238	(.0238)
ABRASIVE KERF LOSS (cm)	0.0047	.0055	.0038	(.0038)
AREA/SLICE (cm^2)	73.8	73.8	73.8	46.6
CUTTING TIME (total hours)	26:30	27:00	26:15	(23:25)
EFFICIENCY (full test)	1.08	1.07	1.01	0.69
(typical)	1.50	1.[illegible]9	1.12	0.70
(maximum)	1.86	1.88	1.70	1.08
ABRASION RATE (cm^3/hr/blade) (full test)	0.0709	.0696	.0669	.0474
(typical)	0.0958	.0777	.0748	.0478
(maximum)	0.1187	.1228	.1135	.0737
PRODUCTIVITY (cm^2/hr/blade) (full test)	2.78	2.73	2.81	1.99
(typical)	3.88	3.05	3.14	2.01
(maximum)	4.81	4.82	4.77	3.10
SLICE TAPER (cm)	+.0015	+.0016	+.0016	--
ABRASIVE UTILIZATION (cm^3/kg)	(29.1)	64.48	124.67	162.6
OIL UTILIZATION (cm^3/liter)	(13.98)	30.9	59.3	78.0

SLICING TEST SUMMARY

PARAMETER \ TEST		2-011	2-012	2-021	2-022
MATERIAL		{100}	{100}	Si {111}	Si
LOAD (gram/blade)		113-170-227	113-170	113	
SLIDING SPEED (cm/sec)		66	67	35.5	
NUMBER OF BLADES CUTTING		179	115	150	
ABRASIVE (grit size)		#800 SiC	#800 SiC	#600 SiC	#600 SiC
OIL VOLUME (liters)		7.6	7.6	7.6	
MIX (kg/liter)		0.48-0.60	0.48	0.48	0.36
KERF LENGTH (cm)		10.0 max	7.62	10.0 max	10.0 max
INGOT HEIGHT (cm)		8.62	7.62	6.83	
BLADE THICKNESS (cm)		0.020	0.020	0.02	0.02
KERF WIDTH (cm)		0.025	0.024	0.0262	
ABRASIVE KERF LOSS (cm)		0.005	0.004	0.0062	
AREA/SLICE (cm^2)		73.8	58.1	61.6	
CUTTING TIME (total hours)		24:20	23:50	54:35	
EFFICIENCY	(full test)	- -	- -	.74	COLLAPSE
	(typical)	1.13	0.65	.96	OF
	(maximum)	1.37	0.87	1.14	SPACERS
ABRASION RATE	(full test)	0.076	0.058	0.0296	PIN
(cm^3/hr/blade)	(typical)	- -	- -	0.0384	&
	(maximum)	- -	- -	0.0456	EPOXY
PRODUCTIVITY	(full test)	3.033	2.437	1.13	
(cm^2/hr/blade)	(typical)	- -	- -	1.46	
	(maximum)	- -	- -	1.74	
SLICE TAPER (cm)		+.0019	+.0016	+.0004	
ABRASIVE UTILIZATION (cm^3/kg)		72.4	44.0	66.36	
OIL UTILIZATION (cm^3/liter)		43.5	21.1	31.85	

SLICING TEST SUMMARY

PARAMETER \ TEST	2-023	2-024	2-025	2-026
MATERIAL	Si {100}	Si {100}	Si {100}	Si {100}
LOAD (gram/blade)	113	225	113	226.8
SLIDING SPEED (cm/sec)	61.3	59.2	61.3	60.1
NUMBER OF BLADES CUTTING	150	125	128	76
ABRASIVE (grit size)	#600 SiC	#600 SiC	#600 SiC	#600 SiC
OIL VOLUME (liters)	7.6	7.6	7.6	7.6
MIX (kg/liter)	0.24	0.48	0.36	.96
KERF LENGTH (cm)	10.0 max	10.0 max	10.0 max	10
INGOT HEIGHT (cm)	6.83	6.83	6.83	10
BLADE THICKNESS (cm)	0.02	0.02	0.02	.020
KERF WIDTH (cm)	0.0251	0.0262	0.0259	.0262
ABRASIVE KERF LOSS (cm)	0.0051	0.0062	0.0059	.0058
AREA/SLICE (cm^2)	72.1	72.1	72.1	77.42
CUTTING TIME (total hours)	27:30	17:10	27:10	13:30
EFFICIENCY (full test)	0.95	0.83	1.00	1.11
(typical)	1.19	1.09	1.07	1.33
(maximum)	1.95	1.35	1.73	1.6927
ABRASION RATE (cm^3/hr/blade) (full test)	0.0658	0.1101	0.0687	.1503
(typical)	0.0821	0.1447	0.0739	.1806
(maximum)	0.1346	0.1792	0.1194	.2299
PRODUCTIVITY (cm^2/hr/blade) (full test)	2.62	4.20	2.65	5.73
(typical)	3.27	5.52	2.85	6.89
(maximum)	5.36	6.84	4.61	8.77
SLICE TAPER (cm)	+0.0011	+.0011	+.0018	+.00080
ABRASIVE UTILIZATION (cm^3/kg)	148.8	64.7	87.3	21.13
OIL UTILIZATION (cm^3/liter)	35.7	31.1	31.4	20.

SLICING TEST SUMMARY

PARAMETER \ TEST		2-031	2-041	3-001	3-002
MATERIAL		{111}	Si {100}	{111}	{111}
LOAD (gram/blade)		113	113	57-85	28-46
SLIDING SPEED (cm/sec)		67	67.1	68	68
NUMBER OF BLADES CUTTING		125	118	150	145
ABRASIVE (grit size)		#600 SiC	#600 B_4C	#600 SiC	#600 SiC
OIL VOLUME (liters)		7.6	7.6	7.6	7.6
MIX (kg/liter)		0.48-0.72	0.48	0.24	0.24
KERF LENGTH (cm)		10.0 max	10.0 max	10 max	7.62
INGOT HEIGHT (cm)		8.62	8.3 cm	8.8	7.62
BLADE THICKNESS (cm)		0.020	0.02	.010	.010
KERF WIDTH (cm)		0.025	0.0284	(.018)	(.018)
ABRASIVE KERF LOSS (cm)		0.005	0.0084	(.008)	(.008)
AREA/SLICE (cm^2)		73.8	72.1	DNF	DNF
CUTTING TIME (total hours)		19:55	14:50	DNF	DNF
EFFICIENCY	(full test)	1.23	1.83	- -	- -
	(typical)	1.68	2.07	1.60	1.70
	(maximum)	2.43	3.18	1.80	1.81
ABRASION RATE (cm^3/hr/blade)	(full test)	0.093	0.1380	- -	- -
	(typical)	0.127	0.1564	- -	- -
	(maximum)	0.183	0.2403	- -	- -
PRODUCTIVITY (cm^2/hr/blade)	(full test)	3.71	4.86	- -	- -
	(typical)	5.07	5.51	- -	- -
	(maximum)	7.33	8.46	- -	- -
SLICE TAPER (cm)		+.0043	+.0009	- -	- -
ABRASIVE UTILIZATION (cm^3/kg)		42.1	66.23	- -	- -
OIL UTILIZATION (cm^3/liter)		30.3	31.79	- -	- -

SLICING TEST SUMMARY

PARAMETER \ TEST		3-021	3-031	3-032	3-033
MATERIAL		Si {111}	Si {111}	Si {100}	Si {100}
LOAD (gram/blade)		57	85	85	85
SLIDING SPEED (cm/sec)		65.8	62.7	60.9	60.4
NUMBER OF BLADES CUTTING		145	136	96	114
ABRASIVE (grit size)		#600 SiC	#600 SiC	#600 SiC	#600 SiC
OIL VOLUME (liters)		7.6	7.6	7.6	7.6
MIX (kg/liter)		0.48	0.48	0.48	0.24
KERF LENGTH (cm)		7.62	7.62	10.0 max	10.0 max
INGOT HEIGHT (cm)		5.40	5.31	8.3	8.3
BLADE THICKNESS (cm)		0.010	0.015	0.015	0.015
KERF WIDTH (cm)		(0.015)	0.023	0.0216	0.0202
ABRASIVE KERF LOSS (cm)		(0.005)	0.008	0.0066	0.0052
AREA/SLICE (cm^2)		41.1	40.5	72.1	72.1
CUTTING TIME (total hours)		23:10	17:00	26:05	28:50
EFFICIENCY	(full test)	0.71	1.03	1.16	0.99
	(typical)	0.86	1.15	1.45	1.13
	(maximum)	1.61	1.65	2.43	1.73
ABRASION RATE	(full test)	0.0266	0.0547	0.0597	0.0505
(cm^3/hr/blade)	(typical)	0.0335	0.0611	0.0748	0.0578
	(maximum)	0.0626	0.0876	0.1253	0.0885
PRODUCTIVITY	(full test)	1.77	2.38	2.76	2.50
(cm^2/hr/blade)	(typical)	2.23	2.66	3.46	2.86
	(maximum)	4.18	3.81	5.80	4.38
SLICE TAPER (cm)		+0.012	-0.0003	+.0018	+.0020
ABRASIVE UTILIZATION (cm^3/kg)		22.9	34.6	41.0	91.0
OIL UTILIZATION (cm^3/liter)		10.9	16.6	19.7	21.8

SLICING TEST SUMMARY

PARAMETER \ TEST		3-034	3-035	3-036	3-041
MATERIAL		Si (100)	Si (100)	Si	Si (100)
LOAD (gram/blade)		141.75	85.05	113.40	57
SLIDING SPEED (cm/sec)		60.7	60.0	60.7	
NUMBER OF BLADES CUTTING		80	118	97	
ABRASIVE (grit size)		#600 SiC	#600 SiC	#600 SiC	#600 SiC
OIL VOLUME (liters)		7.6	7.6	7.6	7.6
MIX (kg/liter)		.36	.36	.48	0.24
KERF LENGTH (cm)		10	10	10	
INGOT HEIGHT (cm)		10	10	6.19	
BLADE THICKNESS (cm)		.015	.015	.015	0.010
KERF WIDTH (cm)		.0224	.0213	.0223	
ABRASIVE KERF LOSS (cm)		.0071	.0061	.0071	
AREA/SLICE (cm^2)		77.42	77.42	56.39	
CUTTING TIME (total hours)		19:45	29:30	26:15	
EFFICIENCY	(full test)	1.02	1.10	0.698	BROKE IN PRECONDITIONING
	(typical)	1.22	1.45	.7735	
	(maximum)	1.7458	2.0966	1.1299	
ABRASION RATE (cm^3/hr/blade)	(full test)	.0878	.0559	.0479	
	(typical)	.1046	.07373	.0531	
	(maximum)	.1497	.1066	.0775	
PRODUCTIVITY (cm^2/hr/blade)	(full test)	3.92	2.26	2.15	
	(typical)	4.67	3.46	2.38	
	(maximum)	6.68	5.00	3.48	
SLICE TAPER (cm)		+.00157	+.00153	+.00013	
ABRASIVE UTILIZATION (cm^3/kg)		50.71	71.12	45.91	
OIL UTILIZATION (cm^3/liter)		18.25	25.60	22.04	

SLICING TEST SUMMARY

PARAMETER \ TEST		P-001	P-002	P-003	P-004
MATERIAL		Si (100)	Si (100)	Si (100)	Si (100)
LOAD (gram/blade)		170	113	113.40	85.05
SLIDING SPEED (cm/sec)		66.8	65.1	60.2	59.6
NUMBER OF BLADES CUTTING		225	225	225	271
ABRASIVE (grit size)		#600 SiC	#600 SiC	#600 SiC	#600 SiC
OIL VOLUME (liters)		7.6	7.6	7.6	7.6
MIX (kg/liter)		0.48	0.36	.48	.36
KERF LENGTH (cm)		10.0 max	10.0 max	10	10
INGOT HEIGHT (cm)		10.0	10.0	10	10
BLADE THICKNESS (cm)		0.0203	0.0203	.020	.015
KERF WIDTH (cm)		0.0257	0.0257	.0262	.0198
ABRASIVE KERF LOSS (cm)		0.0057	0.0254	.0059	.0046
AREA/SLICE (cm^2)		78.5	78.5	77.42	77.42
CUTTING TIME (total hours)		19:00	23:25	25:20	35:15
EFFICIENCY	(full test)	0.94	1.17	1.18	0.861
	(typical)	1.03	1.28	1.38	1.12
	(maximum)	1.37	1.51	1.6617	1.2829
ABRASION RATE	(full test)	0.1062	0.0862	.0801	.0435
(cm^3/hr/blade)	(typical)	0.1166	0.0938	.0939	.0566
	(maximum)	0.1550	0.1107	.1130	.0643
PRODUCTIVITY	(full test)	4.13	3.35	3.06	2.20
(cm^2/hr/blade)	(typical)	4.53	3.65	3.58	2.86
	(maximum)	6.03	4.31	4.31	3.27
SLICE TAPER (cm)		--	--	+.00141	+.00298
ABRASIVE UTILIZATION (cm^3/kg)		124.4	165.9	125.11	151.83
OIL UTILIZATION (cm^3/liter)		59.7	59.7	60.05	54.66

SLICING TEST SUMMARY

PARAMETER \ TEST		P-005
MATERIAL		Si (100)
LOAD (gram/blade)		85.05
SLIDING SPEED (cm/sec)		57.8
NUMBER OF BLADES CUTTING		234
ABRASIVE (grit size)		#600 SiC
OIL VOLUME (liters)		7.6
MIX (kg/liter)		.36
KERF LENGTH (cm)		10
INGOT HEIGHT (cm)		10
BLADE THICKNESS (cm)		.015
KERF WIDTH (cm)		.0216
ABRASIVE KERF LOSS (cm)		.0064
AREA/SLICE (cm^2)		77.42
CUTTING TIME (total hours)		32:00
EFFICIENCY	(full test)	1.068
	(typical)	1.37
	(maximum)	1.5259
ABRASION RATE (cm^3/hr/blade)	(full test)	.0523
	(typical)	.0671
	(maximum)	.0747
PRODUCTIVITY (cm^2/hr/blade)	(full test)	2.42
	(typical)	3.11
	(maximum)	3.46
SLICE TAPER (cm)		+.00083
ABRASIVE UTILIZATION (cm^3/kg)		143.03
OIL UTILIZATION (cm^3/liter)		51.49

APPENDIX II

PHASE I WAFER CHARACTERIZATION SUMMARY

SUMMARY OF WAFER CHARACTERIZATION

TEST		1-001	1-011	1-012
THICKNESS (AVE)	cm	.0565	0551	0534
STD. DEVIATION	cm	.0020	0017	0045
TOTAL VARIATION (AVE)	cm	.0032	0019	0058
STD. DEVIATION	cm	.0017	0012	0038
STD. DEVIATION (AVE)	cm	.0014	0010	0030
STD. DEVIATION	cm	.0007	0006	0020
VARIATION (AVE WAFER)	cm	.0022	0010	0037
TAPER (AVE WAFER)	cm	.0021	0011	0030
BOW (AVE)	µm	SEE FOLLOWING TABLE	15	8
TAPER (AVE)	µm		26	11
WAVINESS (p-p) (10^{-2}m)	µm		11	48
ROUGHNESS (p-p) (10^{-4}m)	µm		2	2
ROUGHNESS (RMS)	µinch		16-19	19-24
STEPS	µm		4	19

TEST		1-013	1-014	1-015
THICKNESS (AVE)	cm	0573	0502	- -
STD. DEVIATION	cm	0061	0085	- -
TOTAL VARIATION (AVE)	cm	0052	0085	- -
STD. DEVIATION	cm	0053	0050	- -
STD. DEVIATION (AVE)	cm	0028	0045	- -
STD. DEVIATION	cm	0030	0027	- -
VARIATION (AVE WAFER)	cm	0029	0045	- -
TAPER (AVE WAFER)	cm	0018	0039	- -
BOW (AVE)	μm	72	- -	- -
TAPER (AVE)	μm	85	32	- -
WAVINESS (p-p) (10^{-2}m)	μm	15	12	- -
ROUGHNESS (p-p) (10^{-4}m)	μm	1.8	1.8	- -
ROUGHNESS (RMS)	μinch	18-22	16-22	- -
STEPS	μm	13	55	- -

TEST		1-021	1-022	1-023	1-024
THICKNESS (AVE	cm	0536	0555	0535	0569
STD. DEVIATION	cm	0021	0029	0013	0030
TOTAL VARIATION (AVE)	cm	0027	0022	0034	0038
STD. DEVIATION	cm	0022	0014	0016	0023
STD. DEVIATION (AVE)	cm	0014	0012	0018	0020
STD. DEVIATION	cm	0011	0007	0008	0012
VARIATION (AVE WAFER)	cm	0014	0010	0021	0011
TAPER (AVE WAFER)	cm	0007	0003	0012	0011
BOW (AVE)	μm	10	20	13	17
TAPER (AVE)	μm	27	36	22	34
WAVINESS (p-p) (10^{-2}m)	μm	20	5	11	14
ROUGHNESS (p-p) (10^{-4}m)	μm	1	1.5	1.4	2
ROUGHNESS (RMS)	μinch	25-45	14-17	13-16	14-17
STEPS	μm	8	4	14	- -

TEST		1-031	1-032	1-033	1-034
THICKNESS (AVE)	cm	0526	0519	0516	0535
STD. DEVIATION	cm	0022	0044	0051	0035
TOTAL VARIATION (AVE)	cm	0034	0057	0035	0042
STD. DEVIATION	cm	0024	0029	0029	0022
STD. DEVIATION (AVE)	cm	0019	0030	0018	0022
STD. DEVIATION	cm	0012	0015	0014	0011
VARIATION (AVE WAFER)	cm	0026	0039	0018	0018
TAPER (AVE WAFER)	cm	0022	0036	0002	0006
BOW (AVE)	µm	10	- -	28	40
TAPER (AVE)	µm	22	35	29	38
WAVINESS (p-p) (10^{-2}m)	µm	13	9	16	27
ROUGHNESS (p-p) (10^{-4}m)	µm	1.9	1.5	2.0	2.0
ROUGHNESS (RMS)	µinch	18-20	16-17	22-25	35-50
STEPS	µm	4	3	6	21

TEST		1-041	1-042	1-043
THICKNESS (AVE)	cm	- -	0534	0552
STD. DEVIATION	cm	- -	0045	0017
TOTAL VARIATION (AVE)	cm	- -	0046	0022
STD. DEVIATION	cm	- -	0036	0015
STD. DEVIATION (AVE)	cm	- -	0023	0011
STD. DEVIATION	cm	- -	0018	0008
VARIATION (AVE WAFER)	cm	- -	0028	0014
TAPER (AVE WAFER)	cm	- -	0028	0014
BOW (AVE)	μm	- -	23	- -
TAPER (AVE)	μm	- -	44	- -
WAVINESS (p-p) (10^{-2}m)	μm	- -	17	- -
ROUGHNESS (p-p) (10^{-4}m)	μm	- -	2.0	- -
ROUGHNESS (RMS)	μinch	- -	16-19	20-24
STEPS	μm	- -	15	- -

TEST		1-051	1-052	1-053	1-054
THICKNESS (AVE)	cm	0524	0566	0333	0332
STD. DEVIATION	cm	0025	0011	0013	0026
TOTAL VARIATION (AVE)	cm	0043	0016	0044	0018
STD. DEVIATION	cm	0019	0009	0022	0013
STD. DEVIATION (AVE)	cm	0022	0008	0017	0009
STD. DEVIATION	cm	0009	0005	0009	0006
VARIATION (AVE WAFER)	cm	0034	0007	0025	0008
TAPER (AVE WAFER)	cm	0034	0007	0015	0008
BOW (AVE)	μm	17	21	6	8
TAPER (AVE)	μm	29	15	6	7
WAVINESS (p-p) (10^{-2}m)	μm	34	15	14	9
ROUGHNESS (p-p) (10^{-4}m)	μm	2.2	1.5	1.5	1.4
ROUGHNESS (RMS)	μinch	20-22	17-19	15-16	17-19
STEPS	μm	4	40	13	13

TEST		1-061	1-062	1-063
THICKNESS (AVE)	cm	0592	0591	0573
STD. DEVIATION	cm	0007	0014	0027
TOTAL VARIATION (AVE)	cm	0029	0035	0018
STD. DEVIATION	cm	0015	0022	0011
STD. DEVIATION (AVE)	cm	0015	0015	0009
STD. DEVIATION	cm	0008	0009	0005
VARIATION (AVE WAFER)	cm	0020	0013	0009
TAPER (AVE WAFER)	cm	0020	0007	0001
BOW (AVE)	μm	- -	15	44
TAPER (AVE)	μm	- -	52	24
WAVINESS (p-p) (10^{-2}m)	μm	- -	15	18
ROUGHNESS (p-p) (10^{-4}m)	μm	- -	1.1	1.6
ROUGHNESS (RMS)	μinch	14-16	10-12	12-13
STEPS	μm	- -	5	- -

TEST		2-001	2-002	2-003
THICKNESS (AVE)	cm	0245	0334	0318
STD. DEVIATION	cm	0017	0016	0017
TOTAL VARIATION (AVE)	cm	0036	0026	0046
STD. DEVIATION	cm	0014	0014	0009
STD. DEVIATION (AVE)	cm	0011	0013	0024
STD. DEVIATION	cm	0004	0007	0004
VARIATION (AVE WAFER)	cm	0020	0011	0044
TAPER (AVE WAFER)	cm	0006	0011	0027
BOW (AVE)	µm	- -	- -	- -
TAPER (AVE)	µm	20	6	28
WAVINESS (p-p) (10^{-2}m)	µm	88	8	40
ROUGHNESS (p-p) (10^{-4}m)	µm	1.5	1.5	2.0
ROUGHNESS (RMS)	µinch	17-19	15-16	18-19
STEPS	µm	- -	- -	30

(ALSO SEE FOLLOWING TABLE)

TEST		2-004	2-005	2-006A
THICKNESS (AVE)	cm	.0253	0261	0253
STD. DEVIATION	cm	.0037	0015	0022
TOTAL VARIATION (AVE)	cm	0643	0043	0040
STD. DEVIATION	cm	0020	0018	0015
STD. DEVIATION (AVE)	cm	0024	0016	0013
STD. DEVIATION	cm	0009	0007	0006
VARIATION (AVE WAFER)	cm	0020	0015	0016
TAPER (AVE WAFER)	cm	0007	0015	0016
BOW (AVE)	μm	40	--	--
TAPER (AVE)	μm	--	--	30
WAVINESS (p-p) (10^{-2}m)	μm	24	51	23
ROUGHNESS (p-p) (10^{-4}m)	μm	2.4	2.0	2.3
ROUGHNESS (RMS)	μinch	18-20	18-22	15-16
STEPS	μm	--		

TEST		2-006B	2-006C	2-011
THICKNESS (AVE)	cm	0270	DNF	0362
STD. DEVIATION	cm	0029		0040
TOTAL VARIATION (AVE)	cm	0057		0051
STD. DEVIATION	cm	0024		0033
STD. DEVIATION (AVE)	cm	0022		0024
STD. DEVIATION	cm	0009		0016
VARIATION (AVE WAFER)	cm	0017		0019
TAPER (AVE WAFER)	cm	0017		0019
BOW (AVE)	μm	--		--
TAPER (AVE)	μm	--		--
WAVINESS (p-p) (10^{-2}m)	μm	48		24
ROUGHNESS (p-p) (10^{-4}m)	μm	2.3		1.5
ROUGHNESS (RMS)	μinch	14-16		17-18
STEPS	μm	8.5		36

TEST		2-012	2-021	2-022
THICKNESS (AVE)	cm	0374	0246	DNF
STD. DEVIATION	cm	0009	0013	
TOTAL VARIATION (AVE)	cm	0043	0021	
STD. DEVIATION	cm	0010	0009	
STD. DEVIATION (AVE)	cm	0017	0007	
STD. DEVIATION	cm	0005	0003	
VARIATION (AVE WAFER)	cm	0022	0004	
TAPER (AVE WAFER)	cm	0016	0004	
BOW (AVE)	μm	- -	9	
TAPER (AVE)	μm	38	10	
WAVINESS (p-p) (10^{-2}m)	μm	40	16	
ROUGHNESS (p-p) (10^{-4}m)	μm	2.2	1.9	
ROUGHNESS (RMS)	μinch	10-12	15-18	
STEPS	μm	6	28	

TEST		2-023	2-024	2-025
THICKNESS (AVE)	cm	0257	0348	0248
STD. DEVIATION	cm	0030	0025	0011
TOTAL VARIATION (AVE)	cm	0049	0041	0043
STD. DEVIATION	cm	0035	0015	0019
STD. DEVIATION (AVE)	cm	0018	0016	0017
STD. DEVIATION	cm	0011	0006	0007
VARIATION (AVE WAFER)	cm	0023	0018	0020
TAPER (AVE WAFER)	cm	0013	0010	0018
BOW (AVE)	μm	--	--	68
TAPER (AVE)	μm	22	19	35
WAVINESS (p-p) (10^{-2}m)	μm	16	38	15
ROUGHNESS (p-p) (10^{-4}m)	μm	2	3	3
ROUGHNESS (RMS)	μinch	21-24	16-19	15-18
STEPS	μm	--	--	--

TEST		2-026	2-031	2-041
THICKNESS (AVE)	cm	03485	0355	0326
STD. DEVIATION	cm	00196	0058	0016
TOTAL VARIATION (AVE)	cm	00546	0100	0042
STD. DEVIATION	cm	00249	0043	0018
STD. DEVIATION (AVE)	cm	00206	0038	0015
STD. DEVIATION	cm	00104	0015	0006
VARIATION (AVE WAFER)	cm	00137	0049	0009
TAPER (AVE WAFER)	cm	00079	0043	0009
BOW (AVE)	μm		- -	--
TAPER (AVE)	μm		- -	--
WAVINESS (p-p) (10^{-2}m)	μm		50	38
ROUGHNESS (p-p) (10^{-4}m)	μm		2.0	2.6
ROUGHNESS (RMS)	μinch		13-15	17-19
STEPS	μin		- -	41

TEST		3-021	3-031	3-032
THICKNESS (AVE)	cm	0394	0331	0343
STD. DEVIATION	cm	0047	0020	0019
TOTAL VARIATION (AVE)	cm	0171	0027	0046
STD. DEVIATION	cm	0111	0011	0027
STD. DEVIATION (AVE)	cm	0067	0010	0018
STD. DEVIATION	cm	0044	0005	0011
VARIATION (AVE WAFER)	cm	0122	0003	0020
TAPER (AVE WAFER)	cm	0122	0003	0018
BOW (AVE)	μm	--	--	50
TAPER (AVE)	μm	27	--	--
WAVINESS (p-p) (10^{-2}m)	μm	62	13	70
ROUGHNESS (p-p) (10^{-4}m)	μm	2.3	2.2	30
ROUGHNESS (RMS)	μinch	22-24	17-22	14-16
STEPS	μm	62	2	30

TEST		3-033	3-034	3-035
THICKNESS (AVE)	cm	0255	03366	02441
STD. DEVIATION	cm	0018	00157	00135
TOTAL VARIATION (AVE)	cm	0044	00340	00320
STD. DEVIATION	cm	0021	00127	00155
STD. DEVIATION (AVE)	cm	0017	00135	00119
STD. DEVIATION	cm	0009	00053	00610
VARIATION (AVE WAFER)	cm	0022	00183	00196
TAPER (AVE WAFER)	cm	0019	00157	00152
BOW (AVE)	μm	--		SEE FOLLOWING TABLE
TAPER (AVE)	μm	21		
WAVINESS (p-p) (10^{-2}m)	μm	62		
ROUGHNESS (p-p) (10^{-4}m)	μm	3		
ROUGHNESS (RMS)	μinch	24-28		
STEPS	μm	--		

TEST		3-036	P-001	P-002
THICKNESS (AVE)	cm	02339	0048	0303
STD. DEVIATION	cm	00185	0007	0015
TOTAL VARIATION (AVE)	cm	00272	0047	0036
STD. DEVIATION	cm	00109	0015	0014
STD. DEVIATION (AVE)	cm	00094	0017	0014
STD. DEVIATION	cm	00041	0006	0006
VARIATION (AVE WAFER)	cm	00107	--	--
TAPER (AVE WAFER)	cm	00013	--	--
BOW (AVE)	µm		--	--
TAPER (AVE)	µm		--	10
WAVINESS (p-p) (10^{-2}m)	µm		--	29
ROUGHNESS (p-p) (10^{-4}m)	µm		--	25
ROUGHNESS (RMS)	µinch		17-20	13-17
STEPS	µm		--	--

TEST		P-003	P-004	P-005
THICKNESS (AVE)	cm	02456	02600	02921
STD. DEVIATION	cm	00264	00279	00414
TOTAL VARIATION (AVE)	cm	00549	00483	00744
STD. DEVIATION	cm	00274	00302	00231
STD. DEVIATION (AVE)	cm	00203	00216	00318
STD. DEVIATION	cm	00112	00117	00107
VARIATION (AVE WAFER)	cm	00196	00338	00460
TAPER (AVE WAFER)	cm	00152	00300	00213
BOW (AVE)	µm	SEE FOLLOWING TABLE	SEE FOLLOWING TABLE	SEE FOLLOWING TABLE
TAPER (AVE)	µm			
WAVINESS (p-p) (10^{-2}m)	µm			
ROUGHNESS (p-p) (10^{-4}m)	µm			
ROUGHNESS (RMS)	µinch			
STEPS	µm			

SUMMARY OF WAFER CHARACTERIZATION
(Non-Contact Gauging)

TEST		1-001	2-001	3-035
SLICE	Diameter (cm)	(10)	10	10
	Area (cm^2)	82.6	77.4	77.4
	Thickness (μ)	565	245	244
VERTICAL TAPER	Average (μ)	57	49	39
	Maximum	100	58	74
	Minimum	22	35	16
HORIZONTAL TAPER	Average (μ)	7	16	13
	Maximum	12	24	19
	Minimum	1	9	6
VERTICAL BOW-TOP	Average (μ)	63	94	57
	Maximum	108	107	100
	Minimum	30	77	23
HORIZONTAL BOW-TOP	Average (μ)	19	34	57
	Maximum	45	53	79
	Minimum	8	17	15
VERTICAL BOW-BOTTOM	Average (μ)	24	80	46
	Maximum	40	96	59
	Minimum	10	59	29
HORIZONTAL BOW-BOTTOM	Average (μ)	17	39	49
	Maximum	43	59	64
	Minimum	2	25	24
VERTICAL BOW-CL	Average (μ)	78	170	97
	Maximum	135	192	136
	Minimum	23	133	42
HORIZONTAL BOW-CL	Average (μ)	36	72	106
	Maximum	90	110	142
	Minimum	9	29	39

SUMMARY OF WAFER CHARACTERIZATION

(Non-Contact Gauging)

TEST		P-003	P-004	P-005
SLICE	Diameter (cm)	10	10	10
	Area (cm^2)	77.4	77.4	77.4
	Thickness (μ)	246	260	291
VERTICAL TAPER	Average (μ)	47	53	74
	Maximum	89	98	118
	Minimum	18	16	34
HORIZONTAL TAPER	Average (μ)	11	11	6
	Maximum	24	22	13
	Minimum	3	4	2
VERTICAL BOW-TAPER	Average (μ)	97	44	95
	Maximum	165	88	236
	Minimum	42	14	25
HORIZONTAL BOW-TOP	Average (μ)	79	52	71
	Maximum	108	75	112
	Minimum	45	25	24
VERTICAL BOW-BOTTOM	Average (μ)	113	51	111
	Maximum	160	78	148
	Minimum	87	21	85
HORIZONTAL BOW-BOTTOM	Average (μ)	72	50	71
	Maximum	95	78	120
	Minimum	34	31	33
VERTICAL BOW-CL	Average (μ)	205	79	194
	Maximum	327	127	360
	Minimum	140	37	85
HORIZONTAL BOW-CL	Average (μ)	152	101	143
	Maximum	193	144	229
	Minimum	80	65	54

APPENDIX III

PHASE II SLICING TEST SUMMARY

SLICING TEST SUMMARY

PARAMETER	TEST	2-1-01	2-1-02	2-1-03	2-1-04
Material		100 Si	100 Si	100 Si	100 Si
Size	(mm)	100	100	100	100
Area/Slice	(cm^2)	78.54	78.54	78.54	78.54
Blade Thickness	(mm)	0.15 x 6.35	0.15 x 6.35	0.15 x 6.35	0.15 x 6.35
Spacer Thickness	(mm)	0.36	0.36	0.36	0.36
Blade Height	(mm)	6.4	6.4	6.4	6.4
Number of Blades		150	150	152	150
Load	(gram/blade)	85	85	85	127.6
Sliding Speed	(cm/sec)	61.6	64.5	63.7	- -
Abrasive	(type/grit size)	#600 SiC	#600 SiC	#600 Sic	- -
Oil Volume	(liters)	7.6 PC	7.6 PC	7.6 PC	- -
Mix	(kg/liter)	0.36	0.24	0.18	- -
Slice Thickness	(mm)	0.273	0.272	0.284	- -
Kerf Width	(mm)	0.234	0.236	0.224	- -
Abrasive Kerf Loss	(mm)	0.084	0.086	0.074	- -
Cutting Time	(hours)	41.6	72.3	43.[illegible]	- -
Efficiency	(full test)	0.8433	0.4759	0.7599	- -
	(typical)	1.0738	0.7023	0.9414	- -
	(maximum)	1.5969	1.7077	1.2364	- -
Abrasion Rate	(full test)	0.044	0.026	0.041	- -
(cm^3/hr/bl)	(typical)	0.056	0.038	0.051	- -
	(maximum)	0.083	0.093	0.067	- -
Productivity	(full test)	1.89	1.09	1.81	- -
(cm^2/hr/bl)	(typical)	2.39	1.61	2.28	- -
	(maximum)	3.55	3.94	2.99	- -
Yield		138/149 93%	128/149 86%	0/151 0%	0%
Slice Taper	(mm)	0.054	0.092	- -	- -
Slice Bow	(mm)	0.061	0.160	- -	- -
Abrasive Utilization	(cm^3/kg)	100.75	152.43	195.48	- -
Oil Utilization	(cm^3/liter)	36.27	36.58	35.19	- -
Blade Wear Ratio	(cm^3/cm^3)	0.051	0.051	0.058	- -

SLICING TEST SUMMARY

PARAMETER	TEST	2-1-05	2-1-06	2-1-07	2-1-08
Material		- -	100 Si	100 Si	100 Si
Size	(mm)	- -	100	100	100
Area/Slice	(cm^2)	- -	78.5	78.5	78.5
Blade Thickness	(mm)	- -	0.15 x 6.35	0.15 x 6.35	0.15 x 6.35
Spacer Thickness	(mm)	- -	0.36	0.36	0.36
Blade Height	(mm)	- -	6.35	6.35	6.35
Number of Blades		- -	150	150	
Load	(gram/blade)	- -	85	85	
Sliding Speed	(cm/sec)	- -	62.7	65.5	
Abrasive	(type/grit size)	- -	#600 SiC	#600 SiC	#600 SiC
Oil Volume	(liters)	- -	7.6 PC	7.6 PC	7.6 PC
Mix	(kg/liter)	- -	0.36	0.36	0.36
Slice Thickness	(mm)	- -	0.277	0.297	
Kerf Width	(mm)	- -	0.231	0.211	
Abrasive Kerf Loss	(mm)	- -	0.081	0.061	
Cutting Time	(hours)	- -	35.4	42.9	
Efficiency	(full test)	- -	0.9603	0.7030	
	(typical)	- -	1.2775	0.8108	
	(maximum)	- -	1.5011	0.9817	
Abrasion Rate	(full test)	- -	0.051	0.039	
(cm^3/hr/bl)	(typical)	- -	0.068	0.045	
	(maximum)	- -	0.080	0.054	
Productivity	(full test)	- -	2.22	1.83	
(cm^2/hr/bl)	(typical)	- -	2.94	2.13	
	(maximum)	- -	3.46	2.56	
Yield		- -	96 64%	119 80%	0%
Slice Taper	(mm)	- -	0.064	0.055	
Slice Bow	(mm)	- -	0.085	0.059	
Abrasive Utilization	(cm^3/kg)	- -	99.58	90.83	
Oil Utilization	(cm^3/liter)	- -	35.85	32.70	
Blade Wear Ratio	(cm^3/cm^3)	- -	0.050	0.040	

SLICING TEST SUMMARY

PARAMETER TEST	2-1-09	2-1-10	2-2-01	2-2-02
Material	100 Si	100 Si	100 Si	100 Si
Size (mm)	100	100	100	100
Area/Slice (cm^2)	78.5	78.5	78.5	78.5
Blade Thickness (mm)	0.15 x 6.35	0.15 x 6.35	0.15 x 6.35	0.15 x 6.35
Spacer Thickness (mm)	0.36	0.36	0.36	0.36
Blade Height (mm)	6.35	6.35	6.35	6.35
Number of Blades		145	10	10
Load (gram/blade)		85	- -	- -
Sliding Speed (cm/sec)		61.7	- -	- -
Abrasive (type/grit size)	#600 SiC	#600 SiC	#600 SiC	#600 SiC
Oil Volume (liters)	7.6 PC	7.6 PC	7.6 PC	7.6 PC
Mix (kg/liter)	0.36	0.36	0.36	0.36
Slice Thickness (mm)		0.287	0.282	0.321
Kerf Width (mm)		0.221	0.226	0.187
Abrasive Kerf Loss (mm)		0.071	0.076	0.037
Cutting Time (hours)		41.33	- -	- -
Efficiency (full test)		0.8037	- -	- -
(typical)		0.9916	- -	- -
(maximum)		1.3894	- -	- -
Abrasion Rate (full test)		0.042	- -	- -
(cm^3/hr/bl) (typical)		0.052	- -	- -
(maximum)		0.073	- -	- -
Productivity (full test)		1.90	- -	- -
(cm^2/hr/bl) (typical)		2.35	- -	- -
(maximum)		3.30	- -	- -
Yield	0%	130/144 90%	7 70%	3 30%
Slice Taper (mm)		0.052	- -	- -
Slice Bow (mm)		0.046	- -	- -
Abrasive Utilizacion (cm^3/kg)		92.03	6.47	5.39
Oil Utilization (cm^3/liter)		33.13	2.33	1.94
Blade Wear Ratio (cm^3/cm^3)		0.047	- -	- -

SLICING TEST SUMMARY

PARAMETER	TEST	2-3-01	2-3-02	2-3-03	2-3-04
Material		{100} Si	{100} Si	{100} Si	{100} Si
Size	(mm)	100	100	100	100
Area/Slice	(cm^2)	78.54	78.54	78.54	78.54
Blade Thickness	(mm)	0.15 x 6.35	0.15 x 6.35	0.15 x 6.35	0.15 x 6.35
Spacer Thickness	(mm)	0.41	0.30	0.36	0.41
Blade Height	(mm)	6.4	6.4	6.4	6.4
Number of Blades		150	155	270	137
Load	(gram/blade)	85	85	85	85
Sliding Speed	(cm/sec)	67.7	64.6	61.9	71.30
Abrasive	(type/grit size)	#500 SiC	#600 SiC	#600 SiC	#500/600/800S
Oil Volume	(liters)	7.6 (PC)	7.6 (LUB)	716 (LUB)	7.6 (PC)
Mix	(kg/liter)	0.36	0.36	0.36	0.36 Total
Slice Thickness	(mm)	0.320	- -	0.320	0.313
Kerf Width	(mm)	0.239	- -	0.188	0.246
Abrasive Kerf Loss	(mm)	0.086	- -	0.036	0.094
Cutting Time	(hours)	24.5	27.8	32.4	22.1
Efficiency	(full test)	1.34		0.87	1.45
	(typical)	1.49	- -	1.12	1.66
	(maximum)	1.69	- -	1.30	1.94
Abrasion Rate	(full test)	0.077	- -	0.046	0.087
(cm^3/hr/bl)	(typical)	0.09	- -	0.06	0.100
	(maximum)	0.10	- -	0.07	0.117
Productivity	(full test)	3.21	2.83	2.42	3.55
(cm^2/hr/bl)	(typical)	3.57	- -	3.12	4.08
	(maximum)	4.05	- -	3.63	4.76
Yield		100/149 (67%)	0/154 (0%)	20-30%	113/136(83%)
Slice Taper	(mm)	0.039	- -		0.040
Slice Bow	(mm)	0.034	- -		0.051
Abrasive Utilization	(cm^3/kg)	102.9	89.0	145.7	96.7
Oil Utilization	(cm^3/liter)	37.0	32.0	52.5	34.8
Blade Wear Ratio	(cm^3/cm^3)	0.039	0.049	0.060	0.046

SLICING TEST SUMMARY

PARAMETER TEST	2-3-05	2-3-06	2-3-07	2-3-08
Material	100 Si	100 Si	100 Si	100 Si
Size (mm)	100	100	100	100
Area/Slice (cm^2)	78.54	78.54	78.54	78.54
Blade Thickness (mm)	0.15	0.15 x 6.35	0.15 x 6.35	0.15 x 6.35
Spacer Thickness (mm)	0.36	0.36	0.36	0.36
Blade Height (mm)	6.4	6.4	6.4	6.4
Number of Blades	134	270	131	150
Load (gram/blade)	85	85	85	85
Sliding Speed (cm/sec)	66.2	63.76		61.15
Abrasive (type/grit size)	#600/800 SiC	#600 SiC	#600/800/ 1000 Sic	#600/800/ 1000 SiC
Oil Volume (liter)	7.6 PC	7.6 Lub.	7.6 PC	7.6 PC
Mix (kg/liter)	0.36 Total	0.24	0.18 Total	0.36 Total
Slice Thickness (mm)	0.315	0.292		0.320
Kerf Width (mm)	0.193	0.216		0.188
Abrasive Kerf Loss (mm)	0.041	0.064		0.038
Cutting Time (hours)	22.1	34.25	23.20	44.10
Efficiency (full test)	1.23	0.93		0.656
(typical)	1.41	1.15		0.812
(maximum)	1.49	1.27		0.939
Abrasion Rate (cm^3/hr/bl) (full test)	0.069	.050		.034
(typical)	0.079	.062		.042
(maximum)	0.084	.069		.049
Productivity (cm^2/hr/bl) (full test)	3.55	2.29	3.39	1.78
(typical)	4.09	2.87		2.23
(maximum)	4.35	3.19		2.60
Yield	38/132 29%	52/269 19%	4/130 3%	17/149 11%
Slice Taper (mm)		.065		.101
Slice Bow (mm)		.054		.107
Abrasive Utilization (cm^3/kg)	74.2	251.3		81.1
Oil Utilization (cm^3/liter)	26.7	60.3		29.2
Blade Wear Ratio (cm^3/cm^3)	0.063	.054		.067

SLICING TEST SUMMARY

PARAMETER	TEST	2-3-09	2-3-10	2-3-11	2-3-12
Material		100 Si	100 Si	100 Si	100 Si
Size	(mm)	100	100	100	100
Area/Slice	(cm^2)	78.54	78.54	78.54	78.54
Blade Thickness	(mm)	0.15 x 6.35	0.15 x 6.35	0.15 x 6.35	0.15 x 6.35
Spacer Thickness	(mm)	0.36	0.41	0.36	- -
Blade Height	(mm)	6.4	6.4	6.4	6.4
Number of Blades		136	131	150	150
Load	(gram/blade)	85	85	85	85
Sliding Speed	(cm/sec)	64.44		- -	- -
Abrasive	(type/grit size)	#600 SiC	#600 SiC	#600 SiC	- -
Oil Volume	(liters)	7.6 Lub.	7.6 Lub.	7.6 Lub.	- -
Mix	(kg/liter)	0.12	0.06	0.12	- -
Slice Thickness	(mm)	0.304		- -	- -
Kerf Width	(mm)	0.204		- -	- -
Abrasive Kerf Loss	(mm)	0.052		- -	- -
Cutting Time	(hours)	36.20	44.55	32.7	- -
Efficiency	(full test)	0.81		- -	- -
	(typical)	1.06		- -	- -
	(maximum)	1.28		- -	- -
Abrasion Rate	(full test)	.044		- -	- -
(cm^3/hr/bl)	(typical)	.058		- -	- -
	(maximum)	.070		- -	- -
Productivity	(full test)	2.17	1.76	- -	- -
(cm^2/hr/bl)	(typical)	2.84		- -	- -
	(maximum)	3.43		- -	- -
Yield		16/135 12%	5/130 4%	0/149 0%	- -
Slice Taper	(mm)	.078		- -	- -
Slice Bow	(mm)	.168		- -	- -
Abrasive Utilization	(cm^3/kg)	239.2		- -	- -
Oil Utilization	(cm^3/liter)	28.7		- -	- -
Blade Wear Ratio	(cm^3/cm^3)	.064		- -	- -

SLICING TEST SUMMARY

PARAMETER	TEST	2-3-13	2-3-14	2-3-15	2-3-16
Material		100 Si	100 Si	100 Si	100 Si
Size	(mm)	100	100	100	100
Area/Slice	(cm^2)	78.54	78.54	78.54	78.54
Blade Thickness	(mm)	0.15 x 6.35	0.15 x 6.35	- -	0.15 x 6.35
Spacer Thickness	(mm)	- -	- -	- -	0.36
Blade Height	(mm)	6.4	6.4	- -	6.35
Number of Blades		153	136	- -	123
Load	(gram/blade)	85	85	- -	85
Sliding Speed	(cm/sec)	- -	- -	- -	- -
Abrasive	(type/grit size)	- -	- -	- -	#600 SiC
Oil Volume	(liters)	- -	- -	- -	7.6
Mix	(kg/liter)	- -	- -	- -	0.36
Slice Thickness	(mm)	- -	- -	- -	- -
Kerf Width	(mm)	- -	- -	- -	- -
Abrasive Kerf Loss	(mm)	- -	- -	- -	- -
Cutting Time	(hours)	- -	- -	- -	- -
Efficiency	(full test)	- -	- -	- -	- -
	(typical)	- -	- -	- -	- -
	(maximum)	- -	- -	- -	- -
Abrasion Rate	(full test)	- -	- -	- -	- -
(cm^3/hr/bl)	(typical)	- -	- -	- -	- -
	(maximum)	- -	- -	- -	- -
Productivity	(full test)	- -	- -	- -	- -
(cm^2/hr/bl)	(typical)	- -	- -	- -	- -
	(maximum)	- -	- -	- -	- -
Yield		- -	- -	- -	- -
Slice Taper	(mm)	- -	- -	- -	- -
Slice Bow	(mm)	- -	- -	- -	- -
Abrasive Utilization	(cm^3/kg)	- -	- -	- -	- -
Oil Utilization	(cm^3/liter)	- -	- -	- -	- -
Blade Wear Ratio	(cm^3/cm^3)	- -	- -	- -	- -

SLICING TEST SUMMARY

PARAMETER	TEST	2-3-17	2-3-18	2-3-19	2-3-20
Material		100 Si	100 Si	100 Si	100 Si
Size	(mm)	100	100	100	100
Area/Slice	(cm^2)	78.54	78.54	78.54	78.54
Blade Thickness	(mm)	0.15 x 6.35	0.15	0.15	0.15
Spacer Thickness	(mm)	0.36	0.36	0.36	0.36
Blade Height	(mm)	6.35	6.35	6.35	6.35
Number of Blades		145	150	150	150
Load	(gram/blade)	85	85	85	85
Sliding Speed	(cm/sec)	53.43	65	65	65
Abrasive	(type/grit size)	#600 SiC	#600 SiC	#600 SiC	#600 SiC
Oil Volume	(liters)	7.6 M.O.	7.6 WBV IV	7.6 WBV V	7.6 M.O + Lard
Mix	(kg/liter)	0.36	0.36	0.36	0.36
Slice Thickness	(mm)	0.309			
Kerf Width	(mm)	0.201			
Abrasive Kerf Loss	(mm)	0.051			
Cutting Time	(hours)	40.25			
Efficiency	(full test)	0.8618			
	(typical)	0.8298			
	(maximum)	1.6734			
Abrasion Rate	(full test)	0.039			
(cm^3/hr/bl)	(typical)	0.038			
	(maximum)	0.076			
Productivity	(full test)	1.95			
(cm^2/hr/bl)	(typical)	1.89			
	(maximum)	3.78			
Yield		32 22%	0	0	
Slice Taper	(mm)	0.091			
Slice Bow	(mm)	0.071			
Abrasive Utilization	(cm^3/kg)	83.53			
Oil Utilization	(cm^3/liter)	30.07			
Blade Wear Ratio	(cm^3/cm^3)	0.057			

SLICING TEST SUMMARY

PARAMETER / TEST	2-3-21	2-3-22	2-3-23	2-3-24
Material	100 Si	100 Si	100 Si	100 Si
Size (mm)	100	100	100	100
Area/Slice (cm^2)	78.54	78.54	78.54	78.54
Blade Thickness (mm)	0.15 x 6.35	0.15	0.15 x 6.35	
Spacer Thickness (mm)	0.36	0.36	0.36	
Blade Height (mm)	6.35	6.35	6.35	
Number of Blades	156	150	150	
Load (gram/blade)	85	85	85	
Sliding Speed (cm/sec)	65.34	65	62.10	
Abrasive (type/grit size)	Norton 500	#600 SiC	#600 SiC	ASSIGNED TO WATER, LOW BLADE STRESS: NOT RUN
Oil Volume (liters)	7.6	7.6 D. W.	7.6 Min.Oil/L	
Mix (kg/liter)	0.36	0.36	0.36	
Slice Thickness (mm)	0.242		0.266	
Kerf Width (mm)	0.266		0.242	
Abrasive Kerf Loss (mm)	0.116		0.092	
Cutting Time (hours)	11.33		36.75	
Efficiency (full test)	3.325		0.9886	
(typical)	1.699		1.3175	
(maximum)	3.6173		1.6590	
Abrasion Rate (cm^3/hr/bl) (full test)	0.184		0.052	
(typical)	0.094		0.069	
(maximum)	0.200		0.087	
Productivity (cm^2/hr/bl) (full test)	6.93		2.14	
(typical)	3.53		2.85	
(maximum)	7.52		3.59	
Yield	113 73%	0	18/150 12%	
Slice Taper (mm)	0.039		0.120	
Slice Bow (mm)	0.047		0.118	
Abrasive Utilization (cm^3/kg)	119.08		104.17	
Oil Utilization (cm^3/liter)	42.87		37.50	
Blade Wear Ratio (cm^3/cm^3)	0.040		0.042	

SLICING TEST SUMMARY

PARAMETER	TEST	2-3-25	2-3-26	2-3-27	2-3-28
Material		100 Si	100 Si	100 Si	Si
Size	(mm)	100	100	100	100 dia
Area/Slice	(cm^2)	78.5	78.5	78.5	78.5
Blade Thickness	(mm)	0.15 x 6.35	0.15 x 6.35	0.15 x 6.35	0.15
Spacer Thickness	(mm)	0.36	0.36	0.36	0.36
Blade Height	(mm)	6.35	6.35	6.35	6.35
Number of Blades		150	150	146	150
Load	(gram/blade)	85	85	85	85
Sliding Speed	(cm/sec)	61.03	63.39	63.57	58.16
Abrasive	(tyoe/grit size)	#600 SiC	#600 SiC	#600 SiC	SiC/#600
Oil Volume	(liters)	7.6 Lard/M.oi	7.6 100 SUS M. Oil	7.6 Lard/Min.	7.6
Mix	(kg/liter)	0.36	0.36	0.48	0.48
Slice Thickness	(mm)	0.282	0.238	0.263	0.278
Kerf Width	(mm)	0.226	0.270	0.245	0.230
Abrasive Kerf Loss	(mm)	0.076	0.120	0.095	0.080
Cutting Time	(hours)	61.0	61.08	26.42	38.33
Efficiency	(full test)	0.561	0.6519	1.356	0.954
	(typical)	0.804	1.0009	1.383	1.293
	(maximum)	1.2593	3.8872	1.8459	1.686
Abrasion Rate	(full test)	0.029	0.035	0.073	0.047
(cm^3/hr/bl)	(typical)	0.042	0.054	0.074	0.064
	(maximum)	0.065	0.209	0.099	0.083
Productivity	(full test)	1.287	1.29	2.971	2.049
(cm^2/hr/bl)	(typical)	1.860	2.00	3.025	2.784
	(maximum)	2.879	7.74	4.047	3.611
Yield		73/150 49%	109/149 73%	7/146 5%	66%
Slice Taper	(mm)	0.092	0.102	0.047	0.087
Slice Bow	(mm)	0.128	0.128	0.038	0.099
Abrasive Utilization	(cm^3/kg)	97.19	116.19	76.85	7[illegible].23
Oil Utilization	(cm^3/liter)	34.99	41.83	36.89	35.63
Blade Wear Ratio	(cm^3/cm^3)	0.049	0.049	0.042	0.042

SLICING TEST SUMMARY

PARAMETER TEST	2-3-29	2-3-30	2-3-31	2-3-32
Material	Si	Si	Si	Si
Size (mm)	100 Dia	100 Dia	100 Dia	100 Dia
Area/Slice (cm^2)	78.5	78.5	78.5	78.5
Blade Thickness (mm)	0.15	0.15	0.15	0.15
Spacer Thickness (mm)	0.36	0.36	0.36	0.36
Blade Height (mm)	6.35	6.35	6.35	6.35
Number of Blades	150	150	150	150
Load (gram/blade)	85	85	85	85
Sliding Speed (cm/sec)	64.2	64.2	64.2	64.2
Abrasive (type/grit size)	SiC/#600	SiC/#600	SiC/#600	SiC/#600
Oil Volume (liters)	6.3*	6.3	6.3*	6.3*
Mix (kg/liter)	0.36	0.36	0.36	0.36
Slice Thickness (mm)		0.260		
Kerf Width (mm)		0.248		
Abrasive Kerf Loss (mm)		0.098		
Cutting Time (hours)		30.33		
Efficiency (full test)		1.178		
(typical)		1.474		
(maximum)		2.317		
Abrasion Rate (full test)		0.064		
(cm^3/hr/bl) (typical)		0.080		
(maximum)		0.126		
Productivity (full test)		2.590		
(cm^2/hr/bl) (typical)		3.220		
(maximum)		5.072		
Yield		99%		
Slice Taper (mm)		0.051		
Slice Bow (mm)		0.044		
Abrasive Utilization (cm^3/kg)		129.03		
Oil Utilization (cm^3/liter)		46.45		
Blade Wear Ratio (cm^3/cm^3)		0.040		
	*W&B #1	*Norton MCA 132	*W&B #2698	*100 SUS M.O & W&B #2213

SLICING TEST SUMMARY

PARAMETER TEST	2-3-33	2-3-34	2-3-35	2-3-36
Material	100 Si	100 Si	Si	Si
Size (mm)	100	100	100 Dia	100 Dia
Area/Slice (cm^2)	78.54	78.54	78.5	78.5
Blade Thickness (mm)	0.15	0.15	0.15	0.15
Spacer Thickness (mm)	0.36	0.36	0.36	0.36
Blade Height (mm)	6.35	6.35	6.35	6.35
Number of Blades	150	150	150	150
Load (gram/blade)	85	85	85	85
Sliding Speed (cm/sec)	65	65	64.2	64.2
Abrasive (type/grit size)	#600 SiC *	#600 SiC	SiC/#600	SiC/#600*
Oil Volume (liters)	7.6 PC	7.6 M.O.*	6.3*	6.3(100 SUS)
Mix (kg/liter)	0.36	0.36	0.36	0.36
Slice Thickness (mm)	0.276			
Kerf Width (mm)	0.234			
Abrasive Kerf Loss (mm)	0.084			
Cutting Time (hours)	28.7			
Efficiency (full test)				
(typical)				
(maximum)				
Abrasion Rate (cm^3/hr/bl) (full test)				
(typical)				
(maximum)				
Productivity (cm^2/hr/bl) (full test)				
(typical)				
(maximum)				
Yield	149/149 100%	0	0	0
Slice Taper (mm)	0.063			
Slice Bow (mm)	0.131			
Abrasive Utilization (cm^3/kg)				
Oil Utilization (cm^3/liter)				
Blade Wear Ratio (cm^3/cm^3)				
	*33% recycled	* + Lard + surfactant	*H_2O + VCI-309	* treated

SLICING TEST SUMMARY

PARAMETER TEST	2-3-37	2-3-38	2-4-01	2-4-02
Material	100 Si	100 Si	{100} Si	{100} Si
Size (mm)	100	100	100	100
Area/Slice (cm^2)	78.54	78.54	78.54	78.54
Blade Thickness (mm)	0.15	0.15	0.15 x 6.35	0.15 x 6.35
Spacer Thickness (mm)	0.36	0.36	0.36	0.41
Blade Height (mm)	6.35	6.35	6.4	6.4
Number of Blades	150	150	165	150
Load (gram/blade)	85	85	85	85
Sliding Speed (cm/sec)	65	65	64.8	64.8
Abrasive (type/grit size)	#600 SiC	#600 SiC *	#600 SiC	#600 SiC
Oil Volume (liters)	7.6 WBV VI	7.6 PC	7.6	7.6
Mix (kg/liter)	0.36	0.30	0.36	0.36
Slice Thickness (mm)			0.314	0.358
Kerf Width (mm)			0.194	0.201
Abrasive Kerf Loss (mm)			0.042	0.049
Cutting Time (hours)			22.4	22.4
Efficiency (full test)			1.24	1.28
(typical)			1.47	1.50
(maximum)			1.67	1.80
Abrasion Rate (cm^3/hr/bl) (full test)			0.068	0.070
(typical)			0.08	0.08
(maximum)			0.09	0.10
Productivity (cm^2/hr/bl) (full test)			3.51	3.51
(typical)			4.16	4.10
(maximum)			4.72	4.92
Yield	0	138/149 93%	97/164 (59%)	75/144 (50%)
Slice Taper (mm)			0.074	0.079
Slice Bow (mm)			0.072	0.056
Abrasive Utilization (cm^3/kg)			91.9	86.5
Oil Utilization (cm^3/liter)			33.1	31.2
Blade Wear Ratio (cm^3/cm^3)			0.053	0.055

* 33% recycled

SLICING TEST SUMMARY

PARAMETER TEST		2-4-03	2-4-04	2-4-05	2-4-06
Material		100 Si	100 Si	100 Si	100 Si
Size	(mm)	100(Wafers)*	100	100	100
Area/Slice	(cm^2)	4 (2 x 2)	78.54	78.54	78.54
Blade Thickness	(mm)		0.15 x 6.35	0.20 x 6.35	0.15 x 6.35
Spacer Thickness	(mm)		0.41	0.41	0.41
Blade Height	(mm)		6.4	6.4	6.4
Number of Blades			271	78	205
Load	(gram/blade)		85	113.4	85
Sliding Speed	(cm/sec)		65.3	61.14	65.77
Abrasive	(type/grit size)		#600 SiC	#600 SiC	#600 SiC
Oil Volume	(liters)		7.6	7.6 PC	7.6 PC
Mix	(kg/liter)		0.36	0.48	0.36
Slice Thickness	(mm)		0.322	0.333	0.351
Kerf Width	(mm)		0.237	0.277	0.208
Abrasive Kerf Loss	(mm)		0.087	0.074	0.058
Cutting Time	(hours)		26.55	36.50	40.3
Efficiency	(full test)		1.25	0.87	0.7360
	(typical)		1.53	1.42	1.1027
	(maximum)		1.733	1.85	1.6696
Abrasion Rate	(full test)		.069	.060	0.041
(cm^3/hr/bl)	(typical)		.085	.098	0.061
	(maximum)		.096	.128	0.093
Productivity	(full test)		2.91	2.15	1.95
(cm^2/hr/bl)	(typical)		3.59	3.54	2.93
	(maximum)		4.06	4.62	4.47
Yield			78/270 29%	42/77 55%	130/204 64%
Slice Taper	(mm)		0.044	.035	0.117
Slice Bow	(mm)		0.046	.057	0.112
Abrasive Utilization	(cm^3/kg)		184.2	46.5	122.4
Oil Utilization	cm^3/liter)		66.3	22.3	44.07
Blade Wear Ratio	(cm^3/cm^3)		.052		0.058

* dicing

SLICING TEST SUMMARY

PARAMETER	TEST	2-5-01	2-5-02	2-5-03	2-5-04
Material		{100} Si	{100} Si	100 Si	100 Si
Size	(mm)	100	100	100	100
Area/Slice	(cm^2)	78.54	78.54	78.54	78.54
Blade Thickness	(mm)	0.15 x 6.35	0.15 x 6.35	0.15 x 6.35	0.15 x 6.35
Spacer Thickness	(mm)	0.30	0.41	0.41	0.41
Blade Height	(mm)	6.4	6.4	6.4	6.4
Number of Blades		120	150	125	136
Load	(gram/blade)	85	85	113.4	85
Sliding Speed	(cm/sec)	63.5	66.9	65.73	65.21
Abrasive	(type/grit size)	#600 SiC	#600 SiC	#600 SiC	#600 SiC
Oil Volume	(liters)	7.6	7.6	7.6 PC	7.6 PC
Mix	(kg/liter)	0.36	0.36	0.48	0.36
Slice Thickness	(mm)	- -	0.334	0.341	0.330
Kerf Width	(mm)	- -	0.225	0.269	0.229
Abrasive Kerf Loss	(mm)	- -	0.073	0.069	0.076
Cutting Time	(hours)	23.4	23.0	25.05	65.[illegible]5
Efficiency	(full test)	- -	1.36	1.13	0.49
	(typical)	- -	1.47	1.30	1.33
	(maximum)	- -	2.05	1.66	2.06
Abrasion Rate	(full test)	- -	0.077	0.084	.027
(cm^3/hr/bl)	(typical)	- -	0.08	0.097	.073
	(maximum)	- -	0.12	0.123	.114
Productivity	(full test)	3.36	3.42	3.14	1.20
(cm^2/hr/bl)	(typical)	- -	3.70	3.61	3.19
	(maximum)	- -	5.16	4.58	4.98
Yield		0/119 (0%)	63/149 (42%)	124/124 100%	96/135 71%
Slice Taper	(mm)	- -	0.069	[illegible]	.090
Slice Bow	(mm)	- -	0.051	0.030	.137
Abrasive Utilization	(cm^3/kg)	68.9	96.9	72.3	89.4
Oil Utilization	(cm^3/liter)	24.8	34.9	34.7	32.2
Blade Wear Ratio	(cm^3/cm^3)	0.047	0.049	0.048	.048

SLICING TEST SUMMARY

PARAMETER TEST	2-5-05	2-5-06	2-5-07	2-5-08
Material	100 Si	100 Si	100 Si	100 Si
Size (mm)	100	100	100	100
Area/Slice (cm^2)	78.54	78.54	78.54	- -
Blade Thickness (mm)	0.15 x 6.35	0.2	0.15 x 6.35	0.15 x 12.70
Spacer Thickness (mm)	0.36	0.36, 0.41	0.36	0.46 - 0.56
Blade Height (mm)	6.4	6.4	6.4	12.7
Number of Blades	150	150	150	116
Load (gram/blade)	≤ 85	113.4	85	113.4
Sliding Speed (cm/sec)	61.8	64	63.8	- -
Abrasive (type/grit size)	#600 SiC	#600 SiC	#600 SiC	#600 SiC
Oil Volume (liters)	7.6 PC	7.6 PC	7.6 PC	7.6 PC
Mix (kg/liter)	0.36	0.48	0.36	0.48
Slice Thickness (mm)	0.290		0.267	- -
Kerf Width (mm)	0.218		0.241	- -
Abrasive Kerf Loss (mm)	0.068		0.091	- -
Cutting Time (hours)	76.7		32.3	- -
Efficiency (full test)	0.4203		1.0918	- -
(typical)	0.6895		1.1546	- -
(maximum)	1.2566		1.4184	- -
Abrasion Rate (full test)	0.022		0.059	- -
(cm^3/hr/bl) (typical)	0.017		0.062	- -
(maximum)	* 0.060		0.077	- -
Productivity (full test)	1.02		2.43	- -
(cm^2/hr/bl) (typical)	0.78		2.57	- -
(maximum)	2.75		3.20	- -
Yield	100/149 67%	0	35/149 23%	0/115 0%
Slice Taper (mm)	0.055		0.098	- -
Slice Bow (mm)	0.154		0.101	- -
Abrasive Utilization (cm^3/kg)	93.87		103.77	- -
Oil Utilization (cm^3/liter)	33.79		37.36	- -
Blade Wear Ratio (cm^3/cm^3)	0.050		0.045	- -

SLICING TEST SUMMARY

PARAMETER TEST		2-5-09	2-5-10	2-5-11	2-5-12
Material		100 Si	100 Si	100 Si	100 Si
Size	(mm)	127	100	100	127
Area/Slice	(cm^2)	126.7	78.54	78.54	126.7
Blade Thickness	(mm)	0.15 x 6.35	0.15 x 6.35	0.15 x 6.35	0.15 x 6.35
Spacer Thickness	(mm)	0.41	0.41	0.30	0.41
Blade Height	(mm)	6.35	6.35	6.35	6.35
Number of Blades		137	150	166	136
Load	(gram/blade)	85	85	85	85
Sliding Speed	(cm/sec)	61.22	65.28	60.74	1
Abrasive	(type/grit size)	#600 SiC	#600 SiC	#600 SiC	#600 SiC
Oil Volume	(liters)	7.6 PC	7.6 PC	7.6 PC	7.6 PC
Mix	(kg/liter)	0.36	0.36	0.36	0.36
Slice Thickness	(mm)	0.351	0.317	0.235	- -
Kerf Width	(mm)	0.208	0.242	0.222	- -
Abrasive Kerf Loss	(mm)	0.058	0.092	0.072	- -
Cutting Time	(hours)	[illegible]2.8	36.4	35.25	- -
Efficiency	(full test)	0.9643	0.9405	0.9525	- -
	(typical)	1.776	1.153	1.385	- -
	(maximum)	2.1949	1.7089	1.5698	- -
Abrasion Rate	(full test)	0.050	0.052	0.049	- -
(cm^3/hr/bl)	(typical)	0.092	0.064	0.066	- -
	(maximum)	0.114	0.094	0.081	- -
Productivity	(full test)	2.400	2.16	2.23	- -
(cm^2/hr/bl)	(typical)	4.42	2.64	2.97	- -
	(maximum)	5.48	3.88	3.65	- -
Yield		73 54%	149 100%	127 77%	0 0%
Slice Taper	(mm)	- -	0.071	0.065	- -
Slice Bow	(mm)	- -	0.041	0.075	- -
Abrasive Utilization	(cm^3/kg)	132.1	104.2	105.7	- -
Oil Utilization	(cm^3/liter)	47.57	37.52	38.04	- -
Blade Wear Ratio	(cm^3/cm^3)	0.049	0.046	0.052	- -

SLICING TEST SUMMARY

PARAMETER	TEST	2-5-13	2-5-14	2-5-15	2-5-16
Material		100 Si	100 SI	100 Si	100 Si
Size	(mm)	50.8 (½)	100	100	100
Area/Slice	(cm^2)	39.27	78.54	78.54	78.54
Blade Thickness	(mm)	0.10	0.20	0.15	0.20
Spacer Thickness	(mm)	0.41	0.30	0.41	0.30
Blade Height	(mm)	4.75	6.35	6.35	6.35
Number of Blades		150	150	135	150
Load	(gram/blade)	56.7	113.4	85	85
Sliding Speed	(cm/sec)	64.15	65.25	62.62	62.65
Abrasive	(type/grit size)	#600 Sic	#600 SiC	#600 SiC	#600 SiC
Oil Volume	(liters)	7.6 PC	7.6 PC	7.6 PC	7.6 PC
Mix	(kg/liter)	0.36	0.36	0.36	0.36
Slice Thickness	(mm)	0.356	0.252	0.308	0.278
Kerf Width	(mm)	0.152	0.256	0.251	0.230
Abrasive Kerf Loss	(mm)	0.052	0.056	0.101	0.030
Cutting Time	(hours)	21.75	27.33	35.25	32.9
Efficiency	(full test)	0.7725	1.0037	1.0558	1.0365
	(typical)	0.7567	1.230	1.197	1.252
	(maximum)	0.9936	1.4031	1.9502	1.8992
Abrasion Rate	(full test)	0.028	0.074	0.056	0.055
(cm^3/hr/bl)	(typical)	0.027	0.091	0.063	0.066
	(maximum)	0.036	0.103	0.103	0.101
Productivity	(full test)	1.81	2.87	2.23	2.39
(cm^2/hr/bl)	(typical)	1.78	3.55	2.51	2.87
	(maximum)	2.37	4.02	4.10	4.39
Yield		- -	123 83%	124 93%	108 72%
Slice Taper	(mm)	- -	0.054	0.065	0.060
Slice Bow	(mm)	- -	0.047	0.067	0.066
Abrasive Utilization	(cm^3/kg)	32.81	110.3	97.35	98.87
Oil Utilization	(cm^3/liter)	11.81	29.69	35.05	35.59
Blade Wear Ratio	(cm^3/cm^3)	0.058	0.050	0.046	0.060

SLICING TEST SUMMARY

PARAMETER	TEST	2-5-17	2-5-18	2-5-19	2-5-20
Material		100 Si	100 Si	100 Si	100 Si
Size	(mm)	100	100	100	100
Area/Slice	(cm^2)	78.54	78.54	78.54	78.54
Blade Thickness	(mm)	0.15	0.15	0.15	0.10
Spacer Thickness	(mm)	0.36	0.36	0.36	0.41
Blade Height	(mm)	6.35	6.35	6.35	4.8
Number of Blades		150	146	300	147
Load	(gram/blade)	85	85	85	85
Sliding Speed	(cm/sec)	62.91	63.79	63.56	64
Abrasive	(type/grit size)	#600 SiC	#600 SiC	#600 SiC	#600 SiC
Oil Volume	(liters)	7.6 PC	7.6 PC	7.6 PC	7.6 PC
Mix	(kg/liter)	0.36	0.36	0.36	0.36
Slice Thickness	(mm)	0.296	0.297	0.270	
Kerf Width	(mm)	0.212	0.211	0.238	
Abrasive Kerf Loss	(mm)	0.062	0.061	0.088	
Cutting Time	(hours)	32.5	37.25	31.0	115
Efficiency	(full test)	0.9571	0.8144	1.1145	
	(typical)	1.138	1.074	1.1823	
	(maximum)	1.6694	1.4001	1.5045	
Abrasion Rate	(full test)	0.051	0.044	0.060	
(cm^3/hr/bl)	(typical)	0.061	0.058	0.064	
	(maximum)	0.089	0.076	0.081	
Productivity	(full test)	2.42	2.11	2.53	
(cm^2/hr/bl)	(typical)	2.88	2.75	2.69	
	(maximum)	4.20	3.60	3.40	
Yield		128 86%	113 78%	241 81%	0
Slice Taper	(mm)	0.057	0.064	0.049	
Slice Bow	(mm)	0.066	0.059	0.075	
Abrasive Utilization	(cm^3/kg)	91.43	88.38	204.74	
Oil Utilization	(cm^3/liter)	32.92	31.81	73.71	
Blade Wear Ratio	(cm^3/cm^3)	0.054	0.054	0.049	

SLICING TEST SUMMARY

PARAMETER TEST	2-5-21	2-5-22	2-6-01	2-6-02
Material	Si	Si	100 Si	100 Si
Size (mm)	100	100	100	100
Area/Slice (cm^2)	78.5	78.5	78.54	78.54
Blade Thickness (mm)	0.10	0.10	0.15 x 6.35	0.15 x 6.35
Spacer Thickness (mm)	0.30	0.30	0.36	0.36
Blade Height (mm)	4.76	4.76	6.4	6.4
Number of Blades	150	150	150	138
Load (gram/blade)	- - *	- - *	127.6/85	85
Sliding Speed (cm/sec)	64.2	64.2	63.42	
Abrasive (type/grit size)	SiC/#600	SiC/#600	#600 SiC	#600 SiC
Oil Volume (liters)	7.6	7.6	7.6 PC	7.6 PC
Mix (kg/liter)	0.36	0.30	0.36	0.24
Slice Thickness (mm)			0.287	0.300
Kerf Width (mm)			0.221	0.208
Abrasive Kerf Loss (mm)			0.068	0.056
Cutting Time (hours)			22.55	12.35
Efficiency (full test)			1.15	
(typical)			1.59	
(maximum)			2.00	
Abrasion Rate (full test)			.077	
(cm^3/hr/bl) (typical)			.107	
(maximum)			.134	
Productivity (full test)			3.48	
(cm^2/hr/bl) (typical)			4.84	
(maximum)			6.06	
Yield	0	0	120/149 81%	0/137 0%
Slice Taper (mm)			.075	
Slice Bow (mm)			.020	
Abrasive Utilization (cm^3/kg)			95.3	
Oil Utilization (cm^3/liter)			34.3	
Blade Wear Ratio (cm^3/cm^3)			.054	

*cut rate 0.64 μm/sec (2-5-21)

* cut rate 0.64 μm/sec (2-5-22)

SLICING TEST SUMMARY

PARAMETER	TEST	2-6-03	2-6-04	2-6-05	2-7-01
Material		100 Si	100 Si	100 Si	100 Si
Size	(mm)	100	100	100	100
Area/Slice	(cm^2)	78.54	78.54	78.54	78.54
Blade Thickness	(mm)	0.15 x 6.35	0.15 x 6.35	0.15	0.20
Spacer Thickness	(mm)	0.36	0.36	0.36	0.41
Blade Height	(mm)	6.4	6.4	6.4	6.35
Number of Blades		150	150	300	131
Load	(gram/blade)	85	85	85	- - *
Sliding Speed	(cm/sec)	63.24	62.23	64	64
Abrasive	(type/grit size)	#600 SiC	#600 SiC	#600 SiC	#600 SiC
Oil Volume	(liters)	7.6 PC	7.6 PC	7.6 PC	34.1 PC
Mix	(kg/liter)	0.36	0.36	0.36	0.36
Slice Thickness	(mm)	0.274	0.267		0.301
Kerf Width	(mm)	0.234	0.241		0.309
Abrasive Kerf Loss	(mm)	0.082	0.091		0.109
Cutting Time	(hours)	28.20	30.50		- -
Efficiency	(full test)	1.21	1.16		- -
	(typical)	1.64	1.75		- -
	(maximum)	1.91	2.09		- -
Abrasion Rate	(full test)	.065	.061		- -
(cm^3/hr/bl)	(typical)	.088	.092		- -
	(maximum)	.102	.110		- -
Productivity	(full test)	2.79	2.53		- -
(cm^2/hr/bl)	(typical)	3.76	3.82		- -
	(maximum)	4.36	4.56		- -
Yield		80/149 54%	99/149 66%	0	106 82%
Slice Taper	(mm)	.060	.079		0.059
Slice Bow	(mm)	.059	.086		0.194
Abrasive Utilization	(cm^3/kg)	100.8	103.9		25.89
Oil Utilization	(cm^3/liter)	36.3	37.4		9.32
Blade Wear Ratio	(cm^3/cm^3)	.046	.047		- -

* .64 μm/m cut rate

SLICING TEST SUMMARY

PARAMETER TEST	2-7-02	2-7-03	2-7-04	2-7-05
Material	100 Si	100 Si	100 Si	Si
Size (mm)	100	100	100	100 dia
Area/Slice (cm^2)	78.5	78.5	78.5	78.5
Blade Thickness (mm)	0.20	0.15	0.15	0.15
Spacer Thickness (mm)	0.41	0.36	0.36	0.36
Blade Height (mm)	6.35	6.35	6.35	6.35
Number of Blades	131	975	95	975
Load (gram/blade)	- - *	- - *	- - *	85
Sliding Speed (cm/sec)	64	64	64	- -
Abrasive (type/grit size)	#600 SiC	#600 SiC	#600 SiC	SiC/#600
Oil Volume (liters)	37.9	37.9	37.9	37.9
Mix (kg/liter)	0.36	0.36	0.36	0.36
Slice Thickness (mm)			0.299	0.285
Kerf Width (mm)			0.208	0.224
Abrasive Kerf Loss (mm)			0.058	0.074
Cutting Time (hours)			36.8	41.58
Efficiency (full test)				
(typical)				
(maximum)				
Abrasion Rate (cm^3/hr/bl) (full test)			0.113	0.042
(typical)				
(maximum)				
Productivity (cm^2/hr/bl) (full test)			2.14	1.889
(typical)				
(maximum)				
Yield	0 (halted)	0	348 36%	31%
Slice Taper (mm)			0.082	0.105
Slice Bow (mm)			0.066	0.162
Abrasive Utilization (cm^3/kg)			296.52	125.44
Oil Utilization (cm^3/liter)			106.7	45.16
Blade Wear Ratio (cm^3/cm^3)				- -
	* .64 μm/min cut rate	* .64 μm/min cut rate	* .64 μm/min cut rate	

SLICING TEST SUMMARY

PARAMETER	TEST	2-7-06	2-7-07	2-7-08	2-7-09
Material		100 Si	100 Si	100 Si	100 Si
Size	(mm)	100	100	100	100
Area/Slice	(cm^2)	78.5	78.5	78.5	78.5
Blade Thickness	(mm)	0.15	0.10	0.15	0.15
Spacer Thickness	(mm)	0.36	0.41	0.36	0.36
Blade Height	(mm)	6.35	4.76	6.35	6.35
Number of Blades		940	1000	975	975
Load	(gram/blade)	85	56	84	84
Sliding Speed	(cm/sec)	64.2	64	64	64
Abrasive	(type/grit size)	SiC/#600			
Oil Volume	(liters)	37.9			
Mix	(kg/liter)	0.36		28	30.5
Slice Thickness	(mm)	0.267			
Kerf Width	(mm)	0.241			
Abrasive Kerf Loss	(mm)	0.091			
Cutting Time	(hours)	38.83			
Efficiency	(full test)	- -			
	(typical)	- -			
	(maximum)	- -			
Abrasion Rate	(full test)	0.049			
(cm^3/hr/bl)	(typical)	- -			
	(maximum)	- -			
Productivity	(full test)	2.023			
(cm^2/hr/bl)	(typical)	- -			
	(maximum)	- -			
Yield		90%/74% *	0	40-50% est.	20-30% est.
Slice Taper	(mm)	0.078			
Slice Bow	(mm)	0.085			
Abrasive Utilization	(cm^3/kg)	130.56			
Oil Utilization	(cm^3/liter)	47.0			
Blade Wear Ratio	(cm^3/cm^3)	- -			

* before/after cleaning

SLICING TEST SUMMARY

PARAMETER	TEST	2-7-10	2-7-11		
Material		100 Si	100 Si		
Size	(mm)	100	100		
Area/Slice	(cm^2)	78.54	78.54		
Blade Thickness	(mm)	0.10	0.15		
Spacer Thickness	(mm)	0.30	0.30		
Blade Height	(mm)	4.76	6.35		
Number of Blades		1165	1015		
Load	(gram/blade)	56.8	84		
Sliding Speed	(cm/sec)	64	64		
Abrasive	(type/grit size)	#600 SiC	#600 SiC		
Oil Volume	(liters)	37.9	37.9		
Mix	(kg/liter)	0.36	0.36		
Slice Thickness	(mm)				
Kerf Width	(mm)				
Abrasive Kerf Loss	(mm)				
Cutting Time	(hours)	28.5	27.2		
Efficiency	(full test)				
	(typical)				
	(maximum)				
Abrasion Rate	(full test)				
(cm^3/hr/bl)	(typical)				
	(maximum)				
Productivity	(full test)				
(cm^2/hr/bl)	(typical)				
	(maximum)				
Yield		0	0		
Slice Taper	(mm)				
Slice Bow	(mm)				
Abrasive Utilization	(cm^3/kg)				
Oil Utilization	(cm^3/liter)				
Blade Wear Ratio	(cm^3/cm^3)				

APPENDIX IV

PHASE II WAFER CHARACTERIZATION SUMMARY

WAFER THICKNESS CHARACTERIZATION SUMMARY

PARAMETER	TEST		2-1-01	2-1-02	2-1-03	2-1-06
SLICE	Diameter	(mm)	100	100	100	100
	Area	(cm^2)	78.5	78.5	78.5	78.5
THICKNESS	Average	μ	273.2	270.6	283.9	276.6
	Std. Dev.	μ	27.2	17.3	36.9	35.0
TOTAL VARIATION	Average	μ	52.7	84.8	64.8	56.7
	Std. Dev.	μ	30.3	11.4	37.6	23.9
STD. DEVIATION	Average	μ	20.1	31.7	28.8	20.8
	Std. Dev.	μ	12.0	5.8	17.4	8.7
VERTICAL TTV	Average	μ	53.7	91.9	- -	64.2
	Maximum	μ	126.5	131.6	- -	123.3
	Minimum	μ	22.8	74.7	- -	28.1
HORIZONTAL TTV	Average	μ	17.4	12.4	- -	13.6
	Maximum	μ	24.7	22.8	- -	40.4
	Minimum	μ	10.3	3.2	- -	3.2
VERTICAL BOW	Average	μ	67.9	170.2	- -	91.4
	Maximum	μ	127.6	218.3	- -	166.6
	Minimum	μ	25.9	105.3	- -	24.9
HORIZONTAL BOW	Average	μ	17.5	47.4	- -	38.4
	Maximum	μ	30.3	78.0	- -	82.1
	Minimum	μ	5.3	20.4	- -	19.8
VERTICAL CL BOW	Average	μ	122.9	319.7	- -	169.1
	Maximum	μ	161.3	406.6	- -	255.8
	Minimum	μ	70.3	207.3	- -	61.4
HORIZONTAL CL BOW	Average	μ	42.4	91.6	- -	78.3
	Maximum	μ	64.3	147.6	- -	154.5
	Minimum	μ	12.3	32.4	- -	31.7

WAFER THICKNESS CHARACTERIZATION SUMMARY

PARAMETER	TEST		2-1-07	2-1-10	2-2-01	2-2-02
SLICE	Diameter	(mm)	100	100	100	100
	Area	(cm^2)	78.5	78.5	78.5	78.5
THICKNESS	Average	μ	296.9	286.7	282.4	320.6
	Std. Dev.	μ	30.0	26.6	23.7	27.6
TOTAL VARIATION	Average	μ	46.8	54.4	38.0	57.9
	Std. Dev.	μ	18.8	17.4	7.8	37.9
STD. DEVIATION	Average	μ	16.6	20.1	13.6	19.6
	Std. Dev.	μ	7.5	7.1	3.9	14.2
VERTICAL TTV	Average	μ	55.0	51.9	57.6	63.6
	Maximum	μ	104.6	93.1	83.2	92.3
	Minimum	μ	21.7	23.2	39.5	23.3
HORIZONTAL TTV	Average	μ	14.2	14.7	11.4	16.4
	Maximum	μ	32.3	29.8	16.0	20.3
	Minimum	μ	3.7	7.2	7.4	11.8
VERTICAL BOW	Average	μ	63.8	47.7	63.3	48.3
	Maximum	μ	100.8	86.9	99.9	61.4
	Minimum	μ	28.5	6.3	18.0	25.9
HORIZONTAL BOW	Average	μ	14.7	15.7	15.4	17.8
	Maximum	μ	26.4	31.1	32.2	20.2
	Minimum	μ	4.7	3.8	7.1	15.9
VERTICAL CL BOW	Average	μ	117.6	92.3	125.4	40.2
	Maximum	μ	[illegible]	140.6	169.4	45.2
	Minimum	μ	51.5	28.9	68.9	31.5
HORIZONTAL CL BOW	Average	μ	24.5	32.1	44.2	24.9
	Maximum	μ	40.5	59.1	65.4	49.9
	Minimum	μ	8.1	10.1	15.3	12.2

WAFER THICKNESS CHARACTERIZATION SUMMARY

PARAMETER	TEST		2-3-01	2-3-03	2-3-04	2-3-06
SLICE	Diameter	(mm)	100	100	100	100
	Area	(cm^2)	78.5	78.5	78.5	78.5
THICKNESS	Average	μ	320	320	313	292.1
	Std. Dev.	μ	24	71	18	39.7
TOTAL VARIATION	Average	μ	34	91	36	60.4
	Std. Dev.	μ	14	58	22	21.2
STD. DEVIATION	Average	μ	12	38	14	23.8
	Std. Dev.	μ	6	25	9	8.7
VERTICAL TTV	Average	μ	40	- -	40	65.4
	Maximum	μ	99	- -	120	111.9
	Minimum	μ	13	- -	24	32.9
HORIZONTAL TTV	Average	μ	16	- -	10	18.6
	Maximum	μ	31	- -	24	38.3
	Minimum	μ	5	- -	3	6.2
VERTICAL BOW	Average	μ	40	- -	53	52.6
	Maximum	μ	112	- -	157	117.6
	Minimum	μ	8	- -	28	18.4
HORIZONTAL BOW	Average	μ	15	- -	16	63.9
	Maximum	μ	58	- -	40	86.2
	Minimum	μ	4	- -	6	24.0
VERTICAL CL BOW	Average	μ	68	- -	102	108.7
	Maximum	μ	141	- -	216	209.7
	Minimum	μ	36	- -	55	38.6
HORIZONTAL CL BOW	Average	μ	29	- -	31	139.4
	Maximum	μ	99	- -	57	195.2
	Minimum	μ	8	- -	16	40.2

WAFER THICKNESS CHARACTERIZATION SUMMARY

PARAMETER	TEST		2-3-01	2-3-03	2-3-04	2-3-06
SLICE	Diameter	(mm)	100	100	100	100
	Area	(cm^2)	78.5	78.5	78.5	78.5
THICKNESS	Average	μ	320	320	313	292.1
	Std. Dev.	μ	24	71	18	39.7
TOTAL VARIATION	Average	μ	34	91	36	60.4
	Std. Dev.	μ	14	58	22	21.2
STD. DEVIATION	Average	μ	12	38	14	23.8
	Std. Dev.	μ	6	25	9	8.7
VERTICAL TTV	Average	μ	40	- -	40	65.4
	Maximum	μ	99	- -	120	111.9
	Minimum	μ	13	- -	24	32.9
HORIZONTAL TTV	Average	μ	16	- -	10	18.6
	Maximum	μ	31	- -	24	38.3
	Minimum	μ	5	- -	3	6.2
VERTICAL BOW	Average	μ	40	- -	53	52.6
	Maximum	μ	112	- -	157	117.6
	Minimum	μ	8	- -	28	18.4
HORIZONTAL BOW	Average	μ	15	- -	16	63.9
	Maximum	μ	58	- -	40	86.2
	Minimum	μ	4	- -	6	24.0
VERTICAL CL BOW	Average	μ	68	- -	102	108.7
	Maximum	μ	141	- -	216	209.7
	Minimum	μ	36	- -	55	38.6
HORIZONTAL CL BOW	Average	μ	29	- -	31	139.4
	Maximum	μ	99	- -	57	195.2
	Minimum	μ	8	- -	16	40.2

WAFER THICKNESS CHARACTERIZATION SUMMARY

PARAMETER	TEST		2-3-08	2-3-09	2-3-17	2-3-21
SLICE	Diameter	(mm)	100	100	100	100
	Area	(cm^2)	78.5	78.5	78.5	78.5
THICKNESS	Average	μ	319.5	303.7	308.7	242.1
	Std. Dev.	μ	34.0	38.0	21.1	18.2
TOTAL VARIATION	Average	μ	58.9	57.6	82.3	41.2
	Std. Dev.	μ	18.3	37.0	39.5	9.0
STD. DEVIATION	Average	μ	20.8	20.4	32.0	14.9
	Std. Dev.	μ	7.2	15.8	15.5	3.3
VERTICAL TTV	Average	μ	100.8	78.2	91.0	39.1
	Maximum	μ	140.6	226.7	207.4	71.6
	Minimum	μ	79.1	45.6	42.4	26.7
HORIZONTAL TTV	Average	μ	26.4	17.5	12.8	15.9
	Maximum	μ	35.7	46.8	24.3	39.2
	Minimum	μ	18.1	7.0	5.5	4.2
VERTICAL BOW	Average	μ	118.0	159.0	83.0	40.5
	Maximum	μ	161.0	173.5	191.9	68.2
	Minimum	μ	70.9	144.7	38.4	14.3
HORIZONTAL BOW	Average	μ	41.7	30.7	26.9	31.1
	Maximum	μ	64.2	50.9	88.3	52.7
	Minimum	μ	26.7	12.6	8.4	9.2
VERTICAL CL BOW	Average	μ	214.1	335.3	142.0	93.2
	Maximum	μ	365.2	392.3	254.7	157.0
	Minimum	μ	81.2	171.9	29.5	41.3
HORIZONTAL CL BOW	Average	μ	70.1	43.3	46.8	59.0
	Maximum	μ	107.6	65.4	173.9	95.2
	Minimum	μ	20.5	27.8	16.7	18.3

WAFER THICKNESS CHARACTERIZATION SUMMARY

PARAMETER	TEST		2-3-23	2-3-25	2-3-26	2-3-27 *
SLICE	Diameter	(mm)	100	100	100	100
	Area	(cm^2)	78.5	78.5	78.5	78.5
THICKNESS	Average	μ	266.0	282.3	238.0	263.5
	Std. Dev.	μ	55.5	44.7	34.0	33.7
TOTAL VARIATION	Average	μ	113.6	79.3	91.6	42.4
	Std. Dev.	μ	41.1	32.4	23.8	8.8
STD. DEVIATION	Average	μ	44.9	30.2	36.9	15.1
	Std. Dev.	μ	15.9	13.5	10.1	3.1
VERTICAL TTV	Average	μ	119.6	91.8	101.8	46.7
	Maximum	μ	210.4	183.7	120.7	60.2
	Minimum	μ	40.4	38.8	34.9	32.0
HORIZONTAL TTV	Average	μ	22.3	16.1	15.8	12.6
	Maximum	μ	50.2	41.4	35.9	22.6
	Minimum	μ	6.8	1.5	2.9	6.4
VERTICAL BOW	Average	μ	107.6	123.5	132.8	43.2
	Maximum	μ	271.6	214.0	211.5	58.1
	Minimum	μ	43.5	62.2	28.4	15.9
HORIZONTAL BOW	Average	μ	24.7	21.2	29.5	23.7
	Maximum	μ	40.5	51.2	45.7	56.0
	Minimum	μ	12.0	5.6	9.7	8.9
VERTICAL CL BOW	Average	μ	235.2	255.3	256.5	76.8
	Maximum	μ	523.6	450.1	343.8	110.2
	Minimum	μ	88.2	141.2	34.3	57.4
HORIZONTAL CL BOW	Average	μ	43.8	42.6	56.5	48.3
	Maximum	μ	71.4	118.2	98.1	95.7
	Minimum	μ	12.6	10.9	23.9	10.6

* 7 wafers

WAFER THICKNESS CHARACTERIZATION SUMMARY

PARAMETER	TEST		2-3-28	2-3-30	2-3-33	2-4-01
SLICE	Diameter	(mm)	100	100	100	100
	Area	(cm^2)	78.5	78.5	78.5	78.5
THICKNESS	Average	μ	278.2	259.7	275.9	314
	Std. Dev.	μ	48.5	28.6	20.3	33
TOTAL VARIATION	Average	μ	76.7	48.3	56.9	62
	Std. Dev.	μ	32.4	16.6	23.0	23
STD. DEVIATION	Average	μ	29.7	16.8	20.3	26
	Std. Dev.	μ	13.0	5.0	9.3	11
VERTICAL TTV	Average	μ	86.7	50.9	62.9	74
	Maximum	μ	160.8	86.1	102.8	150
	Minimum	μ	34.7	25.1	28.8	30
HORIZONTAL TTV	Average	μ	20.3	17.2	18.4	16
	Maximum	μ	42.8	30.4	38.4	33
	Minimum	μ	6.7	5.6	7.1	4
VERTICAL BOW	Average	μ	121.8	53.0	82.8	82
	Maximum	μ	267.1	255.7	140.7	140
	Minimum	μ	42.0	11.3	35.3	29
HORIZONTAL BOW	Average	μ	28.8	23.2	40.0	19
	Maximum	μ	72.4	132.7	81.8	46
	Minimum	μ	7.5	2.8	6.6	4
VERTICAL CL BOW	Average	μ	197.7	87.8	181.1	144
	Maximum	μ	368.0	330.2	274.4	204
	Minimum	μ	57.3	30.9	103.5	80
HORIZONTAL CL BOW	Average	μ	46.3	48.2	69.5	33
	Maximum	μ	111.8	245.7	140.0	67
	Minimum	μ	10.1	6.2	23.9	11

WAFER THICKNESS CHARACTERIZATION SUMMARY

PARAMETER	TEST		2-4-02	2-4-04	2-4-05	2-4-06
SLICE	Diameter	(mm)	100	100	100	100
	Area	(cm^2)	78.5	78.5	78.5	78.5
THICKNESS	Average	μ	358	322	332.6	350.4
	Std. Dev.	μ	56	21.7	21.7	47.7
TOTAL VARIATION	Average	μ	66	35.6	63.8	96.7
	Std. Dev.	μ	43	23.3	19.7	50.3
STD. DEVIATION	Average	μ	28	13.7	24.6	36.0
	Std. Dev.	μ	19	10.2	7.8	19.3
VERTICAL TTV	Average	μ	79	44.0	65.9	116.9
	Maximum	μ	184	137.2	102.1	222.2
	Minimum	μ	22	17.4	34.3	42.2
HORIZONTAL TTV	Average	μ	13	9.0	15.3	21.0
	Maximum	μ	30	17.7	34.3	39.8
	Minimum	μ	4	1.9	6.6	2.8
VERTICAL BOW	Average	μ	69	36.6	56.8	121.3
	Maximum	μ	132	109.0	95.8	185.4
	Minimum	μ	13	11.5	30.09	42.3
HORIZONTAL BOW	Average	μ	18	15.7	53.4	34.2
	Maximum	μ	46	30.8	101.0	62.9
	Minimum	μ	7	6.5	8.7	3.2
VERTICAL CL BOW	Average	μ	101	91.7	113.3	224.7
	Maximum	μ	182	306.9	164.4	339.2
	Minimum	μ	28	15.9	81.3	61.8
HORIZONTAL CL BOW	Average	μ	32	29.2	109.7	65.3
	Maximum	μ	79	55.3	203.8	88.5
	Minimum	μ	14	8.6	19.4	23.2

WAFER THICKNESS CHARACTERIZATION SUMMARY

PARAMETER	TEST		2-5-02	2-5-03	2-5-05	2-5-07
SLICE	Diameter	(mm)	100	100	100	100
	Area	(cm^2)	78.5	78.5	78.5	78.5
THICKNESS	Average	μ	334	341.1	288.4	265.8
	Std. Dev.	μ	36	21.0	19.2	20.3
TOTAL VARIATION	Average	μ	65	35.1	52.2	66.0
	Std. Dev.	μ	28	14.9	19.4	20.2
STD. DEVIATION	Average	μ	25	13.3	17.8	25.3
	Std. Dev.	μ	12	6.3	7.9	8.5
VERTICAL TTV	Average	μ	69	44.3	54.9	97.9
	Maximum	μ	118	72.5	96.8	144.8
	Minimum	μ	32	21.8	22.3	73.5
HORIZONTAL TTV	Average	μ	14	11.5	9.7	18.4
	Maximum	μ	21	18.5	21.7	37.8
	Minimum	μ	7	4.3	2.5	9.8
VERTICAL BOW	Average	μ	61	36.1	163.3	79.2
	Maximum	μ	159	70.6	182.8	140.4
	Minimum	μ	17	16.1	121.5	61.7
HORIZONTAL BOW	Average	μ	20	24.1	12.9	17.1
	Maximum	μ	46	35.7	25.8	30.8
	Minimum	μ	4	5.5	3.4	9.0
VERTICAL CL BOW	Average	μ	102	60.3	307.3	201.9
	Maximum	μ	211	102.3	338.4	350.9
	Minimum	μ	20	31.6	261.5	127.7
HORIZONTAL CL BOW	Average	μ	38	48.7	29.2	34.1
	Maximum	μ	73	74.3	46.8	55.8
	Minimum	μ	16	14.9	13.8	14.2

WAFER THICKNESS CHARACTERIZATION SUMMARY

PARAMETER	TEST		2-5-09	2-5-10	2-5-11	2-5-13
SLICE	Diameter	(mm)	127	100	100	50½
	Area	(cm^2)	126.7	78.5	78.5	39.3
THICKNESS	Average	μ	350.5	316.8	235.4	355.6
	Std. Dev.	μ	33.0	45.4	33.8	53.3
TOTAL VARIATION	Average	μ	104.1	73.1	62.5	53.3
	Std. Dev.	μ	53.3	47.1	26.6	40.6
STD. DEVIATION	Average	μ	35.6	26.6	23.7	25.4
	Std. Dev.	μ	17.8	16.6	11.2	17.8
VERTICAL TTV	Average	μ	- -	70.8	65.3	- -
	Maximum	μ	- -	180.9	123.7	- -
	Minimum	μ	- -	14.9	26.9	- -
HORIZONTAL TTV	Average	μ	- -	20.3	13.1	- -
	Maximum	μ	- -	41.6	23.9	- -
	Minimum	μ	- -	8.0	4.6	- -
VERTICAL BOW	Average	μ	- -	38.9	77.9	- -
	Maximum	μ	- -	69.3	149.3	- -
	Minimum	μ	- -	8.1	33.1	- -
HORIZONTAL BOW	Average	μ	- -	11.3	45.0	- -
	Maximum	μ	- -	21.1	82.1	- -
	Minimum	μ	- -	2.9	11.4	- -
VERTICAL CL BOW	Average	μ	- -	82.0	149.3	- -
	Maximum	μ	- -	141.5	332.7	- -
	Minimum	μ	- -	33.8	42.9	- -
HORIZONTAL CL BOW	Average	μ	- -	27.1	89.7	- -
	Maximum	μ	- -	55.4	192.8	- -
	Minimum	μ	- -	8.6	15.1	- -

WAFER THICKNESS CHARACTERIZATION SUMMARY

PARAMETER	TEST		2-5-14	2-5-15	2-5-16	2-5-17
SLICE	Diameter	(mm)	100	100	100	100
	Area	(cm^2)	78.5	78.5	78.5	78.5
THICKNESS	Average	μ	252.0	307.6	278.5	295.6
	Std. Dev.	μ	31.6	32.5	33.1	18.2
TOTAL VARIATION	Average	μ	49.6	48.0	54.8	50.0
	Std. Dev.	μ	27.9	19.9	25.3	23.4
STD. DEVIATION	Average	μ	17.7	17.5	19.6	19.4
	Std. Dev.	μ	10.9	7.3	9.8	10.0
VERTICAL TTV	Average	μ	53.8	64.8	60.1	56.7
	Maximum	μ	148.4	116.0	121.9	116.8
	Minimum	μ	24.7	36.0	33.3	34.3
HORIZONTAL TTV	Average	μ	12.6	14.5	15.9	12.7
	Maximum	μ	51.2	25.3	26.5	37.2
	Minimum	μ	1.6	8.2	8.4	4.3
VERTICAL BOW	Average	μ	52.0	74.2	67.2	63.8
	Maximum	μ	111.6	115.5	102.1	89.3
	Minimum	μ	10.6	35.1	28.2	21.0
HORIZONTAL BOW	Average	μ	13.4	17.1	31.4	49.2
	Maximum	μ	27.1	32.4	47.8	117.5
	Minimum	μ	1.6	4.4	16.5	7.8
VERTICAL CL BOW	Average	μ	93.0	133.2	132.2	132.0
	Maximum	μ	139.1	190.6	168.4	212.6
	Minimum	μ	53.2	63.9	69.9	40.3
HORIZONTAL CL BOW	Average	μ	24.1	37.7	67.1	106.9
	Maximum	μ	49.9	64.0	114.4	241.0
	Minimum	μ	9.9	17.2	19.1	30.8

WAFER THICKNESS CHARACTERIZATION SUMMARY

PARAMETER	TEST		2-5-19	2-5-18	2-6-03	2-6-04
SLICE	Diameter	(mm)	100	100	100	100
	Area	(cm^2)	78.5	78.5	78.5	78.5
THICKNESS	Average	μ	270.2	297.3	273.6	267
	Std. Dev.	μ	20.8	23.7	18.4	28.8
TOTAL VARIATION	Average	μ	51.4	51.1	45.9	61.8
	Std. Dev.	μ	16.0	21.0	22.5	21.1
STD. DEVIATION	Average	μ	19.3	18.2	16.8	24.2
	Std. Dev.	μ	6.3	7.5	9.1	9.5
VERTICAL TTV	Average	μ	49.0	64.4	60.1	78.6
	Maximum	μ	90.3	135.3	127.4	121.9
	Minimum	μ	18.7	30.4	32.0	34.9
HORIZONTAL TTV	Average	μ	11.3	14.9	7.8	13.6
	Maximum	μ	21.5	42.9	20.4	27.7
	Minimum	μ	6.1	2.6	2.2	4.0
VERTICAL BOW	Average	μ	71.3	70.1	51.5	85.1
	Maximum	μ	112.6	129.0	73.3	157.4
	Minimum	μ	28.3	32.7	26.6	19.4
HORIZONTAL BOW	Average	μ	21.5	50.7	18.4	21.0
	Maximum	μ	41.1	84.5	38.9	47.3
	Minimum	μ	7.8	17.8	7.2	2.5
VERTICAL CL BOW	Average	μ	149.3	117.5	117.0	172.2
	Maximum	μ	222.9	232.7	157.3	397.3
	Minimum	μ	89.6	43.0	45.7	64.9
HORIZONTAL CL BOW	Average	μ	45.1	99.7	40.7	40.9
	Maximum	μ	88.3	252.4	70.8	93.1
	Minimum	μ	16.2	23.1	19.6	7.0

WAFER THICKNESS CHARACTERIZATION SUMMARY

PARAMETER	TEST		2-7-01	2-7-04		
SLICE	Diameter	(mm)	100	100		
	Area	(cm^2)	78.5	78.5		
THICKNESS	Average	μ	300.7	299.3		
	Std. Dev.	μ	14.7	28.2		
TOTAL VARIATION	Average	μ	57.0	72.1		
	Std. Dev.	μ	15.3	40.9		
STD. DEVIATION	Average	μ	18.7	27.3		
	Std. Dev.	μ	4.5	18.0		
VERTICAL TTV	Average	μ	58.8	82.4		
	Maximum	μ	83.9	156.9		
	Minimum	μ	32.8	21.1		
HORIZONTAL TTV	Average	μ	15.7	15.0		
	Maximum	μ	24.1	33.6		
	Minimum	μ	6.9	3.1		
VERTICAL BOW	Average	μ	206.0	63.5		
	Maximum	μ	248.0	96.3		
	Minimum	μ	76.7	29.8		
HORIZONTAL BOW	Average	μ	15.7	17.0		
	Maximum	μ	31.3	32.1		
	Minimum	μ	6.7	4.4		
VERTICAL CL BOW	Average	μ	388.3	132.0		
	Maximum	μ	488.7	205.8		
	Minimum	μ	146.9	83.2		
HORIZONTAL CL BOW	Average	μ	21.8	26.7		
	Maximum	μ	39.4	78.5		
	Minimum	μ	7.0	7.8		

APPENDIX V

DATA FOR SOLAR CELL EFFICIENCY AS A FUNCTION OF AMOUNT ETCHED

TABLE AI

EFFICIENCIES FOR WAFERS ETCHED IN PLANAR ETCH. (DASHES INDICATE BROKEN WAFERS. UNDERLINES INDICATE WAFERS IGNORED AT 95%+ CONFIDENCE LEVEL.)

LOT	P-007-01	P-007-02	P-007-03
AMOUNT REMOVED (per side)	0 μm	2.6 μm	4.6 μm
WAFER			
1	3.7	- -	- -
2	3.3	- -	8.6
3	2.6	6.1	9.7
4	<u>5.7</u>	7.1	- -
5	- -	7.5	7.4
6	2.9	4.2	6.1
7	2.9	3.0	- -
8	3.7	7.5	9.5
9	3.8	- -	9.1
10	3.1	8.9	8.7
11	3.2	4.3	9.5
12	- -	7.7	7.8
13	3.3	- -	6.7
14	<u>1.9</u>	7.0	8.3
15	- -	6.5	9.7
16	<u>8.6</u>	2.4	8.8
17	3.6	6.3	9.0
18	3.6	5.4	8.1
19	3.7	4.2	7.1
20	3.6	5.6	- -
MEAN	3.4	5.9	8.4
STD. DEV.	0.4	1.8	1.1

TABLE AI
(continued)

EFFICIENCIES FOR WAFERS ETCHED IN PLANAR ETCH. (DASHES INDICATE BROKEN WAFERS. UNDERLINES INDICATE WAFERS IGNORED AT 95%+ CONFIDENCE LEVEL.)

LOT	P-007-04	P-007-05	P-007-06	P-007-07
AMOUNT REMOVED (per side)	7.0 μm	8.1 μm	12 μm	15 μm
WAFER				
1	10.3	10.4	10.6	10.6
2	9.3	10.7	11.0	- -
3	6.0	- -	10.1	10.5
4	10.2	9.2	10.8	10.5
5	5.6	8.8	10.1	8.3
6	9.8	8.6	10.0	10.5
7	7.1	- -	10.5	10.5
8	10.4	7.6	- -	10.9
9	9.8	7.8	10.5	10.2
10	6.4	10.4	10.7	11.0
11	10.4	- -	10.4	10.2
12	- -	6.6	10.7	11.0
13	10.6	10.5	10.7	10.4
14	8.3	- -	10.4	10.8
15	10.7	10.1	- -	8.8
16	10.4	10.3	<u>6.4</u>	9.0
17	6.7	6.3	10.2	10.6
18	10.1	9.5	10.2	9.8
19	9.6	4.2	10.2	9.7
20	10.5	10.5	<u>8.6</u>	10.0
MEAN	9.1	8.8	10.4	10.2
STD. DEV.	1.8	1.9	0.3	0.8

TABLE AI
(concluded)

EFFICIENCIES FOR WAFERS ETCHED IN PLANAR ETCH. (DASHES INDICATE BROKEN WAFERS. UNDERLINES INDICATE WAFERS IGNORED AT 95%+ CONFIDENCE LEVEL.)

LOT	P-007-08	P-007-09	P-007-10	P-007-11	P-007-12
AMOUNT REMOVED (per side)	19 μm	32 μm	44 μm	53 μm	61 μm
WAFER					
1	10.8	8.5	10.1	- -	6.0
2	10.5	11.0	8.6	8.3	9.7
3	10.6	11.0	- -	9.6	4.9
4	6.4	9.6	10.8	8.2	8.3
5	6.6	11.1	11.0	6.2	10.1
6	4.5	4.9	5.4	- -	6.9
7	- -	8.4	11.3	8.8	5.9
8	- -	10.9	10.2	8.3	8.6
9	6.9	9.5	9.3	6.9	6.0
10	- -	9.5	8.5	6.5	7.5
11	5.6	11.0	8.8	8.2	- -
12	10.3	11.0	- -	9.6	7.5
13	- -	10.5	11.1	9.2	10.0
14	- -	5.8	8.0	7.0	9.4
15	11.1	5.0	8.8	7.0	5.7
16	6.1	- -	10.2	10.7	4.9
17	10.5	9.5	11.0	10.3	10.2
18	10.0	5.8	10.5	10.6	6.7
19	11.0	7.7	11.0	3.8	7.1
20	4.8	10.7	10.2	6.4	7.8
MEAN	8.4	9.0	10.0	8.1	7.5
STD. DEV.	2.5	2.2	0.71	1.8	1.8

TABLE AII

EFFICIENCIES FOR WAFERS ETCHED IN TRANSENE SOLAR CELL ETCH (TEXTURE ETCH). (DASHES INDICATE BROKEN WAFERS. UNDERLINES INDICATE WAFERS IGNORED AT 95%+ CONFIDENCE LEVEL.)

LOT	P-008-01	P-008-02	P-008-03	P-008-04
AMOUNT REMOVED (per side)	0 μm	1.5 μm	2.9 μm	6.3 μm
WAFER				
1	3.6	6.5	8.3	5.8
2	3.3	- -	6.0	8.4
3	3.0	7.2	6.0	- -
4	- -	5.2	7.9	5.9
5	3.5	- -	- -	5.2
6	3.5	- -	9.7	4.5
7	- -	6.7	6.8	- -
8	4.1	5.9	8.6	- -
9	- -	7.1	5.4	7.1
10	3.1	6.4	8.3	7.6
11	3.4	6.8	7.6	6.1
12	- -	5.2	7.9	- -
13	3.4	7.0	- -	9.4
14	3.9	5.8	8.5	4.3
15	3.7	7.0	9.7	8.6
16	- -	7.2	5.1	7.2
17	2.9	8.5	8.6	9.2
18	3.2	7.0	6.7	6.6
19	- -	5.4	6.3	8.7
20	3.0	6.1	9.2	8.2
MEAN	3.4	6.5	7.6	7.1
STD. DEV.	0.4	0.9	1.4	1.6

TABLE AII
(continued)

EFFICIENCIES FOR WAFERS ETCHED IN TRANSENE SOLAR CELL ETCH (TEXTURE ETCH). (DASHES INDICATE BROKEN WAFERS. UNDERLINES INDICATE WAFERS IGNORED AT 95%+ CONFIDENCE LEVEL.)

LOT	P-008-05	P-008-06	P-008-07	P-008-08
AMOUNT REMOVED (per side)	7.6 μm	10 μm	16 μm	16 μm
WAFER				
1	8.7	9.8	8.2	6.6
2	6.1	9.1	- -	- -
3	- -	- -	- -	8.7
4	6.2	9.9	- -	5.4
5	- -	9.3	8.4	10.0
6	7.3	7.4	9.1	- -
7	8.8	- -	- -	- -
8	- -	6.0	- -	5.3
9	8.4	- -	9.4	8.6
10	- -	8.5	8.4	- -
11	8.1	4.9	<u>5.6</u>	6.2
12	8.1	9.4	- -	7.8
13	- -	8.1	8.3	5.6
14	5.1	8.5	9.9	- -
15	8.3	9.0	9.0	4.1
16	8.8	9.0	9.0	8.1
17	3.9	9.6	8.9	- -
18	7.6	10.3	8.8	6.7
19	8.1	8.6	7.7	8.9
20	4.5	7.8	7.8	4.9
MEAN	7.2	8.5	8.7	7.1
STD. DEV.	1.6	1.4	0.6	1.8

TABLE AII
(concluded)

EFFICIENCIES FOR WAFERS ETCHED IN TRANSENE SOLAR CELL ETCH (TEXTURE ETCH). (DASHES INDICATE BROKEN WAFERS. UNDERLINES INDICATE WAFERS IGNORED AT 95%+ CONFIDENCE LEVEL.)

LOT	P-008-09	P-008-10	P-008-11	P-008-12
AMOUNT REMOVED (per side)	25 μm	30 μm	40 μm	52 μm
WAFER				
1	7.7	10.2	8.8	9.1
2	- -	- -	- -	9.9
3	6.5	- -	5.3	- -
4	10.2	8.6	8.9	6.0
5	- -	- -	- -	6.5
6	6.7	8.1	4.7	5.5
7	9.0	6.4	7.2	- -
8	4.6	7.4	- -	7.6
9	9.5	5.0	- -	8.0
10	7.8	- -	8.2	5.2
11	9.3	7.9	7.5	9.9
12	8.0	3.6	5.5	- -
13	5.9	8.9	5.1	8.8
14	6.9	8.2	- -	- -
15	8.9	6.3	5.1	4.5
16	4.3	5.6	5.0	6.0
17	5.4	7.5	6.2	7.4
18	5.4	7.5	4.5	6.7
19	6.9	5.8	9.2	4.3
20	4.5	- -	5.3	8.5
MEAN	7.1	7.1	6.4	7.1
STD. DEV.	1.8	1.7	1.7	1.8

APPENDIX VI

NEW TECHNOLOGY

A "Multiple Blade Alignment Device" consisting of four rack gears engaging with the blades (as described in the text) was reported to JPL as an item of new technology. A "Bounce Fixture" to reduce end-of-stroke shock loads was also reported.

APPENDIX VII

ENGINEERING DRAWINGS AND SKETCHES

(Lab Saw)

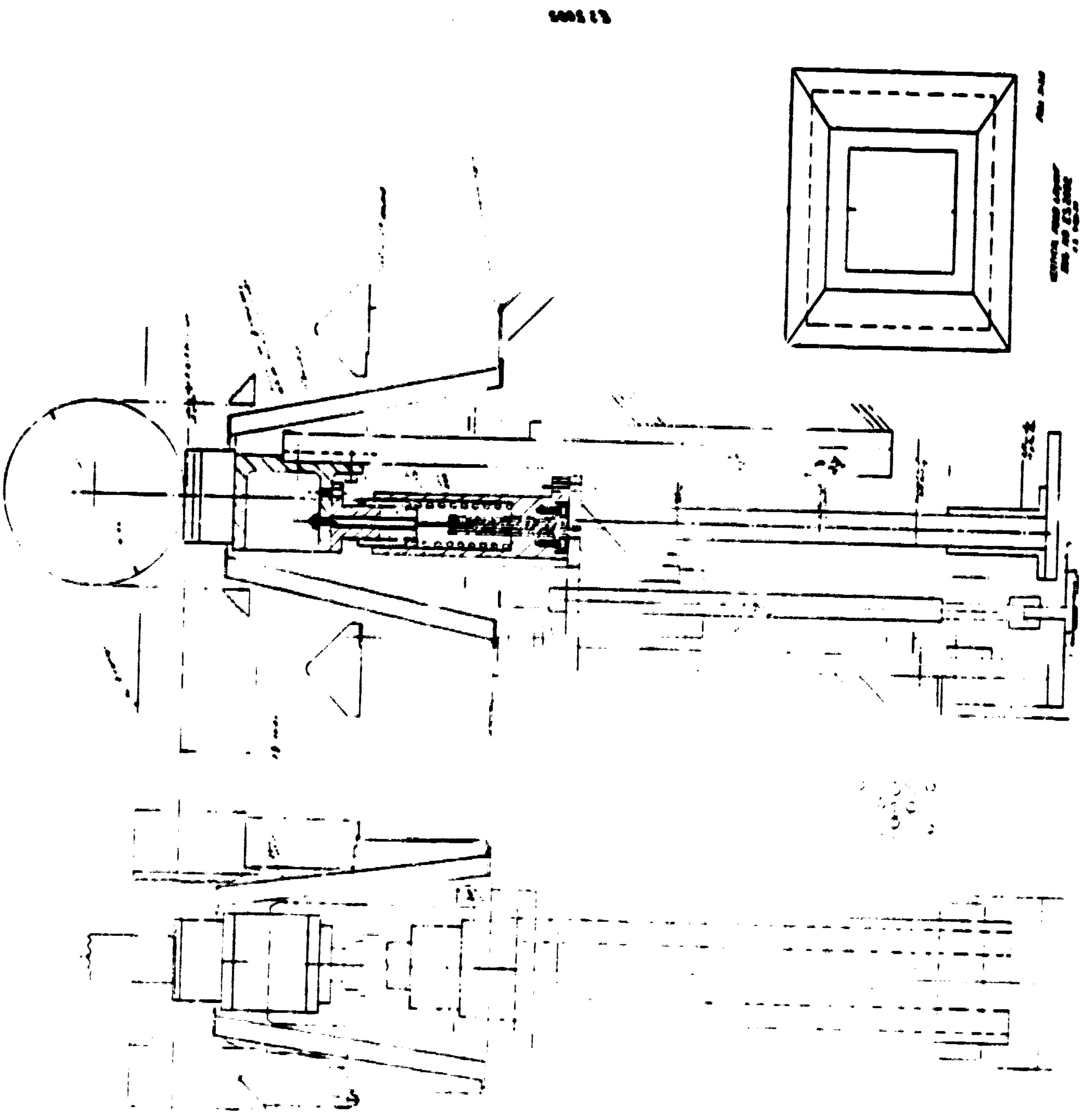

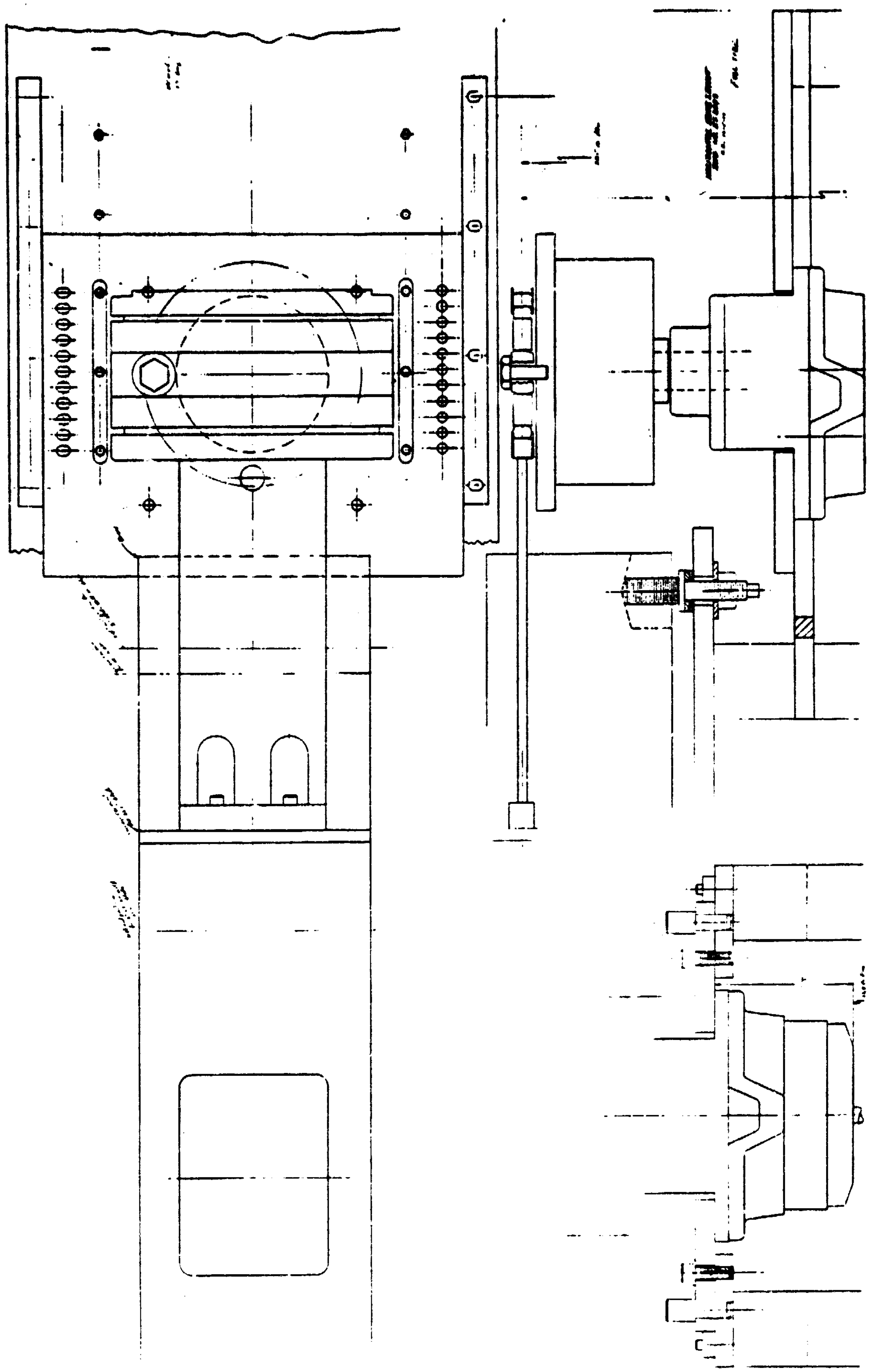

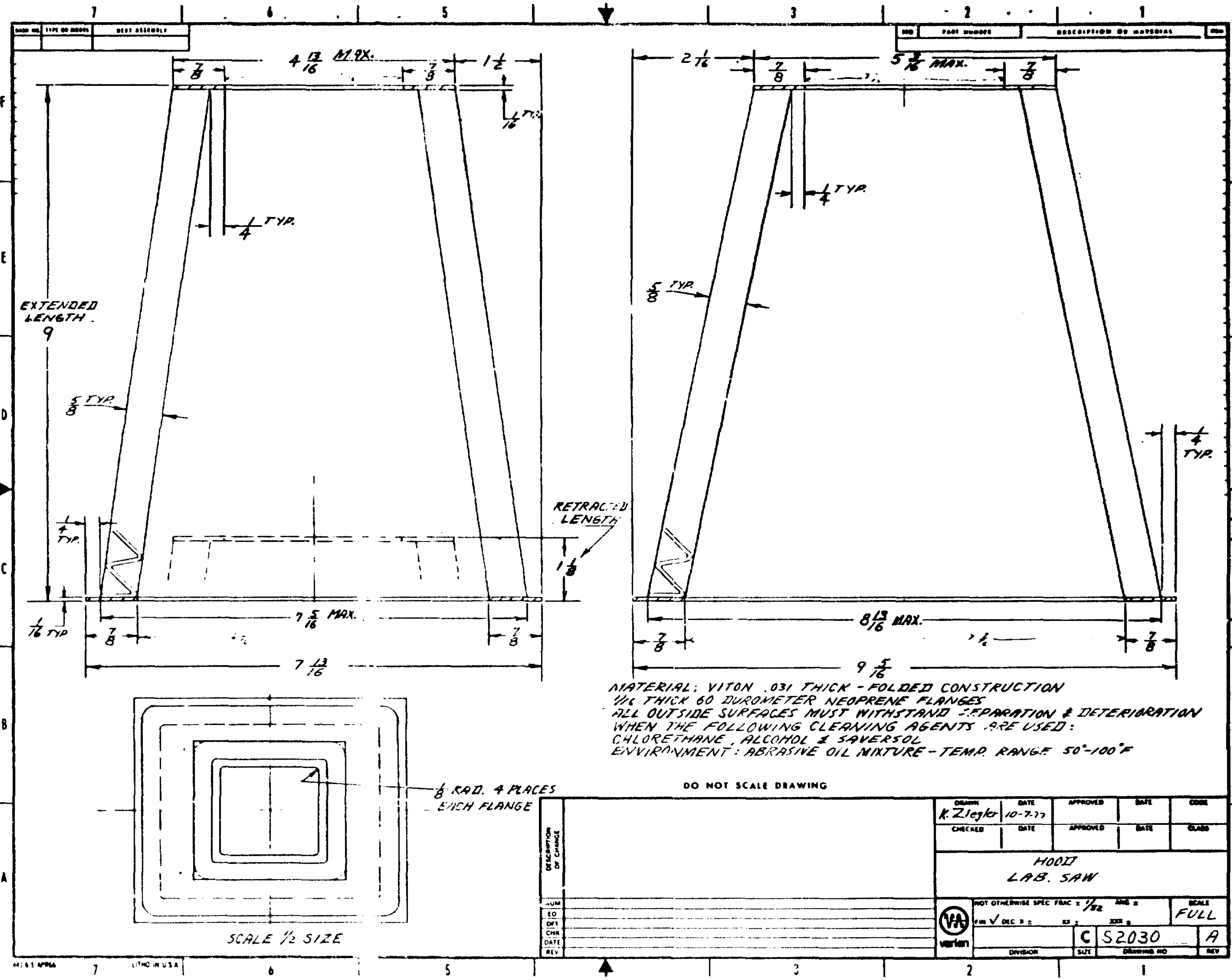
4 13/16 MAX.
1 1/2
2 1/16
5 3/16 MAX.
7/8
1/4 TYP.
1/16 TYP.
5/8 TYP.
EXTENDED LENGTH 9
RETRACTED LENGTH
1 1/8
1/4 TYP.
1/16 TYP
7 5/16 MAX.
8 13/16 MAX.
7 13/16
9 5/16
MATERIAL: VITON .031 THICK - FOLDED CONSTRUCTION
1/16 THICK 60 DUROMETER NEOPRENE FLANGES
ALL OUTSIDE SURFACES MUST WITHSTAND SEPARATION & DETERIORATION
WHEN THE FOLLOWING CLEANING AGENTS ARE USED:
CHLORETHANE, ALCOHOL & SAVERSOL
ENVIRONMENT: ABRASIVE OIL MIXTURE - TEMP. RANGE 50°-100°F
1/8 RAD. 4 PLACES EACH FLANGE
SCALE 1/2 SIZE
DO NOT SCALE DRAWING
DRAWN K. Ziegler DATE 10-7-77
HOOD
LAB. SAW
SCALE FULL
C S2030 A
varian
LITHO IN U.S.A.

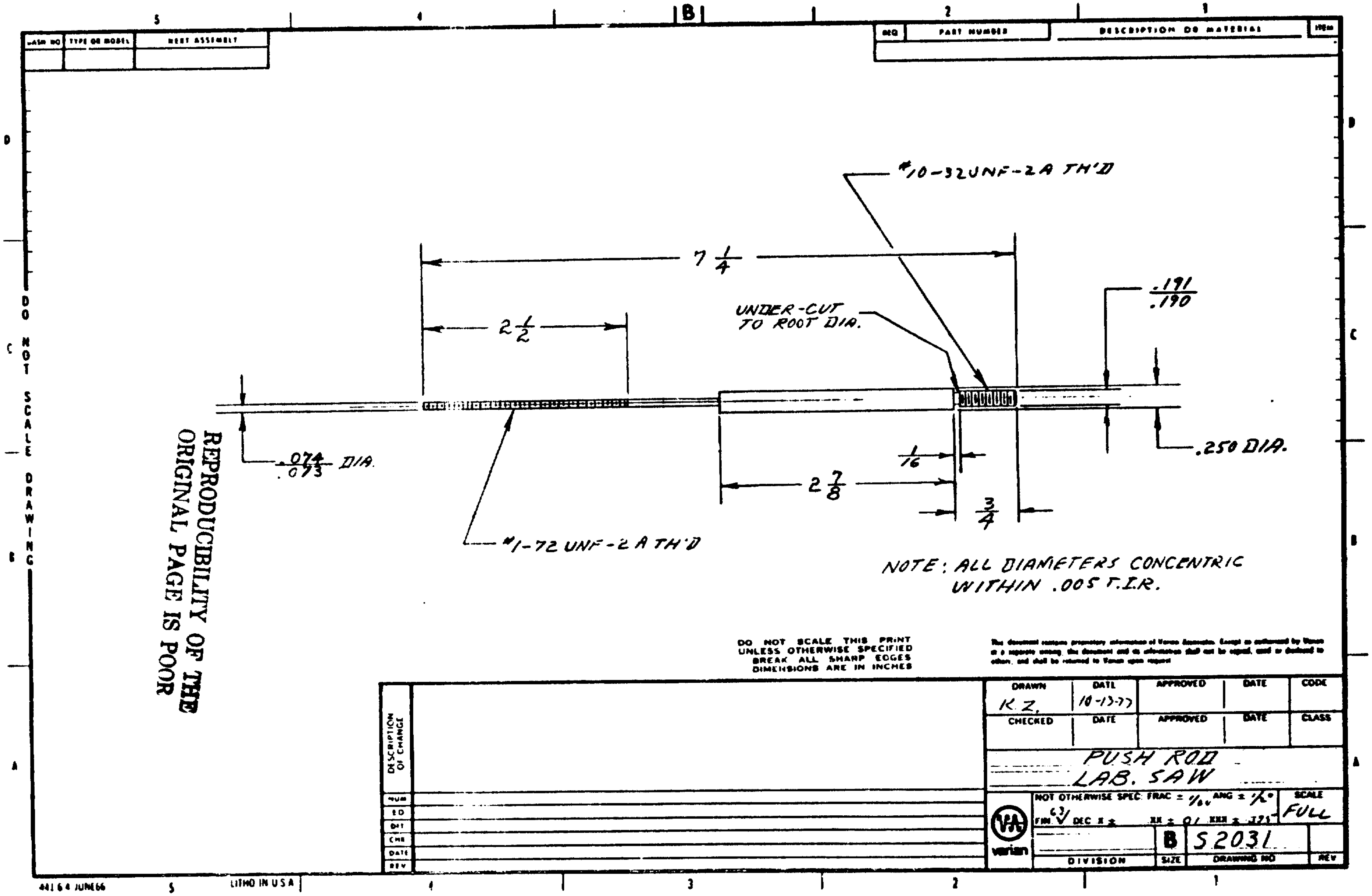

#10-32UNF-2A TH'D
7 1/4
2 1/2
UNDER-CUT
TO ROOT DIA.
.191
.190
.250 DIA.
.074
.073 DIA.
1/16
2 7/8
3/4
#1-72 UNF-2A TH'D
NOTE: ALL DIAMETERS CONCENTRIC
WITHIN .005 T.I.R.
DO NOT SCALE DRAWING
DO NOT SCALE THIS PRINT
UNLESS OTHERWISE SPECIFIED
BREAK ALL SHARP EDGES
DIMENSIONS ARE IN INCHES
DASH NO
TYPE OR MODEL
NEXT ASSEMBLY
REQ
PART NUMBER
DESCRIPTION OR MATERIAL
ITEM
DESCRIPTION OF CHANGE
DRAWN
K.Z.
DATE
10-13-77
CHECKED
APPROVED
CODE
CLASS
PUSH ROD
LAB. SAW
SCALE
FULL
varian
DIVISION
SIZE
B
S2031
DRAWING NO
REV
LITHO IN U.S.A.

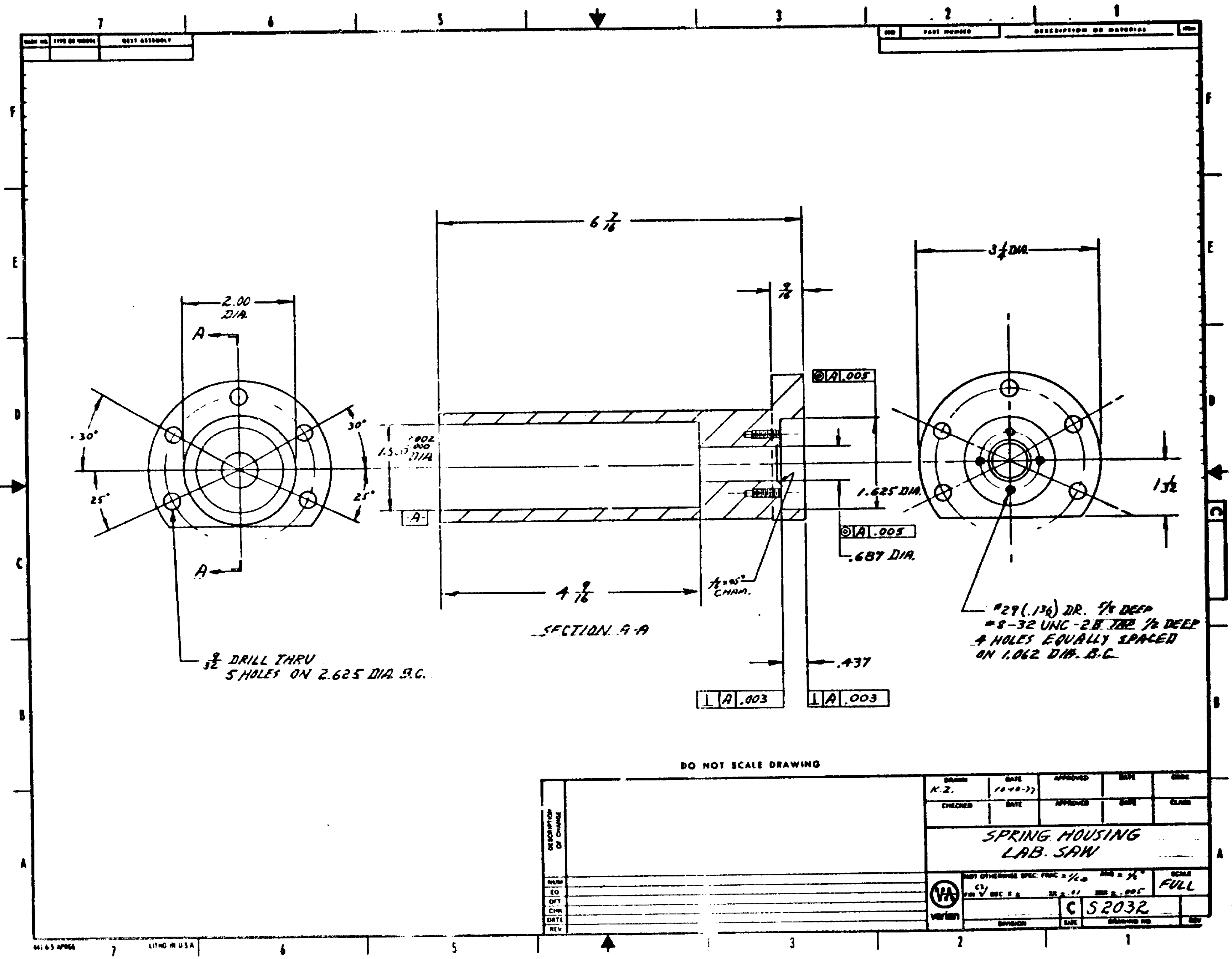

2.00 DIA
A
30°
25°
9/32 DRILL THRU
5 HOLES ON 2.625 DIA B.C.
6 7/16
4 9/16
SECTION A-A
A
.005
.003
1/16 x 45° CHAM.
1.625 DIA.
.687 DIA.
.437
9/16
3 1/2 DIA.
1 1/32
#29 (.136) DR. 5/8 DEEP
#8-32 UNC-2B TAP 1/2 DEEP
4 HOLES EQUALLY SPACED
ON 1.062 DIA. B.C.
DO NOT SCALE DRAWING
DRAWN K.Z.
DATE 10-10-77
CHECKED
SPRING HOUSING
LAB. SAW
FULL
C S2032
varian
LITHO IN U.S.A.

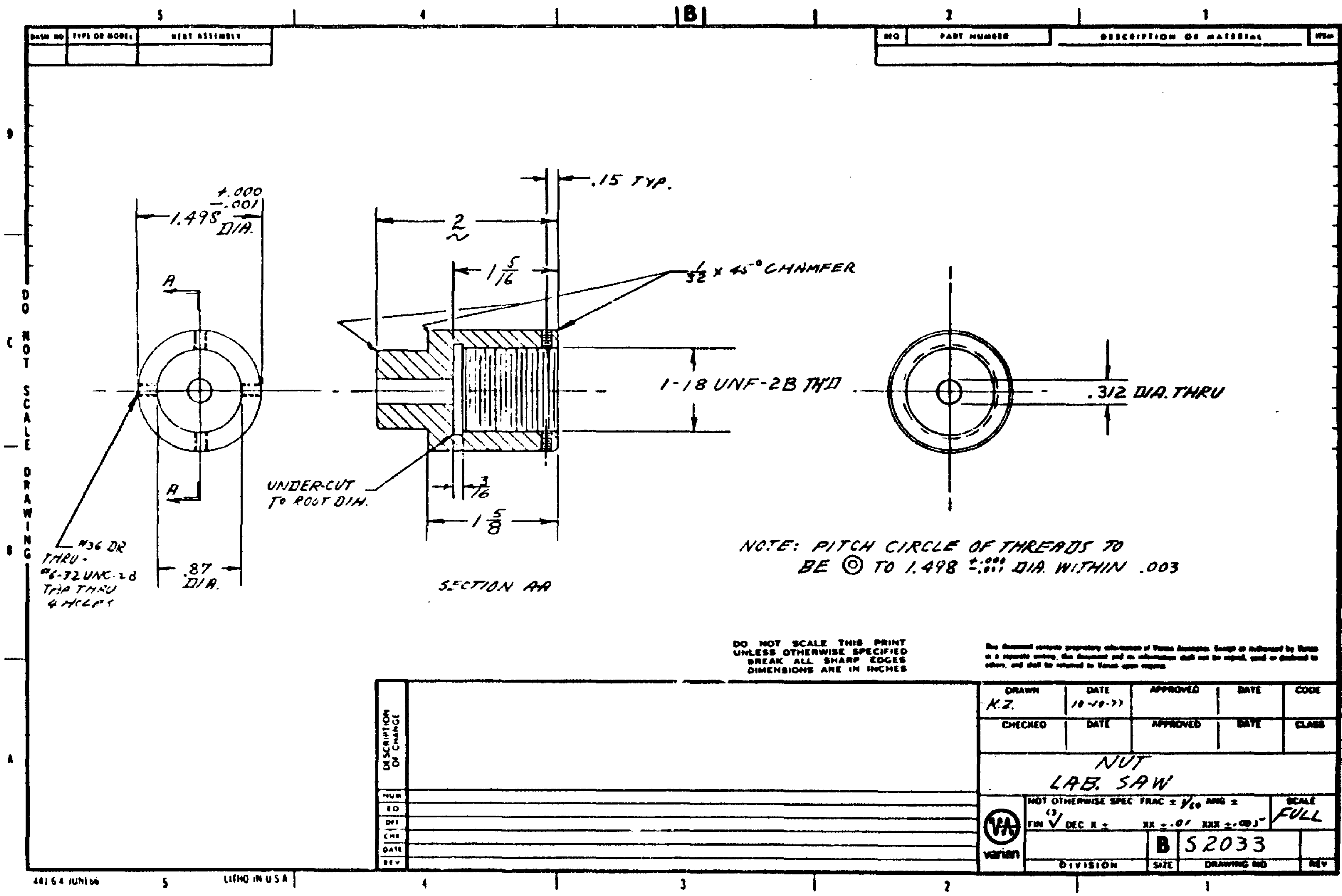

DO NOT SCALE DRAWING
DASH NO | TYPE OR MODEL | NEXT ASSEMBLY
NO | PART NUMBER | DESCRIPTION OF MATERIAL | ITEM
1.495 +.000 -.001 DIA.
.87 DIA.
A
A
#36 DR THRU - #6-32 UNC-2B TAP THRU 4 HOLES
2
1 5/16
.15 TYP.
1/32 x 45° CHAMFER
1-18 UNF-2B THD
UNDER-CUT TO ROOT DIA.
3/16
1 5/8
SECTION AA
.312 DIA. THRU
NOTE: PITCH CIRCLE OF THREADS TO BE ◎ TO 1.498 +.000 -.001 DIA. WITHIN .003
DO NOT SCALE THIS PRINT UNLESS OTHERWISE SPECIFIED BREAK ALL SHARP EDGES DIMENSIONS ARE IN INCHES
DESCRIPTION OF CHANGE
NUM
EO
DFT
CHK
DATE
REV
DRAWN K.Z.
DATE 10-10-77
APPROVED
DATE
CODE
CHECKED
DATE
APPROVED
DATE
CLASS
NUT
LAB. SAW
NOT OTHERWISE SPEC FRAC ± 1/64 ANG ±
FIN ∇ DEC X ± XX ±.01 XXX ±.003
SCALE FULL
varian
DIVISION
SIZE B
DRAWING NO 52033
REV
4416 4 JUN66
LITHO IN U S A

REPRODUCIBILITY OF THE ORIGINAL PAGE IS POOR

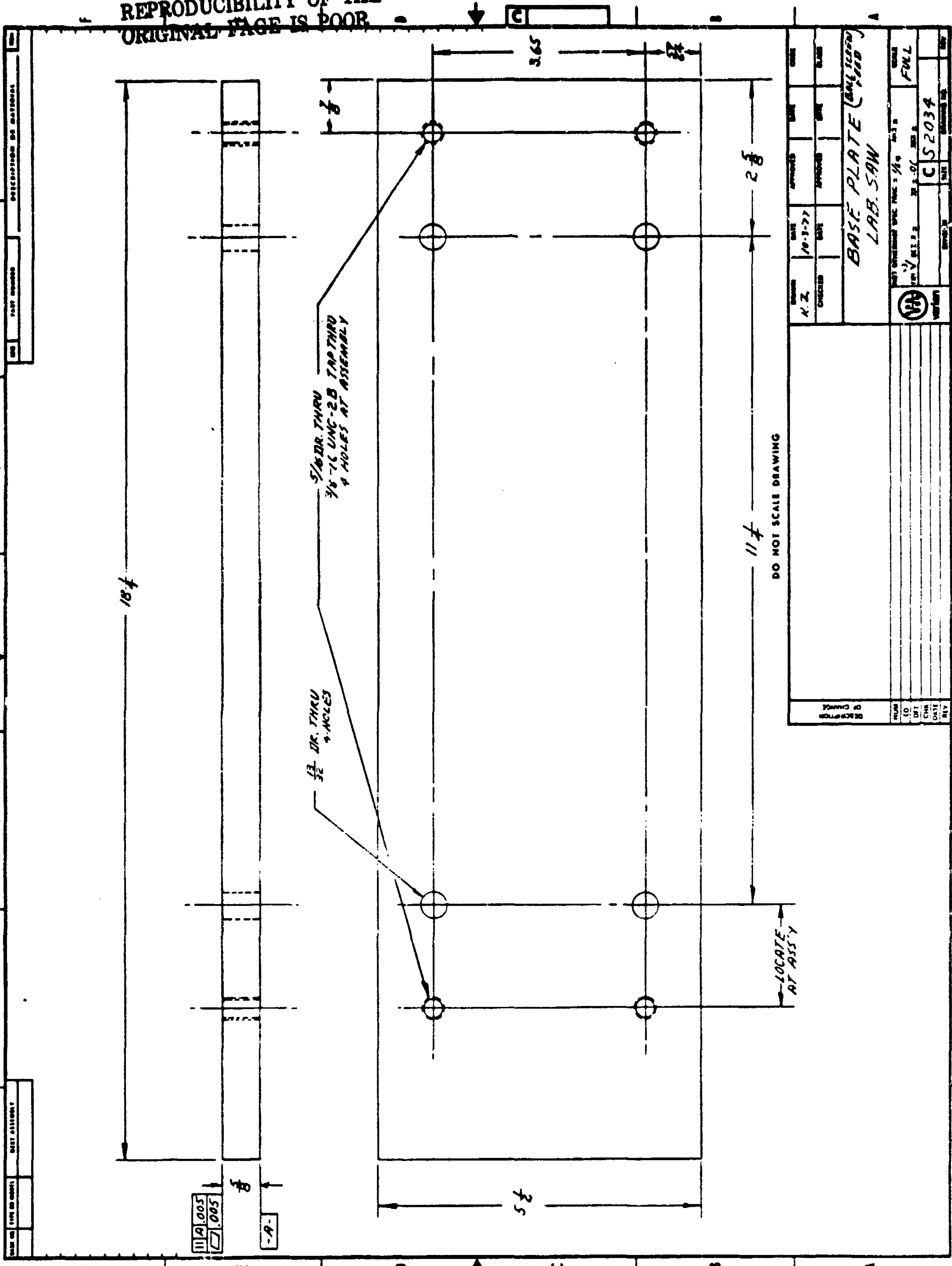

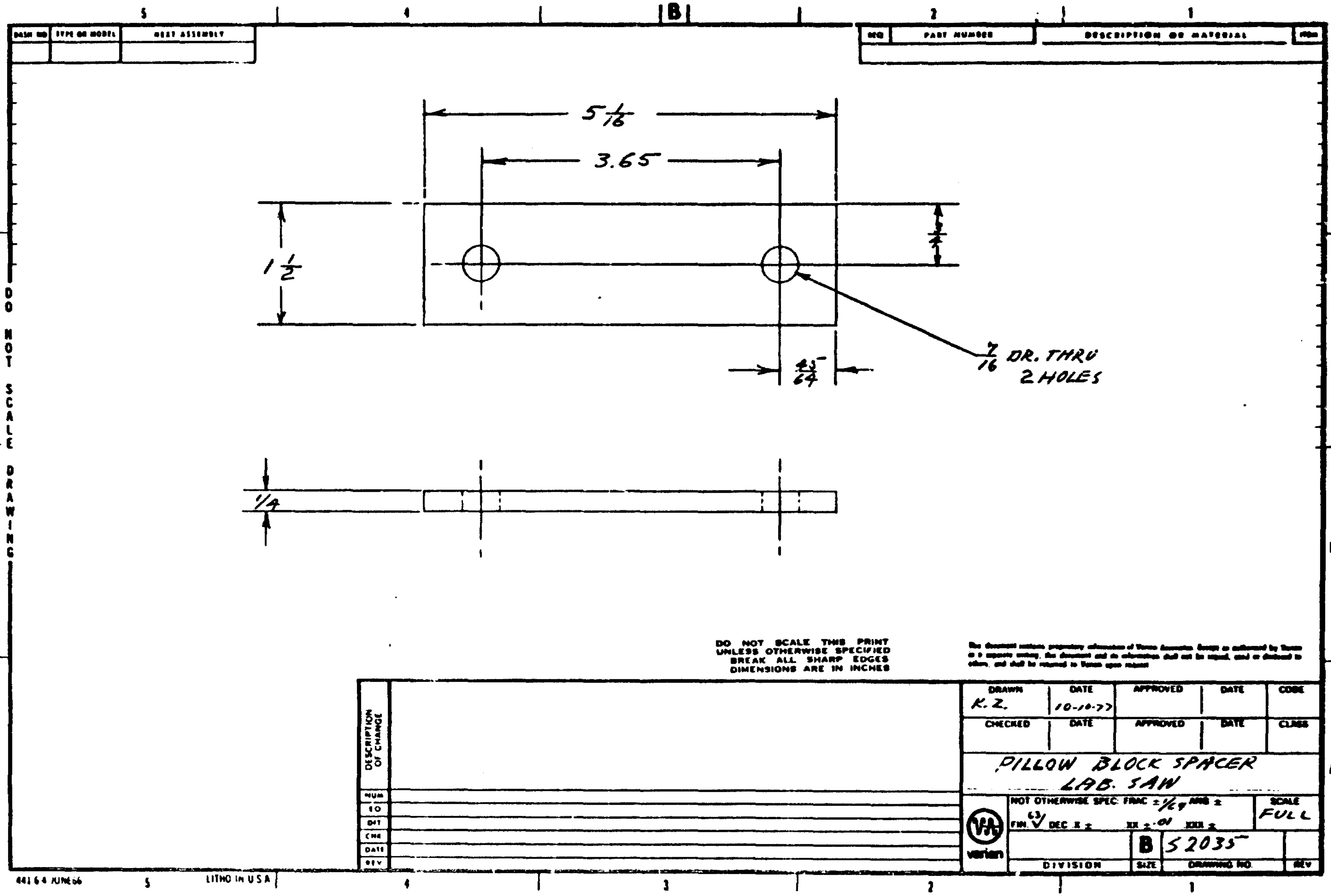
5 1/16
3.65
1 1/2
3/4
43/64
7/16 DR. THRU 2 HOLES
1/4
DO NOT SCALE DRAWING
DO NOT SCALE THIS PRINT UNLESS OTHERWISE SPECIFIED BREAK ALL SHARP EDGES DIMENSIONS ARE IN INCHES
DRAWN K.Z.
DATE 10-10-77
PILLOW BLOCK SPACER
LAB. SAW
NOT OTHERWISE SPEC: FRAC ±1/64
XX ±.01
SCALE FULL
varian
B
52035
LITHO IN U.S.A.

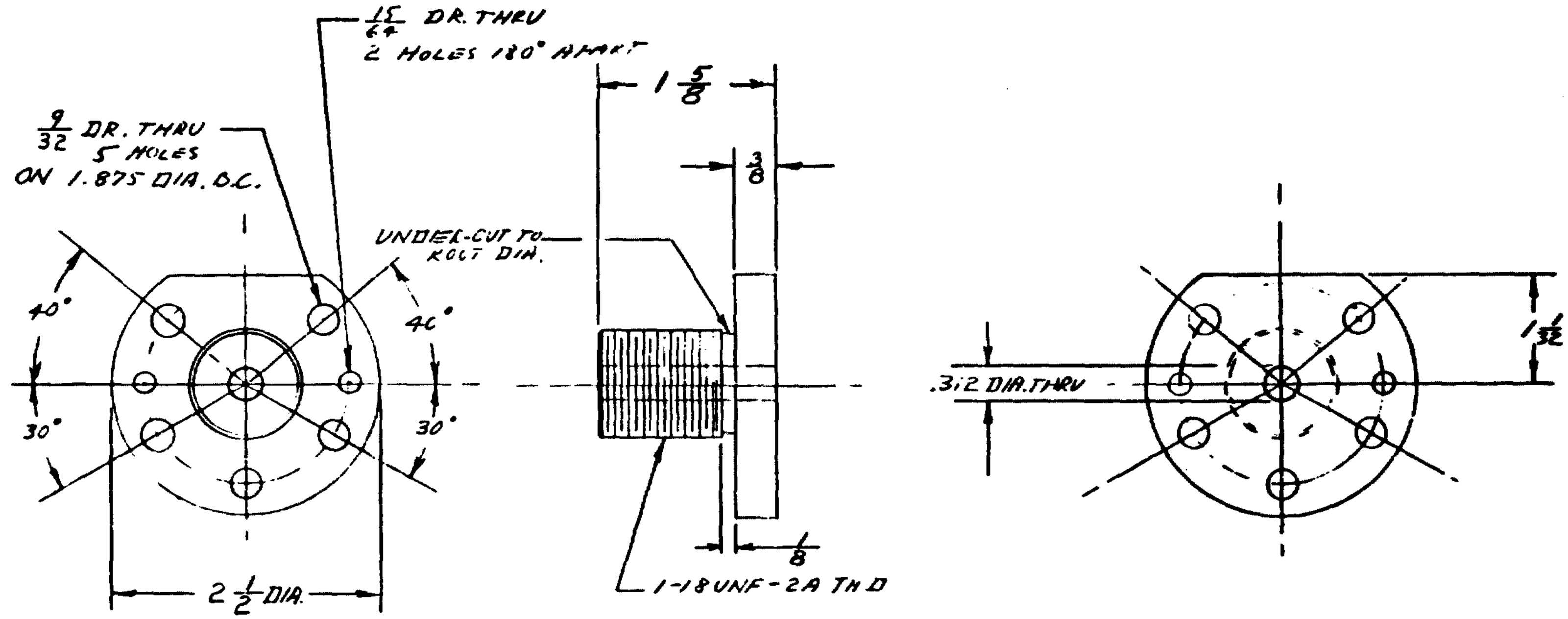

DO NOT SCALE DRAWING

DO NOT SCALE THIS PRINT
UNLESS OTHERWISE SPECIFIED
BREAK ALL SHARP EDGES
DIMENSIONS ARE IN INCHES

DASH NO	TYPE OR MODEL	NEXT ASSEMBLY

REQ	PART NUMBER	DESCRIPTION OR MATERIAL	ITEM

DRAWN	DATE	APPROVED	DATE	CODE
KZ.	10-11-77			
CHECKED	DATE	APPROVED	DATE	CLASS

TAKE-UP SCREW
LAB. SAW

NOT OTHERWISE SPEC FRAC ± 1/64 ANG ± 1/2° FIN 63 DEC X ± XX ± .01 XXX ± .005
SCALE FULL

varian

DIVISION	SIZE	DRAWING NO	REV
	B	S 2036	

DESCRIPTION OF CHANGE

NUM / EO / DFT / CHK / DATE / REV

44164 JUNE66 LITHO IN U.S.A

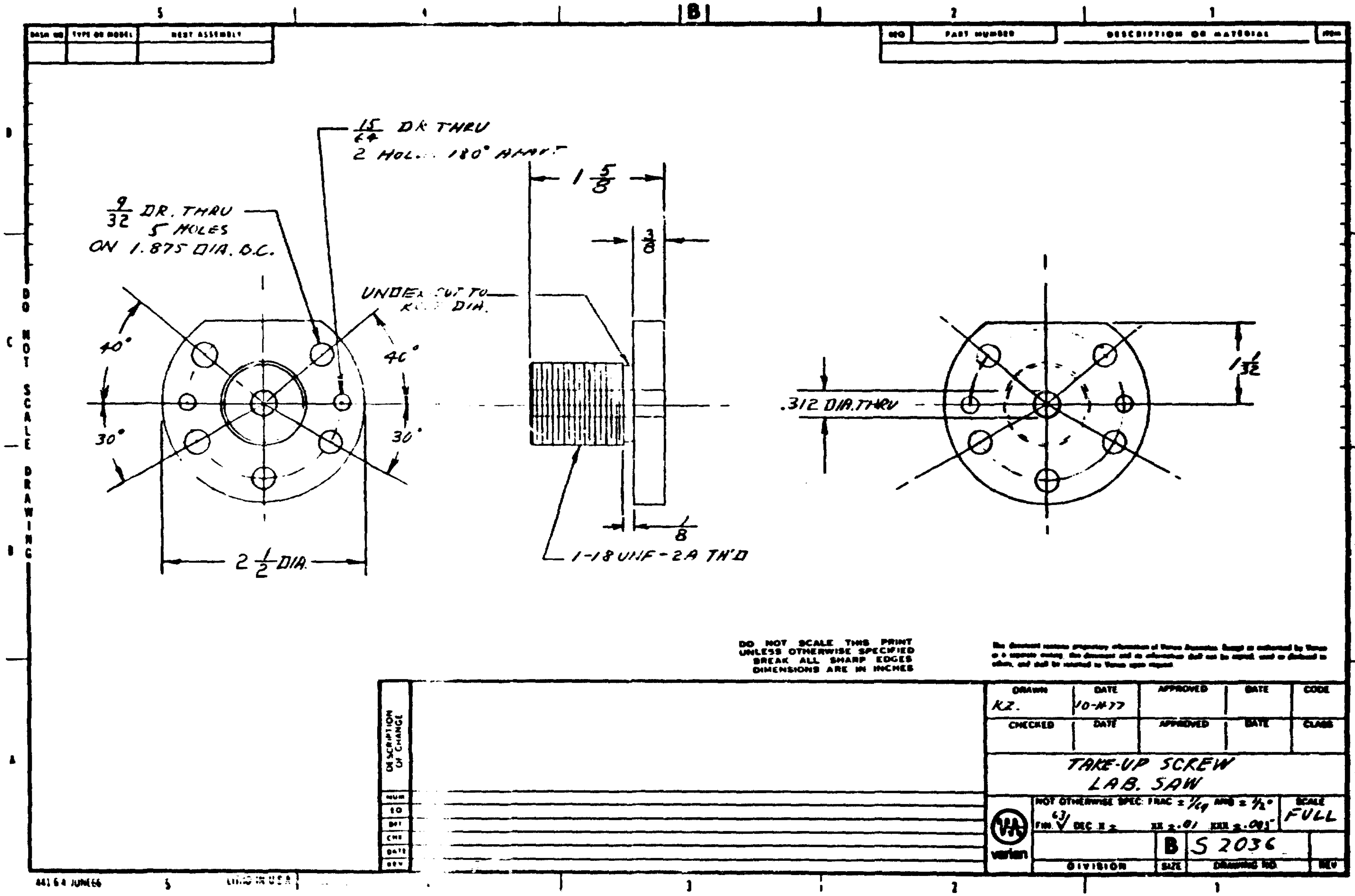

15/64 DR THRU
2 HOL... 180° APART
9/32 DR. THRU
5 HOLES
ON 1.875 DIA. B.C.
40°
40°
30°
30°
2 1/2 DIA.
UNDERCUT TO
DIA.
1 5/8
3/8
1/8
1-18 UNF-2A TH'D
.312 DIA. THRU
1 1/32
DO NOT SCALE DRAWING
DO NOT SCALE THIS PRINT
UNLESS OTHERWISE SPECIFIED
BREAK ALL SHARP EDGES
DIMENSIONS ARE IN INCHES
DASH NO.
TYPE OR MODEL
NEXT ASSEMBLY
REQ
PART NUMBER
DESCRIPTION OR MATERIAL
ITEM
DESCRIPTION OF CHANGE
DRAWN
K.Z.
DATE
10-11-77
CHECKED
APPROVED
CODE
CLASS
TAKE-UP SCREW
LAB. SAW
SCALE
FULL
varian
DIVISION
SIZE
B
DRAWING NO.
S 2036
REV

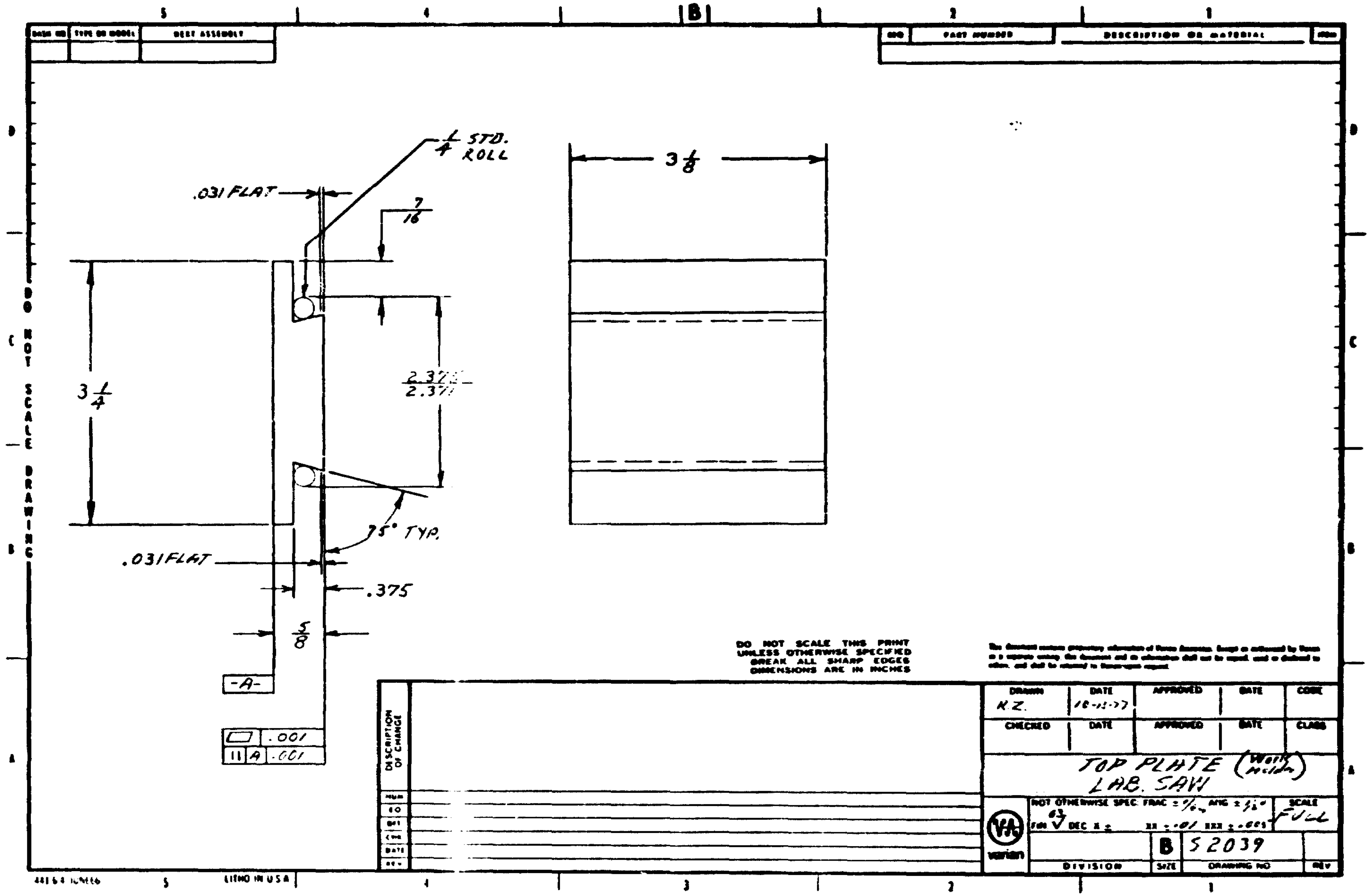

1/4 STD. ROLL
.031 FLAT
7/16
3 1/8
3 1/4
2.37
75° TYP.
.031 FLAT
.375
5/8
-A-
.001
A .001
DO NOT SCALE DRAWING
DO NOT SCALE THIS PRINT
UNLESS OTHERWISE SPECIFIED
BREAK ALL SHARP EDGES
DIMENSIONS ARE IN INCHES
DESCRIPTION OF CHANGE
DRAWN K.Z.
DATE 10-12-77
CHECKED
APPROVED
DATE
CODE
CLASS
TOP PLATE (Work Holder)
LAB. SAW
SCALE FULL
B
52039
DIVISION
SIZE
DRAWING NO
REV
varian
LITHO IN U.S.A.

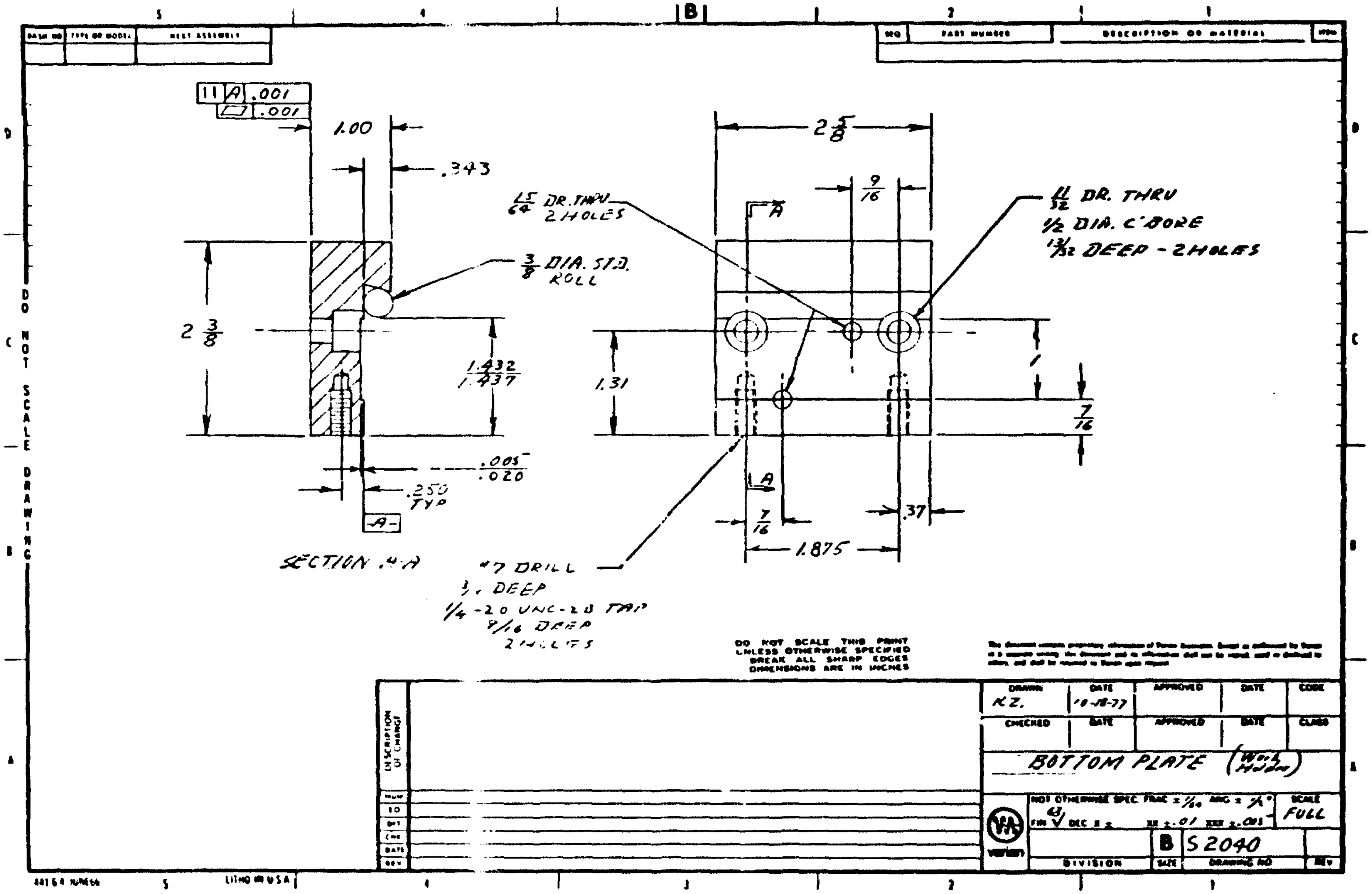
11 A .001
.001
1.00
.343
2 3/8
3/8 DIA. STD. ROLL
1.432 / 1.437
.005 / .020
.250 TYP
-A-
SECTION A-A
#7 DRILL
3/4 DEEP
1/4-20 UNC-2B TAP
9/16 DEEP
2 HOLES
2 5/8
9/16
25/64 DR. THRU
2 HOLES
11/32 DR. THRU
1/2 DIA. C'BORE
13/32 DEEP - 2 HOLES
1.31
1
7/16
.37
1.875
DO NOT SCALE THIS PRINT
UNLESS OTHERWISE SPECIFIED
BREAK ALL SHARP EDGES
DIMENSIONS ARE IN INCHES
DO NOT SCALE DRAWING
DRAWN K.Z.
DATE 10-18-77
CHECKED
APPROVED
BOTTOM PLATE (Work Holder)
FULL
B S2040
DIVISION
LITHO IN U.S.A.

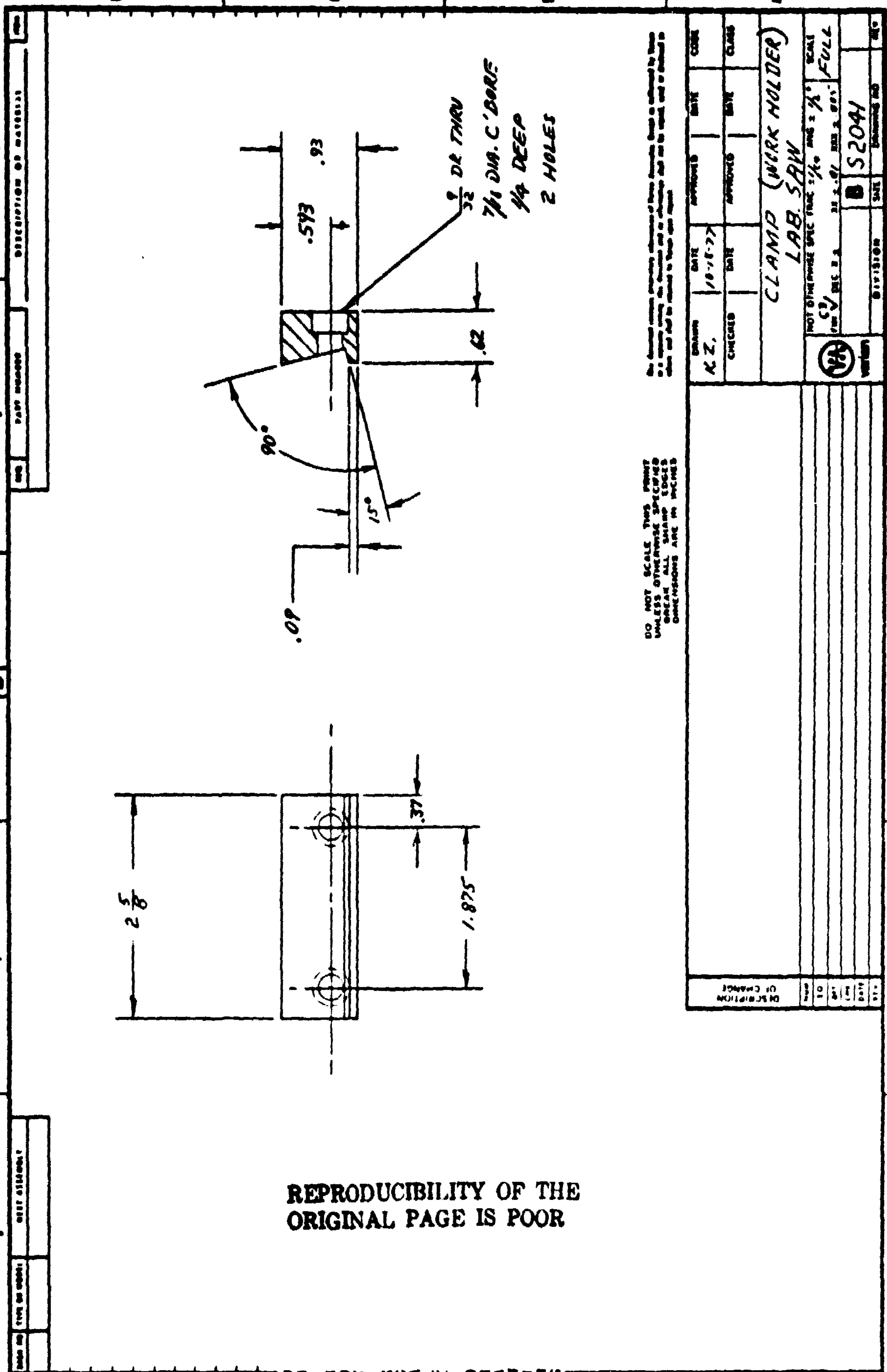
9/32 DR THRU
7/16 DIA. C'BORE
1/4 DEEP
2 HOLES
.593
.93
.62
90°
15°
.09
2 5/8
.37
1.875
DO NOT SCALE THIS PRINT
UNLESS OTHERWISE SPECIFIED
BREAK ALL SHARP EDGES
DIMENSIONS ARE IN INCHES
DRAWN R.Z.
DATE 10-15-77
CHECKED
CLAMP (WORK HOLDER)
LAB. SAW
SCALE FULL
B
S2041

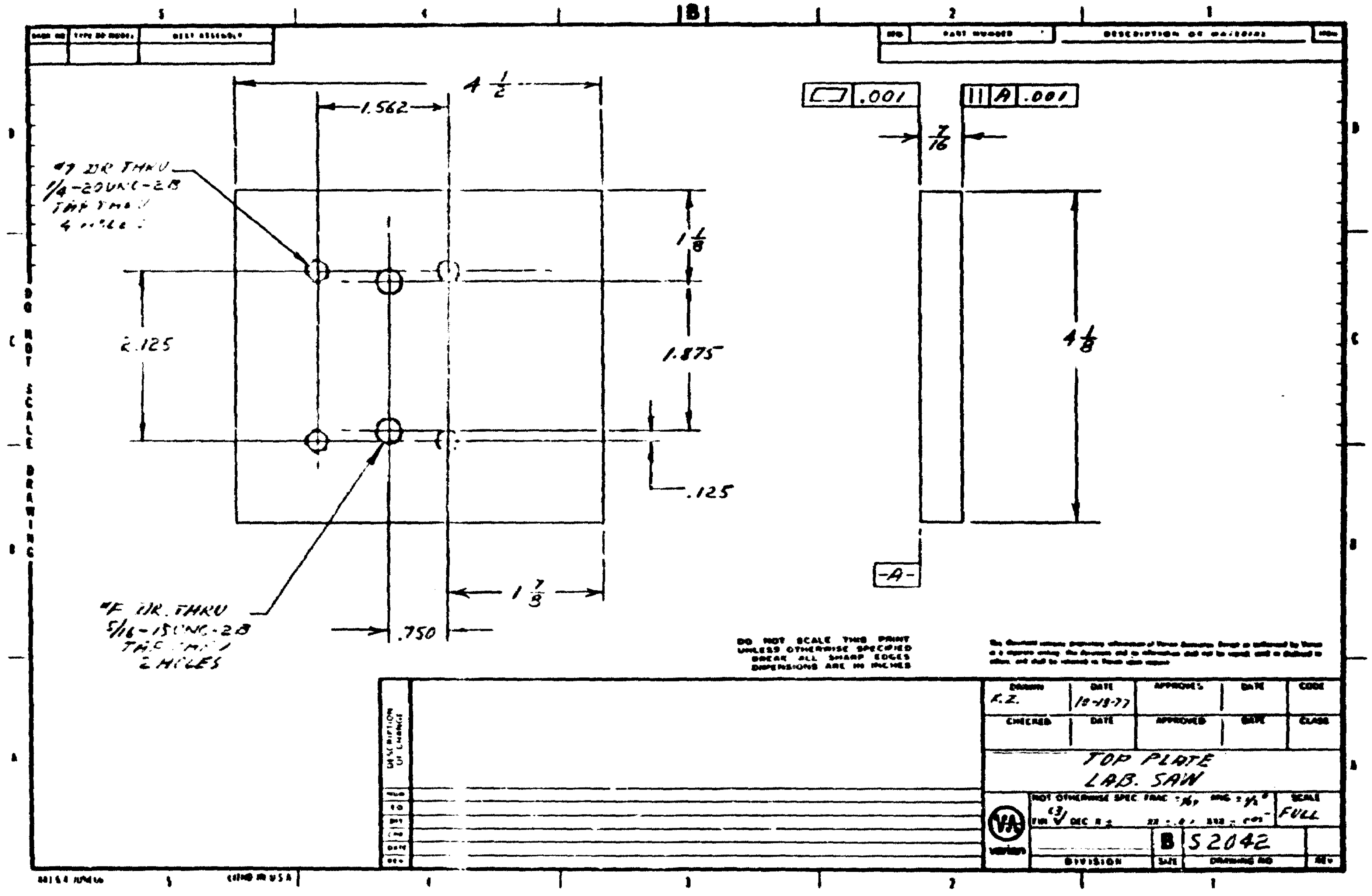
4 1/2
1.562
#7 DR THRU
1/4-20UNC-2B
TAP THRU
4 HOLES
2.125
1 1/8
1.875
.125
1 7/8
.750
#F DR. THRU
5/16-18UNC-2B
TAP THRU
2 HOLES
.001
A .001
7/16
4 1/8
-A-
DO NOT SCALE THIS PRINT
UNLESS OTHERWISE SPECIFIED
BREAK ALL SHARP EDGES
DIMENSIONS ARE IN INCHES
DO NOT SCALE DRAWING
DRAWN K.Z.
DATE 10-13-77
TOP PLATE
LAB. SAW
SCALE FULL
B
S2042
DRAWING NO
varian

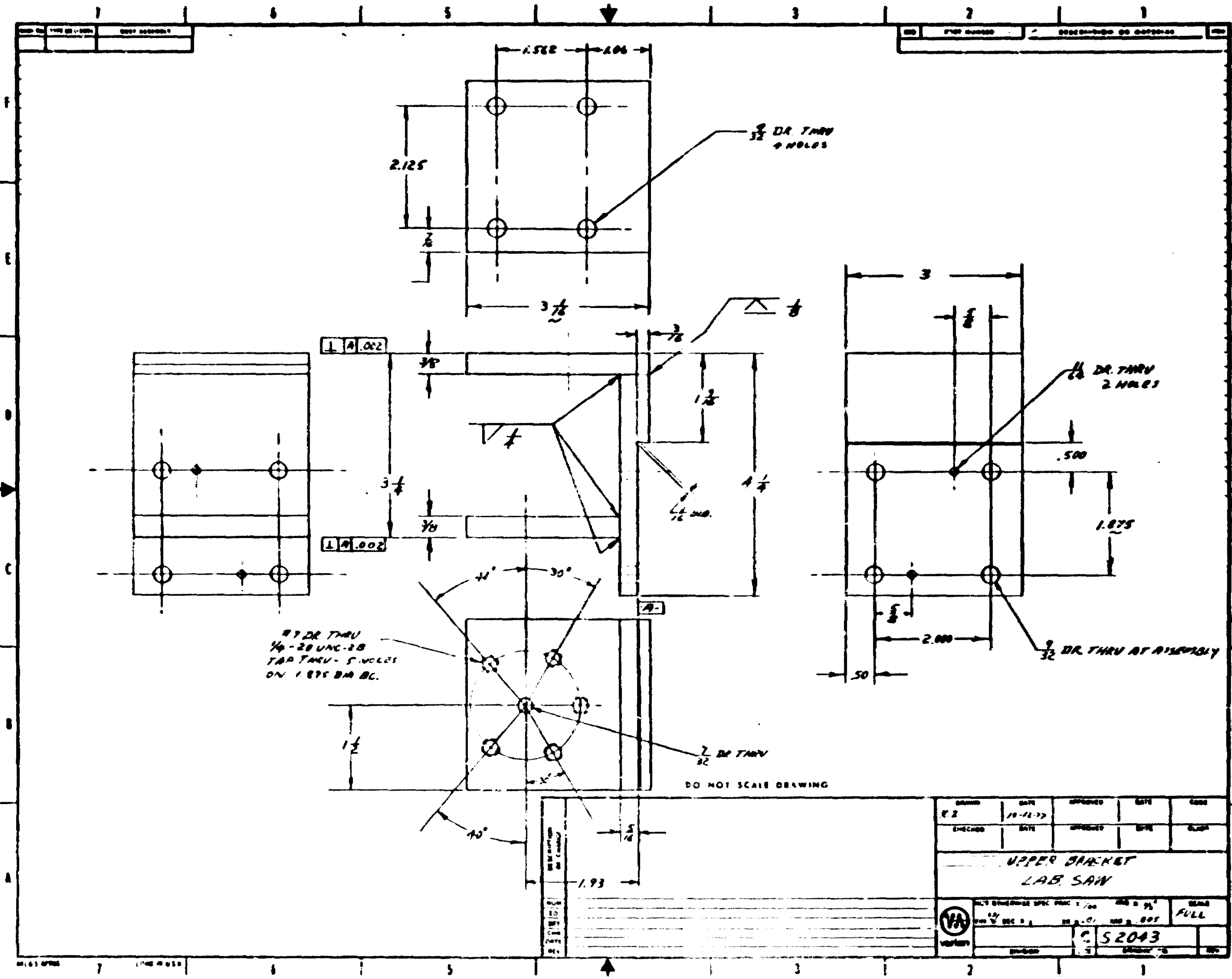

9/32 DR. THRU 4 HOLES
11/64 DR. THRU 2 HOLES
9/32 DR. THRU AT ASSEMBLY
#7 DR. THRU
1/4-20 UNC-2B TAP THRU - 5 HOLES ON 1.875 DIA BC.
7/32 DR. THRU
DO NOT SCALE DRAWING
UPPER BRACKET
LAB. SAW
FULL
C 52043

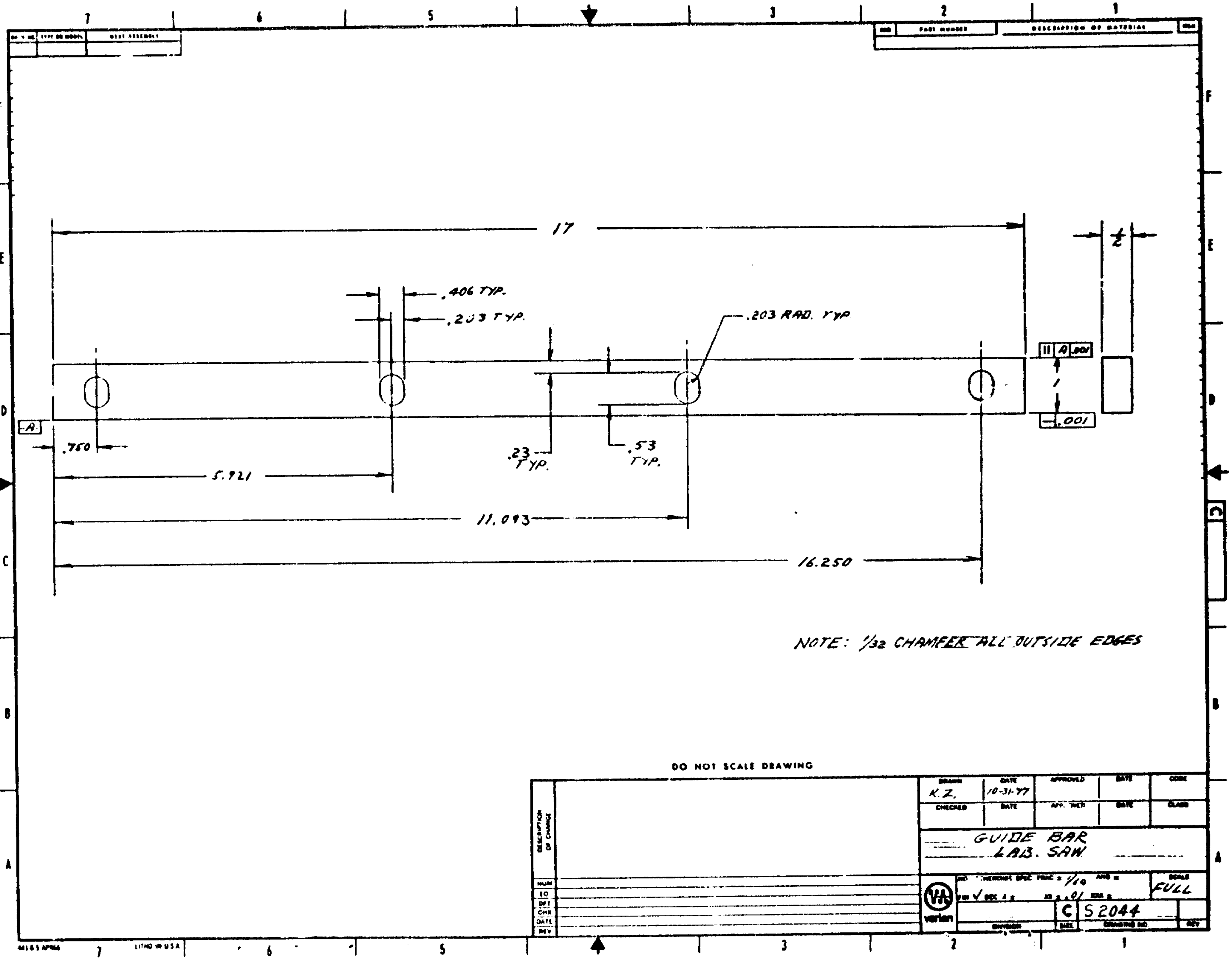
17
1/2
.406 TYP.
.203 TYP.
.203 RAD. TYP.
A
.001
.750
.23 TYP.
.53 TYP.
5.921
11.093
16.250
NOTE: 1/32 CHAMFER ALL OUTSIDE EDGES
DO NOT SCALE DRAWING
DRAWN K.Z.
DATE 10-31-77
GUIDE BAR
LAB. SAW
SCALE FULL
C
S 2044
varian

DASH NO	TYPE OR MODEL	NEXT ASSEMBLY

NO	PART NUMBER	DESCRIPTION OR MATERIAL	ITEM

DO NOT SCALE DRAWING

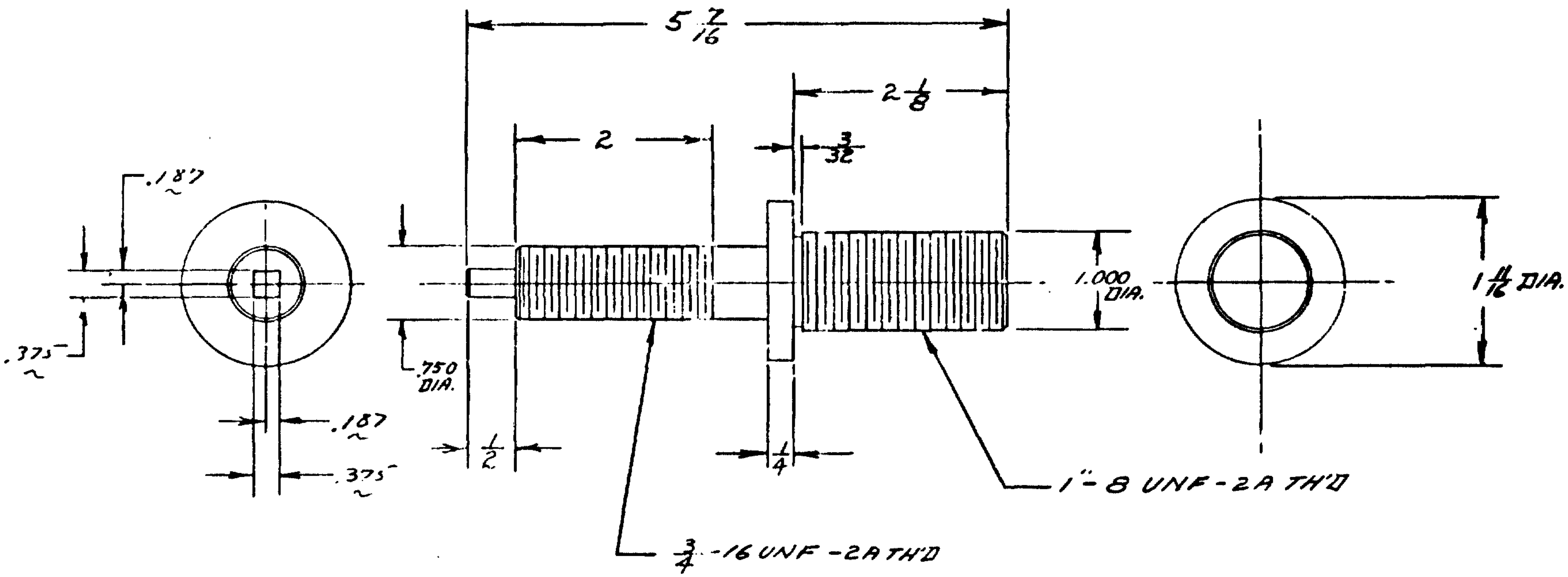

DRAWN	DATE	APPROVED	DATE	CODE
R.Z.	11-1-77			
CHECKED	DATE	APPROVED	DATE	CLASS

JACKING SCREW
LAB. SAW

NOT OTHERWISE SPEC: FRAC ± 1/64 ANG ±
FIN √ DEC .X ± .XX ± .01 .XXX ± .005

SCALE FULL

varian

DIVISION	SIZE	DRAWING NO	REV
	B	S 2045	

DESCRIPTION OF CHANGE — NUM, ED, DFT, CHK, DATE, REV

44164 JUNE66 LITHO IN U.S.A.

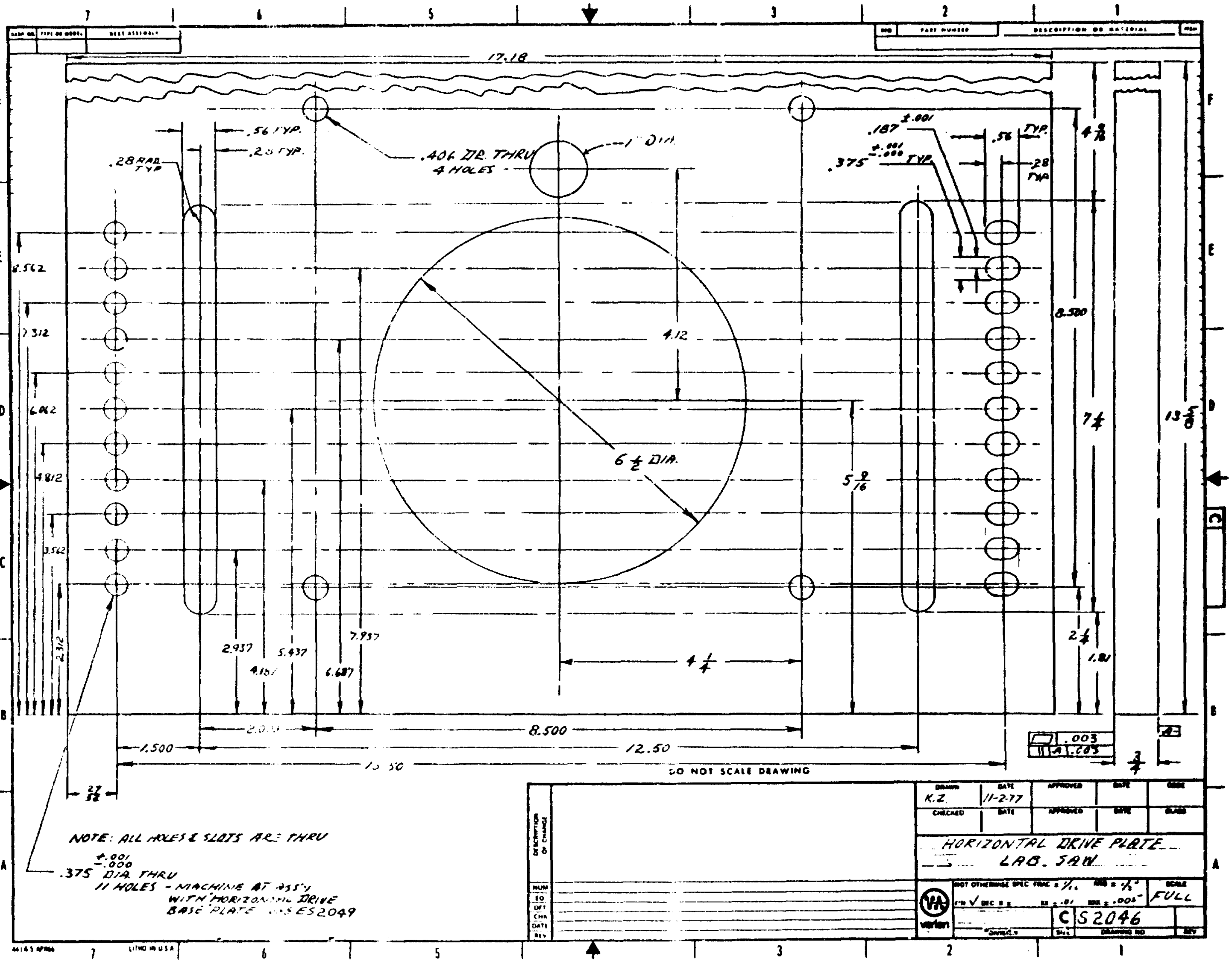
17.18
.56 TYP.
.25 TYP.
.28 RAD. TYP
.406 DR. THRU 4 HOLES
1" DIA.
.187 ±.001
.375 +.001 -.000 TYP.
.56 TYP.
.28 TYP
4 9/16
8.562
7.312
6.062
4.812
3.562
2.312
4.12
6 1/2 DIA.
8.500
7 1/4
13 5/8
5 9/16
2.937
4.187
5.437
6.687
7.937
4 1/4
2 1/4
1.81
1.500
8.500
12.50
.003
A .005
3/4
27/32
DO NOT SCALE DRAWING
NOTE: ALL HOLES & SLOTS ARE THRU
.375 +.001 -.000 DIA THRU
11 HOLES - MACHINE AT ASS'Y WITH HORIZONTAL DRIVE BASE PLATE
ES2049
DRAWN K.Z.
DATE 11-2-77
CHECKED
DATE
APPROVED
HORIZONTAL DRIVE PLATE
LAB. SAW
varian
SCALE FULL
C S2046
DRAWING NO
REV
LITHO IN U.S.A.

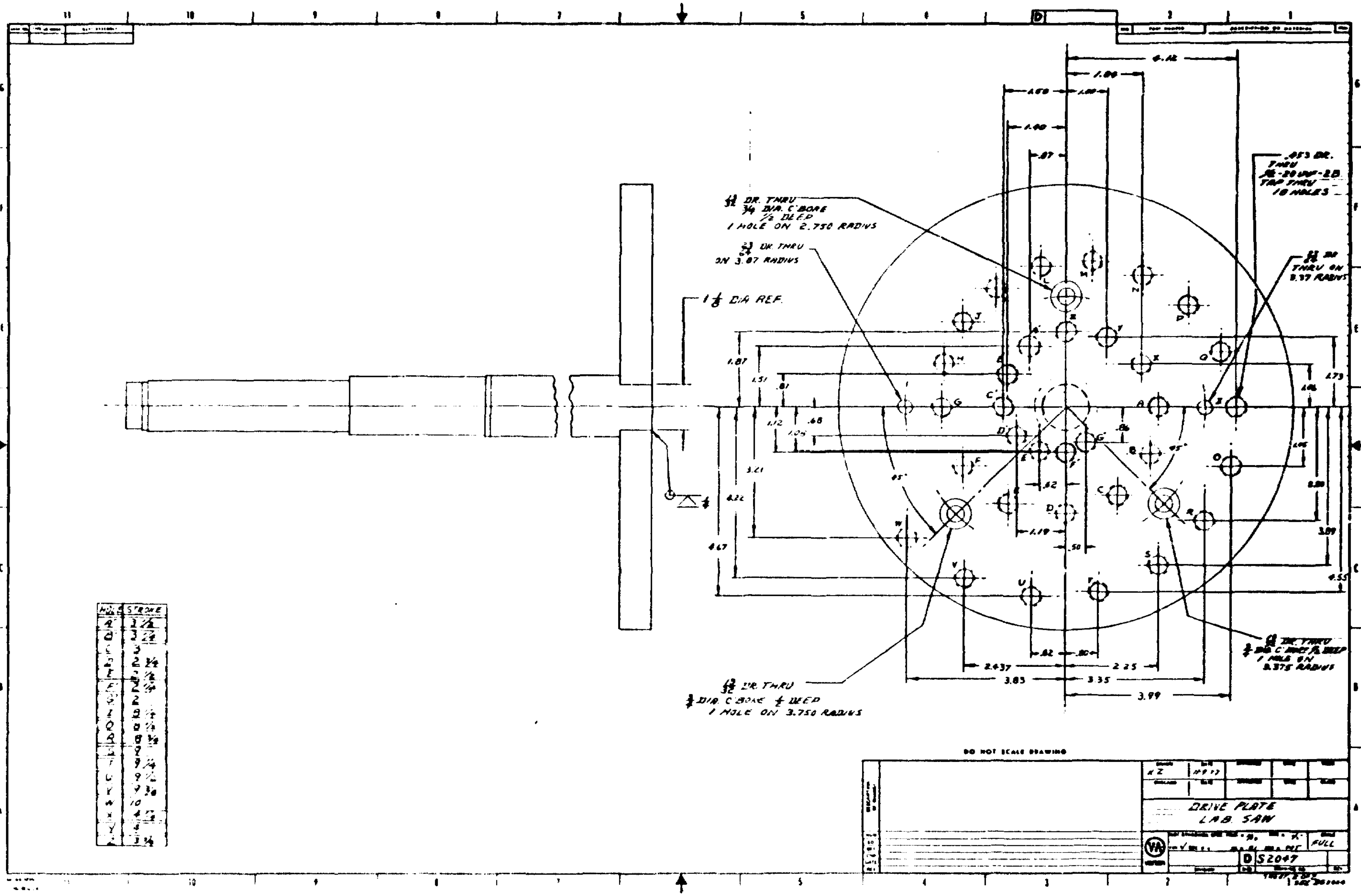

HOLE	STROKE
A	3 1/2
B	3 1/4
C	3
D	2 3/4
E	2 1/2
F	2 1/4
G	2
[illegible]	[illegible]
O	8 1/4
R	8 1/2
S	9
T	9 1/4
U	9 1/2
V	9 3/4
W	10
X	4 1/2
Y	4
Z	3 3/4

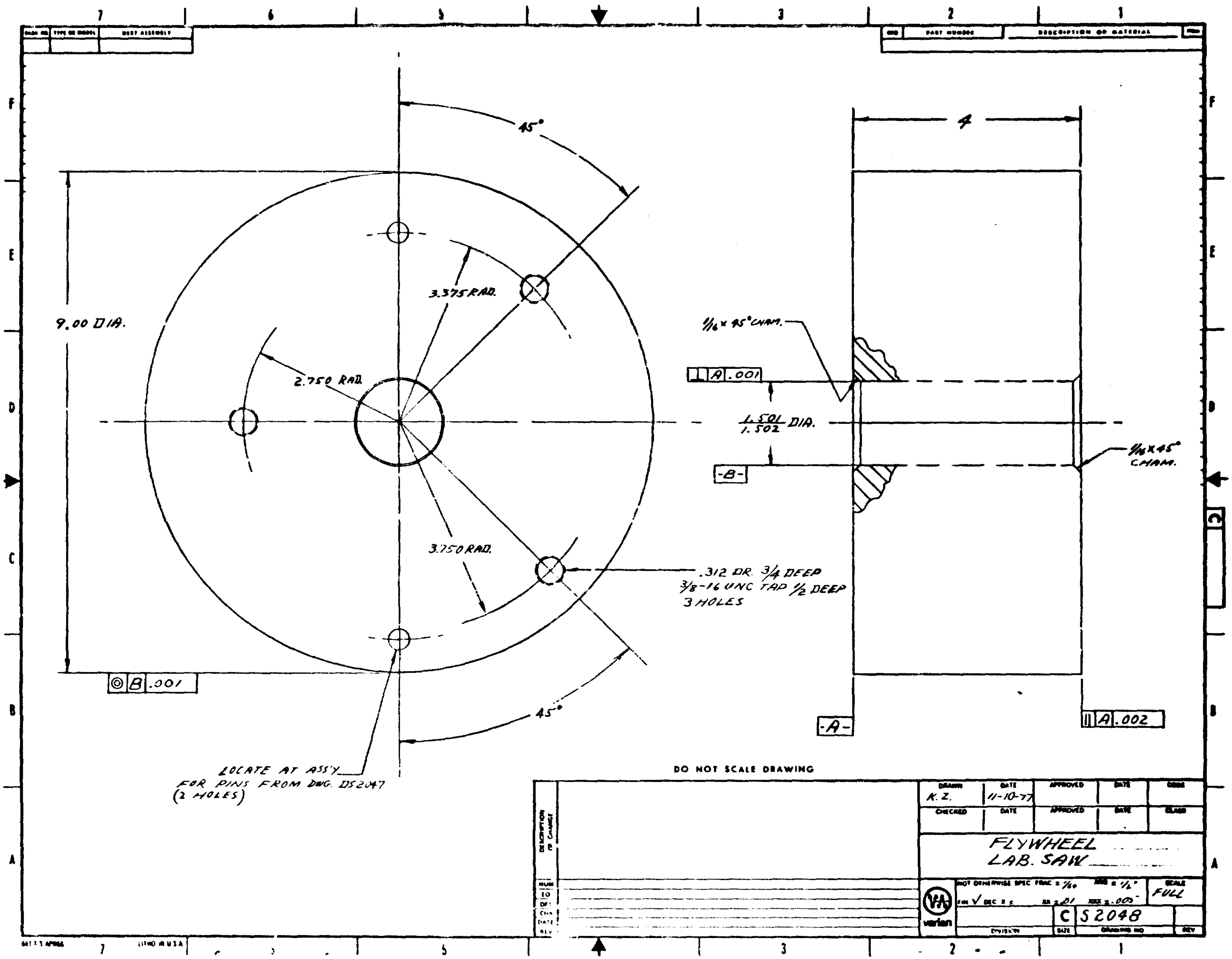

9.00 DIA.
45°
3.375 RAD.
2.750 RAD.
3.750 RAD.
.312 DR. 3/4 DEEP
3/8-16 UNC TAP 1/2 DEEP
3 HOLES
45°
LOCATE AT ASS'Y
FOR PINS FROM DWG. DS2047
(2 HOLES)
◎ B .001
4
1/16 x 45° CHAM.
⊥ A .001
1.501
1.502 DIA.
-B-
1/16 x 45° CHAM.
-A-
∥ A .002
DO NOT SCALE DRAWING
DRAWN K. Z.
DATE 11-10-77
CHECKED
DATE
APPROVED
FLYWHEEL
LAB. SAW
SCALE FULL
varian
C S2048

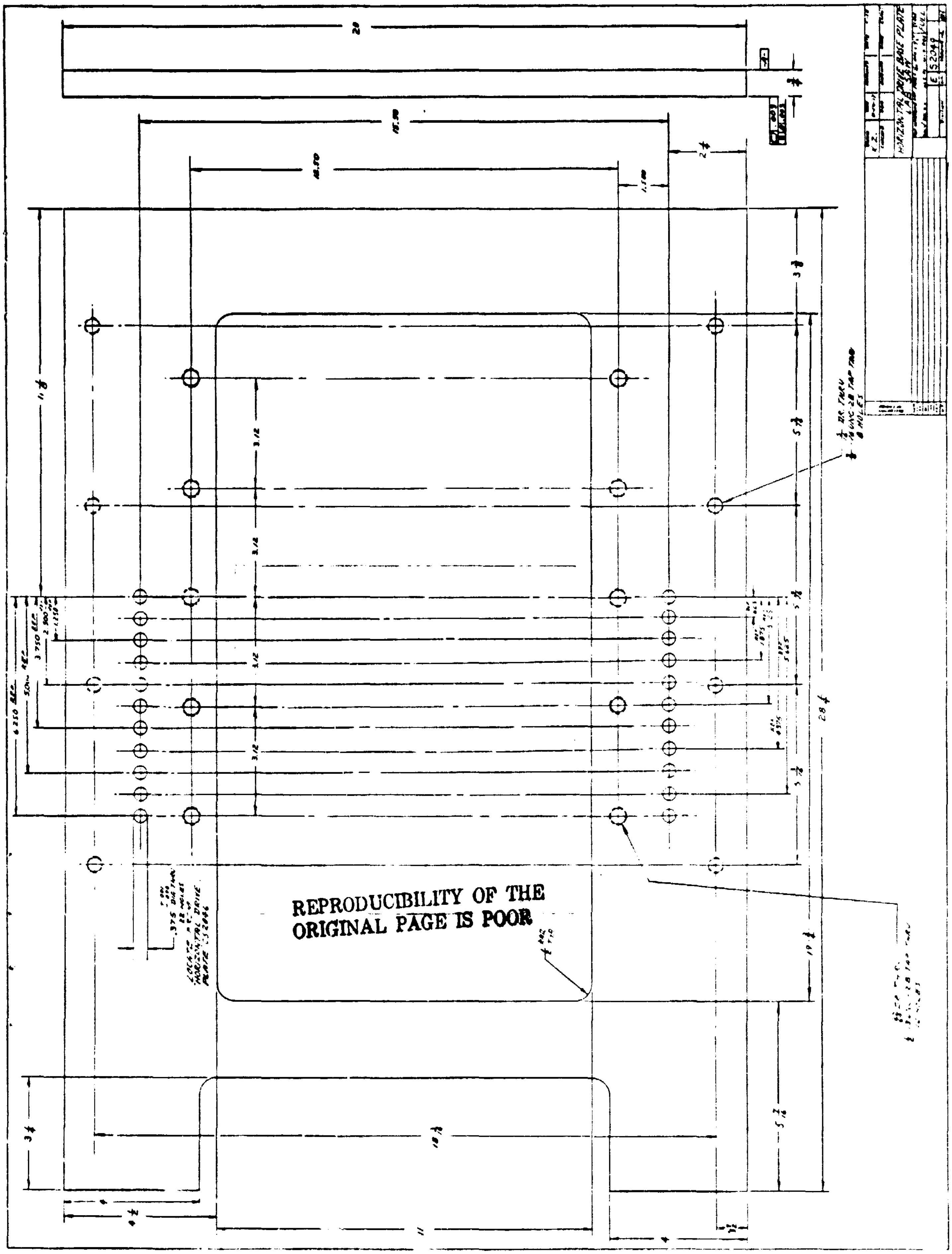

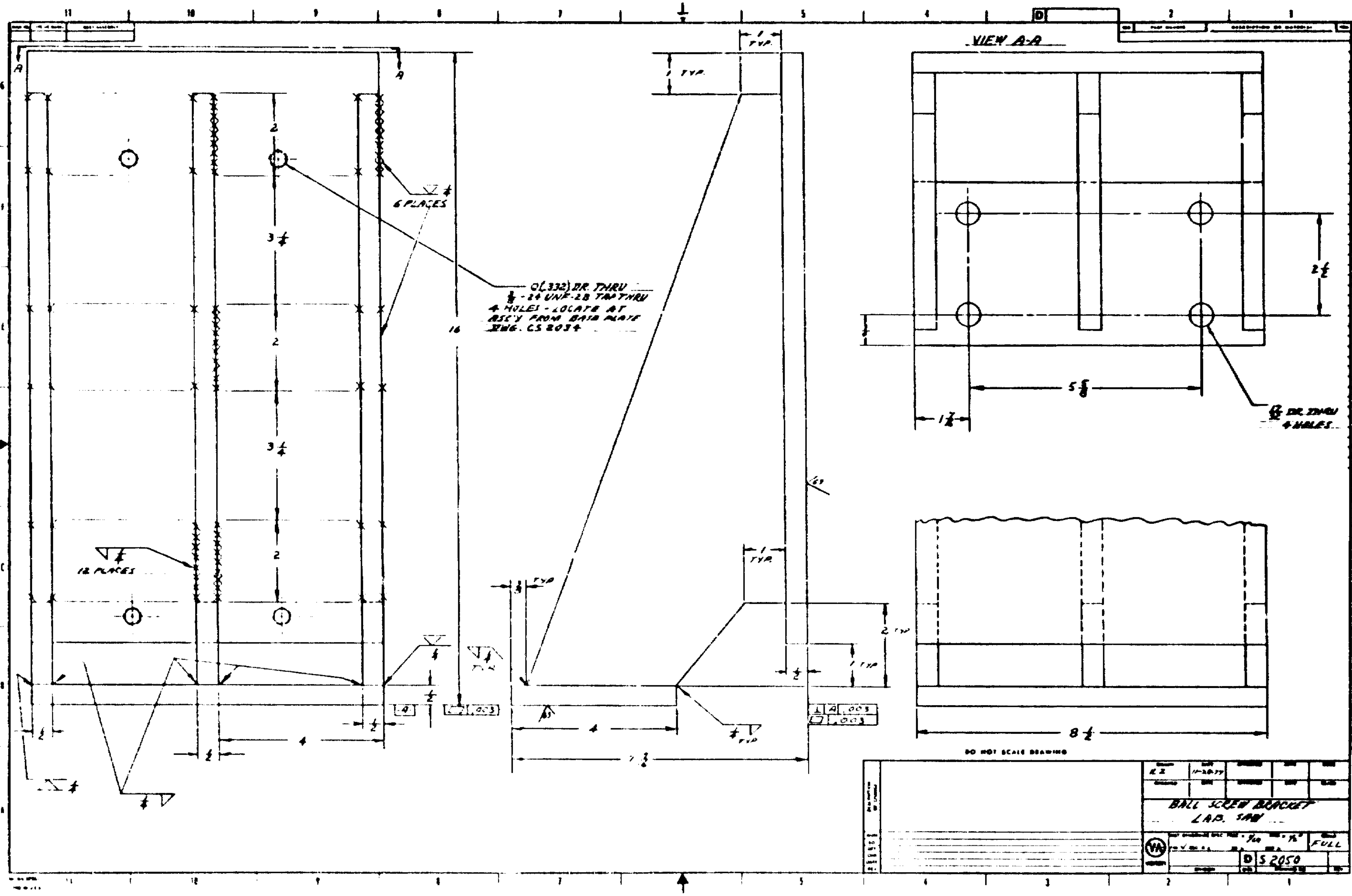
VIEW A-A
Q(.332) DR. THRU
1/4 - 28 UNF-2B TAP THRU
4 HOLES - LOCATE AT
ASS'Y FROM BASE PLATE
DWG. CS 2034
6 PLACES
12 PLACES
DO NOT SCALE DRAWING
BALL SCREW BRACKET
LAB. SAW
FULL
D S 2050

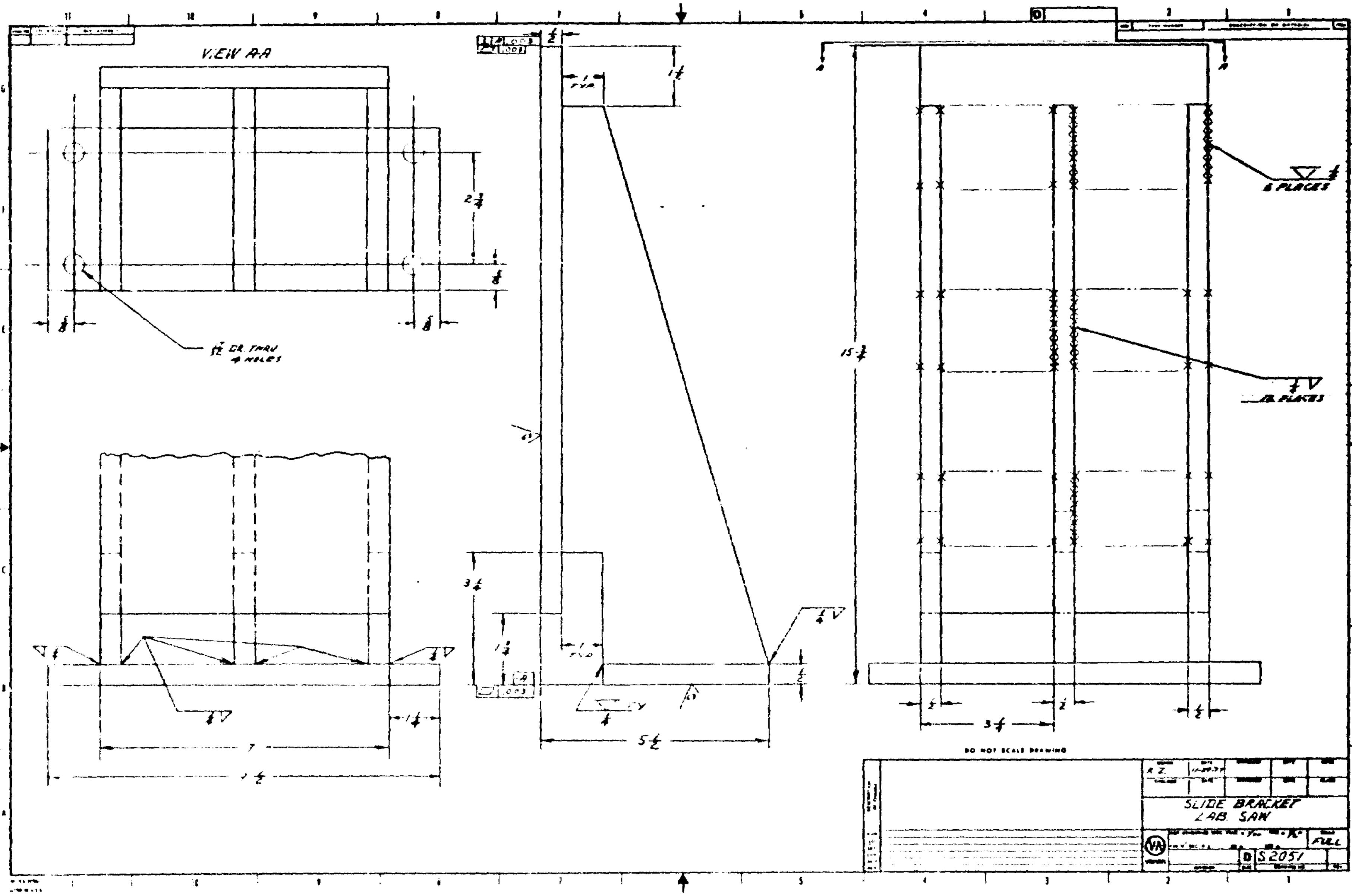

VIEW AA
$1\frac{1}{2}$ DR THRU 4 HOLES
8 PLACES
12 PLACES
DO NOT SCALE DRAWING
SLIDE BRACKET
LAB SAW
FULL
S2051

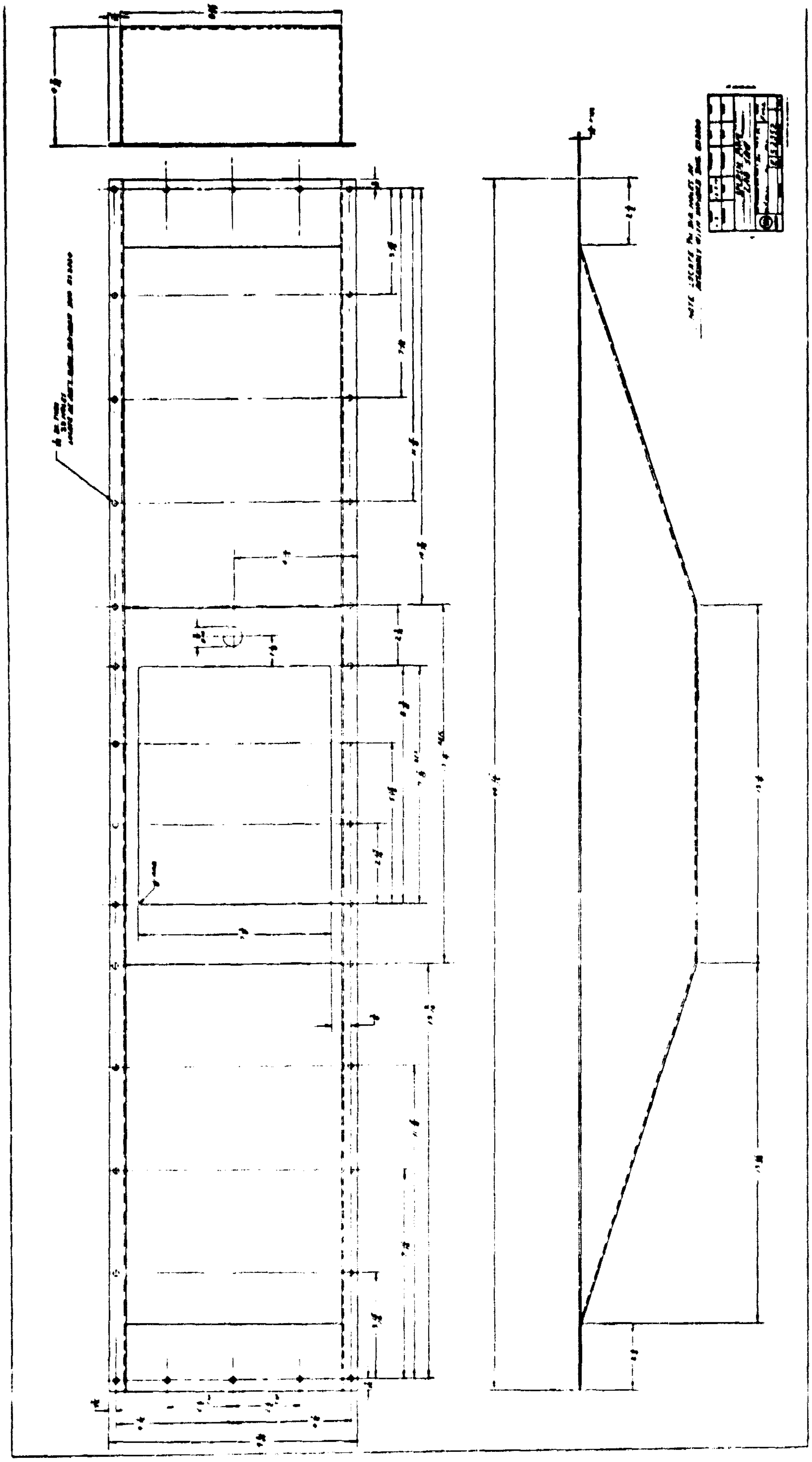

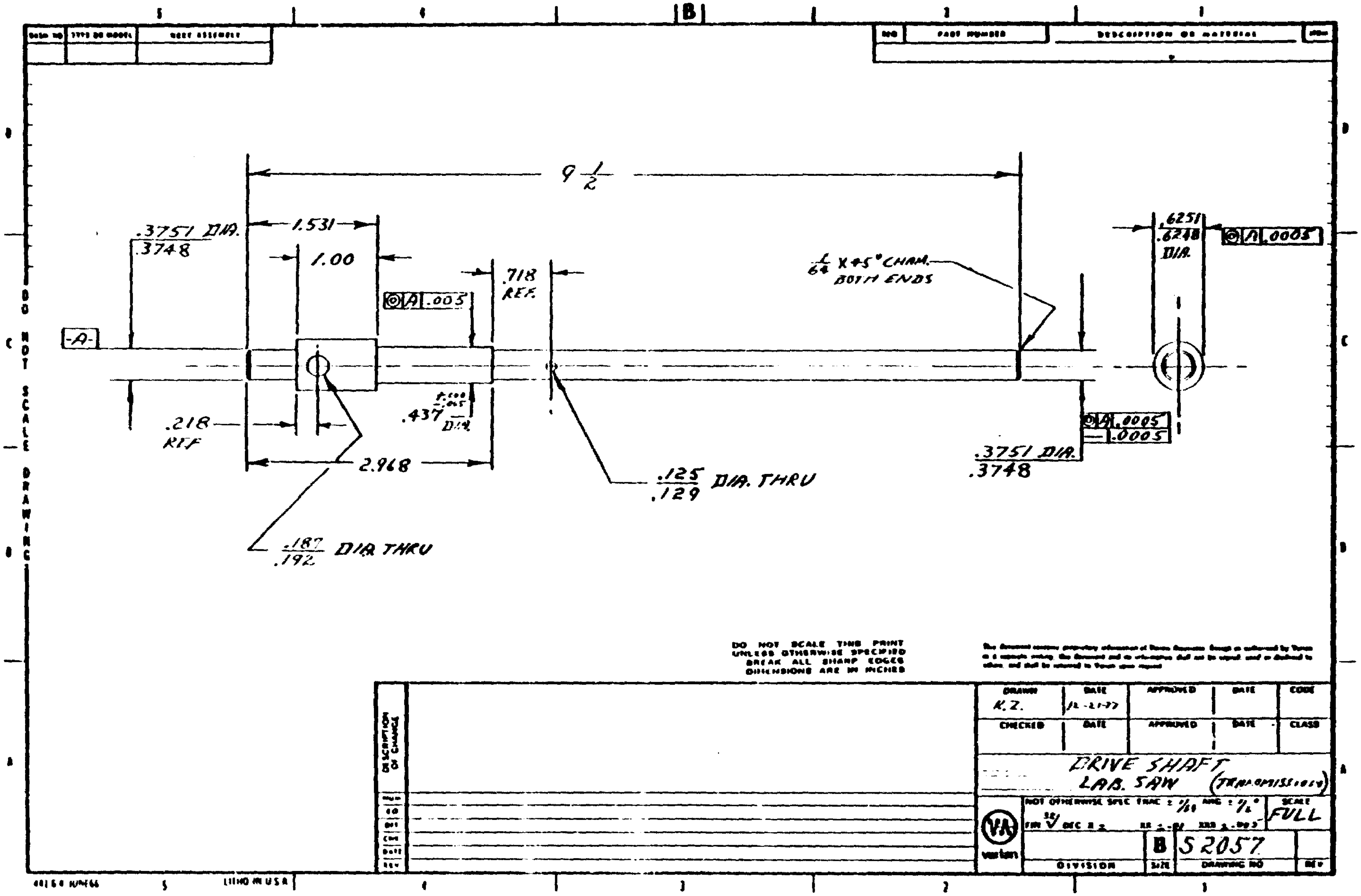

DO NOT SCALE DRAWING
9 1/2
.3751 DIA.
.3748
1.531
1.00
.718 REF.
-A-
.218 REF
.437 DIA
2.968
.125
.129 DIA. THRU
.187
.192 DIA THRU
1/64 X 45° CHAM. BOTH ENDS
.6251
.6248 DIA.
.0005
.005
DO NOT SCALE THIS PRINT UNLESS OTHERWISE SPECIFIED BREAK ALL SHARP EDGES DIMENSIONS ARE IN INCHES
DESCRIPTION OF CHANGE
DRAWN K.Z.
DATE
CHECKED
APPROVED
CODE
CLASS
DRIVE SHAFT
LAB. SAW (TRANSMISSION)
SCALE FULL
varian
DIVISION
SIZE B
DRAWING NO 5 2057
REV
LITHO IN U.S.A.

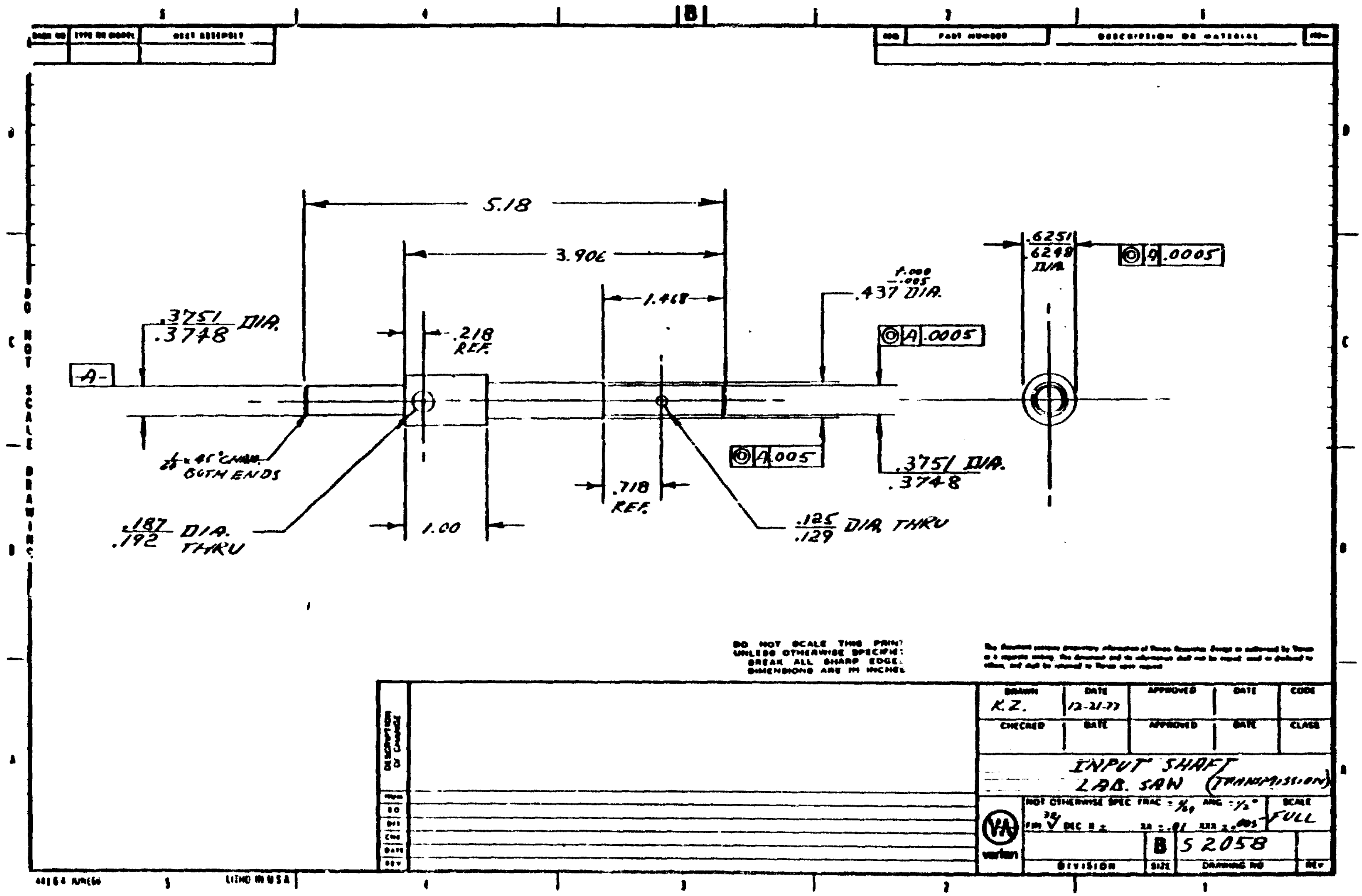
5.18
3.906
1.468
.3751 / .3748 DIA.
-A-
.218 REF.
+.000 / -.005 .437 DIA.
A .0005
.6251 / .6249 DIA.
A .0005
1/32 x 45° CHAM. BOTH ENDS
.187 / .192 DIA. THRU
1.00
A .005
.718 REF.
.125 / .129 DIA. THRU
.3751 / .3748 DIA.
DO NOT SCALE THIS PRINT
UNLESS OTHERWISE SPECIFIED:
BREAK ALL SHARP EDGES
DIMENSIONS ARE IN INCHES
DRAWN K.Z.
DATE 12-21-77
CHECKED
APPROVED
CODE
CLASS
INPUT SHAFT
LAB. SAW (TRANSMISSION)
SCALE FULL
B 52058
DIVISION
SIZE
DRAWING NO
REV
DESCRIPTION OF CHANGE
LITHO IN U.S.A.

DASH NO	TYPE OR MODEL	NEXT ASSEMBLY	REQ	PART NUMBER	DESCRIPTION OR MATERIAL	ITEM

A

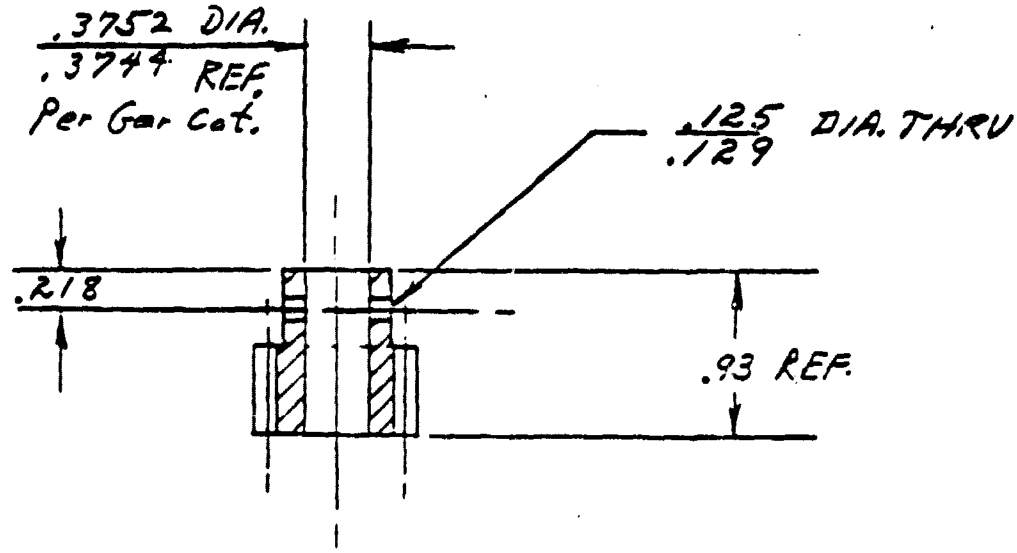

DO NOT SCALE DRAWING

DO NOT SCALE THIS PRINT
UNLESS OTHERWISE SPECIFIED
BREAK ALL SHARP EDGES
DIMENSIONS ARE IN INCHES

DRAWN	DATE	APPROVED	DATE	CODE
R.Z.	12-21-77			
CHECKED	DATE	APPROVED	DATE	CLASS

16T - .800 P.D. - 20 D.P. - 20° BOSTON GEAR
LAB. SAW (CAT. NO. YB16)
(TRANSMISSION)

NOT OTHERWISE SPEC FRAC ± ANG ± 1/2° SCALE FULL
FIN 63√ DEC X ± XX ± .01 XXX ± .005

varian

DIVISION	SIZE	DRAWING NO.	REV
	A	S2059	

DESCRIPTION OF CHANGE

NUM	
EO	
DFT	
CHK	
DATE	
REV	

LITHO IN U.S.A.

DASH NO	TYPE OR MODEL	NEXT ASSEMBLY	REQ	PART NUMBER	DESCRIPTION OR MATERIAL	ITEM

A

DO NOT SCALE DRAWING

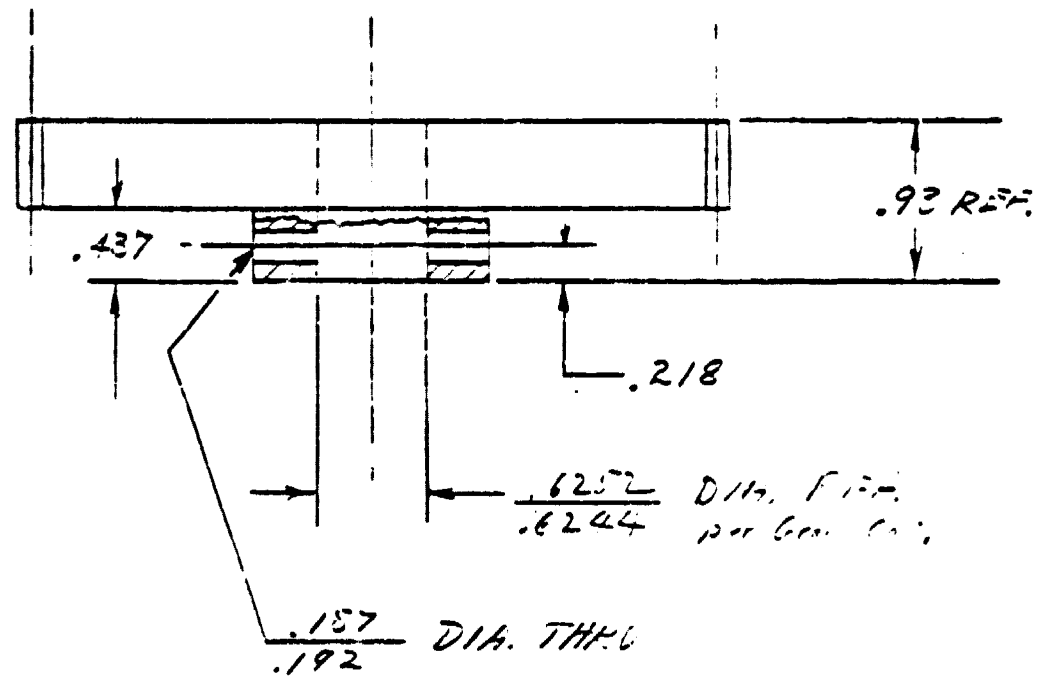

DO NOT SCALE THIS PRINT
UNLESS OTHERWISE SPECIFIED
BREAK ALL SHARP EDGES
DIMENSIONS ARE IN INCHES

LITHO IN U.S.A.

DESCRIPTION OF CHANGE

DRAWN	DATE	APPROVED	DATE	CODE
K.Z	12-21-77			
CHECKED	DATE	APPROVED	DATE	CLASS

80T - 4.000 P.D. - 20 D.P. - 20° [illegible]
LAB. SAW (CAT. NO. VA30)

NUM	
EO	
DFT	
CHK	
DATE	
REV	

NOT OTHERWISE SPEC FRAC = ±/ ANG = ±/ SCALE FULL
FIN 63 DEC X = XX = .01 XXX = .005

varian

DIVISION	SIZE	DRAWING NO	REV
	A	S 2060	

DASH NO	TYPE OR MODEL	NEXT ASSEMBLY	REQ	PART NUMBER	DESCRIPTION OR MATERIAL	ITEM

A

DO NOT SCALE DRAWING

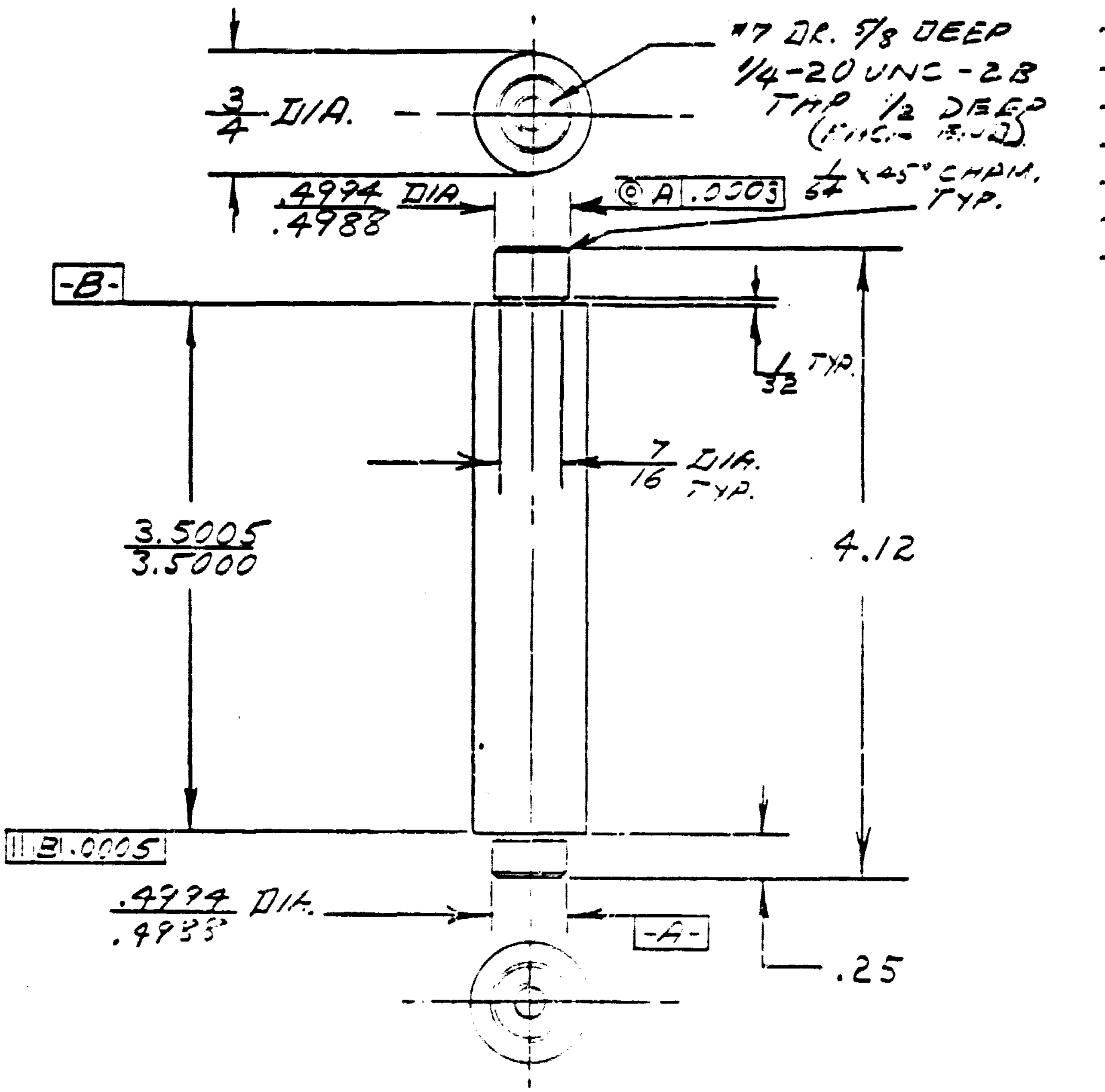

DO NOT SCALE THIS PRINT
UNLESS OTHERWISE SPECIFIED
BREAK ALL SHARP EDGES
DIMENSIONS ARE IN INCHES

DRAWN	DATE	APPROVED	DATE	CODE
KZ	12-17-77			
CHECKED	DATE	APPROVED	DATE	CLASS

PLATE SPACER [illegible]
[illegible]

DESCRIPTION OF CHANGE

NUM	
EO	
DFT	
CHK	
DATE	
REV	

NOT OTHERWISE SPEC FRAC ± 1/64 ANG ± 1/2° SCALE FULL
FIN 32 DEC X ± XX ± .01 XXX ± .005

varian

DIVISION	SIZE	DRAWING NO	REV
	A	S 2061	

LITHO IN U.S.A.

DASH NO.	TYPE OR MODEL	NEXT ASSEMBLY	REQ	PART NUMBER	DESCRIPTION OR MATERIAL	ITEM

A

DO NOT SCALE DRAWING

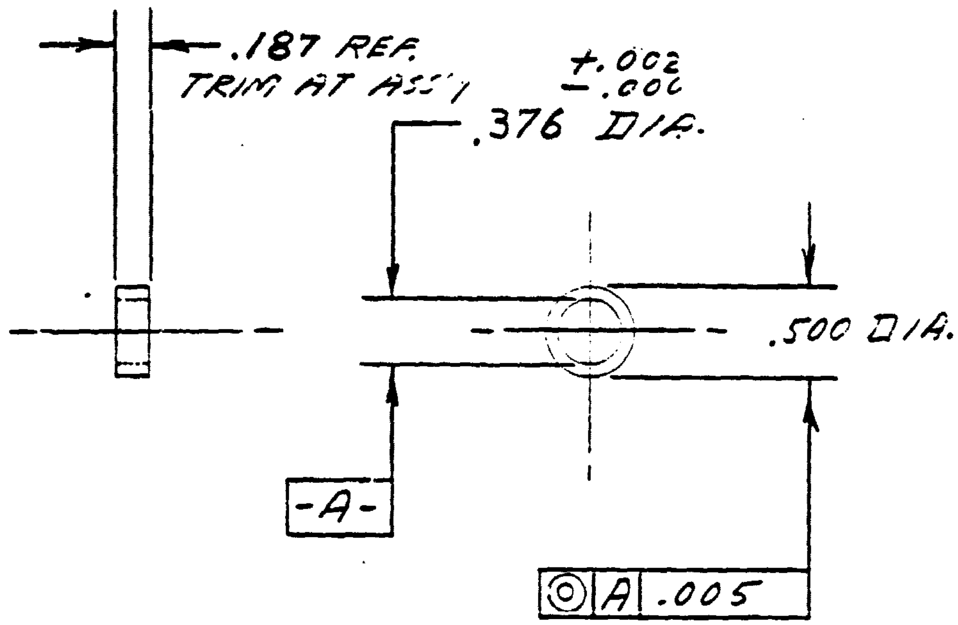

DO NOT SCALE THIS PRINT
UNLESS OTHERWISE SPECIFIED
BREAK ALL SHARP EDGES
DIMENSIONS ARE IN INCHES

DESCRIPTION OF CHANGE: C-5

NUM	
EO	
DFT	
CHK	
DATE	
REV	

DRAWN	DATE	APPROVED	DATE	CODE
K.Z.	12-21-77			
CHECKED	DATE	APPROVED	DATE	CLASS

SPACER (TRANSMISSION)
LAB. SAW

NOT OTHERWISE SPEC: FRAC ± 1/64 ANG ± 1/2°
FIN 32 √ DEC X ± XX ± .01 XXX ± .005

SCALE: FULL

varian

DIVISION	SIZE	DRAWING NO	REV
	A	52062	

DASH NO	TYPE OR MODEL	NEXT ASSEMBLY	REQ	PART NUMBER	DESCRIPTION OR MATERIAL	ITEM

A

DO NOT SCALE DRAWING

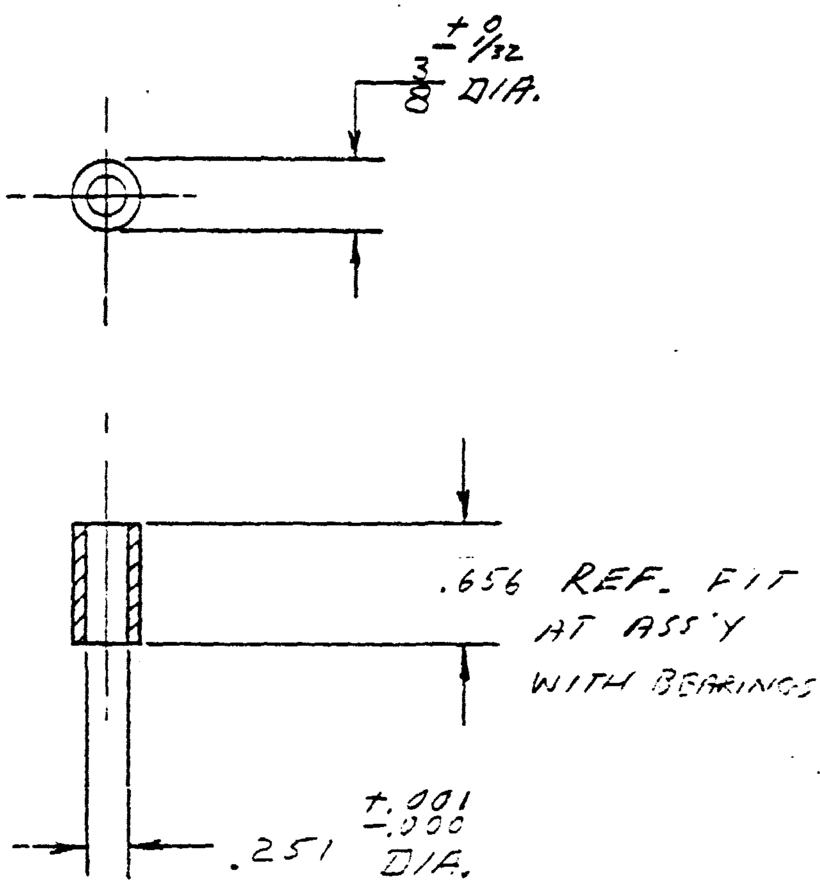

DO NOT SCALE THIS PRINT
UNLESS OTHERWISE SPECIFIED
BREAK ALL SHARP EDGES
DIMENSIONS ARE IN INCHES

DRAWN	DATE	APPROVED	DATE	CODE
K. Z.	1-9-73			
CHECKED	DATE	APPROVED	DATE	CLASS

BEARING SPACER (TRANSMISSION) LAB. SAW

NOT OTHERWISE SPEC FRAC $\pm 1/64$ ANG $\pm 1/2°$ — SCALE: FULL

FIN $\sqrt{32}$ DEC X ± XX ± .01 XXX ± .005

varian

DIVISION	SIZE	DRAWING NO.	REV
	A	S 2063	

DESCRIPTION OF CHANGE

NUM	
EO	
DFT	
CHK	
DATE	
REV	

LITHO IN U.S.A.

441-3 MAY

DASH NO.	TYPE OR MODEL	NEXT ASSEMBLY	REQ	PART NUMBER	DESCRIPTION OR MATERIAL	ITEM

A

DO NOT SCALE DRAWING

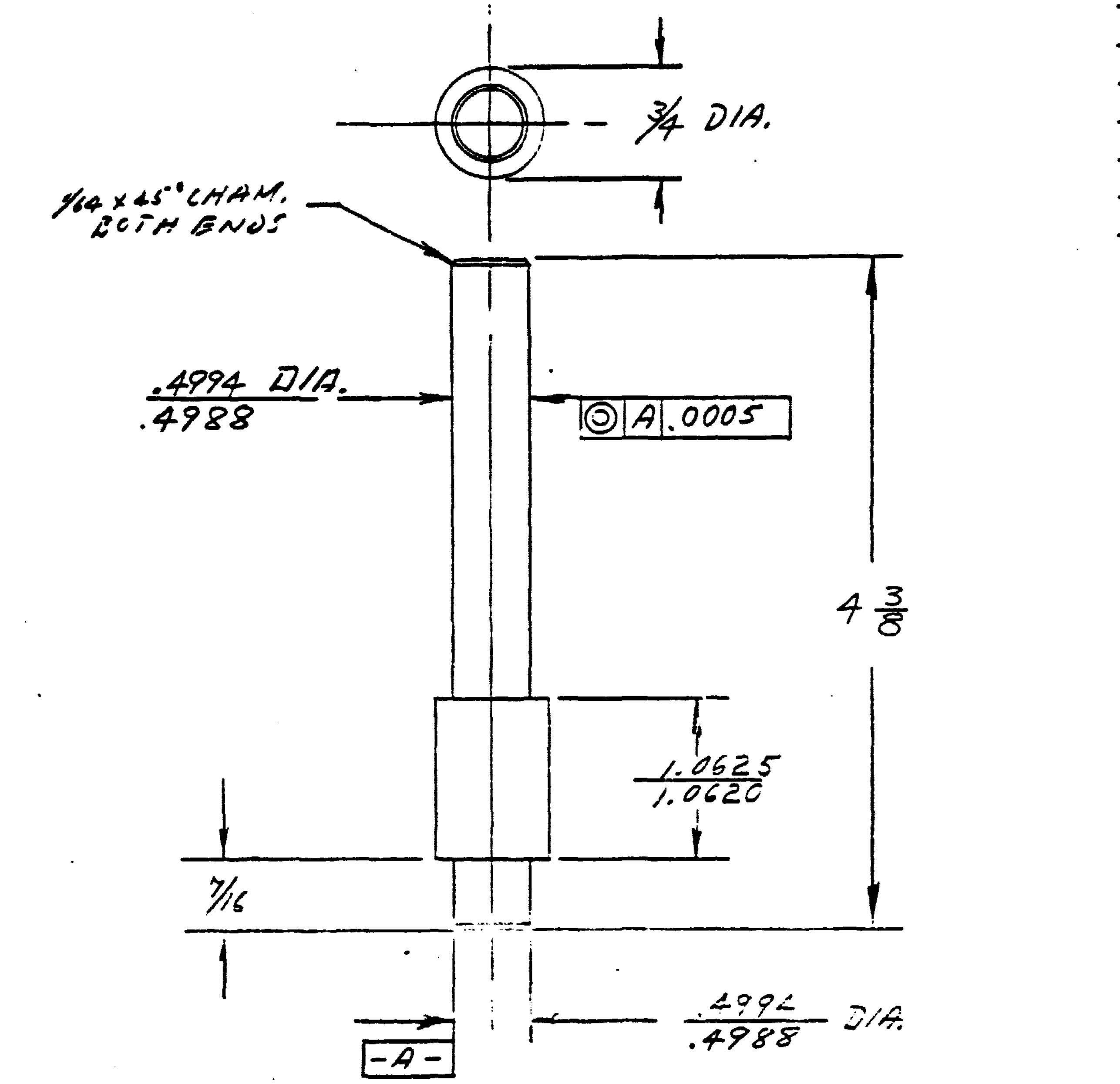

DO NOT SCALE THIS PRINT
UNLESS OTHERWISE SPECIFIED
BREAK ALL SHARP EDGES
DIMENSIONS ARE IN INCHES

DRAWN	DATE	APPROVED	DATE	CODE
K. Z.	1-9-78			
CHECKED	DATE	APPROVED	DATE	CLASS

SHIFT PIVOT (TRANSMISSION)
LAB. SAW

NOT OTHERWISE SPEC. FRAC ± 1/64 ANG ± 1/2° | SCALE FULL
FIN 63 ✓ DEC X ± XX ± .01 XXX ± .005

varian

DIVISION	SIZE	DRAWING NO.	REV
	A	52064	

DESCRIPTION OF CHANGE

NUM	
EO	
DFT	
CHK	
DATE	
REV	

DASH NO.	TYPE OR MODEL	NEXT ASSEMBLY	REQ	PART NUMBER	DESCRIPTION OR MATERIAL	ITEM

A

DO NOT SCALE DRAWING

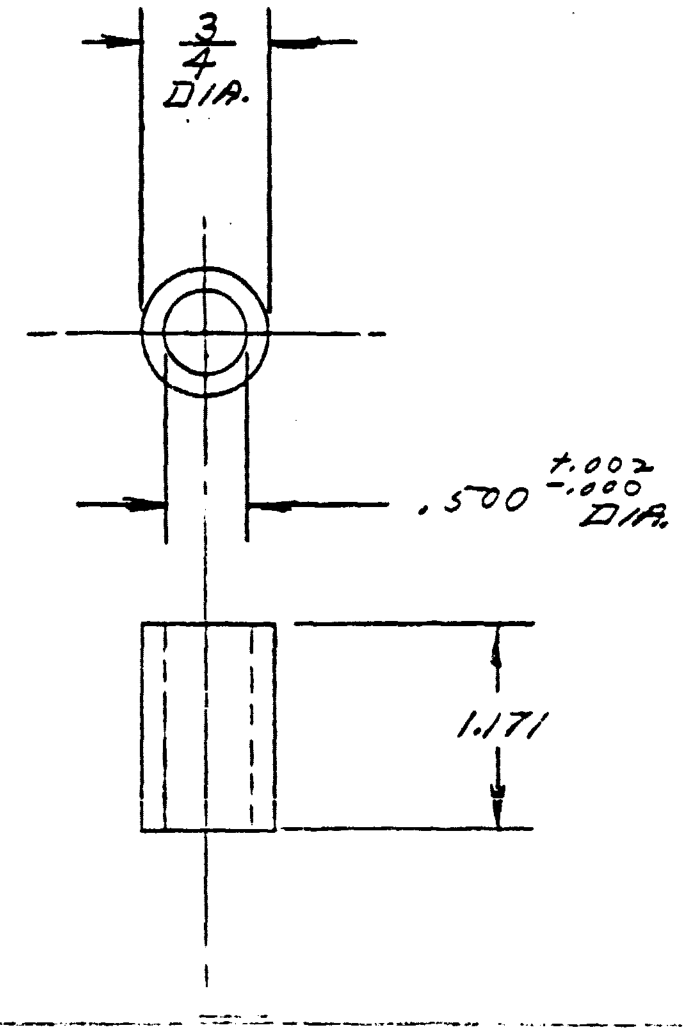

DO NOT SCALE THIS PRINT
UNLESS OTHERWISE SPECIFIED
BREAK ALL SHARP EDGES
DIMENSIONS ARE IN INCHES

DRAWN	DATE	APPROVED	DATE	CODE
CHECKED	DATE	APPROVED	DATE	CLASS

SHAFT PIVOT SPACER
LAB. SAW (TRANSMISSION)

NOT OTHERWISE SPEC. FRAC ± 1/64 ANG ± 1/2° FIN 63√ DEC X ± XX ± .01 XXX ± .005

SCALE FULL

varian

DIVISION	SIZE	DRAWING NO	REV
	A	52065	

DESCRIPTION OF CHANGE	
NUM	
EO	
DFT	
CHK	
DATE	
REV	

DASH NO.	TYPE OR MODEL	NEXT ASSEMBLY	REQ	PART NUMBER	DESCRIPTION OR MATERIAL	ITEM

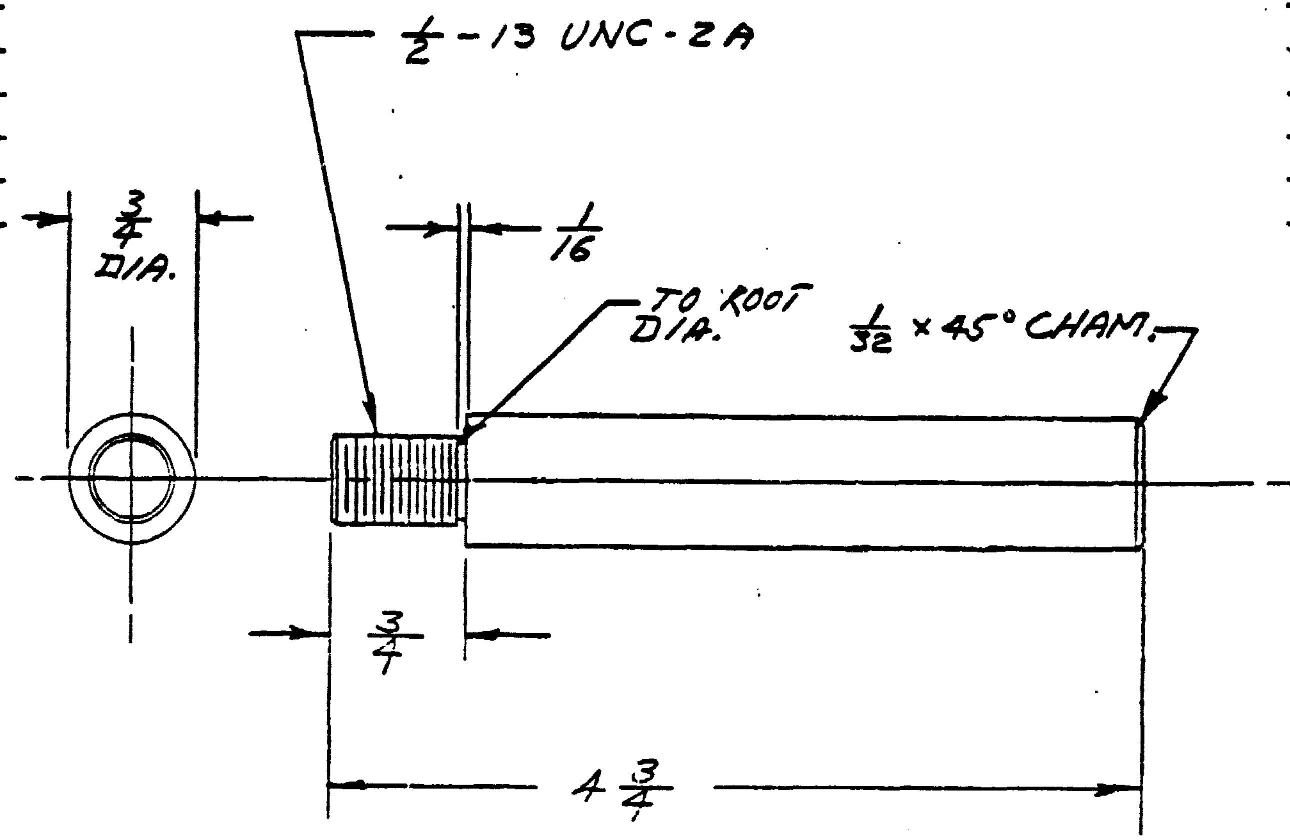

A

DO NOT SCALE DRAWING

DO NOT SCALE THIS PRINT
UNLESS OTHERWISE SPECIFIED
BREAK ALL SHARP EDGES
DIMENSIONS ARE IN INCHES

DRAWN	DATE	APPROVED	DATE	CODE
K.Z.	1-9-78			
CHECKED	DATE	APPROVED	DATE	CLASS

SHIFT HANDLE
LAB. SAW (TRANSMISSION)

NOT OTHERWISE SPEC: FRAC ± 1/64, ANG ± 1/2°
FIN 63 √ DEC X = XX ± .01 XXX ± .005

SCALE FULL

varian

DIVISION	SIZE	DRAWING NO.	REV
	A	52066	

DESCRIPTION OF CHANGE

NUM	
EO	
...	
CHK	
DATE	
REV	

DASH NO	TYPE OR MODEL	NEXT ASSEMBLY	REQ	PART NUMBER	DESCRIPTION OR MATERIAL	ITEM

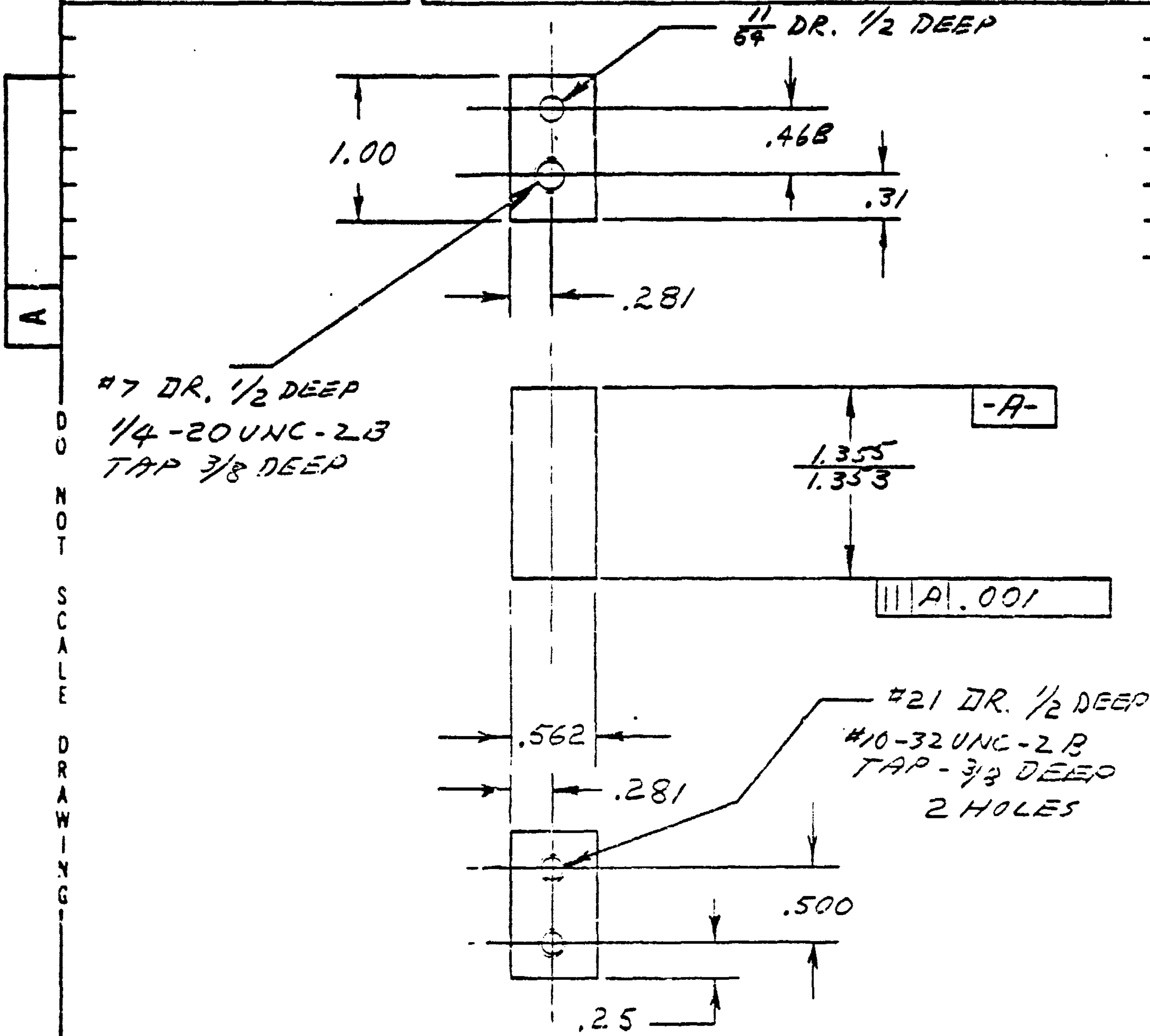

DO NOT SCALE DRAWING

DO NOT SCALE THIS PRINT
UNLESS OTHERWISE SPECIFIED
BREAK ALL SHARP EDGES
DIMENSIONS ARE IN INCHES

DRAWN	DATE	APPROVED	DATE	CODE
K.Z.	1-9-78			
CHECKED	DATE	APPROVED	DATE	CLASS

SHIFT SPACER
LAB. SAW

NOT OTHERWISE SPEC FRAC ± 1/64 ANG ± 1/2° | SCALE
FIN 63 DEC X ± XX ± .01 XXX ± .005 | FULL

varian

DIVISION	SIZE	DRAWING NO	REV
	A	52067	

DESCRIPTION OF CHANGE	
NUM	
EO	
DFT	
CHK	
DATE	
REV	

LITHO IN U.S.A.
41163 REV

DASH NO.	TYPE OR MODEL	NEXT ASSEMBLY	REQ	PART NUMBER	DESCRIPTION OR MATERIAL	ITEM

A

DO NOT SCALE DRAWING

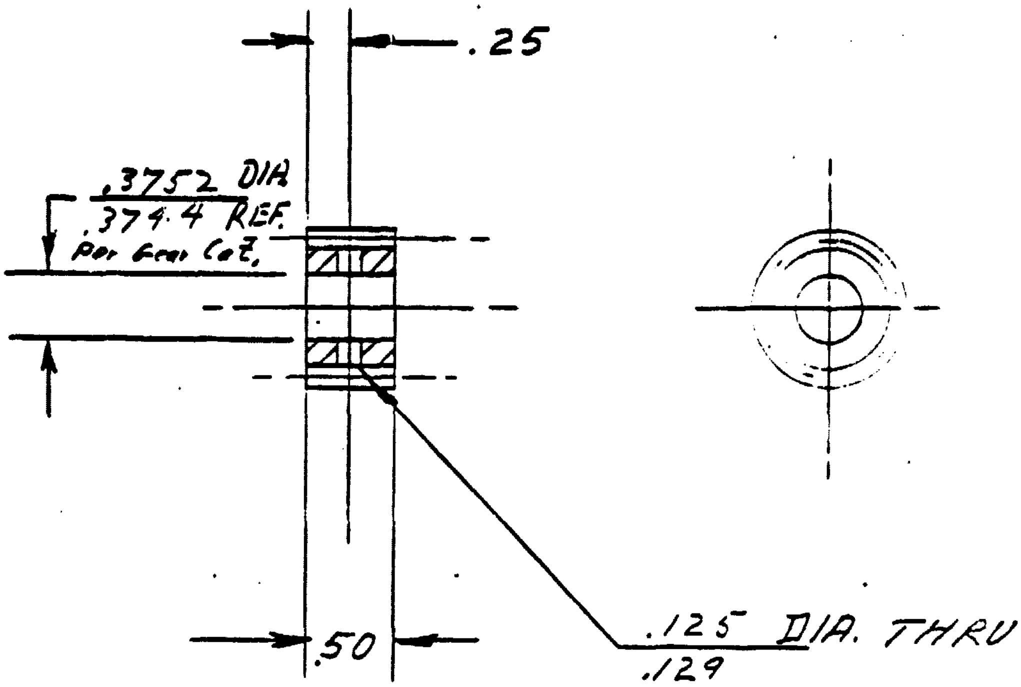

DO NOT SCALE THIS PRINT
UNLESS OTHERWISE SPECIFIED
BREAK ALL SHARP EDGES
DIMENSIONS ARE IN INCHES

DRAWN	DATE	APPROVED	DATE	CODE
K.Z.	1-9-78			
CHECKED	DATE	APPROVED	DATE	CLASS

16 T - .800 P.D. - 20 D.P. - 20° BOSTON GEAR
(SHIFT GEAR) LAB. SAW (CAT. NO. YA16) (+ BANC DIMENSIONS)

NOT OTHERWISE SPEC. FRAC = 1/64 ANG = 1/2 °
FIN. 63 √ DEC X = XX = .01 XXX = .005

SCALE: FULL

varian

DIVISION	SIZE	DRAWING NO.	REV
	A	S 2068	

DESCRIPTION OF CHANGE

NUM	
EO	
DFT	
CHK	
DATE	
REV	

LITHO IN U.S.A.

4163 MAP

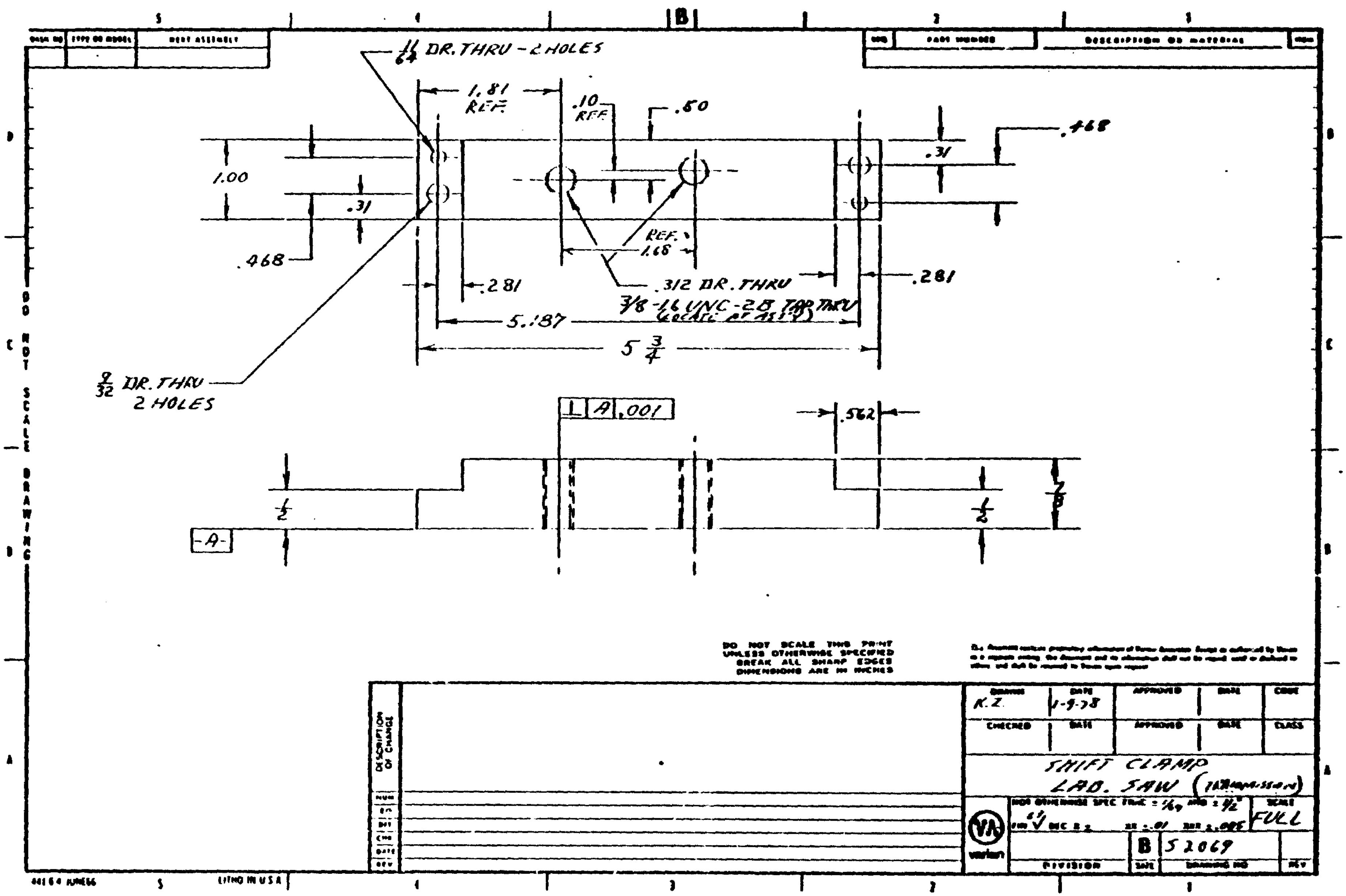

11/64 DR. THRU - 2 HOLES
1.81 REF.
.10 REF.
.50
.468
1.00
.31
.31
.468
REF. 1.68
.281
.281
.312 DR. THRU
3/8-16 UNC-2B TAP THRU
5.187
5 3/4
9/32 DR. THRU 2 HOLES
⊥ A .001
.562
1/2
1/2
7/8
-A-
DO NOT SCALE THIS PRINT
UNLESS OTHERWISE SPECIFIED
BREAK ALL SHARP EDGES
DIMENSIONS ARE IN INCHES
DESCRIPTION OF CHANGE
DRAWN K.Z.
DATE 1-9-78
APPROVED
CHECKED
SHIFT CLAMP
LAB. SAW
SCALE FULL
B 52069
DRAWING NO
DIVISION
varian
LITHO IN U.S.A.

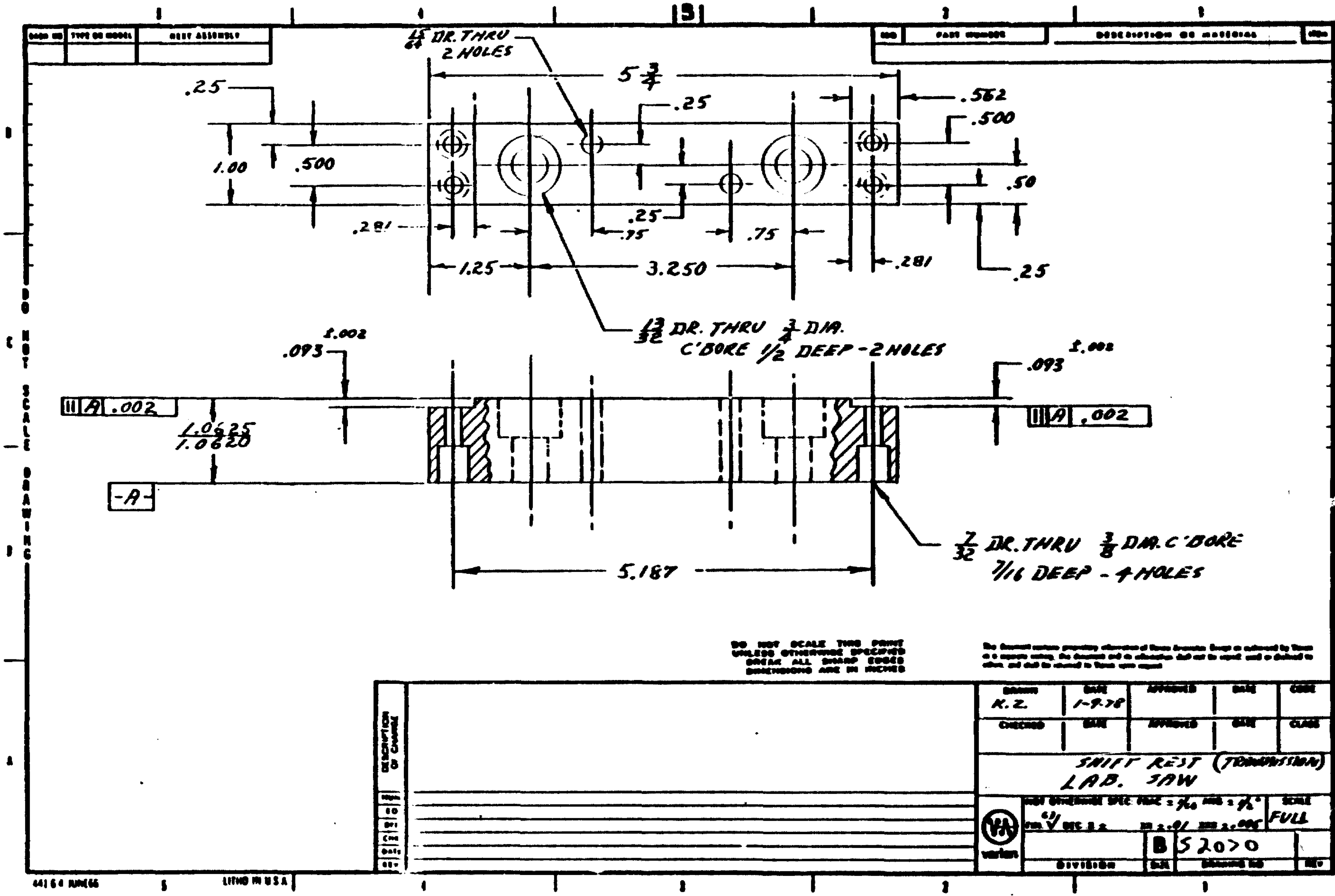
45/64 DR. THRU 2 HOLES
5 3/4
.25
.500
1.00
.281
1.25
3.250
.75
.562
.50
13/32 DR. THRU 3/4 DIA. C'BORE 1/2 DEEP - 2 HOLES
.093 ±.002
.002
1.0625
1.0620
-A-
7/32 DR. THRU 3/8 DIA. C'BORE 7/16 DEEP - 4 HOLES
5.187
DO NOT SCALE THIS PRINT
UNLESS OTHERWISE SPECIFIED
BREAK ALL SHARP EDGES
DIMENSIONS ARE IN INCHES
DESCRIPTION OF CHANGE
DRAWN K.Z.
DATE 1-9-78
CHECKED
APPROVED
SHIFT REST (TRANSMISSION)
LAB. SAW
SCALE FULL
varian
B 520>0
DIVISION
DRAWING NO
REV
DO NOT SCALE DRAWING
LITHO IN U.S.A.

DASH NO	TYPE OR MODEL	NEXT ASSEMBLY	REQ	PART NUMBER	DESCRIPTION OR MATERIAL	ITEM

DO NOT SCALE DRAWING

A

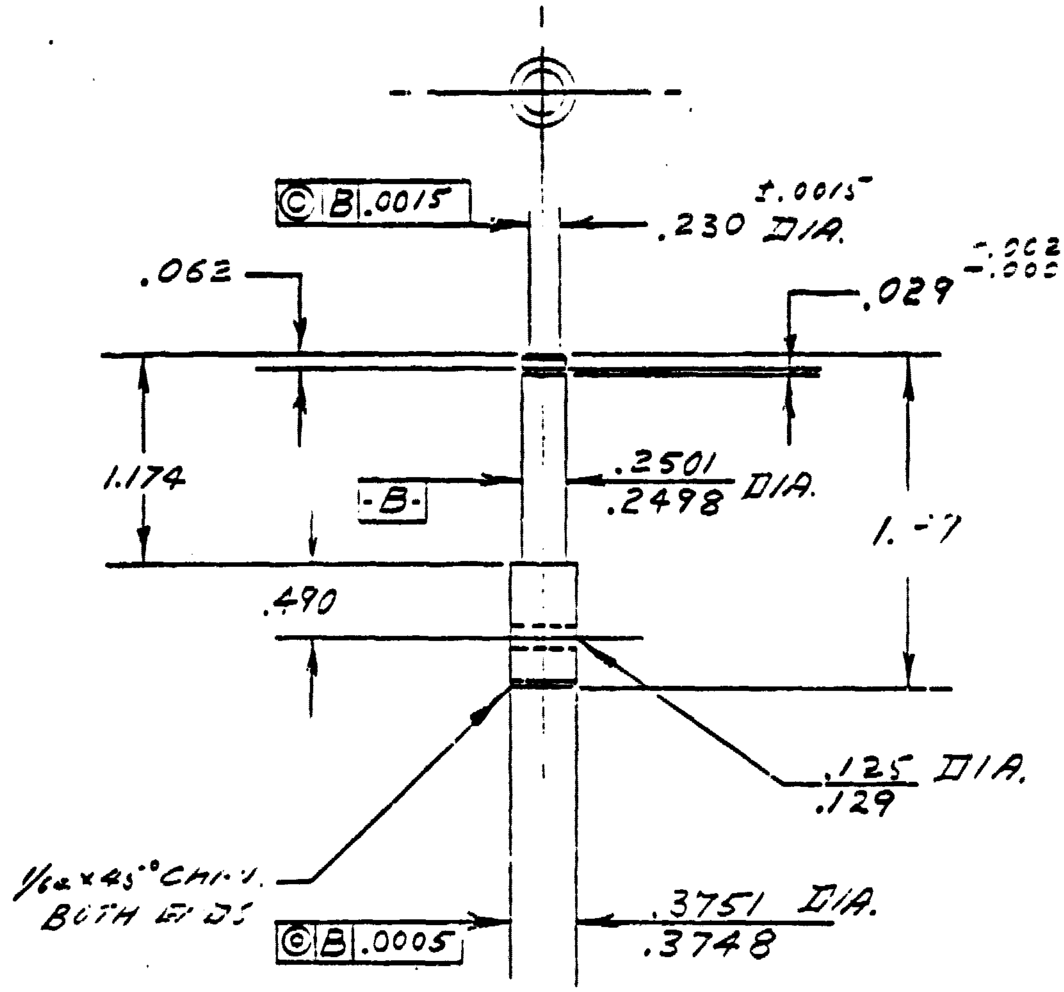

DO NOT SCALE THIS PRINT
UNLESS OTHERWISE SPECIFIED
BREAK ALL SHARP EDGES
DIMENSIONS ARE IN INCHES

DRAWN	DATE	APPROVED	DATE	CODE
K.Z.	1-10-78			
CHECKED	DATE	APPROVED	DATE	CLASS

HIGH SPEED SHAFT
LAB. SAW (TRANSMISSION)

NOT OTHERWISE SPEC FRAC ± 1/64 ANG ± 1/2°
FIN 32 DEC X ± XX ± .01 XXX ± .005

SCALE FULL

varian

DIVISION	SIZE	DRAWING NO	REV
	A	52071	

DESCRIPTION OF CHANGE

NUM	
EO	
DFT	
CHK	
DATE	
REV	

DASH NO	TYPE OR MODEL	NEXT ASSEMBLY	REQ	PART NUMBER	DESCRIPTION OR MATERIAL	ITEM

A

DO NOT SCALE DRAWING

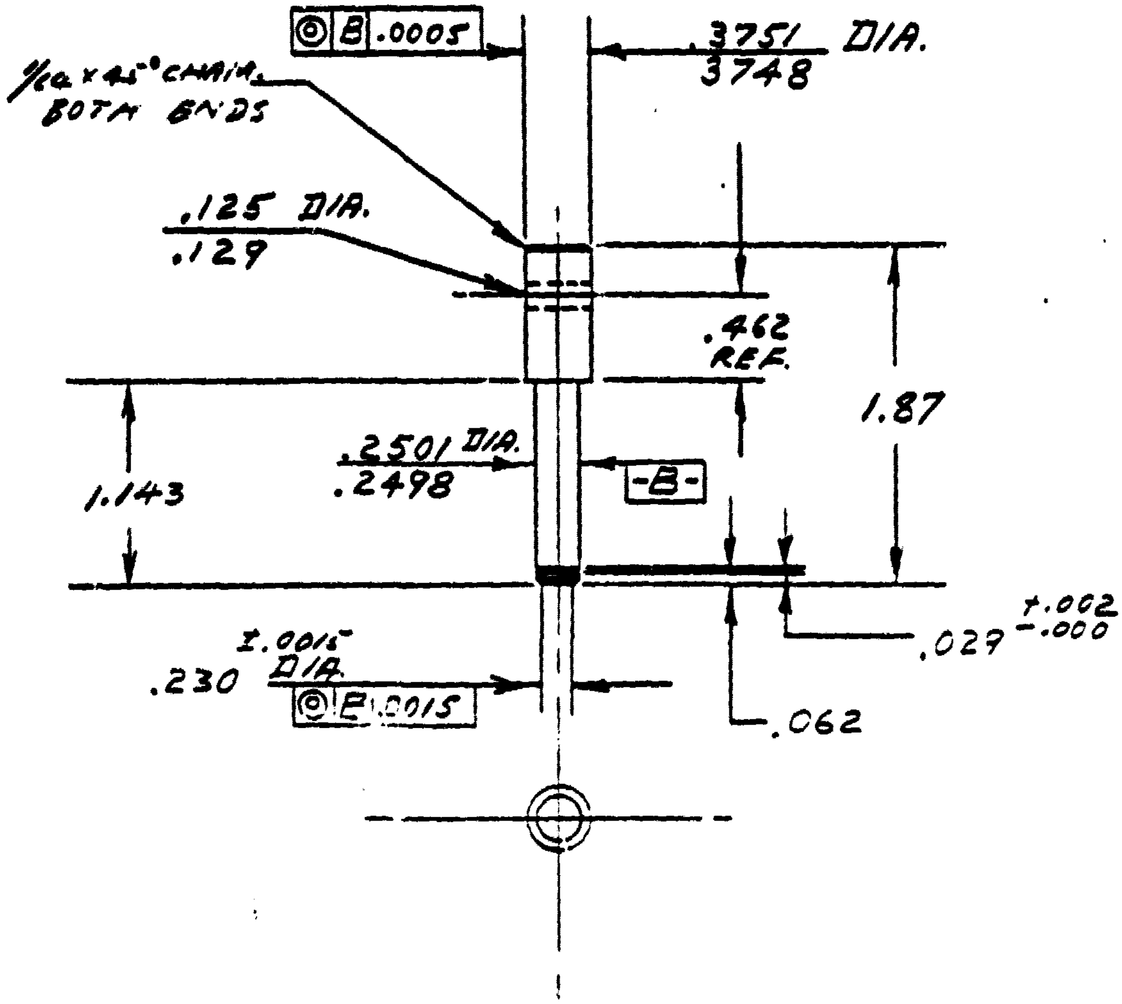

DO NOT SCALE THIS PRINT
UNLESS OTHERWISE SPECIFIED
BREAK ALL SHARP EDGES
DIMENSIONS ARE IN INCHES

This document contains proprietary information of Varian Associates. Except as authorized by Varian in a separate writing, this document and its information shall not be copied, used or disclosed to others, and shall be returned to Varian upon request.

DRAWN	DATE	APPROVED	DATE	CODE
K. Z	1-10-78			
CHECKED	DATE	APPROVED	DATE	CLASS

LOW SPEED SHAFT
LAB. SAW (TRANSMISSION)

NOT OTHERWISE SPEC FRAC = ± 1/64 ANG = ± ... SCALE FULL
FIN 32 DEC X = XX = XXX =

varian

DIVISION	SIZE	DRAWING NO	REV
	A	5 2072	

DESCRIPTION OF CHANGE

NUM
EO
DFT
CHK
DATE
REV

LITHO IN U.S.A.

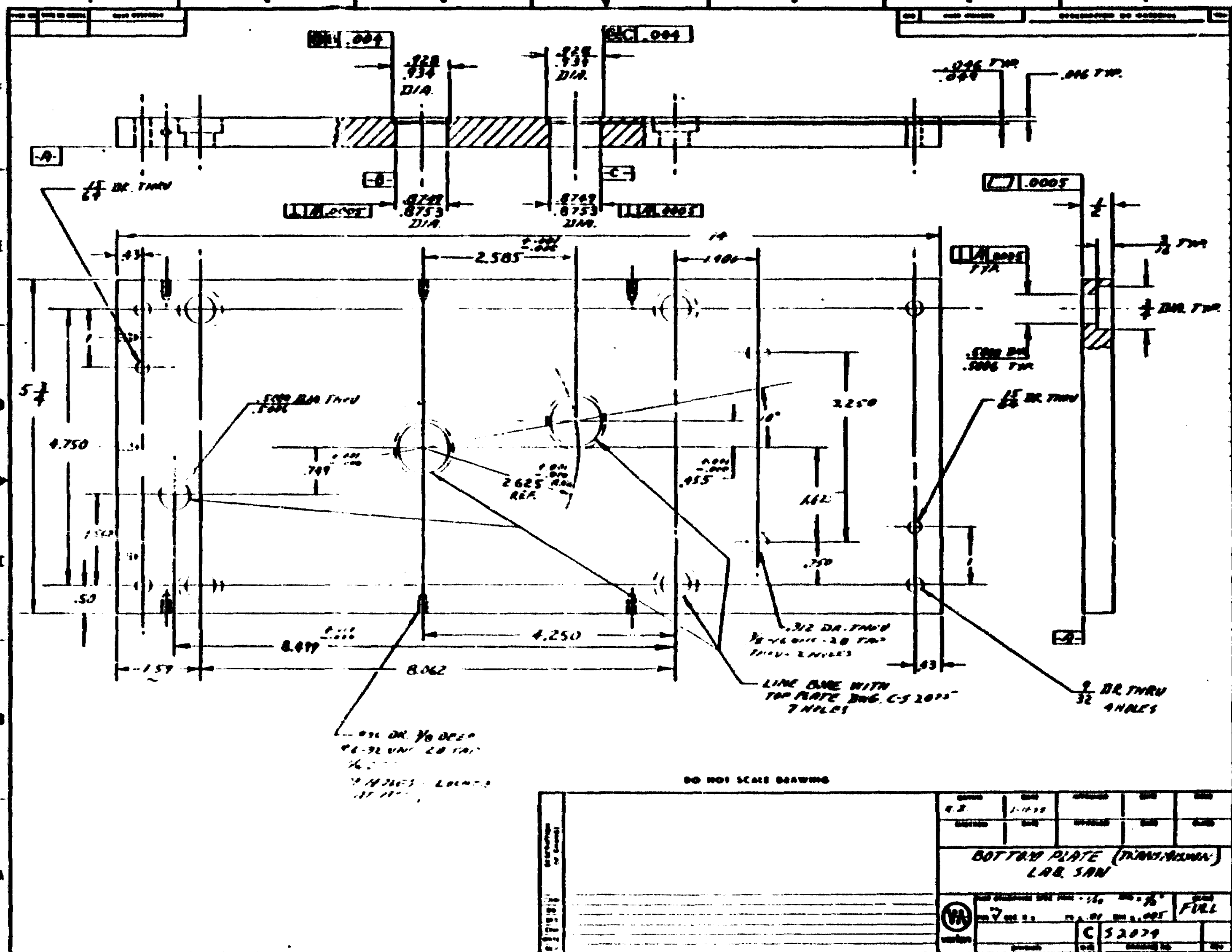

DO NOT SCALE DRAWING
BOTTOM PLATE (TRANSMISSION)
LAB SAW
FULL
C 52079
.750
4.750
2.585
4.250
8.062
8.499
2.625 REF.
2.250
.312 DR. THRU
LINE BORE WITH TOP PLATE DWG. C-52075 7 HOLES
9/32 DR. THRU 4 HOLES
15/64 DR. THRU
.0005
DIA.

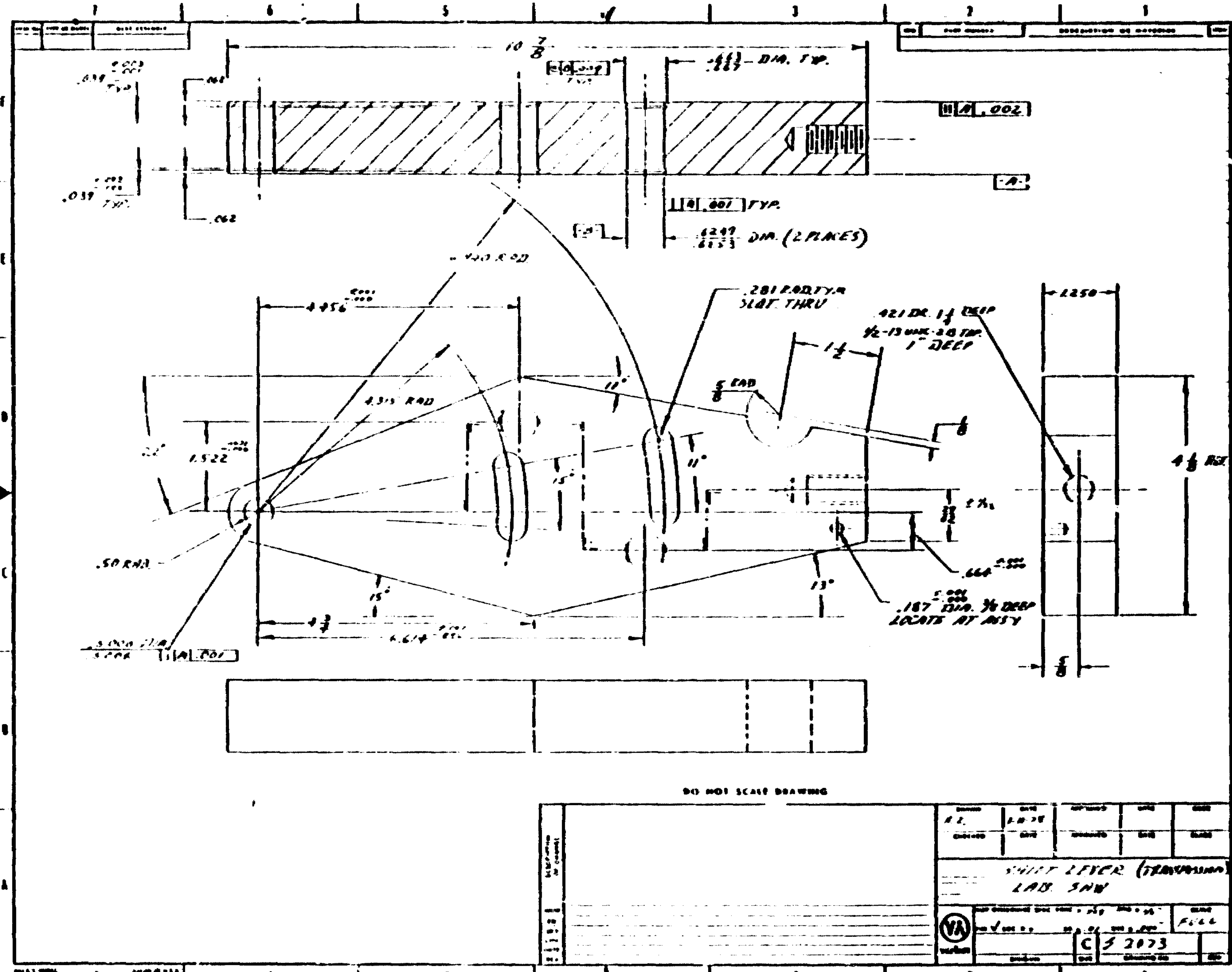
10 7/8
.421 DR. 1 1/4 DEEP
1/2-13 UNC-2B TAP 1" DEEP
.281 RAD. TYP. SLOT THRU
5/8 RAD
4.315 RAD
.50 RAD.
.187 DIA. 3/8 DEEP
LOCATE AT ASSY
.6249 DIA. (2 PLACES)
.250
4 1/8 REF.
DO NOT SCALE DRAWING
SHIFT LEVER (TRANSMISSION)
LAB SAW
FULL
C 5 2073

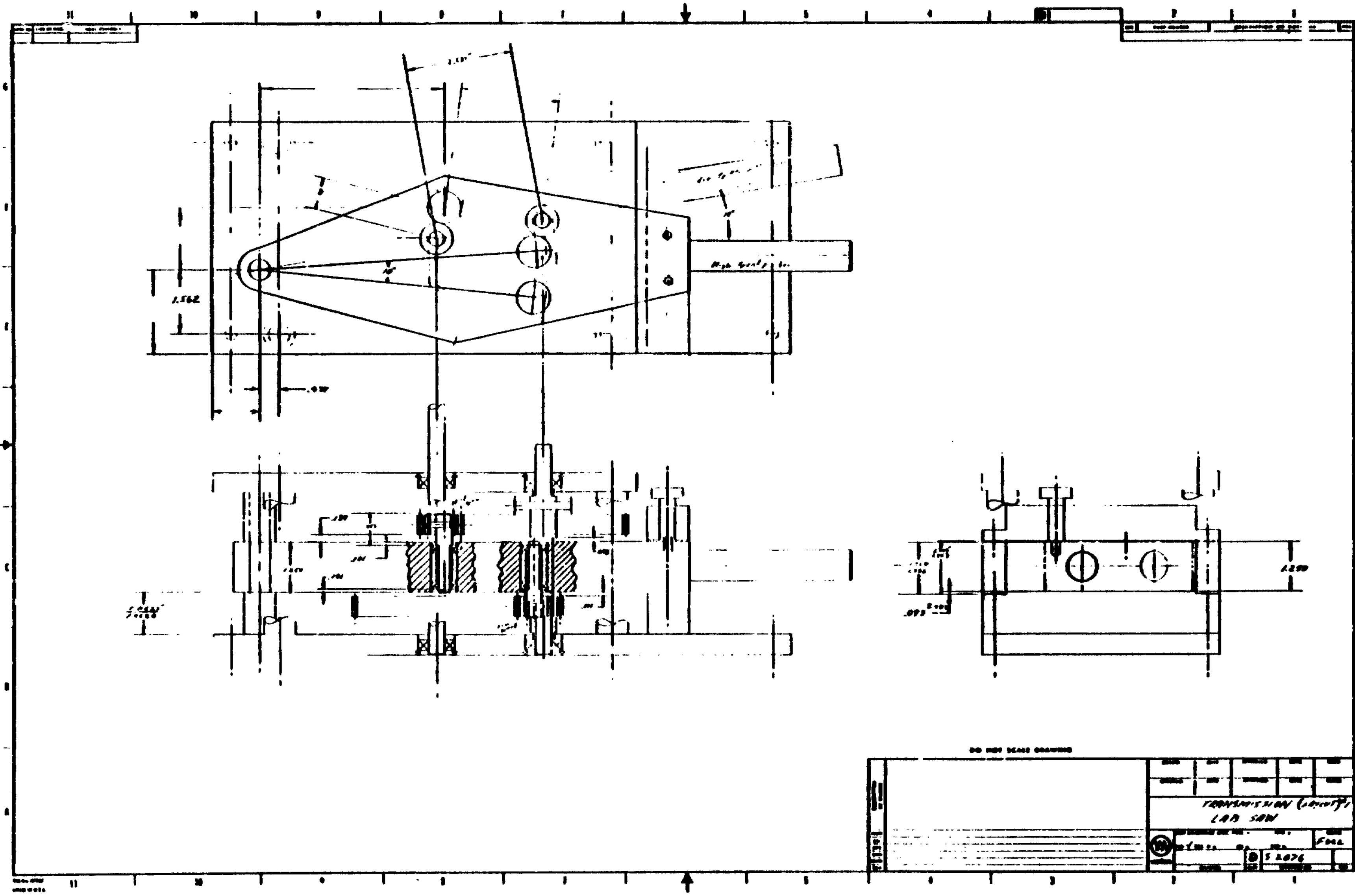

DO NOT SCALE DRAWING
TRANSMISSION (LAYOUT)
LAB SAW
FULL
B
S 2076
1.562

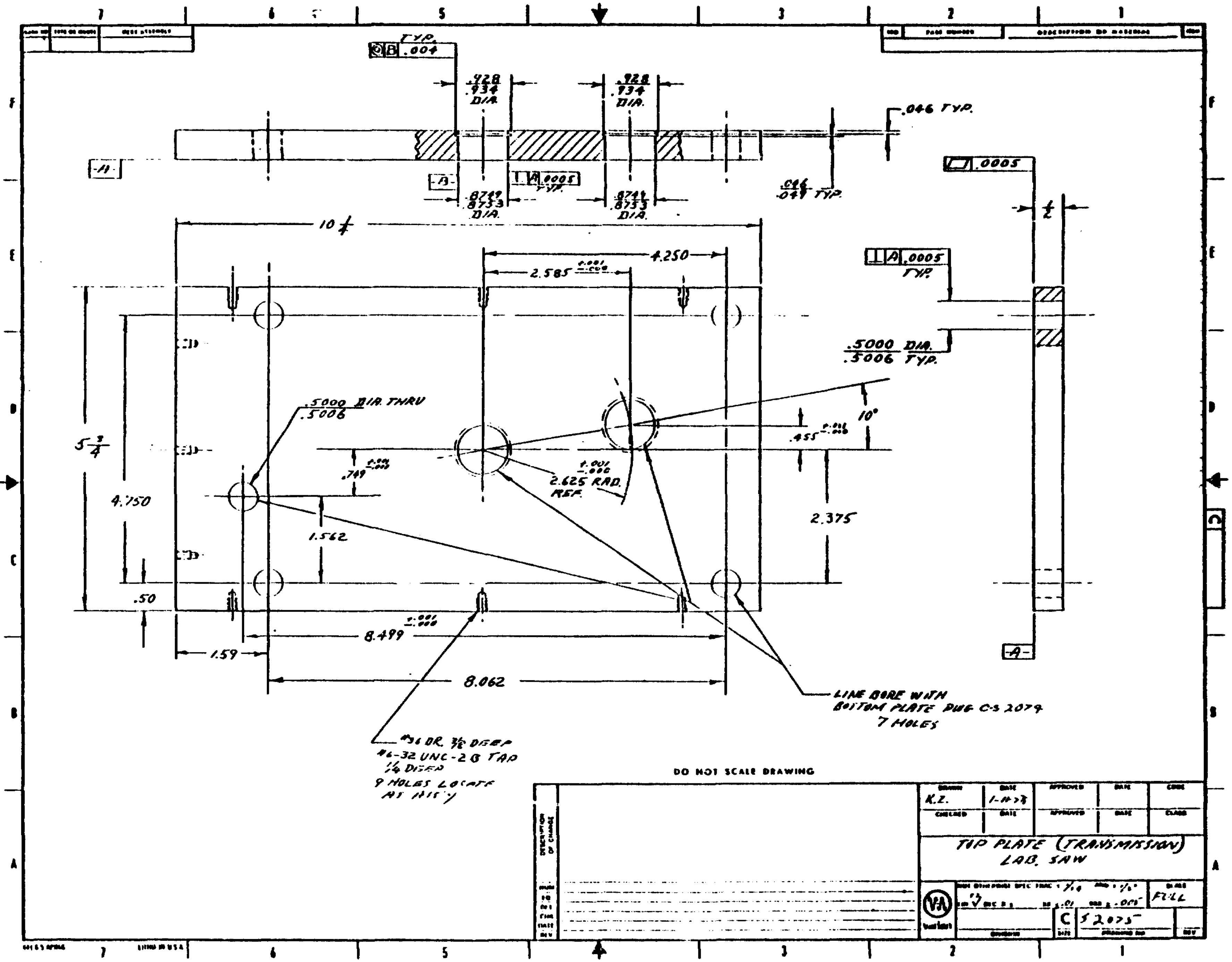

.004 TYP.
.928
.934
DIA.
.046 TYP.
.0005
.8749
.8753
DIA.
.046
.047 TYP.
10 1/4
4.250
2.585
.0005 TYP.
.5000 DIA.
.5006 TYP.
.5000 DIA. THRU
.5006
10°
.455
5 3/4
.749
2.625 RAD. REF.
4.750
1.562
2.375
.50
8.499
1.59
8.062
LINE BORE WITH BOTTOM PLATE DWG C-S 2079
7 HOLES
#36 DR. 3/8 DEEP
#6-32 UNC-2B TAP
1/4 DEEP
9 HOLES LOCATE AT ASS'Y
DO NOT SCALE DRAWING
K.Z.
1-11-73
TIP PLATE (TRANSMISSION)
LAB. SAW
FULL
C
52075

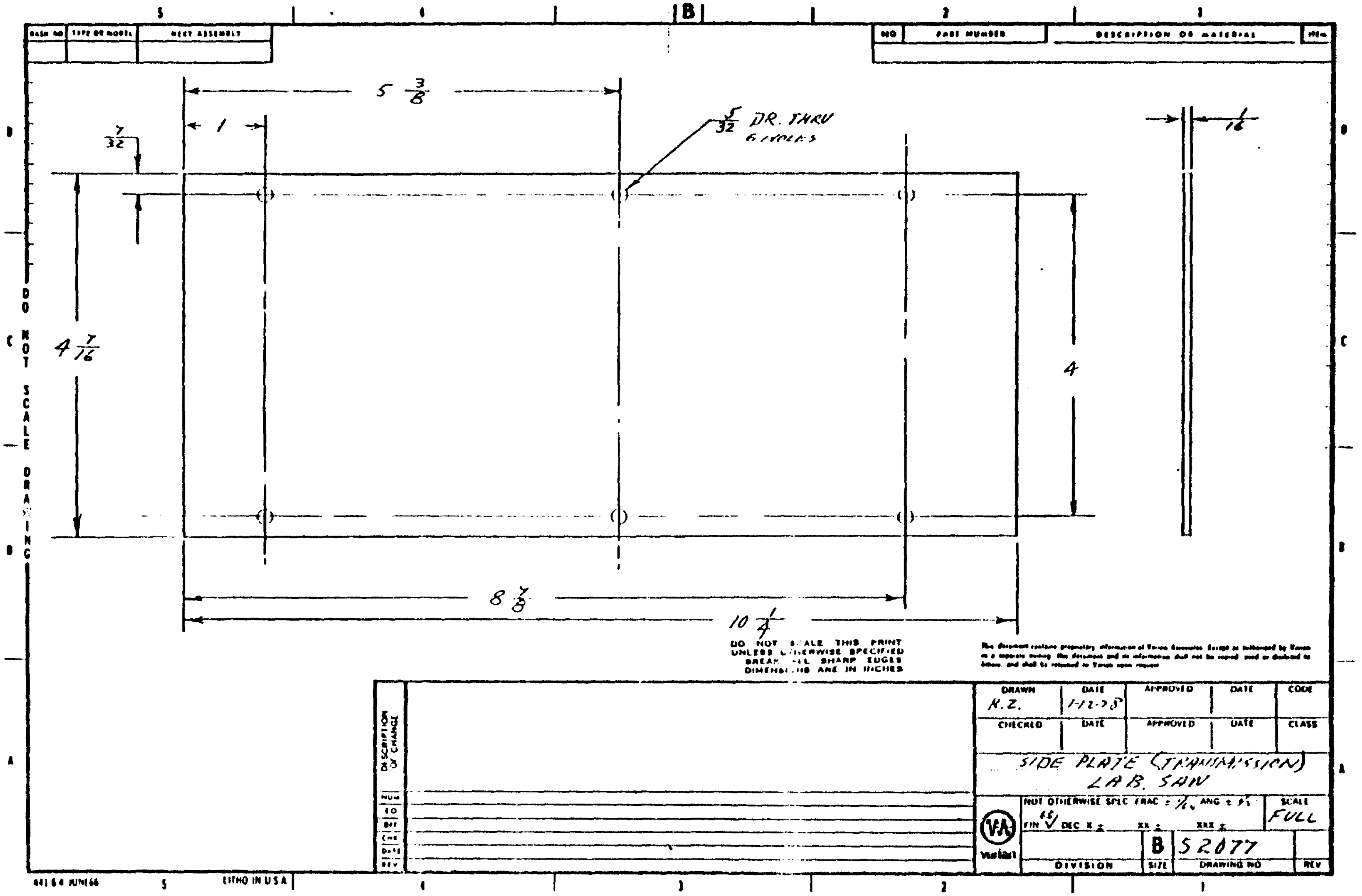

DASH NO
TYPE OR MODEL
NEXT ASSEMBLY
NO
PART NUMBER
DESCRIPTION OF MATERIAL
ITEM
5 3/8
1
7/32
5/32 DR. THRU
6 HOLES
1/16
4 7/16
4
8 7/8
10 1/4
DO NOT SCALE DRAWING
DO NOT SCALE THIS PRINT
UNLESS OTHERWISE SPECIFIED
BREAK ALL SHARP EDGES
DIMENSIONS ARE IN INCHES
DESCRIPTION OF CHANGE
NUM
DRAWN
N.Z.
DATE
1-12-78
CHECKED
DATE
APPROVED
DATE
APPROVED
DATE
CODE
CLASS
SIDE PLATE (TRANSMISSION)
LAB. SAW
NOT OTHERWISE SPEC FRAC ± 1/64 ANG ± 1/2°
FIN 63 DEC X ± XX ± XXX ±
SCALE
FULL
Varian
DIVISION
SIZE
B
DRAWING NO
52077
REV
44164 JUN66
LITHO IN U S A

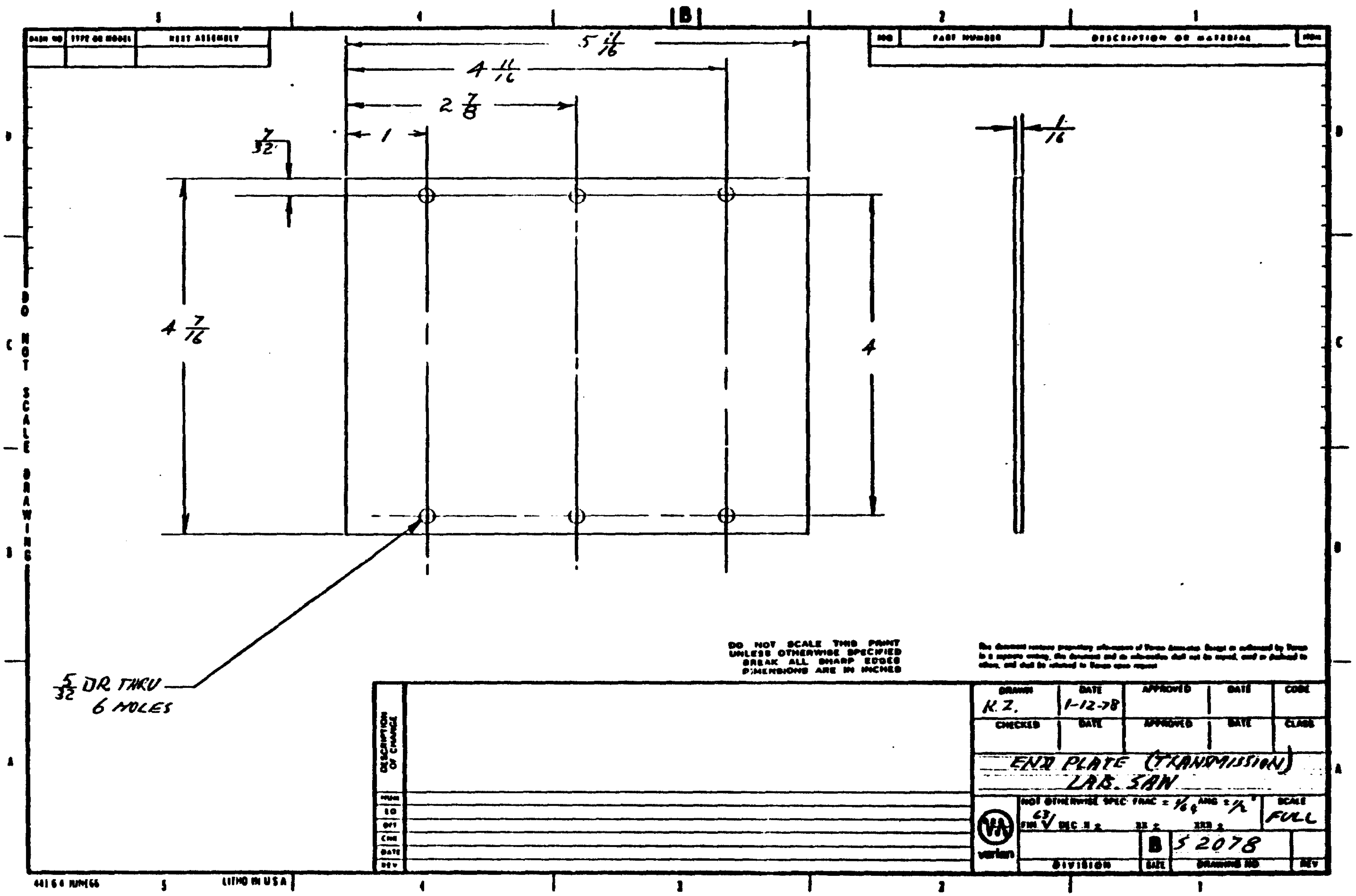
5 11/16
4 11/16
2 7/8
1
7/32
1/16
4 7/16
4
5/32 DR THRU
6 HOLES
DO NOT SCALE DRAWING
DO NOT SCALE THIS PRINT
UNLESS OTHERWISE SPECIFIED
BREAK ALL SHARP EDGES
DIMENSIONS ARE IN INCHES
DRAWN K.Z.
DATE 1-12-78
CHECKED
APPROVED
END PLATE (TRANSMISSION)
LAB. SAW
SCALE FULL
B 52078
varian
LITHO IN U.S.A.

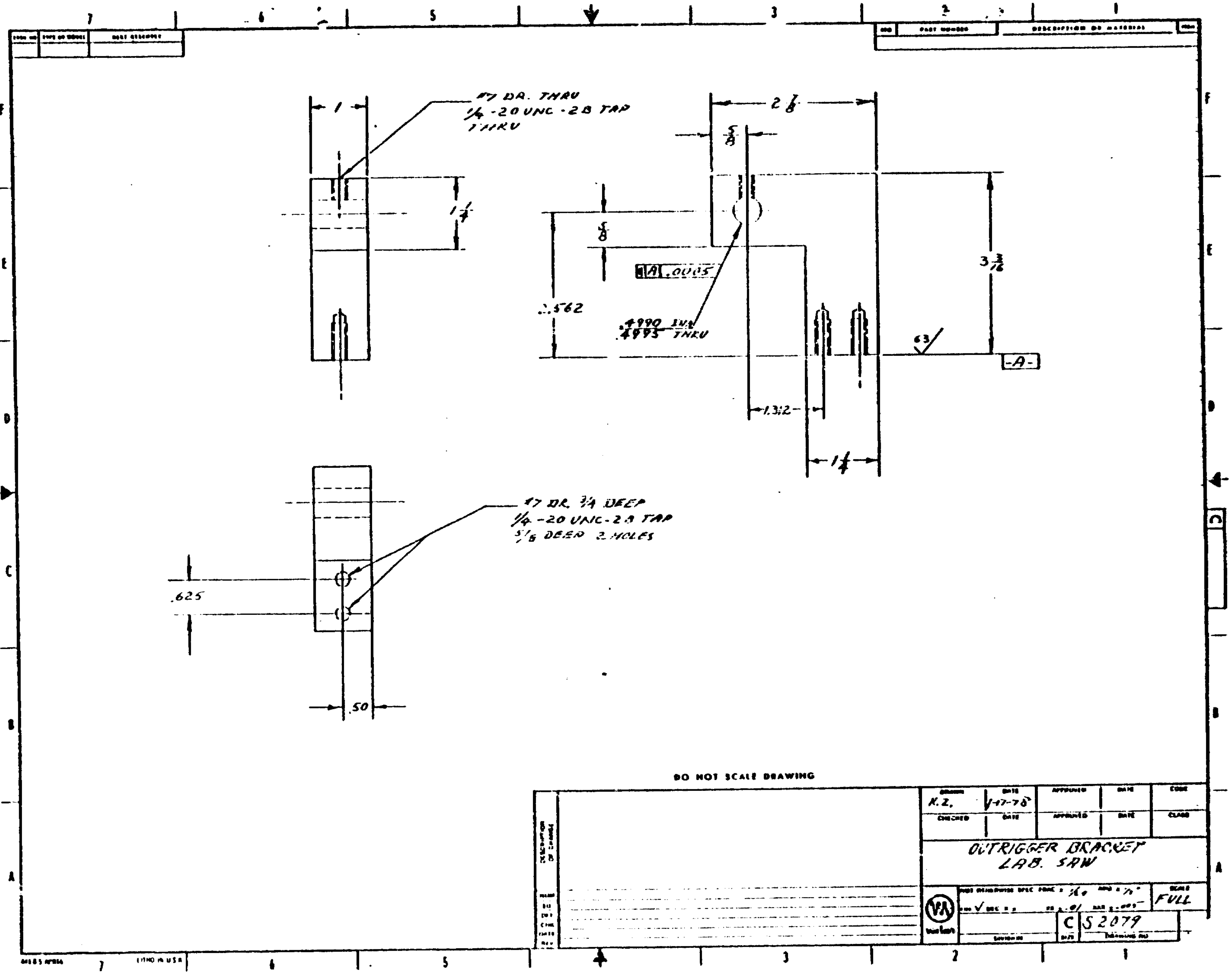
#7 DR. THRU
1/4-20 UNC-2B TAP
THRU
#7 DR. 3/4 DEEP
1/4-20 UNC-2B TAP
5/8 DEEP 2 HOLES
1
1 1/4
2 7/8
5/8
3 3/16
.4990
.4995 THRU
A .0005
-A-
63
.562
1.312
.625
.50
DO NOT SCALE DRAWING
K.Z.
OUTRIGGER BRACKET
LAB. SAW
FULL
C
S 2079

DASH NO.	TYPE OR MODEL	NEXT ASSEMBLY	REQ	PART NUMBER	DESCRIPTION OR MATERIAL	ITEM

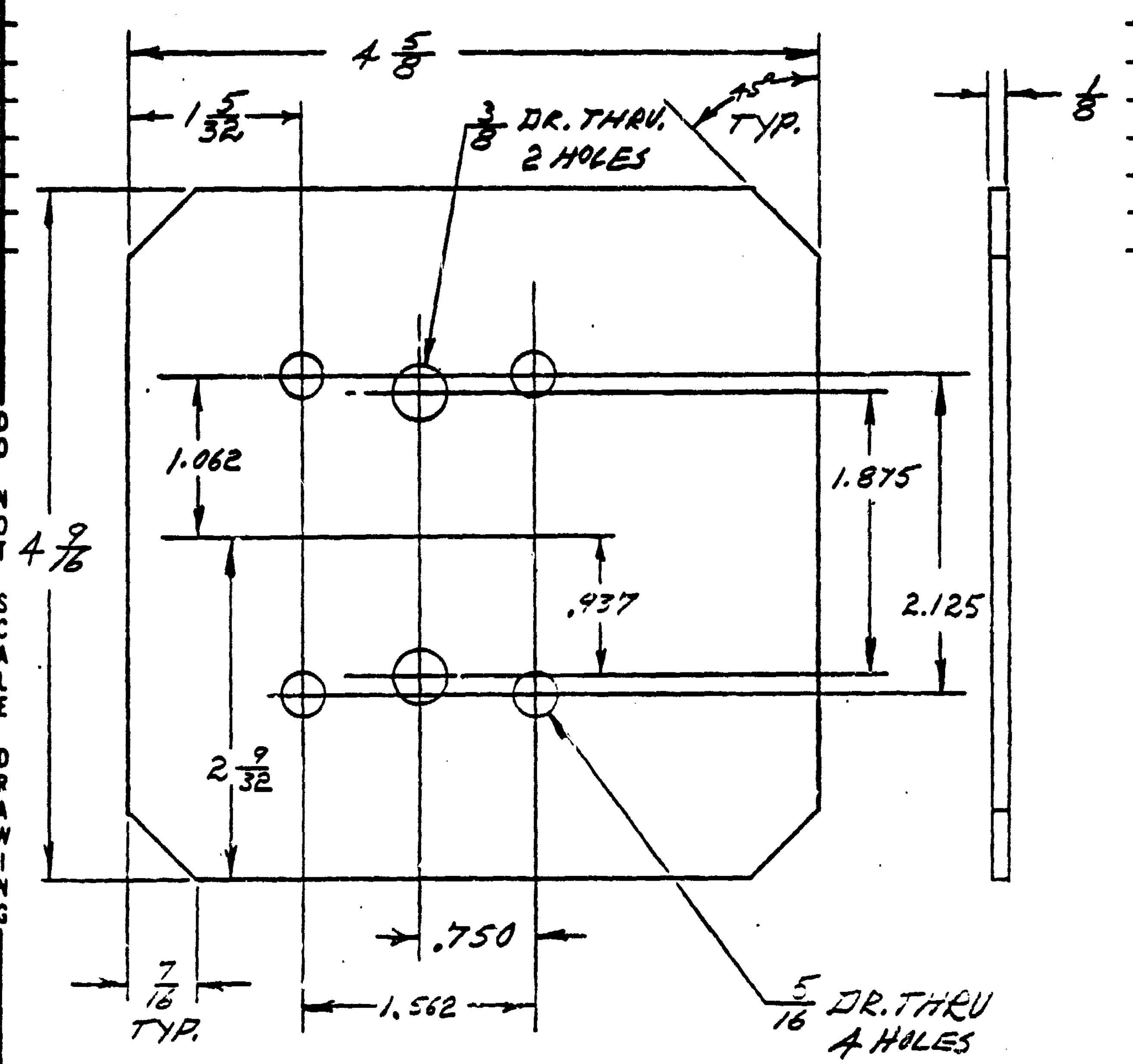

A

DO NOT SCALE DRAWING

DO NOT SCALE THIS PRINT
UNLESS OTHERWISE SPECIFIED
BREAK ALL SHARP EDGES
DIMENSIONS ARE IN INCHES

DRAWN	DATE	APPROVED	DATE	CODE
K.Z.	1-27-78			
CHECKED	DATE	APPROVED	DATE	CLASS

FOOD HOLDER
LAB. SAW

NOT OTHERWISE SPEC: FRAC = ±1/64 ANG = ±1/2° SCALE FULL
FIN ✓ DEC X = XX = ±.01 XXX = ±.005

varian

DIVISION	SIZE	DRAWING NO.	REV
	A	S 2084	

DESCRIPTION OF CHANGE

NUM
EO
DFT
CHK
DATE
REV

LITHO IN U.S.A.

DASH NO.	TYPE OR MODEL	NEXT ASSEMBLY	REQ	PART NUMBER	DESCRIPTION OR MATERIAL	ITEM

A

DO NOT SCALE DRAWING

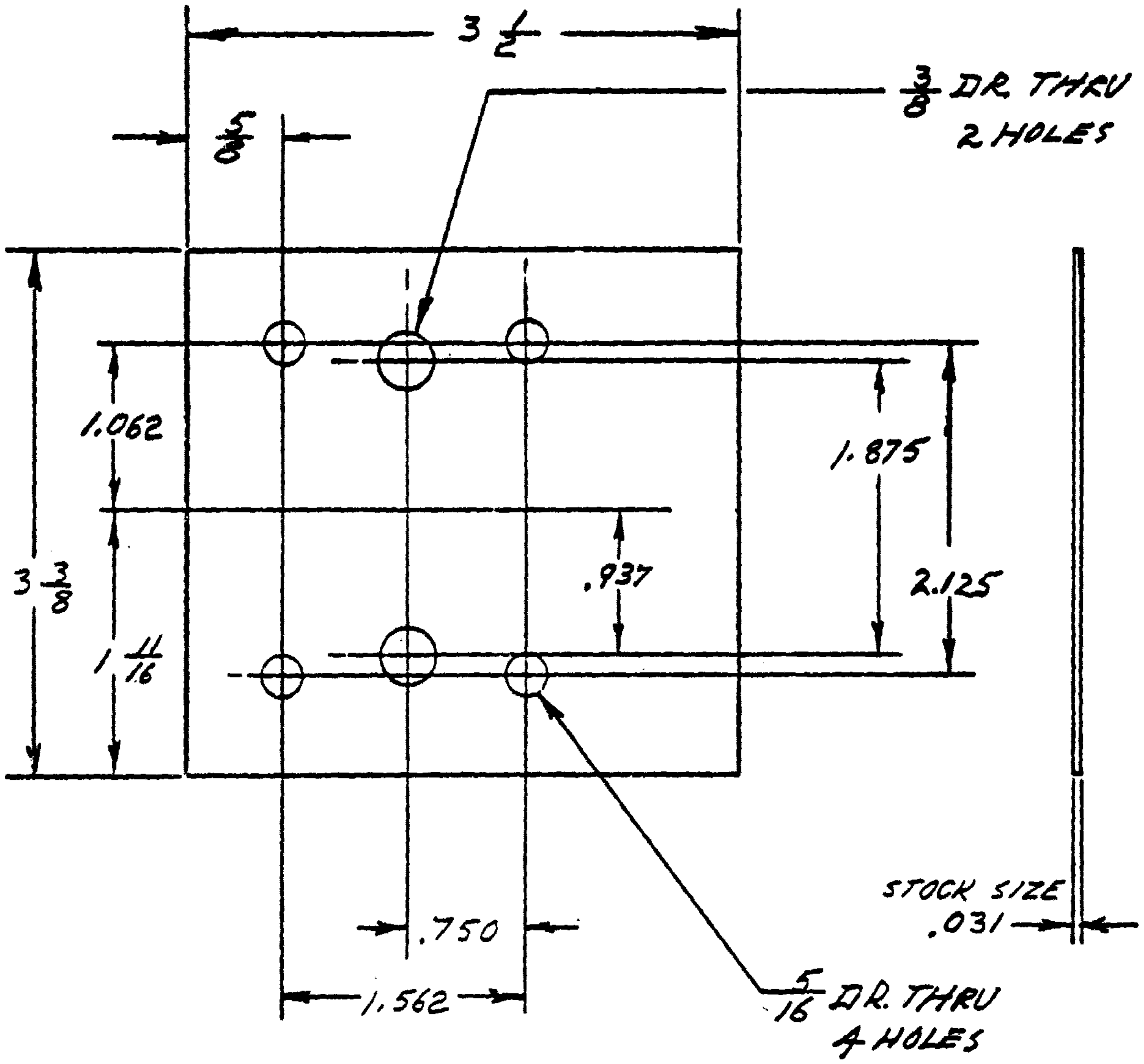

DO NOT SCALE THIS PRINT
UNLESS OTHERWISE SPECIFIED
BREAK ALL SHARP EDGES
DIMENSIONS ARE IN INCHES

DRAWN	DATE	APPROVED	DATE	CODE
K.Z.	1-27-78			
CHECKED	DATE	APPROVED	DATE	CLASS

HOOD HOLDER SPACER
LAB. SAW

NOT OTHERWISE SPEC FRAC ± 1/64 ANG ± 1/2° SCALE FULL
FIN √ DEC .X ± .01 .XX ± .01 .XXX ± .005

varian

DIVISION	SIZE	DRAWING NO.	REV
	A	52085	

DESCRIPTION OF CHANGE

NUM	
EO	
DFT	
CHK	
DATE	
REV	

PRINTED IN U.S.A.

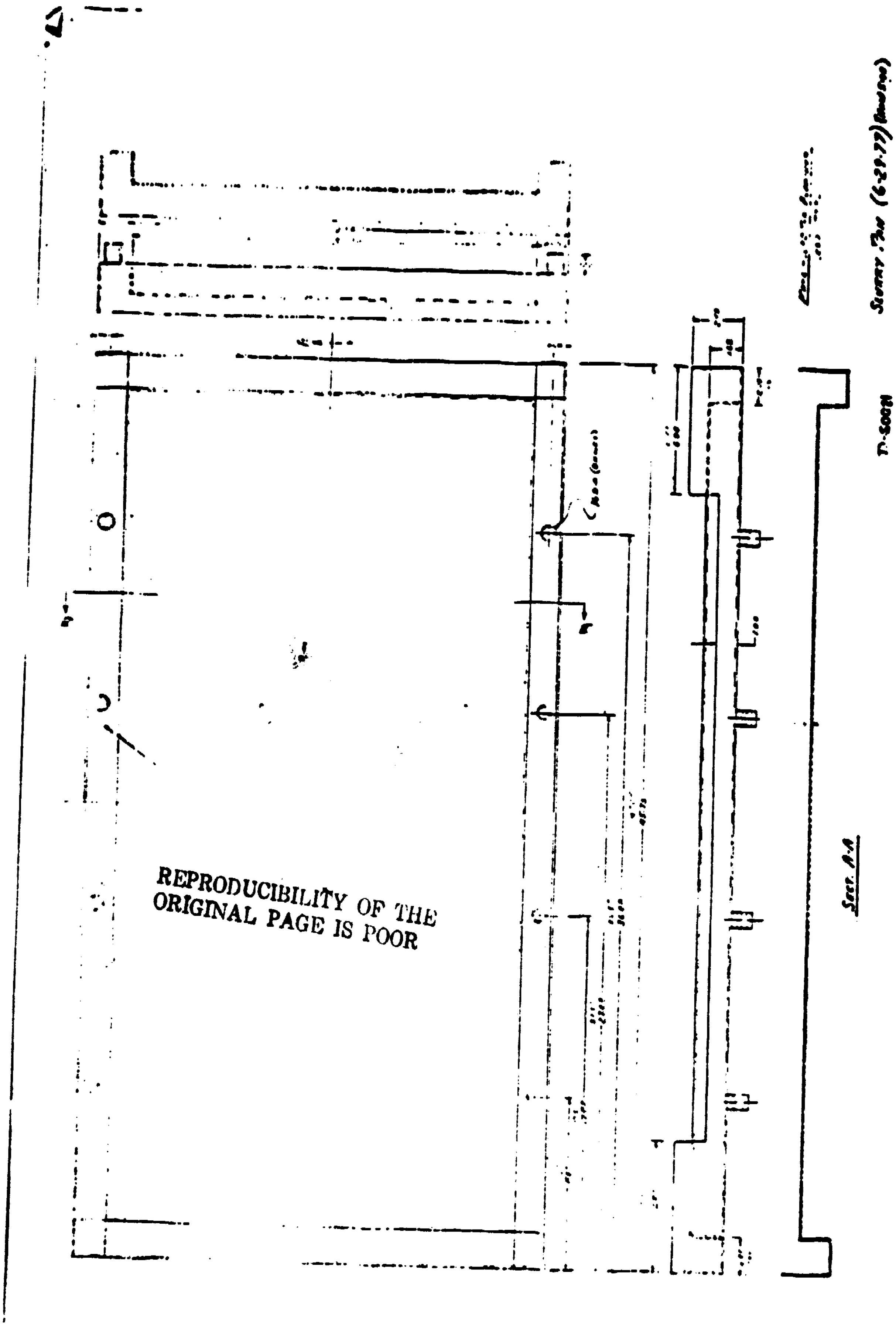
SECT. A-A

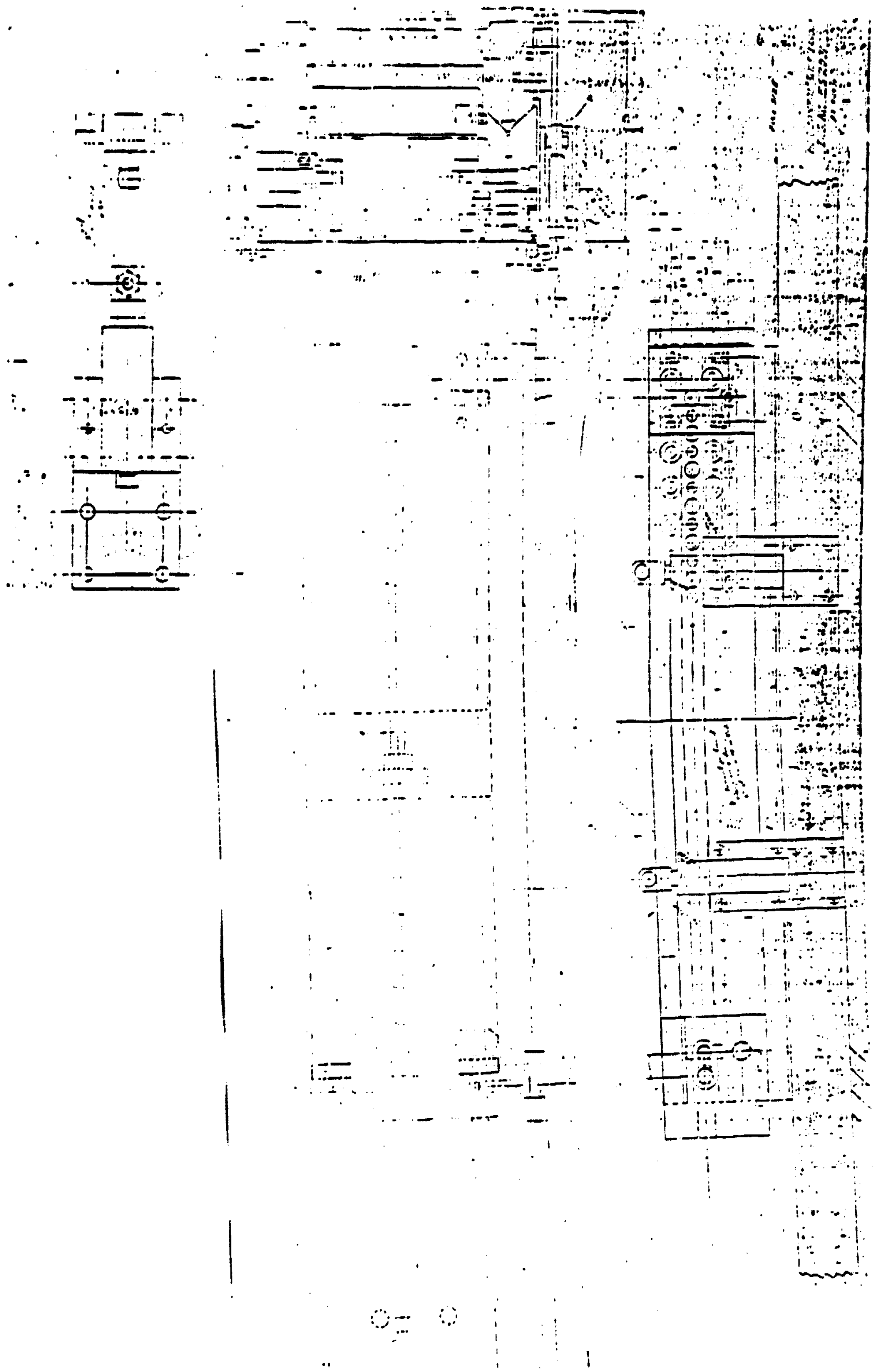

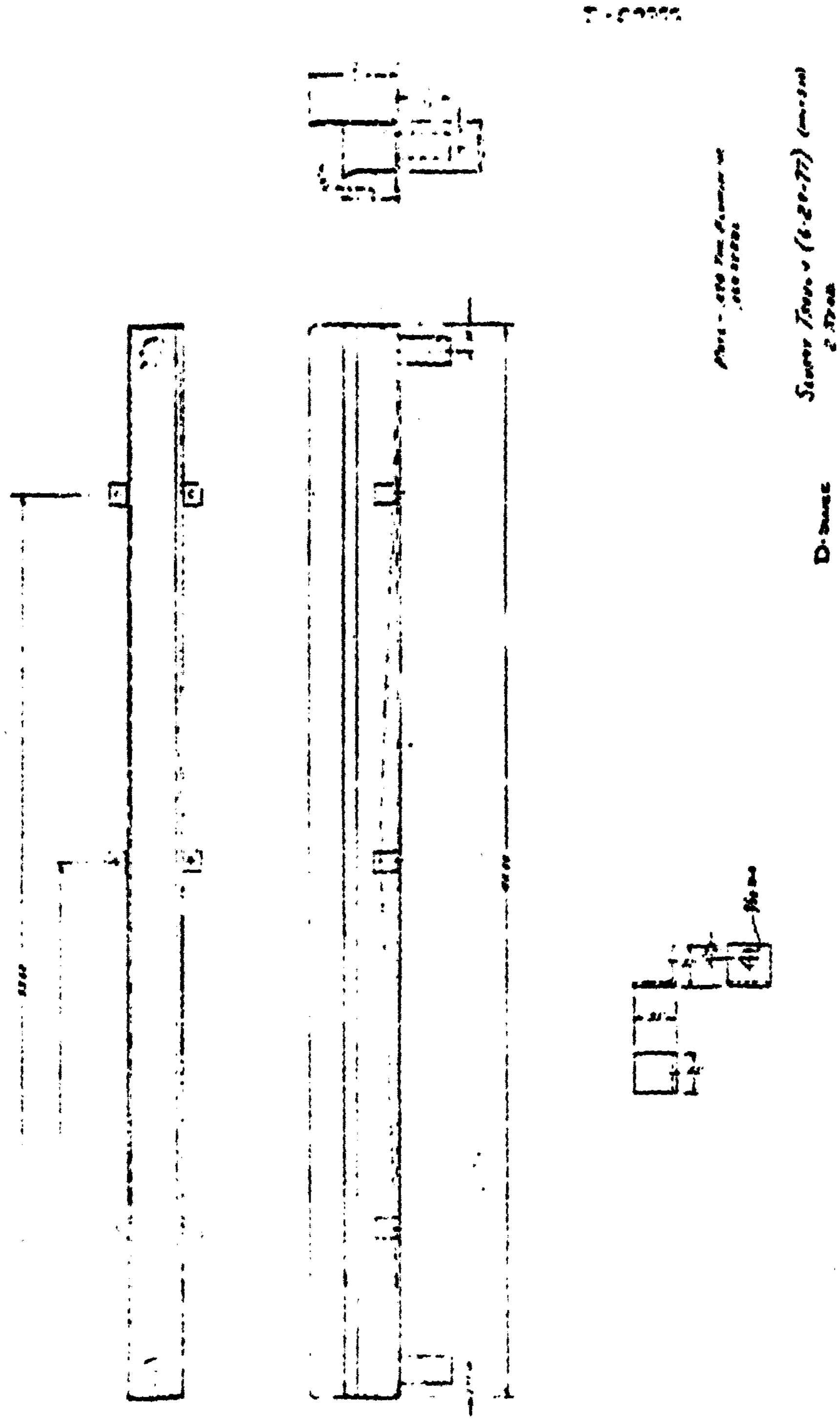

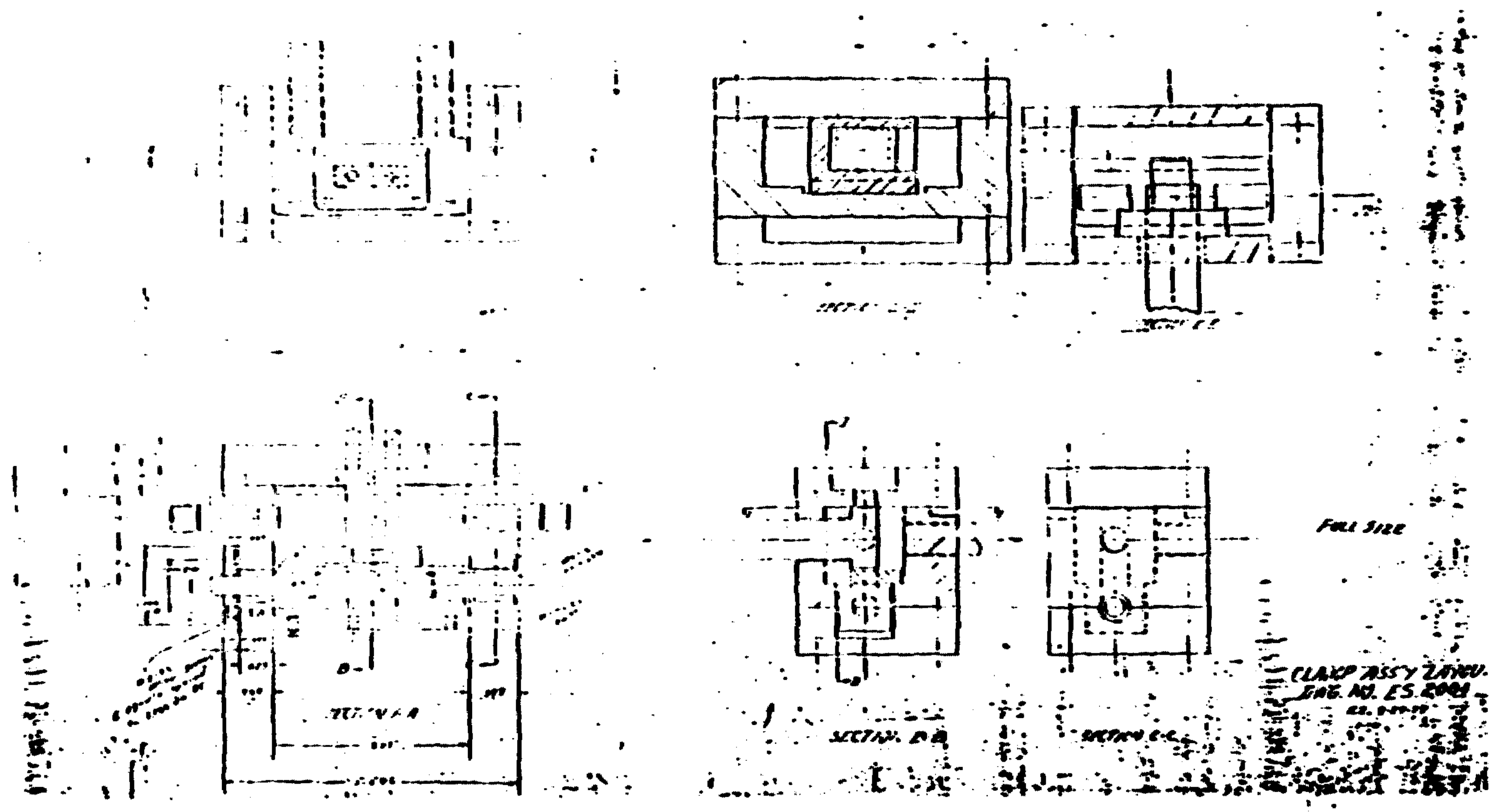
SECTION B-B
SECTION C-C
FULL SIZE
CLAMP ASS'Y LAYOU.
ENG. NO. ES 2001

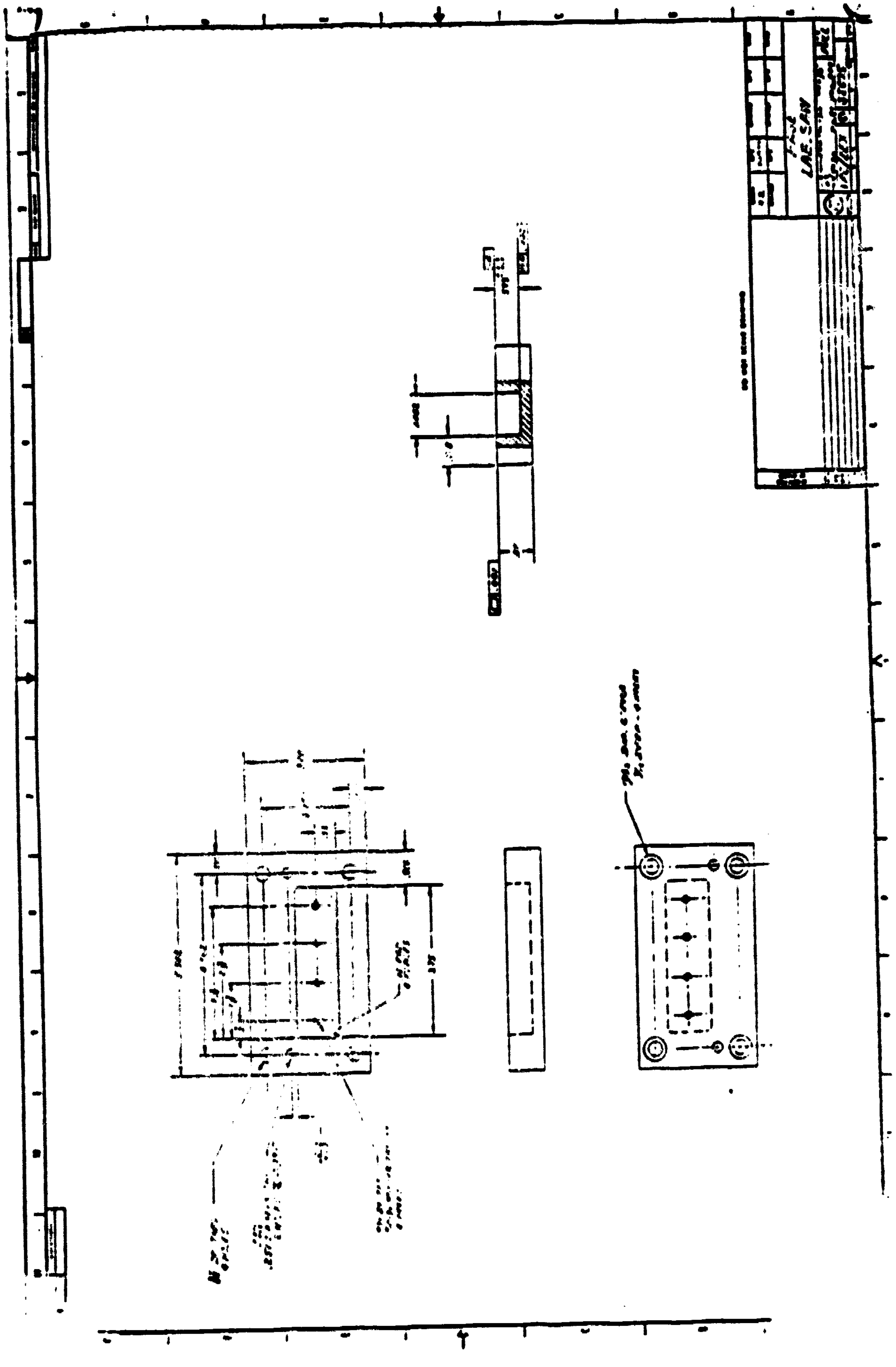

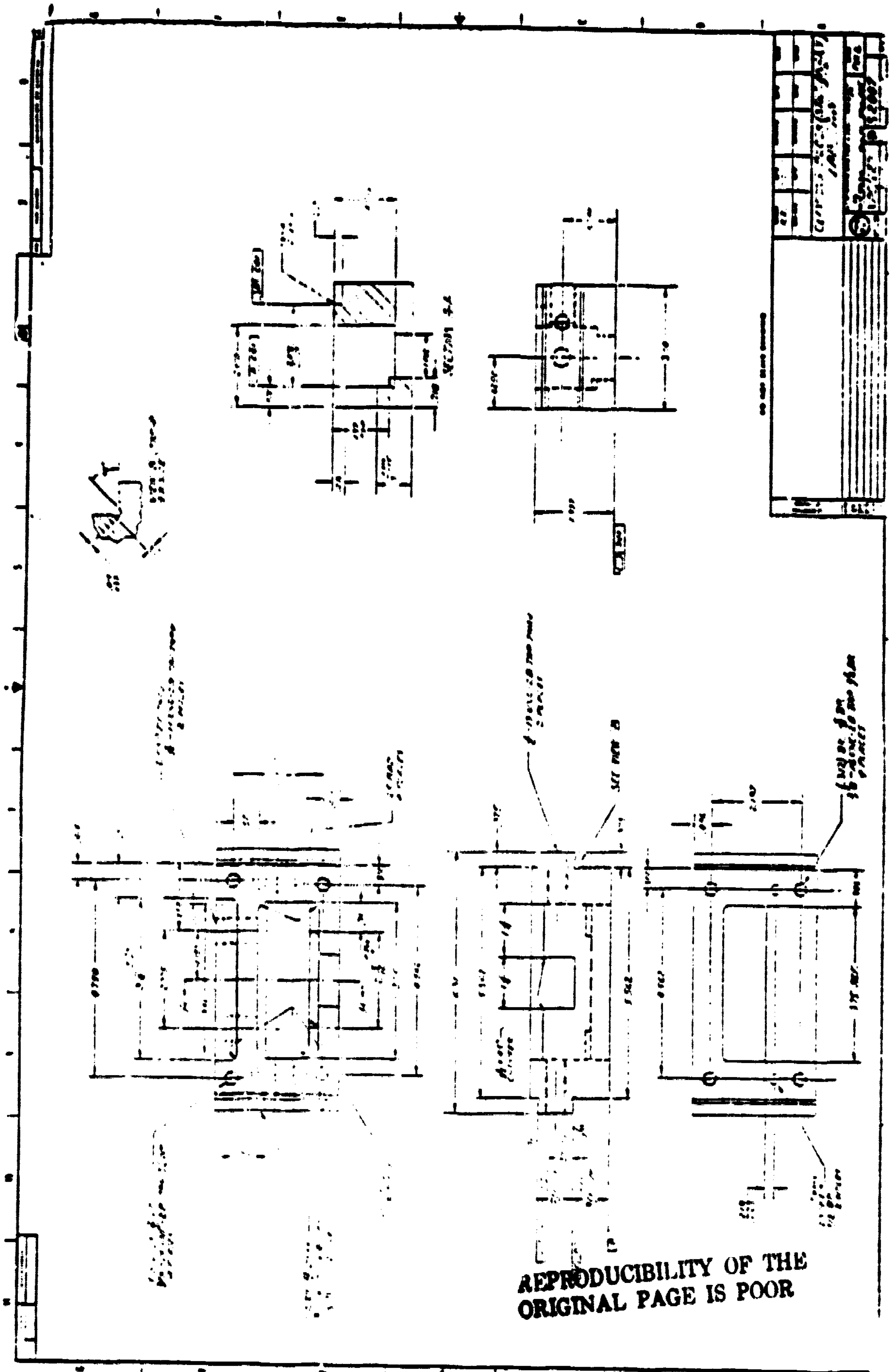

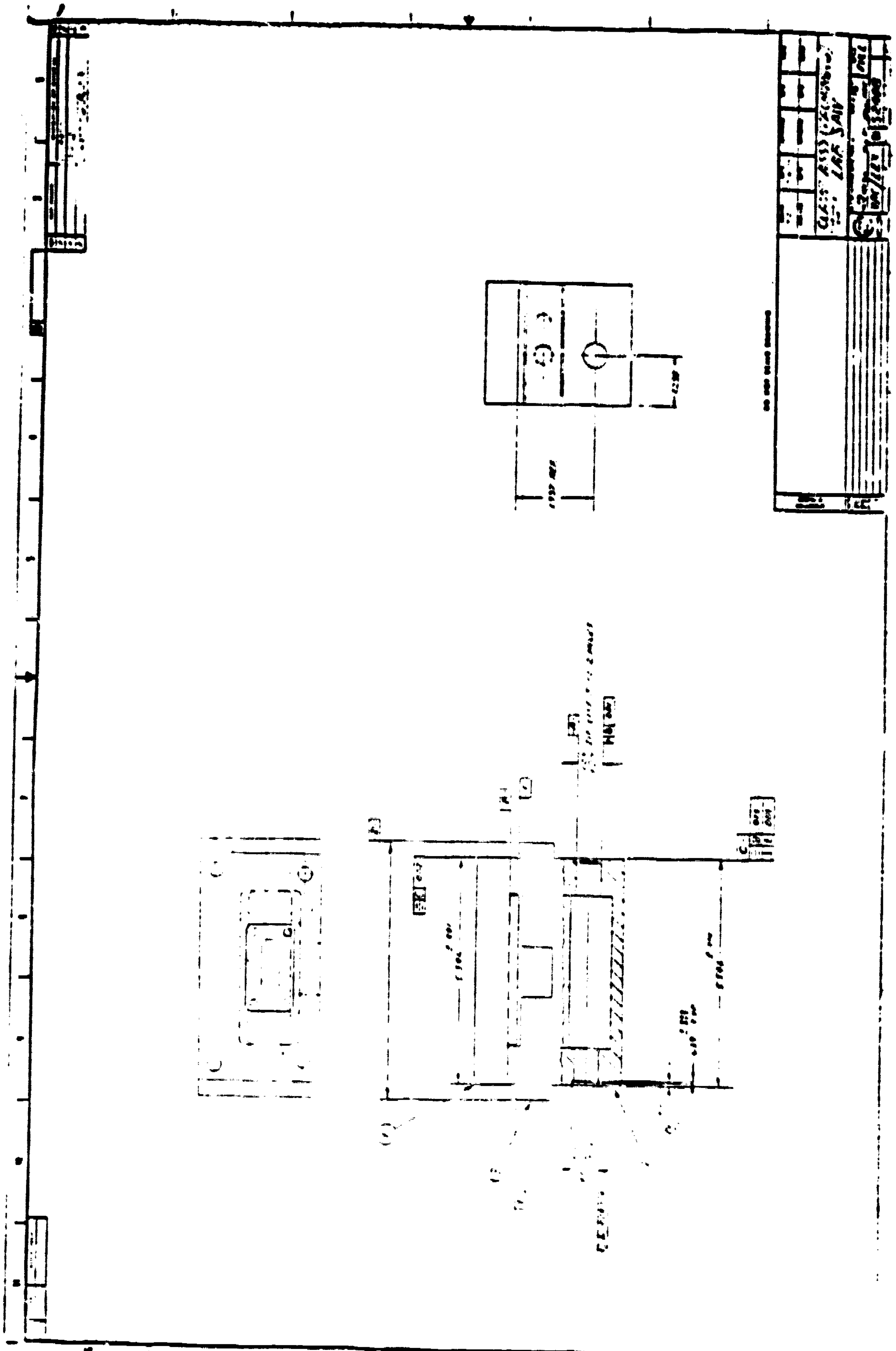

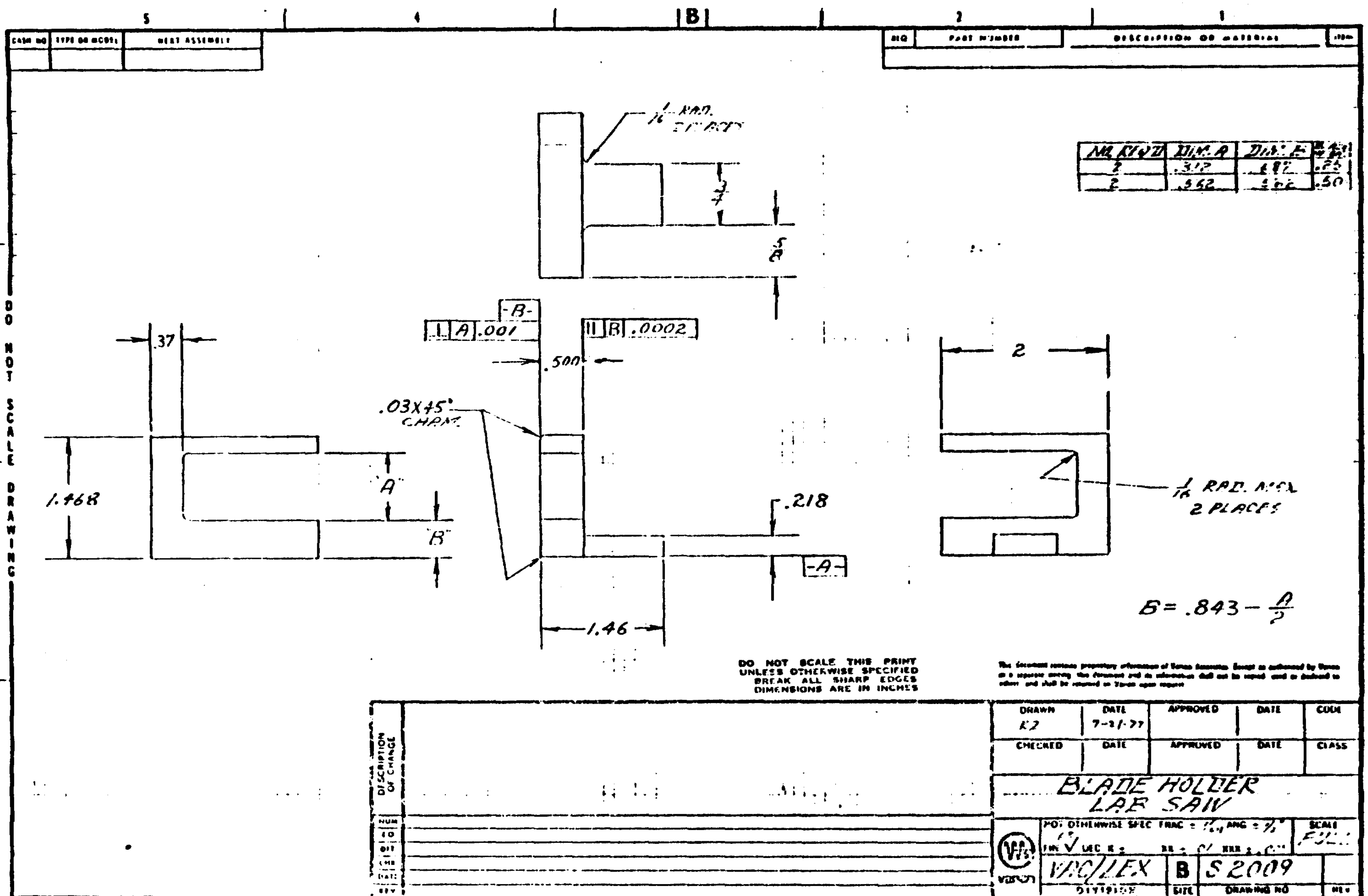
DO NOT SCALE DRAWING
NEXT ASSEMBLY
PART NUMBER
DESCRIPTION OF MATERIAL
1/16 RAD.
3/4
5/8
-B-
A .001
B .0002
.37
.500
.03X45° CHAM.
1.468
"A"
"B"
.218
-A-
1.46
2
1/16 RAD. MAX
2 PLACES
B = .843 - A/2
DO NOT SCALE THIS PRINT UNLESS OTHERWISE SPECIFIED BREAK ALL SHARP EDGES DIMENSIONS ARE IN INCHES
DRAWN
K2
DATE
7-21-77
APPROVED
DATE
CODE
CHECKED
DATE
APPROVED
DATE
CLASS
DESCRIPTION OF CHANGE
BLADE HOLDER
LAB SAW
B
S 2009
SIZE
DRAWING NO

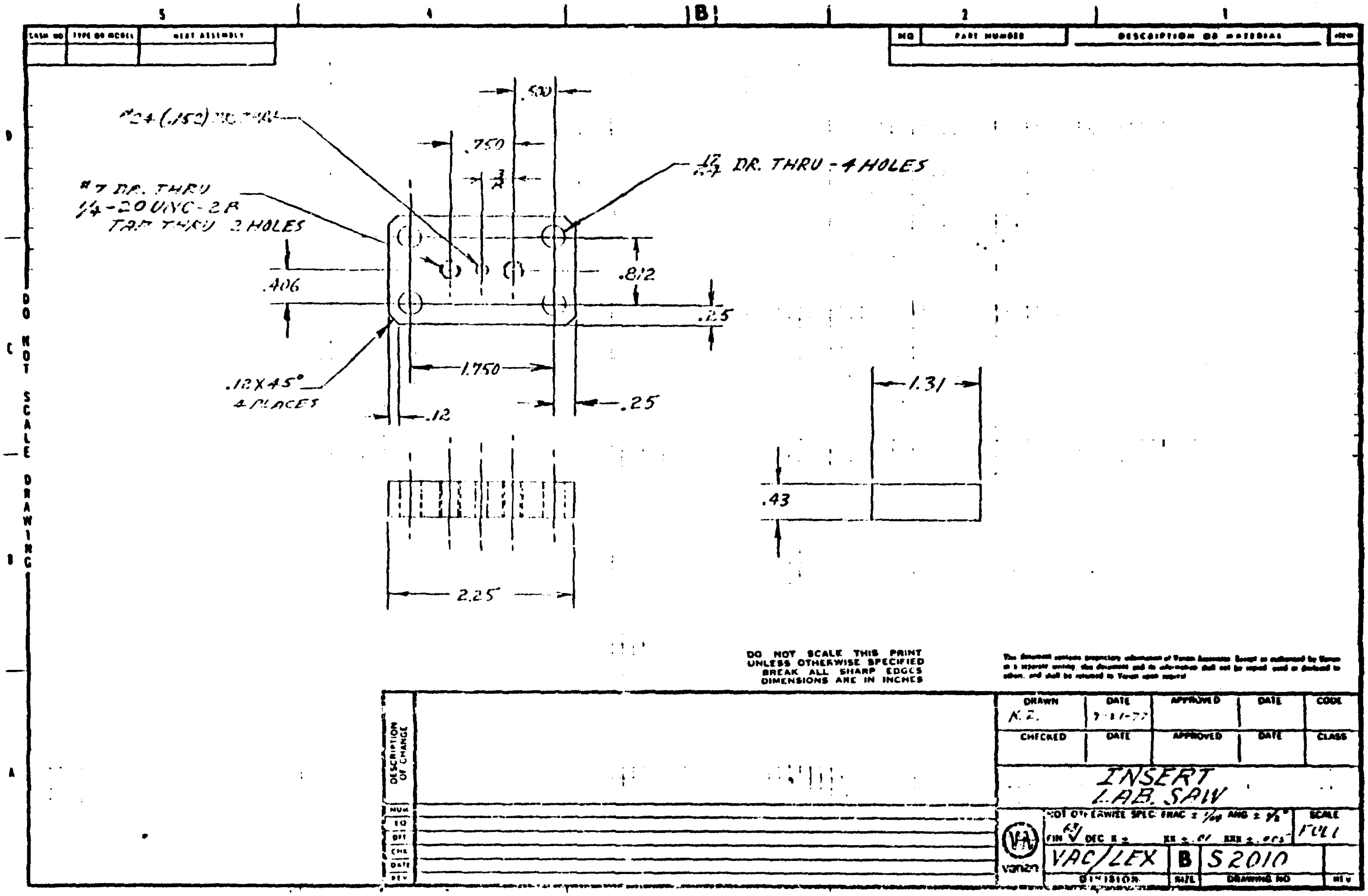

#24 (.152) DR. THRU
#7 DR. THRU
1/4-20 UNC-2B
TAP THRU 2 HOLES
DR. THRU - 4 HOLES
.500
.750
.812
.406
.25
1.750
.12 X 45°
4 PLACES
.12
.25
1.31
.43
2.25
DO NOT SCALE DRAWING
DO NOT SCALE THIS PRINT
UNLESS OTHERWISE SPECIFIED
BREAK ALL SHARP EDGES
DIMENSIONS ARE IN INCHES
DESCRIPTION OF CHANGE
DRAWN
K.Z.
DATE
CHECKED
APPROVED
CODE
CLASS
INSERT
LAB. SAW
SCALE
FULL
VAC/LEX
B
S2010
DIVISION
DRAWING NO
varian

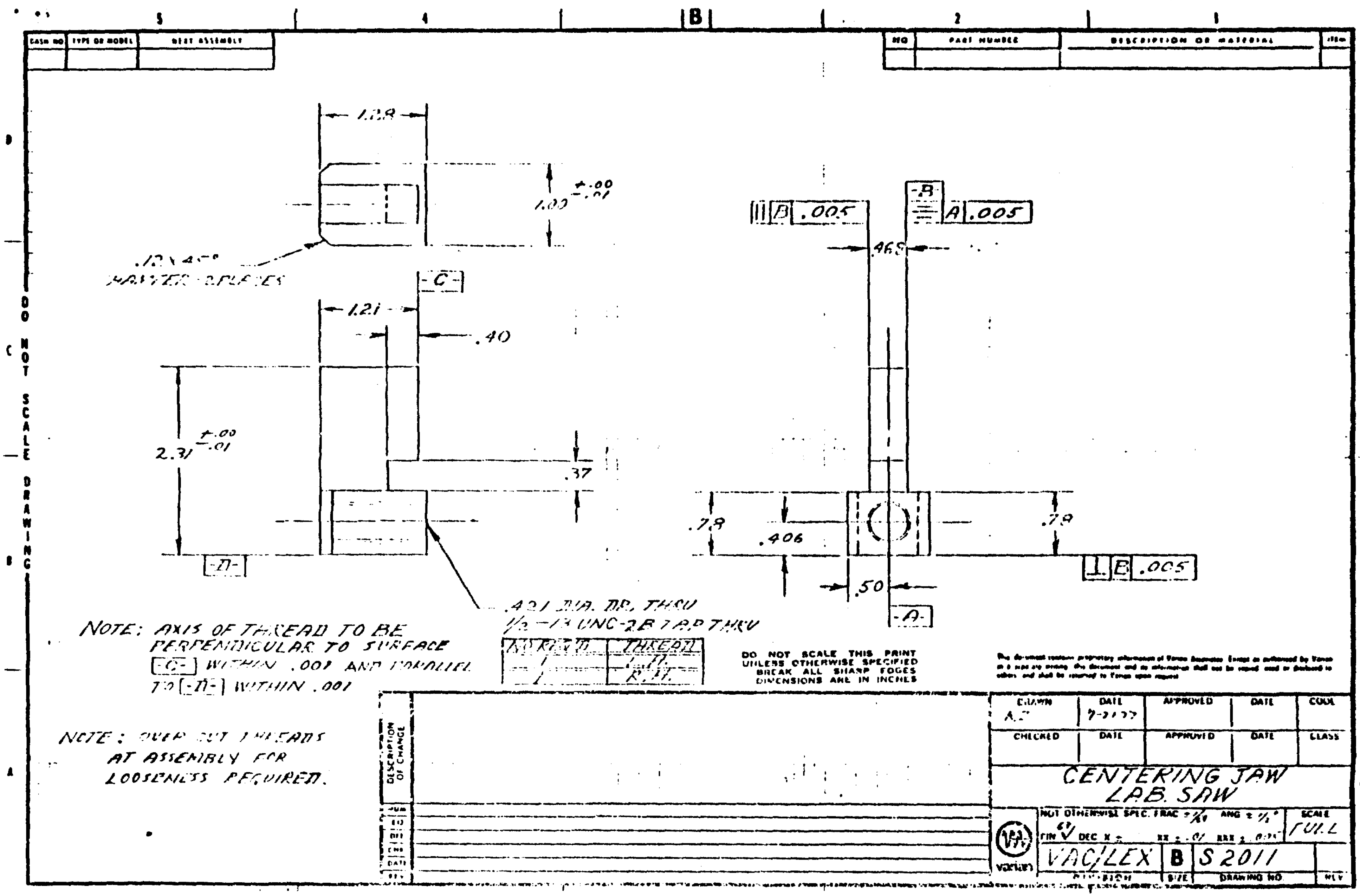

1.28
1.00 +.00 -.01
.12 x 45° CHAMFER 2 PLACES
-C-
1.21
.40
2.31 +.00 -.01
.37
-D-
.421 DIA. DR. THRU
1/2-13 UNC-2B TAP THRU
NOTE: AXIS OF THREAD TO BE PERPENDICULAR TO SURFACE -C- WITHIN .001 AND PARALLEL TO -D- WITHIN .001
NOTE: OVER CUT THREADS AT ASSEMBLY FOR LOOSENESS REQUIRED.
-B-
B .005
A .005
.469
.78
.406
.78
.50
-A-
B .005
DO NOT SCALE THIS PRINT UNLESS OTHERWISE SPECIFIED BREAK ALL SHARP EDGES DIMENSIONS ARE IN INCHES
DRAWN
DATE
APPROVED
DATE
CODE
CHECKED
DATE
APPROVED
DATE
CLASS
CENTERING JAW LAB. SAW
SCALE FULL
VAC/LEX
B
S 2011
DRAWING NO.
SIZE
REV
DESCRIPTION OF CHANGE
NO
PART NUMBER
DESCRIPTION OF MATERIAL
ITEM
DASH NO
TYPE OR MODEL
NEXT ASSEMBLY
DO NOT SCALE DRAWING
varian

DASH NO	TYPE OR MODEL	NEXT ASSEMBLY

NO	PART NUMBER	DESCRIPTION OR MATERIAL	ITEM

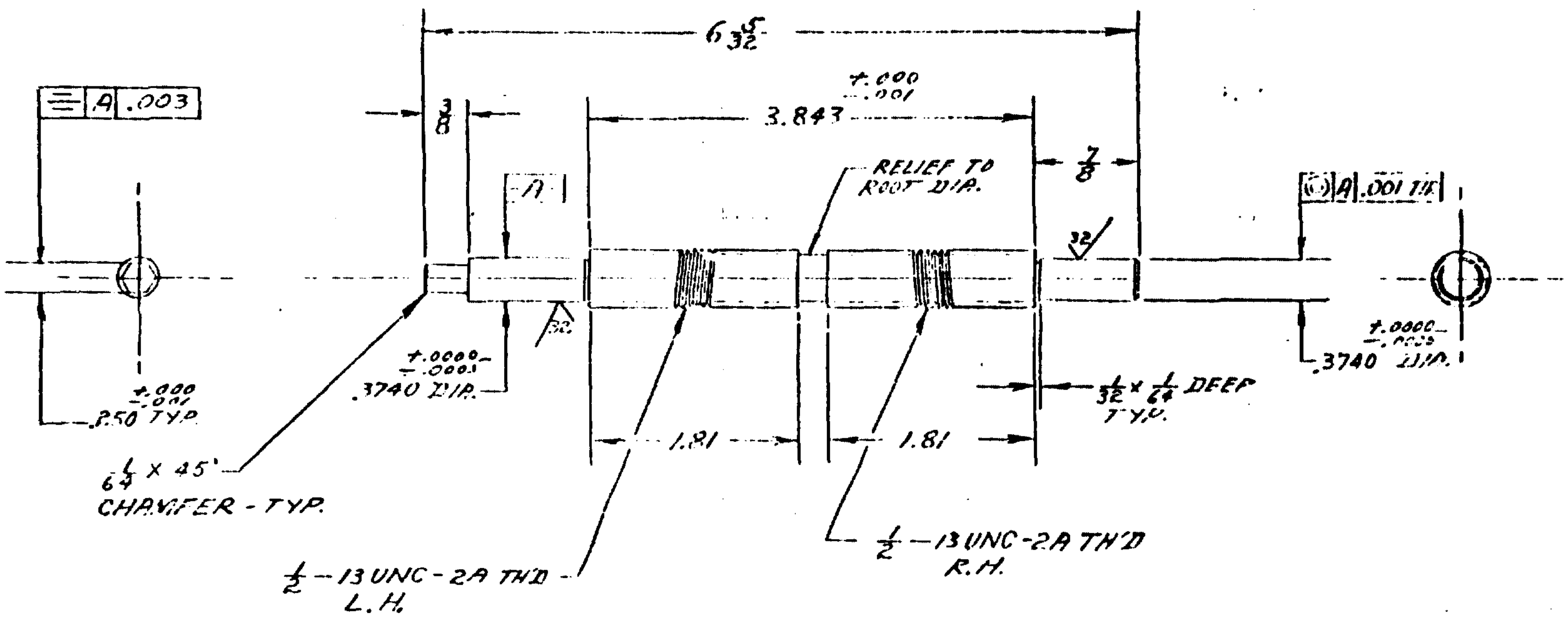

NOTE: PITCH DIA. OF THREADS TO BE CONCENTRIC WITH -A- WITHIN .002 TIR

DO NOT SCALE DRAWING

DO NOT SCALE THIS PRINT
UNLESS OTHERWISE SPECIFIED
BREAK ALL SHARP EDGES
DIMENSIONS ARE IN INCHES

DESCRIPTION OF CHANGE

DRAWN	DATE	APPROVED	DATE	CODE
K.T.	7-11-72			
CHECKED	DATE	APPROVED	DATE	CLASS

CENTERING SCREW
LAB. SAW

NOT OTHERWISE SPEC. FRAC ± 1/64 ANG ± 1/2° — SCALE FULL

VAC/LEX — DIVISION | B — SIZE | S 2012 — DRAWING NO | REV

DASH NO.	TYPE OR MODEL	NEXT ASSEMBLY	REQ	PART NUMBER	DESCRIPTION OR MATERIAL	ITEM

A

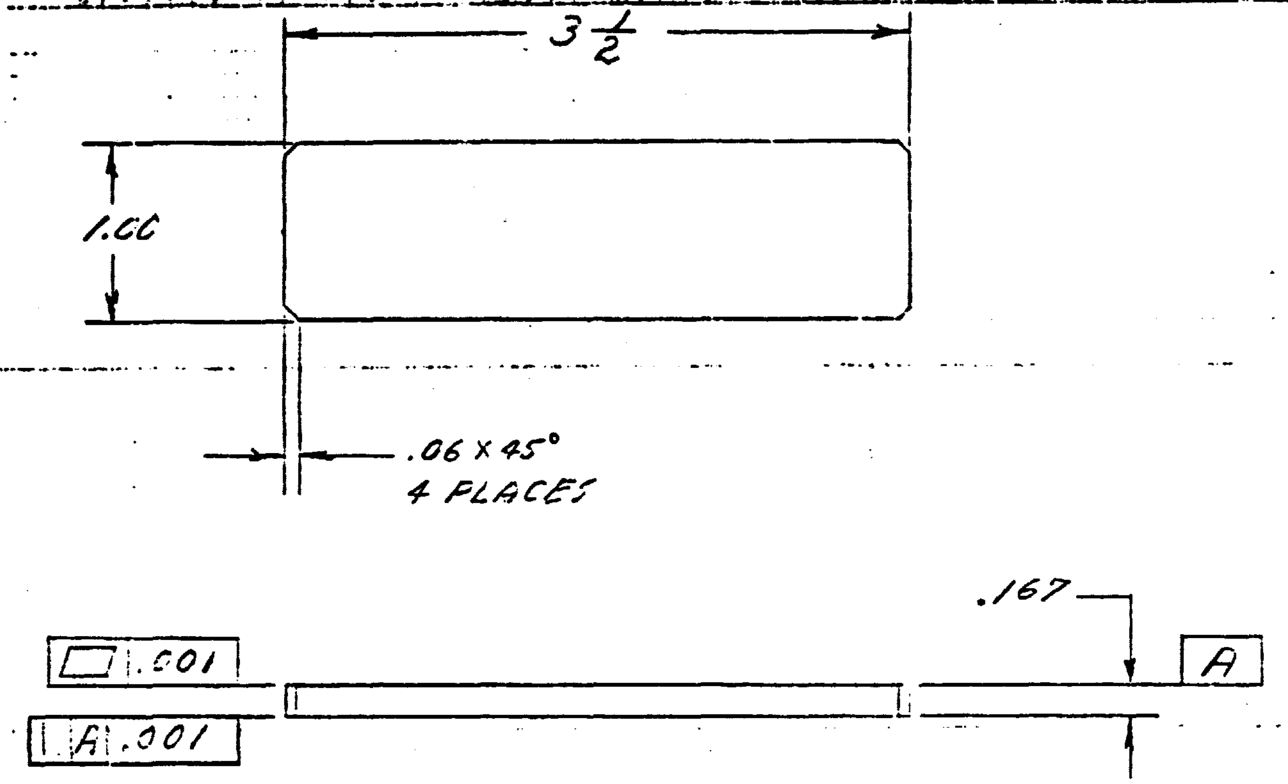

DO NOT SCALE DRAWING

DO NOT SCALE THIS PRINT
UNLESS OTHERWISE SPECIFIED
BREAK ALL SHARP EDGES
DIMENSIONS ARE IN INCHES

DESCRIPTION OF CHANGE	
NUM	
EO	
DFT	
CHK	
DATE	
REV	

DRAWN	DATE	APPROVED	DATE	CODE
K.Z.	7-21-77			
CHECKED	DATE	APPROVED	DATE	CLASS

BOTTOM GIB
LAB SAW

NOT OTHERWISE SPEC: FRAC ± 1/64 ANG ± 1/2° FIN. 63 √ DEC .X ± .XX ± .01 .XXX ± .005 | SCALE FULL

varian

DIVISION	SIZE	DRAWING NO	REV
VAC/LEX	A	S2013	

DASH NO.	TYPE OR MODEL	NEXT ASSEMBLY	REQ	PART NUMBER	DESCRIPTION OR MATERIAL	ITEM

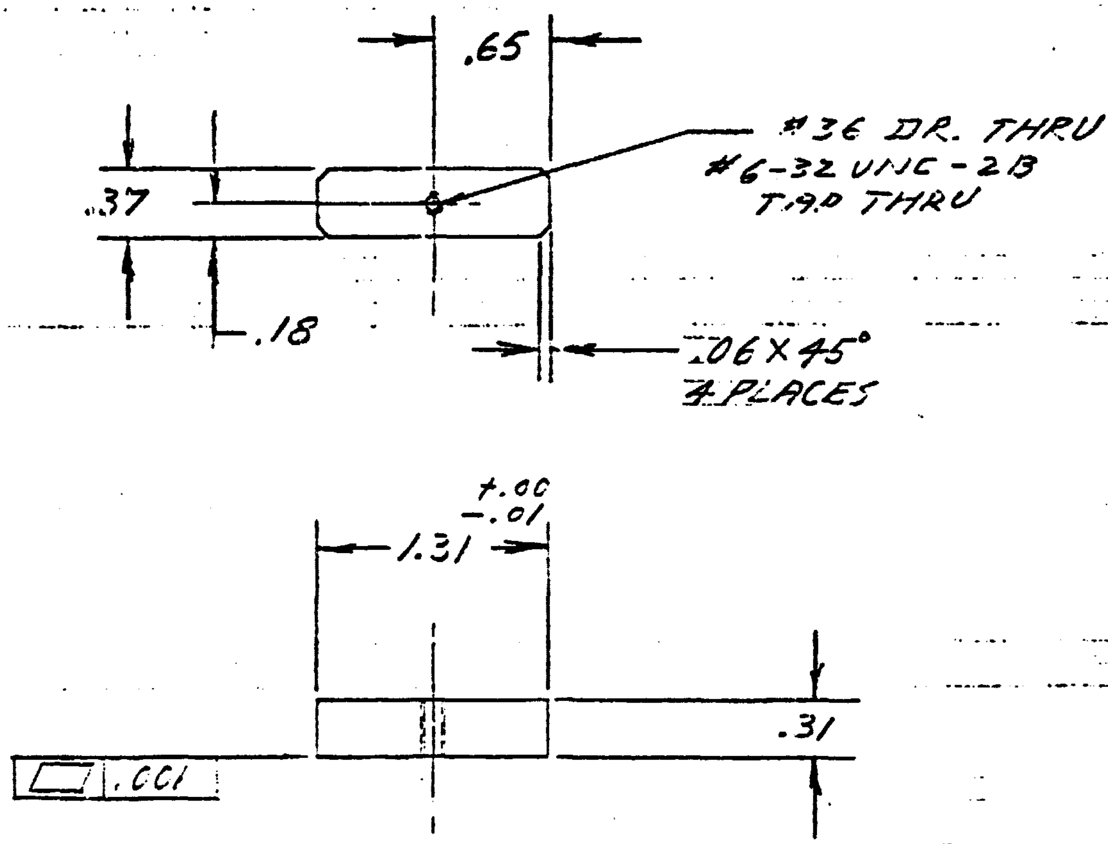

A

DO NOT SCALE DRAWING

DO NOT SCALE THIS PRINT
UNLESS OTHERWISE SPECIFIED
BREAK ALL SHARP EDGES
DIMENSIONS ARE IN INCHES

DRAWN	DATE	APPROVED	DATE	CODE
K.Z.	7-21-77			
CHECKED	DATE	APPROVED	DATE	CLASS

TOP GIB
LAB. SAW

NOT OTHERWISE SPEC: FRAC ± 1/64 ANG ± 1/2° — SCALE FULL

FIN. 63 √ DEC .X ± .XX ± .01 .XXX ± .005

varian

DIVISION	SIZE	DRAWING NO.	REV
VAC/LEX	A	S 2074	

DESCRIPTION OF CHANGE

NUM
EO
DFT
CHK
DATE
REV

DASH NO.	TYPE OR MODEL	NEXT ASSEMBLY	REQ	PART NUMBER	DESCRIPTION OR MATERIAL	ITEM

A

DO NOT SCALE DRAWING

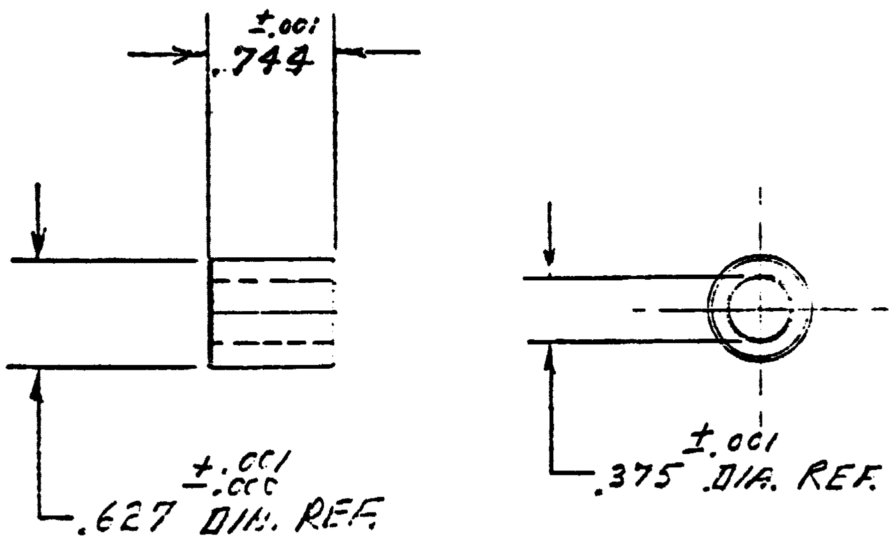

DO NOT SCALE THIS PRINT
UNLESS OTHERWISE SPECIFIED
BREAK ALL SHARP EDGES
DIMENSIONS ARE IN INCHES

DESCRIPTION OF CHANGE

NUM
EO
DFT
CHK
DATE
REV

DRAWN	DATE	APPROVED	DATE	CODE
H.Z.	7-21-77			
CHECKED	DATE	APPROVED	DATE	CLASS

ALTERED BOSTON GEAR BUSHING M610-6
LAB SAW

NOT OTHERWISE SPEC: FRAC ± ANG ± SCALE FULL
FIN. 63 DEC .X ± .XX ± .XXX ±

varian

VAC/LEX	A.	S 2015	
DIVISION	SIZE	DRAWING NO.	REV

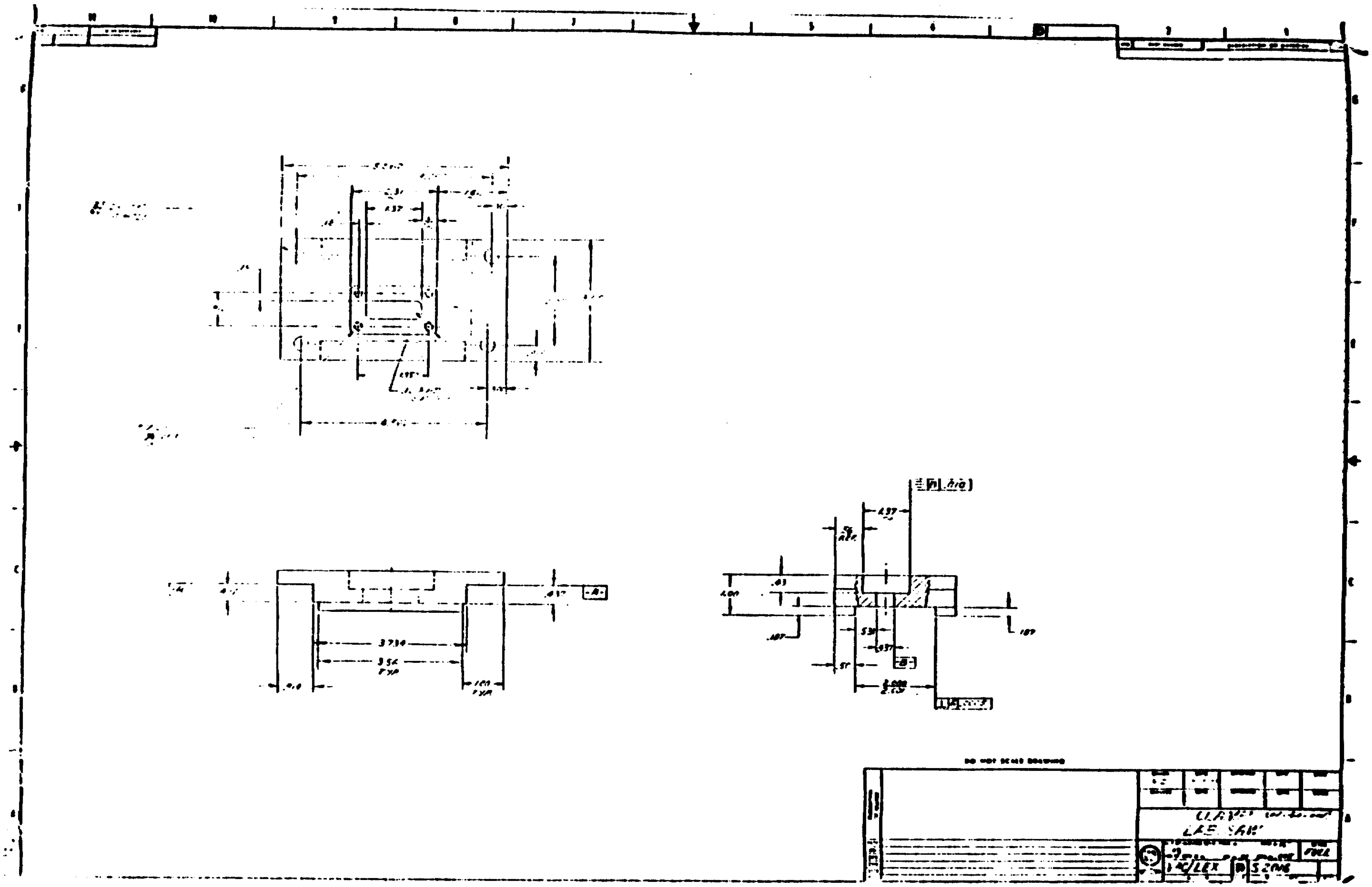

3.734
TYP

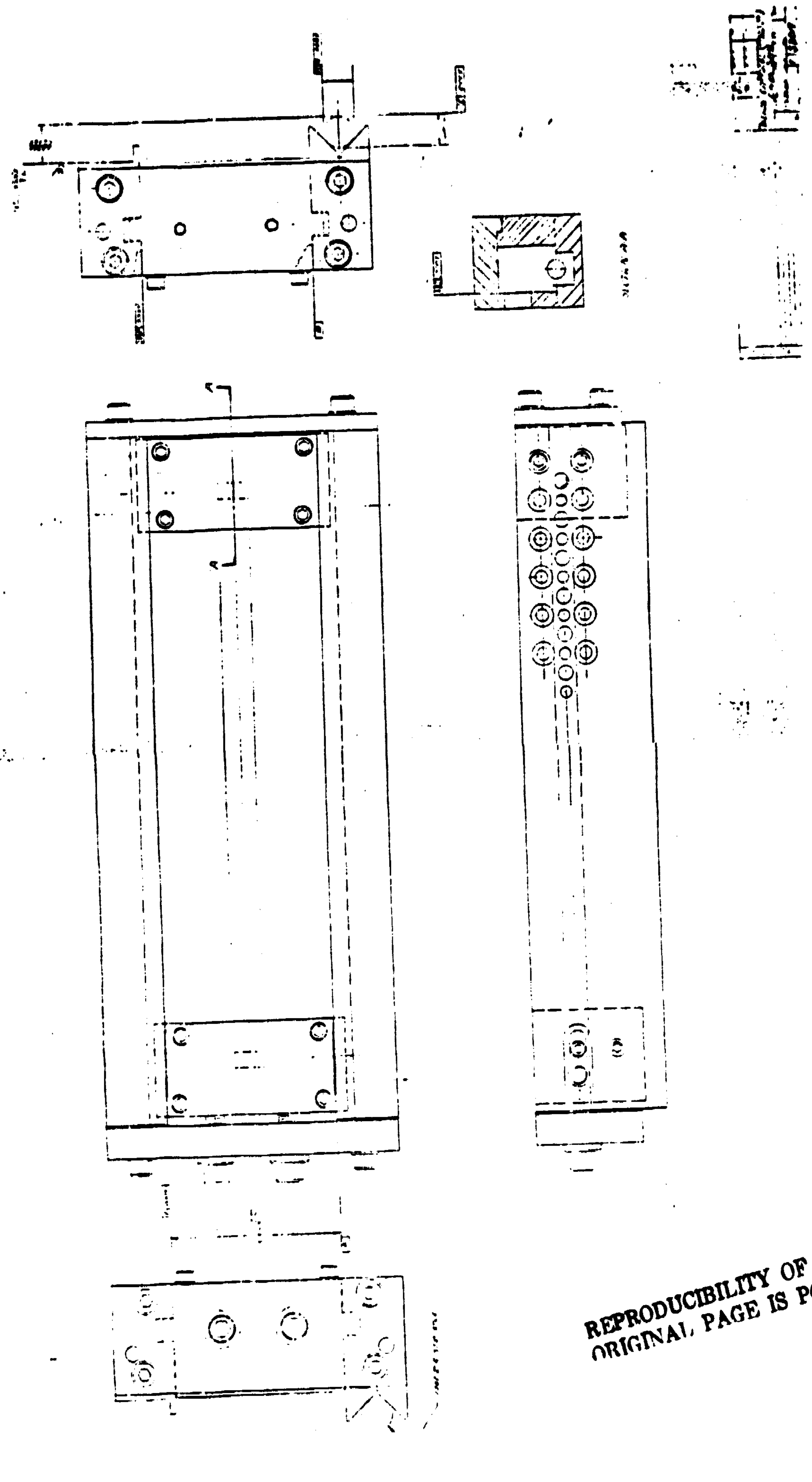

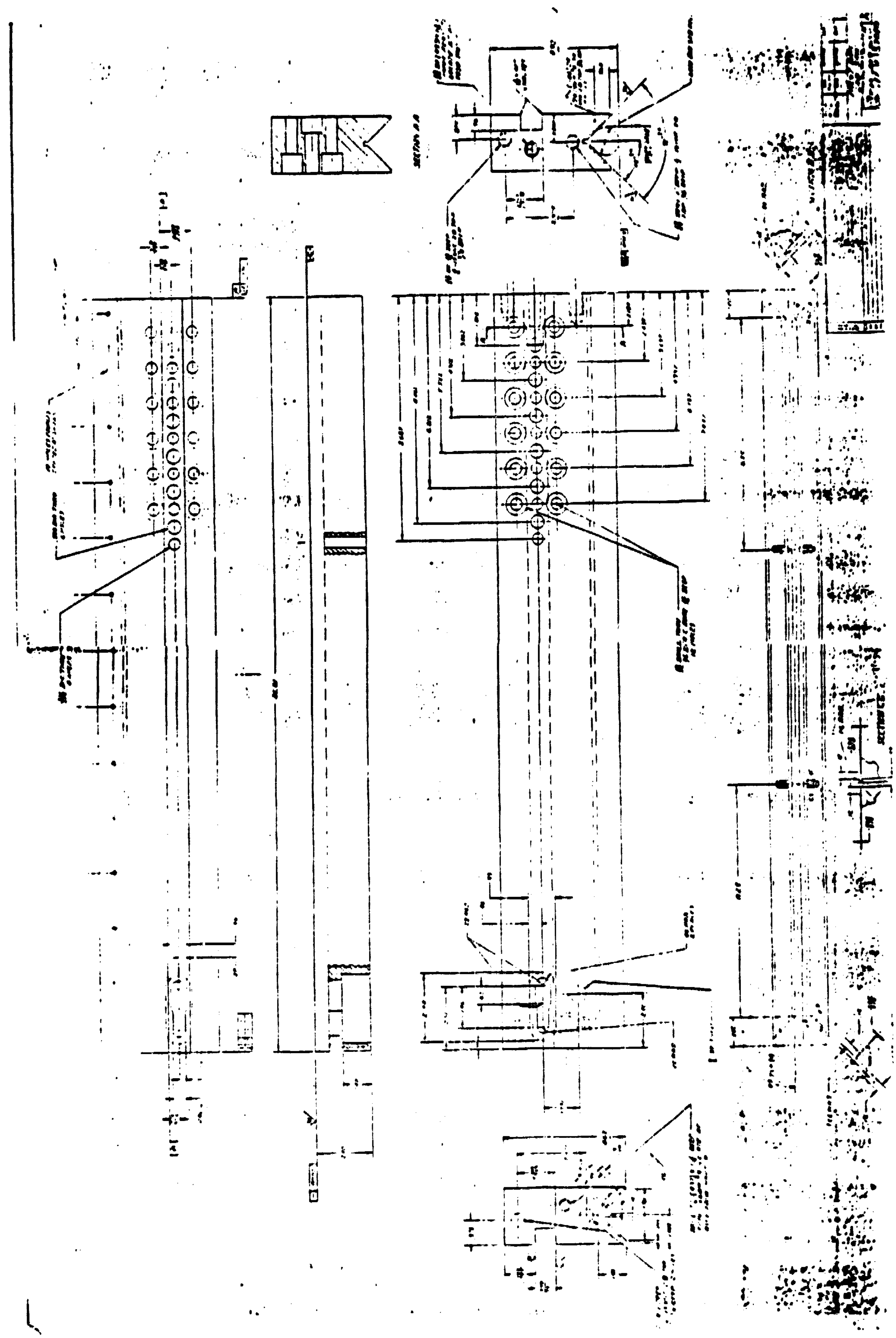

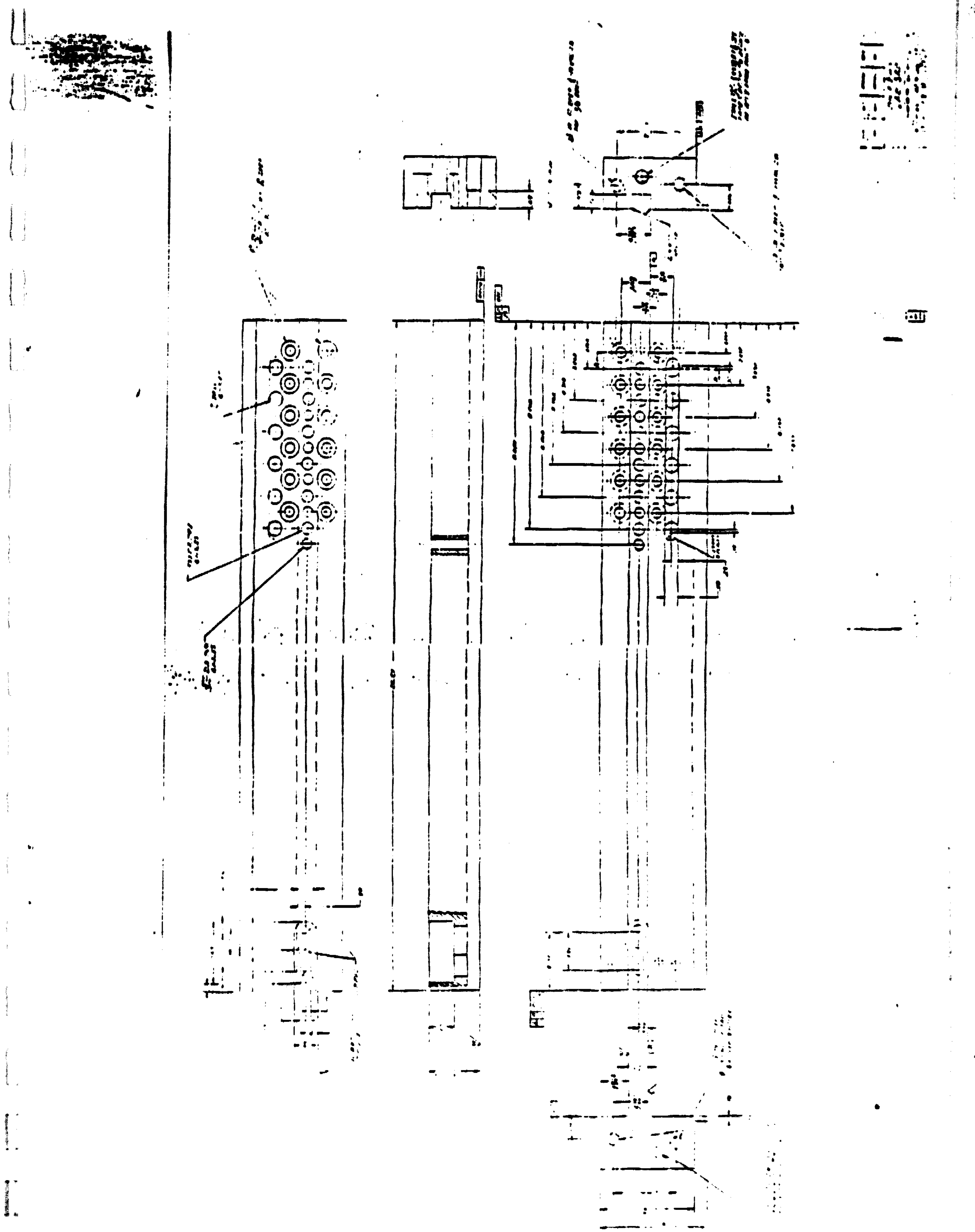

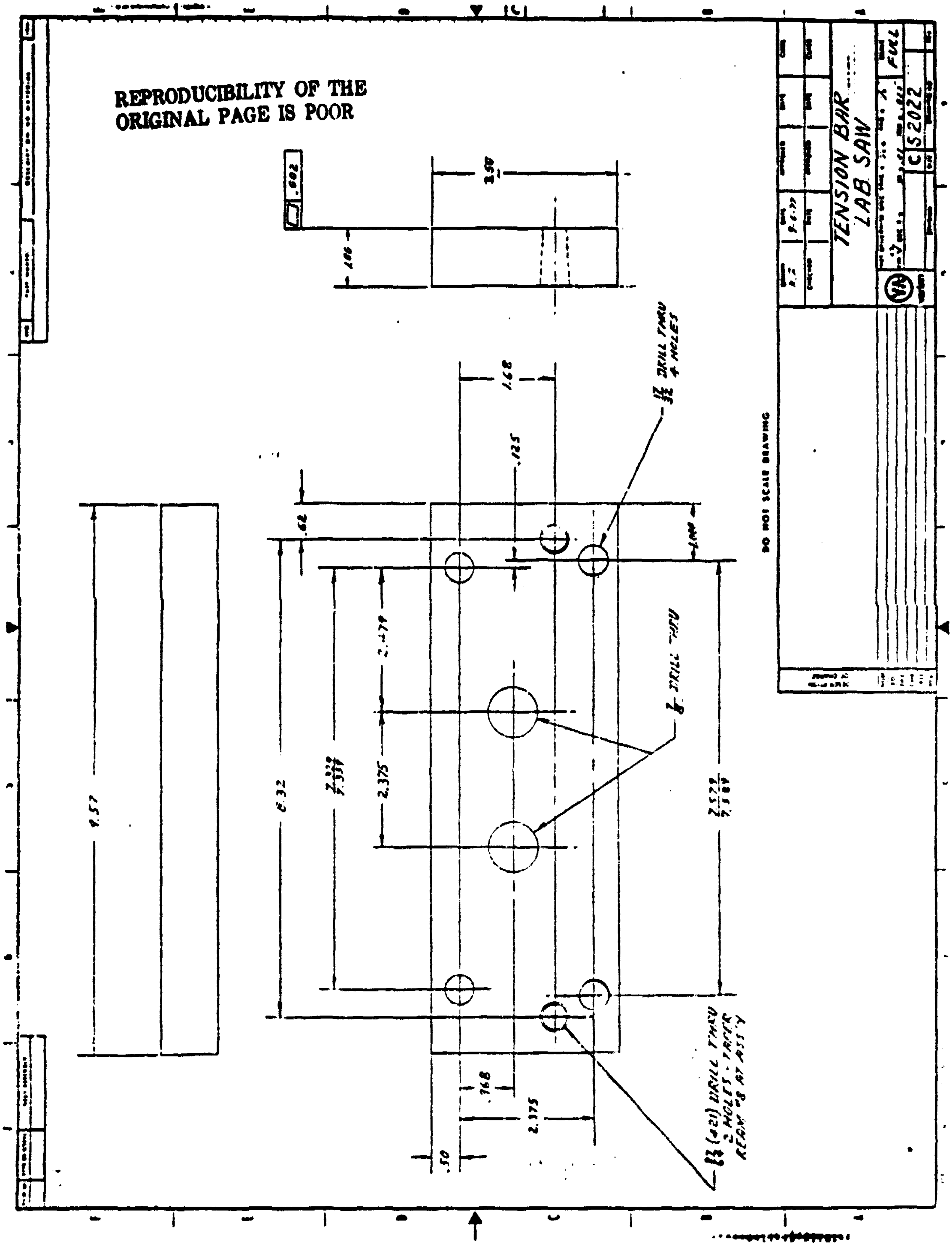
TENSION BAR
LAB SAW
C
S2022
FULL
DO NOT SCALE DRAWING
17/32 DRILL THRU 4 HOLES
1/4 DRILL THRU
3.50
1.68
.125
.62
9.57
6.32
2.375
.50

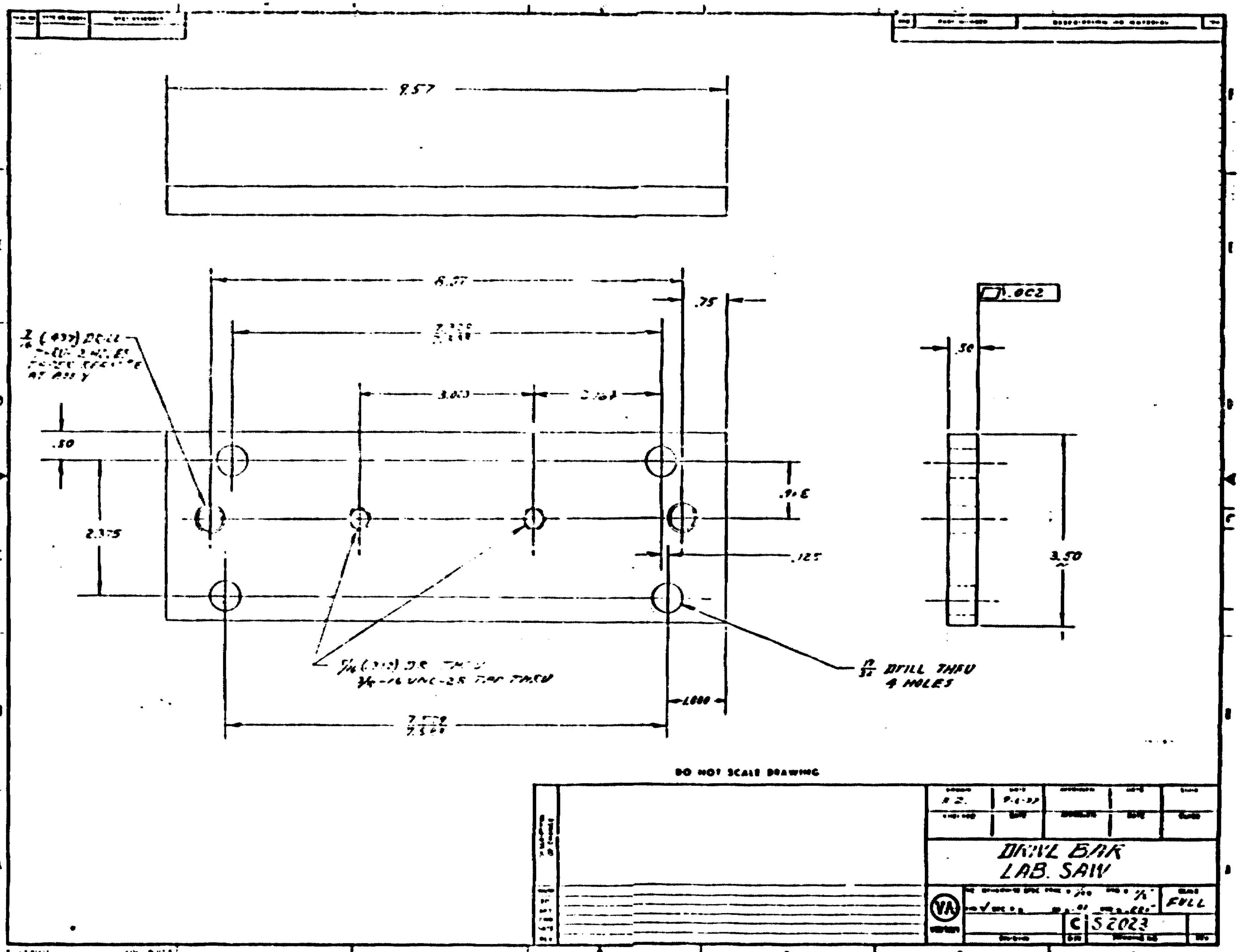
9.57
8.37
.75
.50
3.003
.916
2.375
.125
1.000
3.50
.002
7/16 (.437) DRILL THRU 2 HOLES
5/16 (.313) DR THRU
3/8-16 UNC-2B TAP THRU
11/32 DRILL THRU 4 HOLES
DO NOT SCALE DRAWING
DRILL BAR
LAB. SAW
FULL
C
52023

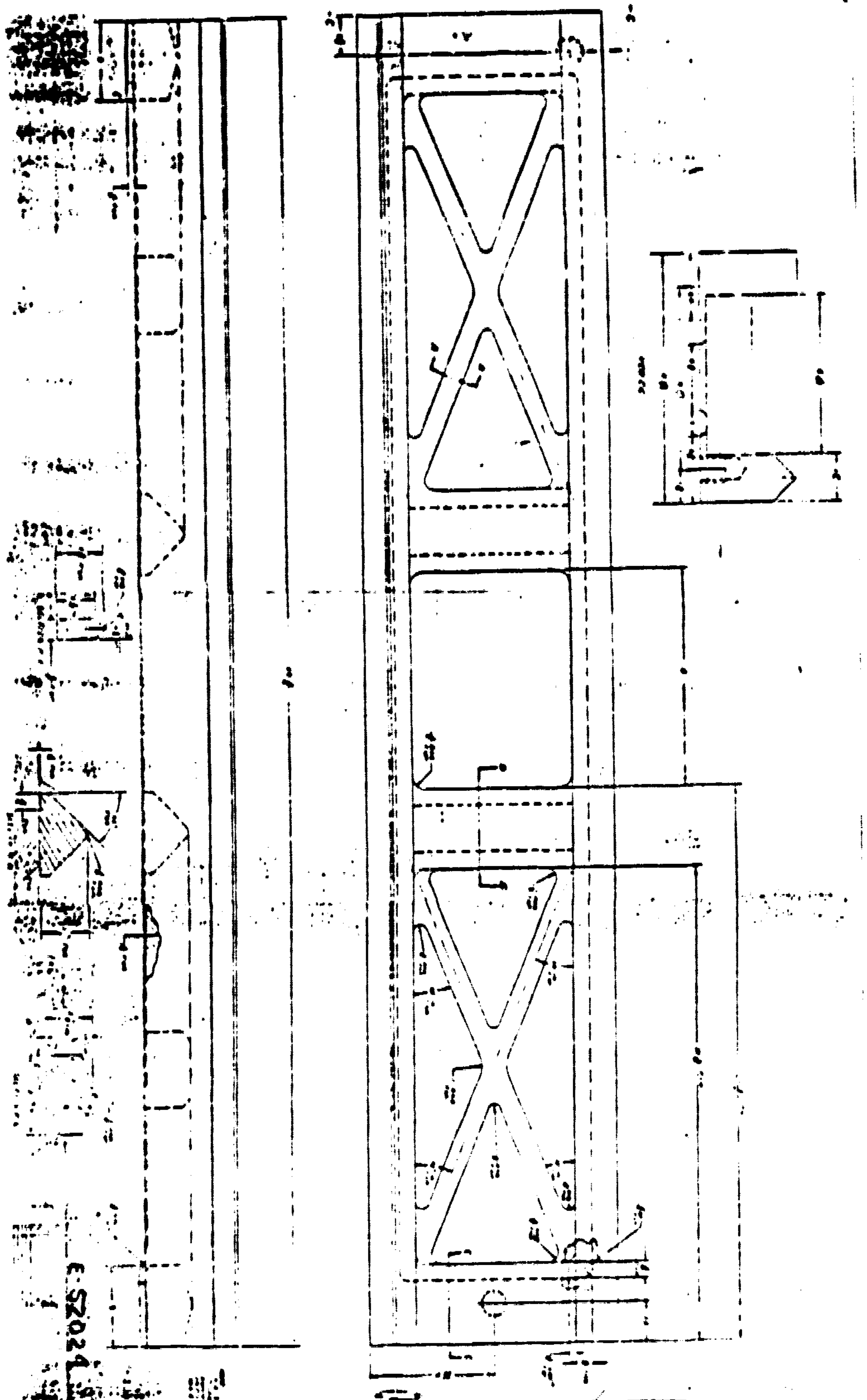

DASH NO.	TYPE OR MODEL	NEXT ASSEMBLY	REQ	PART NUMBER	DESCRIPTION OR MATERIAL	ITEM

A

DO NOT SCALE DRAWING

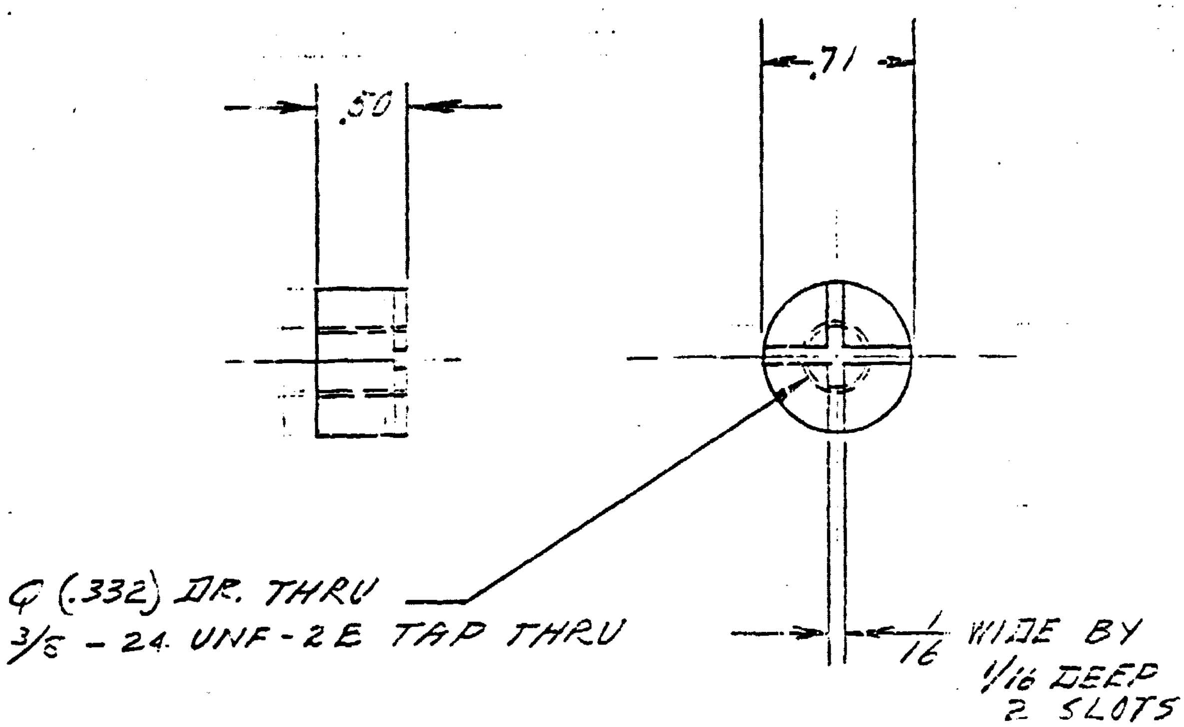

DO NOT SCALE THIS PRINT
UNLESS OTHERWISE SPECIFIED
BREAK ALL SHARP EDGES
DIMENSIONS ARE IN INCHES

DRAWN	DATE	APPROVED	DATE	CODE
K.Z.	9-13-77			
CHECKED	DATE	APPROVED	DATE	CLASS

DESCRIPTION OF CHANGE

NUM
EO
DFT
CHK
DATE
REV

LOADER NUT
LAB. SAW

NOT OTHERWISE SPEC: FRAC ± 1/64 ANG ± 1/2°
FIN 63 √ DEC .X ± .XX ± .01 .XXX ± .005

SCALE FULL

varian

DIVISION	SIZE	DRAWING NO	REV
	A	S2025	

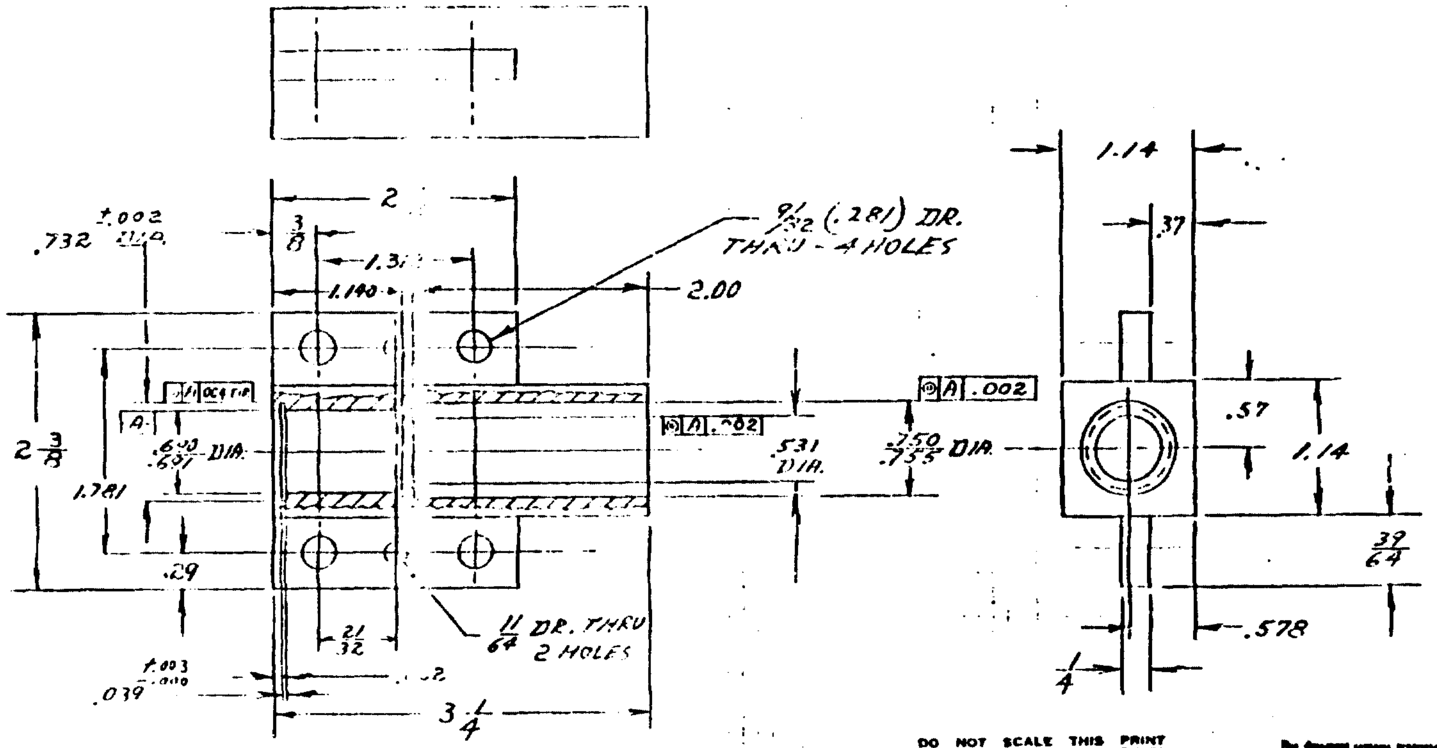

DO NOT SCALE THIS PRINT
UNLESS OTHERWISE SPECIFIED
BREAK ALL SHARP EDGES
DIMENSIONS ARE IN INCHES

DRAWN	DATE	APPROVED	DATE	CODE
K.Z.	7-13-77			
CHECKED	DATE	APPROVED	DATE	CLASS

LOADER HOUSING
LAB. SAW

NOT OTHERWISE SPEC. FRAC ± 1/64 ANG ± 1/2°
SCALE FULL

varian

DIVISION	SIZE	DRAWING NO	REV
	B	S 2026	

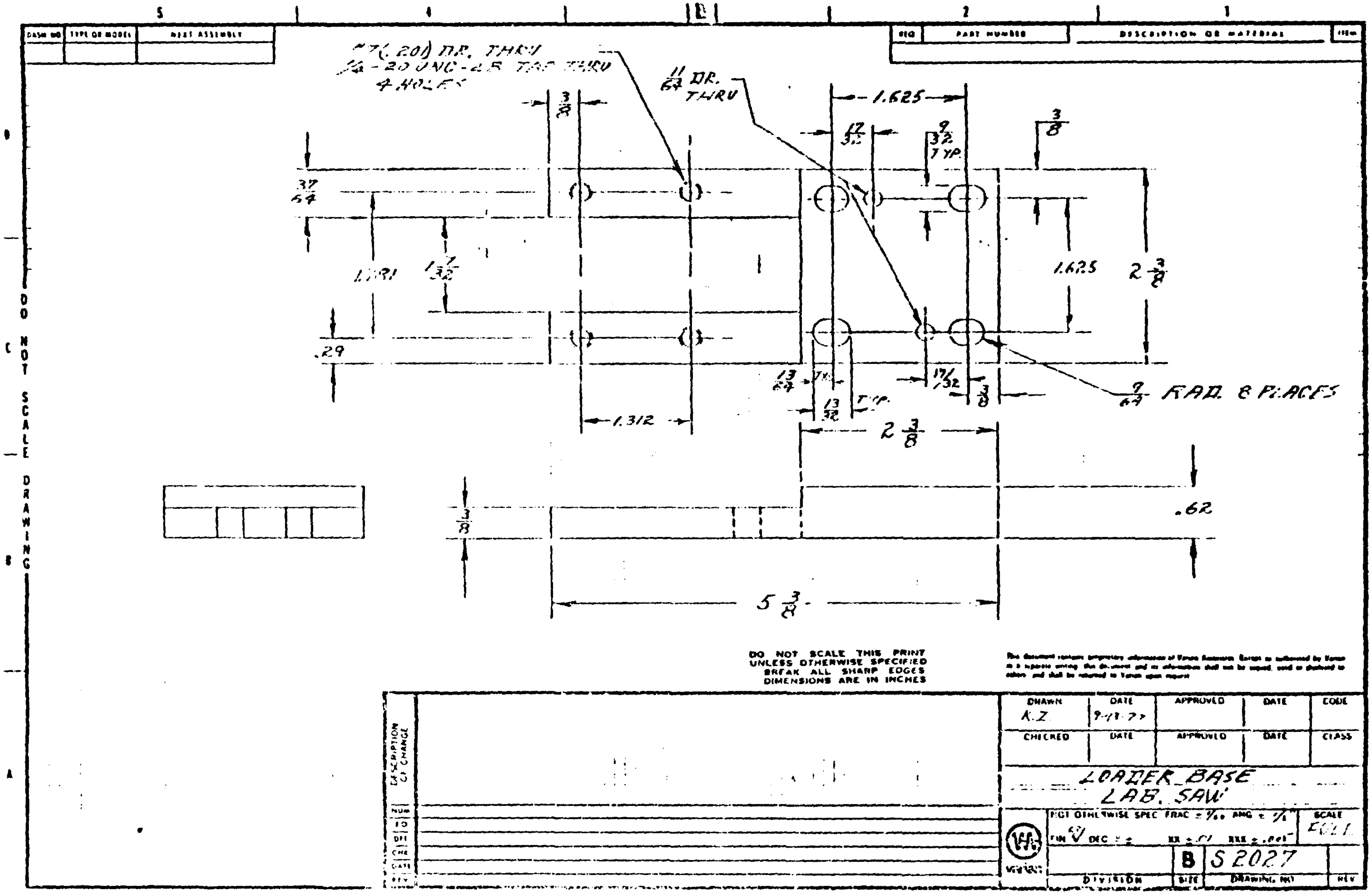
#7(.201) DR. THRU
1/4-20 UNC-2B TAP THRU
4 HOLES
11/64 DR. THRU
9/64 RAD. 8 PLACES
1.625
2 3/8
5 3/8
1.312
.62
.29
3/8
DO NOT SCALE THIS PRINT
UNLESS OTHERWISE SPECIFIED
BREAK ALL SHARP EDGES
DIMENSIONS ARE IN INCHES
DRAWN K.Z.
DATE 9-19-77
LOADER BASE
LAB. SAW
SCALE FULL
B
S 2027
DO NOT SCALE DRAWING

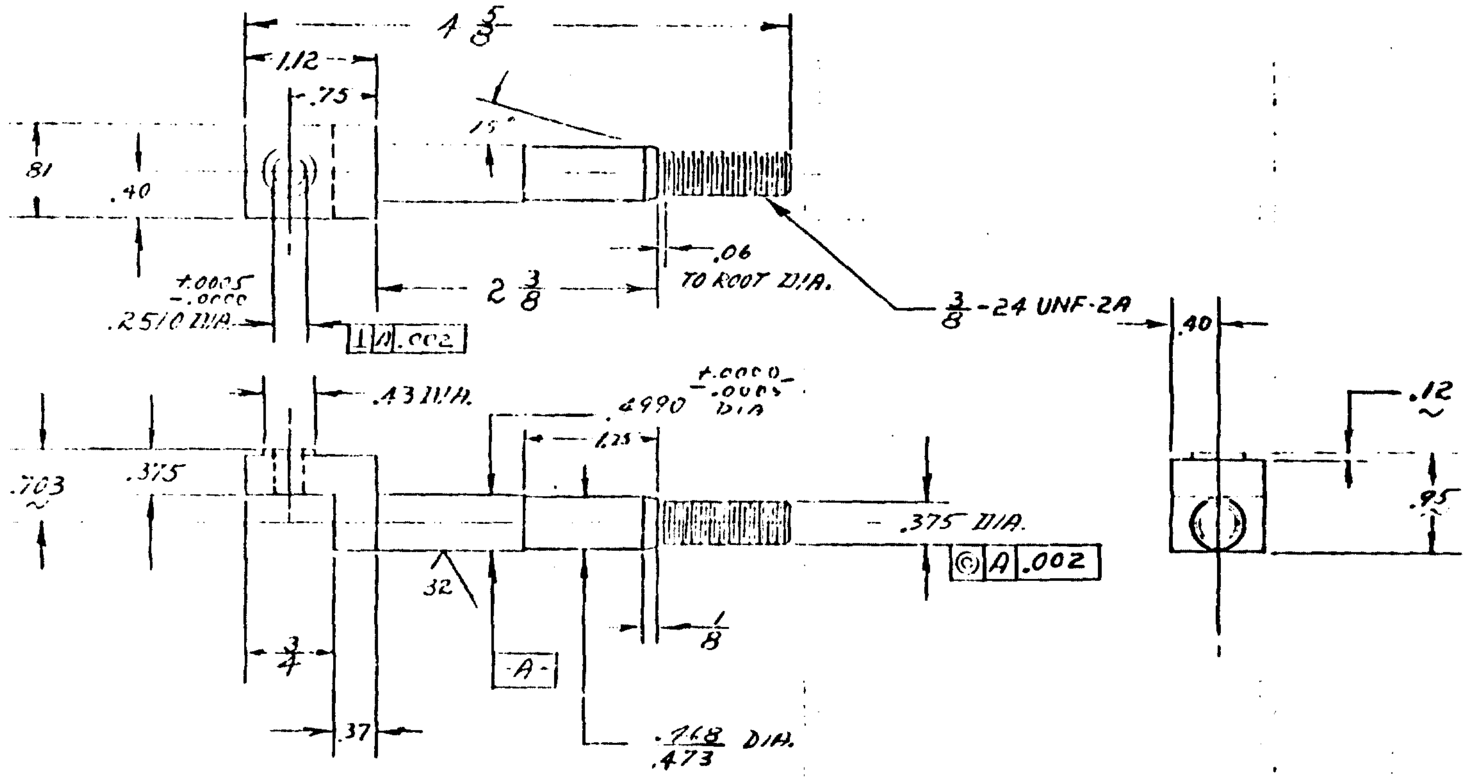

DO NOT SCALE THIS PRINT
UNLESS OTHERWISE SPECIFIED
BREAK ALL SHARP EDGES
DIMENSIONS ARE IN INCHES

DRAWN	DATE	APPROVED	DATE	CODE
K.J.	9-13-71			
CHECKED	DATE	APPROVED	DATE	CLASS

CAMROL HOLDER
LAB. SAW

NOT OTHERWISE SPEC. FRAC ± 1/64, ANG ± 1/2°

FIN. 63 DEC X ± XX ± .01 XXX ± .005

SCALE FULL

varian

DIVISION	SIZE	DRAWING NO	REV
	B	56025	

DO NOT SCALE DRAWING

LITHO IN U.S.A.

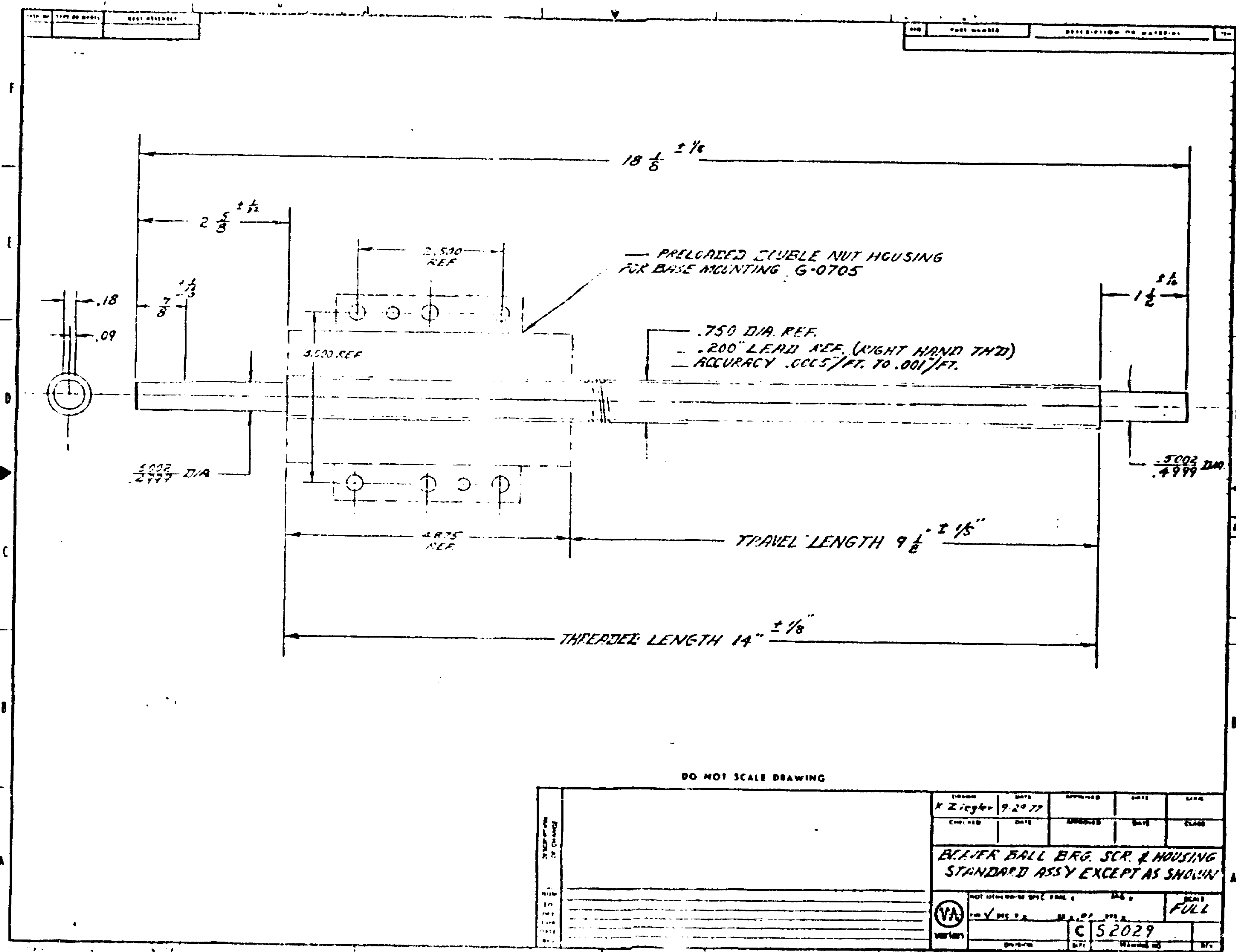

18 1/8 ± 1/8
2 5/8 ± 1/32
2.500 REF
PRELOADED DOUBLE NUT HOUSING FOR BASE MOUNTING G-0705
1 1/2 ± 1/16
.18
.09
7/8 ± 1/32
.750 DIA. REF.
.200" LEAD REF. (RIGHT HAND THD)
ACCURACY .0005"/FT. TO .001"/FT.
3.500 REF
.5002/.4999 DIA.
.5002/.4999 DIA
4.875 REF
TRAVEL LENGTH 9 1/8" ± 1/8"
THREADED LENGTH 14" ± 1/8"
DO NOT SCALE DRAWING
K Ziegler 9-29-77
BEAVER BALL BRG. SCR. & HOUSING
STANDARD ASSY EXCEPT AS SHOWN
FULL
C 52029

APPENDIX VIII

ENGINEERING DRAWINGS AND SKETCHES

(Large Saw)

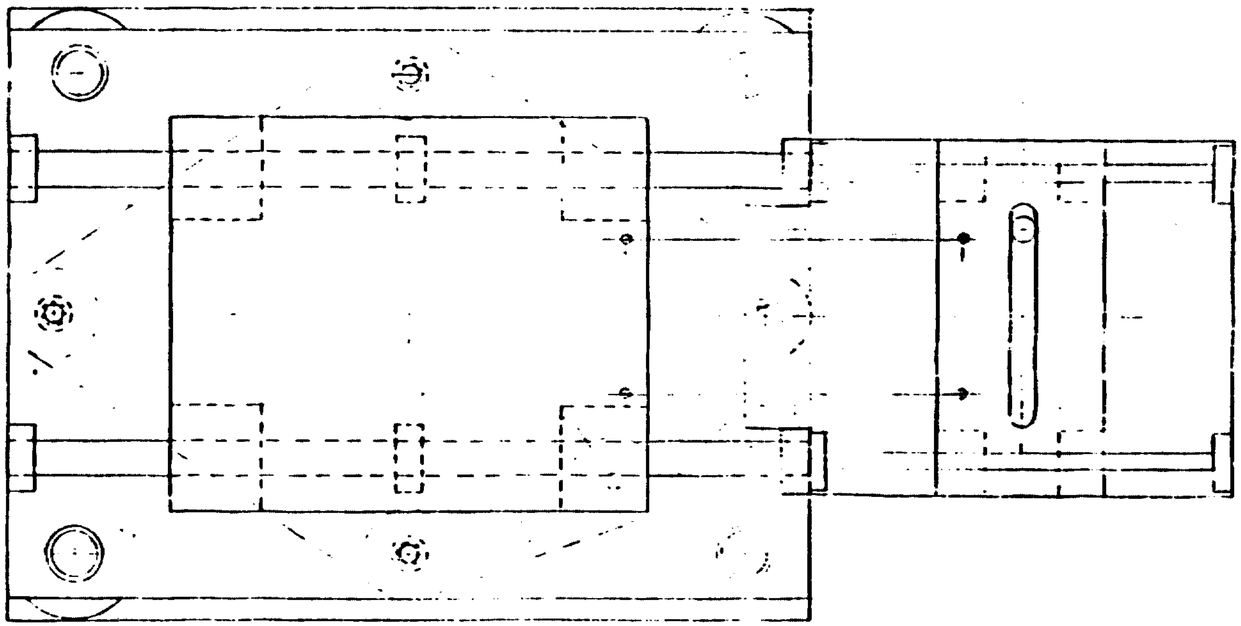

CONCEPT #1

C-50002

LAYOUT #1
SHEET 2

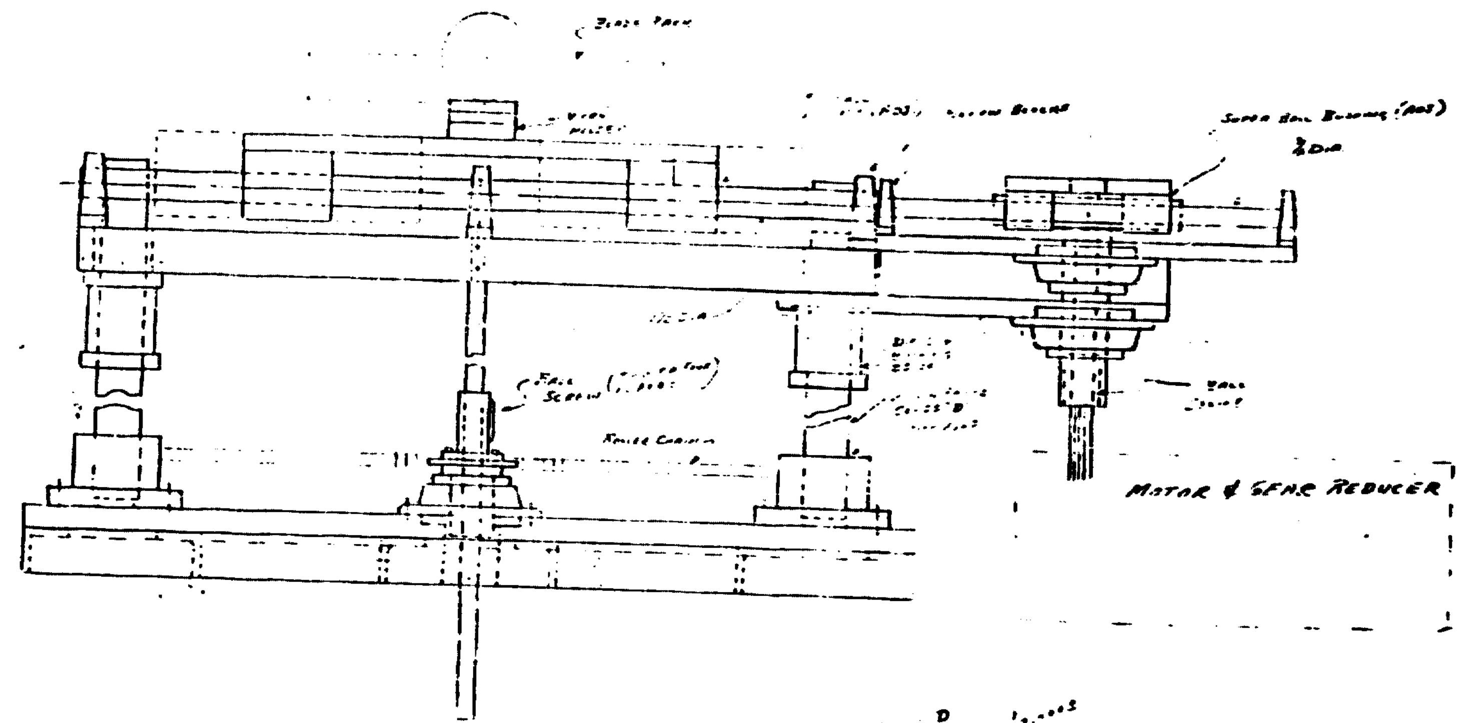

C-SC001

LAYOUT #1
SHEET 1
CONCEPT #1

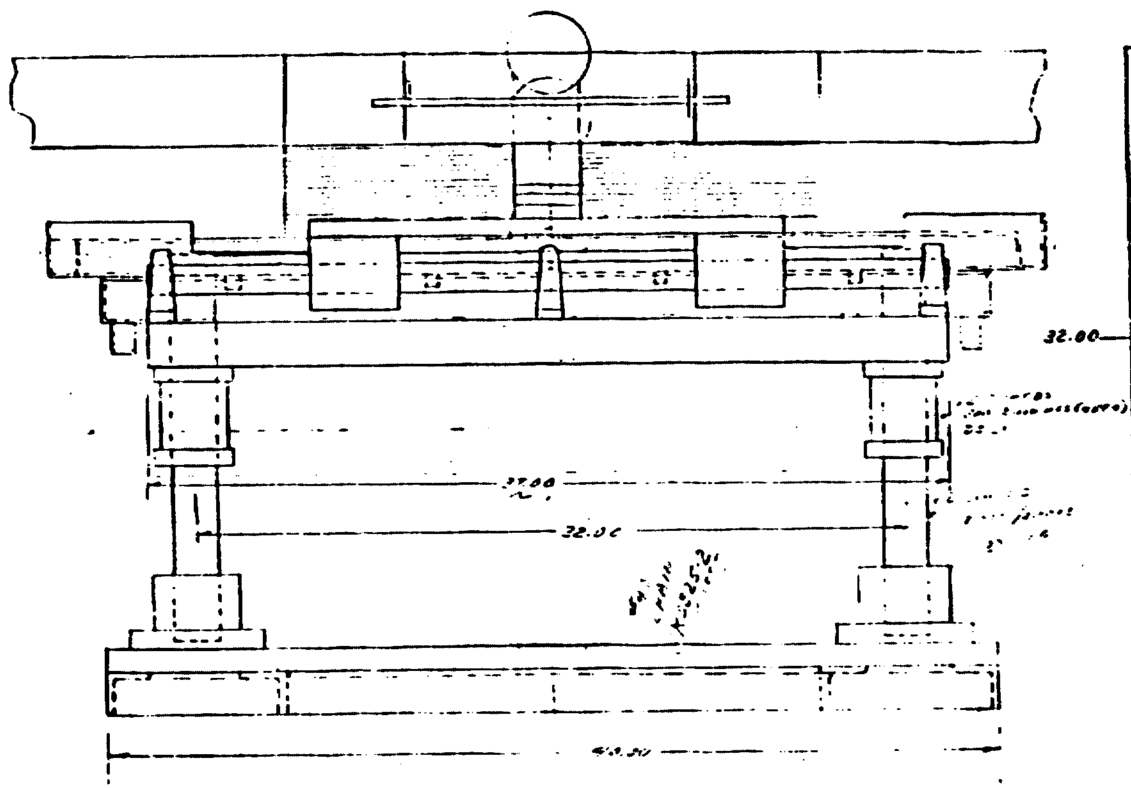

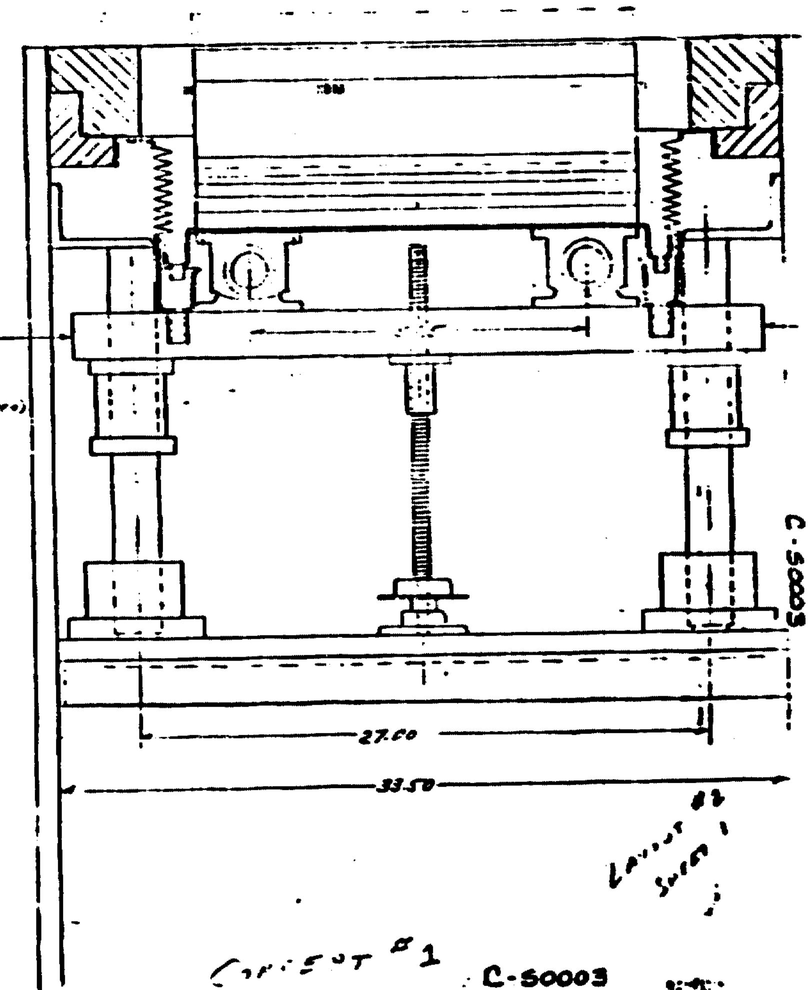

C-50003

J.P.L. II

C-50004

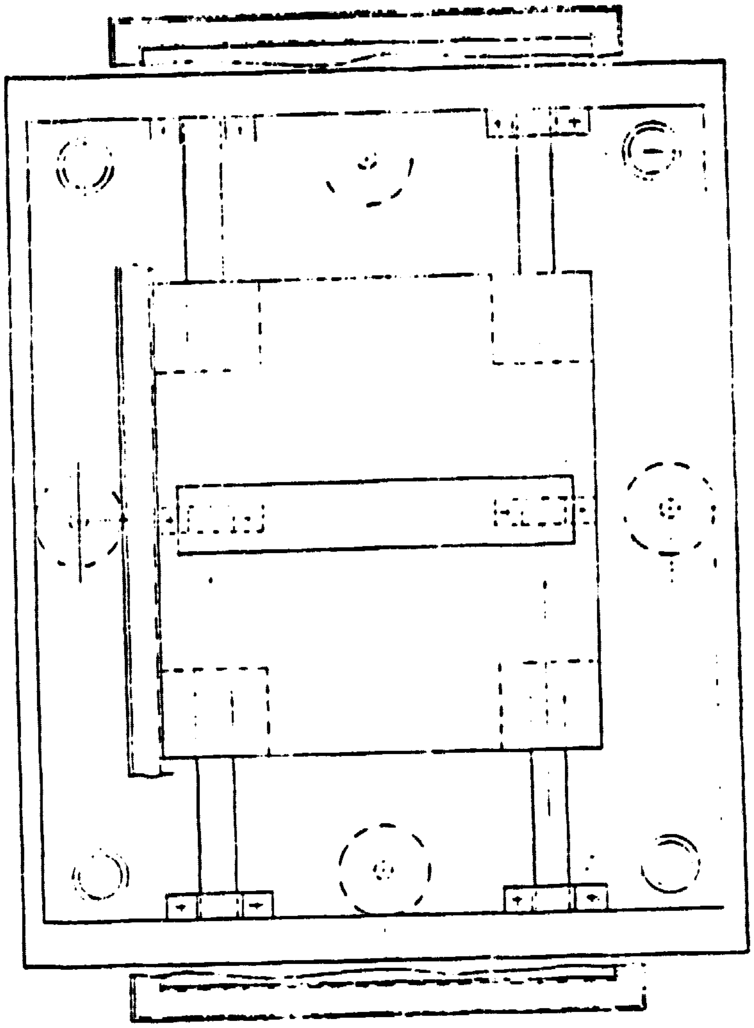

C-50004

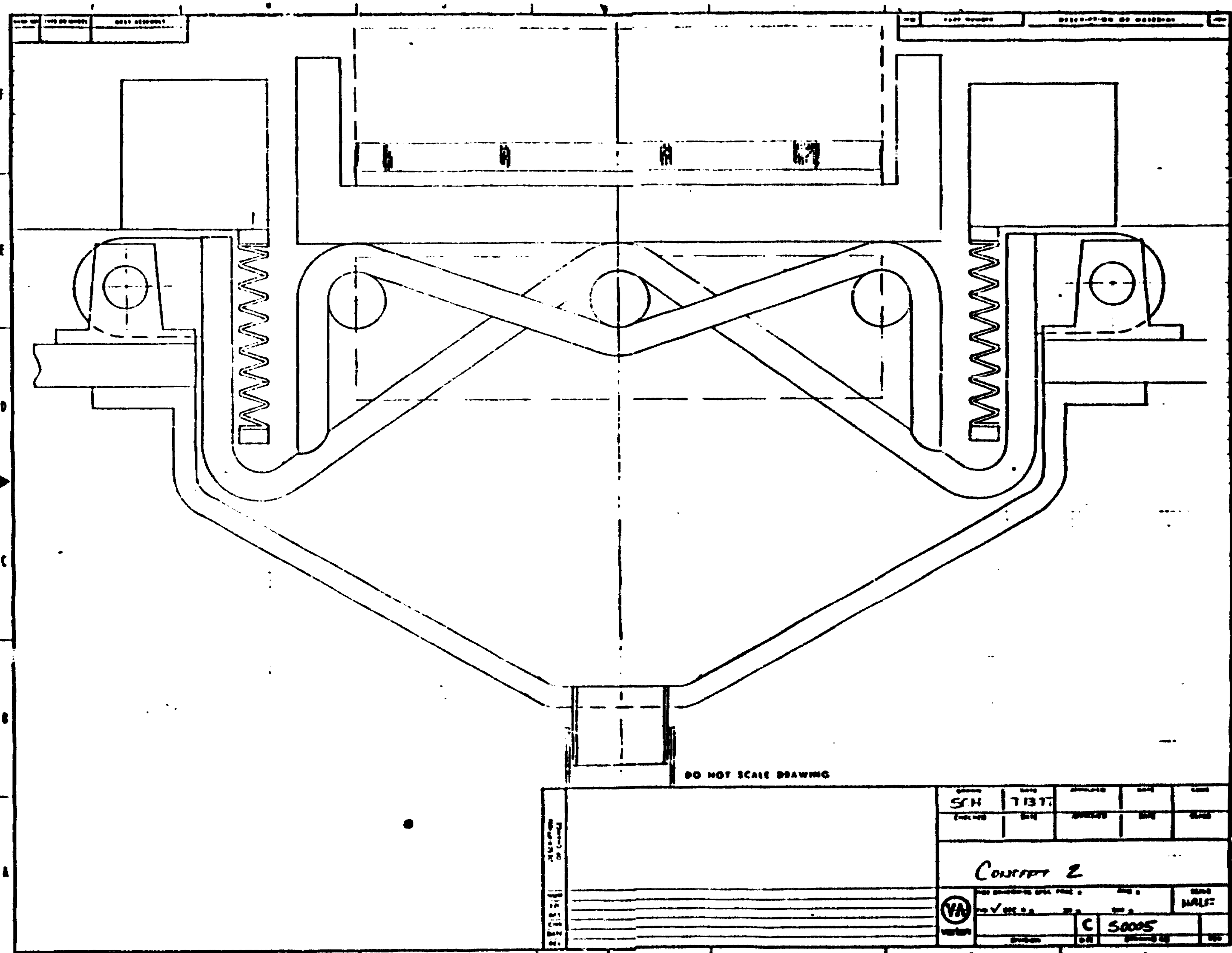
DO NOT SCALE DRAWING
SCH
7 13 72
CONCEPT 2
HALF
C
50005

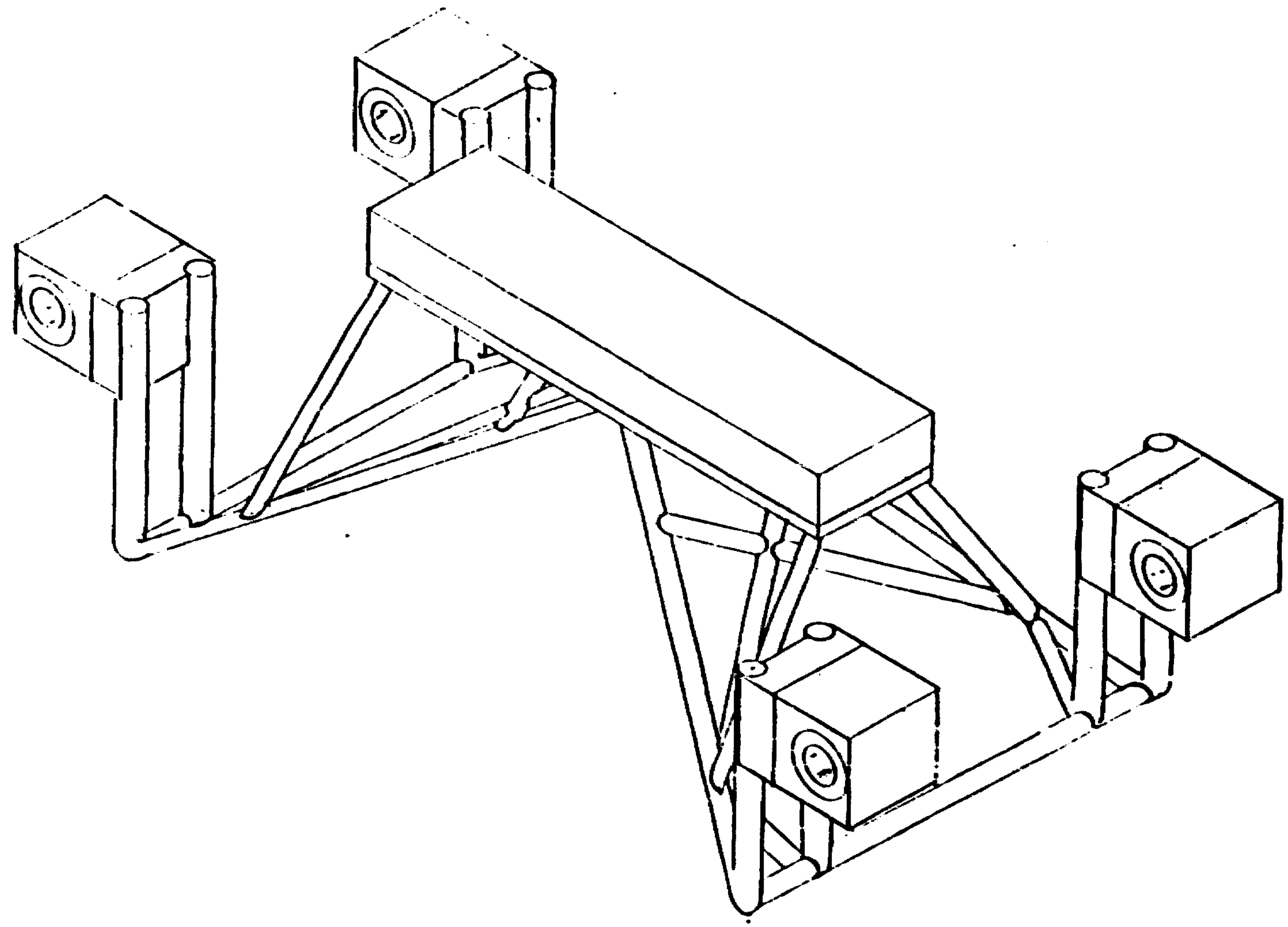

1 of 2

WELLHOLDER FRAME
CONCEPT #2
SCH 7.15

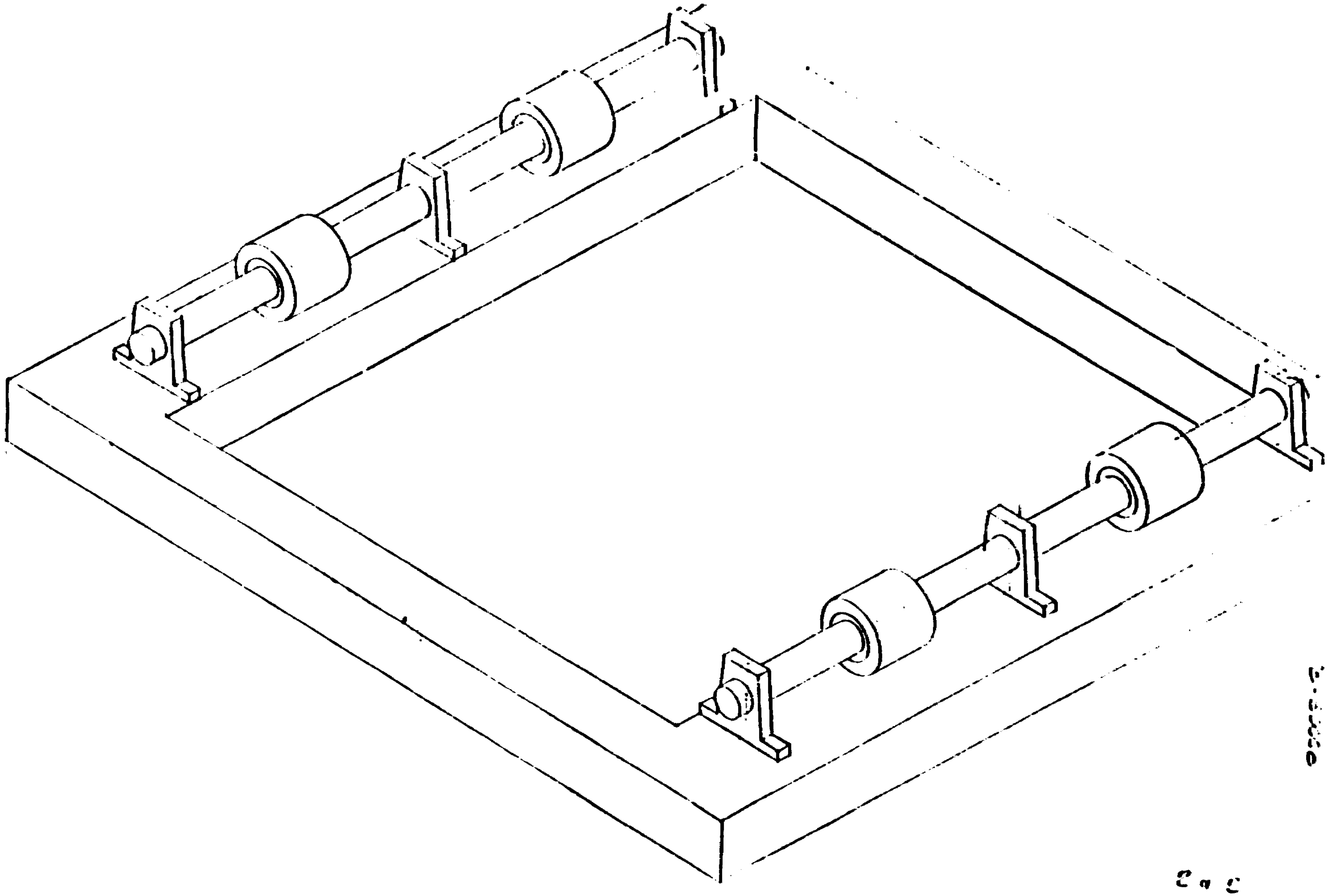

B·5000B

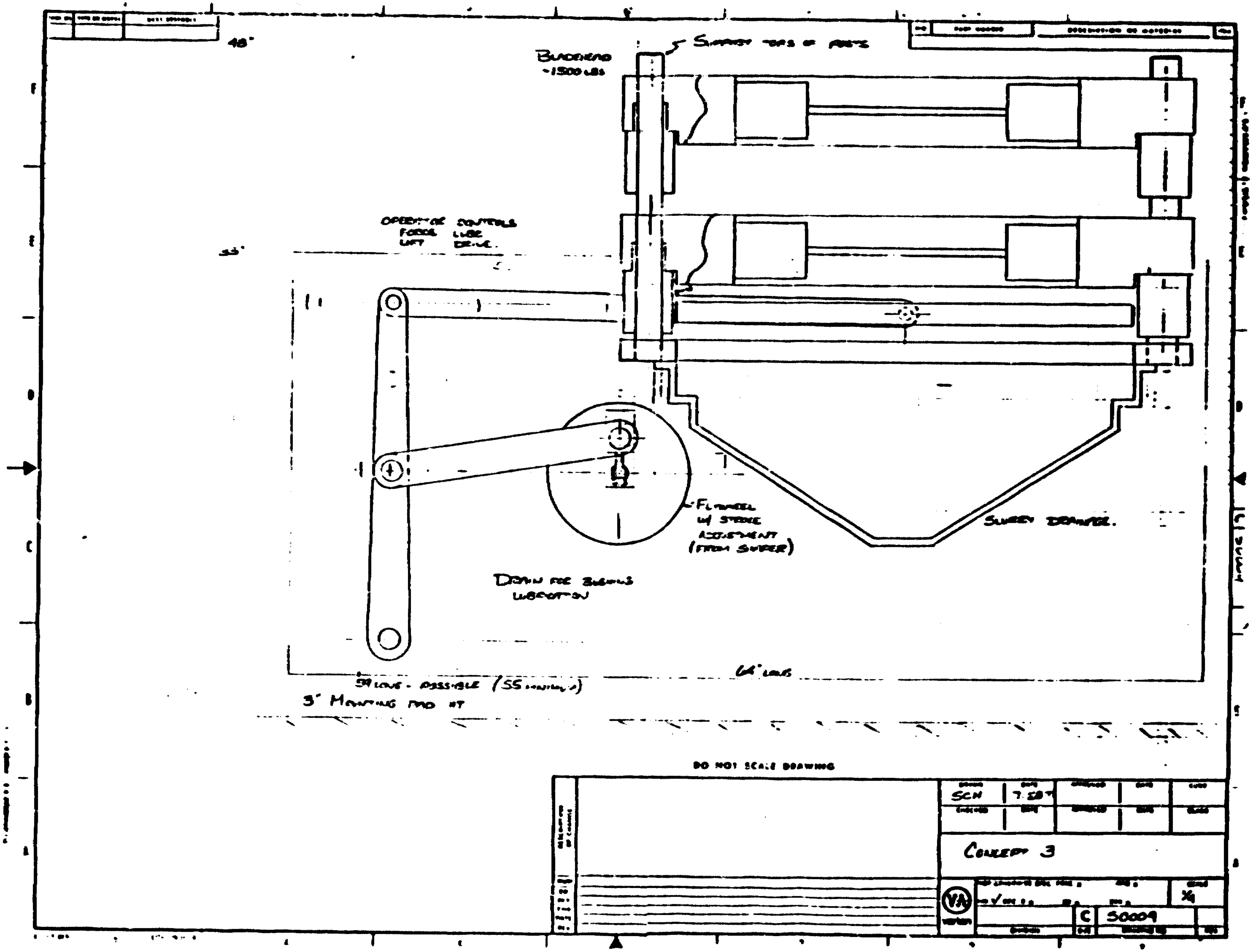

48"
BLADEHEAD
~1500 LBS
SUPPORT TOPS OF POSTS
OPERATOR CONTROLS
FORCE LUBE
LIFT DRIVE
33"
FLYWHEEL
W/ STROKE
ADJUSTMENT
(FROM SWEEP)
SWEEP DRAWER.
DRAIN FOR BEARING
LUBRICATION
59 LONG - POSSIBLE (55 MINIMUM)
3" MOUNTING PAD #7
64" LONG
DO NOT SCALE DRAWING
SCH
7-28-?
CONCEPT 3
C
50009

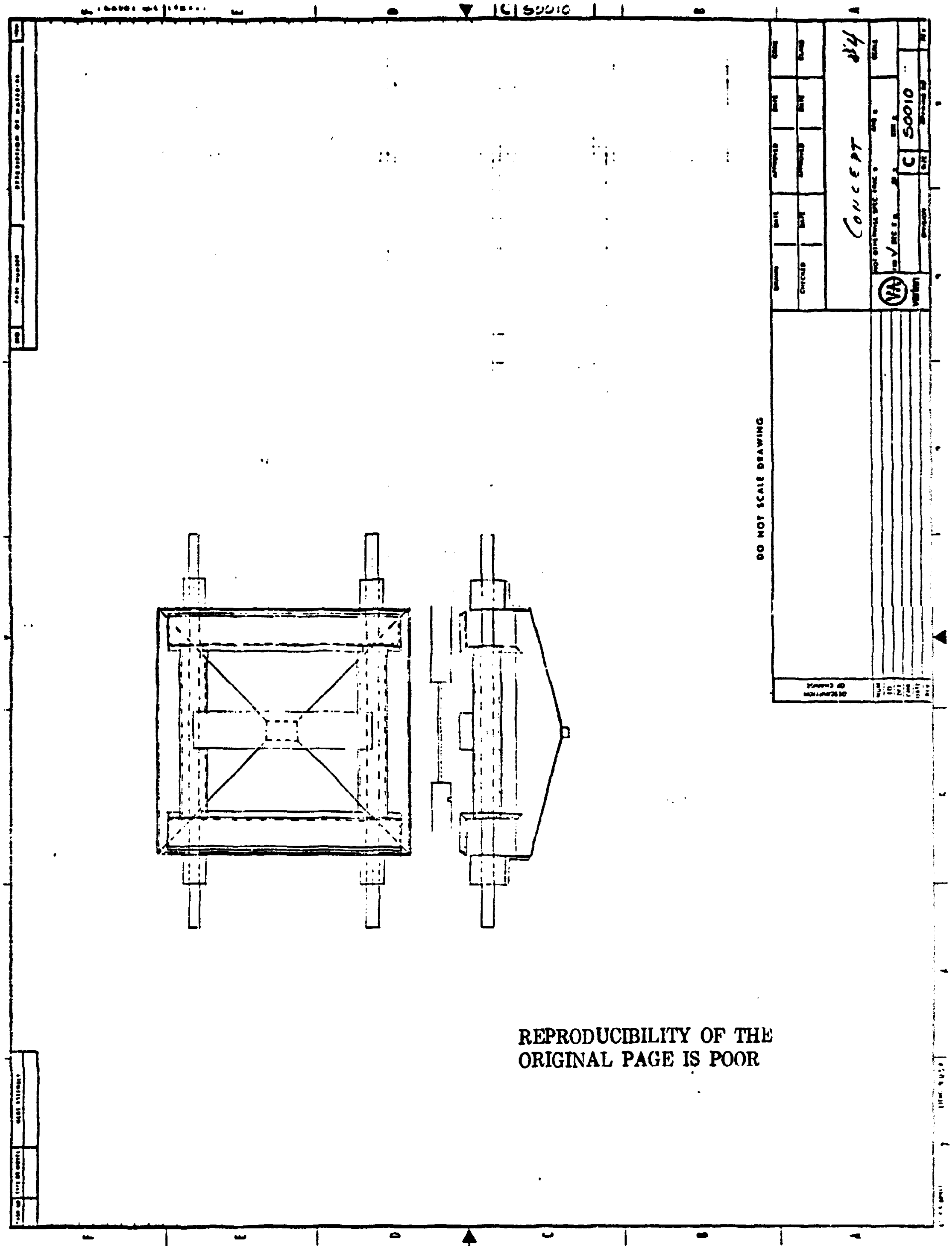

REPRODUCIBILITY OF THE
ORIGINAL PAGE IS POOR

DASH NO.	TYPE OR MODEL	NEXT ASSEMBLY	REQ	PART NUMBER	DESCRIPTION OR MATERIAL	ITEM

A S0011

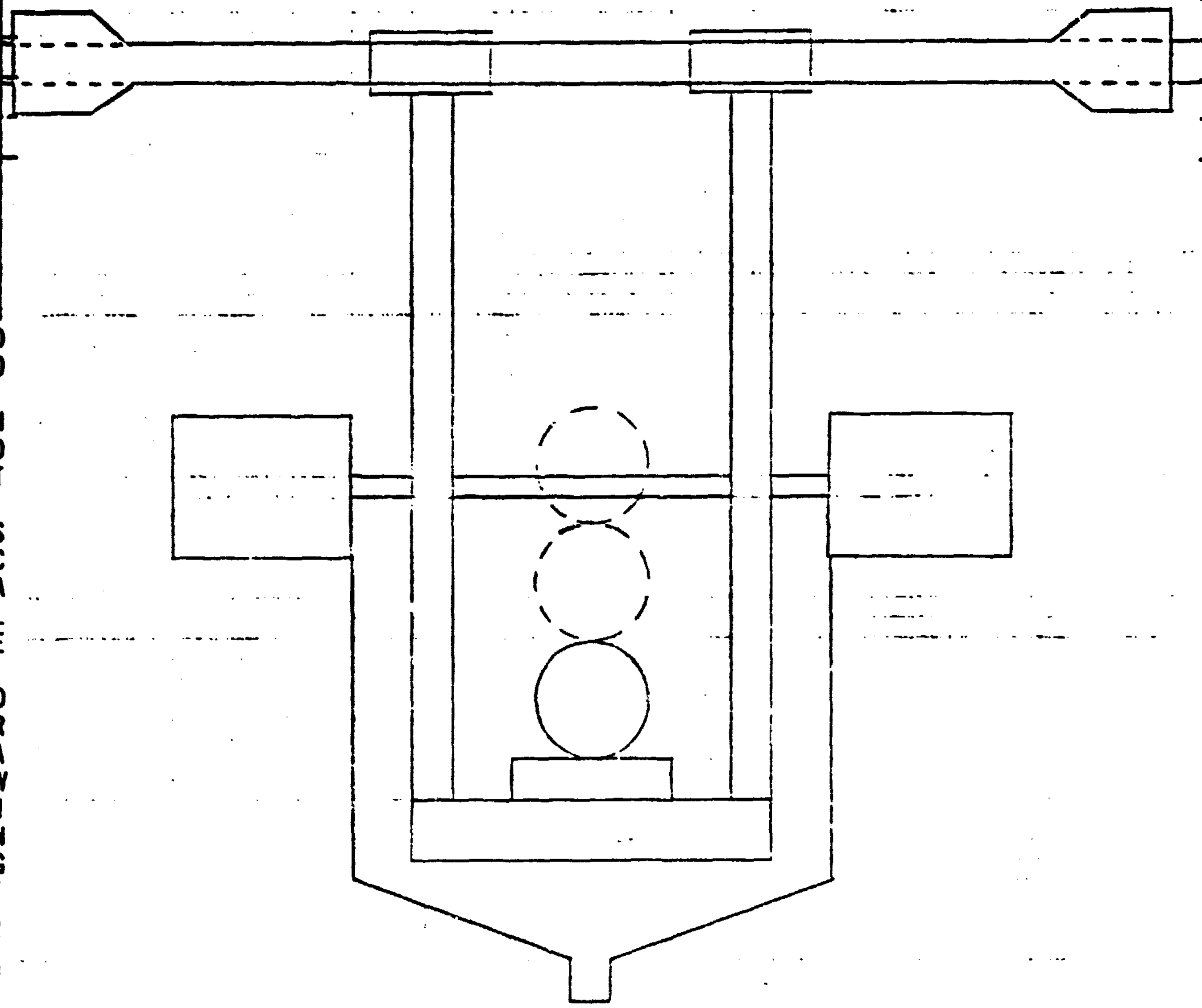

DO NOT SCALE DRAWING

DO NOT SCALE THIS PRINT
UNLESS OTHERWISE SPECIFIED
BREAK ALL SHARP EDGES
DIMENSIONS ARE IN INCHES

DRAWN	DATE	APPROVED	DATE	CODE
PJG				
CHECKED	DATE	APPROVED	DATE	CLASS

MOTION CONCEPT #5

NOT OTHERWISE SPEC: FRAC ± ANG ± SCALE

FIN ✓ DEC .X ± .XX ± .XXX ±

varian

DIVISION	SIZE	DRAWING NO	REV
	A	S0011	

DESCRIPTION OF CHANGE

NUM
EO
DFT
CHK
DATE
REV

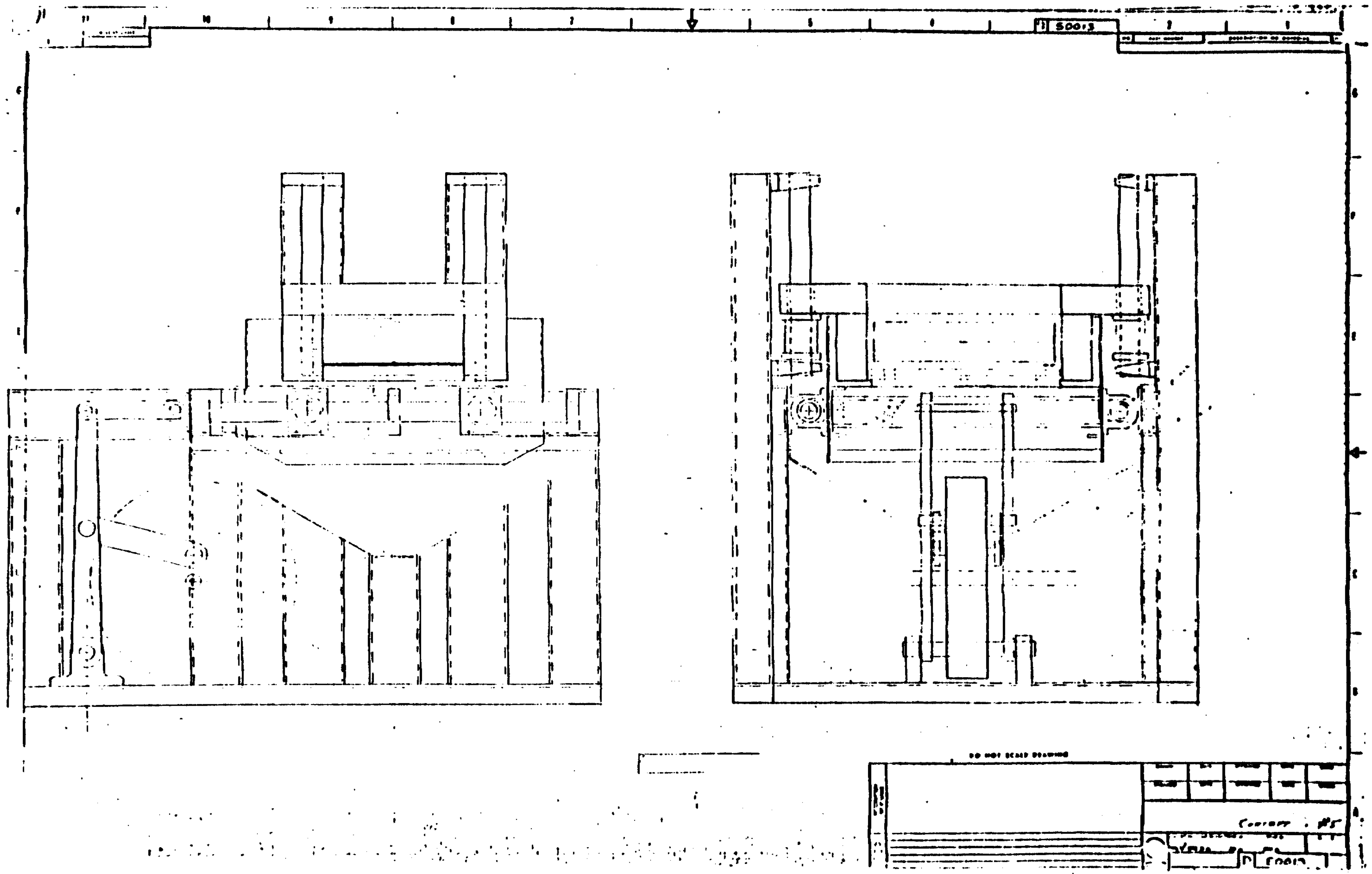
DO NOT SCALE DRAWING

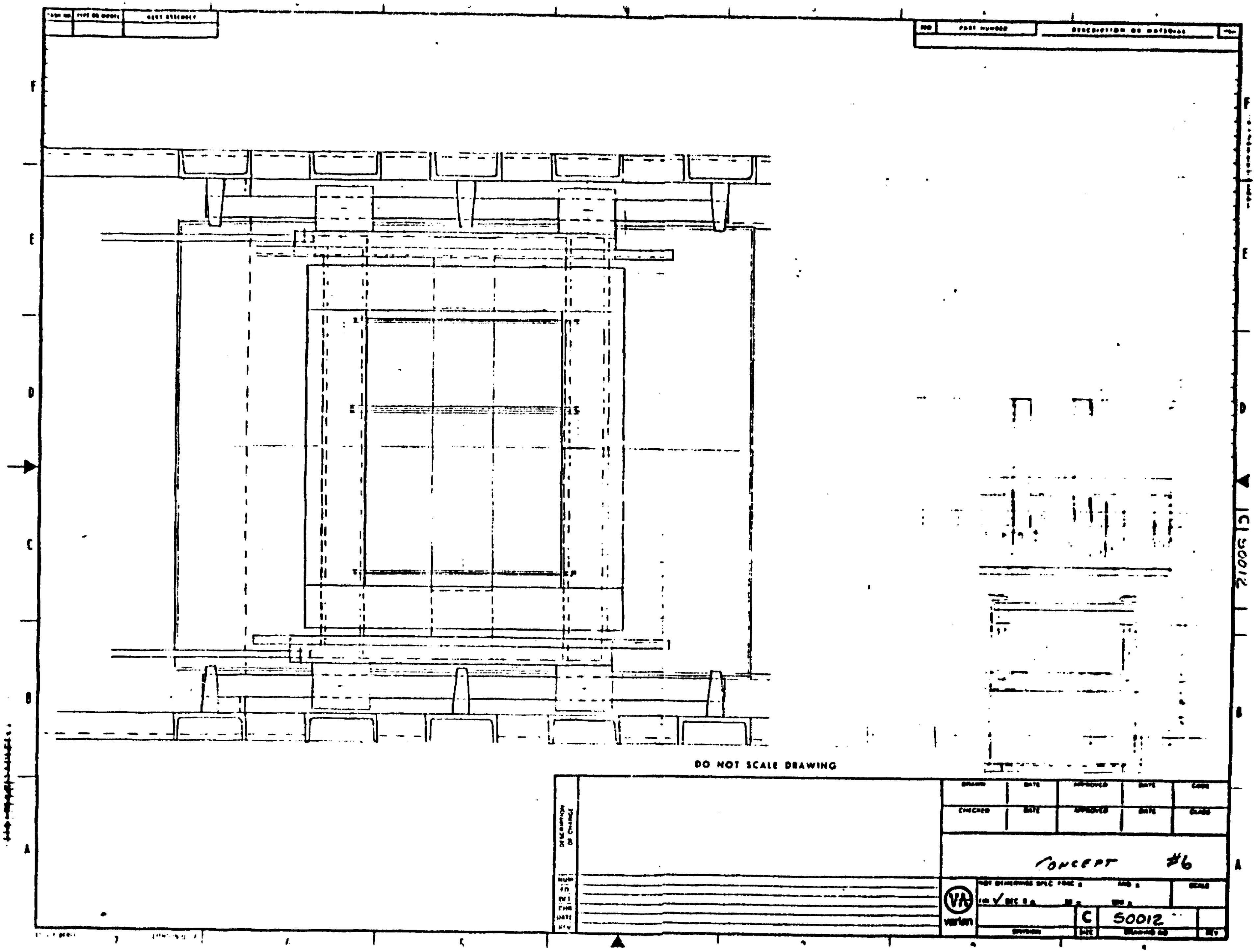
DO NOT SCALE DRAWING
DRAWN
DATE
APPROVED
DATE
CODE
CHECKED
DATE
APPROVED
DATE
CLASS
CONCEPT #6
varian
C
S0012
DESCRIPTION OF CHANGE
PART NUMBER
DESCRIPTION OR MATERIAL
NEXT ASSEMBLY

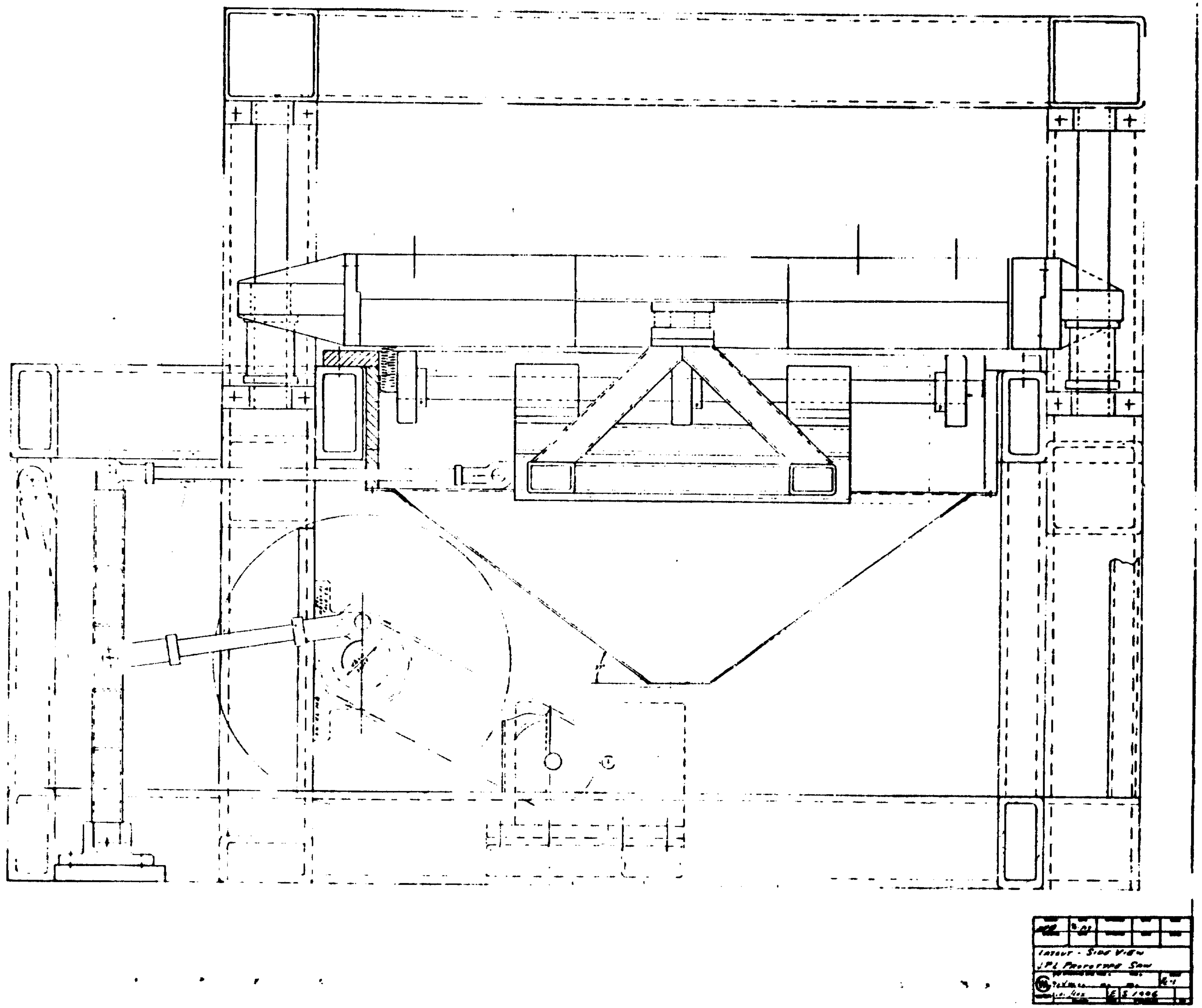
Layout - Side View
JPL Prototype Saw

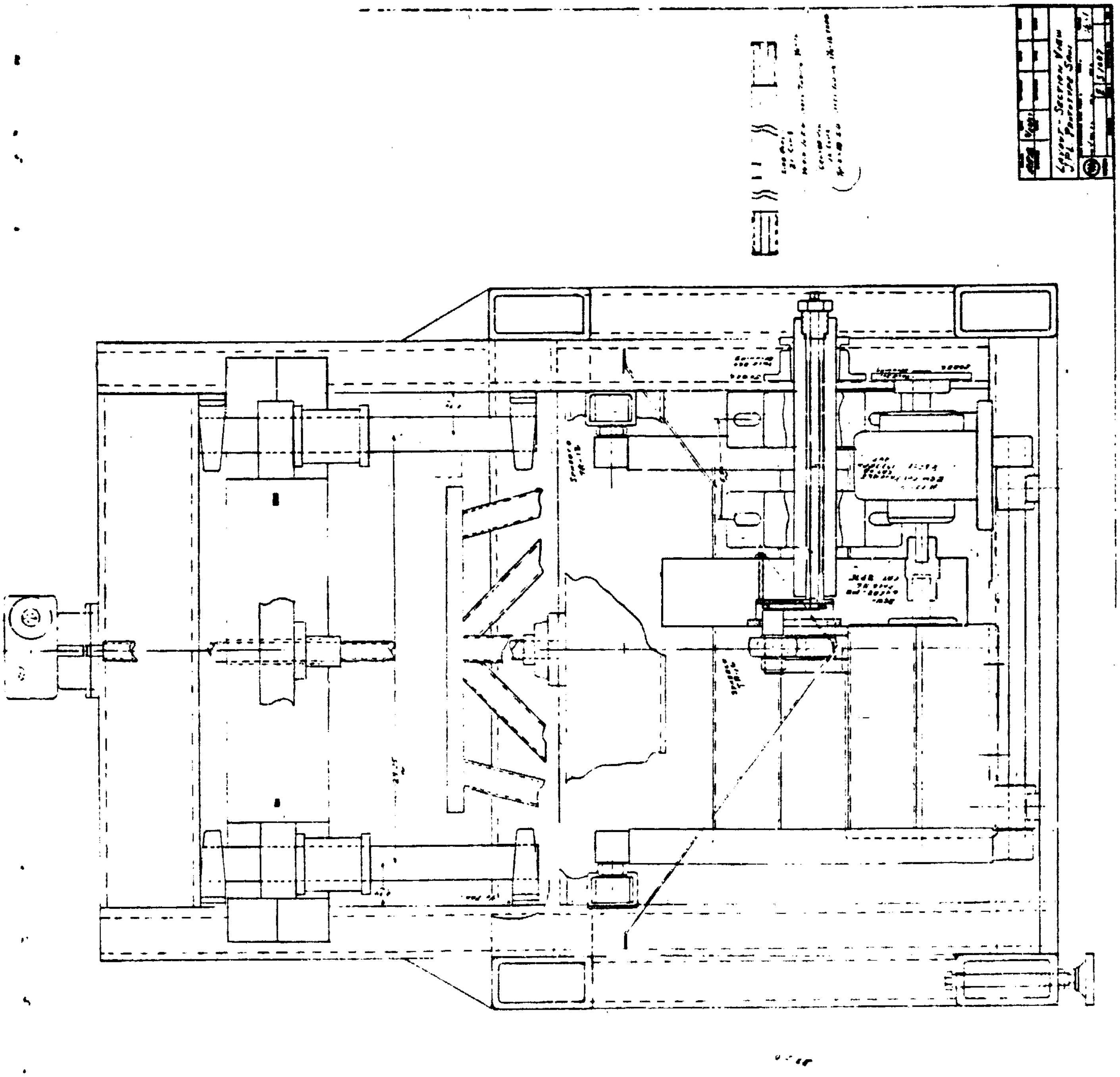

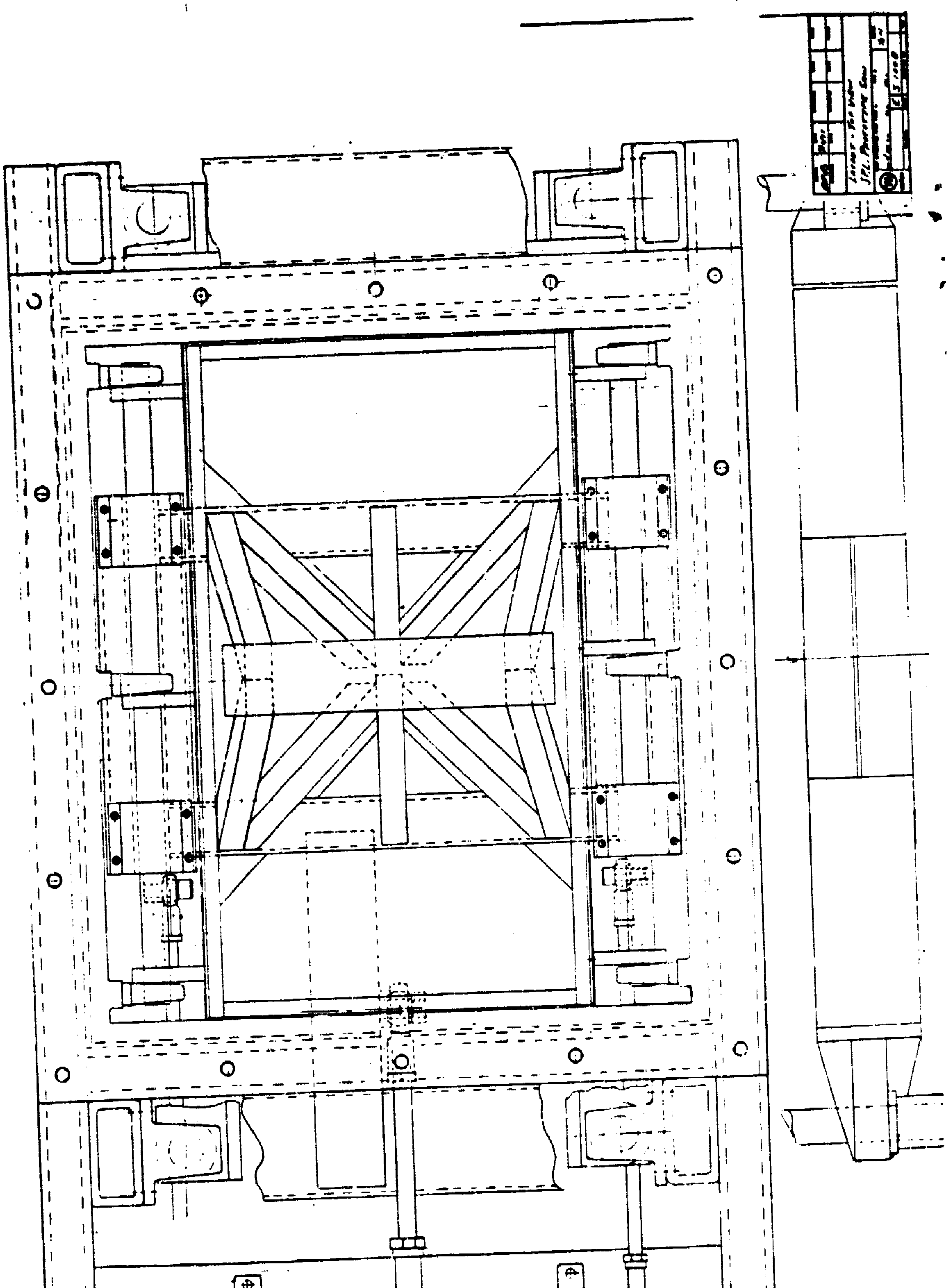
Layout - Top View
J.P.L. Prototype Saw
C
S 1000

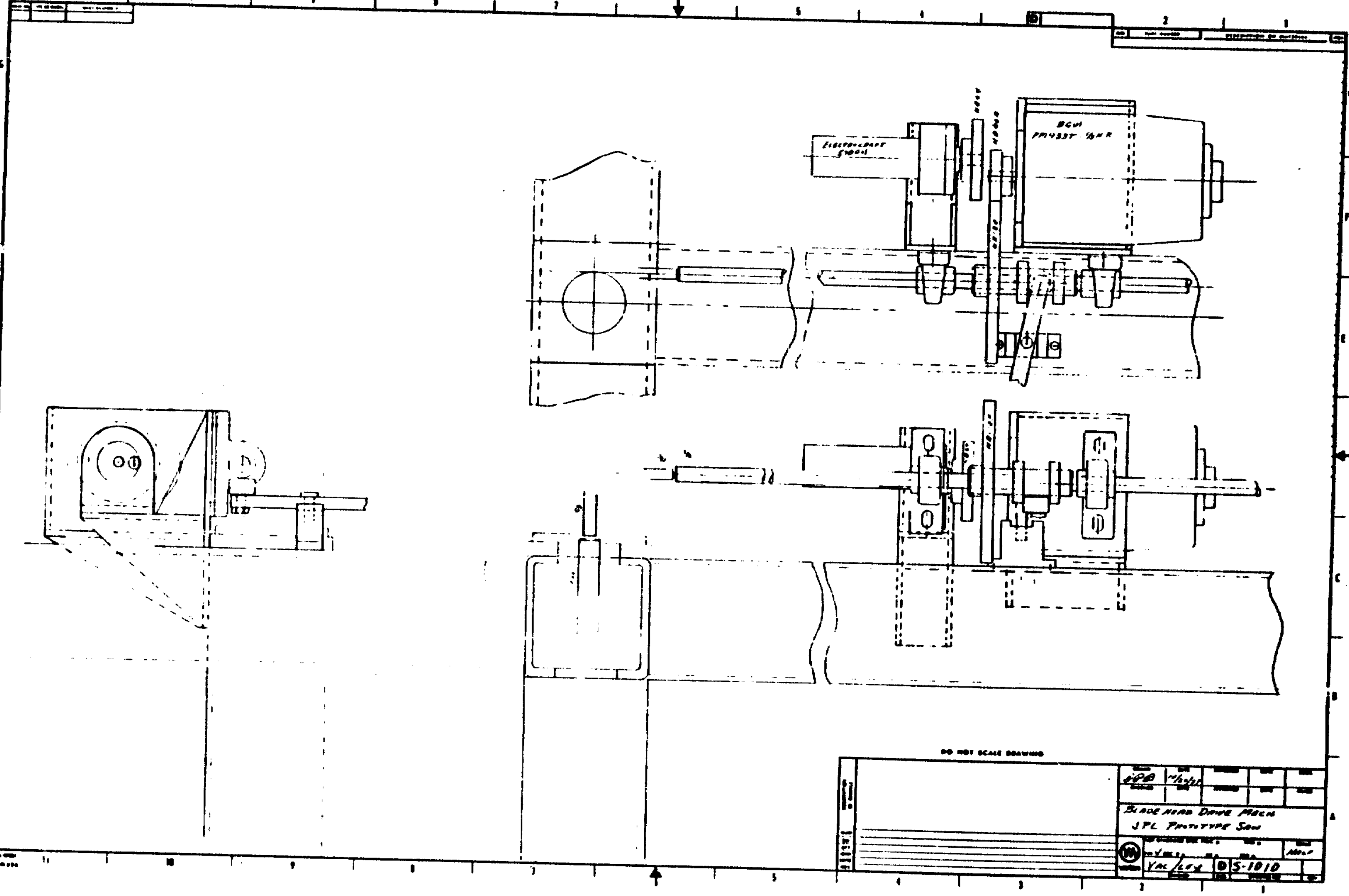

DO NOT SCALE DRAWING

BLADE HEAD DRIVE MECH
JPL PROTOTYPE SAW

D S-1010

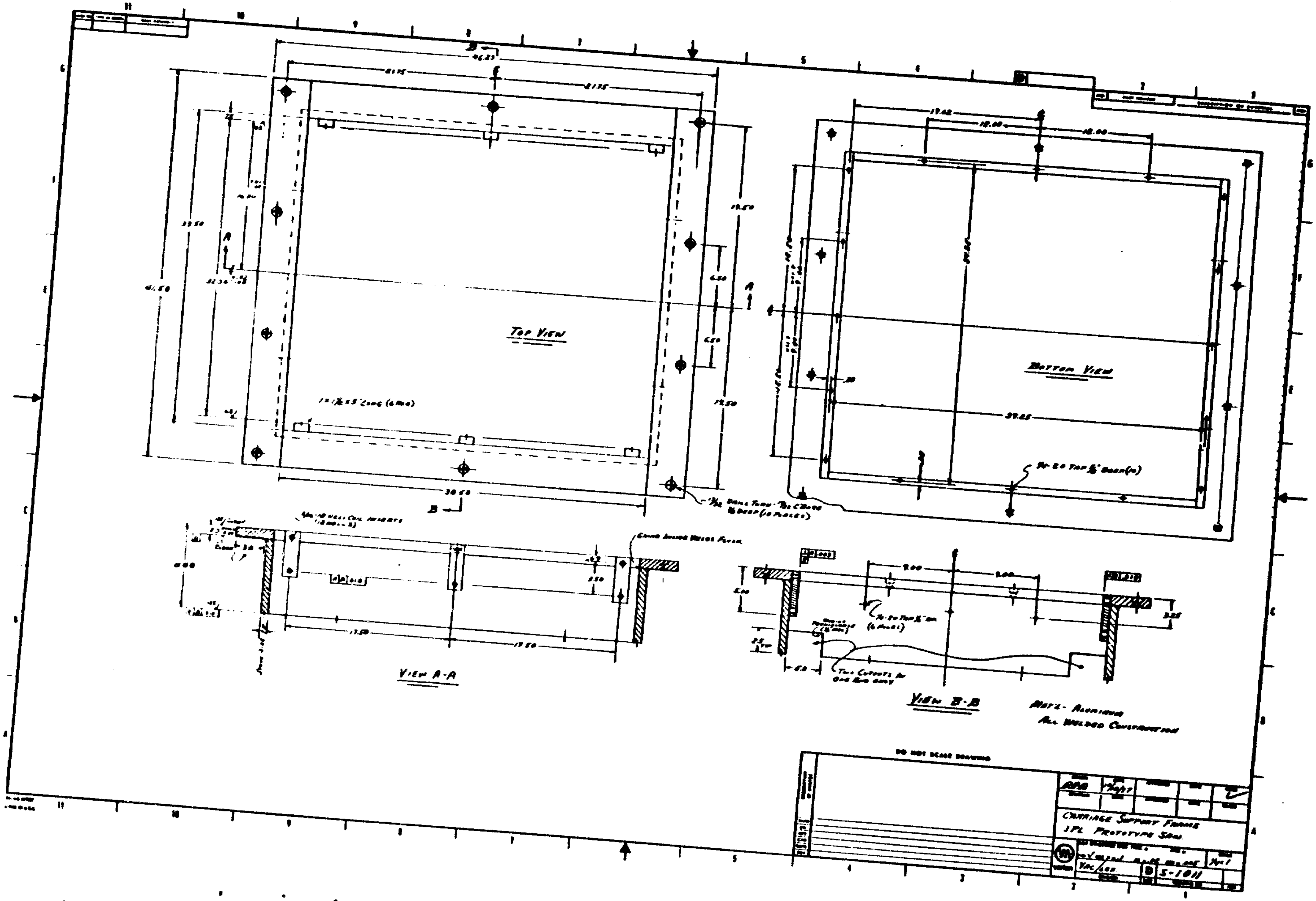

TOP VIEW
BOTTOM VIEW
VIEW A-A
VIEW B-B
MAT'L - ALUMINUM
ALL WELDED CONSTRUCTION
DO NOT SCALE DRAWING
CARRIAGE SUPPORT FRAME
JPL PROTOTYPE SAW
S-1011

REPRODUCIBILITY OF THE ORIGINAL PAGE IS POOR

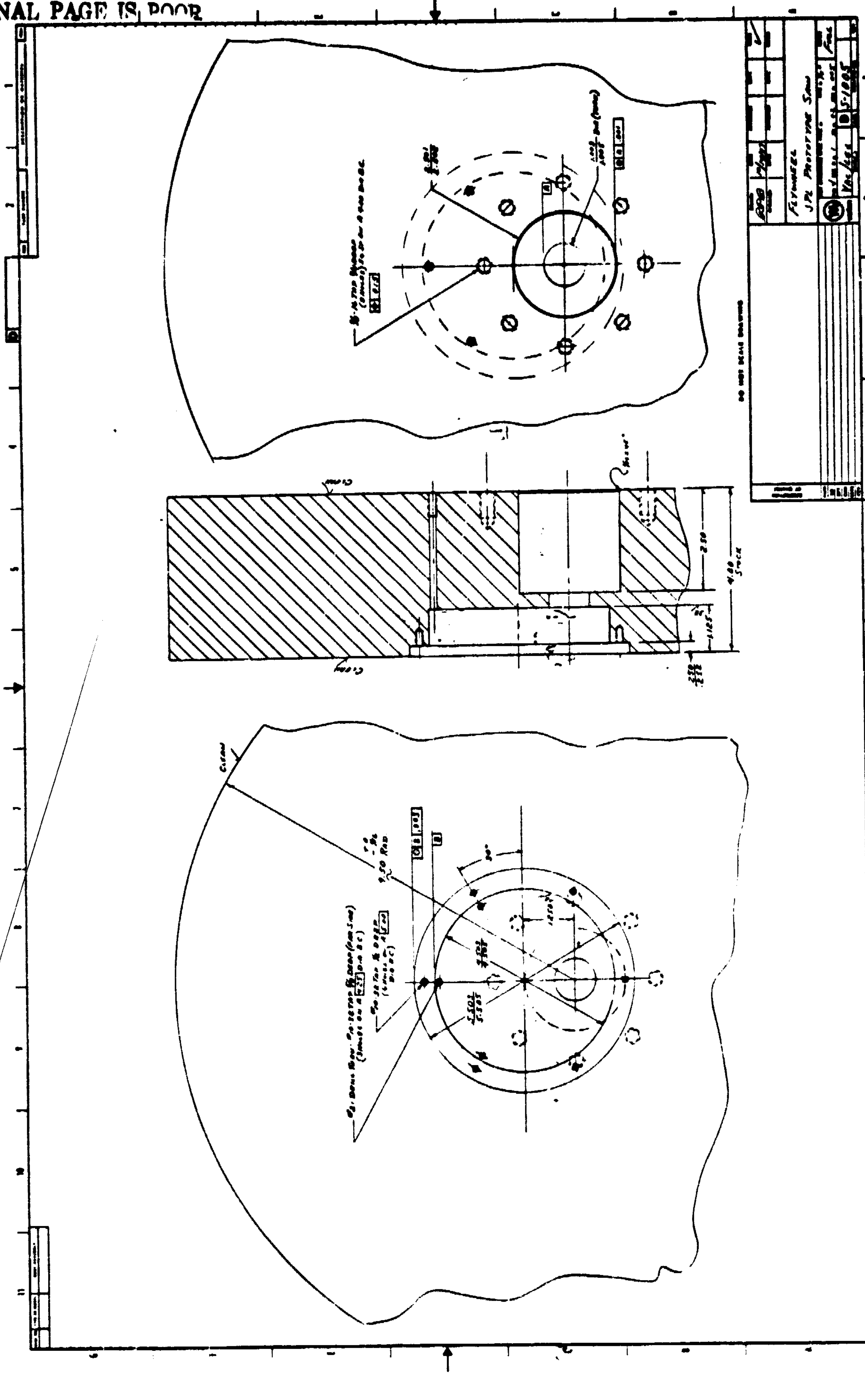

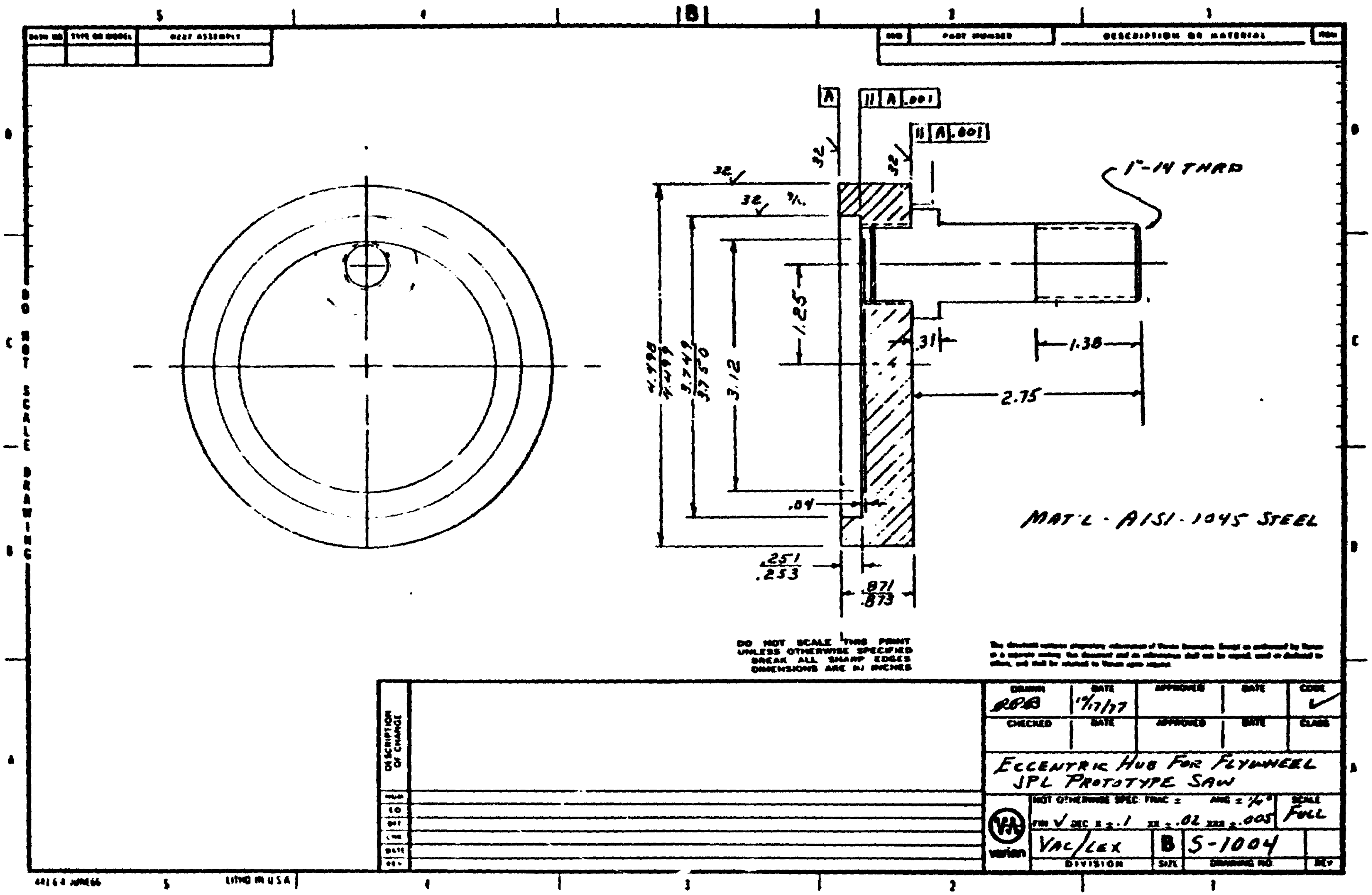
1"-14 THRD
MAT'L - AISI-1045 STEEL
1.38
2.75
.31
1.25
3.12
3.749
3.750
4.498
4.499
.04
.251
.253
.871
.873
A
// A .001
DO NOT SCALE THIS PRINT
UNLESS OTHERWISE SPECIFIED
BREAK ALL SHARP EDGES
DIMENSIONS ARE IN INCHES
DRAWN RPB
DATE 10/17/77
ECCENTRIC HUB FOR FLYWHEEL
JPL PROTOTYPE SAW
SCALE FULL
VAC/LEX
B
S-1004
DIVISION
SIZE
DRAWING NO
varian
DESCRIPTION OF CHANGE
LITHO IN U S A

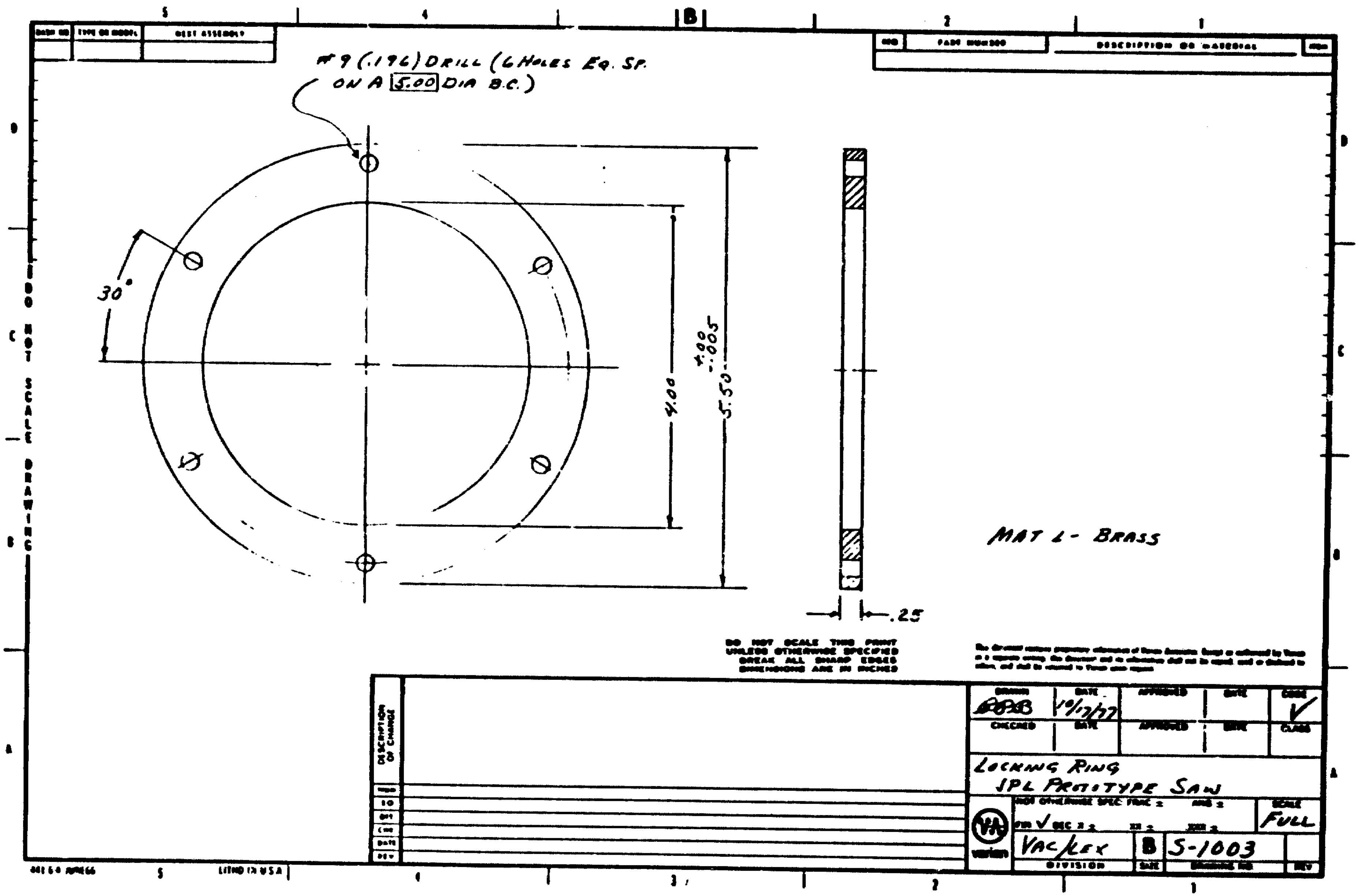
#9 (.196) DRILL (6 HOLES EQ. SP. ON A 5.00 DIA B.C.)
30°
4.00
5.50 +.00 -.005
.25
MAT'L - BRASS
DO NOT SCALE DRAWING
DO NOT SCALE THIS PRINT UNLESS OTHERWISE SPECIFIED BREAK ALL SHARP EDGES DIMENSIONS ARE IN INCHES
DESCRIPTION OF CHANGE
DRAWN 10/13/77
CHECKED
APPROVED
LOCKING RING
JPL PROTOTYPE SAW
SCALE FULL
VAC/LEX
DIVISION
SIZE B
DRAWING NO. S-1003
REV
varian
LITHO IN U.S.A.

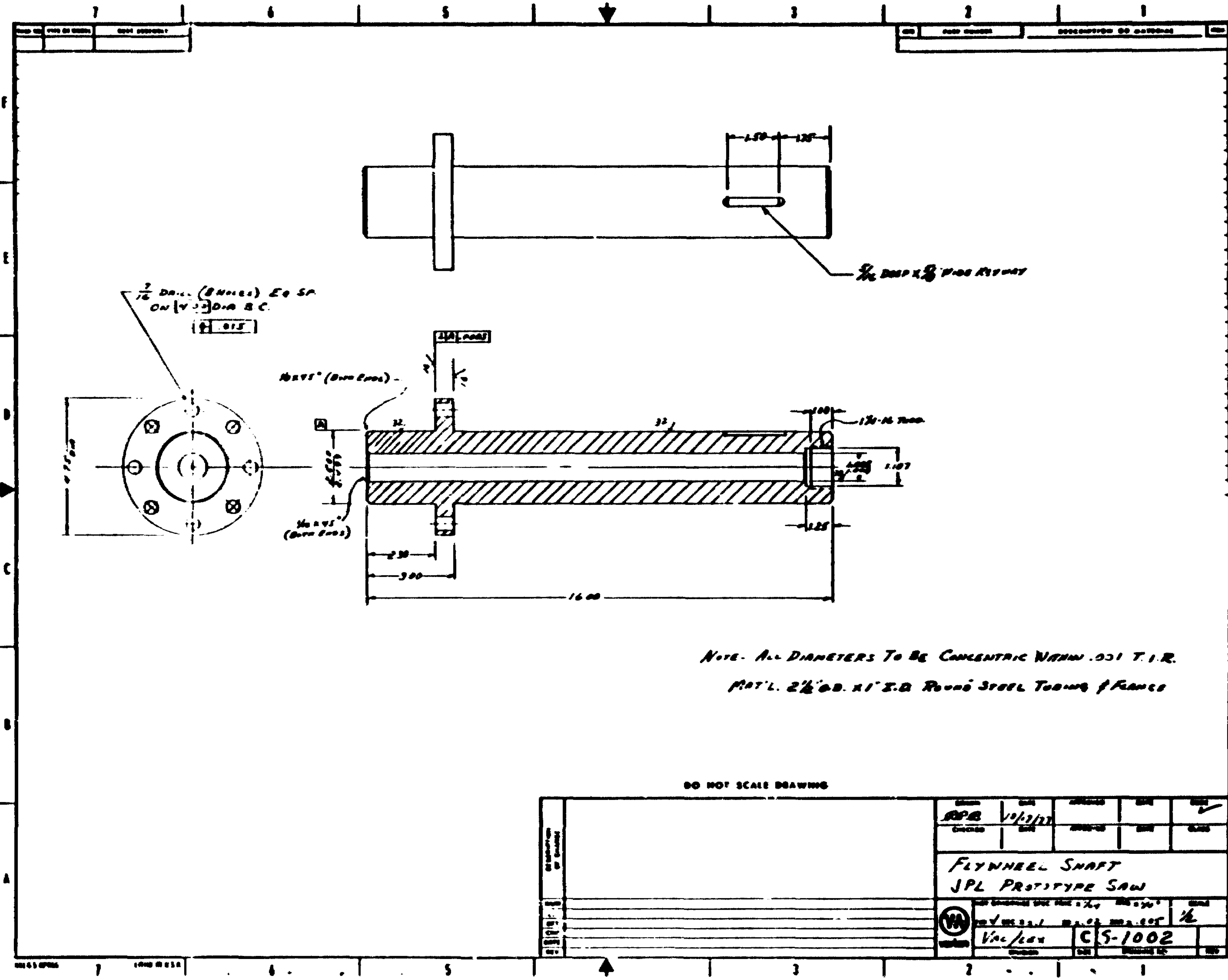

7/16 DRILL (8 HOLES) EQ SP. ON [?] DIA B.C.
5/16 DEEP x 3/8 WIDE KEYWAY
1.50
1.25
16.00
3.00
2.30
1 3/4-16 THRD.
NOTE- ALL DIAMETERS TO BE CONCENTRIC WITHIN .001 T.I.R.
MAT'L. 2 7/8" O.D. x 1" I.D. ROUND STEEL TUBING & FLANGE
DO NOT SCALE DRAWING
FLYWHEEL SHAFT
JPL PROTOTYPE SAW
C
S-1002

DASH NO	TYPE OR MODEL	NEXT ASSEMBLY	REQ	PART NUMBER	DESCRIPTION OR MATERIAL	ITEM

A 5-1012

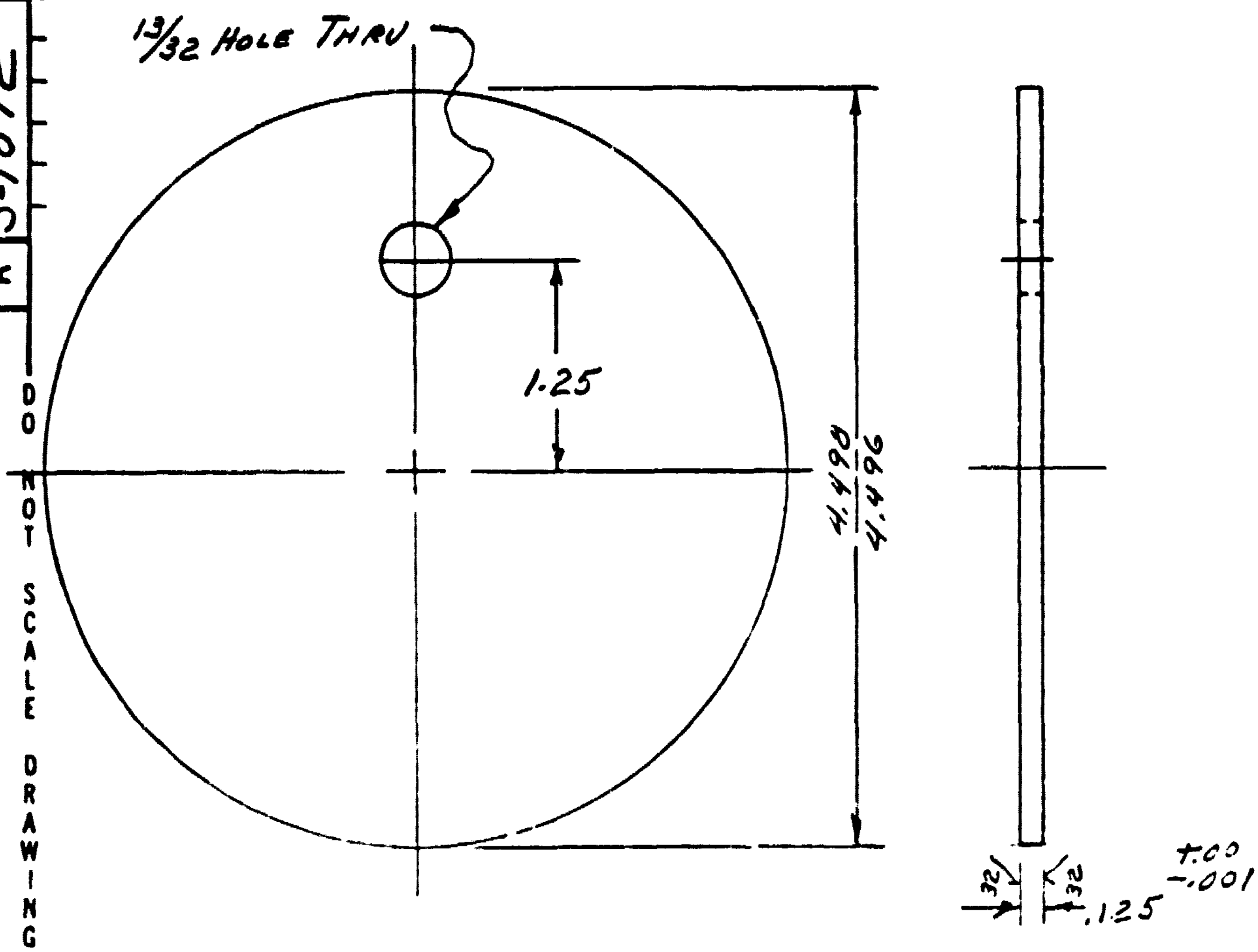

DO NOT SCALE DRAWING

MAT'L - BRASS

DO NOT SCALE THIS PRINT
UNLESS OTHERWISE SPECIFIED
BREAK ALL SHARP EDGES
DIMENSIONS ARE IN INCHES

DRAWN	DATE	APPROVED	DATE	CODE
RPB	10/20/77			✓
CHECKED	DATE	APPROVED	DATE	CLASS

SHIM-STROKE ADJ. MECH.
JPL PROTOTYPE SAW

NOT OTHERWISE SPEC FRAC ±1/64 ANG ±1/2°
FIN ✓ DEC X ± .1 XX ± .02 XXX ± .005

SCALE FULL

varian

DIVISION	SIZE	DRAWING NO.	REV
VAC/LEX	A	5-1012	

DESCRIPTION OF CHANGE	
NUM	
EO	
DFT	
CHK	
DATE	
REV	

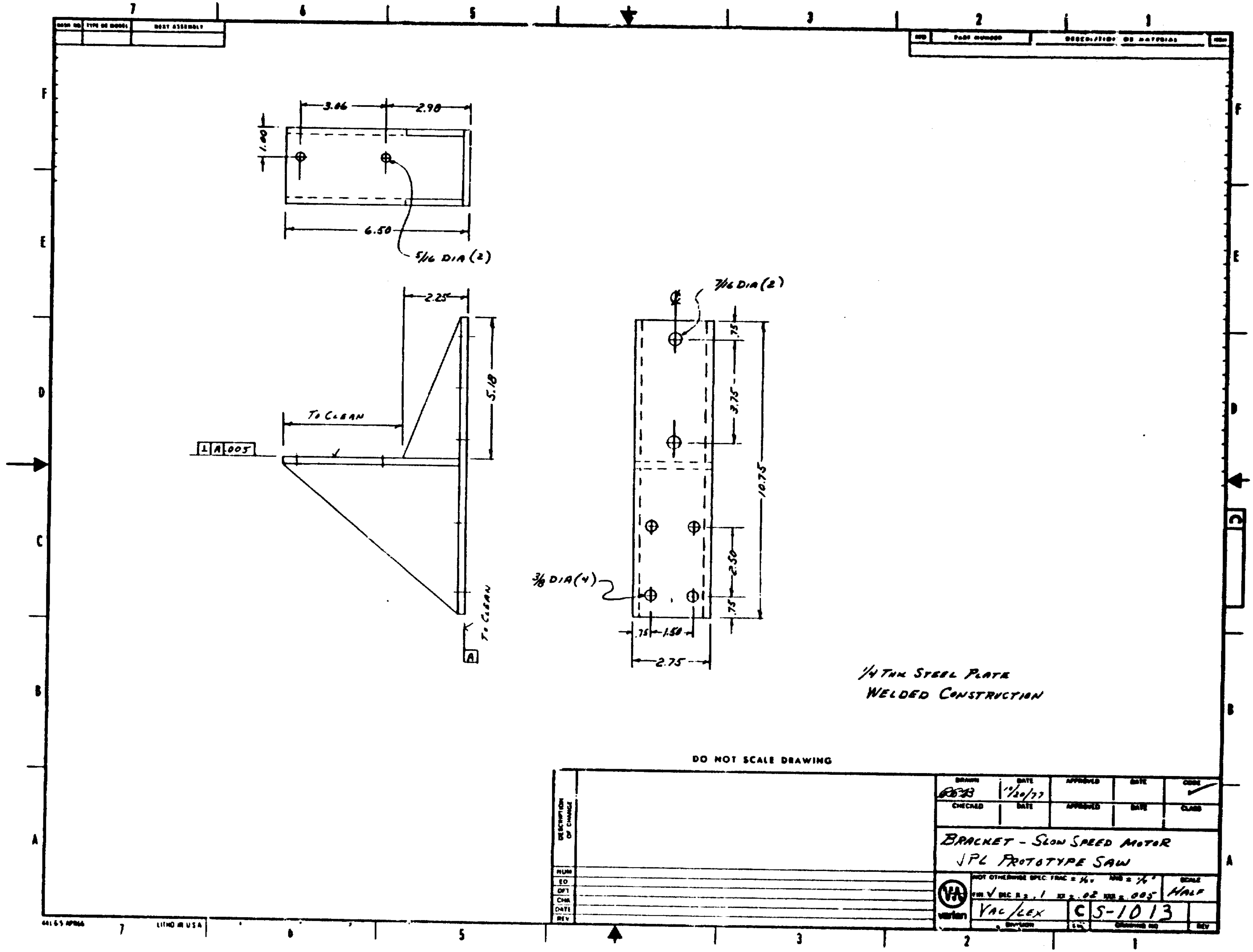
3.06
2.98
1.00
6.50
5/16 DIA (2)
2.25
5.18
TO CLEAN
⊥ A .005
TO CLEAN
A
7/16 DIA (2)
.75
3.75
10.75
2.50
.75
3/8 DIA (4)
.75
1.50
2.75
1/4 THK STEEL PLATE
WELDED CONSTRUCTION
DO NOT SCALE DRAWING
DRAWN
DATE
10/20/77
CHECKED
DATE
APPROVED
DATE
CODE
CLASS
BRACKET - SLOW SPEED MOTOR
JPL PROTOTYPE SAW
varian
VAC/LEX
C S-1013
SCALE HALF
DESCRIPTION OF CHANGE
LITHO IN USA

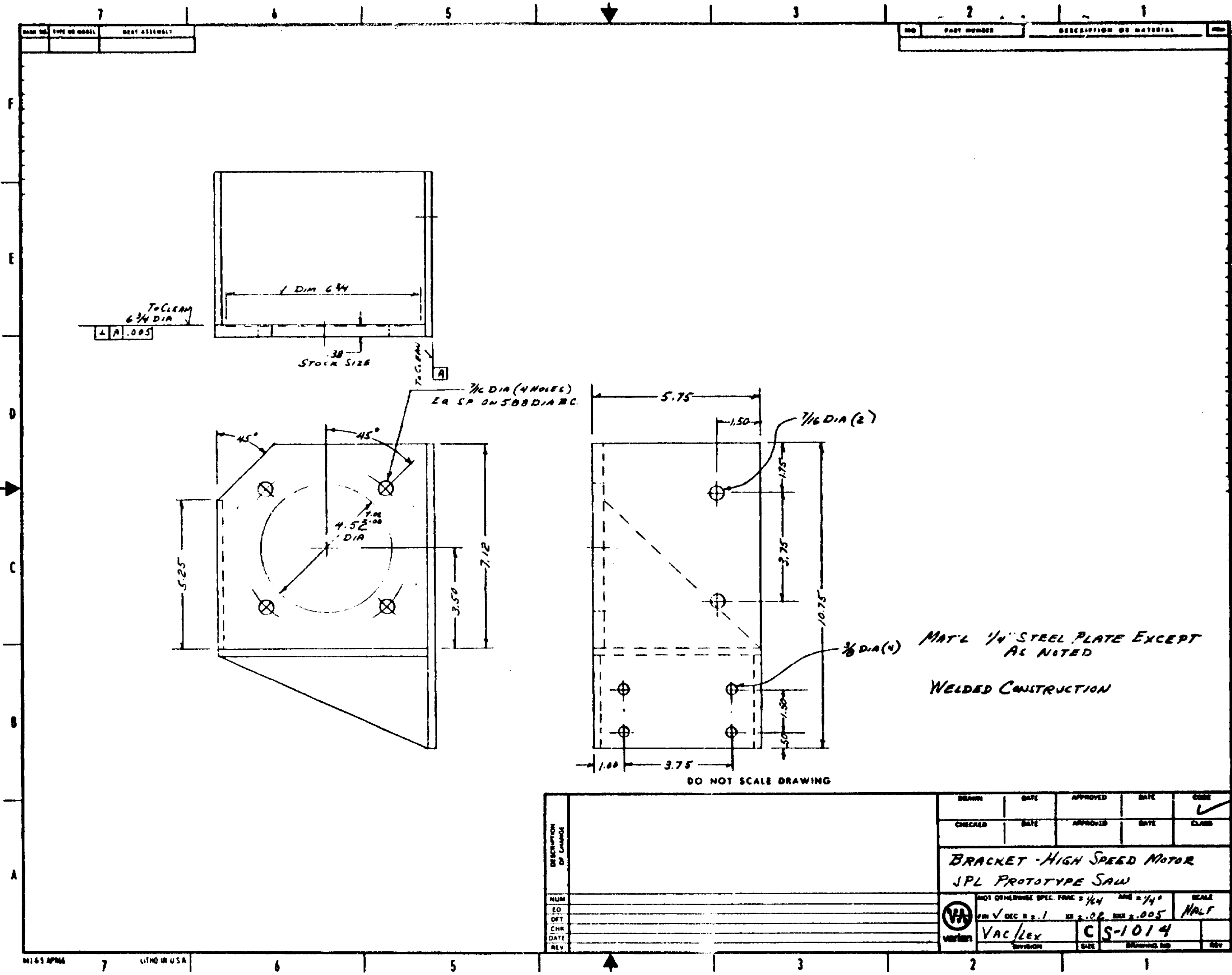

MAT'L 1/4" STEEL PLATE EXCEPT AS NOTED
WELDED CONSTRUCTION
DO NOT SCALE DRAWING
7/16 DIA (4 HOLES) EA SP ON 5.88 DIA B.C.
7/16 DIA (2)
3/8 DIA (4)
4.52 DIA
STOCK SIZE
TO CLEAN 6 3/4 DIA
BRACKET - HIGH SPEED MOTOR
JPL PROTOTYPE SAW
HALF
VAC/LEX
C
S-1014
varian

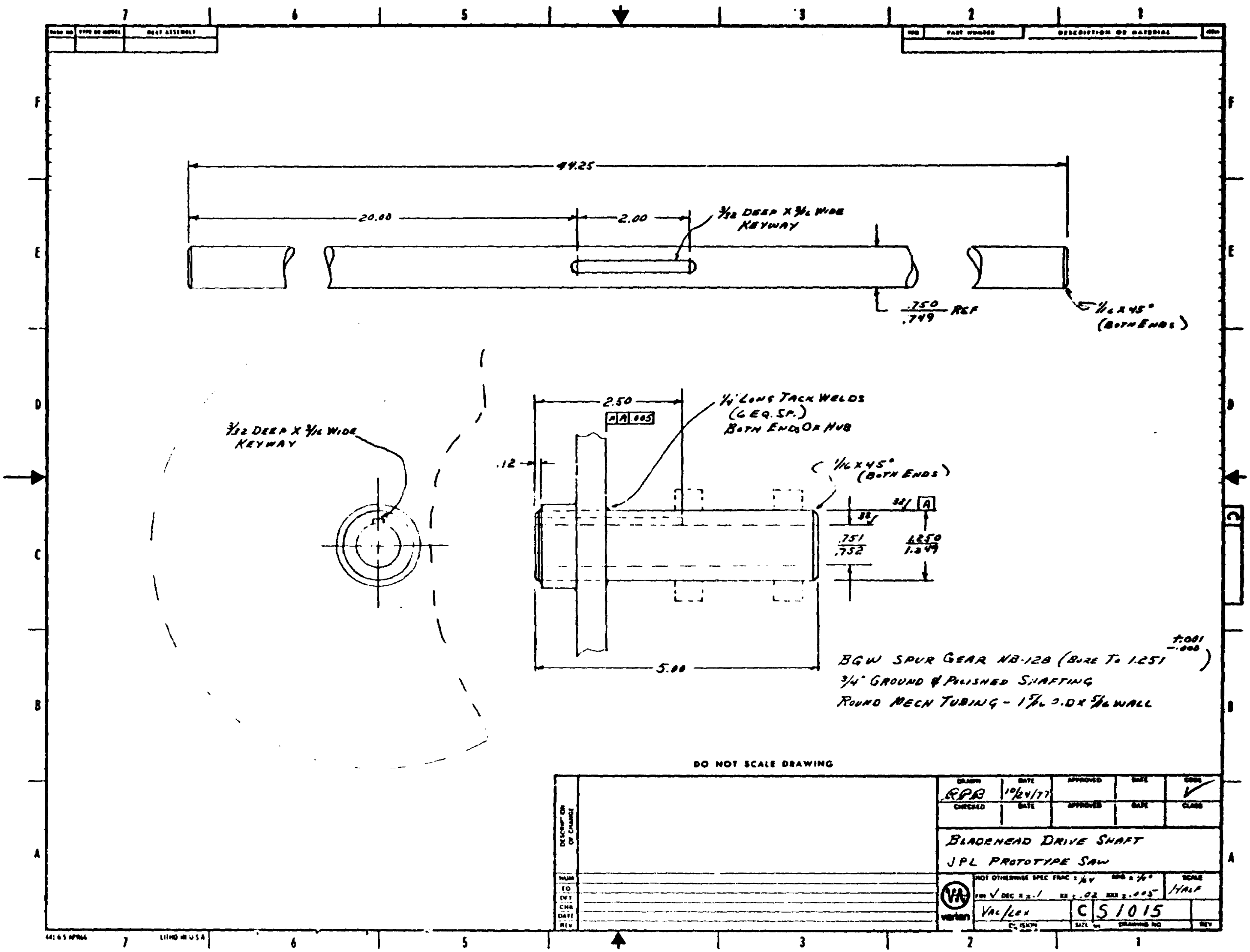

44.25
20.00
2.00
3/32 DEEP X 3/16 WIDE KEYWAY
.750 / .749 REF
1/16 x 45° (BOTH ENDS)
3/32 DEEP X 3/16 WIDE KEYWAY
2.50
1/4" LONG TACK WELDS (6 EQ. SP.) BOTH ENDS OF HUB
.12
1/16 x 45° (BOTH ENDS)
.751 / .752
1.250 / 1.249
5.00
BGW SPUR GEAR NB-128 (BORE TO 1.251 +.001 -.000)
3/4" GROUND & POLISHED SHAFTING
ROUND MECH TUBING - 1 1/4 O.D X 5/16 WALL
DO NOT SCALE DRAWING
DRAWN RPB DATE 10/24/77
CHECKED
BLADEHEAD DRIVE SHAFT
JPL PROTOTYPE SAW
SCALE HALF
VAC/LEX
C S1015
LITHO IN U.S.A.

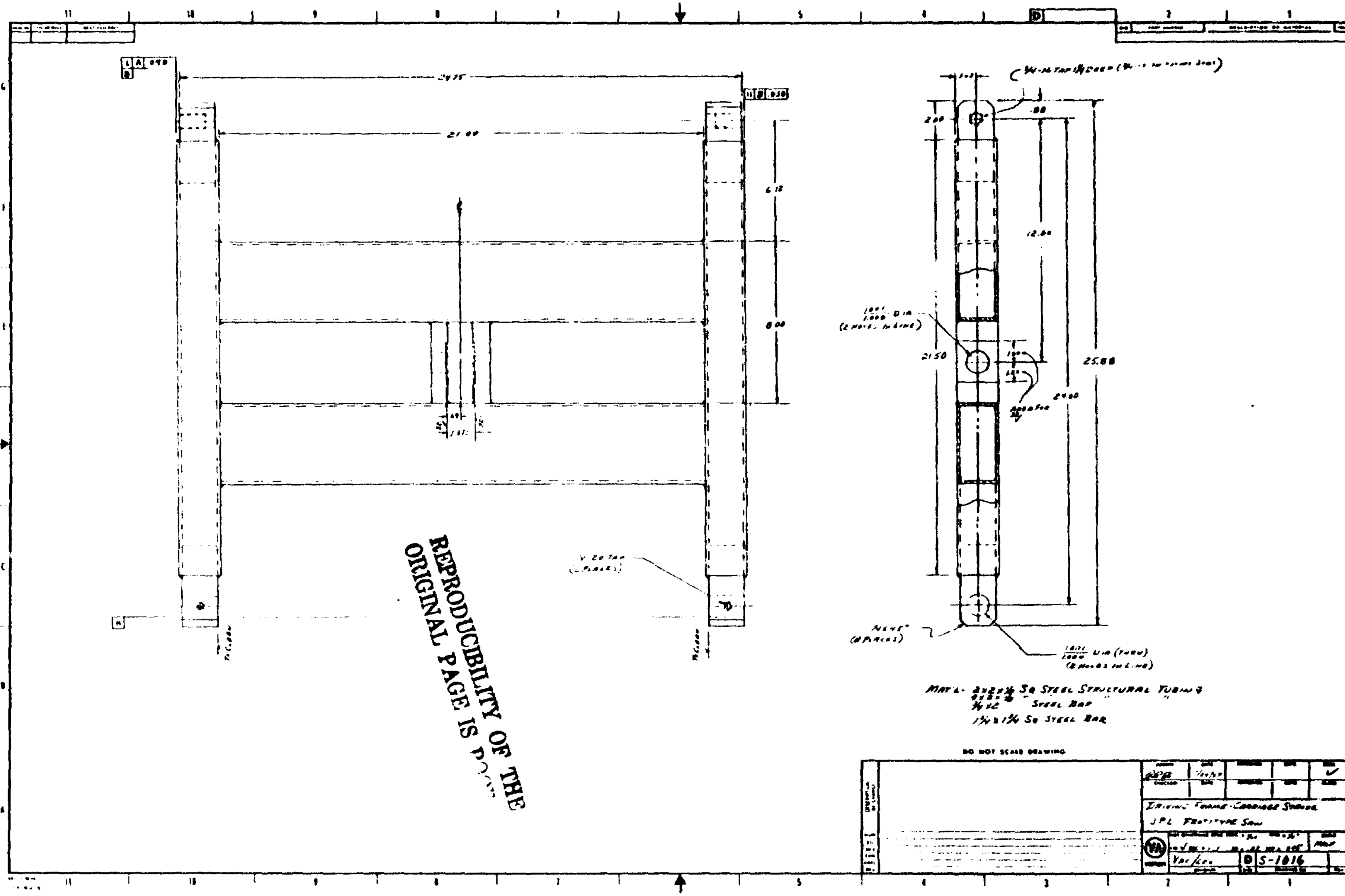
24.75
21.00
6.12
8.00
25.88
24.00
21.50
12.00
2.00
.88
1.50
MAT'L- 2x2x¼ SQ STEEL STRUCTURAL TUBING
1¾x1¾ SQ STEEL BAR
DO NOT SCALE DRAWING
JPL PROTOTYPE SAW
D S-1016

DASH NO.	TYPE OR MODEL	NEXT ASSEMBLY	REQ	PART NUMBER	DESCRIPTION OR MATERIAL	ITEM

A S-1018

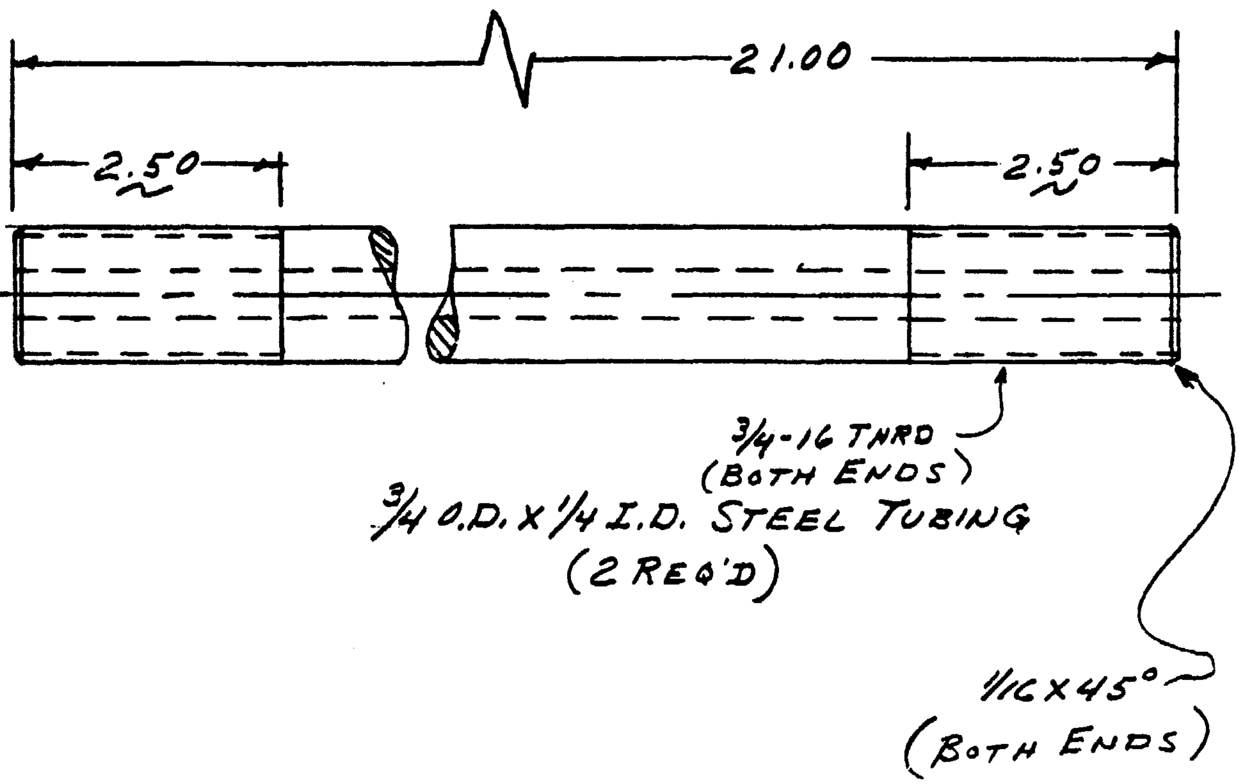

DO NOT SCALE DRAWING

DO NOT SCALE THIS PRINT
UNLESS OTHERWISE SPECIFIED
BREAK ALL SHARP EDGES
DIMENSIONS ARE IN INCHES

DRAWN	DATE	APPROVED	DATE	CODE
RPB	10/24/77			L
CHECKED	DATE	APPROVED	DATE	CLASS

SIDE RODS - CARRIAGE STROKE
JPL PROTOTYPE SAW

DESCRIPTION OF CHANGE

NUM	
EO	
DFT	
CHK	
DATE	
REV	

NOT OTHERWISE SPEC: FRAC ± 1/64 ANG ± 1/4° SCALE FULL
FIN. ✓ DEC .X ± .1 .XX ± .02 .XXX ± .005

varian

DIVISION	SIZE	DRAWING NO.	REV
VAC/LEX	A	S-1018	

DASH NO	TYPE OR MODEL	NEXT ASSEMBLY	REQ	PART NUMBER	DESCRIPTION OR MATERIAL	ITEM

A S1019

DO NOT SCALE DRAWING

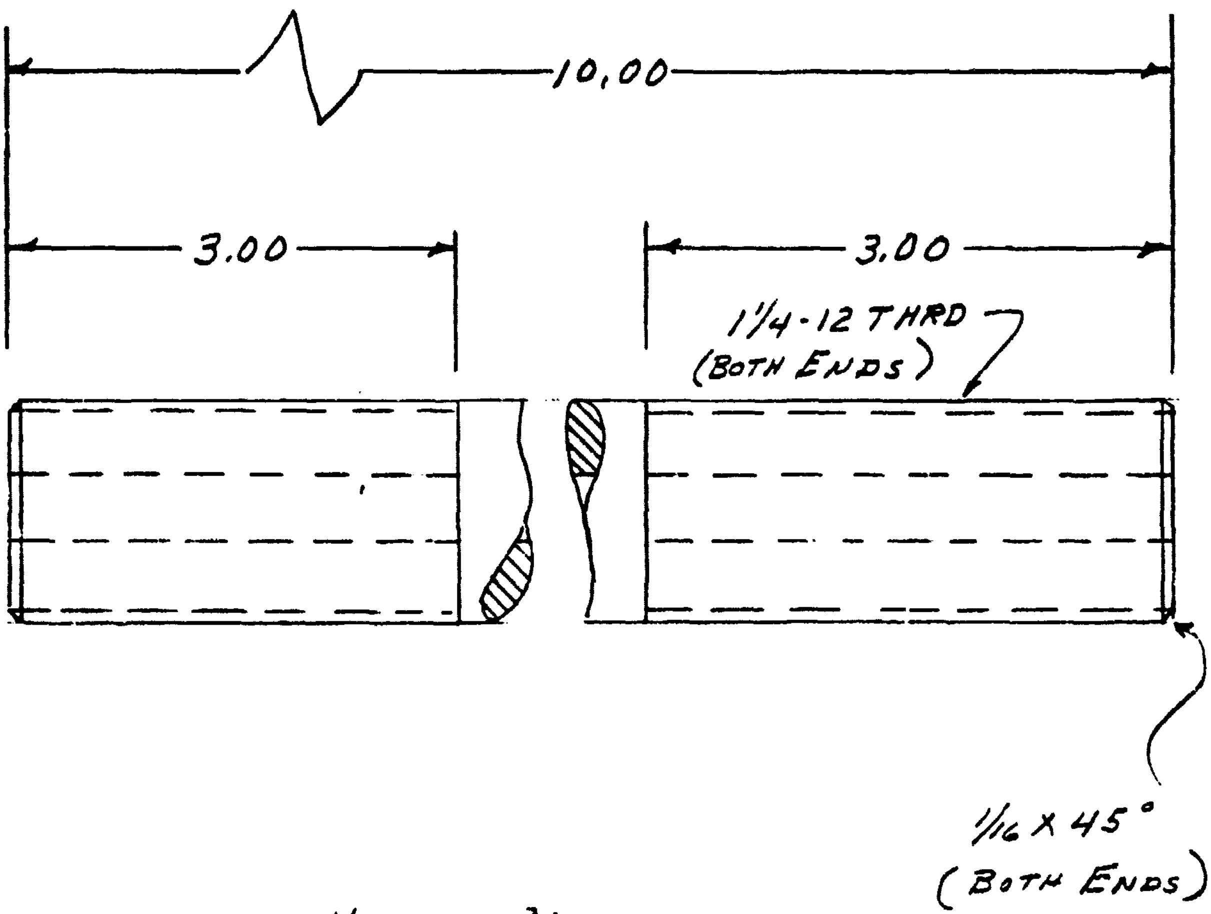

MAT'L - 1¼ O.D. X 3/8 I.D.
STEEL TUBING

DO NOT SCALE THIS PRINT
UNLESS OTHERWISE SPECIFIED
BREAK ALL SHARP EDGES
DIMENSIONS ARE IN INCHES

DRAWN	DATE	APPROVED	DATE	CODE
G.P.B.	10/25/77			✓
CHECKED	DATE	APPROVED	DATE	CLASS

MAIN DRIVE LINK
JPL PROTOTYPE SAW

NOT OTHERWISE SPEC: FRAC ± 1/64 ANG ± 1/4°
FIN. ✓ DEC .X ± .1 .XX ± .02 .XXX ± .005

SCALE FULL

varian

DIVISION	SIZE	DRAWING NO.	REV
VAC/LEX	A	S1019	

DESCRIPTION OF CHANGE

NUM	
EO	
DFT	
CHK	
DATE	
REV	

DESCRIPTION OF MATERIAL
SNAP RING # N5000-244
BEARING - MRC 7305

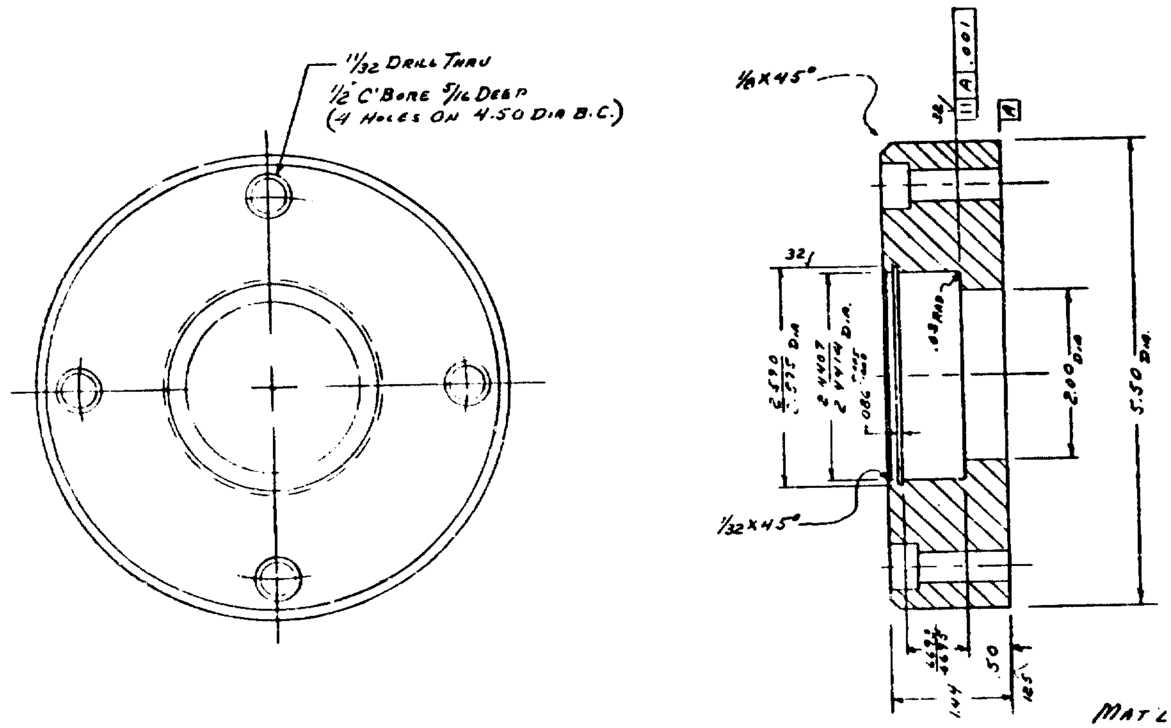

MAT'L. - 5 1/2 DIA STEEL

DO NOT SCALE DRAWING

DRAWN	DATE	APPROVED	DATE	CODE
RPB	11/25/77			
CHECKED	DATE	APPROVED	DATE	CLASS

BEARING MOUNT - BALL SCREW
J.P.L. PROTOTYPE SAW

UNLESS OTHERWISE SPEC: FRAC ± 1/64, ANG ± 1/4°, DEC X ± .1, XX ± .02, XXX ± .005
SCALE: FULL

varian — VAC/LEX

SIZE: C — DRAWING NO: S1020

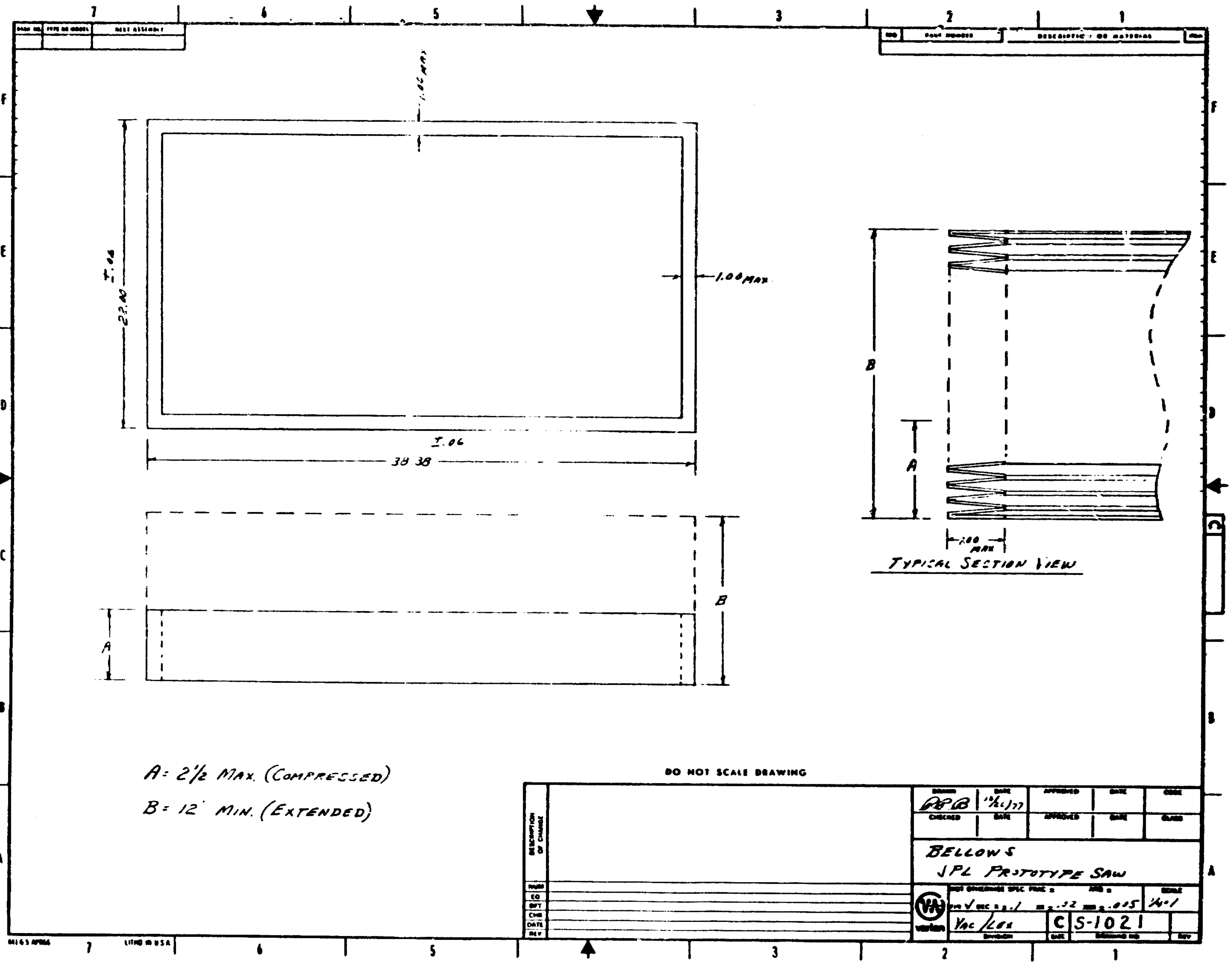
1.00 MAX
1.06 MAX
I.06
22.00
38 38
1.00 MAX
B
A
.100 MAX
TYPICAL SECTION VIEW
A: 2½ MAX. (COMPRESSED)
B: 12" MIN. (EXTENDED)
DO NOT SCALE DRAWING
BELLOWS
JPL PROTOTYPE SAW
RPB 12/21/77
Vac/Lex
C S-1021
¼=1
varian

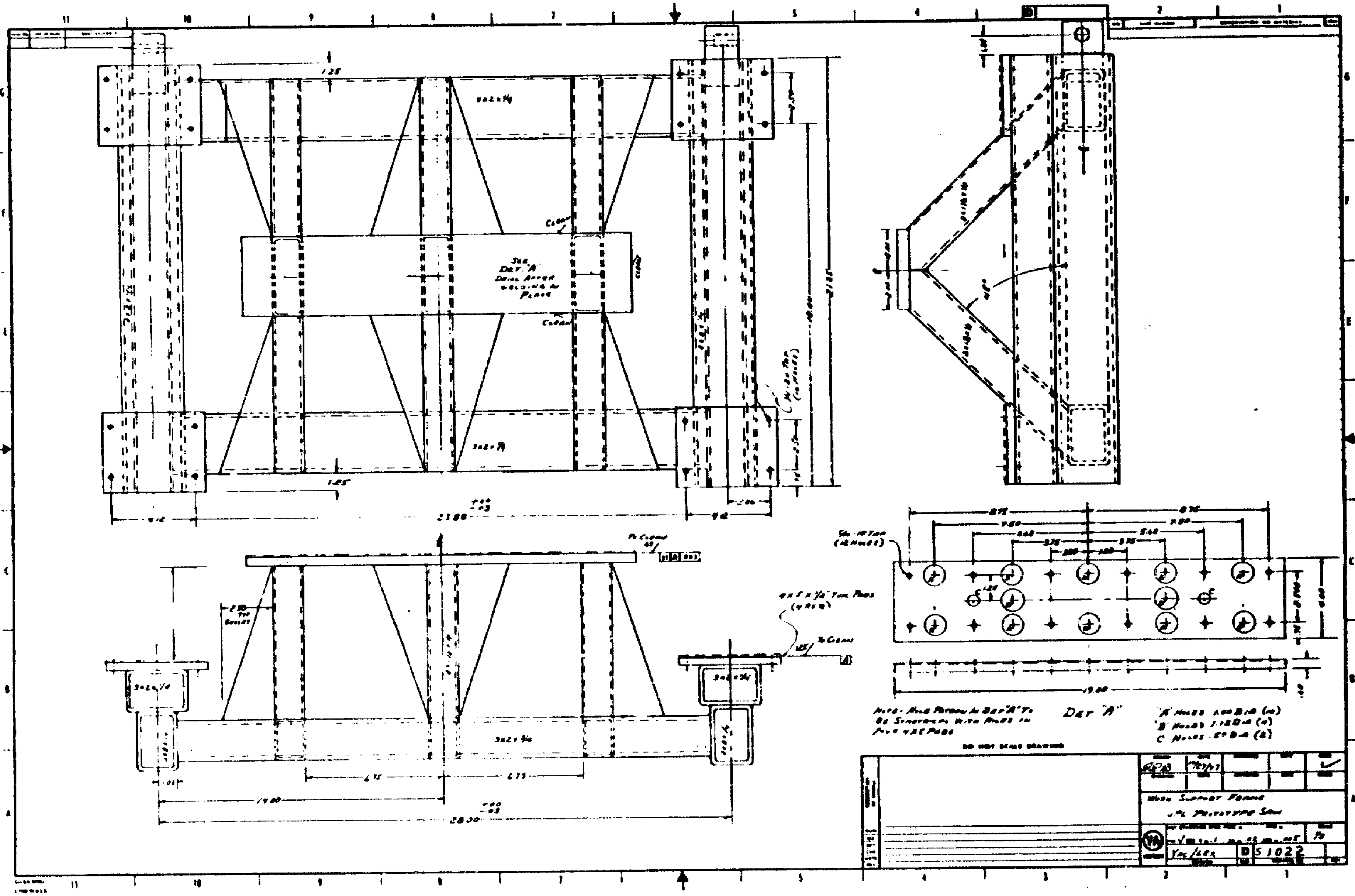
See Det. "A" Drill After Welding in Place
Det. "A"
Note - Hole Pattern in Det "A" To Be Symmetrical With Holes in Five 4x6 Pads
"A" Holes .500 Dia (10)
"B" Holes 1.125 Dia (4)
C Holes .50 Dia (2)
DO NOT SCALE DRAWING
Wood Support Frame
JPL Prototype Saw
D 51022
23.88
28.00
19.00

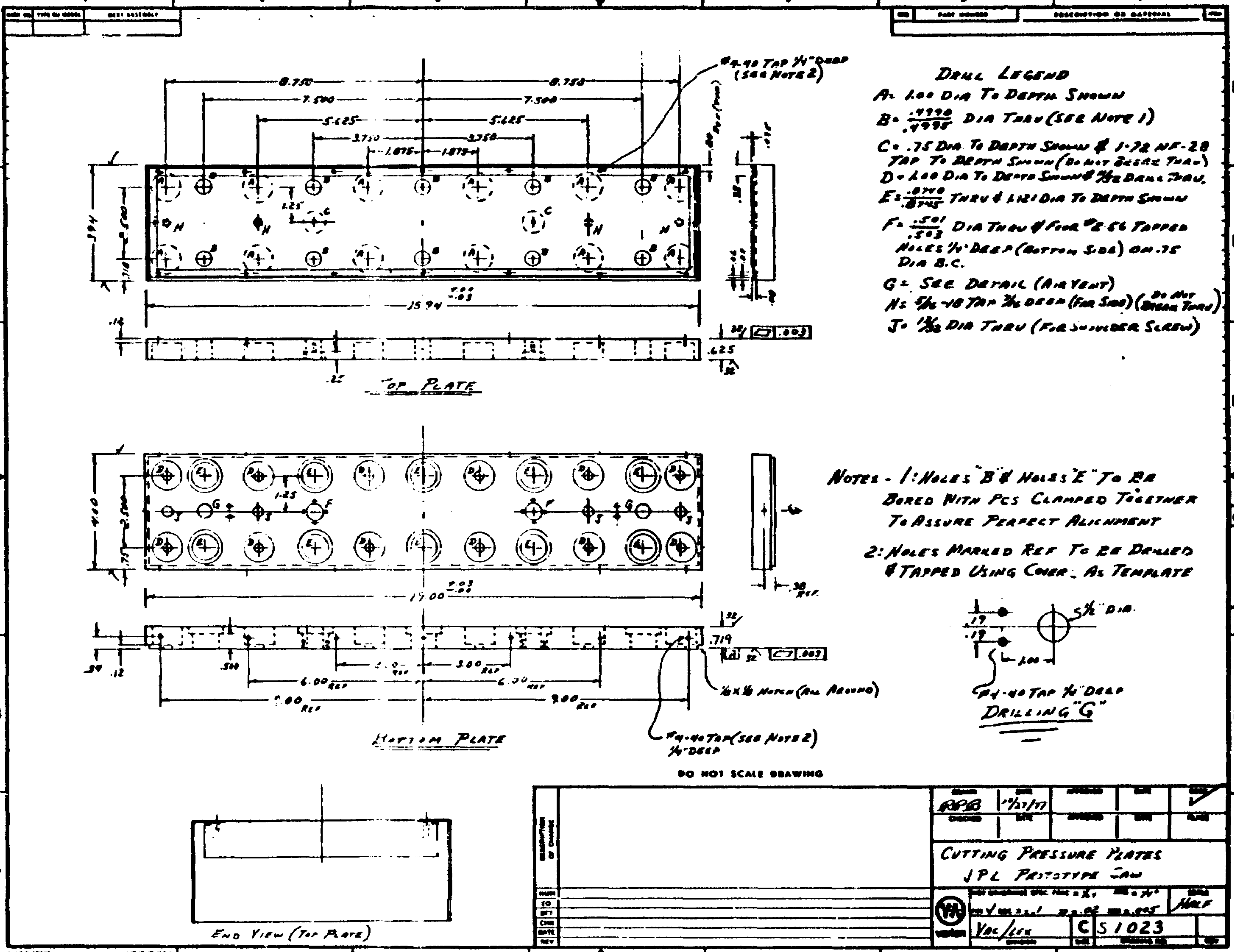
DRILL LEGEND
A= 1.00 DIA TO DEPTH SHOWN
B= .4990/.4995 DIA THRU (SEE NOTE 1)
C= .75 DIA TO DEPTH SHOWN & 1-72 NF-2B TAP TO DEPTH SHOWN (DO NOT BREAK THRU)
D= 1.00 DIA TO DEPTH SHOWN & 11/32 DRILL THRU.
E= .8740/.8745 THRU & 1.121 DIA TO DEPTH SHOWN
F= .501/.503 DIA THRU & FOUR #2-56 TAPPED HOLES 1/4" DEEP (BOTTOM SIDE) ON .75 DIA B.C.
G= SEE DETAIL (AIR VENT)
H= 5/16-18 TAP 3/8 DEEP (FOR SIDE) (DO NOT BREAK THRU)
J= 11/32 DIA THRU (FOR SHOULDER SCREW)
NOTES - 1: HOLES "B" & HOLES "E" TO BE BORED WITH PCS CLAMPED TOGETHER TO ASSURE PERFECT ALIGNMENT
2: HOLES MARKED REF TO BE DRILLED & TAPPED USING COVER AS TEMPLATE
#4-40 TAP 1/4" DEEP (SEE NOTE 2)
TOP PLATE
15.94
BOTTOM PLATE
19.00
1/8 X 1/8 NOTCH (ALL AROUND)
#4-40 TAP (SEE NOTE 2) 1/4" DEEP
5/8" DIA.
#4-40 TAP 1/4" DEEP
DRILLING "G"
DO NOT SCALE DRAWING
END VIEW (TOP PLATE)
CUTTING PRESSURE PLATES
JPL PROTOTYPE SAW
HALF
C S1023

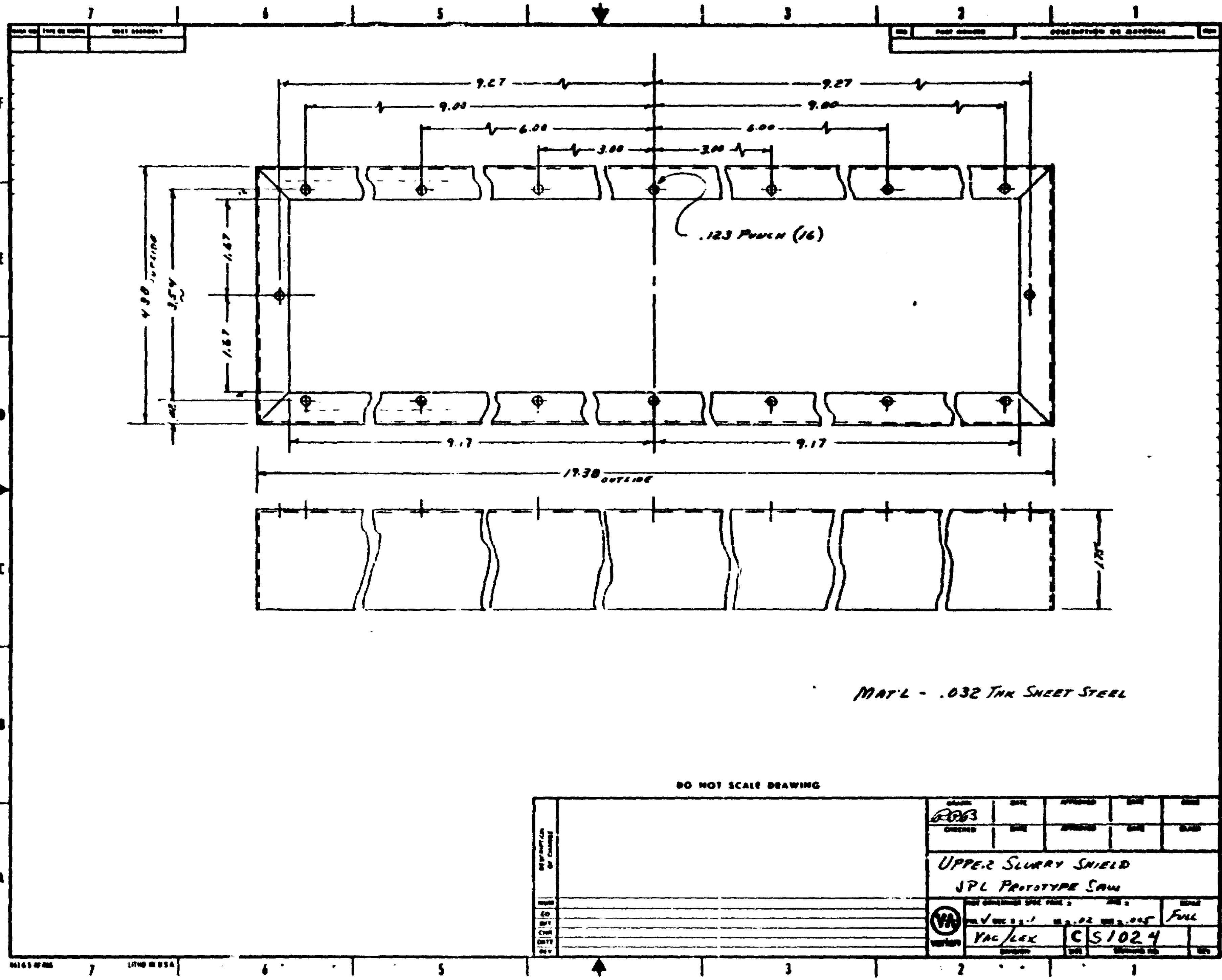
9.27
9.27
9.00
9.00
6.00
6.00
3.00
3.00
.123 PUNCH (16)
4.30 INSIDE
3.54
1.67
1.67
9.17
9.17
19.38 OUTSIDE
1.27
MAT'L - .032 THK SHEET STEEL
DO NOT SCALE DRAWING
UPPER SLURRY SHIELD
JPL PROTOTYPE SAW
FULL
VAC/LEX
C
S1024
varian

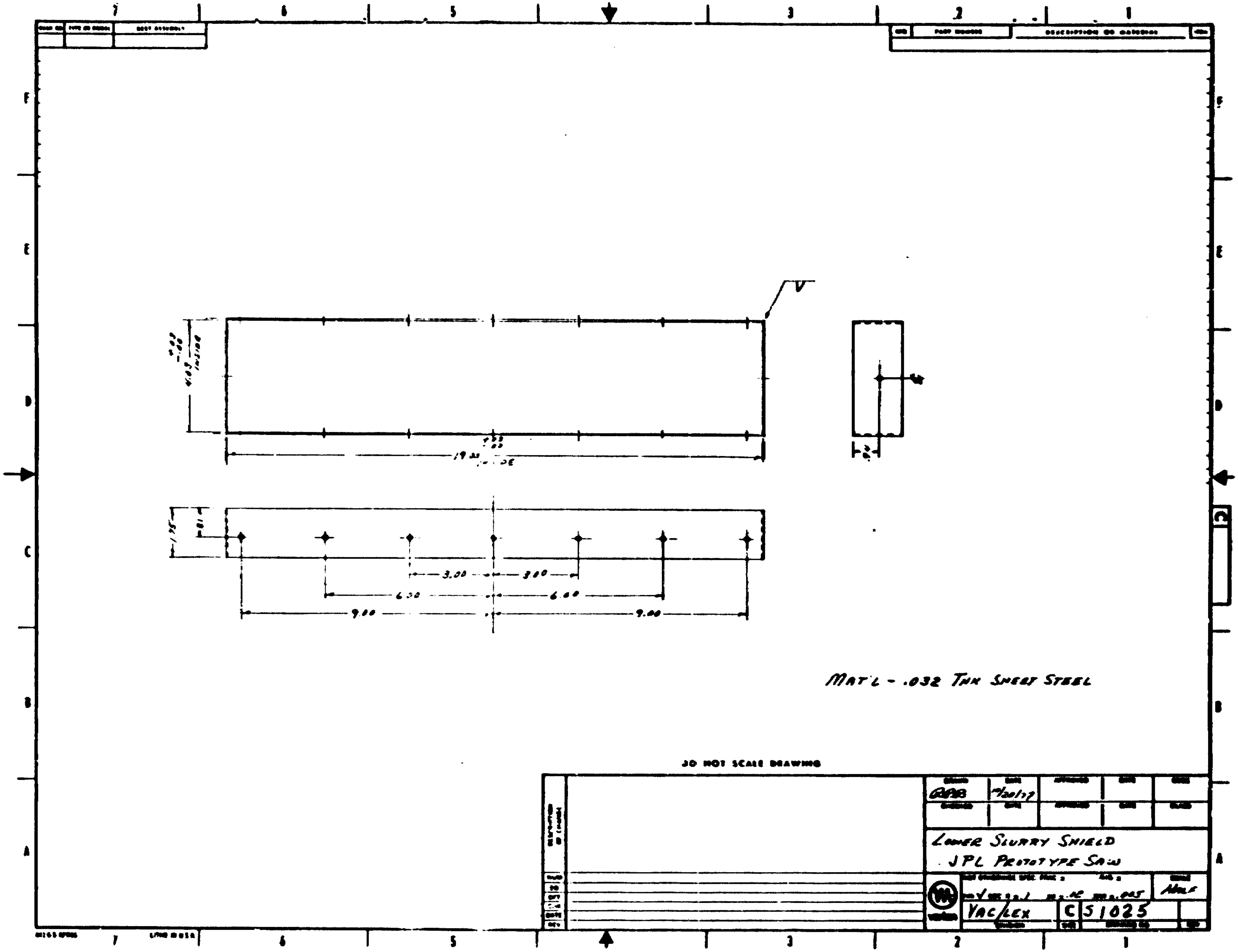

MAT'L - .032 THK SHEET STEEL
DO NOT SCALE DRAWING
3.00
3.00
6.00
6.00
9.00
9.00
19.38
LOWER SLURRY SHIELD
JPL PROTOTYPE SAW
VAC/LEX
C 51025

DASH NO.	TYPE OR MODEL	NEXT ASSEMBLY	REQ	PART NUMBER	DESCRIPTION OR MATERIAL	ITEM
			1		CLAMP TITE COLLAR # 15414 S/S	1

A 51026

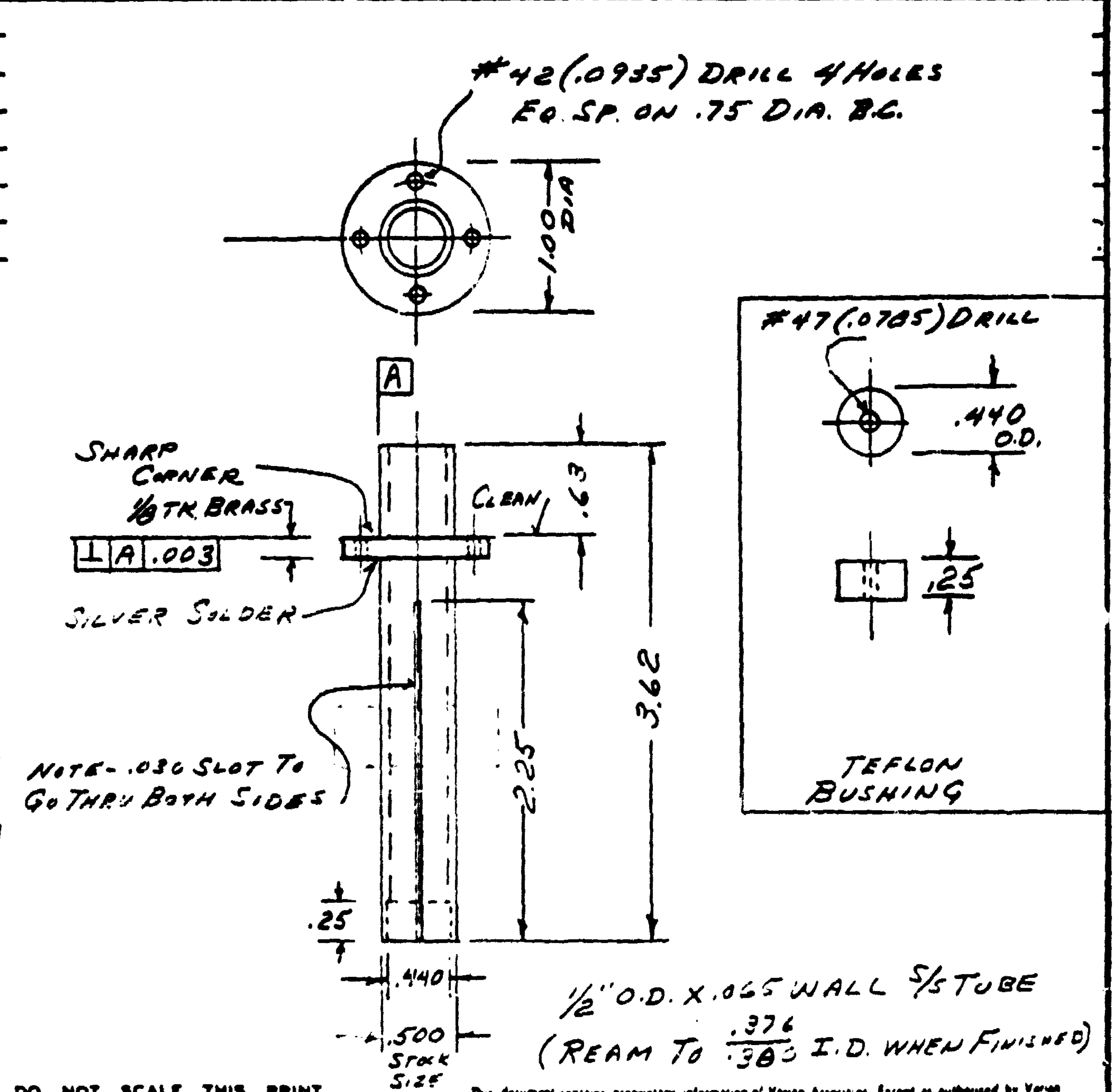

DO NOT SCALE DRAWING

DO NOT SCALE THIS PRINT
UNLESS OTHERWISE SPECIFIED
BREAK ALL SHARP EDGES
DIMENSIONS ARE IN INCHES

DRAWN	DATE	APPROVED	DATE	CODE
RPB				✓
CHECKED	**DATE**	**APPROVED**	**DATE**	**CLASS**

LVDT MOUNTING TUBE
JPL PROTOTYPE SAW

NOT OTHERWISE SPEC: FRAC ± ANG ± SCALE FULL
FIN ✓ DEC X ± .1 XX ± .02 XXX ± .005

DIVISION	SIZE	DRAWING NO.	REV
VAC/LEX	A	51026	

varian

DESCRIPTION OF CHANGE
NUM
EO
DFT
CHK
DATE
REV

DASH NO	TYPE OR MODEL	NEXT ASSEMBLY	REQ	PART NUMBER	DESCRIPTION OR MATERIAL	ITEM

A S-1027

DO NOT SCALE DRAWING

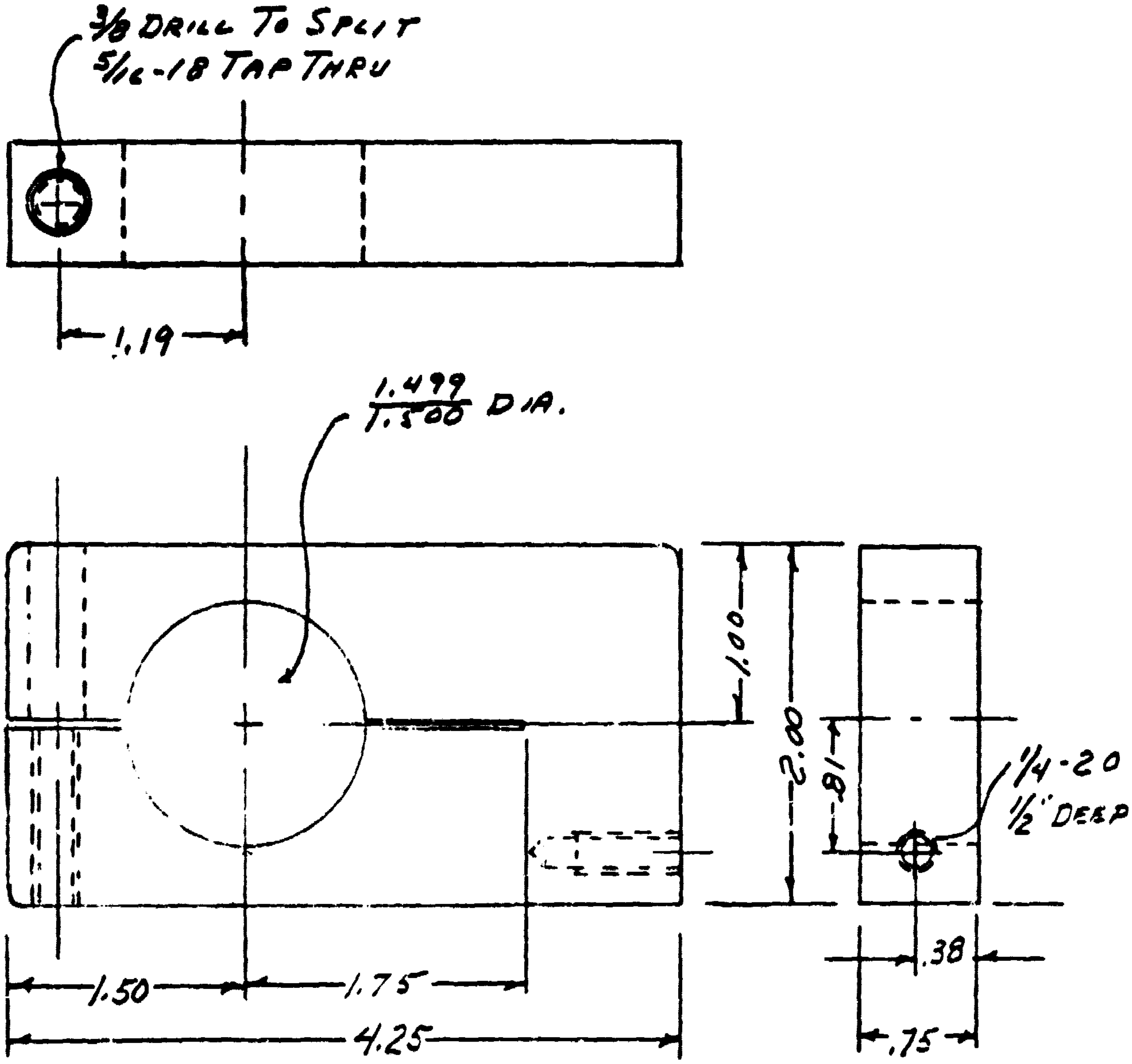

DO NOT SCALE THIS PRINT
UNLESS OTHERWISE SPECIFIED
BREAK ALL SHARP EDGES
DIMENSIONS ARE IN INCHES

DESCRIPTION OF CHANGE	
NUM	
EO	
DFT	
CHK	
DATE	
REV	

DRAWN	DATE	APPROVED	DATE	CODE
RFO	10/20/77			✓
CHECKED	DATE	APPROVED	DATE	CLASS

SLURRY SHIELD SUPPORT
JPL PROTOTYPE SAW

NOT OTHERWISE SPEC: FRAC ± ANG ± SCALE FULL
FIN ✓ DEC X ± .1 XX ± .02 XXX ± .005

varian

DIVISION	SIZE	DRAWING NO.	REV
VAC/LEV	A	S 1027	

DASH NO.	TYPE OR MODEL	NEXT ASSEMBLY	REQ	PART NUMBER	DESCRIPTION OR MATERIAL	ITEM

A 51028

DO NOT SCALE DRAWING

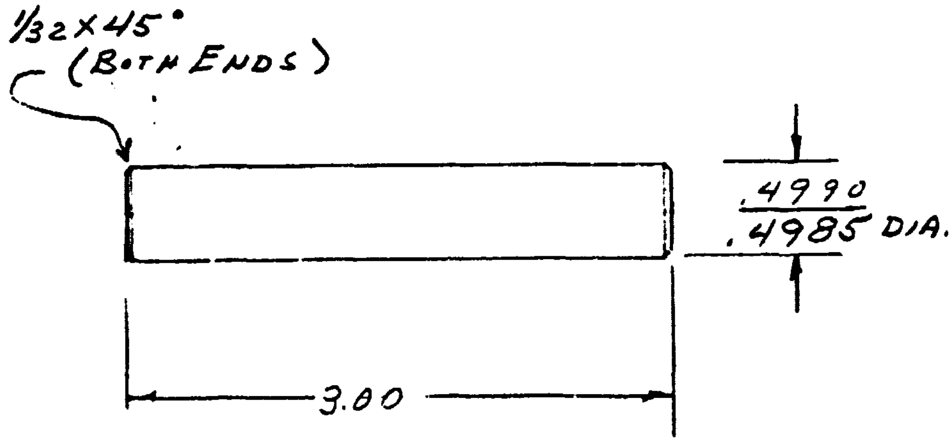

SOLID 60 CASE HARDENED & GROUND
CLASS S" SHAFTING

10 PCS REQ'D.

DO NOT SCALE THIS PRINT
UNLESS OTHERWISE SPECIFIED
BREAK ALL SHARP EDGES
DIMENSIONS ARE IN INCHES

DRAWN	DATE	APPROVED	DATE	CODE
RPB	10/31/77			✓
CHECKED	DATE	APPROVED	DATE	CLASS

DESCRIPTION OF CHANGE

NUM
EO
DFT
CHK
DATE
REV

GUIDE PINS
JPL PROTOTYPE SAW

NOT OTHERWISE SPEC: FRAC ± ANG ±
FIN. ✓ DEC .X ± .XX ± .XXX ±

SCALE: FULL

varian

DIVISION	SIZE	DRAWING NO.	REV
VAC/LEX	A	51028	

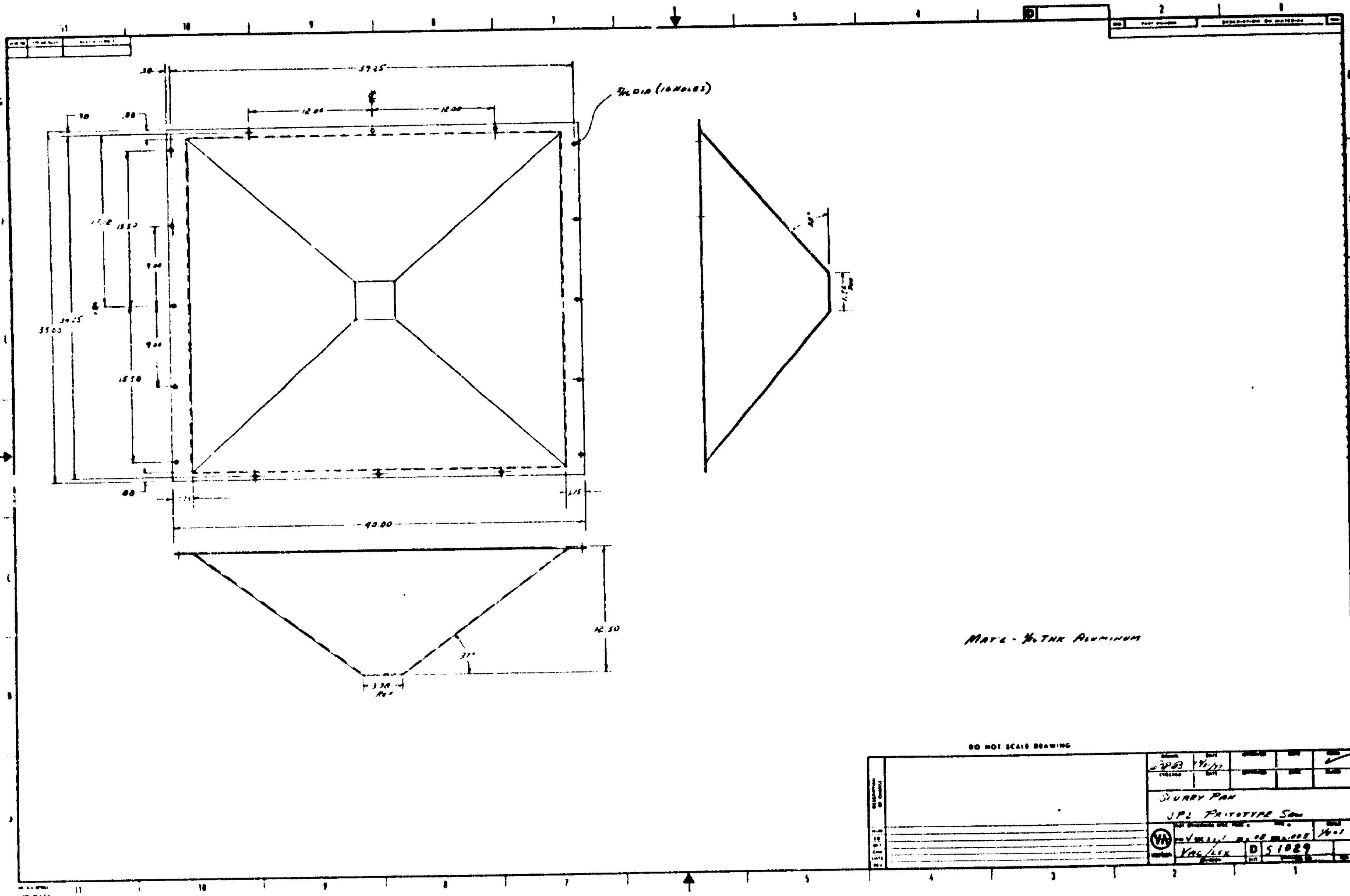

3/16 DIA (16 HOLES)
39.25
12.00
12.00
.38
.70
.88
17.12
15.50
9.00
9.00
15.50
39.25
35.00
.88
1.75
1.75
40.00
12.50
37°
3.78 REF
MAT'L - 1/8 THK ALUMINUM
DO NOT SCALE DRAWING
SLURRY PAN
JPL PROTOTYPE SAW
1/4=1
VAC/LEX
D
51029

DASH NO.	TYPE OR MODEL	NEXT ASSEMBLY	REQ	PART NUMBER	DESCRIPTION OR MATERIAL	ITEM

A S1032

DO NOT SCALE DRAWING

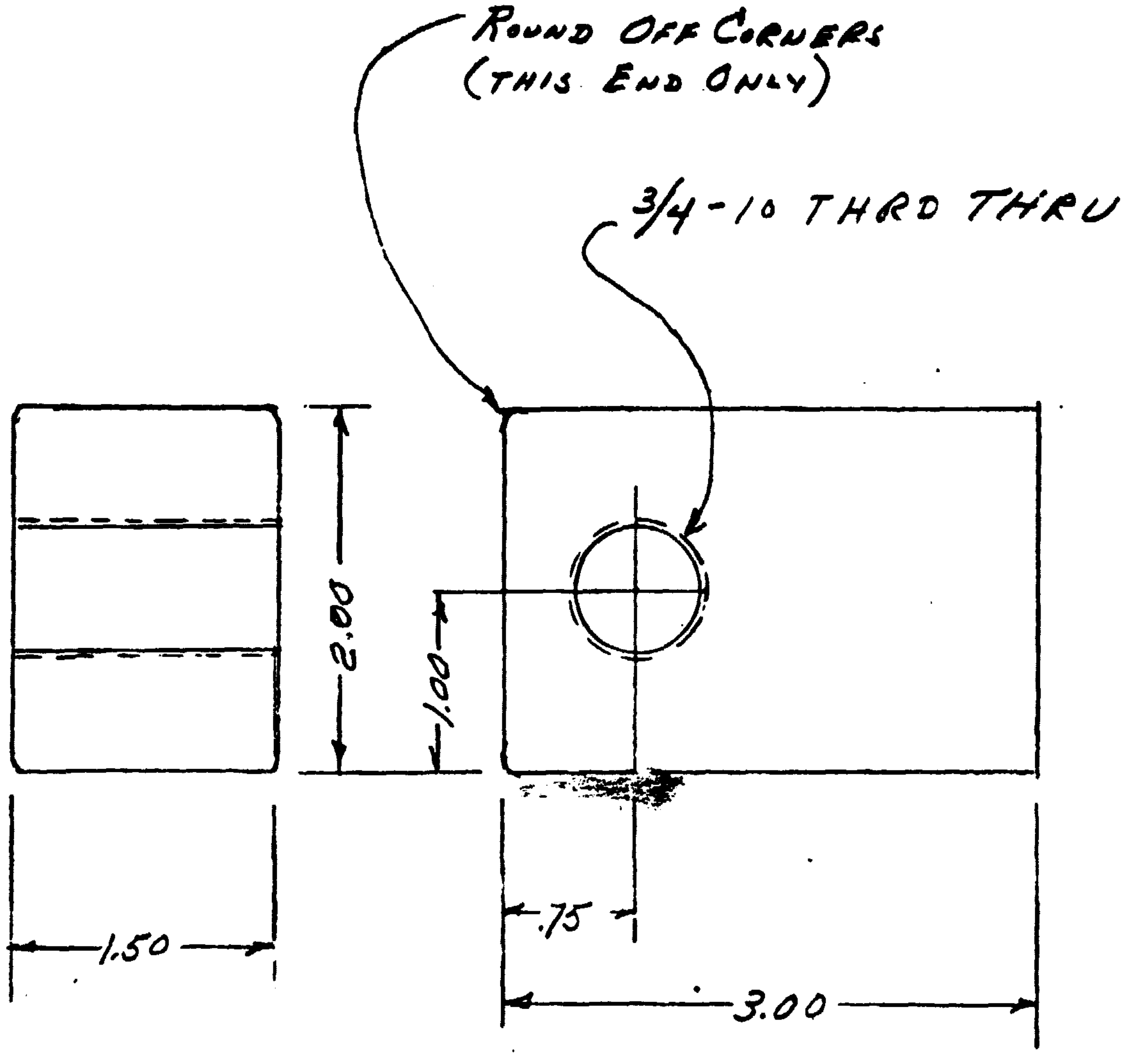

MAT'L - 1½ x 2 M/S

DO NOT SCALE THIS PRINT
UNLESS OTHERWISE SPECIFIED
BREAK ALL SHARP EDGES
DIMENSIONS ARE IN INCHES

DESCRIPTION OF CHANGE

NUM	
EO	
DFT	
CHK	
DATE	
REV	

DRAWN	DATE	APPROVED	DATE	CODE
RPB	11/15/77			✓
CHECKED	DATE	APPROVED	DATE	CLASS

PIVOT BLOCKS
JPL PROTOTYPE

NOT OTHERWISE SPEC: FRAC ± ANG ± SCALE FULL
FIN ✓ DEC X ± XX ± XXX ±

varian

DIVISION	SIZE	DRAWING NO.	REV
VAC/LEX	A	S 1032	

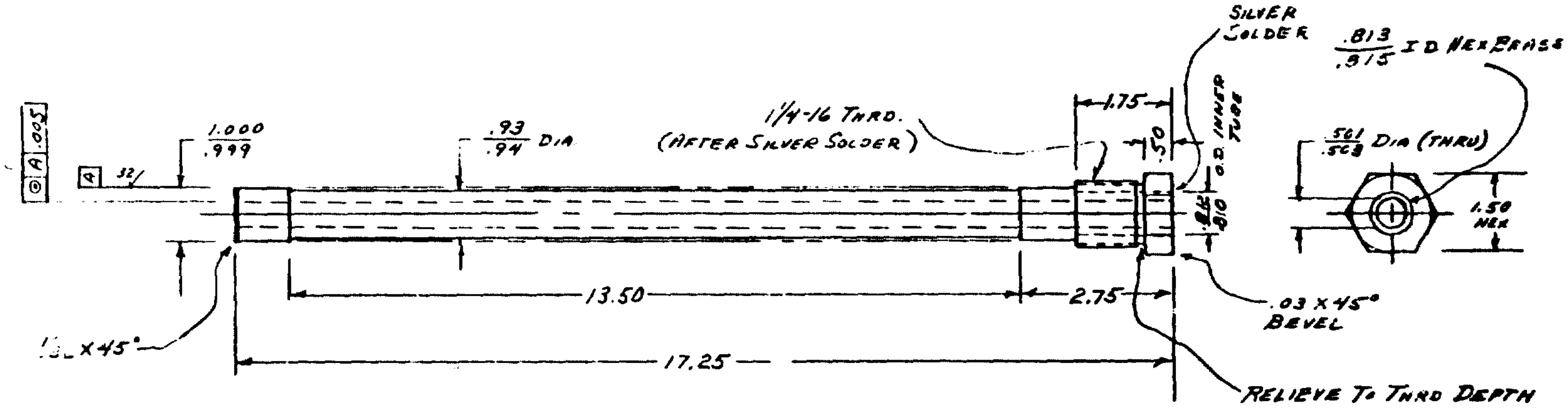

MAT'L - 1" OD X 1/4" WALL HARD BRASS TUBE & 1/2 HEX BRASS

DO NOT SCALE THIS PRINT
UNLESS OTHERWISE SPECIFIED
BREAK ALL SHARP EDGES
DIMENSIONS ARE IN INCHES

DO NOT SCALE DRAWING

DASH NO	TYPE OR MODEL	NEXT ASSEMBLY

NO	PART NUMBER	DESCRIPTION OR MATERIAL	ITEM

DRAWN	DATE	APPROVED	DATE	CODE
RBG	10/10/77			V
CHECKED	DATE	APPROVED	DATE	CLASS

LOCKING SHAFT STROKE ADJ
JPL PROTOTYPE SAW

NOT OTHERWISE SPEC FRAC ± 1/64 ANG ± 1/4° — SCALE 1/2
FIN V DEC X ± .1 XX ± .32 XXX ± .005

varian

DIVISION	SIZE	DRAWING NO.	REV
VAC/LEX	B	C-1033	

DESCRIPTION OF CHANGE — NUM — 10 — DFT — CHK — DATE — REV

44; 6 4 JUNE66 — LITHO IN U S A

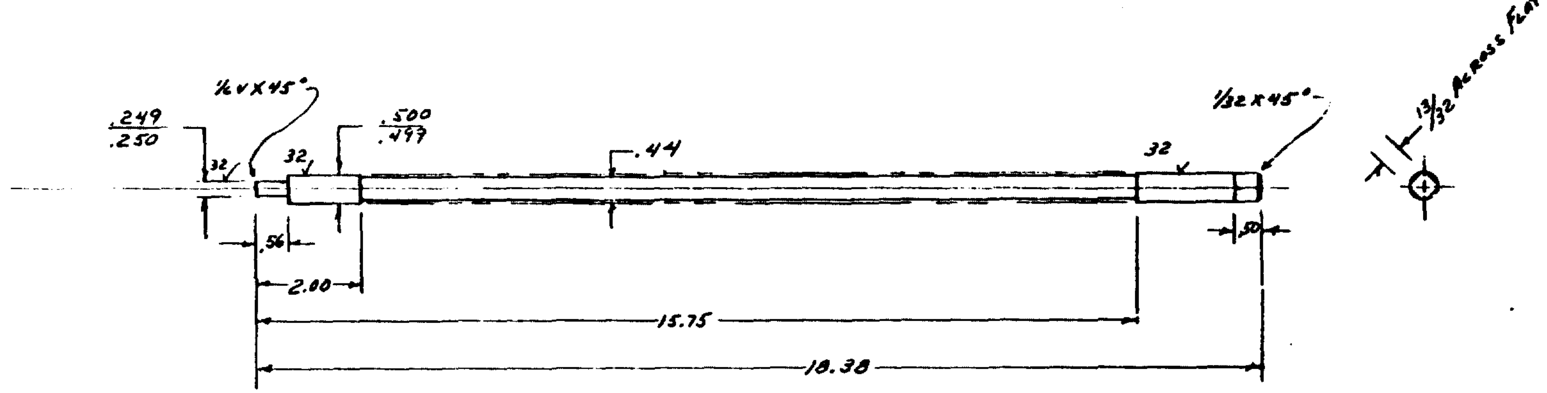

1/2" DIA. DRILL ROD

DO NOT SCALE DRAWING

DO NOT SCALE THIS PRINT
UNLESS OTHERWISE SPECIFIED
BREAK ALL SHARP EDGES
DIMENSIONS ARE IN INCHES

DASH NO	TYPE OR MODEL	NEXT ASSEMBLY

REQ	PART NUMBER	DESCRIPTION OR MATERIAL	ITEM

DRAWN	DATE	APPROVED	DATE	CODE
R.B. Bell	1/18/77			✓
CHECKED	DATE	APPROVED	DATE	CLASS

ADJUSTING SCREW-STROKE ADJ.
JPL PROTOTYPE SAW

NOT OTHERWISE SPEC FRAC ± 1/64 ANG ± 1° — SCALE 1/2
FIN ✓ DEC X ± .1 XX ± .02 XXX ± .005

DIVISION	SIZE	DRAWING NO	REV
VAC/LEX	B	5-1034	

varian

DESCRIPTION OF CHANGE — LTR, EO, DFT, CHK, DATE, REV

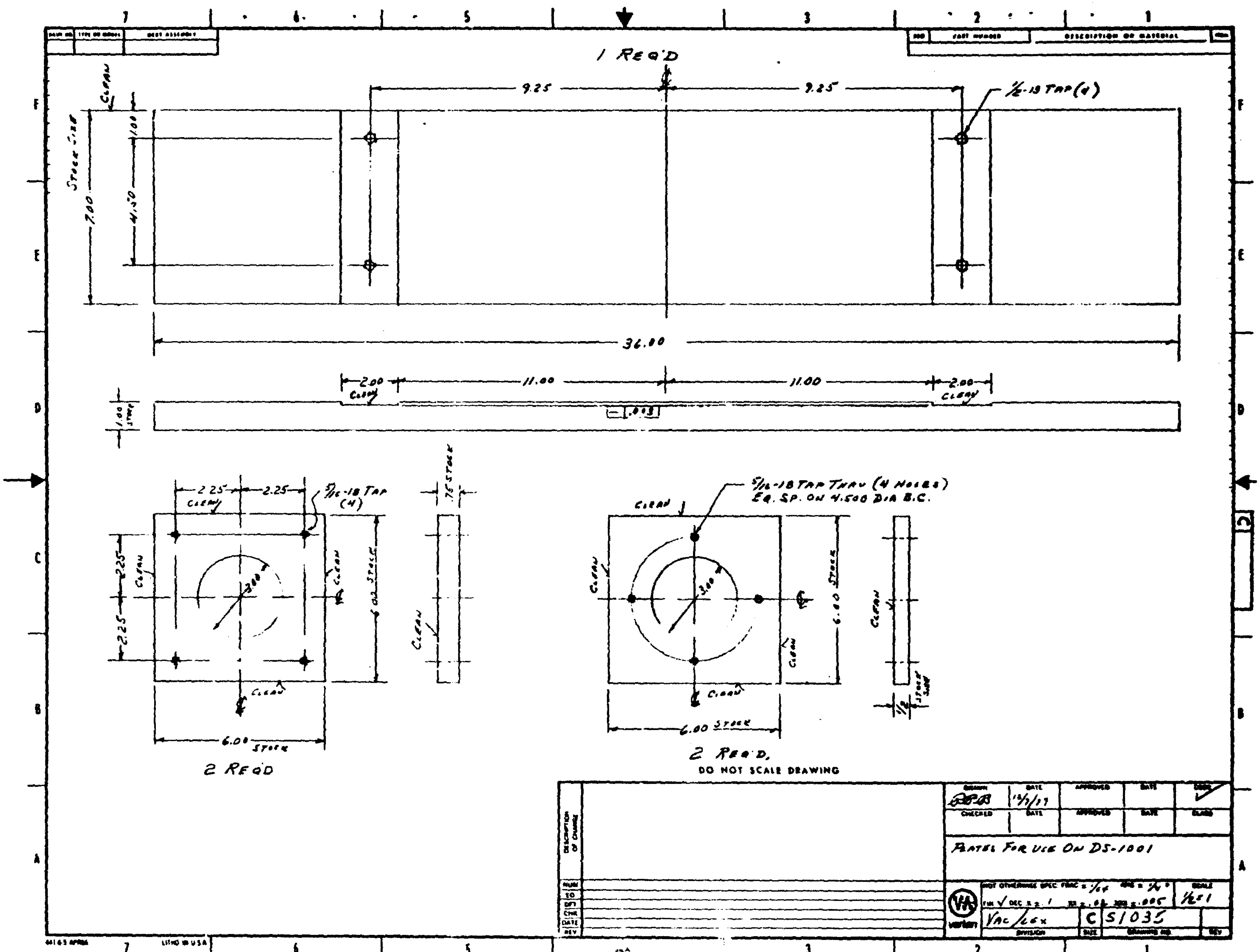
1 REQ'D
9.25
9.25"
1/2-13 TAP (4)
CLEAN
STOCK SIZE
7.00
1.00
4.50
36.00
2.00 CLEAN
11.00
11.00
2.00 CLEAN
1.00 STOCK
2.25"
2.25
5/16-18 TAP (4)
.75 STOCK
6.00 STOCK
2 REQ'D
5/16-18 TAP THRU (4 HOLES) EQ. SP. ON 4.500 DIA B.C.
3.00
2 REQ'D.
DO NOT SCALE DRAWING
DRAWN
DATE
12/7/77
CHECKED
APPROVED
PLATES FOR USE ON DS-1001
SCALE
1/2=1
VAC/LEX
C
51035
DIVISION
SIZE
DRAWING NO.
REV
DESCRIPTION OF CHANGE
PART NUMBER
DESCRIPTION OR MATERIAL
NEXT ASSEMBLY
LITHO IN U.S.A.

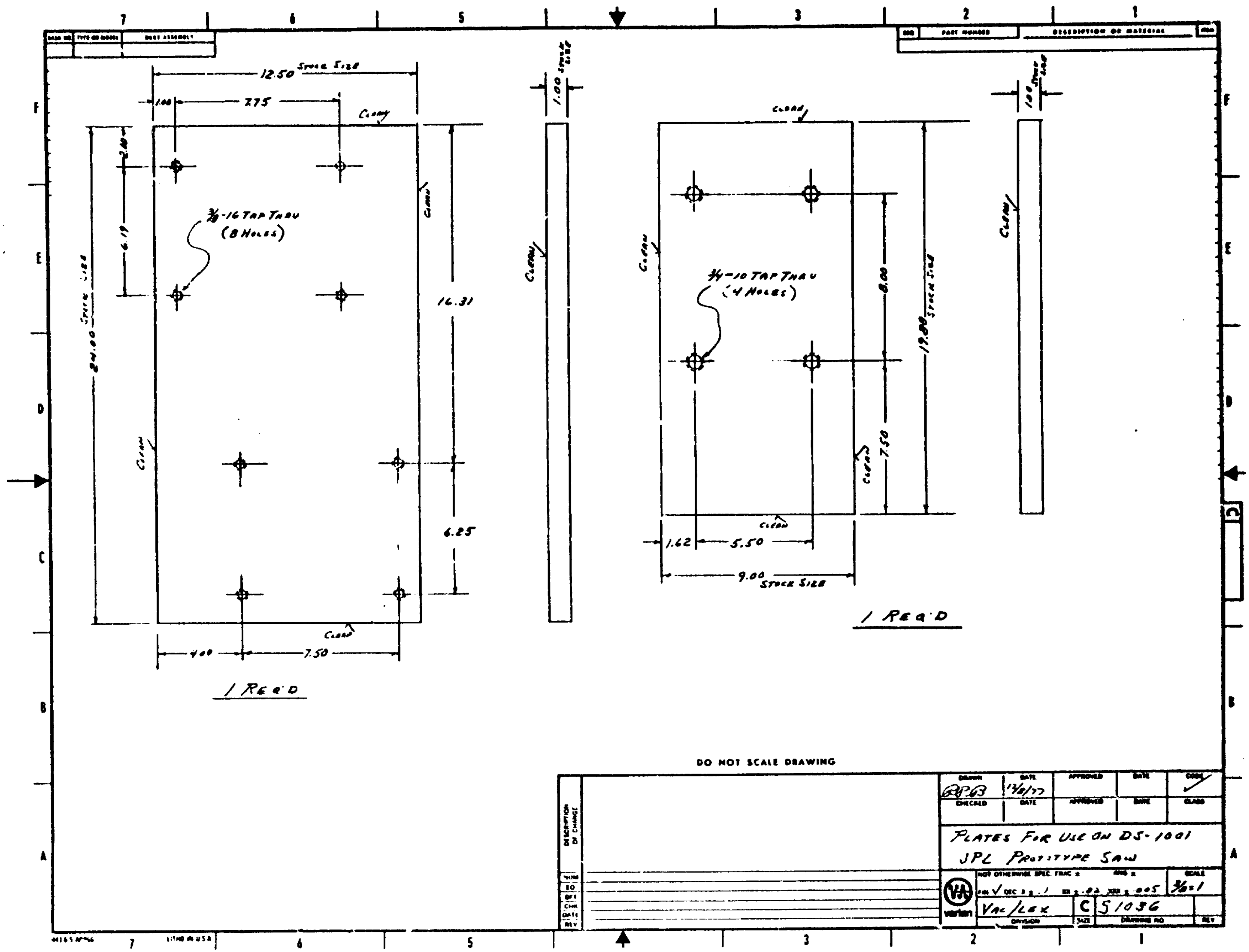
12.50 Stock Size
1.00
7.75
2.00
6.19
24.00 Stock Size
16.31
6.25
4.00
7.50
3/8-16 Tap Thru (8 Holes)
Clean
1 Req'd
1.00 Stock Size
1.00 Stock Size
3/4-10 Tap Thru (4 Holes)
8.00
7.50
19.88 Stock Size
1.62
5.50
9.00 Stock Size
1 Req'd
DO NOT SCALE DRAWING
Plates For Use On DS-1001
JPL Prototype Saw
Drawn RPG
Date 12/8/77
Scale 3/8=1
Vac/Lex
C
51036
varian

DASH NO.	TYPE OR MODEL	NEXT ASSEMBLY	REQ	PART NUMBER	DESCRIPTION OR MATERIAL	ITEM
		DS-1001				

A S-1037

DO NOT SCALE DRAWING

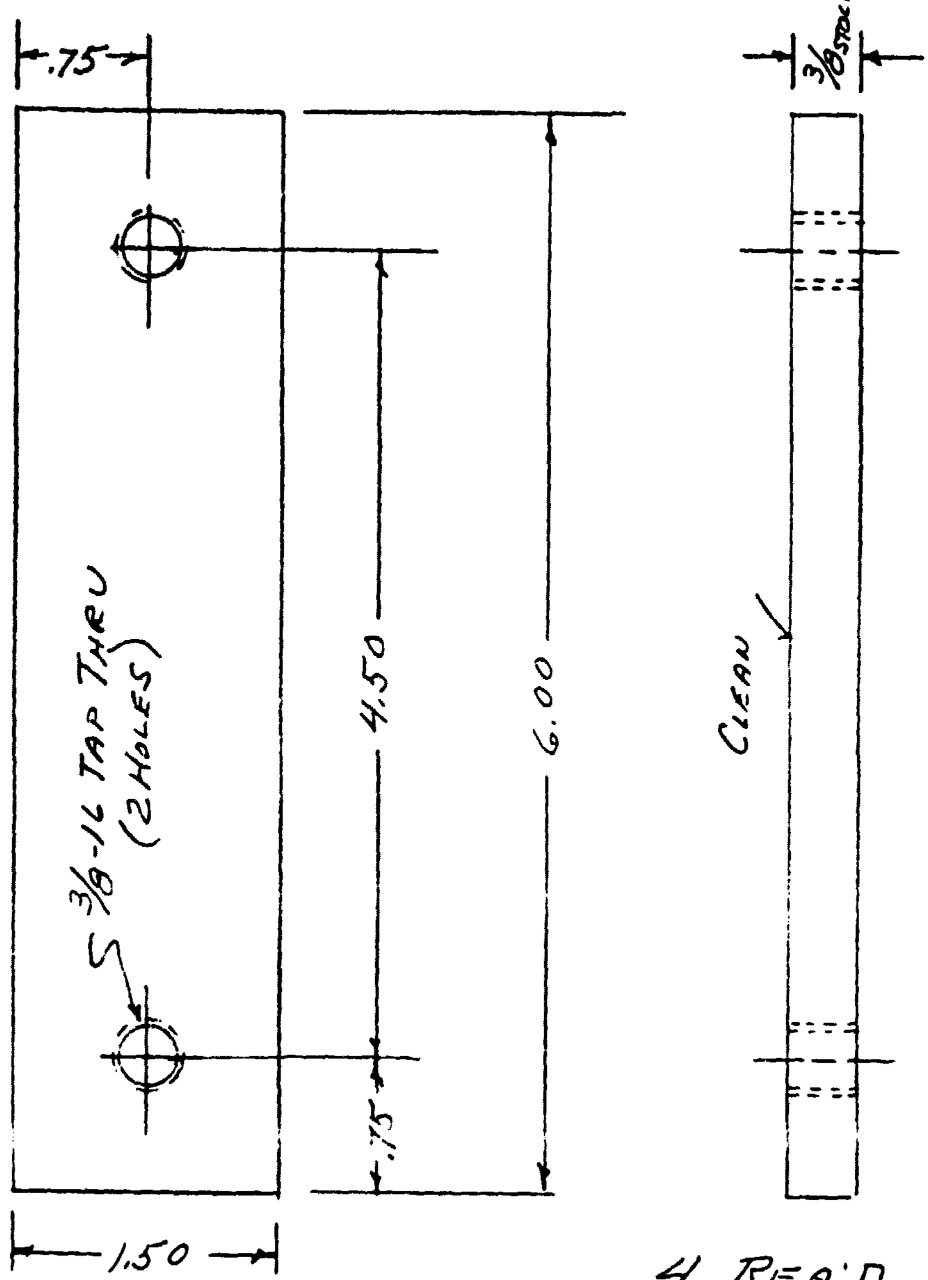

4 REQ'D

DO NOT SCALE THIS PRINT
UNLESS OTHERWISE SPECIFIED
BREAK ALL SHARP EDGES
DIMENSIONS ARE IN INCHES

DRAWN	DATE	APPROVED	DATE	CODE
RBG	12/12/77			
CHECKED	DATE	APPROVED	DATE	CLASS

SHAFT SUPPORT MOUNTING PADS

NOT OTHERWISE SPEC. FRAC ± 1/64 ANG ± 1/4 SCALE FULL
FIN √ DEC X ± .1 XX ± .02 XXX ± .005

DIVISION	SIZE	DRAWING NO	REV
VAC/LEX	A	S-1037	

varian

DESCRIPTION OF CHANGE

NUM	
EO	
DFT	
CHK	
DATE	
REV	

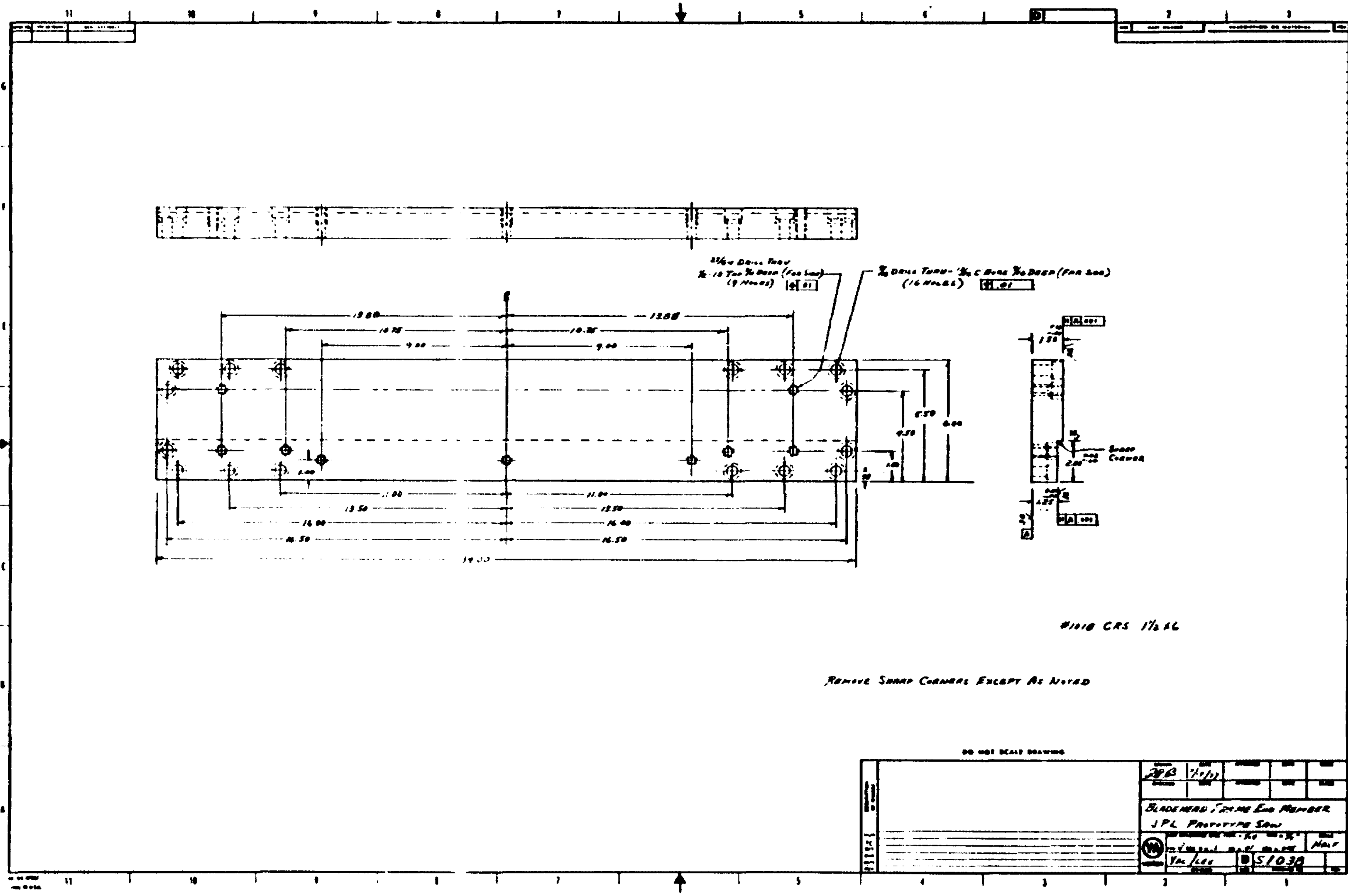

BLADEHEAD FRAME END MEMBER
JPL PROTOTYPE SAW
HALF
D 51030
#1018 CRS 1½ SQ
REMOVE SHARP CORNERS EXCEPT AS NOTED
DO NOT SCALE DRAWING
SHARP CORNER
19.00
12.00
10.75
9.00
11.00
13.50
16.00
16.50
6.00
5.50
4.50
2.00

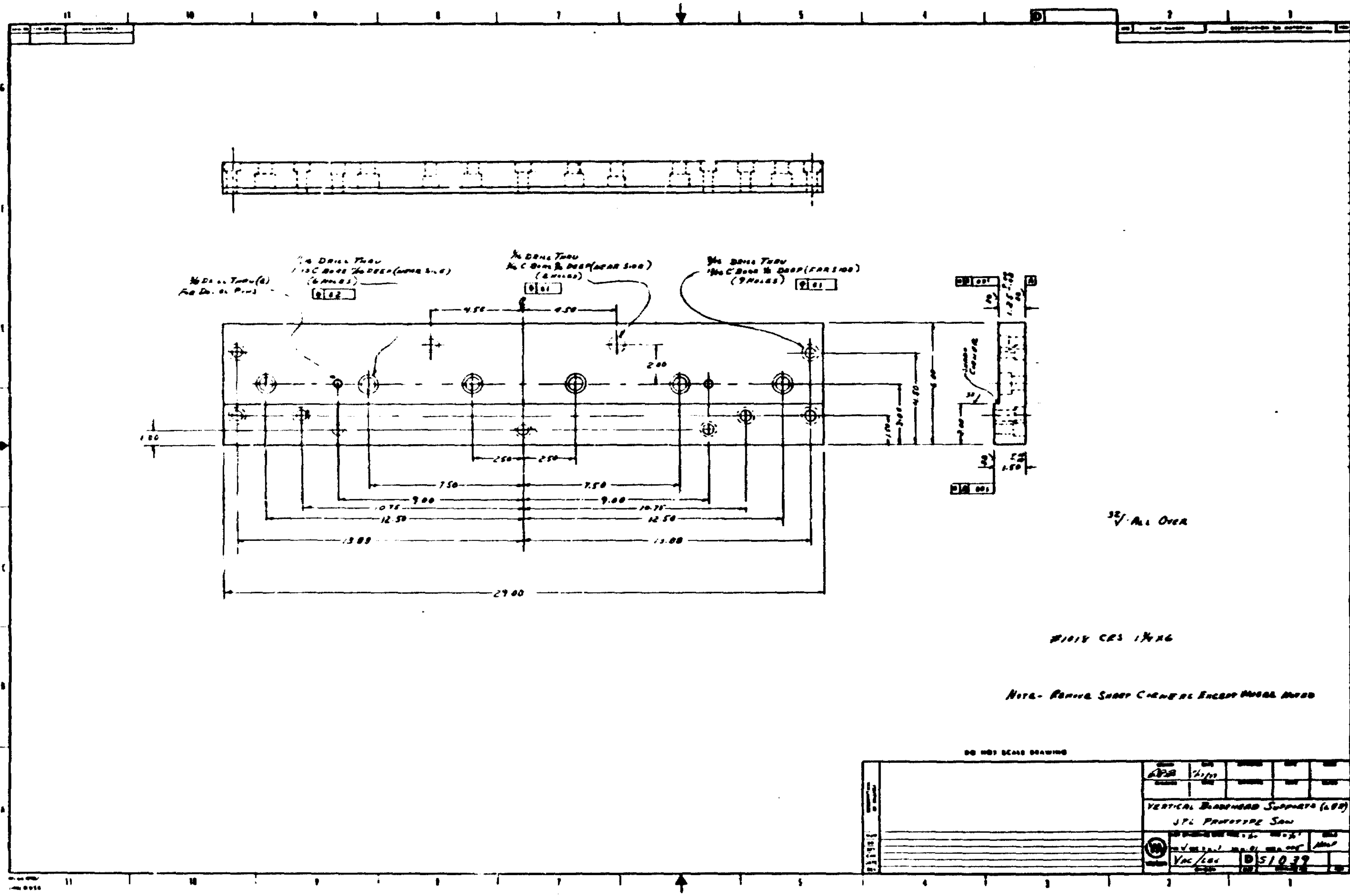

VERTICAL BLADEHEAD SUPPORTS (LBB)
JPL PROTOTYPE SAW
D 51039
32/ ALL OVER
#1018 CRS 1 1/4 x 6
NOTE - REMOVE SHARP CORNERS EXCEPT WHERE NOTED
DO NOT SCALE DRAWING
29.00
13.88
12.50
10.75
9.00
7.50
4.50
2.50
2.00
1.00

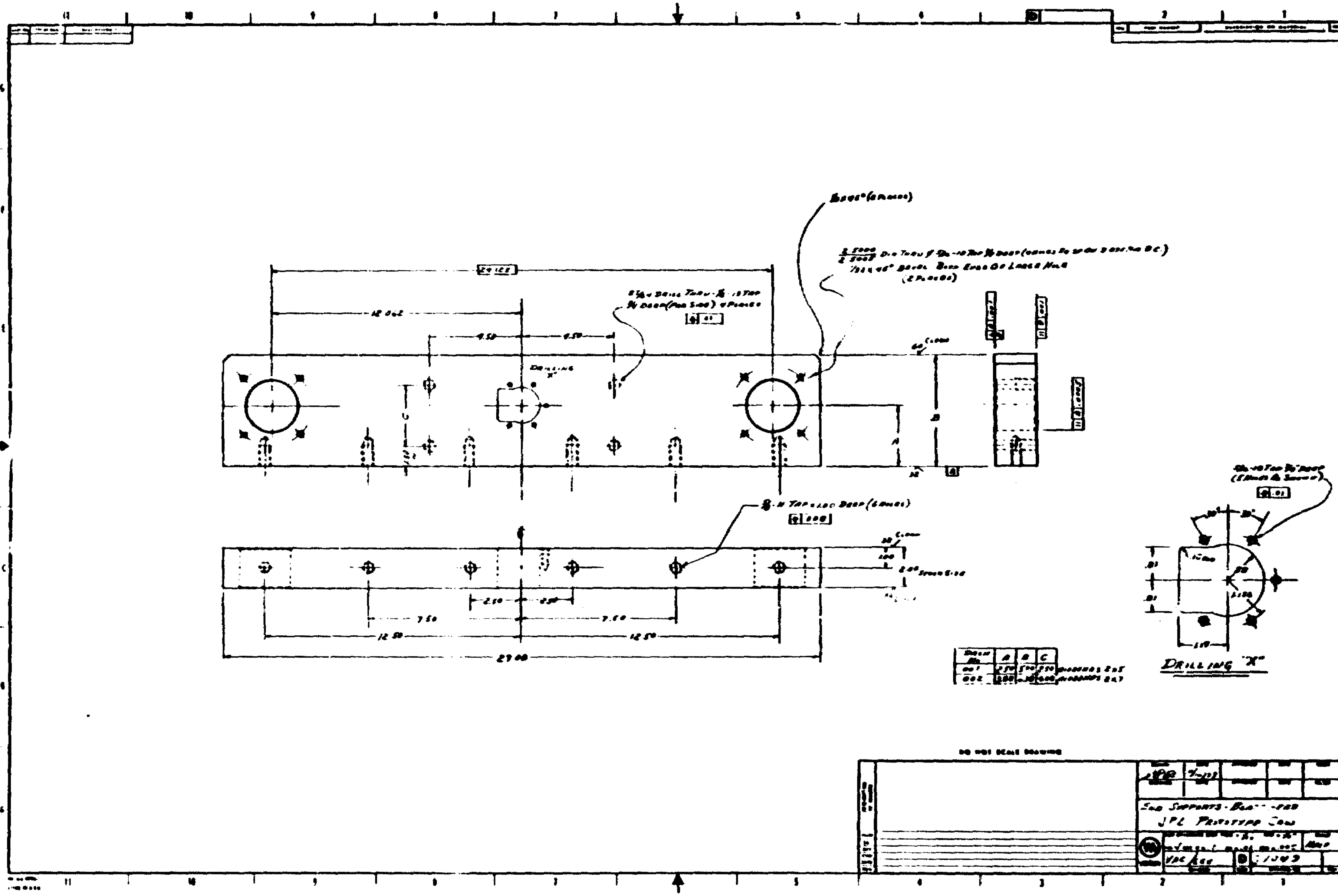
DRILLING "X"
DO NOT SCALE DRAWING
29.00
12.50
7.50
2.50
JPL PROTOTYPE

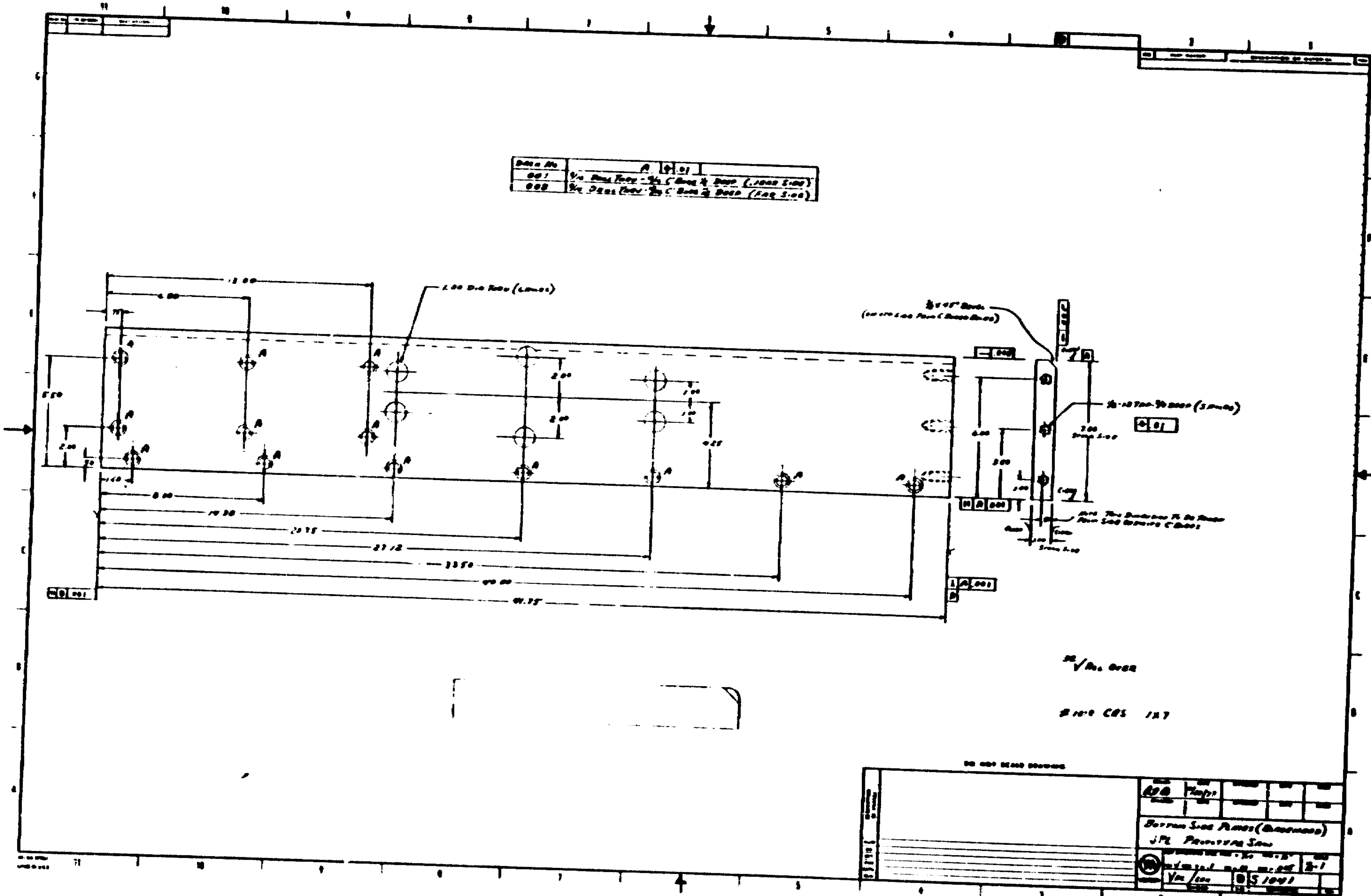
S 1041

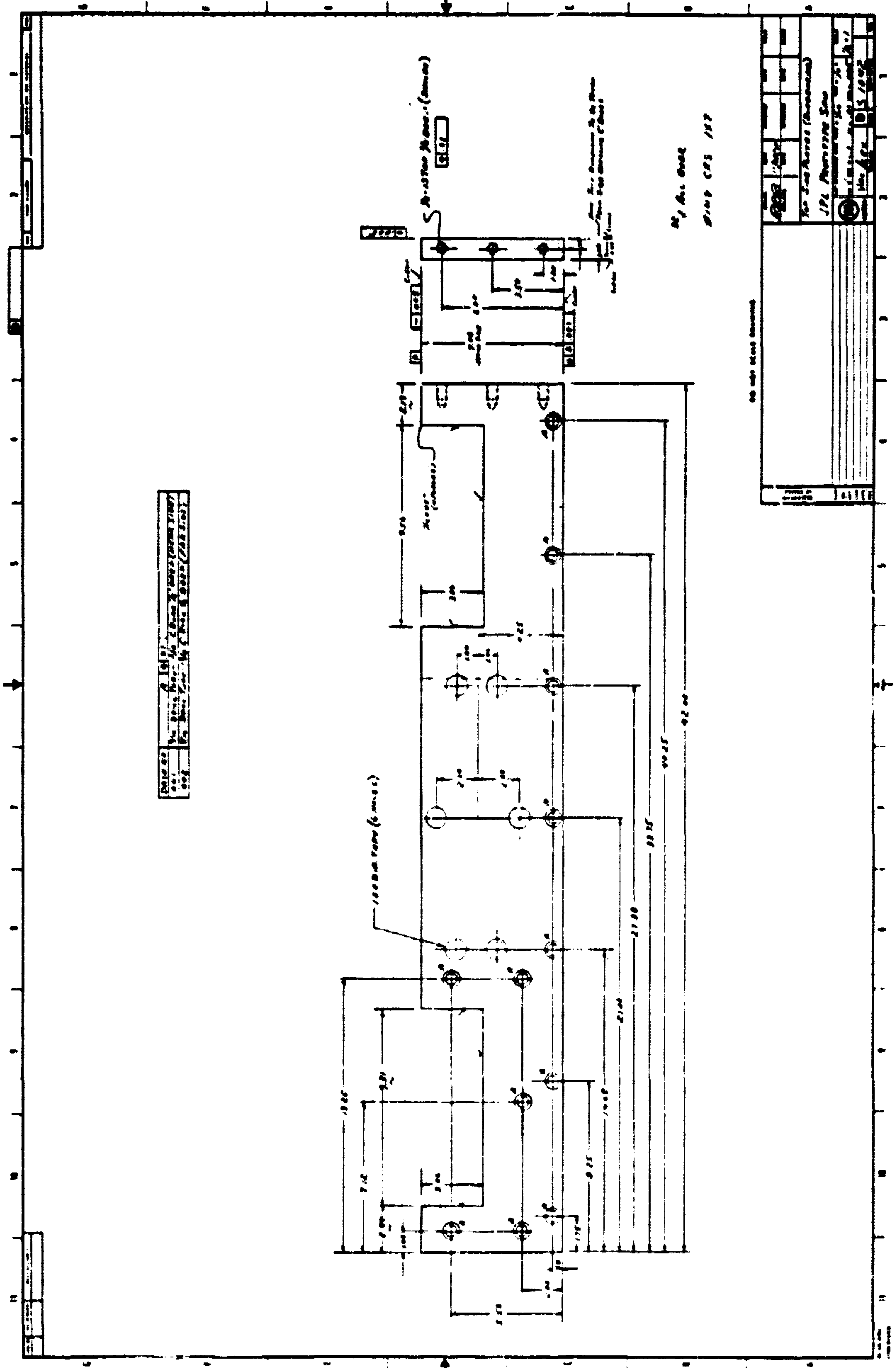

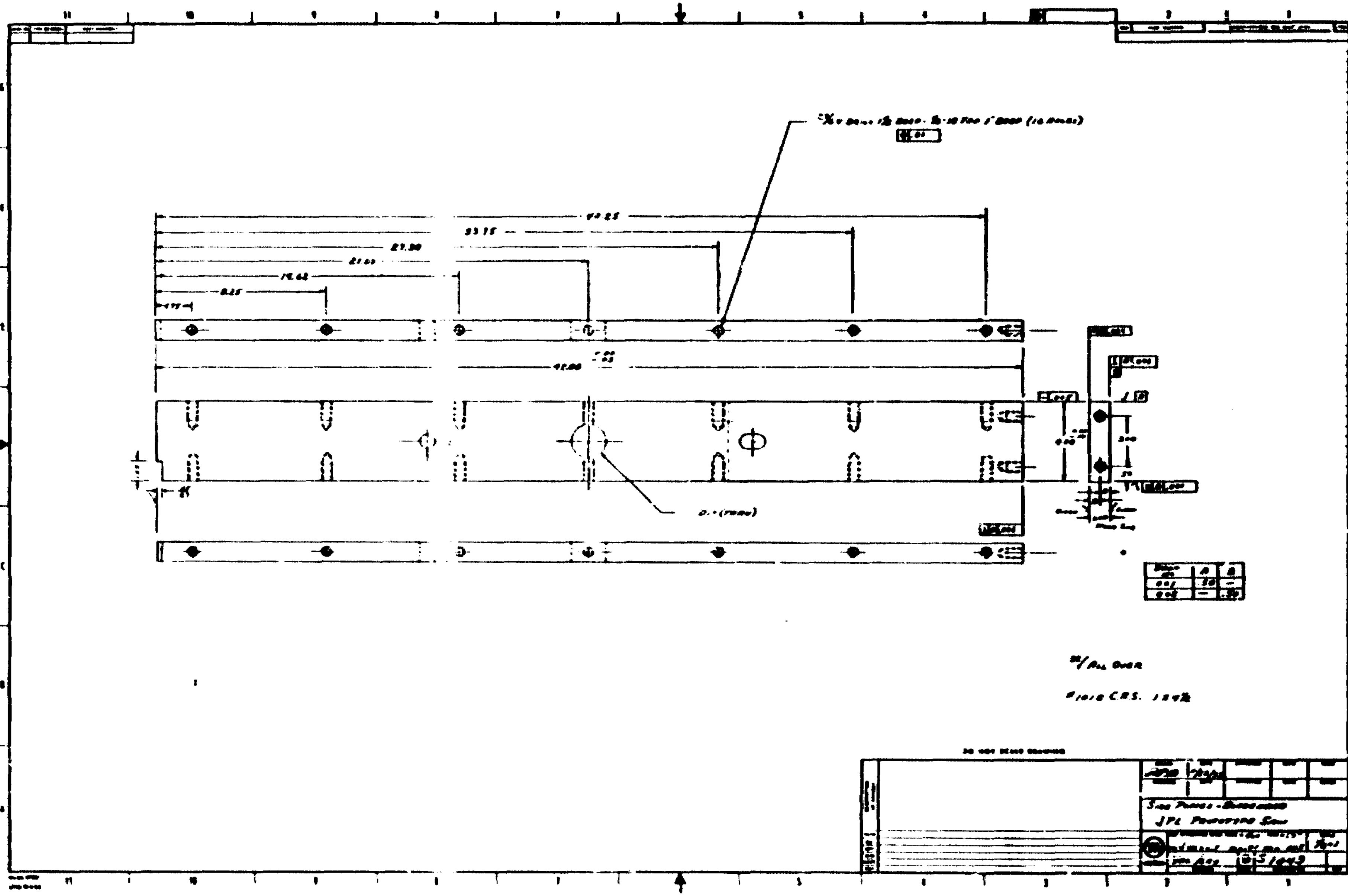

42.25
33.75
27.50
21.00
14.62
8.25
92.00
#1010 C.R.S.

C-6

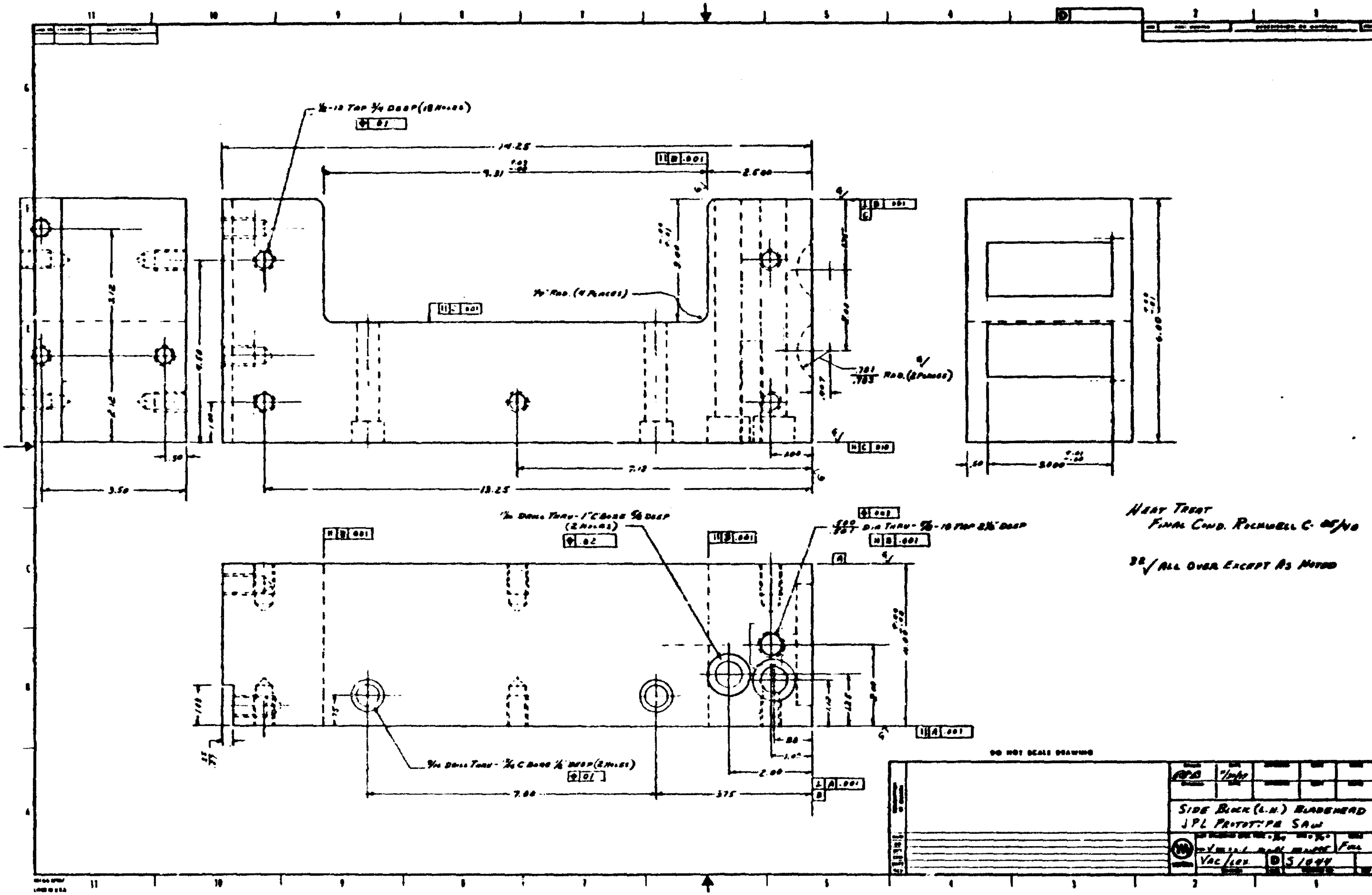

3/8-16 TAP 3/4 DEEP (18 HOLES)
14.25
2.500
3/8" RAD. (4 PLACES)
13.25
7.12
3.50
HEAT TREAT
FINAL COND. ROCKWELL C
32/ ALL OVER EXCEPT AS NOTED
17/32 DRILL THRU - 7/8 C'BORE 1/2 DEEP (2 HOLES)
7.00
3.75
2.00
DO NOT SCALE DRAWING
SIDE BLOCK (L.H.) BLADEHEAD
JPL PROTOTYPE SAW
FULL
5/044

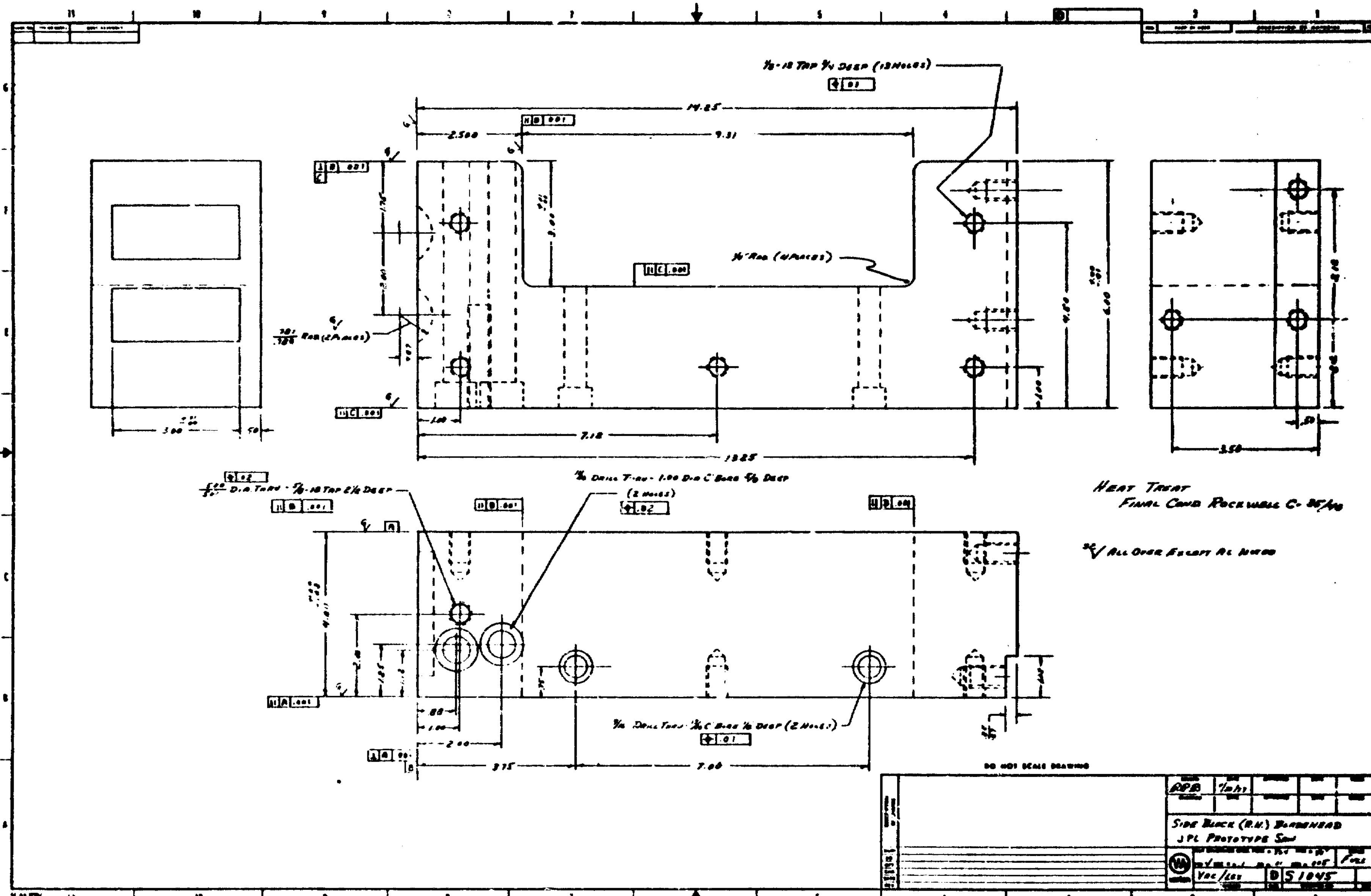

3/8-18 TAP 3/4 DEEP (12 HOLES)
14.25
2.500
9.31
1/4 RAD (4 PLACES)
7.18
13.25
1/4 DRILL THRU - 1.00 DIA C'BORE 5/8 DEEP
(2 HOLES)
3/8-18 TAP 2 1/2 DEEP
9/16 DRILL THRU - 3/4 C'BORE 1/8 DEEP (2 HOLES)
3.75
7.00
HEAT TREAT
FINAL COND ROCKWELL C- 35/40
32 ALL OVER EXCEPT AS NOTED
DO NOT SCALE DRAWING
SIDE BLOCK (R.H.) BULKHEAD
JPL PROTOTYPE SAW
D 51045

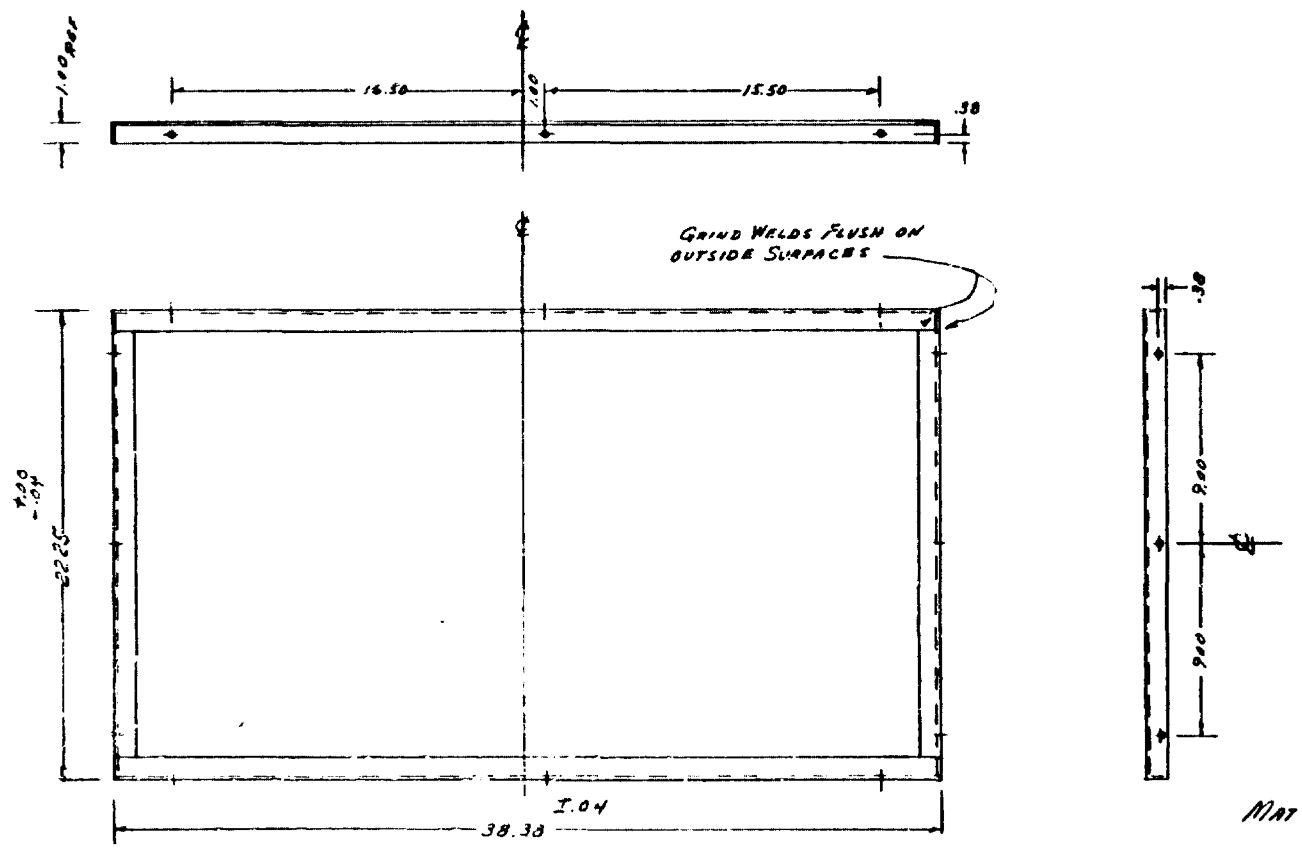

MAT'L 1X1X1/8 STEEL ANGLE

DO NOT SCALE DRAWING

DRAWN	DATE	APPROVED	DATE	MODE
RPG	10/20/77			
CHECKED	DATE	APPROVED	DATE	CLASS

BELLOWS SUPPORT
JPL ...TYPE ...

NOT OTHERWISE SPEC FRAC ± ANG ± | SCALE 1/4=1
DIVISION: VAC/LSY | SIZE: C | DRAWING NO: S 1046 | REV

DESCRIPTION OF CHANGE | NUM | EO | DFT | CHK | DATE | REV

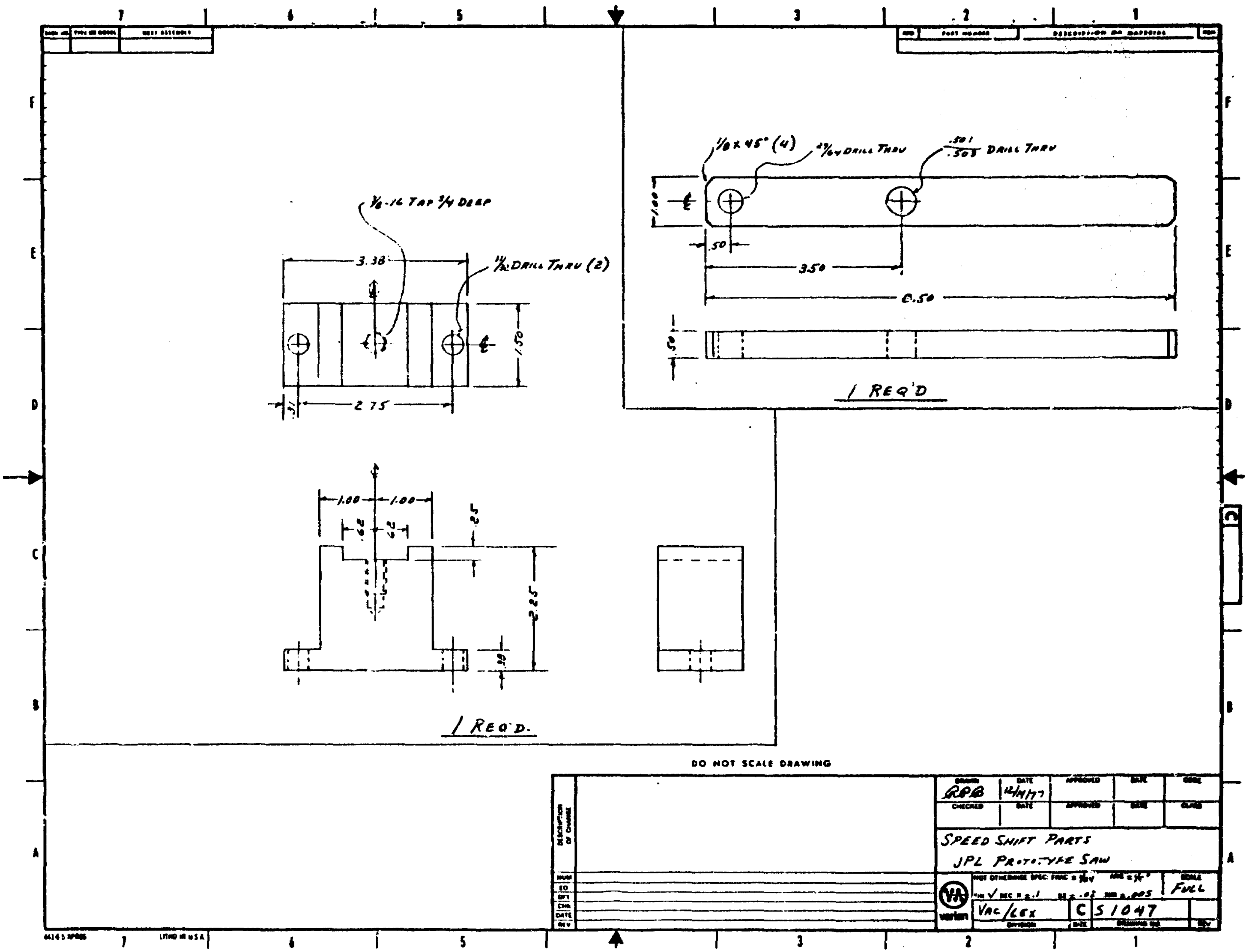

1/8 X 45° (4)
29/64 DRILL THRU
.501
.503 DRILL THRU
1.00
.50
3.50
6.50
.50
1 REQ'D
3/8-16 TAP 3/4 DEEP
11/32 DRILL THRU (2)
3.38
1.50
2.75
1.00
1.00
.62
.62
.25
2.25
1 REQ'D.
DO NOT SCALE DRAWING
RPB
12/14/77
SPEED SHIFT PARTS
JPL PROTOTYPE SAW
FULL
VAC/LEX
C
S1047

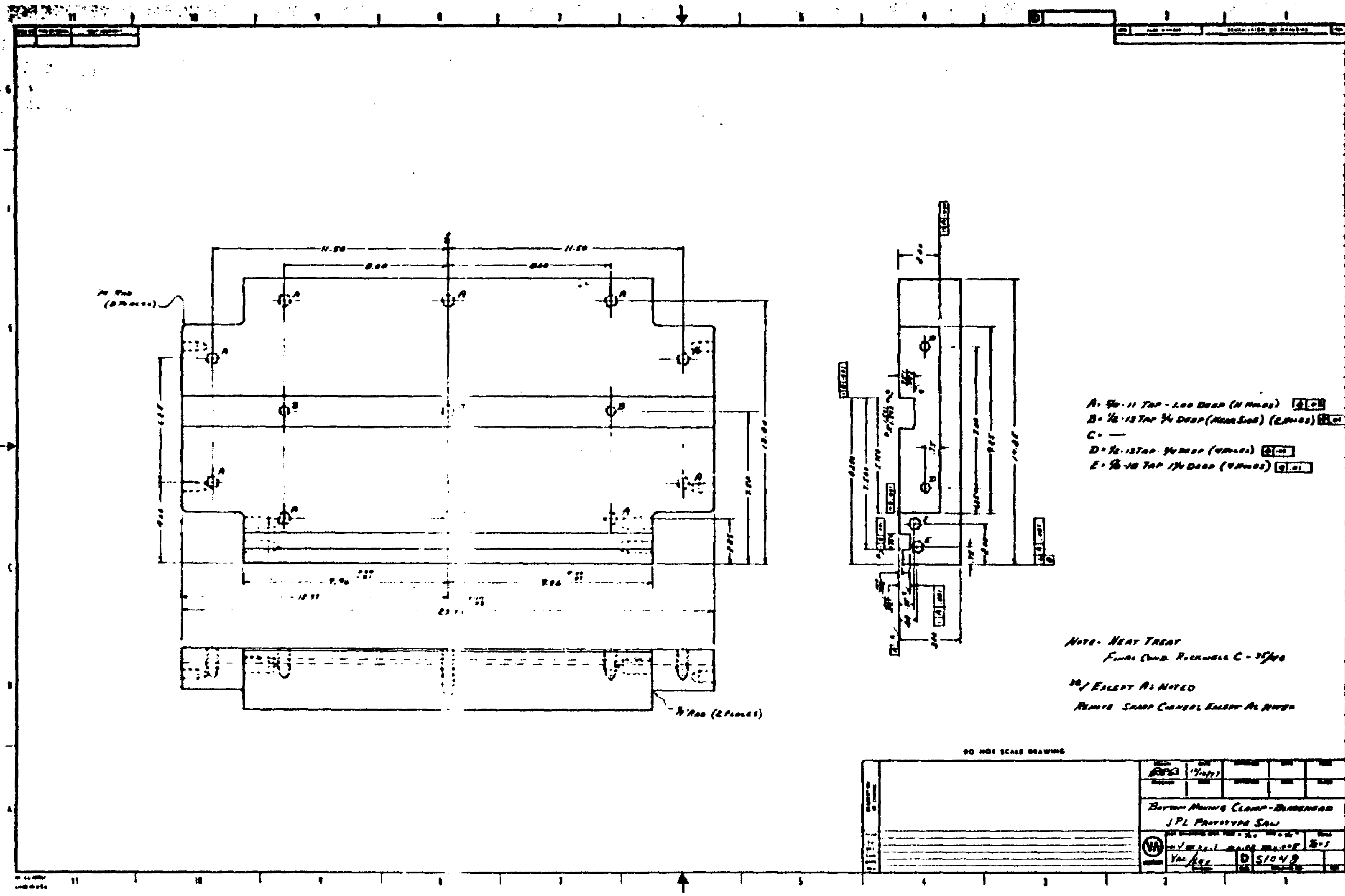

A: 5/8-11 TAP - 1.00 DEEP (11 HOLES)
B: 1/2-13 TAP 3/4 DEEP (NEAR SIDE) (2 HOLES)
C: —
D: 1/2-13 TAP 3/4 DEEP (4 HOLES)
E: 5/8-18 TAP 1 1/4 DEEP (4 HOLES)
NOTE- HEAT TREAT
FINAL COND. ROCKWELL C - 35/40
32/ EXCEPT AS NOTED
REMOVE SHARP CORNERS EXCEPT AS NOTED
DO NOT SCALE DRAWING
BOTTOM MOUNTING CLAMP - BLADEHEAD
JPL PROTOTYPE SAW
D
51048

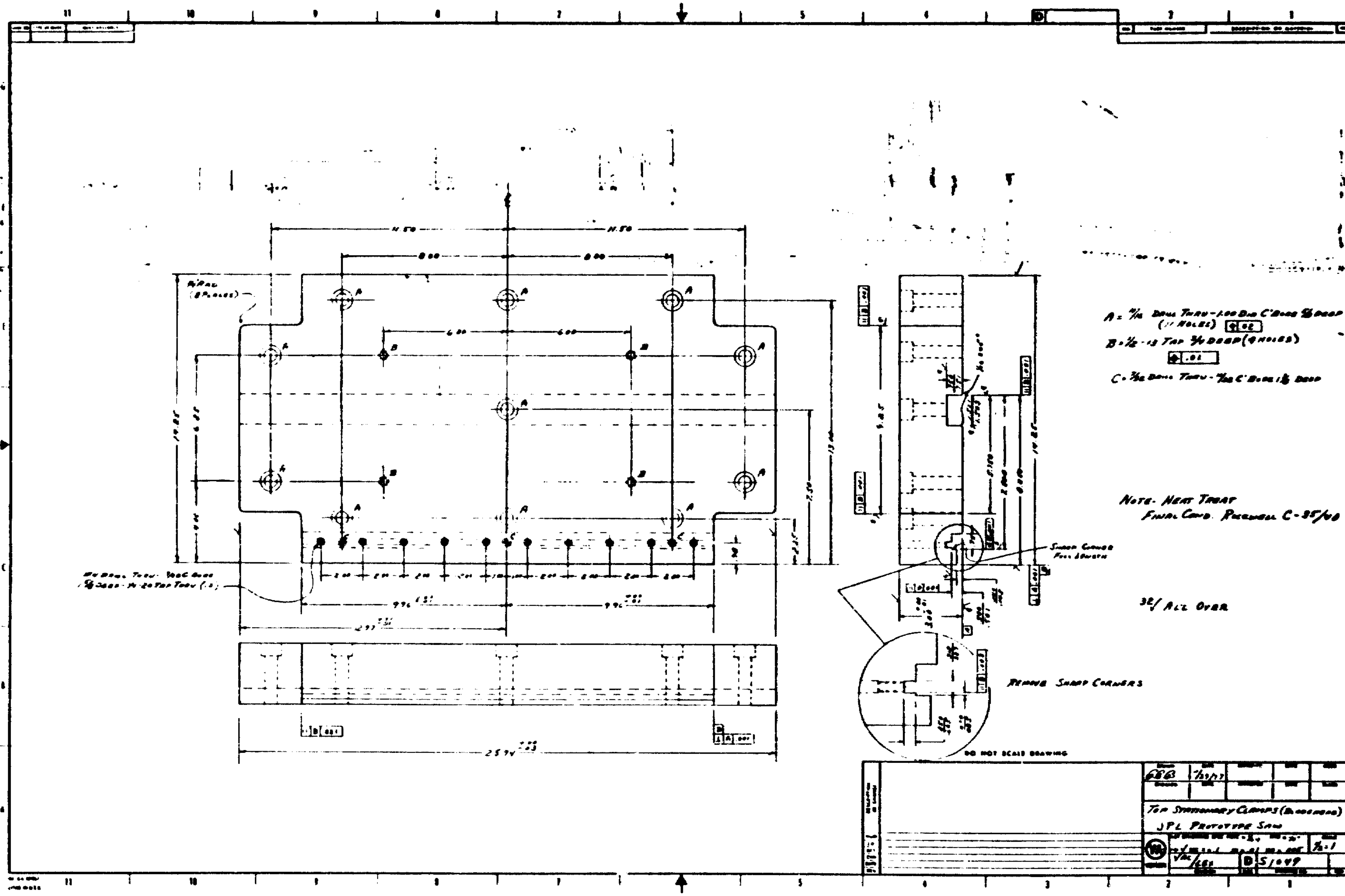
B = 1/2-13 Tap 3/4 Deep (4 Holes)
Note - Heat Treat
Final Cond. Rockwell C-35/40
32/ All Over
Remove Sharp Corners
Do Not Scale Drawing
JPL Prototype Saw
D 51049

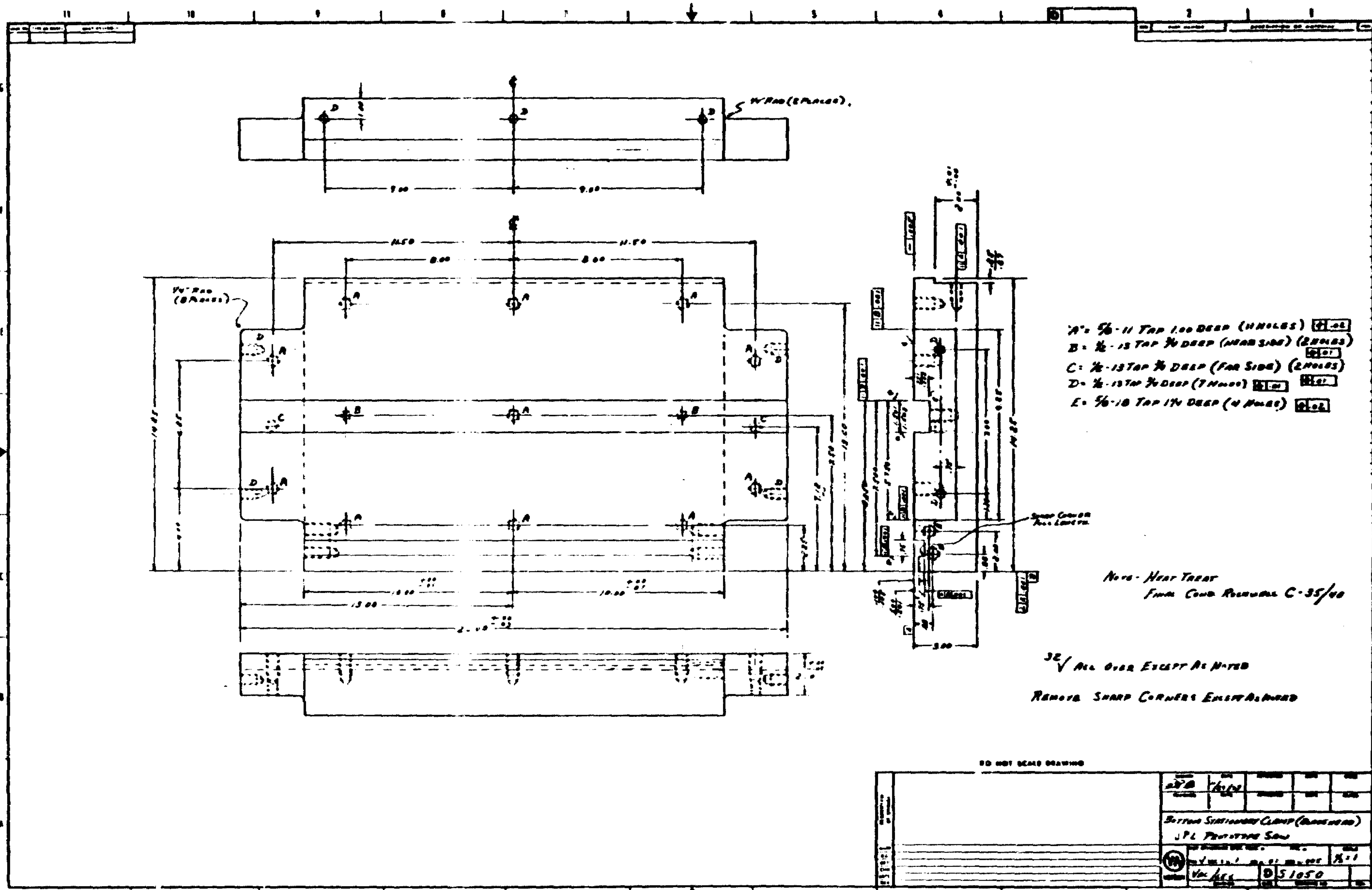
"A" = 5/8-11 TAP 1.00 DEEP (11 HOLES)
B = 1/2-13 TAP 3/4 DEEP (NEAR SIDE) (2 HOLES)
C: 1/2-13 TAP 3/4 DEEP (FAR SIDE) (2 HOLES)
D = 1/2-13 TAP 3/4 DEEP (7 HOLES)
E = 5/8-18 TAP 1 1/4 DEEP (4 HOLES)
NOTE - HEAT TREAT
FINAL COND. ROCKWELL C-35/40
32 ALL OVER EXCEPT AS NOTED
REMOVE SHARP CORNERS EXCEPT AS NOTED
DO NOT SCALE DRAWING
JPL PROTOTYPE SAW
D 51050

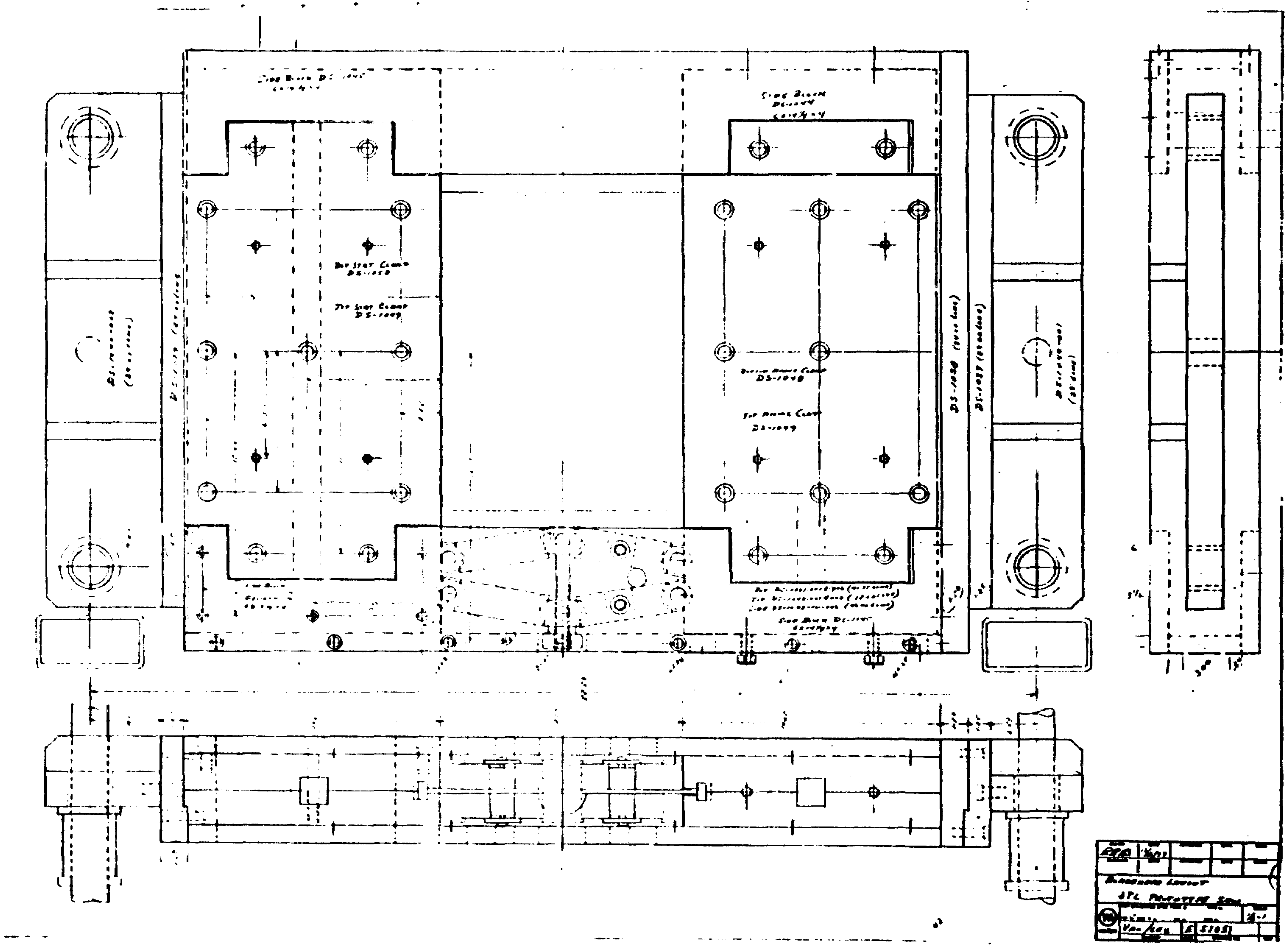
DS-1048
DS-1049
E 5105

DASH NO.	TYPE OR MODEL	NEXT ASSEMBLY	REQ	PART NUMBER	DESCRIPTION OR MATERIAL

A S1052

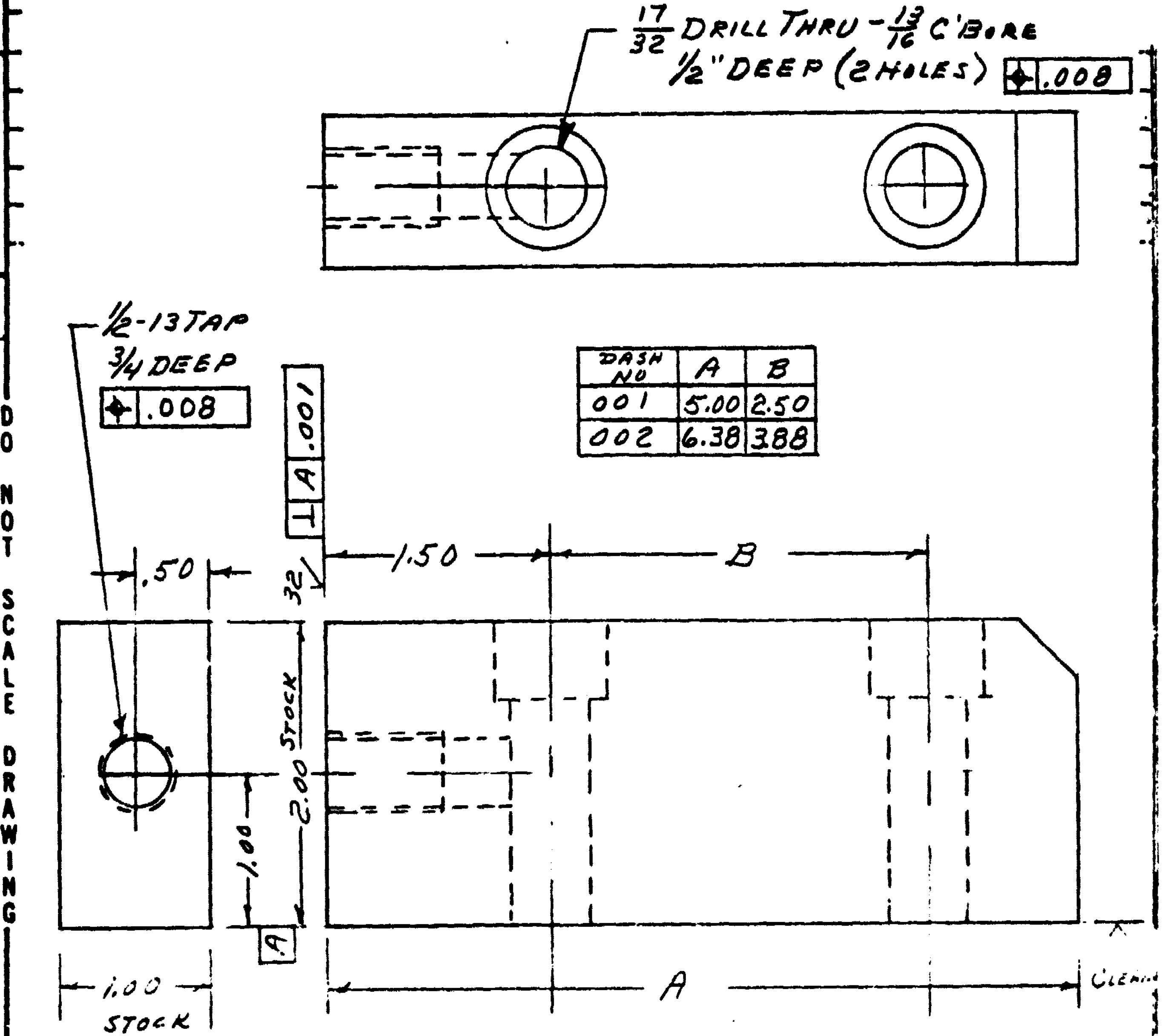

DASH NO	A	B
001	5.00	2.50
002	6.38	3.88

DO NOT SCALE DRAWING

DO NOT SCALE THIS PRINT
UNLESS OTHERWISE SPECIFIED
BREAK ALL SHARP EDGES
DIMENSIONS ARE IN INCHES

DRAWN	DATE	APPROVED	DATE	CODE
RBB	11/17/77			
CHECKED	DATE	APPROVED	DATE	CLASS

GUSSETS - BLADE HEAD
JPL PROTOTYPE SAW

NOT OTHERWISE SPEC: FRAC ± ANG ± SCALE FULL
FIN. ✓ DEC .X ± .XX ± .XXX ±

varian

DIVISION	SIZE	DRAWING NO.
VAC/LEX	A	S1052

DESCRIPTION OF CHANGE

NUM
EO
DFT
CHK
DATE
REV

DASH NO.	TYPE OR MODEL	NEXT ASSEMBLY	REQ	PART NUMBER	DESCRIPTION OR MATERIAL	ITEM

A 51053

DO NOT SCALE DRAWING

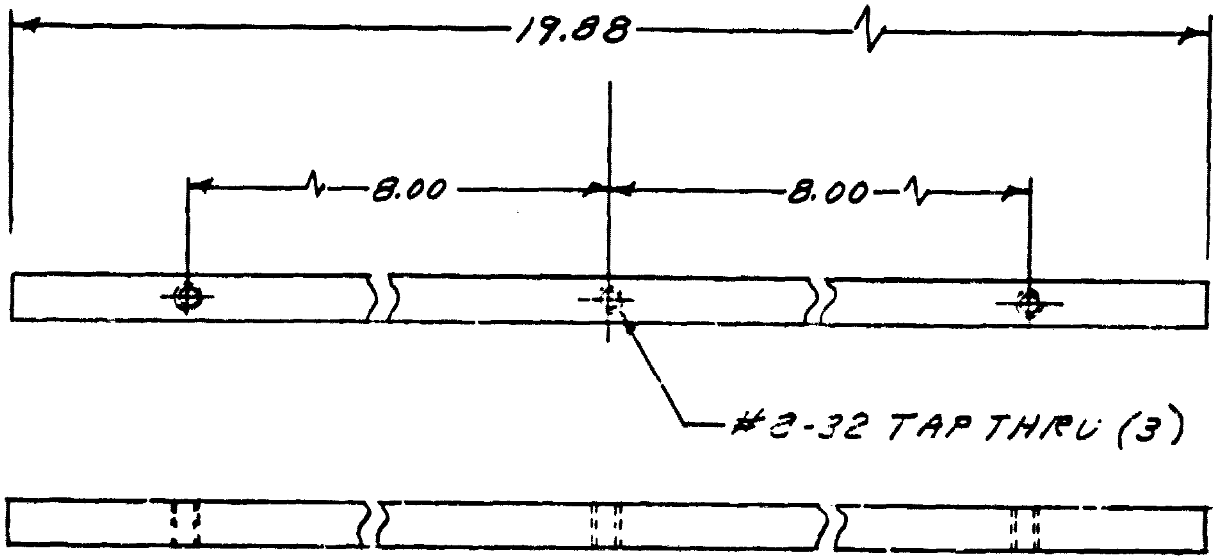

MATL - 1/4" SAE 1020 KEY

(2 REQ'D)

DO NOT SCALE THIS PRINT
UNLESS OTHERWISE SPECIFIED
BREAK ALL SHARP EDGES
DIMENSIONS ARE IN INCHES

DRAWN	DATE	APPROVED	DATE	CODE
RPG3	12/16/77			
CHECKED	DATE	APPROVED	DATE	CLASS

DESCRIPTION OF CHANGE

NUM	
EO	
DFT	
CHK	
DATE	
REV	

SMALL BLADEHEAD KEY
JPL PROTOTYPE SAW

NOT OTHERWISE SPEC FRAC ± 1/64 ANG ± 1/4° — SCALE ~

FIN ✓ DEC X ± .1 XX ± .02 XXX ± .005

varian

DIVISION	SIZE	DRAWING NO	REV
VAC/LEX	A	51053	

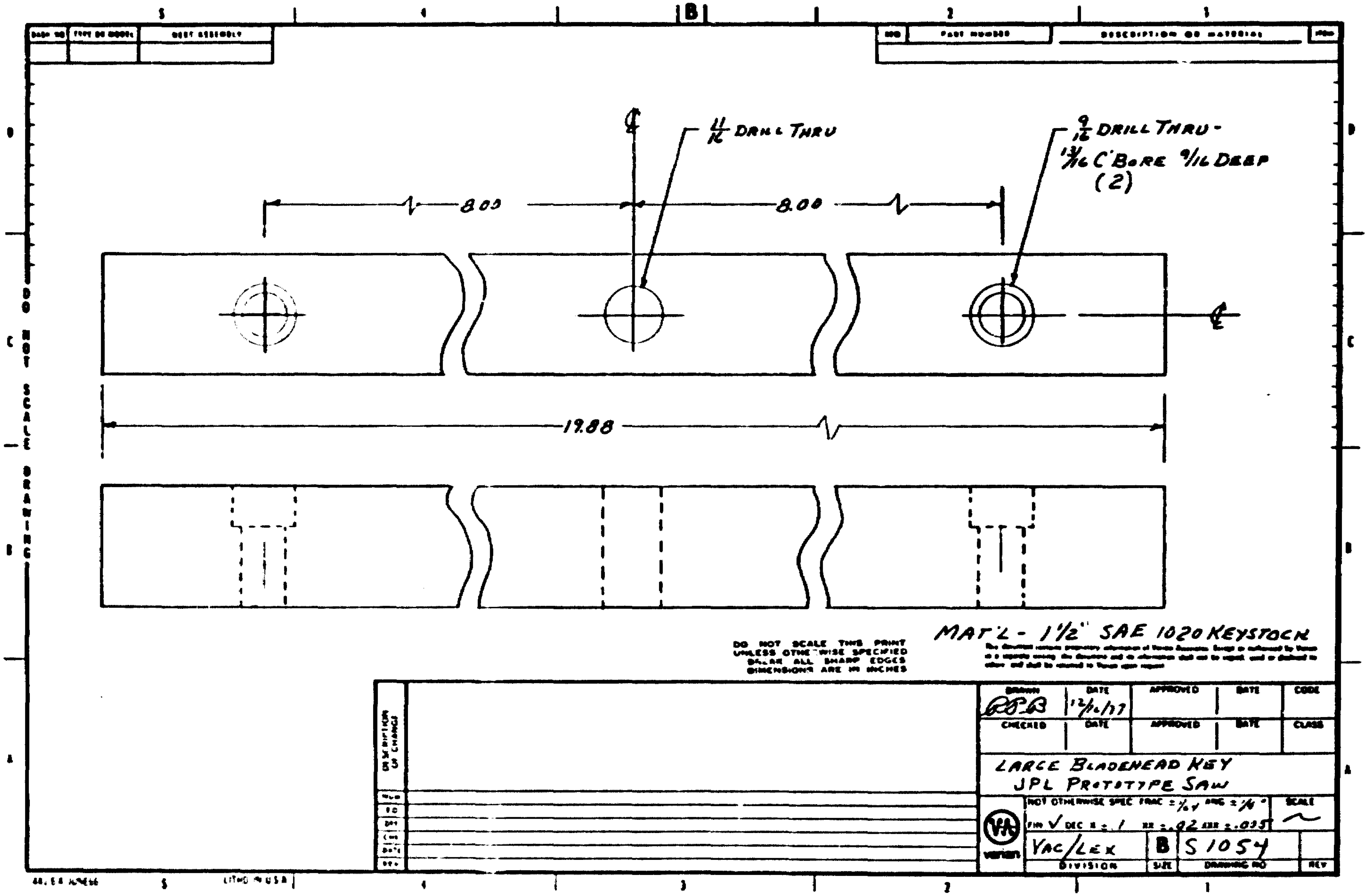

11/16 DRILL THRU
9/16 DRILL THRU - 13/16 C'BORE 9/16 DEEP (2)
8.00
8.00
19.88
MAT'L - 1 1/2" SAE 1020 KEYSTOCK
DO NOT SCALE THIS PRINT
UNLESS OTHERWISE SPECIFIED
BREAK ALL SHARP EDGES
DIMENSIONS ARE IN INCHES
DRAWN
DATE
12/16/77
CHECKED
APPROVED
CODE
CLASS
LARGE BLADEHEAD KEY
JPL PROTOTYPE SAW
NOT OTHERWISE SPEC
SCALE
VAC/LEX
DIVISION
B
S 1054
DRAWING NO
DESCRIPTION OF CHANGE
PART NUMBER
DESCRIPTION OR MATERIAL
NEXT ASSEMBLY
LITHO IN U.S.A.

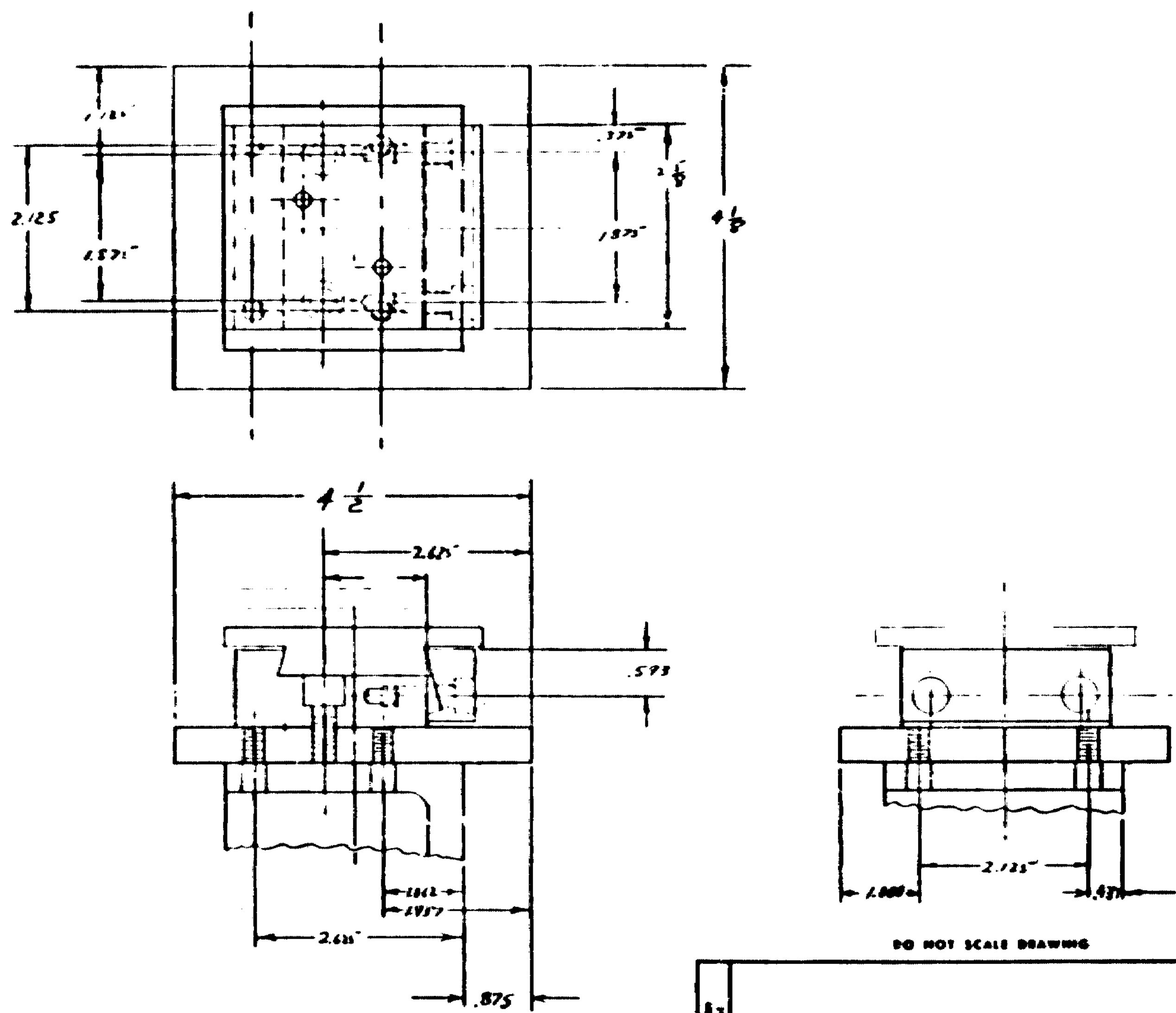

DO NOT SCALE DRAWING

Drawn: KZ	Date: 10-15-73

WORK HOLDER LAYOUT
LAB. SAW

Scale: FULL

C 52053

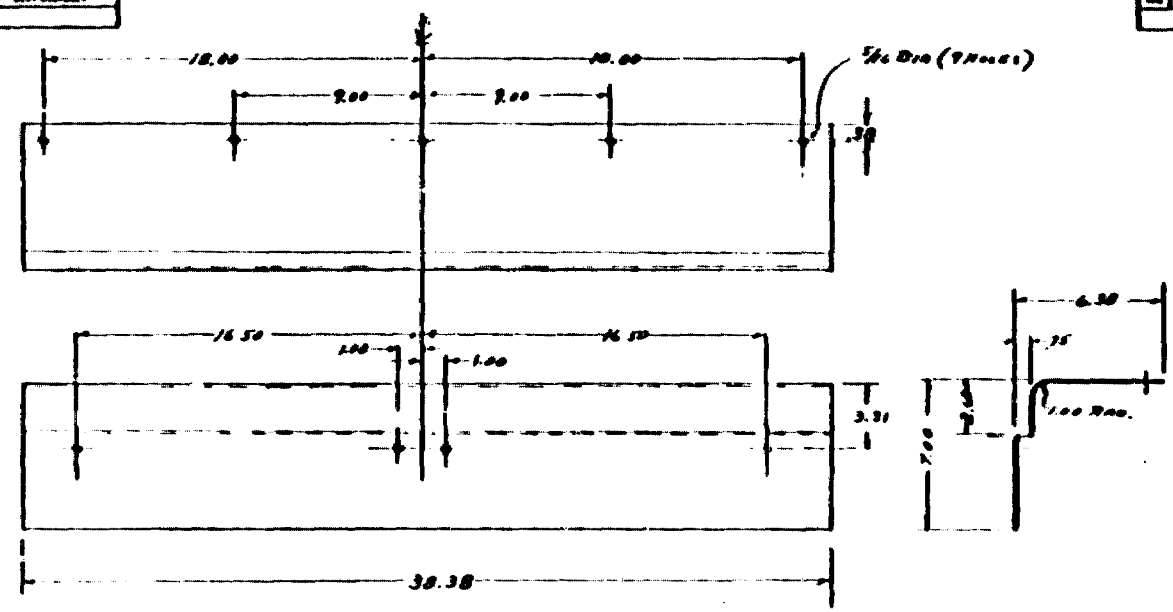

1/16 THK. Sheet Aluminum # 6822-19-063

Remove Sharp Corners

DO NOT SCALE DRAWING

Side Shields

JPL Prototype Saw

Varian

Vac / Lev

C 51055

Scale 1/4 : 1

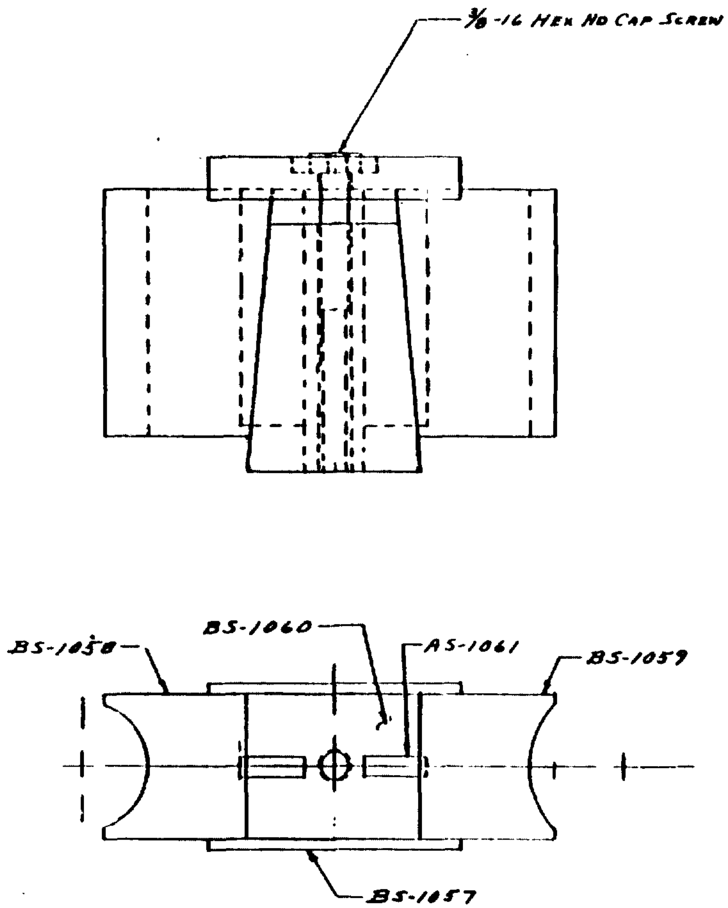

(4 REQ'D)

DO NOT SCALE DRAWING

DRAWN	GBR	DATE	11/23/77	APPROVED	DATE
CHECKED		DATE		APPROVED	DATE

ADJ. TENSIONING BAR (BLADEHEAD)
JPL PROTOTYPE SAW

SCALE: FULL

Vac/Lev — C — S1056

varian

LITHO IN U.S.A.

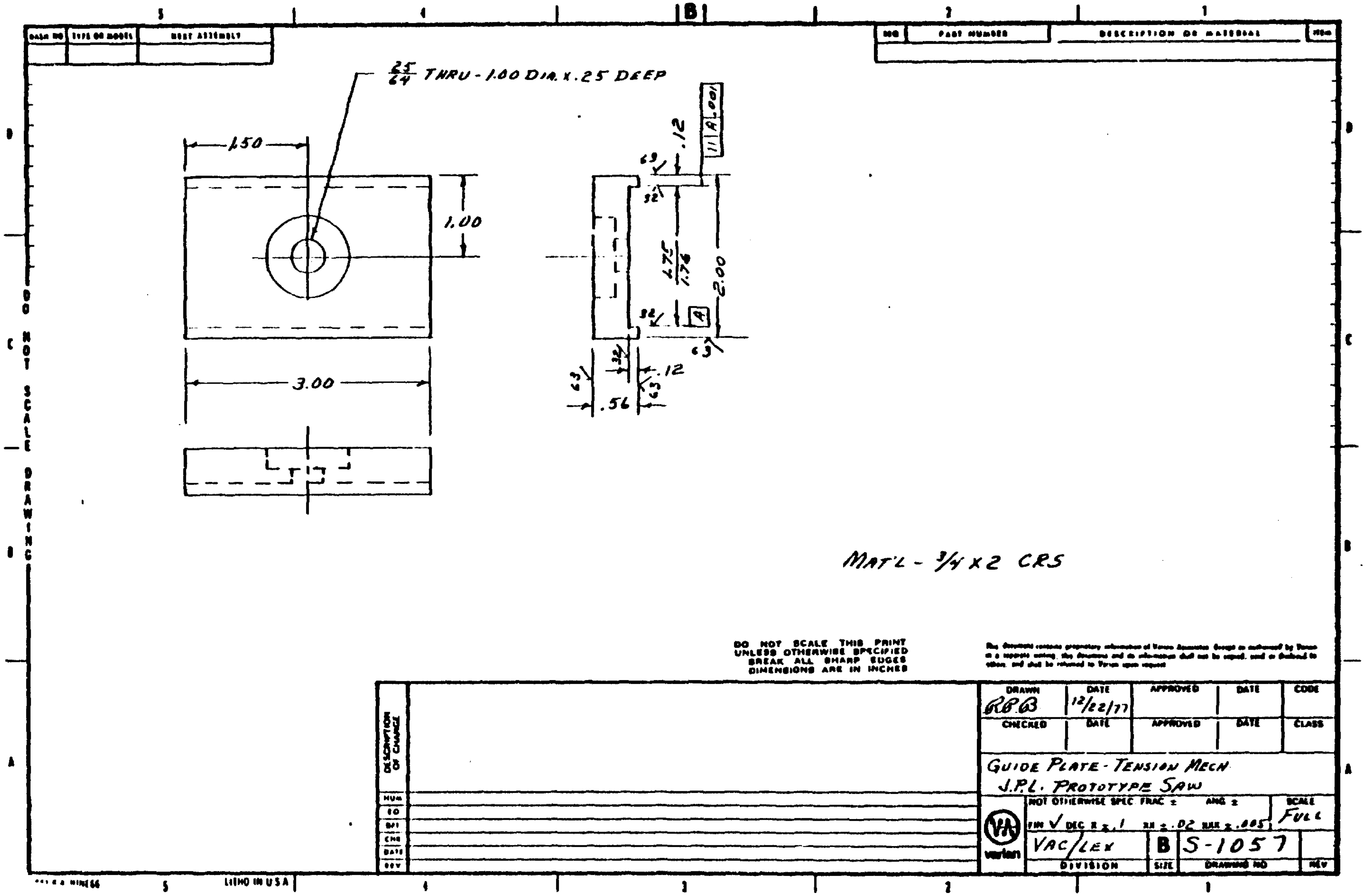

25/64 THRU - 1.00 DIA. X .25 DEEP
1.50
1.00
3.00
.12
.475
1.76
2.00
.56
.12
MAT'L - 3/4 X 2 CRS
DO NOT SCALE THIS PRINT
UNLESS OTHERWISE SPECIFIED
BREAK ALL SHARP EDGES
DIMENSIONS ARE IN INCHES
DO NOT SCALE DRAWING
DRAWN RBB
DATE 12/22/77
CHECKED
APPROVED
CODE
CLASS
GUIDE PLATE - TENSION MECH
J.P.L. PROTOTYPE SAW
SCALE FULL
VAC/LEX
DIVISION
B
S-1057
DRAWING NO
varian
LITHO IN U.S.A.

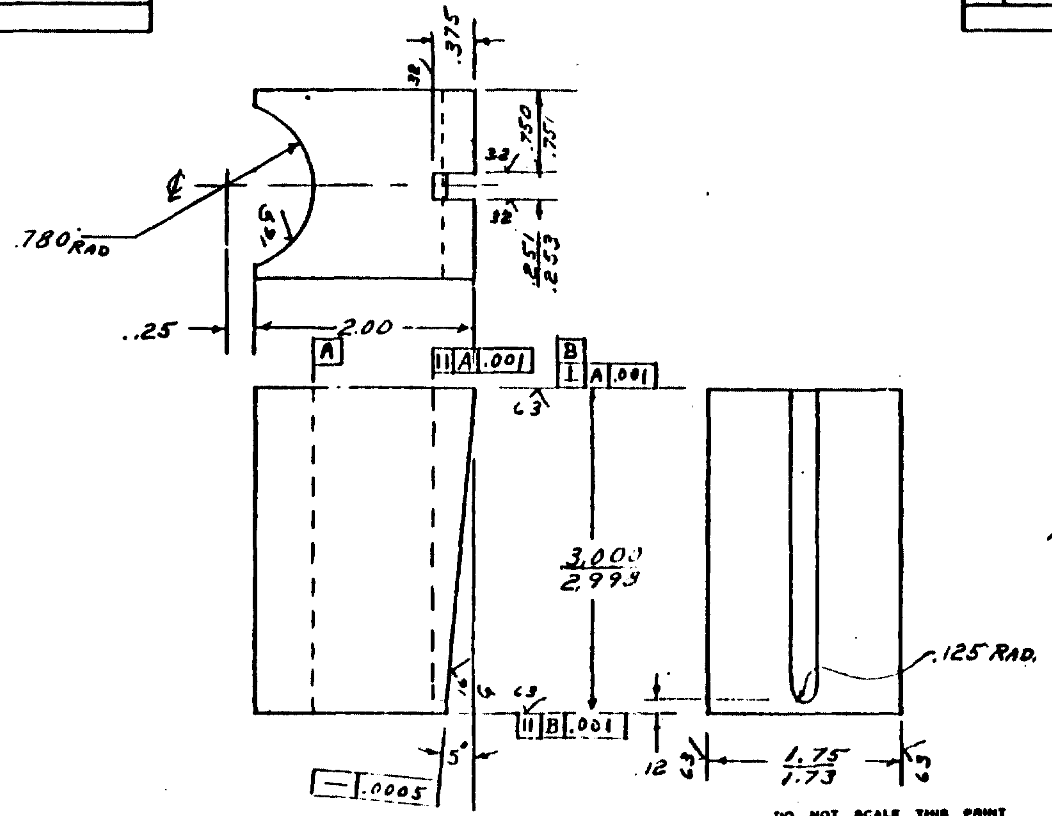

MAT'L - GRAPH - MO

HEAT TREAT TO ROCKWELL C-58-60
BEFORE GRINDING

DO NOT SCALE THIS PRINT
UNLESS OTHERWISE SPECIFIED
BREAK ALL SHARP EDGES
DIMENSIONS ARE IN INCHES

DO NOT SCALE DRAWING

DRAWN	DATE	APPROVED	DATE	CODE
RPB	12/23/77			
CHECKED	DATE	APPROVED	DATE	CLASS

BLOCK - TENSION MECH.
JPL PROTOTYPE SAW

NOT OTHERWISE SPEC: FRAC ± ANG ± 0°2' SCALE FULL
FIN. √ DEC X ±.1 XX ±.01 XXX ±.005

varian VAC/LEX B S1058
DIVISION SIZE DRAWING NO. REV

LITHO IN U.S.A.

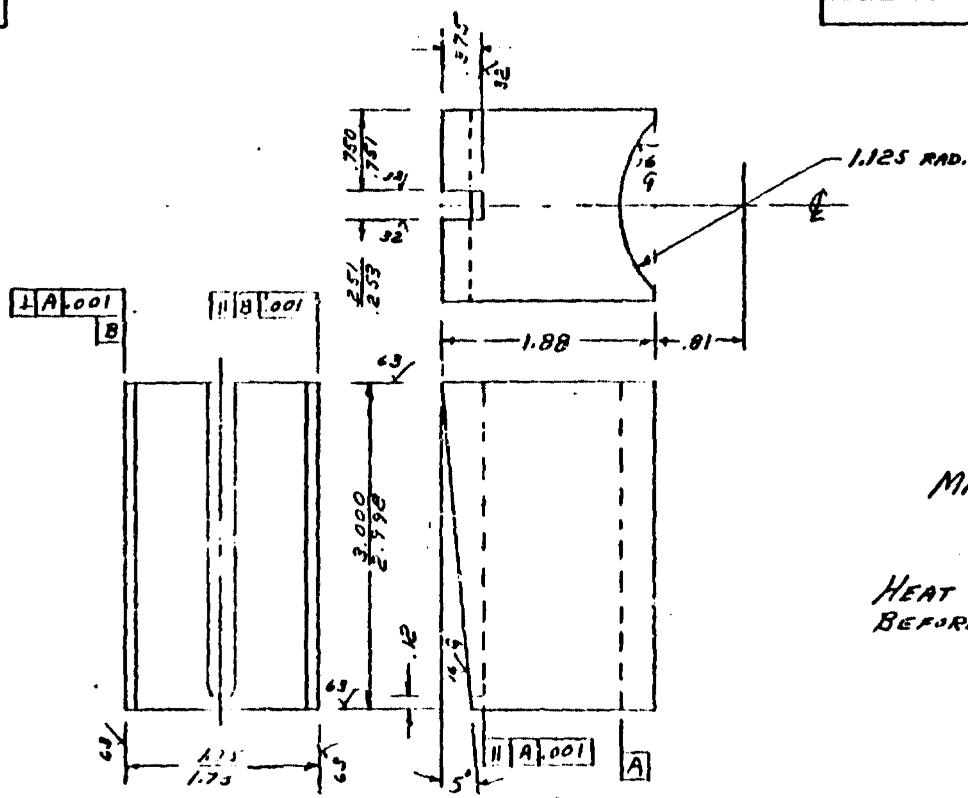

MATL. GRAPH-Mo

HEAT TREAT TO ROCKWELL C-58-60 BEFORE GRINDING

DO NOT SCALE THIS PRINT
UNLESS OTHERWISE SPECIFIED
BREAK ALL SHARP EDGES
DIMENSIONS ARE IN INCHES

DRAWN	DATE	APPROVED	DATE	CODE
RBB	12/22/77			
CHECKED	DATE	APPROVED	DATE	CLASS

BLOCK-TENSION MECH
JPL PROTOTYPE SAW

NOT OTHERWISE SPEC FRAC ± ANG ±0°2' SCALE FULL

DIVISION: VAC/LEX | SIZE: B | DRAWING NO: S 10 5 9

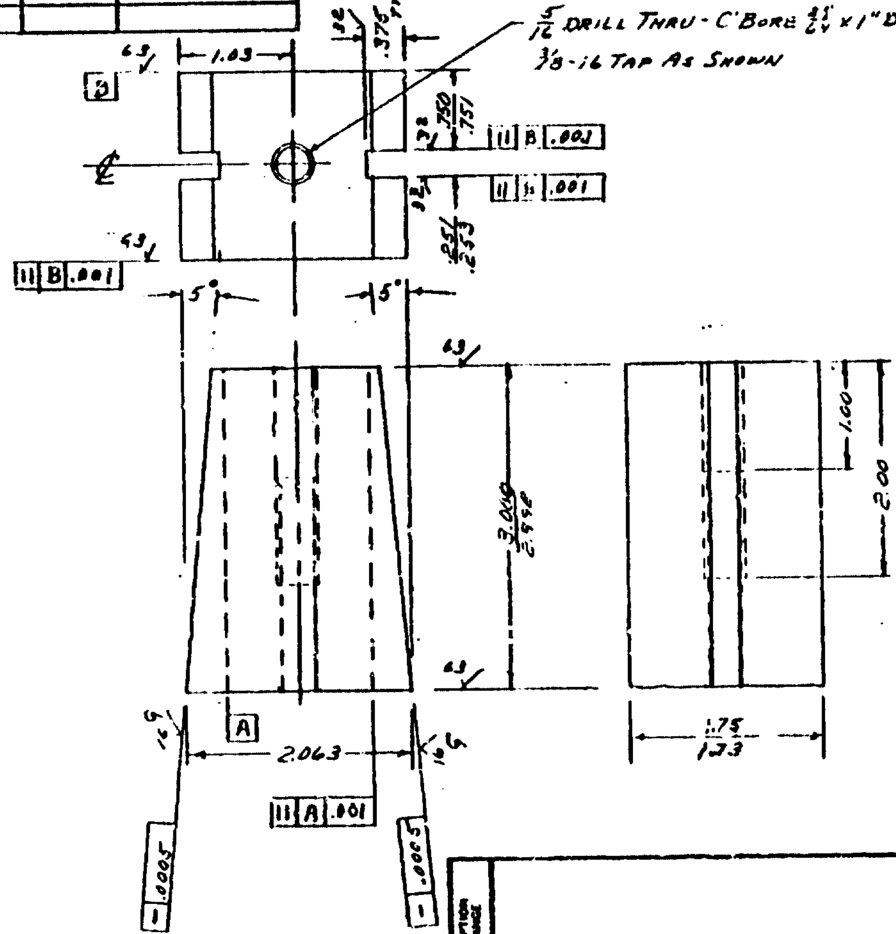

MAT'L - GRAPH - MO

HEAT TREAT TO ROCKWELL C-58-60
BEFORE GRINDING

DO NOT SCALE THIS PRINT
UNLESS OTHERWISE SPECIFIED
BREAK ALL SHARP EDGES
DIMENSIONS ARE IN INCHES

DRAWN	DATE	APPROVED	DATE	CODE
RPB	12/21/77			
CHECKED	DATE	APPROVED	DATE	CLASS

TENSION MECH. WEDGE
JPL PROTOTYPE SAW

NOT OTHERWISE SPEC: FRAC ± ANG ± 0°2' SCALE FULL

DEC X ± .1 XX ± .01 XXX ± .005

varian VAC / LEX — DIVISION; SIZE B; DRAWING NO. S-1060; REV

LITHO IN U.S.A.

5C

DASH NO.	TYPE OR MODEL	NEXT ASSEMBLY	REQ	PART NUMBER	DESCRIPTION OR MATERIAL	ITEM

A S1061

DO NOT SCALE DRAWING

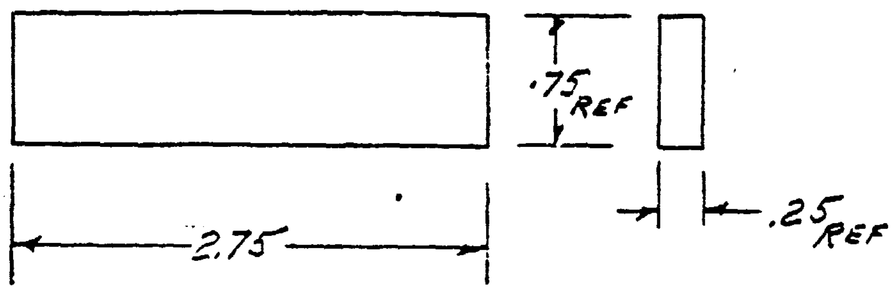

3/4 X 1/4 GROUND FLAT STOCK

(8 REQD)

DO NOT SCALE THIS PRINT
UNLESS OTHERWISE SPECIFIED
BREAK ALL SHARP EDGES
DIMENSIONS ARE IN INCHES

DRAWN	DATE	APPROVED	DATE	CODE
RPB	12/22/77			✓
CHECKED	DATE	APPROVED	DATE	CLASS

KEY - TENSION MECH
JPL PROTOTYPE SAW

NOT OTHERWISE SPEC: FRAC ± ANG ± SCALE FULL
FIN. ✓ DEC .X ±.1 .XX ±.02 .XXX ±.005

varian

DIVISION	SIZE	DRAWING NO.	REV
VAC/LEX	A	S1061	

DESCRIPTION OF CHANGE

NUM	
EO	
DFT	
CHK	
DATE	
REV	

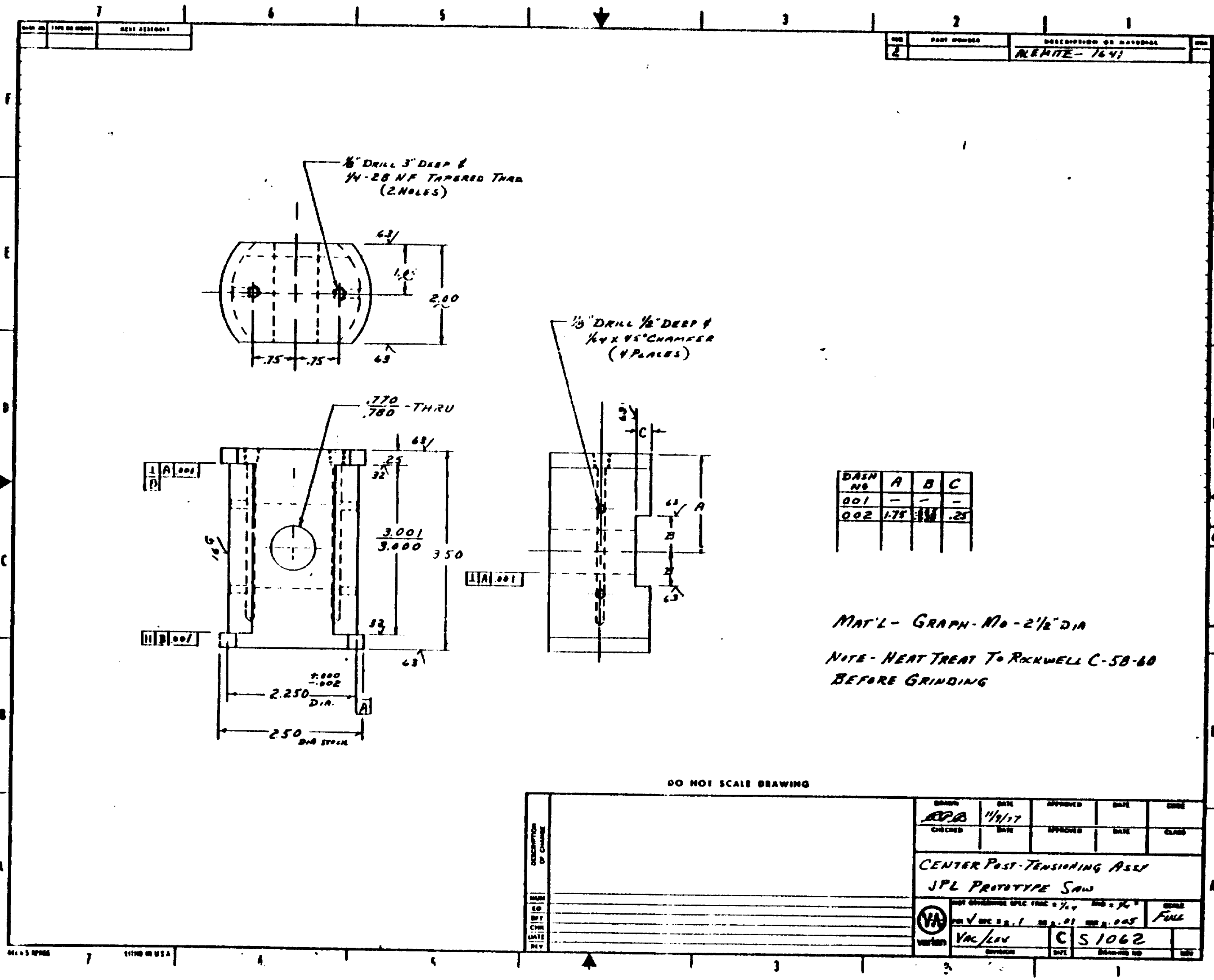

DASH NO	A	B	C
001	—	—	—
002	1.75	[illegible]	.25

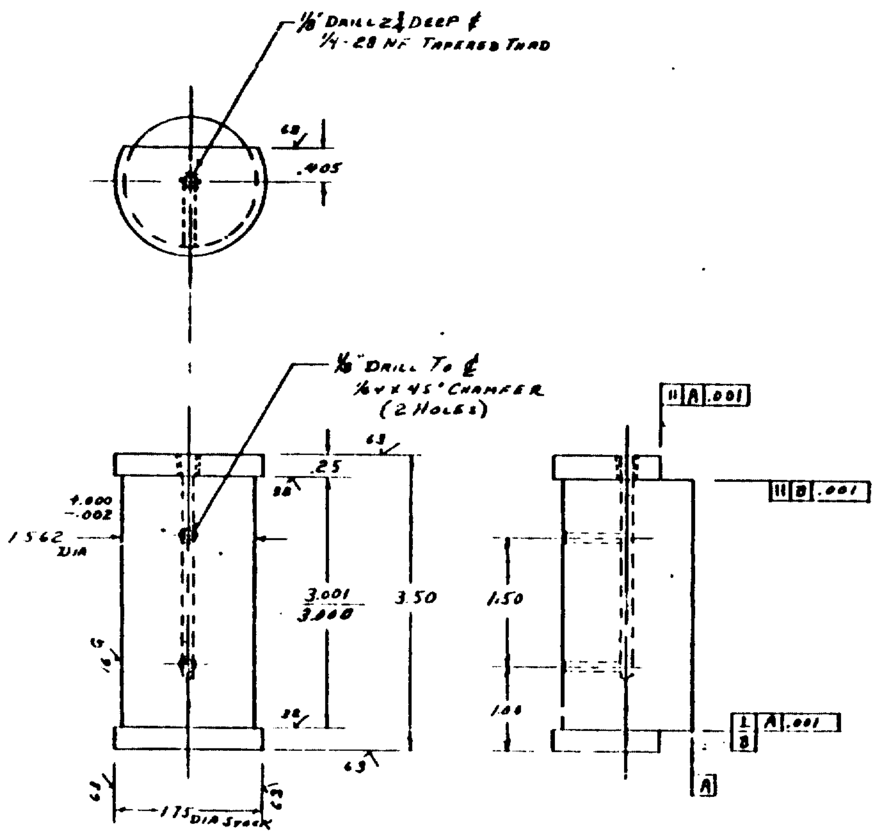

ALGEMITE #1641

MAT'L - GRAPH-MO - 1.75 DIA

NOTE - HEAT TREAT TO ROCKWELL C-58-60
BEFORE GRINDING

DO NOT SCALE DRAWING

DRAWN	RCB
DATE	11/8/77
TITLE	END POST - TENSIONING ASSY. JPL PROTOTYPE SAW
SCALE	FULL
DIVISION	VAC/LEX
SIZE	C
DRAWING NO.	5-4063

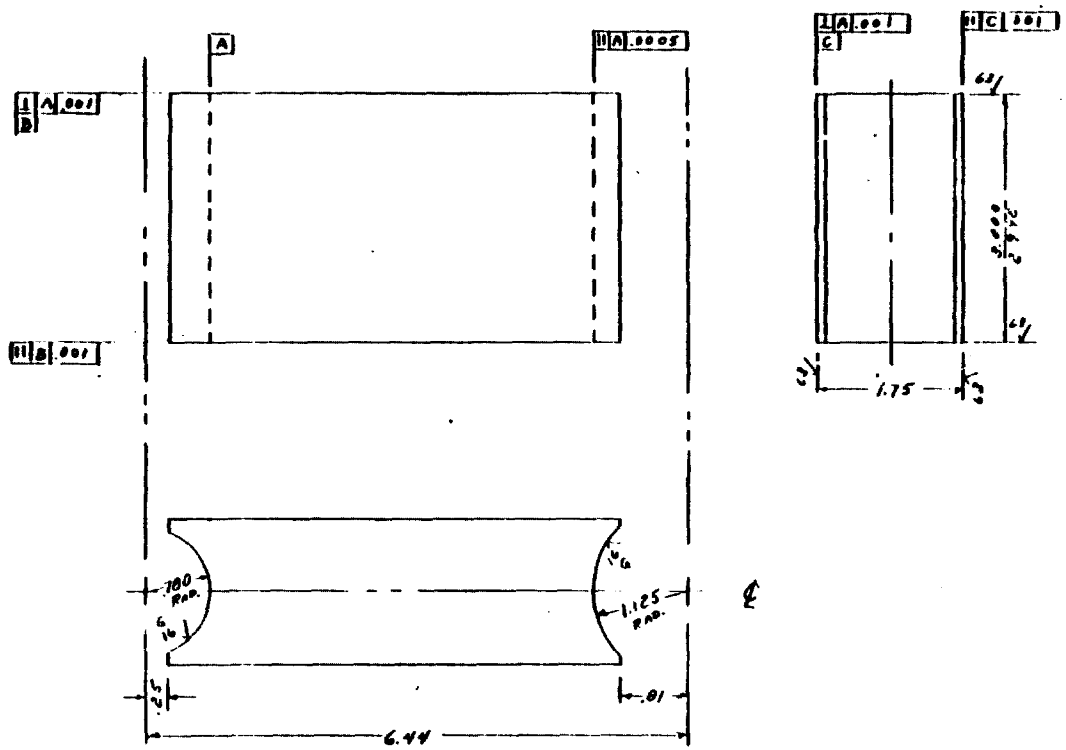

MAT'L - GRAPH-MO

NOTE - HEAT TREAT TO ROCKWELL C-59-62
BEFORE GRINDING

DO NOT SCALE DRAWING

SOLID TENSIONING BAR (BLADEHEAD)
JPL PROTOTYPE SAW

SCALE: FULL

VAC/LEX C S1064

12/20/77

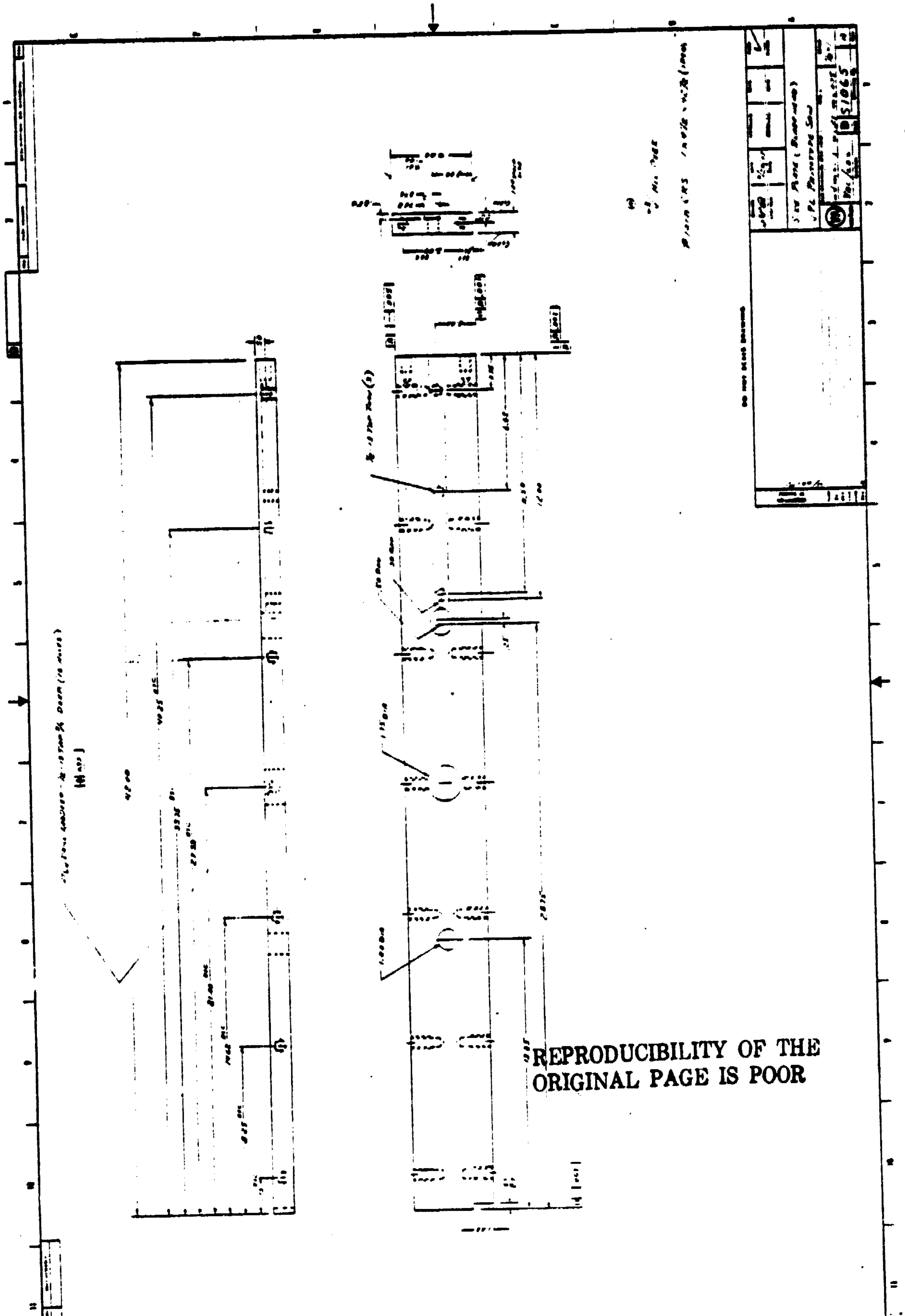

71

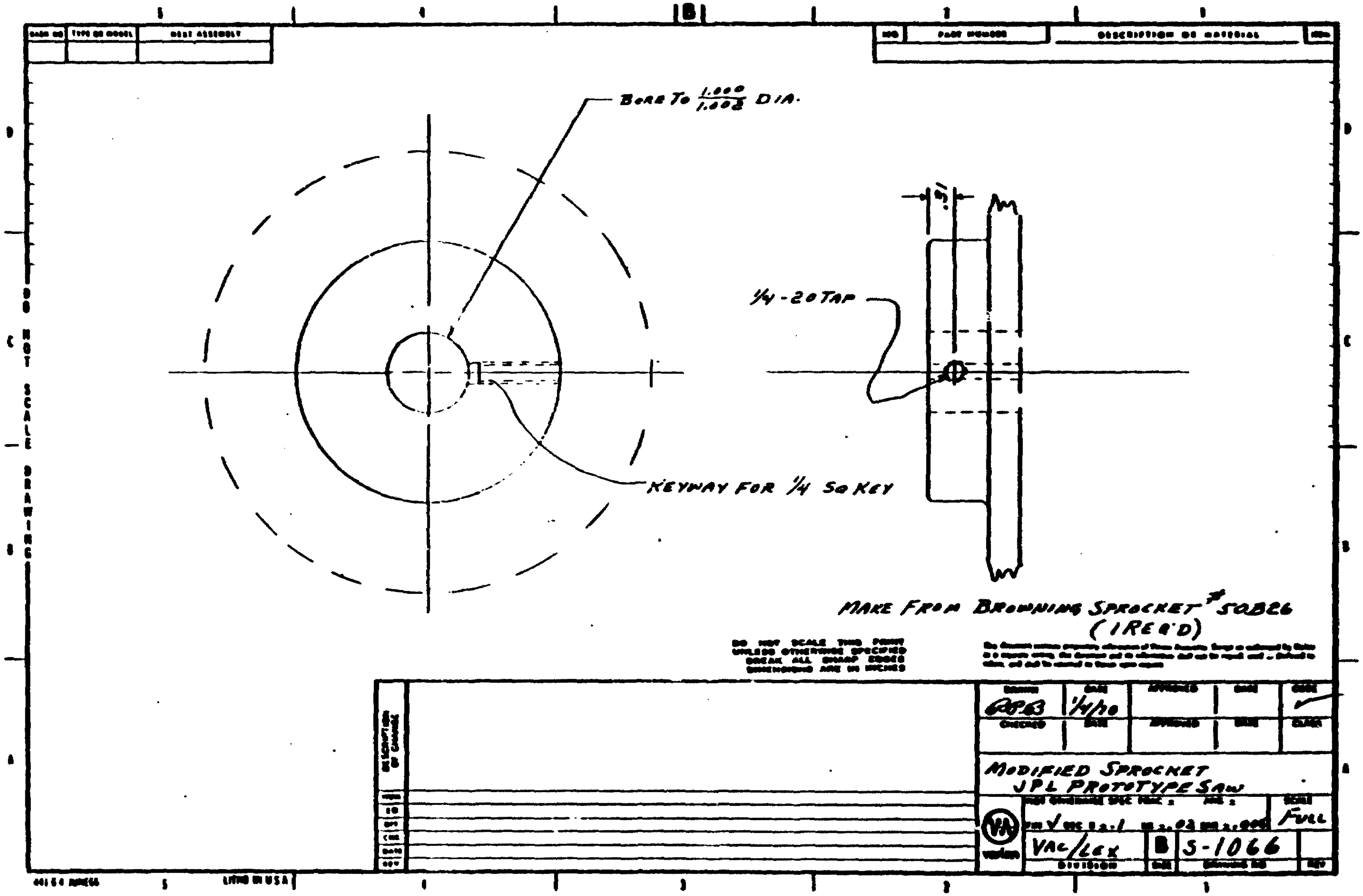

BORE TO $\frac{1.000}{1.002}$ DIA.
1/4-20 TAP
KEYWAY FOR 1/4 SQ KEY
MAKE FROM BROWNING SPROCKET # 50B26
(1 REQ'D)
DO NOT SCALE THIS PRINT
UNLESS OTHERWISE SPECIFIED
BREAK ALL SHARP EDGES
DIMENSIONS ARE IN INCHES
MODIFIED SPROCKET
JPL PROTOTYPE SAW
1/4/70
FULL
VAC/LEX
B
S-1066
DO NOT SCALE DRAWING
LITHO IN U.S.A.

DASH NO	TYPE OR MODEL	NEXT ASSEMBLY	REQ	PART NUMBER	DESCRIPTION OR MATERIAL	ITEM

A S-1067

DO NOT SCALE DRAWING

BORE THIS END TO 5/8 DIA

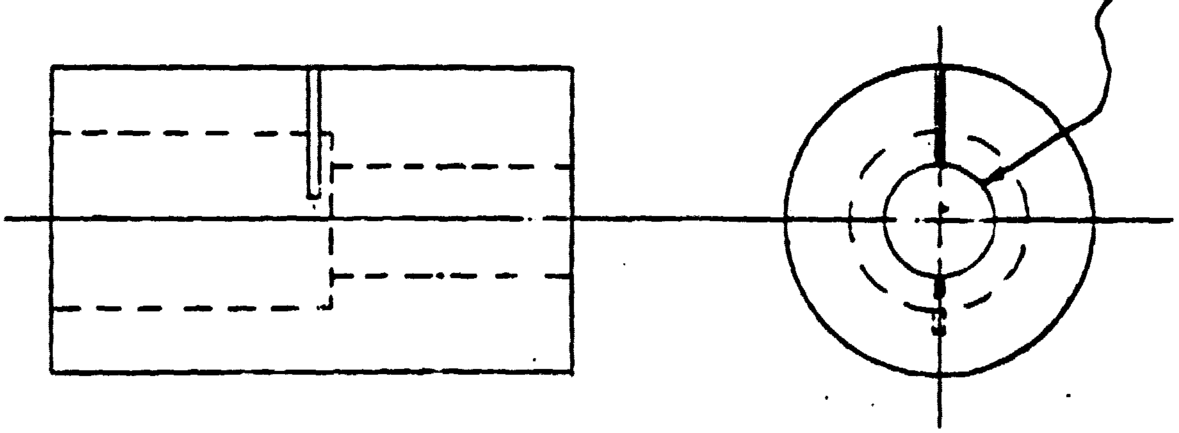

MAKE FROM CLAMP-TITE COUPLING #16232
1" X 1/2"
(2 REQ'D)

DO NOT SCALE THIS PRINT
UNLESS OTHERWISE SPECIFIED
BREAK ALL SHARP EDGES
DIMENSIONS ARE IN INCHES

DRAWN	DATE	APPROVED	DATE	CODE
RPB	1/5/78			✓
CHECKED	DATE	APPROVED	DATE	CLASS

MODIFIED COUPLING
JPL PROTOTYPE SAW

NOT OTHERWISE SPEC. FRAC ± ANG ± SCALE FULL
FIN. ✓ DEC X ± .1 XX ± .02 XXX ± .005

DIVISION	SIZE	DRAWING NO.	REV
VAC/LEX	A	S-1067	

DESCRIPTION OF CHANGE

NUM	
EO	
DFT	
CHK	
DATE	
REV	—

varian

LITHO IN U.S.A.

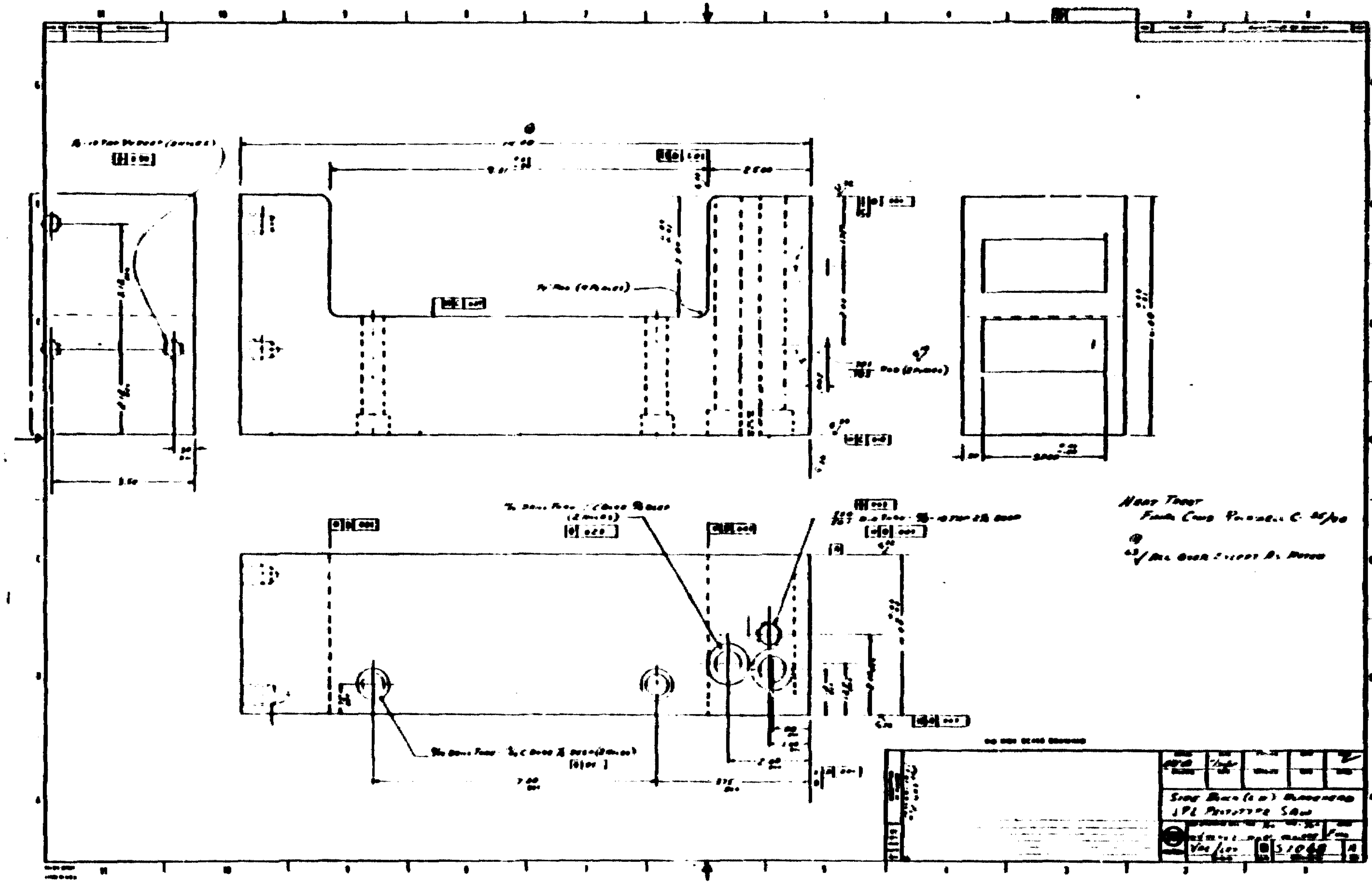

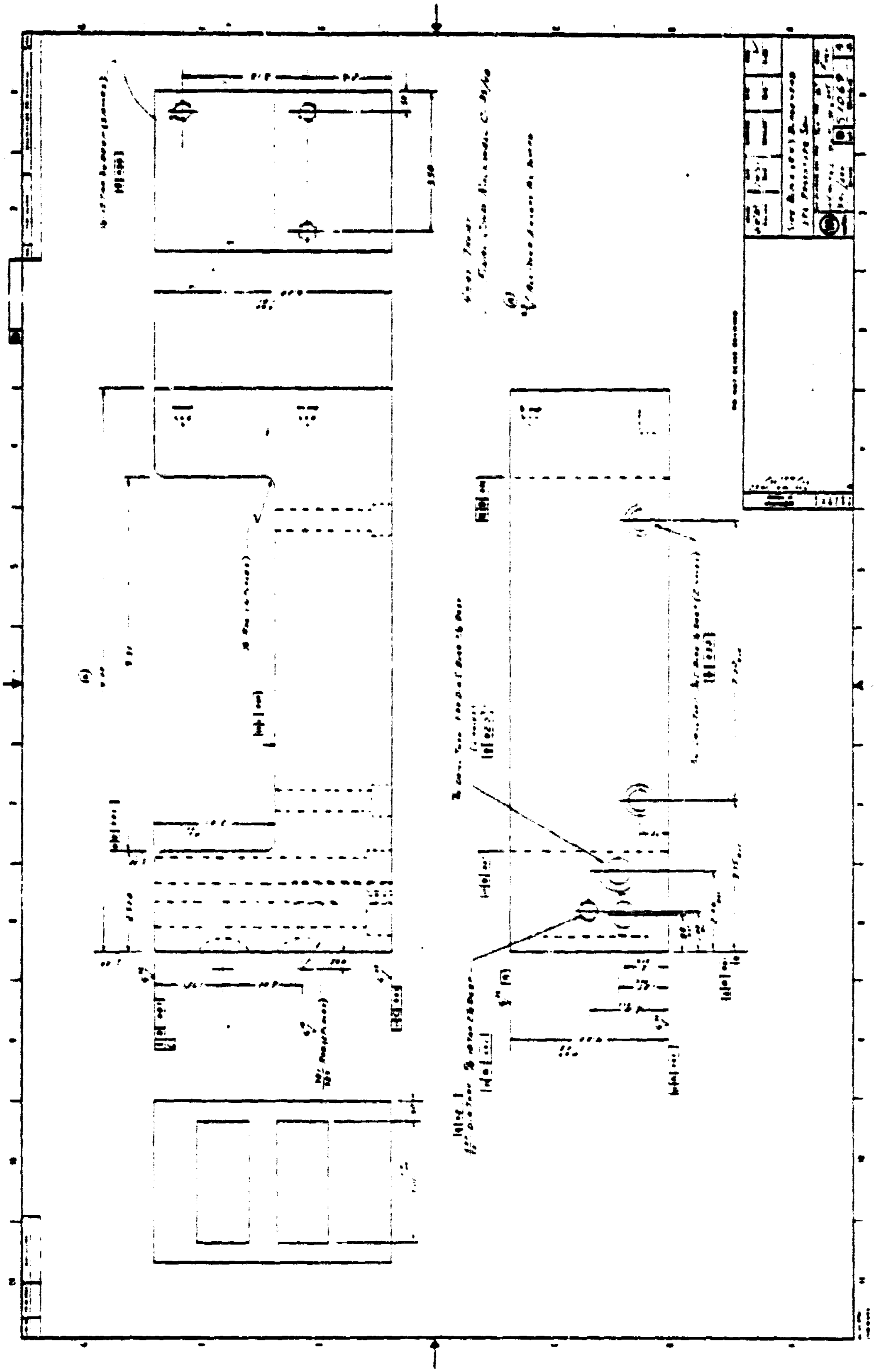

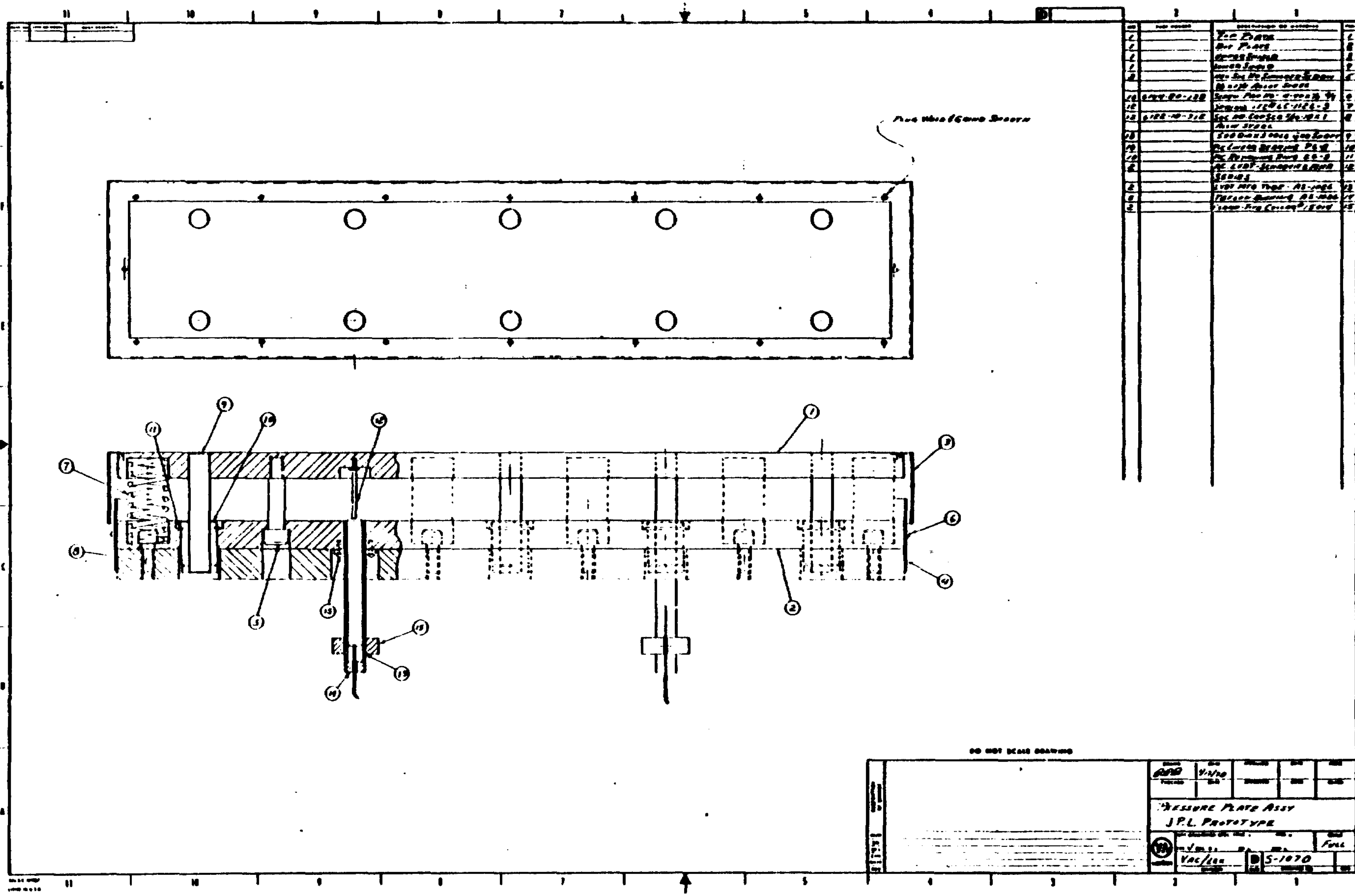
Top Plate
Bot Plate
DO NOT SCALE DRAWING
RESSURE PLATE ASSY
J.P.L. PROTOTYPE
FULL
D
S-1070

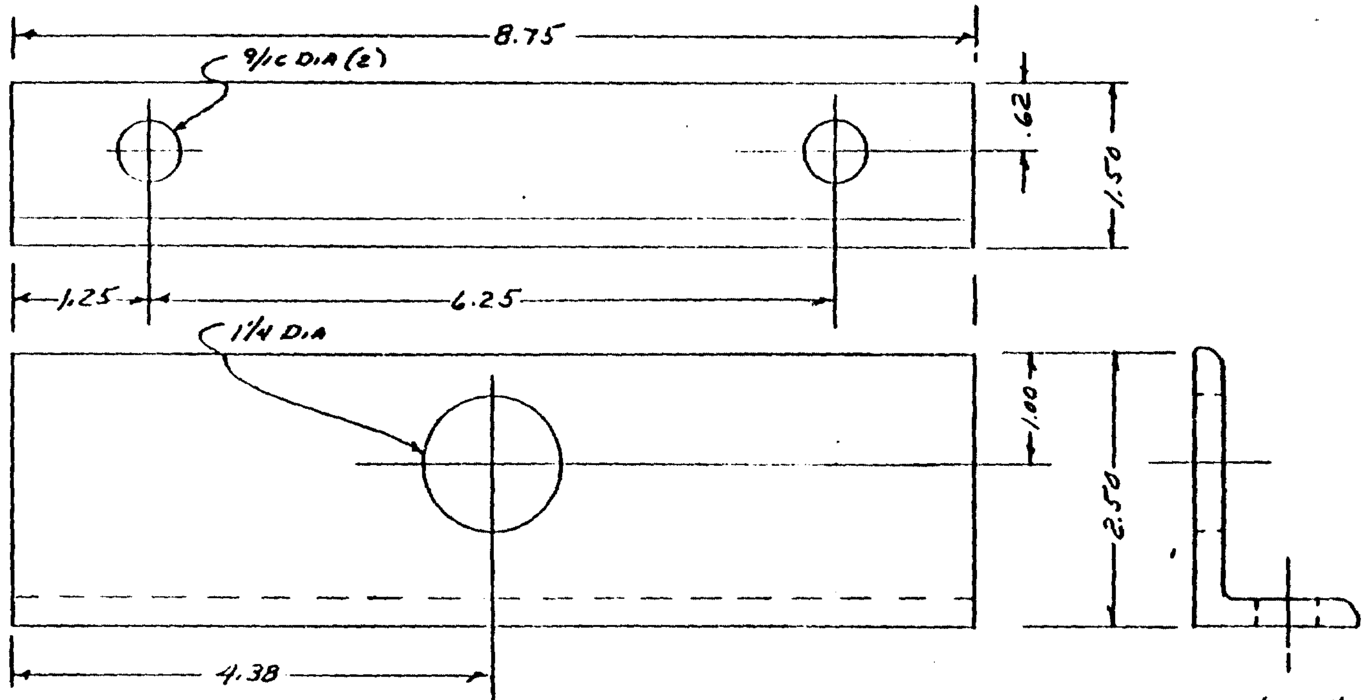

1½ x 2½ x ¼ ANGLE IRON

DO NOT SCALE THIS PRINT
UNLESS OTHERWISE SPECIFIED
BREAK ALL SHARP EDGES
DIMENSIONS ARE IN INCHES

DO NOT SCALE DRAWING

DRAWN	DATE	APPROVED	DATE	CODE
RPB	1/24/70			✓
CHECKED	DATE	APPROVED	DATE	CLASS

TOP CLAMP LIFTING ANGLES
JPL PROTOTYPE SAW

NOT OTHERWISE SPEC. FRAC ± ANG ± SCALE: FULL

FIN ✓ DEC X ± XX ± XXX ±

varian | VAC/LEV | B | 5-1071

DIVISION | SIZE | DRAWING NO | REV

44164 JUNE65 LITHO IN U.S.A.

DASH NO.	TYPE OR MODEL	NEXT ASSEMBLY	REQ	PART NUMBER	DESCRIPTION OR MATERIAL	ITEM

A | S 1072

DO NOT SCALE DRAWING

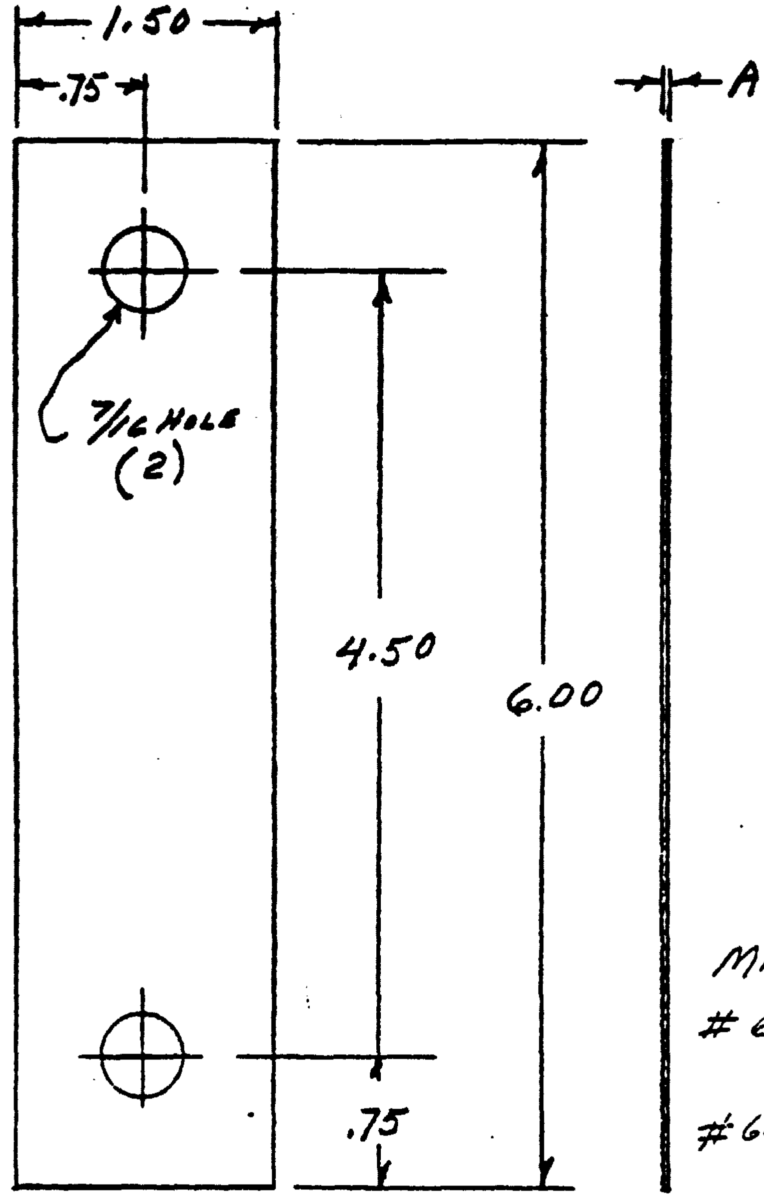

DASH No	A
001	.035
002	.059

MAT'L - M/S
#682220035 (.035)
#6821-25-065 (.059)

DO NOT SCALE THIS PRINT
UNLESS OTHERWISE SPECIFIED
BREAK ALL SHARP EDGES
DIMENSIONS ARE IN INCHES

DRAWN	DATE	APPROVED	DATE	CODE
[illegible]	1/24/78			
CHECKED	DATE	APPROVED	DATE	CLASS

SHIMS - BLADEHEAD
JPL PROTOTYPE

NOT OTHERWISE SPEC: FRAC ± ANG ±
FIN. ✓ DEC X ±.1 XX ±.02 XXX ±.005
SCALE FULL

varian

DIVISION	SIZE	DRAWING NO.	REV
VAC/LEX	A	S 1072	

DESCRIPTION OF CHANGE

NUM	
EO	
DFT	
CHK	
DATE	
REV	

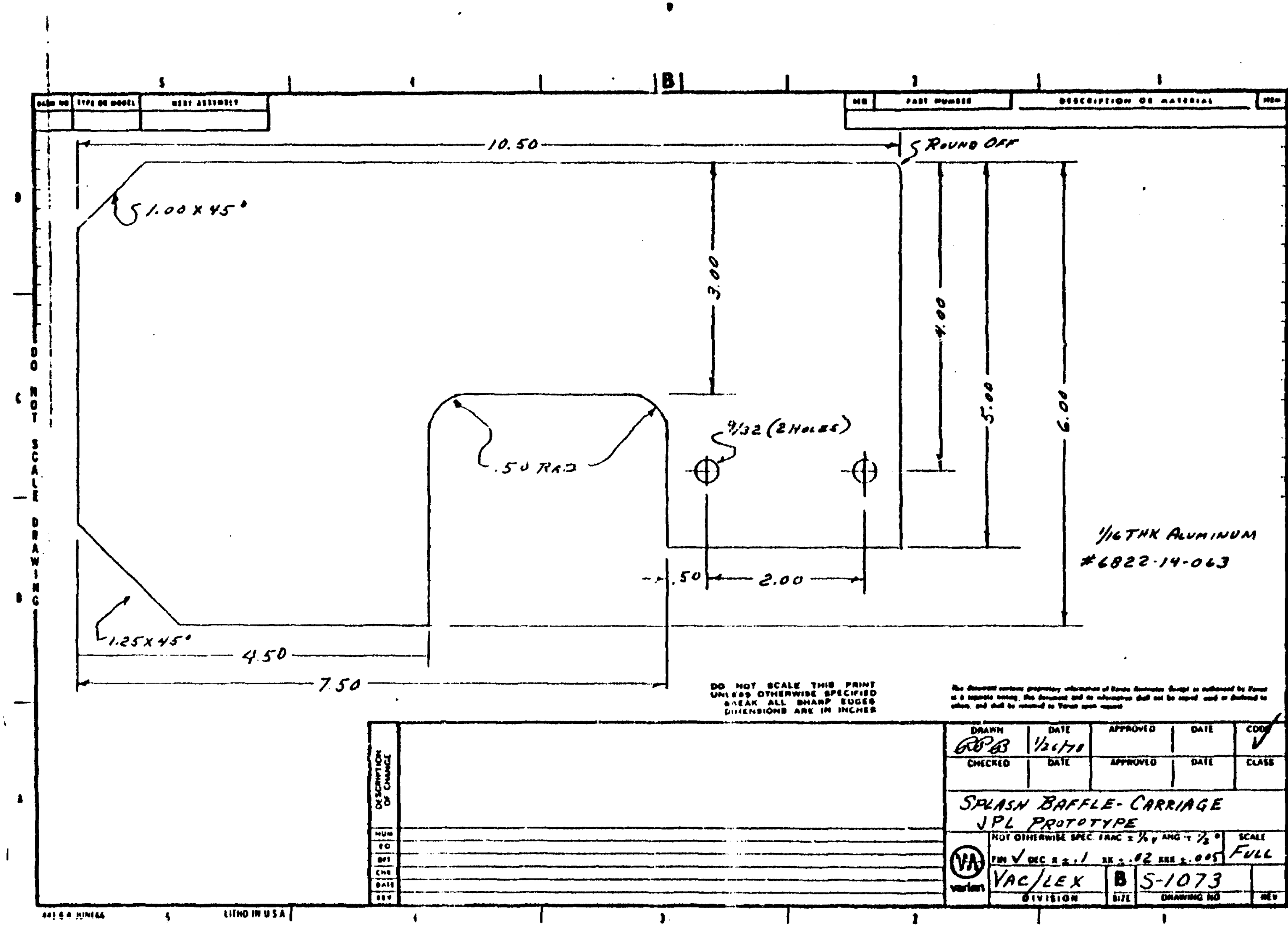

10.50
ROUND OFF
1.00 X 45°
3.00
4.00
5.00
6.00
9/32 (2 HOLES)
.50 RAD
1/16 THK ALUMINUM
#6822-14-063
.50
2.00
1.25 X 45°
4.50
7.50
DO NOT SCALE DRAWING
DO NOT SCALE THIS PRINT
UNLESS OTHERWISE SPECIFIED
BREAK ALL SHARP EDGES
DIMENSIONS ARE IN INCHES
DRAWN
DATE
1/26/70
APPROVED
CODE
CHECKED
CLASS
SPLASH BAFFLE-CARRIAGE
JPL PROTOTYPE
SCALE
FULL
VAC/LEX
DIVISION
B
SIZE
S-1073
DRAWING NO
REV
DESCRIPTION OF CHANGE
NEXT ASSEMBLY
PART NUMBER
DESCRIPTION OF MATERIAL
varian
LITHO IN U.S.A.

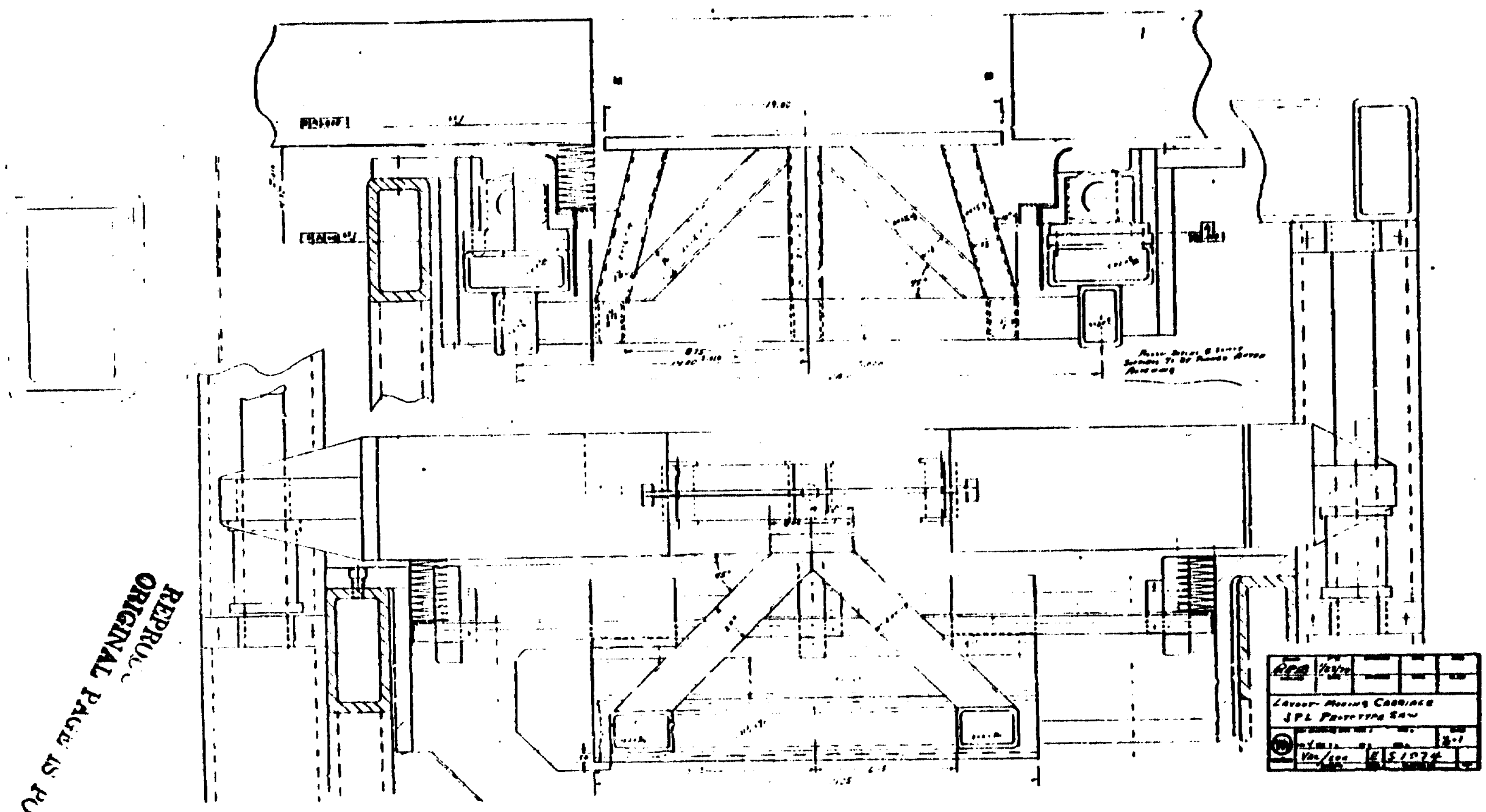
Layout - Moving Carriage
JPL Prototype Saw
2:1
E
51074

DASH NO.	TYPE OR MODEL	NEXT ASSEMBLY	REQ	PART NUMBER	DESCRIPTION OR MATERIAL	ITEM

A 51075

DO NOT SCALE DRAWING

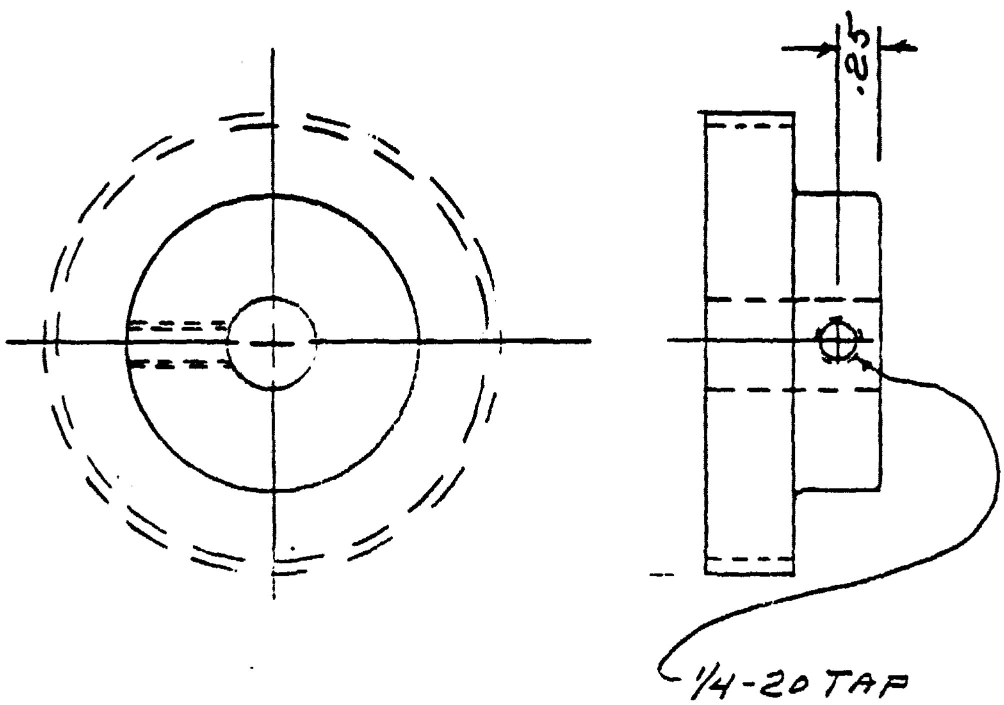

MAT'L - BGW GEAR # NB40A
2 1/2" P.D. 16 PITCH
14 1/2° PRESSURE ANGLE

DRAWN	DATE	APPROVED	DATE	CODE
RPB	1/27/78			✓
CHECKED	DATE	APPROVED	DATE	CLASS

MODIFIED GEAR-SPEED SHIFT
JPL PROTOTYPE

NOT OTHERWISE SPEC: FRAC ± ANG ± SCALE FULL
FIN. ✓ DEC .X ± .XX ± .XXX ±

varian

DIVISION	SIZE	DRAWING NO.	REV
VAC/LEX	A	51075	

DESCRIPTION OF CHANGE

NUM	
EO	
DFT	
CHK	
DATE	
REV	

DASH NO.	TYPE OR MODEL	NEXT ASSEMBLY	REQ	PART NUMBER	DESCRIPTION OR MATERIAL	ITEM

A 51076

DO NOT SCALE DRAWING

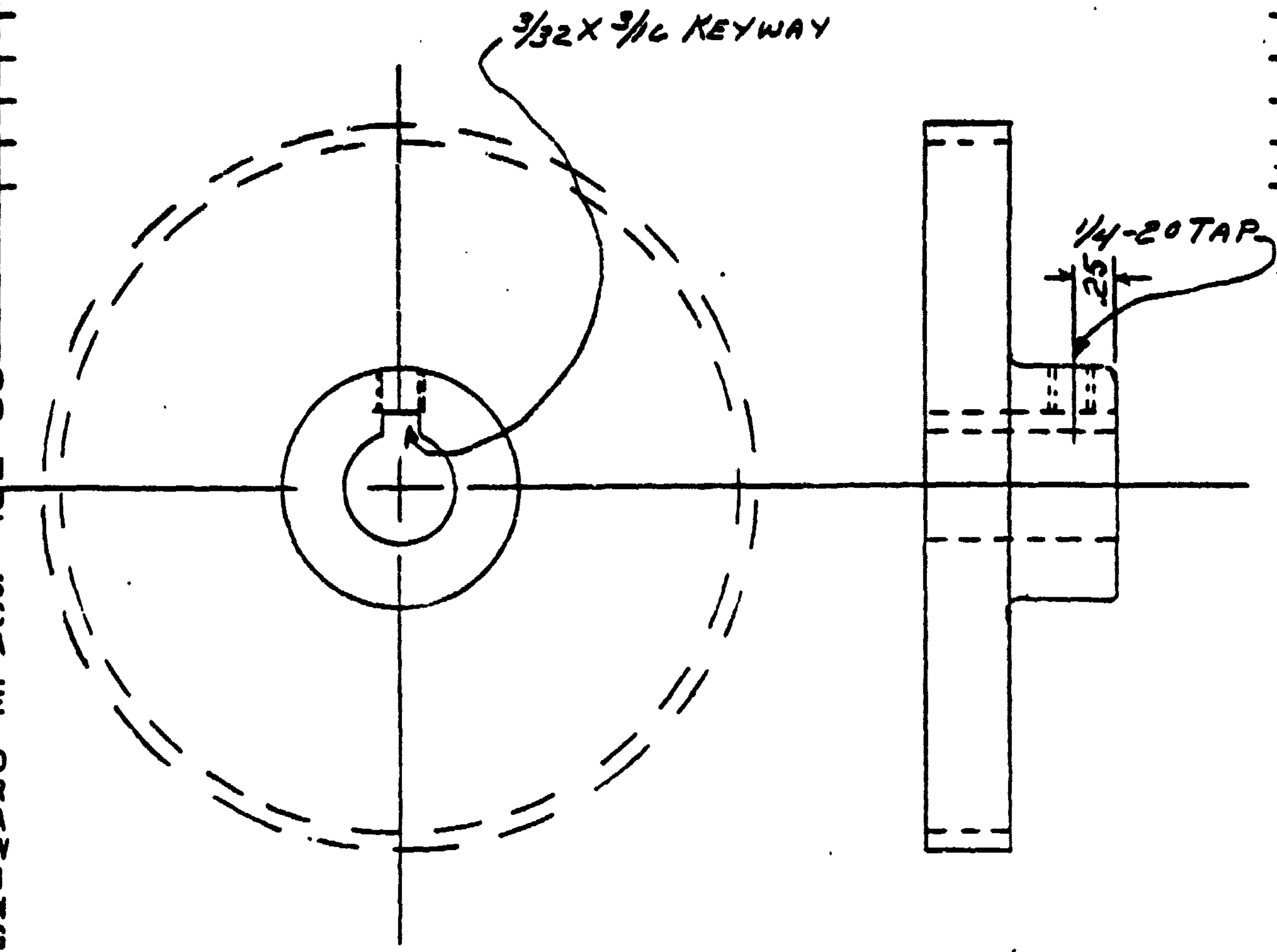

MAT'L - BGW GEAR # NB-128
4" P.D. 16 PITCH 14½° PRESSURE ANGLE

DRAWN	DATE	APPROVED	DATE	CODE
[illegible signature]	1/27/78			✓
CHECKED	**DATE**	**APPROVED**	**DATE**	**CLASS**

MODIFIED GEAR (4") SPEED SHIFT

NOT OTHERWISE SPEC. FRAC ± ANG ± SCALE FULL
FIN. ✓ DEC .X ± .1 .XX ± .02 .XXX ± .005

varian

DIVISION	SIZE	DRAWING NO.	REV
VAC/LEX	A	51076	

DESCRIPTION OF CHANGE

NUM	
EO	
DFT	
CHK	
DATE	
REV	

LITHO IN U.S.A.
41E-3 MAY

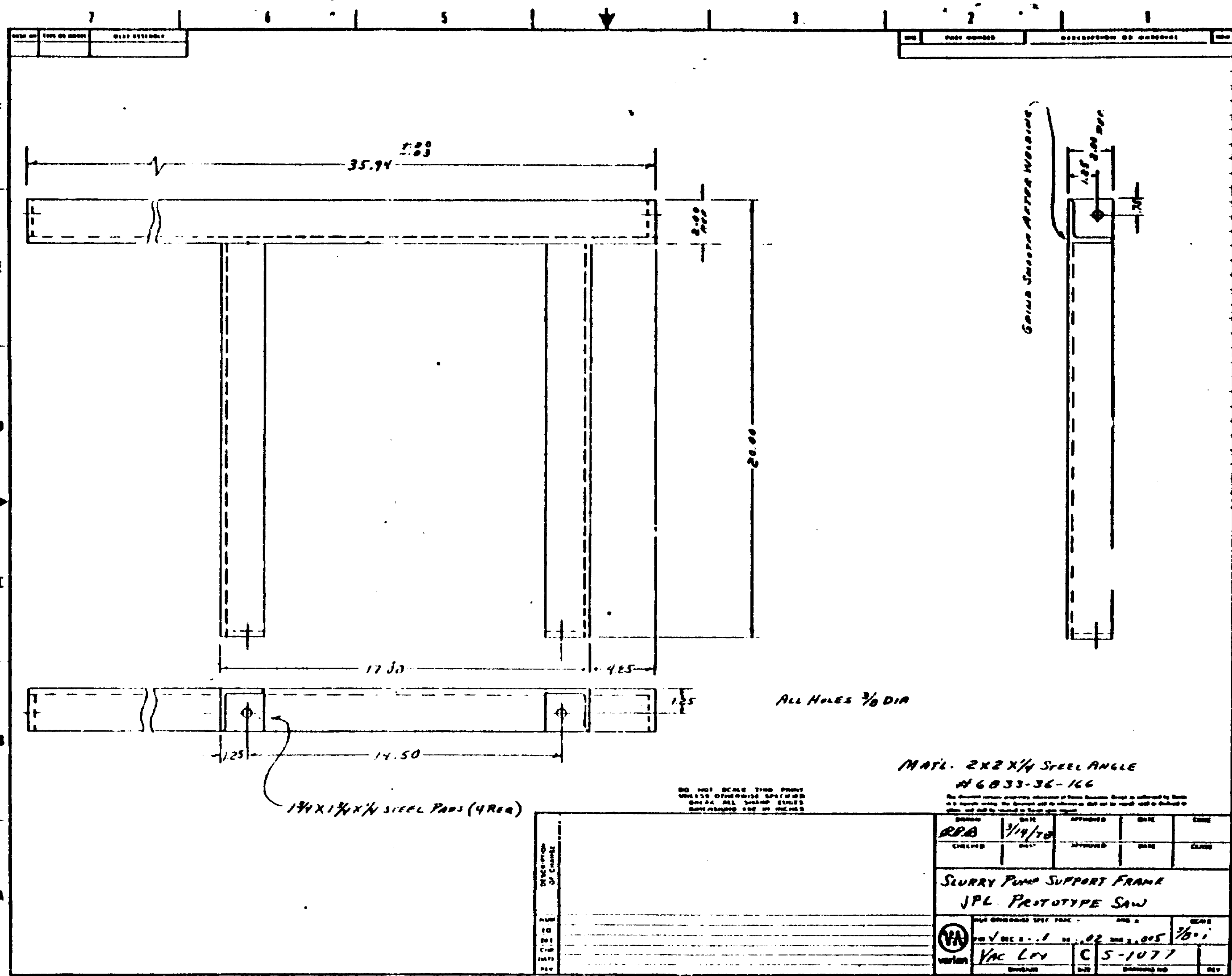

35.94 +.00 -.03
2.00 REF
20.00
17.30
4.25
1.25
14.50
1.25
1¾ X 1¾ X ¼ STEEL PADS (4 REQ)
.38
GRIND SMOOTH AFTER WELDING
ALL HOLES ⅜ DIA
MAT'L. 2 X 2 X ¼ STEEL ANGLE
#6833-36-166
DO NOT SCALE THIS PRINT
RPB
3/19/78
SLURRY PUMP SUPPORT FRAME
JPL PROTOTYPE SAW
varian
VAC LPV
C
S-1077

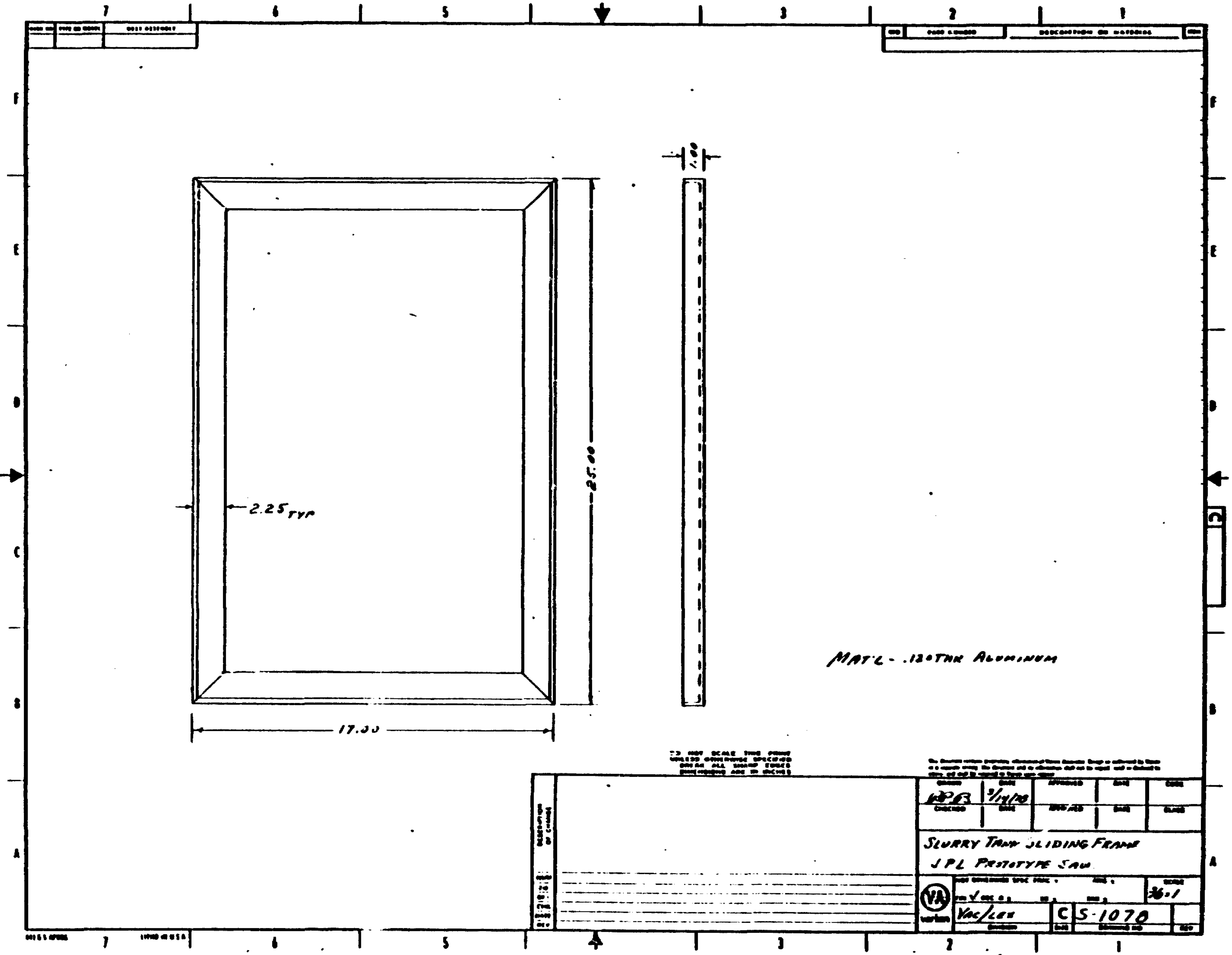

2.25 TYP
25.00
17.50
1.00
MAT'L - .130THK ALUMINUM
SLURRY TANK SLIDING FRAME
JPL PROTOTYPE SAW
9/14/78
VAC/LEX
C
S-1070

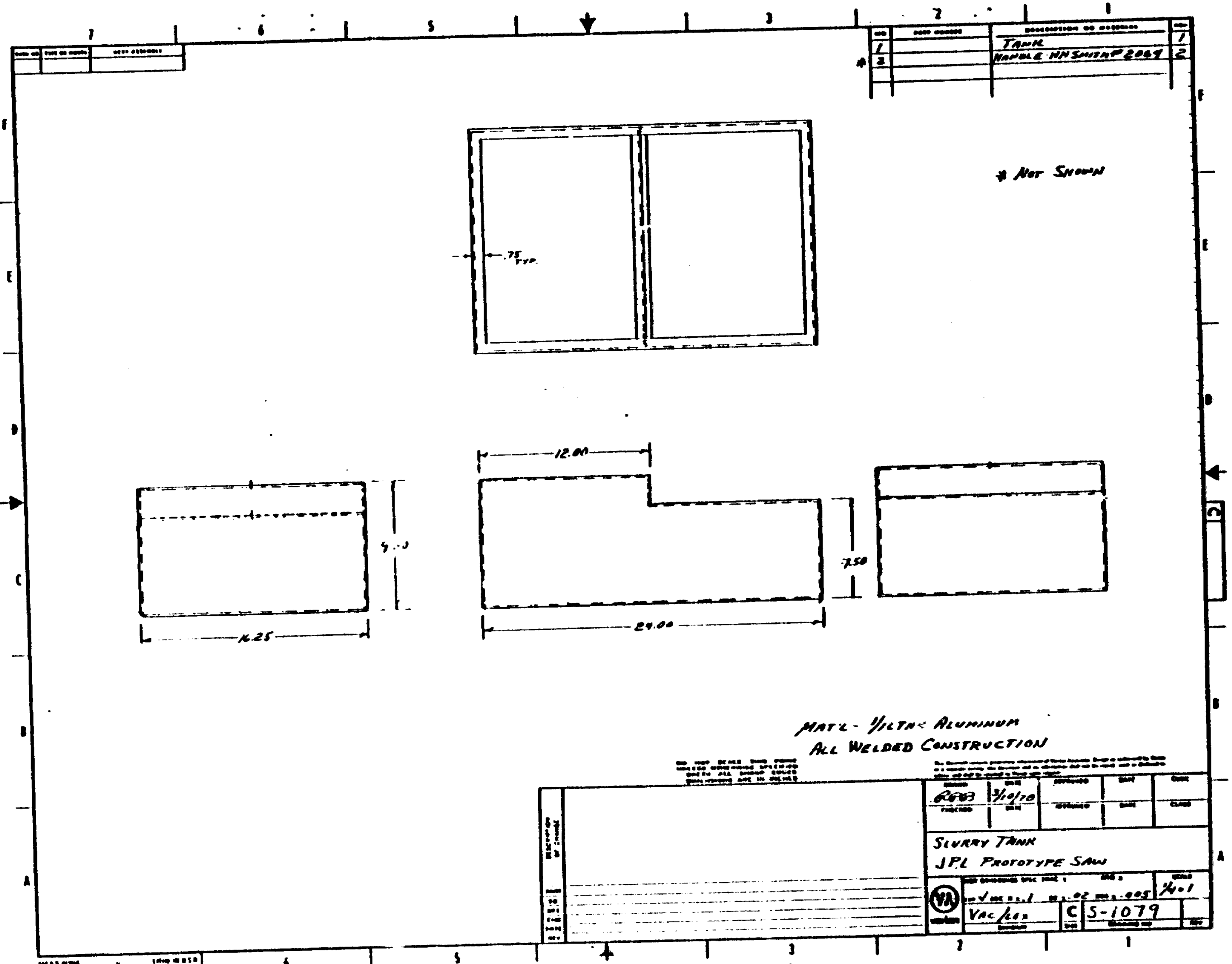

TANK
HANDLE HN SMITH P2069
* NOT SHOWN
.75 TYP.
12.00
7.50
24.00
16.25
MAT'L - 1/8 THK ALUMINUM
ALL WELDED CONSTRUCTION
3/10/70
SLURRY TANK
JPL PROTOTYPE SAW
1/4:1
VAC/LEN
C
S-1079

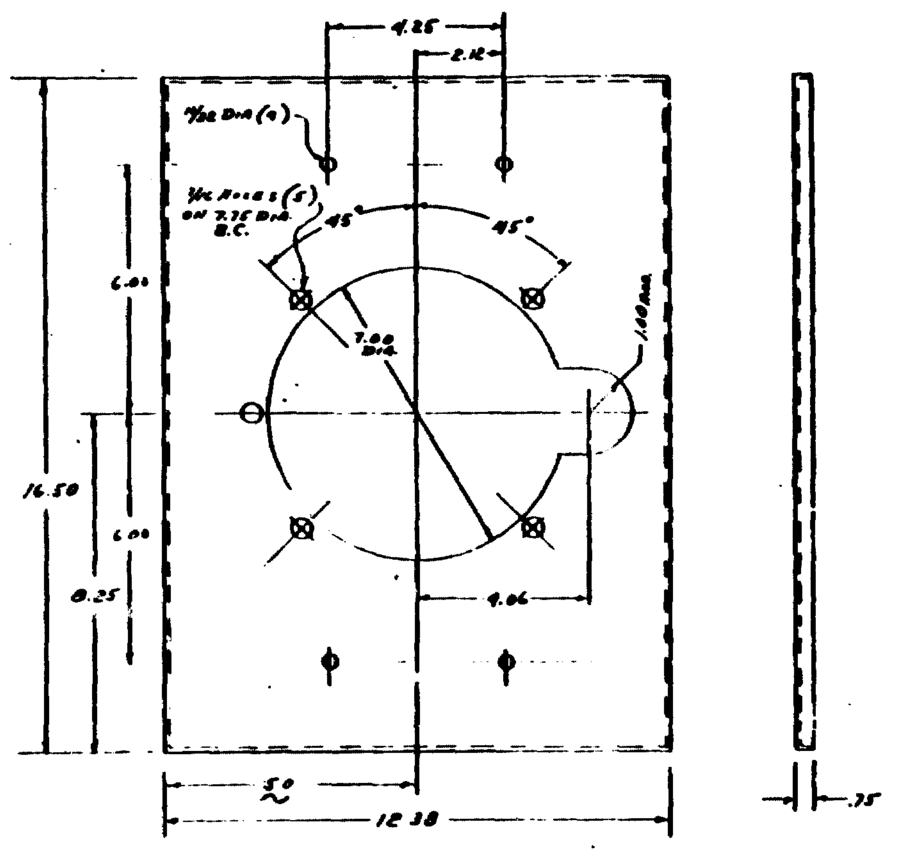

1		COVER	1
2		MODEL - NF SANTO #2052	2

COVER - SLURRY TANK
JPL PROTOTYPE SAW

C | S-1080

Scale 1/2 : 1

B S1082

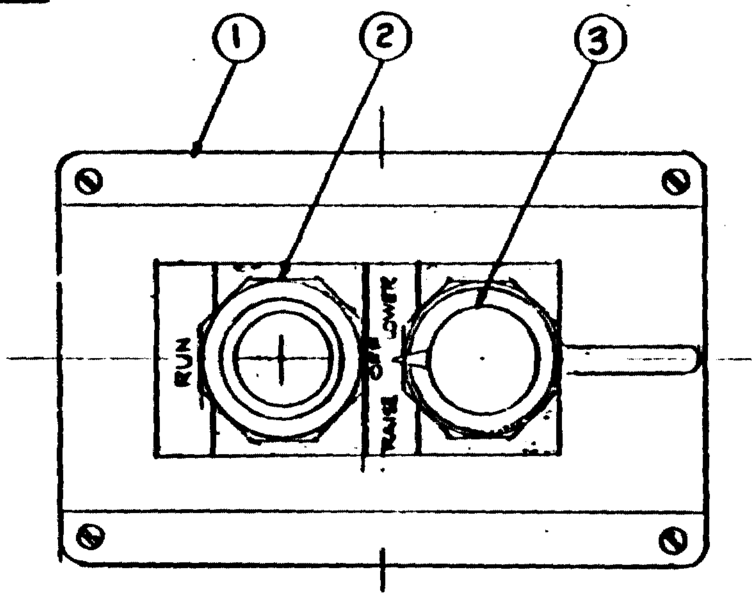

	PART NUMBER	DESCRIPTION OF MATERIAL	ITEM
1		ENCLOSURE-SURFACE MOUNTED NEMA TYPE 13- 2HOLE DIE CAST A-B BUL 800T CAT Nº 800TH2TB	1
1		PILOTLIGHT-120VOLT TRANSF. TYPE GREEN LENS W/LEGEND PLATE "RUN" A-B BUL 800T CAT Nº 800T-P16G	2
1		SELECTOR SWITCH-3POSITION SPRING RETURN FROM BOTH SIDES (1NO-1NC CONTACTS) W/ LEGEND PLATE "RAISE-OFF-LOWER" W/ YELLOW WING LEVER OPERATOR A-B CAT Nº 800TJG141H	3

DO NOT SCALE THIS PRINT

DRAWN CWL	DATE 3-3-78	APPROVED	DATE	CODE
CHECKED	DATE	APPROVED	DATE	CLASS

ENCLOSURE ASSEMBLY
(REMOTE FAST LIFT)

SCALE FULL

LEXINGTON VACUUM

B S1082

DO NOT SCALE DRAWING

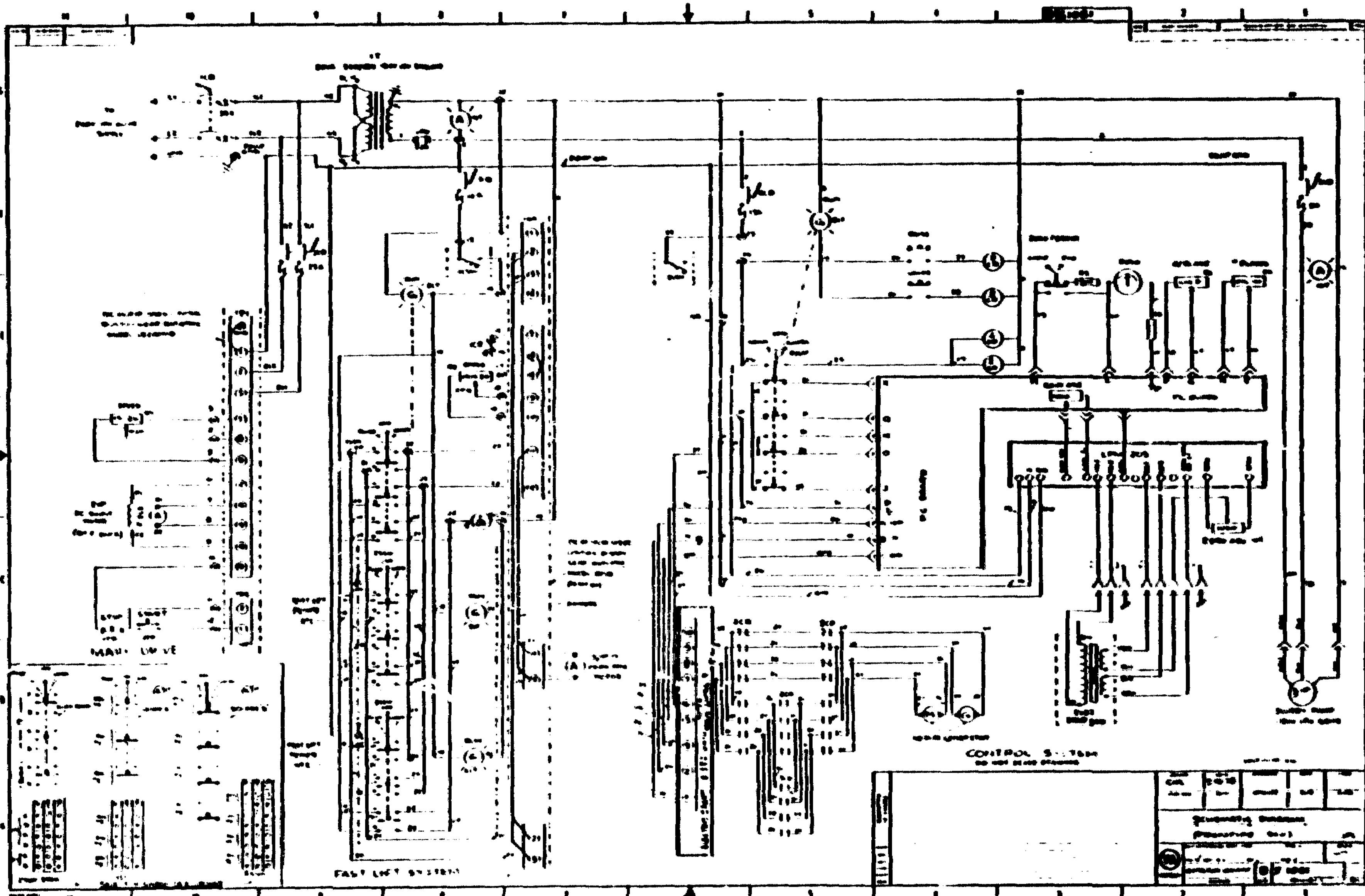
CONTROL SYSTEM
FAST LIFT SYSTEM

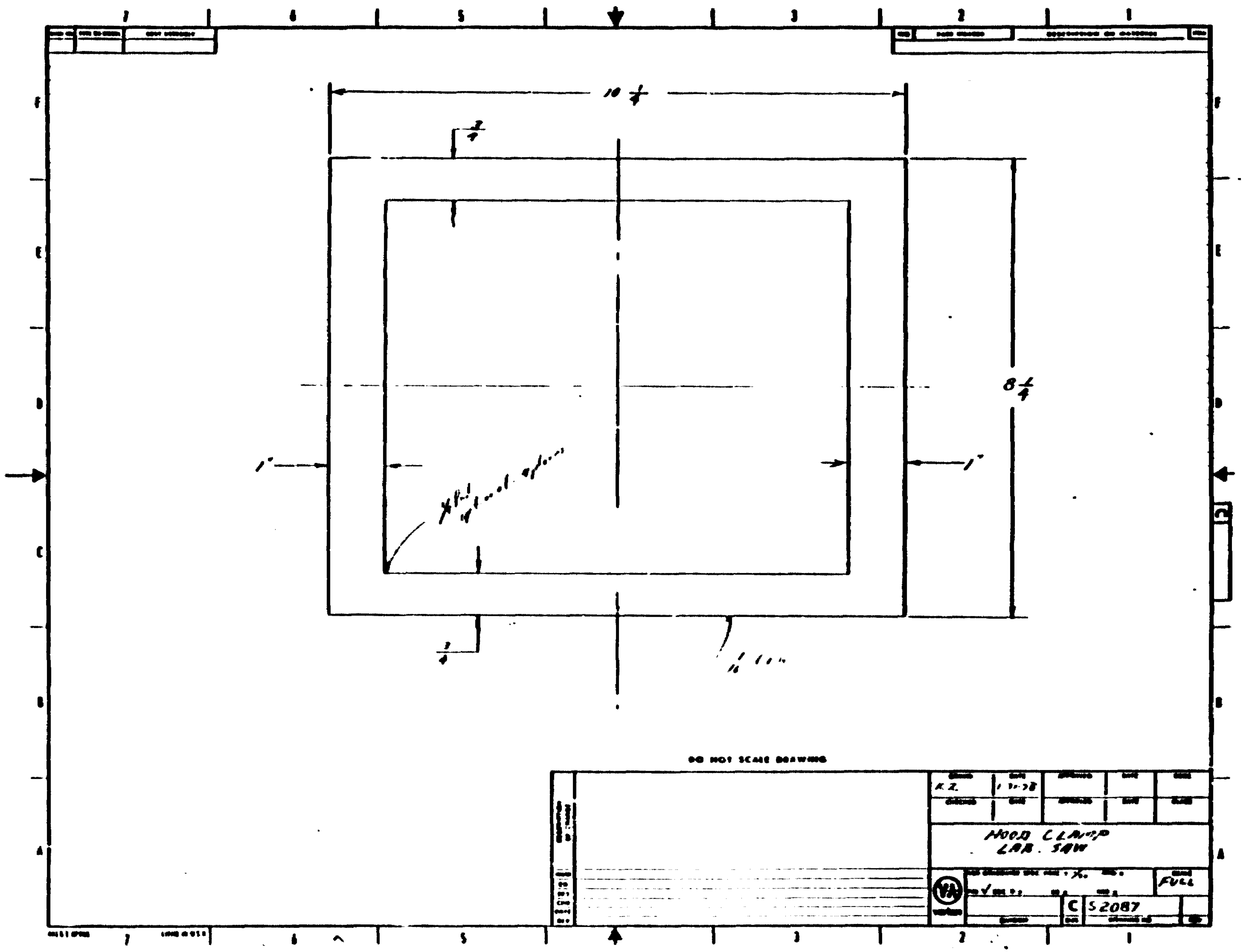
10 1/4
8 1/4
1"
1"
3/4
3/4
DO NOT SCALE DRAWING
K.Z.
HOOD CLAMP
LAB. SAW
FULL
C
S2087

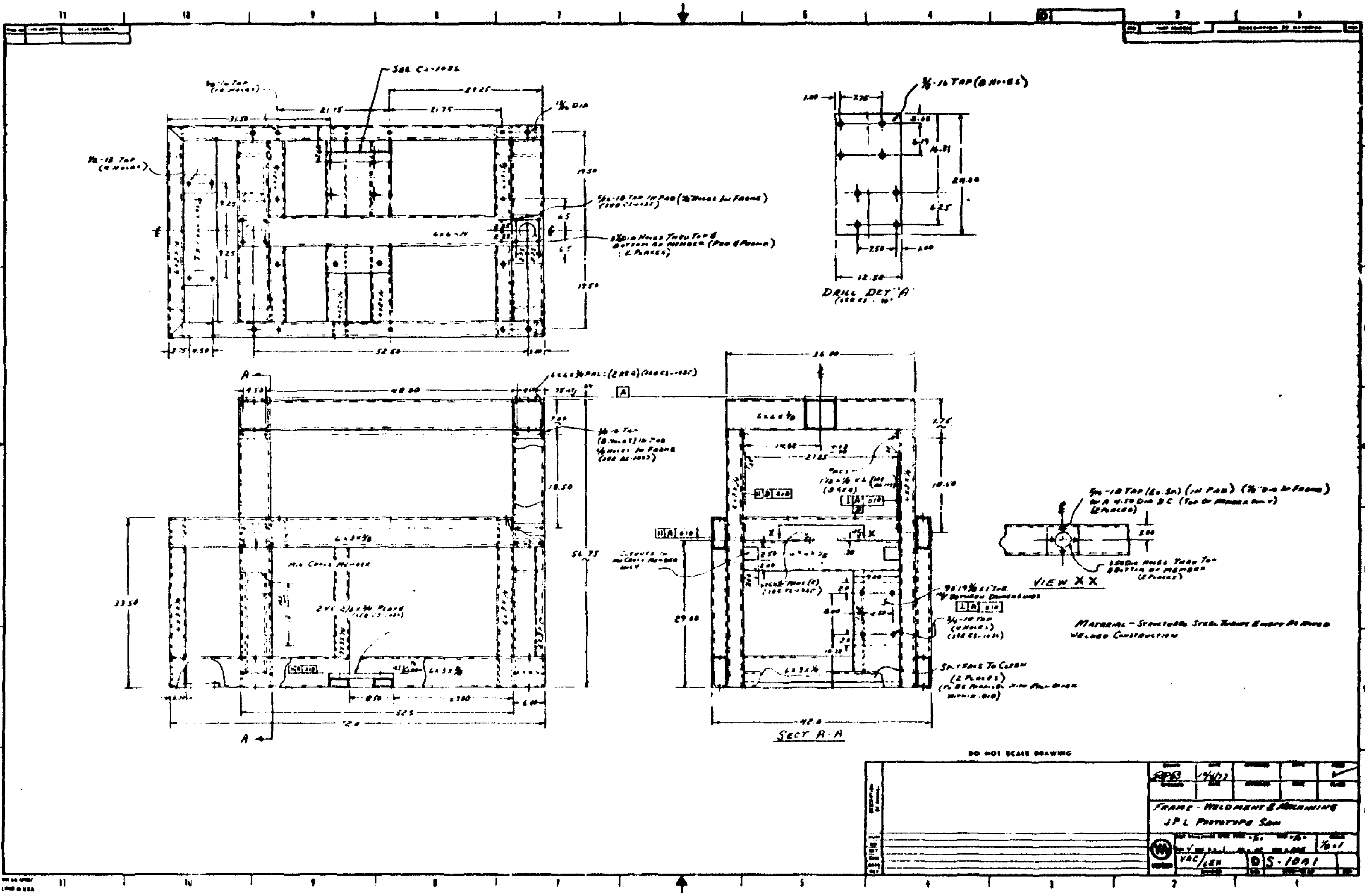

DRILL DET 'A'
VIEW XX
SECT A-A
MATERIAL - STRUCTURAL STEEL TUBING EXCEPT AS NOTED
WELDED CONSTRUCTION
DO NOT SCALE DRAWING
FRAME - WELDMENT & MACHINING
JPL PROTOTYPE SAW
D S-10A1

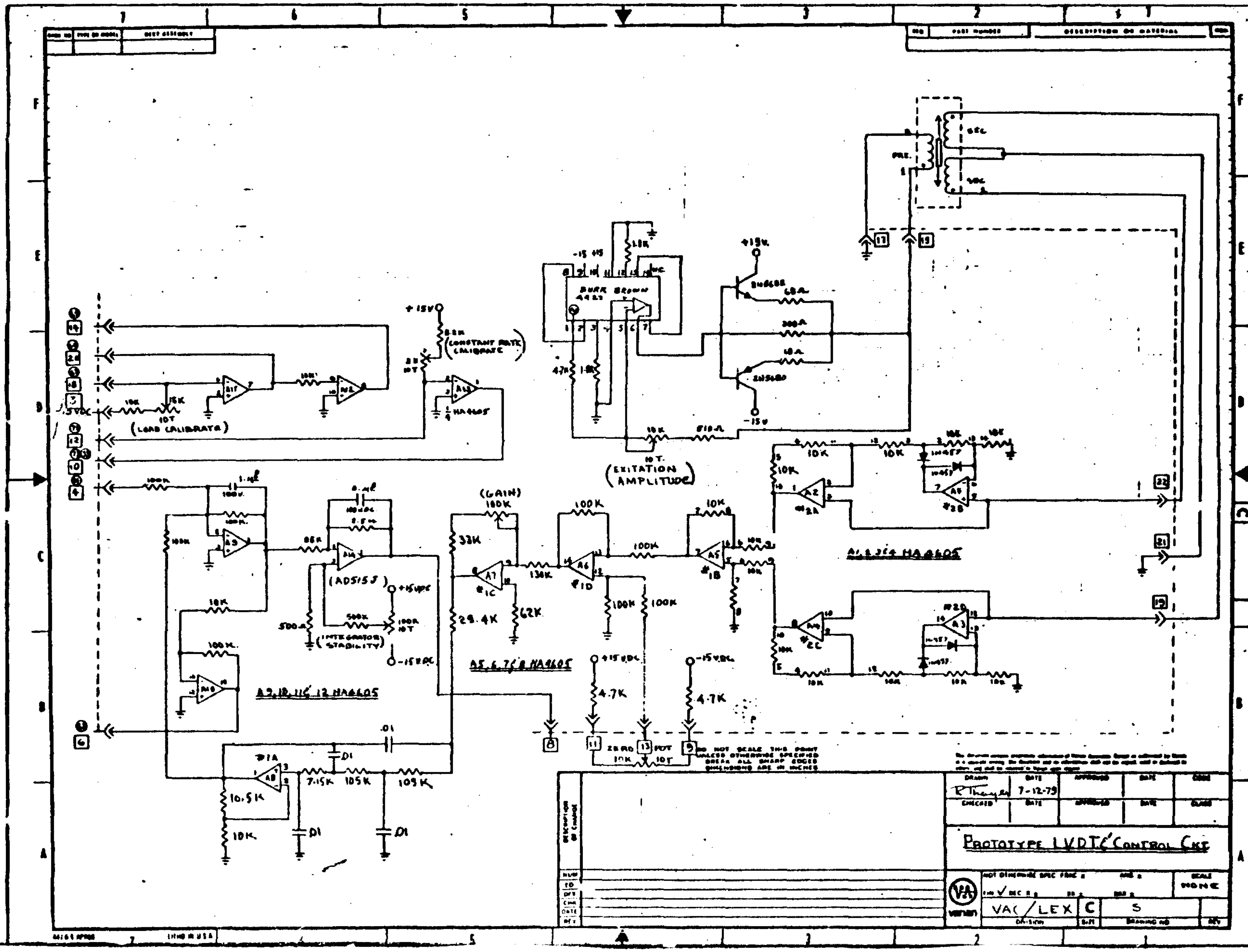
PROTOTYPE LVDT & CONTROL CKT
7-12-79
VAC / LEX
C
5
NONE
(LOAD CALIBRATE)
(CONSTANT RATE CALIBRATE)
(EXITATION AMPLITUDE)
(GAIN)
(AD515J)
(INTEGRATOR STABILITY)
BURR BROWN 4423
2N5680
A1, 2 & 4 HA4605
A5, 6, 7 & 8 HA4605
A9, 10, 11 & 12 HA4605
ZERO POT
DO NOT SCALE THIS PRINT UNLESS OTHERWISE SPECIFIED BREAK ALL SHARP EDGES DIMENSIONS ARE IN INCHES
+15V
-15V
+15VDC
-15VDC
PRI.
SEC.
100K
10K
4.7K
33K
29.4K
62K
130K
105K
7.15K
10.5K
.01
1.5VDC

APPENDIX IX

MILESTONE CHARTS (Phases I and II)

SLICING OF SILICON INTO SHEET MATERIALS

Varian Associates
Lexington Vacuum Division
JPL Contract No. 954374
Starting Date: 1/9/76

1. Background Parameter Study
   - 1.1. Establish standardized cutting format and data collection technique
   - 1.2. Modify saw, measure accuracy, build dynamometer
   - 1.3. Slicing tests - effects of load, speed, slurry, work configuration on rate, wear, wafer accuracy, etc.
   - 1.4. Wafer characterization
2. Theoretical Model
   - 2.1. Parameterize system performance from modified abrasive wear viewpoint
   - 2.2. Establish practical limits to theory - wafer accuracy and thickness, blade instability, abrasive blunting, etc.

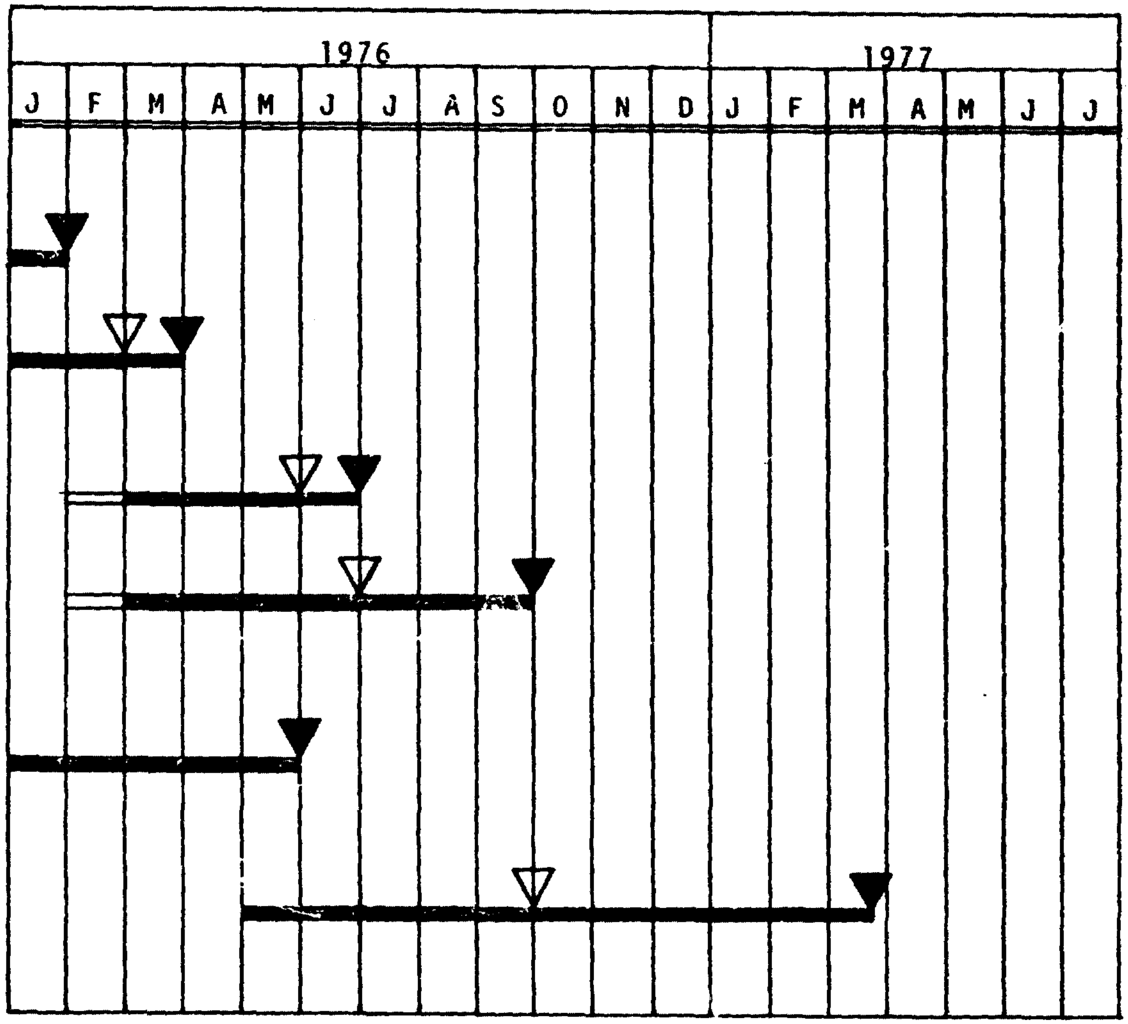

Sch 1/22/76
Updated 6/17/77

3. Load Balancing
   3.1. Build feedback control system - rate and force interaction
   3.2. Cutting performance vs. results of 1.3.
   3.3. Wafer characterization
4. Blade Materials
   4.1. Cutting tests - optimum blade material, thickness, etc. for silicon
   4.2. Wafer characterization
5. Abrasives
   5.1. Cutting tests - optimum size, slurry mix, application technique
   5.2. Wafer characterization
6. Prototype Production Technique
   6.1. Optimize previous results within guidelines of wafer specifications
   6.2. Modify equipment

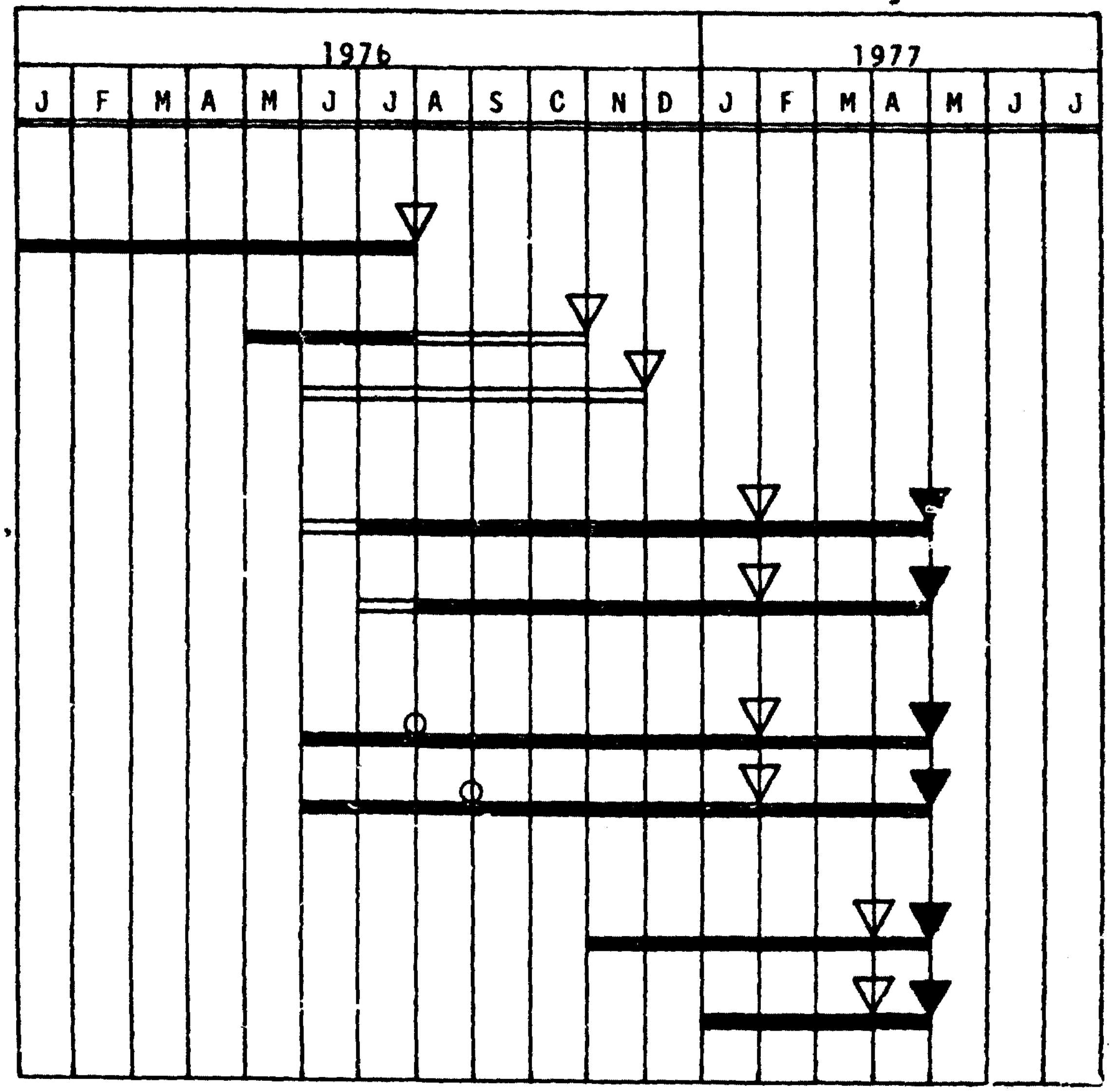

Sch 1/22/76
Updated 6/17/77

7. Evaluation
   - 7.1. Cutting tests with final system
   - 7.2. Economic evaluation, scale-up potential
   - 7.3. Wafer characterization

8. Milestones

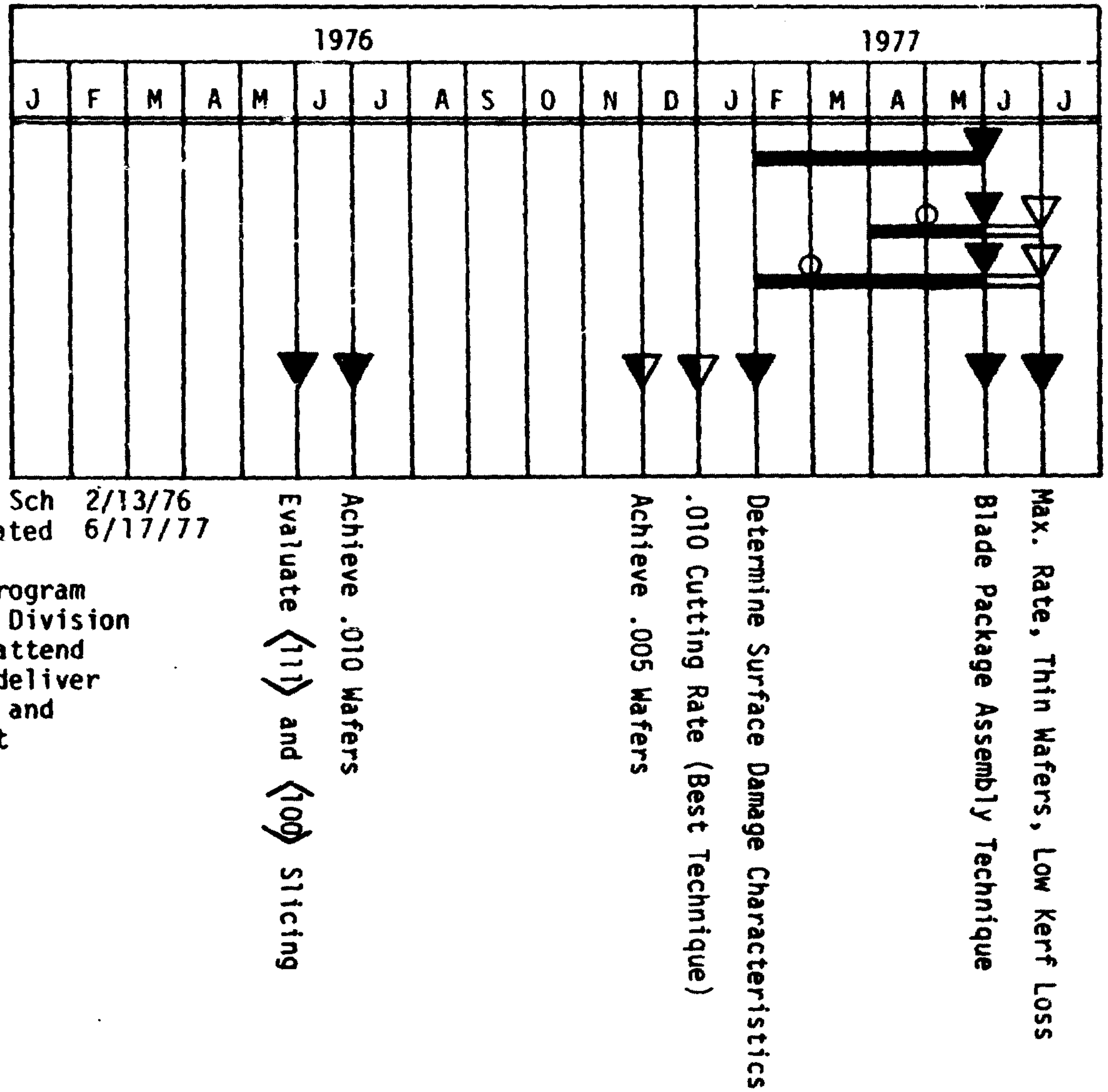

Sch 2/13/76
Updated 6/17/77

NOTE: In addition to the above Program Plan, the Lexington Vacuum Division of Varian Associates will attend the required meetings and deliver the required documentation and samples as per JPL Contract No. 954374.

SLICING OF SILICON INTO SHEET MATERIAL

Varian Associates/Lexington Vacuum Division
JPL Contract 954374
Starting Date: 1/9/76 (I) 5/19/77 (II)

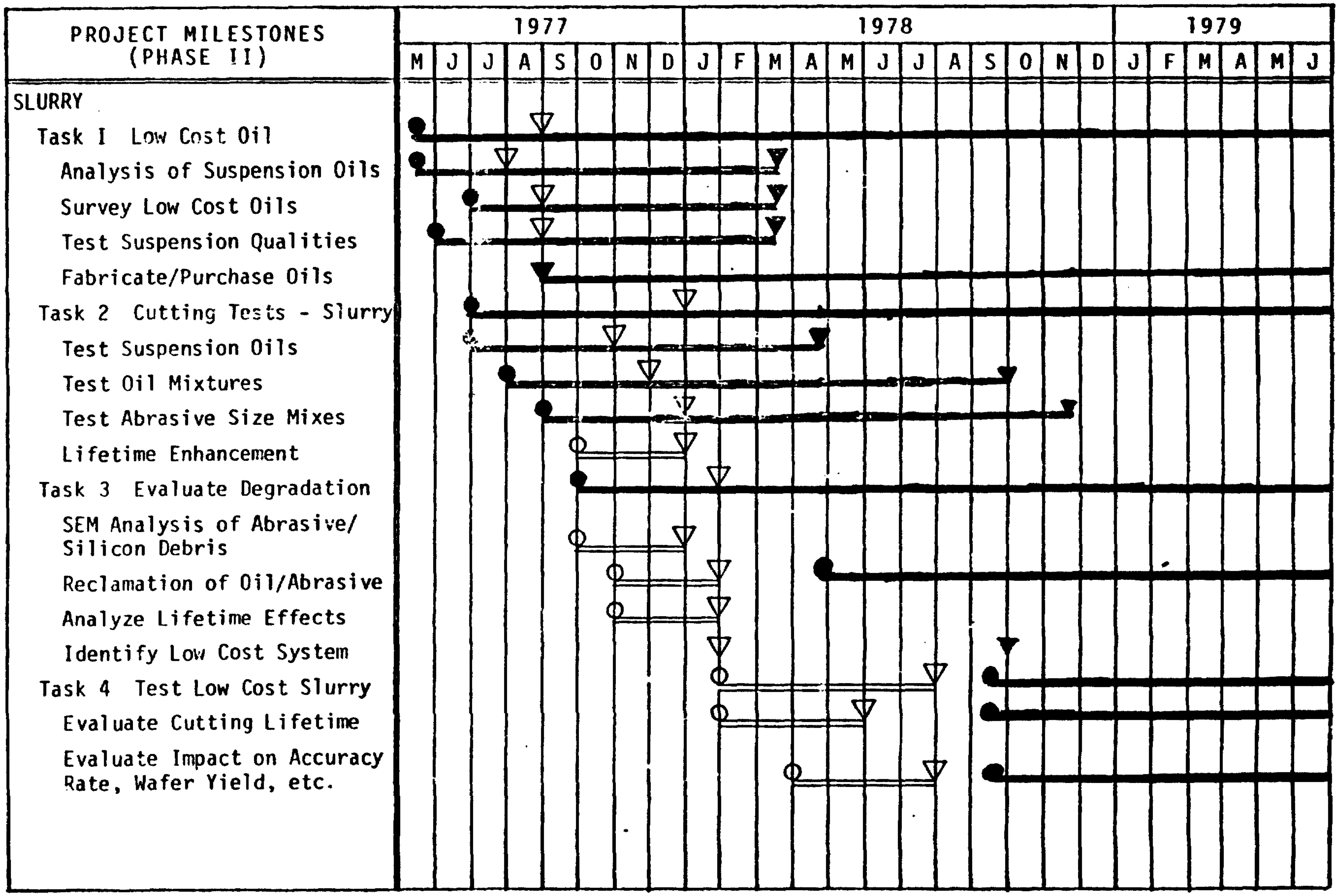

SCH 6/15/77
Updated 5/11/79

SLICING OF SILICON INTO SHEET MATERIAL

Varian Associates/Lexington Vacuum Division
JPL Contract 954374
Starting Date: 1/9/76 (I) 5/19/77 (II)

Phase II
Program Plan

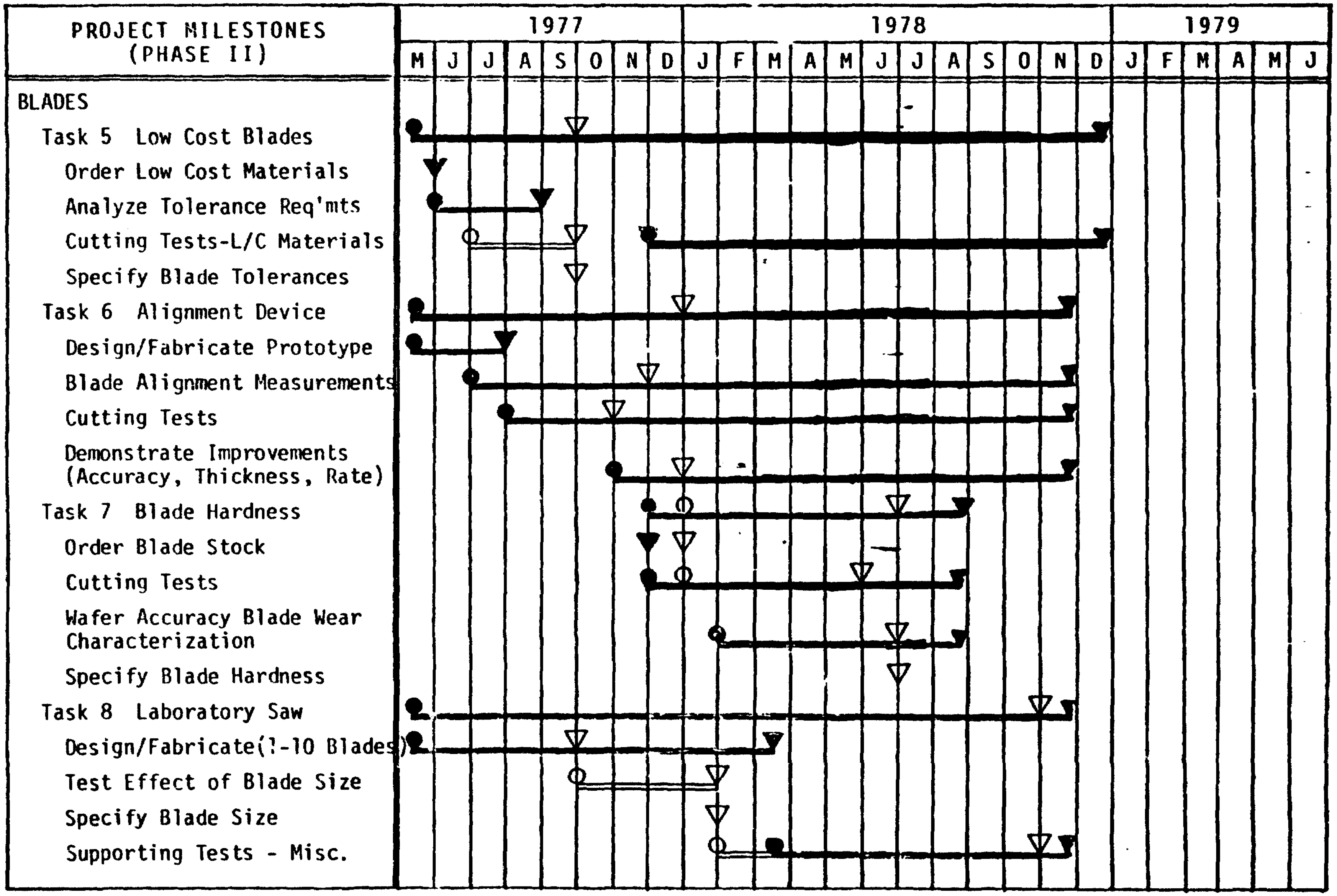

SCH 6/15/77
Updated 5/11/79

SLICING OF SILICON INTO SHEET MATERIAL

Varian Associates/Lexington Vacuum Division
JPL Contract 954374
Starting Date: 1/9/76 (I) 5/19/77 (II)

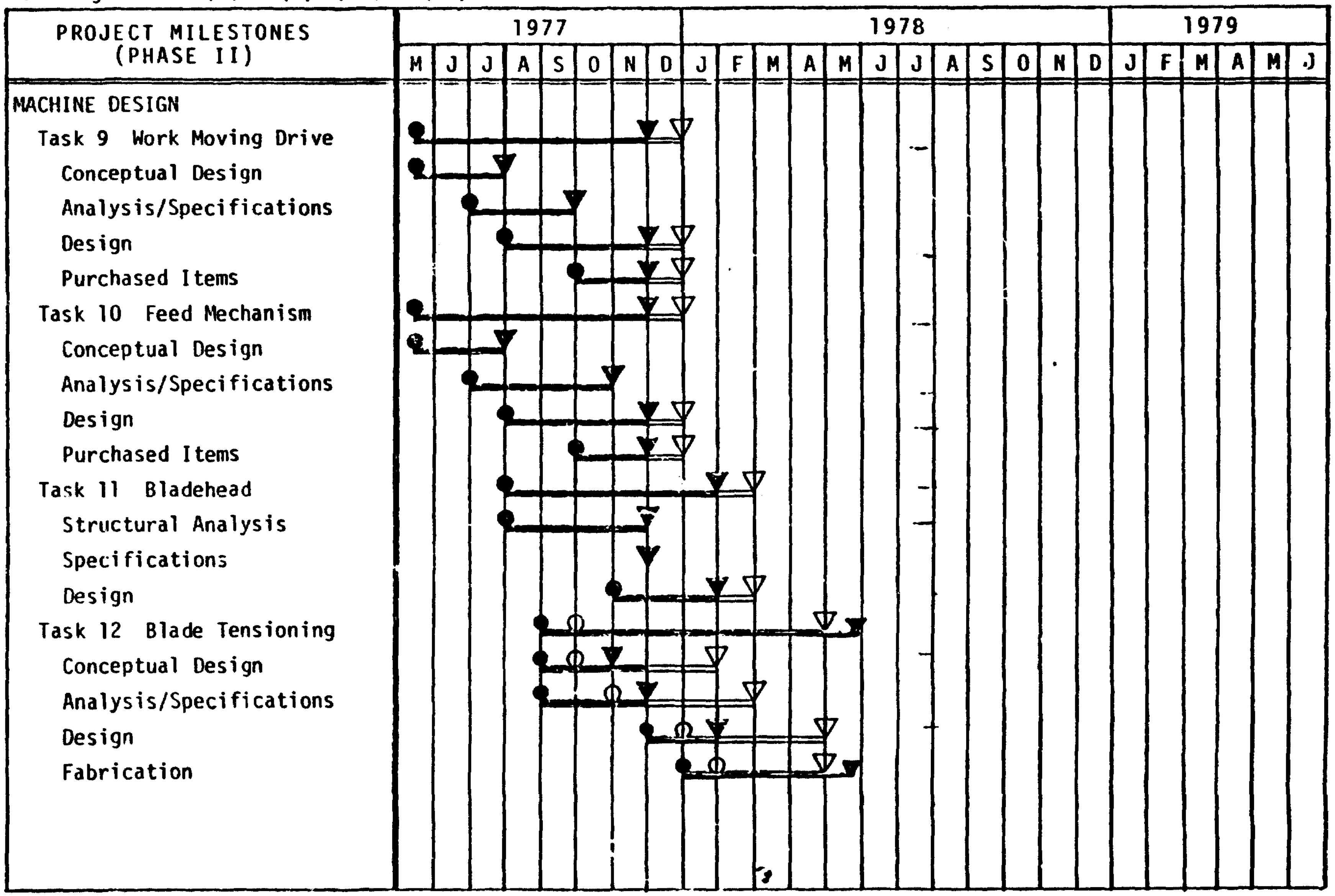

SCH 6/15/77
Updated 5/11/79

SLICING OF SILICON INTO SHEET MATERIAL

Varian Associates/Lexington Vacuum Division
JPL Contract 954374
Starting Date: 1/9/76 (I) 5/19/77 (II)

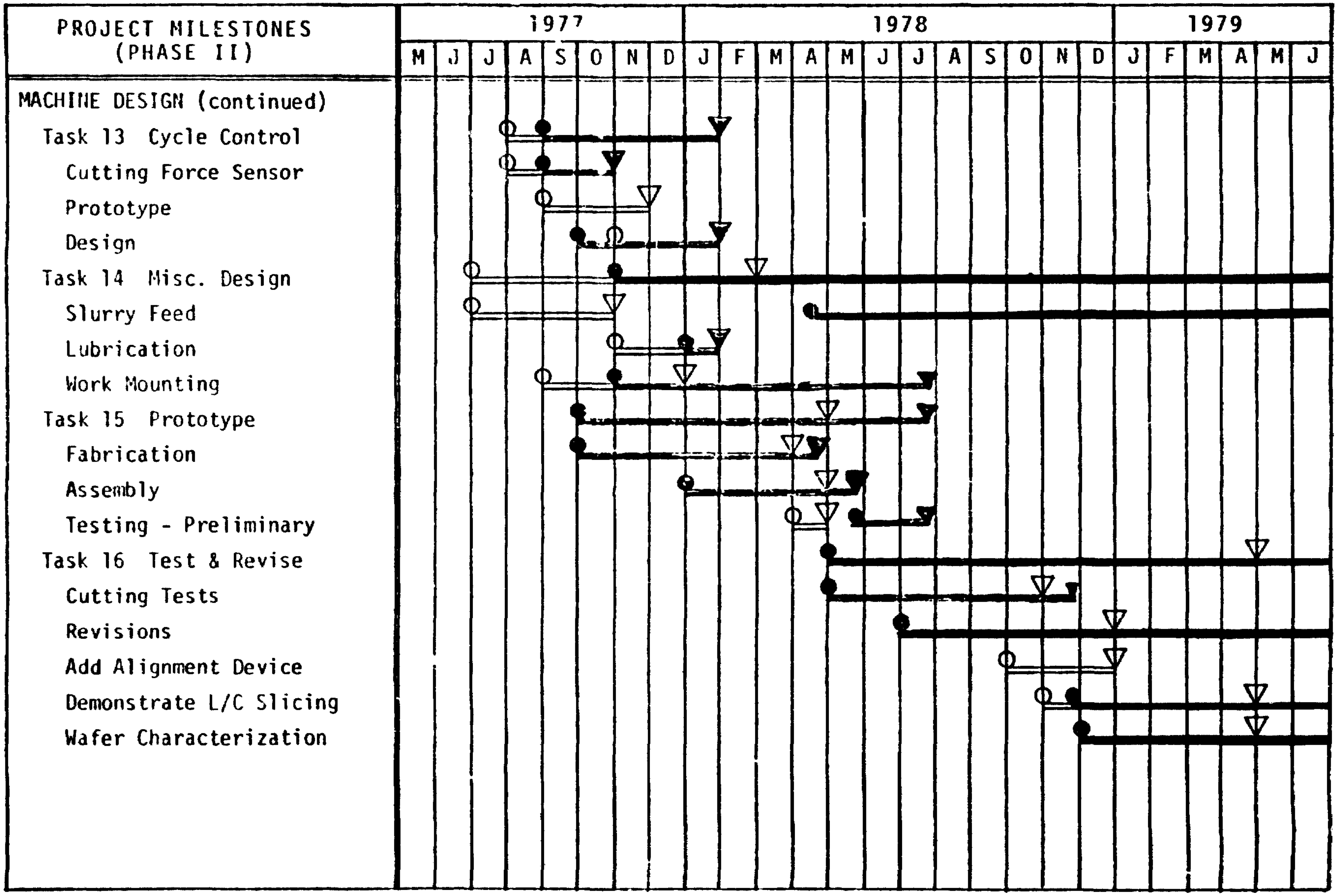

SCH 6/15/77
Updated 5/11/79

SLICING OF SILICON INTO SHEET MATERIAL

Varian Associates/Lexington Vacuum Division
JPL Contract 954374
Starting Date: 1/9/76 (I) 5/19/77 (II)

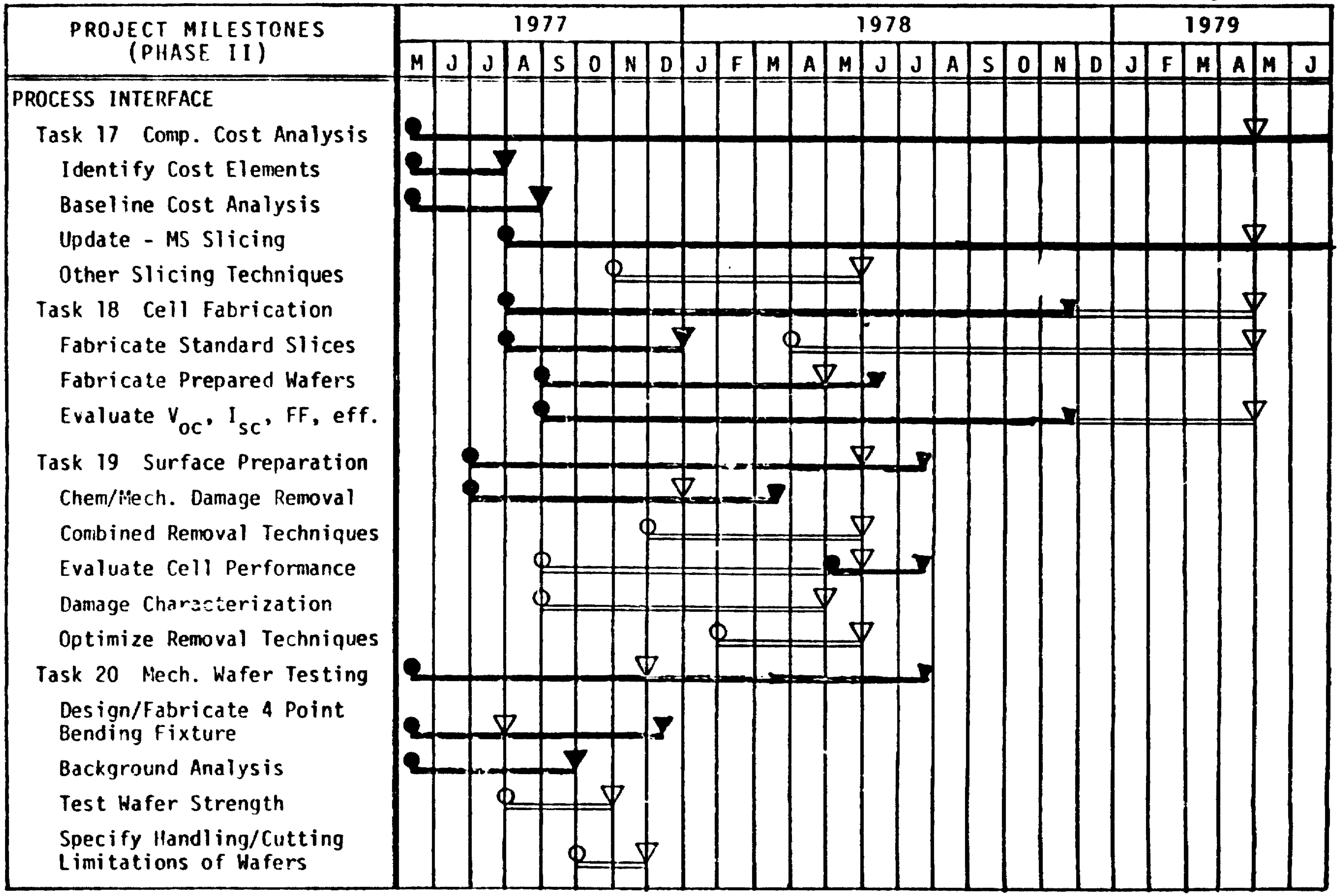

SCH 6/15/77
Updated 5/11/79

SLICING OF SILICON INTO SHEET MATERIAL

Varian Associates/Lexington Vacuum Division
JPL Contract 954374
Starting Date: 1/9/76 (I) 5/19/77 (II)

Phase II
Program Plan

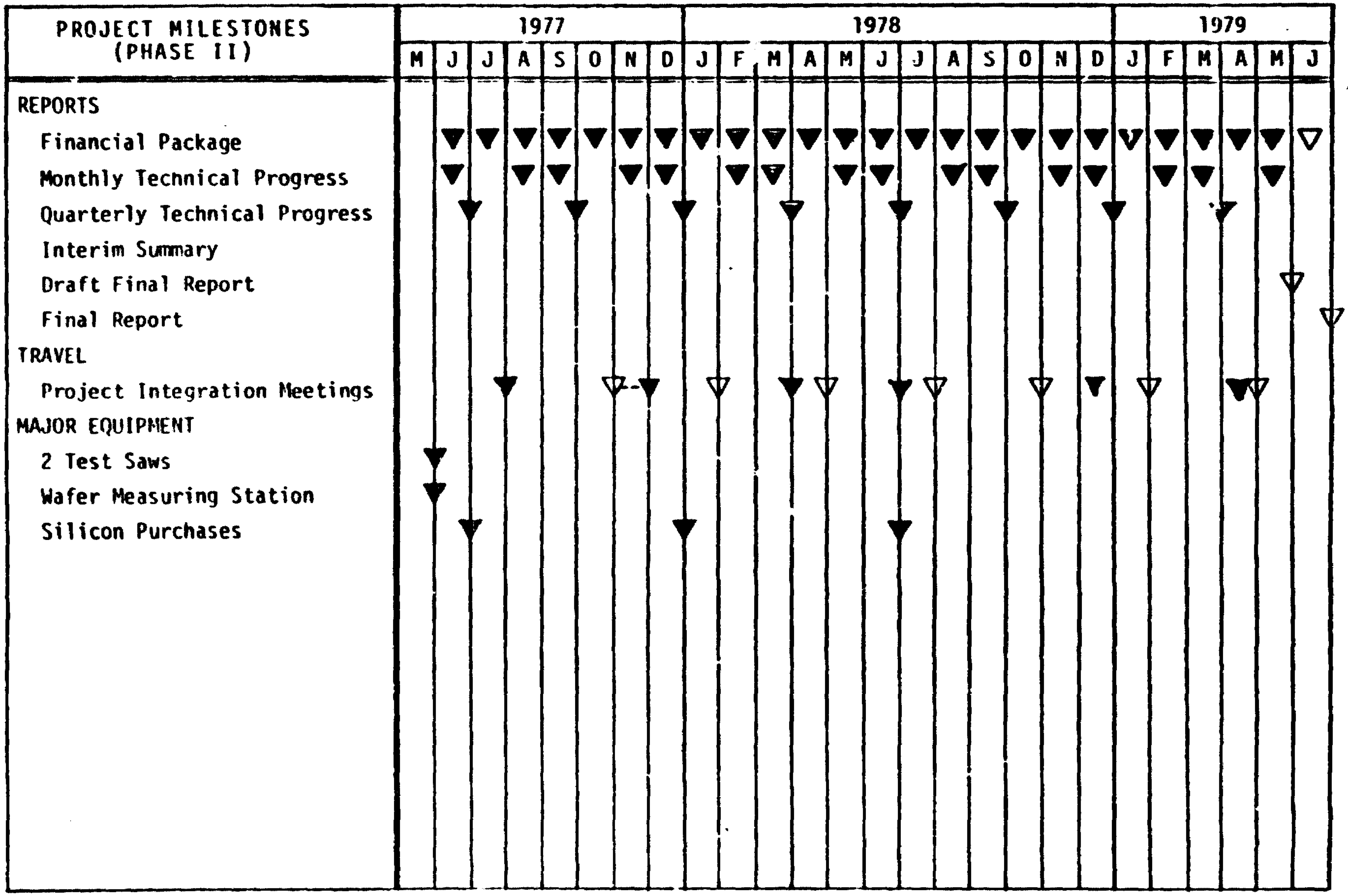

SCH 6/15/77
Updated 5/11/79